12-2013

Hybrid Low-Order Modeling for Conceptual Vehicle Design

Robert Mau
Clemson University, rjmau@outlook.com

HYBRID LOW-ORDER MODELING FOR CONCEPTUAL VEHICLE DESIGN

A Thesis
Presented to
the Graduate School of
ClemsonUniversity

In Partial Fulfillment
of the Requirements for the Degree
Doctor of Philosophy
Automotive Engineering

---

by
Robert John Mau
December 2013

Accepted by:
Dr. Paul J. Venhovens, Committee Chair
Dr. Imtiaz Haque
Dr. Georges Fadel
Dr. Zoran Filipi

ABSTRACT

Design freedom, and particularly the freedom to incorporate innovative designs and strategies, is greatest at the very beginning of vehicle conceptual design. Conversely, this is when the least knowledge of the product exists. As product content decisions are made the level of freedom in the design decreases and the design becomes "locked in." The majority of vehicle lifecycle cost is also set by the end of vehicle conceptual design. This makes it critical to make well-informed and validated decisions in the concept design phase to avoid expensive iterations and redesign in the detailed design phase.

Parametric vehicle modeling permits rapid iteration and optimization of vehicles in the conceptual design phase. A significant portion of vehicle design can be optimized parametrically without knowing specific Computer Aided Design (CAD) based details. Many overall vehicle characteristics such as curb mass, center of gravity location, key dimensions, occupant packaging and cargo volume can all be assessed and improved at the parametric level. Key vehicle performance measures can also be determined to a high level of confidence.

In developing vehicle dimensions for a parametric model it is recommended to build up a vehicle using an "inside-out" approach centered on effective, knowledge-based occupant packaging. This work develops a continuum of dimensional parameters which tie vehicle internal and external dimensions together; it employs a combination of industry standard and author-defined component dimensions which make up overall

vehicle outside dimensions. An effective continuum of functional parameters is also developed.

In order to develop and optimize models for a desired vehicle type and size class, a knowledge base of vehicle typical values for key dimensional parameters has been compiled using a combination of data sources and field measurements. These values provide a useful starting point for the vehicle design optimization process. They also increase optimization effectiveness and ensure that the optimization begins within a valid design space.

This work also develops a parametric modeling, scenario builder and optimization software framework which provides a design and optimization tool for vehicle design with trade-off evaluation tools. These parametric design methods improve design maturity prior to beginning vehicle detailed design.

DEDICATION

This manuscript is dedicated to my wife Katherine, my daughter Jessica and son David for their support and understanding throughout this degree program. I would also like to thank Paul Kumler, who encouraged and supported me in pursuing a doctoral degree through CU-ICAR

I also wish to thank my advisor, Dr. Paul Venhovens, for his support and mentoring. My thanks and appreciation go to Dr. Georges Fadel for his input and feedback on the effective incorporation of optimization methodologies in this work.

TABLE OF CONTENTS

Table of Contents (Continued)

Page

Table of Contents (Continued)

Page

LIST OF TABLES

List of Tables (Continued)

Table Page

List of Tables (Continued)

List of Tables (Continued)

Table Page

List of Tables (Continued)

List of Tables (Continued)

List of Tables (Continued)

Table Page

List of Tables (Continued)

Table Page

LIST OF FIGURES

List of Figures (Continued)

List of Figures (Continued)

List of Figures (Continued)

List of Figures (Continued)

List of Figures (Continued)

List of Figures (Continued)

Figure Page

List of Figures (Continued)

List of Figures (Continued)

List of Figures (Continued)

NOTATION

3-D	Three-Dimensional
$a_1 ... a_4$	Average acceleration for crush zones 1 through 4 for frontal crash model
A40	Torso Angle -- Front. Also referred to as A40-1 (SAE J1100) [1]
A40-1	Torso Angle -- Front (row) (SAE J1100) [1]
A46	Ankle Angle -- Front. Also referred to as A46-1 (SAE J1100) [1]
A46-1	Ankle Angle -- Front (row) (SAE J1100) [1]
A47	Shoe Plane Angle (SAE J1100) [1]
AAA	Automated Aircraft Analysis
a_C_g	Longitudinal distance from Front Wheel Center (FWC) to vehicle Center of Gravity (C_g)
AHP	Accelerator Heel Point (SAE J1100) [1]
ALM	Augmented Lagrange Multiplier
a_{max}	Maximum vehicle acceleration for frontal crush zones 1 through 4
AML	Automated Modeling Language
A_s	Vehicle frontal surface area (m^2)
AutoDSS	Automotive Decision Support System
AWD	All-Wheel Drive
b_Cg	Longitudinal distance from vehicle center of gravity to Rear Wheel Center (RWC)
BiW	Body in White
BMW	BayerischeMotorenWerke AG
BOFRP	Ball of Foot Reference Point (SAE J1100) [1]
CAD	Computer Aided Design
CAE	Computer Aided Engineering
C_d	Vehicle Drag Coefficient
CFR	Code of Federal Regulations
C_g	Center of Gravity

COM	Component Object Model	
CORBA	Common Object Request Broker Architecture	
CSUV	Crossover Sport Utility Vehicle (Unibody / Monococque construction)	
CTC	Curb-to-Curb (turn radius)	
CU-ICAR	Clemson University International Center for Automotive Research	
D102	Turn Diameter, Wall-to-Wall	(SAE J1100) [1]
DARPA	Defense Advanced Research Projects Agency	
DART	Design Analysis Response Tool	
DNA	Deoxyribonucleic Acid	
$E_1 ... E_4$	Energy absorbed in frontal crash for crush zones 1 through 4	
E_{cycle}	Energy required for a given EPA mileage test cycle	
EPA	(U.S.) Environmental Protection Agency	
EPA_{city}	EPA City mileage using UDDS cycle	
$EPA_{highway}$	EPA Highway mileage using FWFET cycle	
$F_1 ... F_4$	Average midrail crush force for frontal crush zones 1 through 4	
F101	Vehicle Footprint	(SAE J1100) [1]
FAA	(U.S.) Federal Aviation Authority	
FANG	Fast Adaptable Next-Generation Ground Vehicle	
FAR	Federal Aviation Regulations	
FEA	Finite Element Analysis	
F_{hybrid}	Hybrid vehicle mass adjustment factor	
F_M	Average midrail crush force	
FMVSS	Federal Motor Vehicle Safety Standard	
f_r	Coefficient of rolling resistance	
FRP	Floor Reference Point	(SAE J1100) [1]
FWD	Front-Wheel Drive	
FWFET	EPA Highway Driving Cycle	
g	Gravitational acceleration (1 "g" = 9.81 m/sec^2)	
GM	General Motors	

H5-1	SgRP to Ground -- Front	(SAE J1100) [1]
H5-2	SgRP to Ground -- Second	(SAE J1100) [1]
H30-1	Seat Height -- Front (Row)	(SAE J1100) [1]
H30-2	Seat Height -- Second (Row)	(SAE J1100) [1]
H30D-2	Seat Height Difference -- First to Second (*H30-2 - H30-1*)	
H37	Headliner Thickness -- Front (Discontinued by SAE)	(SAE J1100) [1]
H38	Headliner Thickness -- Second (Discontinued by SAE)	(SAE J1100) [1]
H61-1	Effective Headroom -- Front	(SAE J1100) [1]
H61-2	Effective Headroom -- Second	(SAE J1100) [1]
H100	Vehicle Height -- Body	(SAE J1100) [1]
H101	Vehicle Height -- Maximum	(SAE J1100) [1]
H111-1	Rocker Panel Height -- Front	(SAE J1100) [1]
H111-2	Rocker Panel Height --Rear	(SAE J1100) [1]
HH-1	"Heel Height" -- vertical distance from H111-1 rocker point to Accelerator heel point (AHP)	
HIC	Head Injury Criteria	
HOTOL	Horizontal Take-Off and Landing	
H-Point	Hip-Point	(SAE J1100) [1]
HC-1	Front Row vertical clearance between driver manikin head and roof headliner surface at driver centerline	
HR-1	Roof panel thickness (author-defined dimension)	
ICAD	Integrated Computer Aided Design	
IDEAS	Integrated Design and Engineering Analysis	
IGES	Initial Graphics Exchange Specification	
IPF	Interior Penalty Function	
IPPD	Integrated Product and Process Development	
IV	Interior Volume	(SAE J1100) [1]
IV1	Passenger Car Interior Volume	(SAE J1100) [1]
J	Jacobian	

kg	kilograms (mass unit)	
kN	kilo-Newton (force unit)	
kph	kilometers per hour	
kW	kiloWatts (power unit)	
L34	Effective Legroom -- Accelerator (driver)	
L50-2	SgRP couple distance, front to second row	(SAE J1100) [1]
L50-3	SgRP couple distance, second to third row	(SAE J1100) [1]
L51-2	Effective Legroom -- Second (row)	(SAE J1100) [1]
L51-3	Effective Legroom -- Third (row)	(SAE J1100) [1]
L99	Also referred to as L99-1	(SAE J1100) [1]
L99-1	Driver's Ball of Foot to SgRP -- Front	(SAE J1100) [1]
L101	Wheelbase	(SAE J1100) [1]
L102	Tire Diameter, Averaged (based on L102-1, L102-2)	(SAE J1100) [1]
L102-1	Tire Size -- Front (Diameter)	(SAE J1100) [1]
L102-2	Tire Size -- Rear (Diameter)	(SAE J1100) [1]
L103	Vehicle Overall Length	(SAE J1100) [1]
L104	Vehicle Overhang -- Front	(SAE J1100) [1]
L105	Vehicle Overhang -- Rear	(SAE J1100) [1]
L113	Front Wheel Centerline to Ball of Foot -- Front	(SAE J1100) [1]
L114	Front Wheel Centerline to SgRP -- Front	(SAE J1100) [1]
L115-1	SgRP--Front to Rear Wheel Centerline	(SAE J1100) [1]
L115-2	SgRP--Second to Rear Wheel Centerline	(SAE J1100) [1]
L_B	Bumper rail length	
lb_f	Pounds (force)	
l_{cycle}	Length of driving cycle in meters (= β_3 parameter)	
L_E	Engine Length	
Li-Ion	Lithium-Ion	
Li-Po	Lithium-Polymer	
L_M	Midrail Length	

m	meter
M_B	Vehicle Body mass
M_{BiW}	Vehicle Body in White mass
MBS	Multi-Body dynamics Solver
M_{Cls}	Vehicle Closure mass
M_{Curb}	Vehicle Curb Mass
M_{Drv}	Vehicle Driveline mass
M_E	Engine Mass
M_{Eng}	Engine Mass
M_{EPA}	EPA vehicle test mass (= vehicle curb mass + 136.36 kg)
MILSPEC	Military Specification
M_{Int}	Interior mass
MIRA	Motor Industry Research Association
MPG	Miles Per Gallon
MPG_{Cycle}	MPG for a given test cycle
mph	Miles per hour
MPV	Multi-Purpose Vehicle (also referred to as "Minivan")
M_{Sprung}	Sprung mass
M_{Susp}	Suspension mass
M_{Uncat}	Uncategorized mass
MVMA	Motor Vehicle Manufacturer's Association
NHTSA	National Highway Traffic Safety Administration
Ni-MH	Nickel-Metal Hydride
Nm	Newton-meter
NVH	Noise, Vibration and Harshness
OEM	Original Equipment Manufacturer
P_{Eng}	Peak Engine Power
P_{Engine}	Peak Engine Power
PLM	Project (Program) Lifecycle Management

PV1	Passenger Volume Index -- Front (row)	(SAE J1100) [1]
PV2	Passenger Volume Index -- Second (row)	(SAE J1100) [1]
QFD	Quality Function Deployment	
R^2	Correlation confidence coefficient	
r_g	Penalty constant	
RWD	Rear-Wheel Drive	
SAV	Space Access Vehicle	
sec	second	
SgRP	Seating Reference Point	(SAE J1100) [1]
SS-1	Seat Span -- Front (Distance between front seat cushion edges)	
SSTO		
STEP	Standard Exchange of Product model data	
SUV	Sport Utility Vehicle (Truck Based / Body on Frame Construction)	
SW16	Averaged Front Cushion Width (Derived from SW16-1)	(SAE J1100) [1]
SW16-1	Cushion Width -- Front (row)	(SAE J1100) [1]
TSTO		
UDDS	EPA Urban Driving Cycle	
UMTRI	University of Michigan Transportation Research Institute	
v_0	Initial vehicle velocity	
V1	Luggage Capacity -- Passenger Cars	(SAE J1100) [1]
$v_1 ... v_4$	Vehicle velocity at end of front crash zones 1 through 4 crush events	
VROOM	Vehicle Related Object Oriented Model	
W3-1	Shoulder Room -- Front (row)	(SAE J1100) [1]
W3-2	Shoulder Room -- Second (row)	(SAE J1100) [1]
W20-1	SgRP Y-Coordinate -- Front	(SAE J1100) [1]
W101	Tread Width (average of front and rear)	(SAE J1100) [1]
W101-1	Tread Width -- Front Tires	(SAE J1100) [1]
W101-2	Tread Width -- Rear Tires	(SAE J1100) [1]
W102	Track Width (average of front and rear)	(SAE J1100) [1]

W102-1	Track Width -- Front Tires	(SAE J1100) [1]
W102-2	Track Width -- Rear Tires	(SAE J1100) [1]
W103	Vehicle Width, Maximum (without outside mirrors)	(SAE J1100) [1]
W117	Body Width at SgRP -- Front (row)	(SAE J1100) [1]
W20-1	SgRP Y-Coordinate -- Front (row)	(SAE J1100) [1]
WB-1	Belt Width -- distance between W3-1 trim point and outside body point along W117 reference line	
WG-1	Gap Width -- distance between front seat cushion edge and W3-1 trim point	
W_{Sp}	Engine specific weight	
WTW	Wall-to-Wall (turn radius)	
X_a	Ankle Point longitudinal distance from Driver Ball of Foot Reference Point	
Ya	Ankle Point vertical distance from Accelerator Heel Point	
β_1	Driving (acceleration) contribution coefficient (Joules / kg)	
β_2	Aerodynamic contribution coefficient (m^3 / sec^2)	
β_3	Rolling resistance contribution coefficient (meters)	
γ	Camber angle	
ΔS	("Delta-S") Offset distance between driver SgRP and front of second row outside passenger foot (can be positive or negative)	
δ_i	Inside steer wheel maximum turn angle	
δ_o	Outside steer wheel turn angle for a given value of δ_i (with Ackerman steering)	
η_{b2w}	Battery-to-wheel efficiency	
η_{t2w}	Tank-to-wheel efficiency	
ρ_{air}	Density of air at 23° C at sea level = 1.225 kg/m^3	
ρ_{fuel}	Energy density of fuel (joules / liter)	
σ	Standard deviation	

CHAPTER ONE

INTEREST / MOTIVATION

The author developed an interest in this topic based on his experiences in industry at an original equipment manufacturer (OEM) and while working at a an automotive supplier. Many of the issues seen at these companies also had to be addressed while working on the Clemson University International Center for Research and Development (CU-ICAR) Deep Orange Pilot Project. The lack of rapid, integrated conceptual design tools at an OEM in the 1990's led to sub-optimal decisions, expensive design and tooling modifications late in the vehicle program and slippage in vehicle launch dates due to late design target changes and design issues which should have been foreseen and avoided. Additionally, the automotive market has changed to a point where a traditional 60-month vehicle development cycle cannot keep pace with changing customer expectations, market conditions and regulatory requirements. The rapidly changing customer market is now driving OEM's to integrate virtual engineering tools and reduce the number of physical prototypes used in its vehicle development process [2]. A suite of integrated design and optimization tools will support shortened product development cycle times leading to better automotive products in a shorter time, saving timing and money while satisfying demanding customers in an increasingly segmented automotive market in the U.S. and internationally.

As shown in Figure 1.1, design freedom, and particularly the freedom to incorporate innovative designs and strategies, is greatest at the very beginning of concept design. Conversely, that is when the least knowledge of the product exists. As product

content decisions are made the level of freedom in the design decreases and the design becomes "locked in." Approximately 70% of the final cost of a vehicle is committed by the end of the conceptual design phase [3,4]. This makes it critical to make well-informed and validated decisions in the concept design phase to avoid expensive iterations and redesign in the detailed design phase.

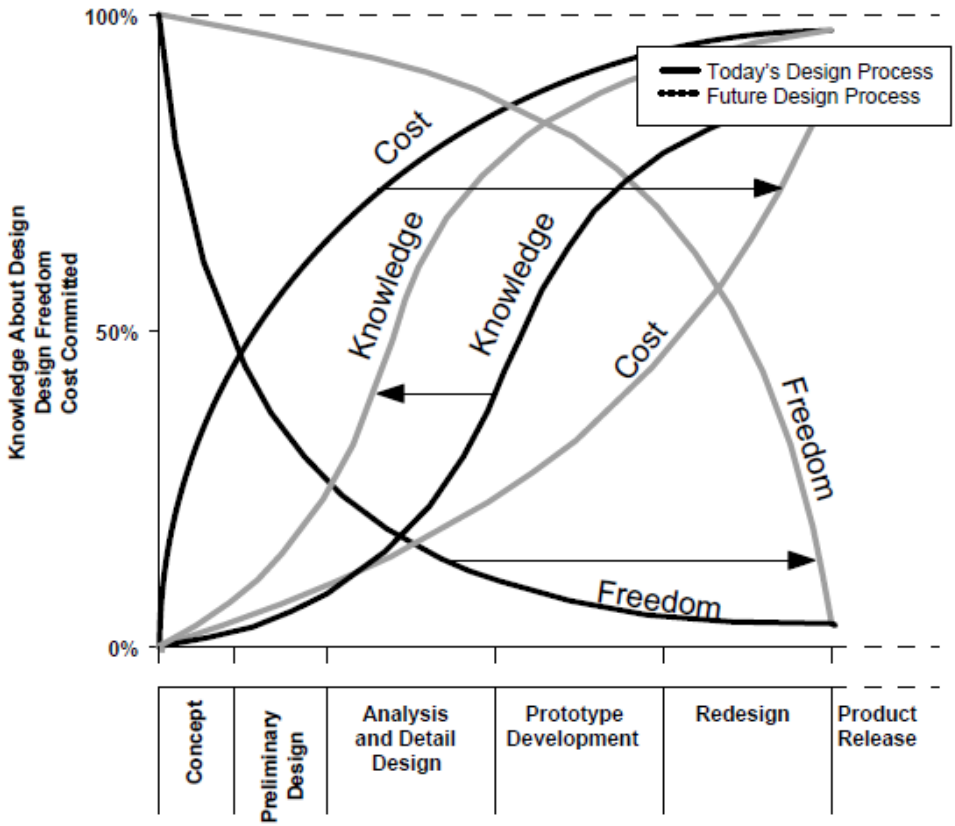

Figure 1.1: Product Knowledge vs. Design Freedom in Design Phases [2]

The automotive industry has become increasingly competitive at an international level. At the same time, automotive design and marketing has changed from a "push" system to a "pull" system dictated by rapidly evolving customer wants and needs. A 60-month vehicle development program, even if it comprehends current customer desires,

will deliver a less appealing vehicle at the end of 5 years; customer preferences and market conditions will have changed drastically in the same time interval. This is accentuated by the rapid rate of new electronic and interactive lifestyle product launches. Customers, particularly those in "Generation Y," are now accustomed to new technology revolutions which occur in the space of months rather than years and extend these high expectations to the automotive industry. A shorter development process will be needed for most vehicle designs to remain relevant in the marketplace [5].

The automotive market is growing increasingly segmented with diverse customer tastes for new features and vehicle segments. In 1964, the Chevrolet Impala set the single-year sales record for one vehicle model with 1,074,925 units sold [6]. A single vehicle style will no longer sell such a large number of units in one year. In 2010 the best-selling vehicle was at 391,000 vehicles (Ford F-150); only 8 models had sales above 200,000 units [7]. In order to achieve economies of scale, OEM's will need to be able to develop multiple vehicle derivatives based on a common platform; these must be co-developed early in the platform design concept process prior to detailed design on each derivative. A multi-disciplinary, multi-objective optimization environment can provide early design maturity of the derivatives and manage trade-offs between derivatives for the benefit of the overall platform.

The Defense Advanced Research Projects Agency (DARPA), in a funding announcement for the Fast Adaptable Next-Generation Ground Vehicle (FANG), noted that the complexity of military systems has increased 3- to 4-fold in the past decade, particularly in the area of aircraft [8]. Combat vehicle and weapons systems have seen

similar complexity increases which cannot be handled by the current MIL-STD-499A military product / system development process, which has been used since 1969 and was developed during the Apollo space program [9].

Current tools which provide dedicated support for the automotive conceptual design phase either do not exist or do not support the task well [4]. Most tools and CAD systems which currently exist are focused on detailed design methods and activities. A suite of integrated, flexible, multi-disciplinary systems which can evaluate multiple design options in multiple levels of detail will save time, money and personnel resources by maturing the design early in the development process with a high degree of confidence. Shorter development times will deliver a fresh, timely product which meets customer wants and needs. Reduced reliance on physical prototypes will remove cost and complexity and eliminate expensive and time-consuming design iterations which now occur in the detailed design phase. Tools which evaluate concepts at the parametric level will provide rapid iteration and convergence on a final design with higher confidence due to the number of targets and requirements which may be considered in parallel.

Such an integrated, multi-disciplinary optimization framework will also be of major value to the Deep Orange Program at CU-ICAR. Deep Orange seeks to develop, design and execute a viable vehicle concept in a 24-month time frame, showcasing innovative and "game-changing" design concepts and production methods using small teams of graduate students. Deep Orange also seeks to understand and manage the risks of such cutting-edge technologies. Concept design methods and tools described herein

can help to quantify and mitigate such risks. The need for tools and methods which support a small team with limited resources and shortened program timing was documented at the completion of the Deep Orange Pilot program in August of 2010 [5].

Problem Statement and Hypotheses

Primary Research Question:

How can a new vehicle concept be designed from various engineering perspectives(often with conflicting properties) early in the development process using simplified models with the overall objective to increase product maturity early in the development process and to reduce costly and time-consuming changes in the (later) detailed design stage?

Primary Hypothesis:

A hybrid set of analytical first-order and low-order parametric models in combination with knowledge-based representations will provide a mathematical environment to balance and optimize (conflicting) concept-relevant vehicle properties prior to the start of the detailed design phase.

Research Question 1:

How can concept-relevant vehicle properties be modeled in their simplest form while capturing their interactions in meeting other (competing) vehicle design targets?

Hypothesis 1:

A hybrid set of analytical first-order and low-order parametric models in combination with knowledge-based surrogate representations can capture concept

relevant vehicle design properties, enabling rapid and accurate engineering analysis/optimization/validation.

Research Question 2:

How can (competing) vehicle properties be optimally balanced for a particular market segment while incorporating desired brand attributes, regulatory requirements and OEM specific constraints?

Hypothesis 2:

Multi-disciplinary optimization using a trade-off function that incorporates customer relevant targets, regulatory requirements and OEM-specific constraints will allow for development of a vehicle design optimized for all considered targets and constraints.

Research Question 3:

What is the best strategy to solve this multi-disciplinary multi-physics problem and resolve internal trade-offs in a transparent, fast and cost-effective manner?

Hypothesis 3:

By applying a multi-objective (non-gradient) optimization with weighting factors based on vehicle brand "DNA" in combination with objective functions based on specific vehicle targets (reflecting Voice of the Customer / Company / Legislator) and inequality constraint equations which define the viable solution space.

Research Question 4:

What is the best way to guarantee traceability and transparency of targets / requirements and achievement of such targets / requirements during the entire product phase?

Hypothesis 4:

Development and implementation of an open-architecture multi-objective plug-and-play framework where simplified first-order / low-order approximation and knowledge-based models can be substituted by more elaborate detailed models will provide traceability and transparency while tracking achievement of targets and requirements.

CHAPTER TWO

RESEARCH OBJECTIVES

The objective of this research is to develop the ability to design, validate and optimize a vehicle concept early in the conceptual design stage of a vehicle development process. The physical and mathematical principles key to developing this ability are explored, developed and organized into an effective methodology. The resulting design framework uses first-order and low-order mathematical models to capture vehicle behaviors sufficiently accurate for the development phase and their sensitivity to a reduced set of critical vehicle design parameters. The vehicle design is optimized for targets representing the Voice of the Customer, Voice of the Company and Voice of the Legislator in addition to specified brand characteristics. It is intended that this framework permits the conduct of numerous design and optimization studies in the space of one day; this represents a significant contrast to detailed design tools which are seeking to shorten weeks-long design studies to a period of a few days for each major iteration.

While these models are an approximation of detailed analysis models such as finite element analysis (FEA) models or physical prototypes, they are selected or developed to ensure a high level of confidence in the results; this permits validation of and confidence in the optimized configuration leading into traditional detailed design activities. This in turn reduces and, in many cases, eliminates iterative detailed design activities, saving time, money and manpower.

The resulting conceptual design tool is also intended to assist the CU-ICAR Deep Orange Program in its efforts to develop and mature a vehicle concept in a 24-month span. The accelerated concept maturation process not only benefits Deep Orange in reaching its objectives, but will also benefit the automotive industry as a whole as it strives to move from a traditional 60-month vehicle development cycle to one which can keep pace with rapidly changing and increasingly segmented customer tastes. It is envisaged that the developed optimization environment will continue to grow and add capability beyond the scope of this current research. As a result, the analysis and optimization framework is developed in such a manner that additional analysis, optimization and interface capabilities can be added in the future.

It is not the intent of this research to develop detailed graphics modeling of the output. There are many existing 3-D modeling tools which already serve this purpose. The optimization framework does, however, output key geometric and functional parameters to a database or spreadsheet format which can be readily used by Deep Orange and other vehicle development teams. Commercial software packages which can read and use the optimization tool outputs include CATIA, SolidWorks and RAMSIS [10].

CHAPTER THREE

STATE OF THE ART

Summary

Several areas of interest have been researched in order to understand all aspects of this work. Specific areas of literature review include parametric and object-oriented design, ontology and integrated / knowledge-based pre-configuration and conceptual design.

These areas have significant overlap. Any parametric or object-oriented model has an implied ontology to some degree. An ontology provides a descriptive data object and describes the relationships between data elements. Integration and use of knowledge-based concepts requires that relationships between fundamental and derivative parameters be established.

Vehicle Development Processes

While each automotive original equipment manufacturer (OEM) uses a different vehicle development process, the differences tend to be due to nomenclature and grouping of tasks; the actual tasks and order of execution are quite similar. Most current vehicle development processes tend to follow a 60-month timeline from concept initiation to full vehicle production. Some OEM's have an advanced concept design or "portfolio" stage which may or may not be counted in the official development process timing. How this "advance work" is counted tends to explain the difference in official OEM vehicle development process length from one company to another.

Calkins, Su and Chan (1998) [4] describe the General Motors design process up to 1993 as having 6 phases: Mission Phase, Functional Requirements and Concept Development Phase, Preliminary Design Phase, Detailed Design Phase, Build, Test and Evaluate Phase and Manufacture, Sell and Service Phase. From 1993 on the GM process is described as a four-phase process: Concept Phase, Final Approval Phase, Production Approval Phase and Development Phase. The Concept Phase is further broken down: Concept Initiation, Concept Requirements, Alternatives Selection, Concept to Division and Design Direction Approval (Styling).

Calkins et al. assert that there are few current tools that effectively support the automotive concept design phase; most tools and CAD systems are focused on detailed design methods and activities. They state that 70% of life-cycle vehicle costs are set in the concept design phase (Figure 3.1, no source given by Calkins, et al.).

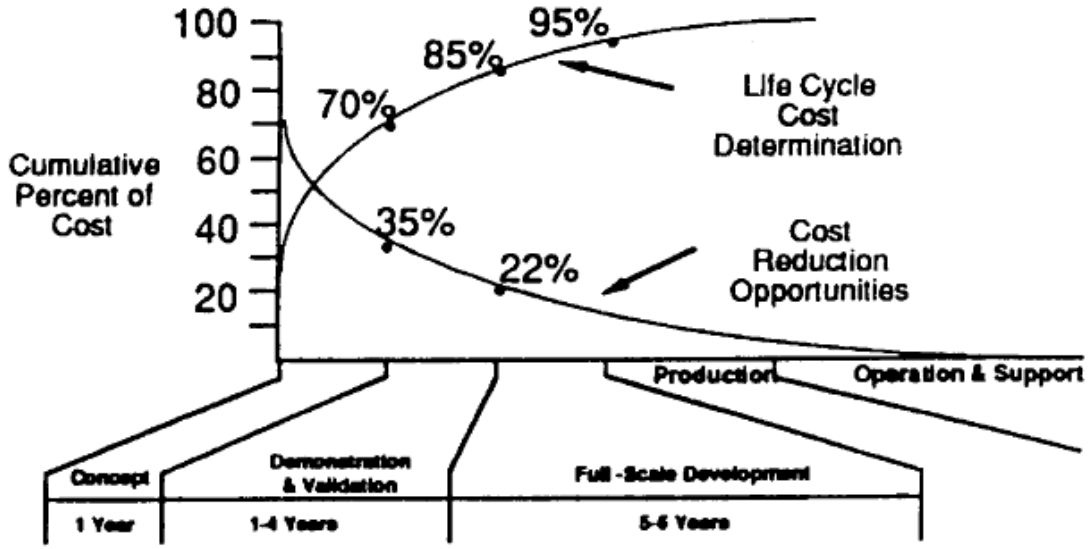

Figure 3.1: Cycle Cost by Development Phase [4]

Most simulation and analysis tools are targeted toward the detailed design phase where detailed CAD models are already available. However, the opportunity for significant design changes are restricted by the body of work amassed and cost already expended in reaching this phase. Most key design decisions are made during the concept development stage. Typically, detailed design tools such as finite element analysis (FEA) are used in concept development using simplified CAD models or modified models from previous vehicle programs. This approach tends to perpetuate a "carryover" mentality to reduce new vehicle development costs that inhibits the use of new and innovative design paths. Multi-body dynamics (MBS) solvers can be used in the concept development phase, but these need to be used in a different manner from the detailed design phase (many iterations with simplified models to rapidly assess design alternatives). Solid-based CAD software can be used to support the concept development phase, but the tendency is to again develop detailed models early in the process and lock in design decisions before all alternatives have been considered. CAD models at this stage should be derived from the output of simple vehicle analysis models rather than serving as the input for concept design models.

Parametric Design and Object-Oriented Design

Colton et al. (1990) at the Georgia Institute of Technology compiled a report [11] which focuses on the requirements for an object-oriented vehicle model and on hierarchical decomposition design methods for automotive vehicles. It explores several aspects of future vehicle design: data modeling, development of an object-oriented vehicle model and methods for making product development decisions.

The report presents their interpretation of a typical (Figure 3.2) and proposed methodology (Figure 3.3) for developing vehicle product specifications.

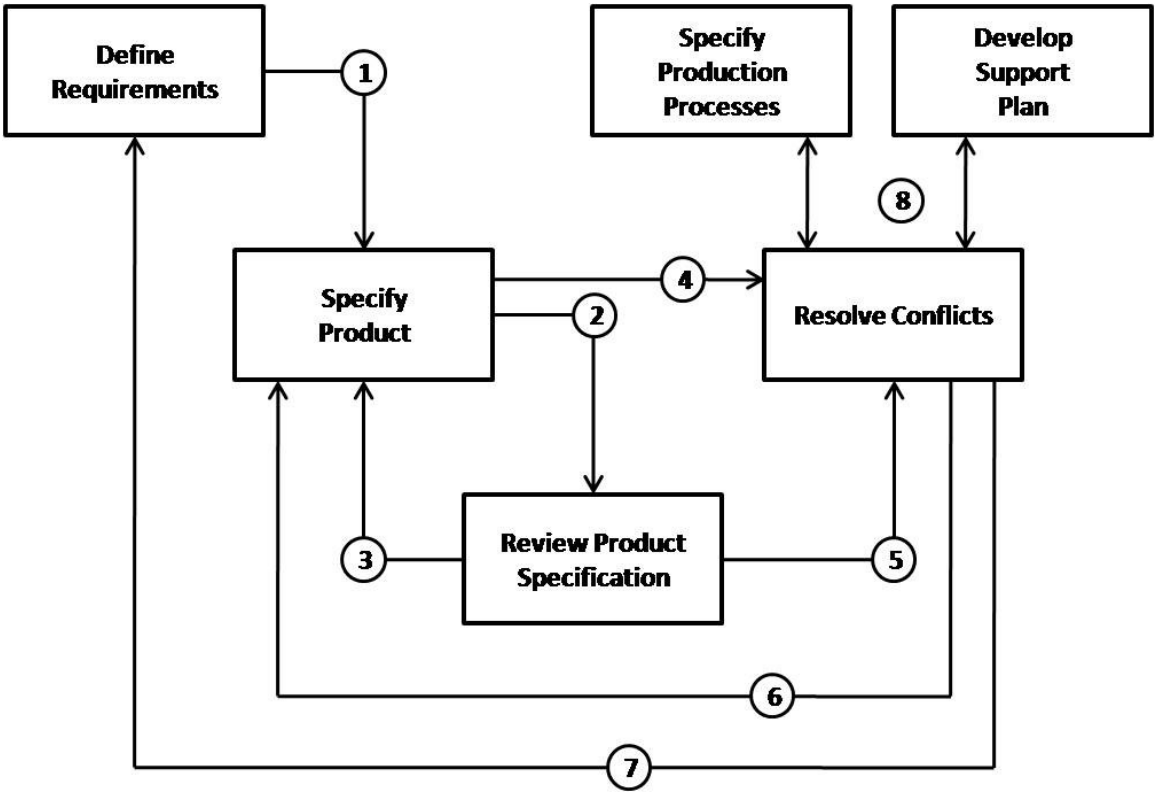

Figure 3.2: Typical Automotive Product Specification Process [11]

The traditional method carries out activities sequentially, with one group defining their activities and resulting specifications and then passing their inputs to the next group. If an irreconcilable issue occurs, the entire process must start over again and cover the same ground enroute to a solution.

The process proposed by Colton et al. (Figure 3.3) first develops parametric product and process models, which can be used to describe and analyze the product. These models can be used to plan the decisions that must be made throughout the specification process and to prioritize the order in which decisions should be made.

Making the right decisions at the right stage in the process can reduce the number of iterations and shorten the time required to develop the final product specifications. This corresponds with the "go slow to go fast," approach wherein more time spent in planning leads to faster and more accurate results in later phases.

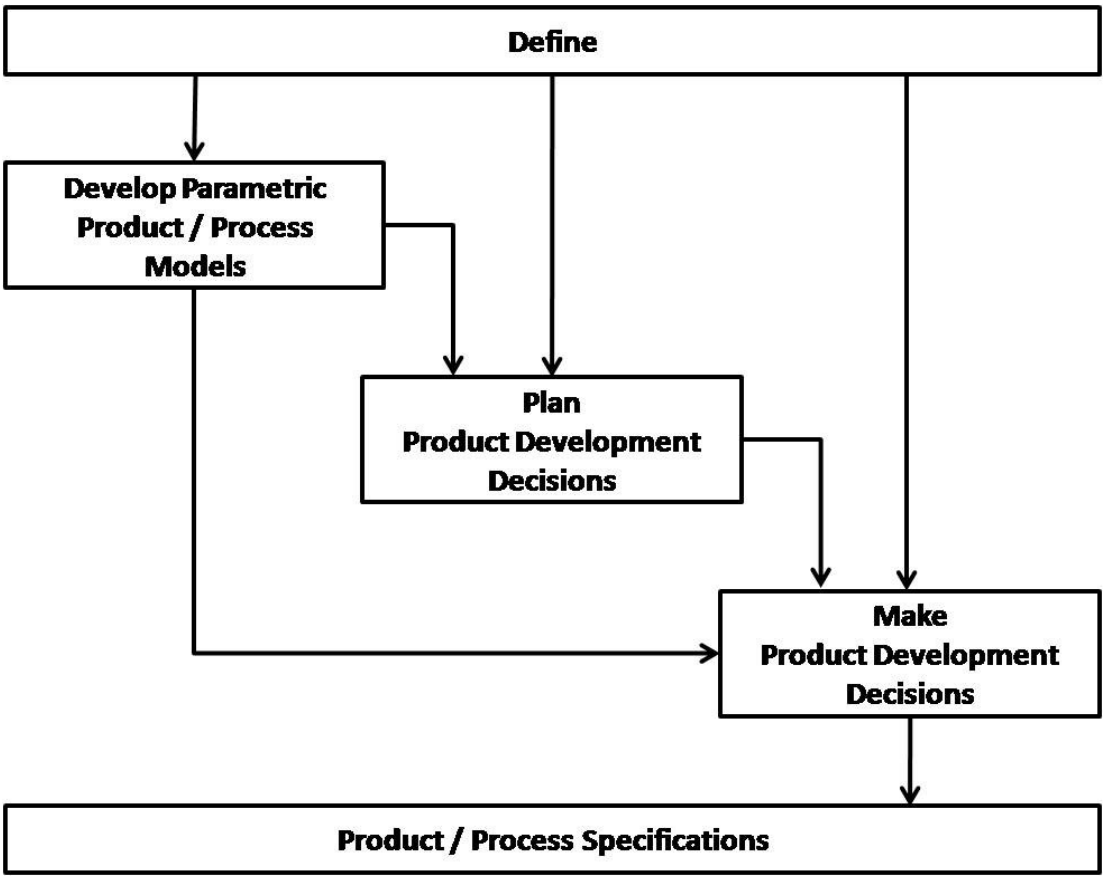

Figure 3.3: Proposed Automotive Product Specification Process [11]

The approach advocated by Colton et al. uses Quality Function Deployment (QFD) tools to develop the "Voice of the Customer" [12]. Their bridge between QFD and the object-oriented system is via a group of 9 baseline parameters, which are used to define the models and their interactions:

- Number of Vehicle Occupants

- Number of Doors
- Engine Size
- Cargo Capability
- Wheelbase
- Drive Type
- Material Percentage (% Metal)
- Silhouette
- Clearance

Due to the interaction between parameters, there is always a level of subjectivity as to which are "base" parameters and which higher order parameters are derivatives of the base values. The terms "silhouette" and "clearance" must be defined in terms of specific measures to make quantitative analysis possible. The authors at one point define silhouette in terms of drag coefficient C_d, but the term is also used in terms of styling and appeal to the customer.

Colton et al. categorize the interactions between these parameters (Figure 3.4) to show how they relate to each other. This determines which parameters are strongly linked and which are independent of each other. In order to perform a multi-objective optimization it is preferable to have all of the base parameters linked to each other--either directly or through one of the other parameters; otherwise there is no common design space to negotiate trade-offs.

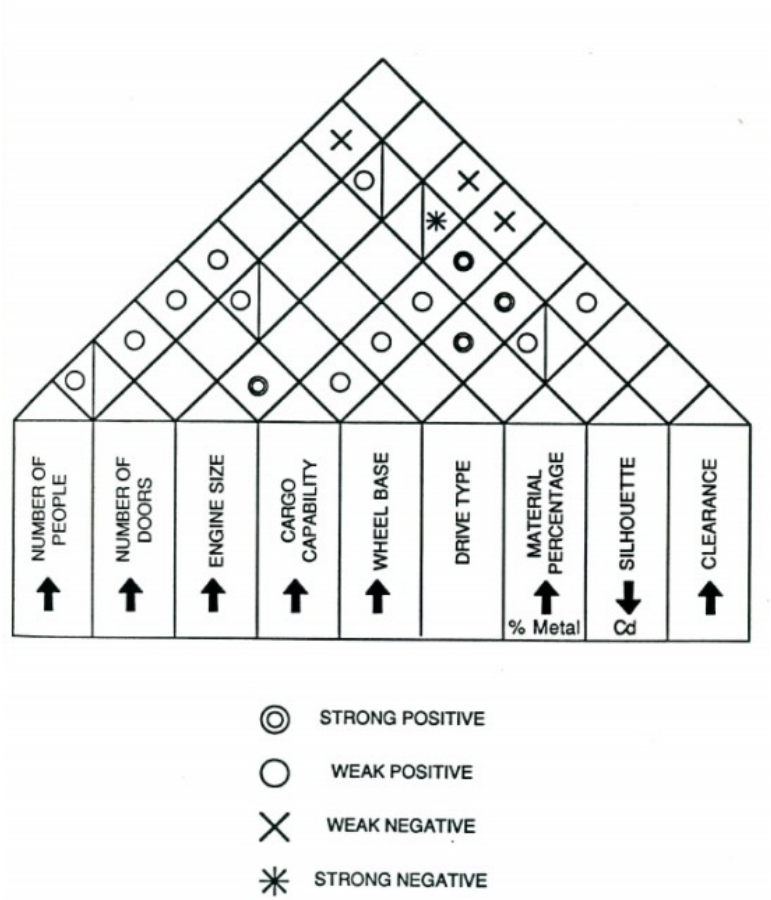

Figure 3.4: Level of Interaction Between Base Vehicle Parameters [11]

The vehicle at the top level is functionally described by the authors as, "a personal system of safe and comfortable transportation," which captures function without presuming specific physical characteristics. A functional decomposition of the vehicle is then conducted through several levels and the functional relationships are mapped (Figure 3.5).

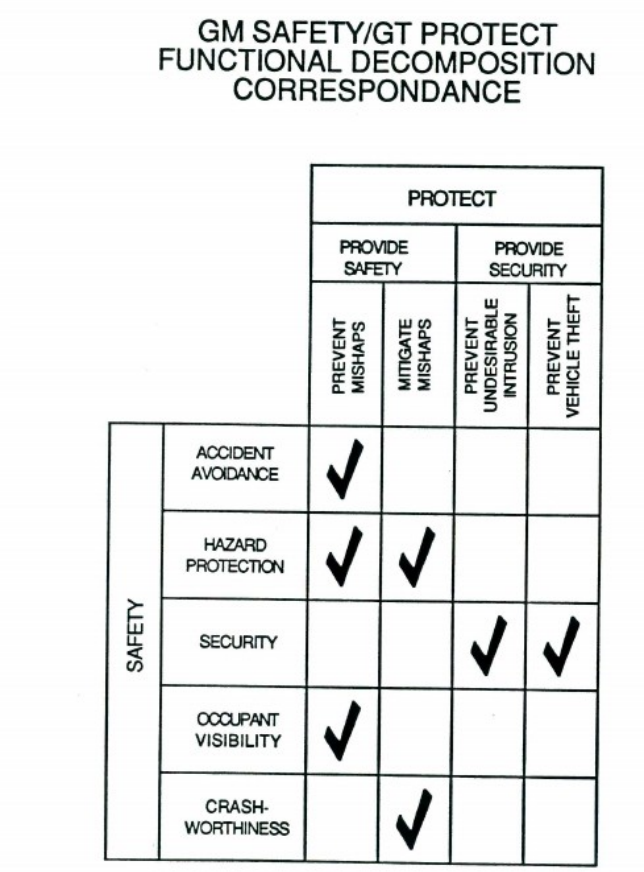

Figure 3.5: Functional Relationship Mapping [11]

When the functions have been defined and mapped to each other, the functions themselves are mapped to the baseline parameters to determine their relationships and degree of interaction at each functional level (Figure 3.6). The functions are then categorized for their level of interaction with each other.

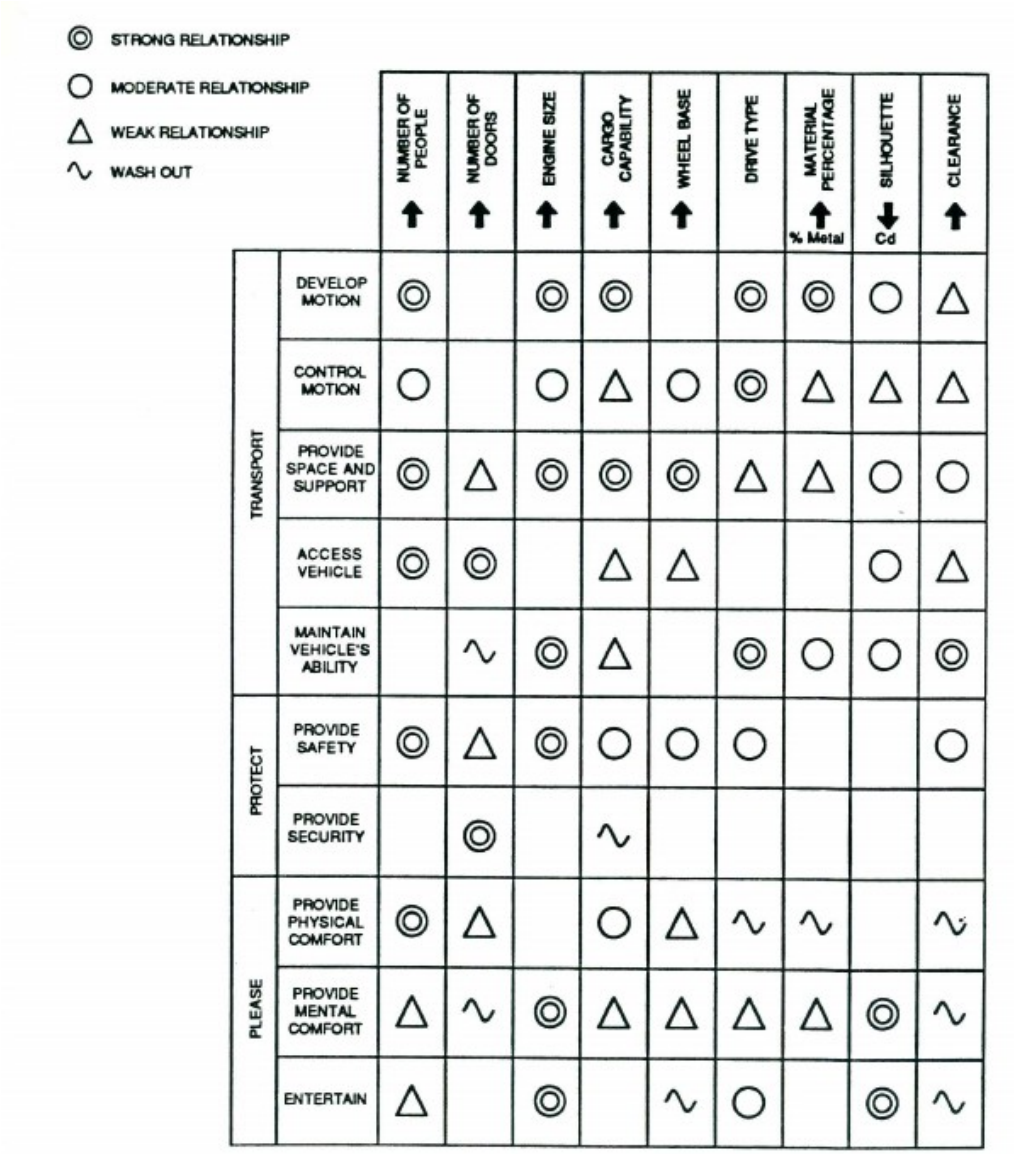

Figure 3.6: Functional Mapping to Base Parameters [11]

There is significant discussion of function vs. form in this report. Function is described as "what an object is intended to do" and form "encompasses the characteristics and physical attributes of that object" [11]. The project spends significant time developing decompositions of both function and form. They also develop several

parametric relationships, which can be used to quantify resultant values for a given set of vehicle parameters.

Two relationships that the report explores are vehicle weight vs. overall vehicle length (Figure 3.7) and engine displacement vs. horsepower (Figure 3.8). In the time since the report was written, a number of effective relationships have been developed for vehicle mass as a function of overall length, width, height and engine power [13]; frontal surface area as a function of overall vehicle height and width [13], vehicle C_g height vs. overall vehicle body height H100 [14], etc. These relationships can be used to develop more specific parametric models and relationships than those available in 1990.

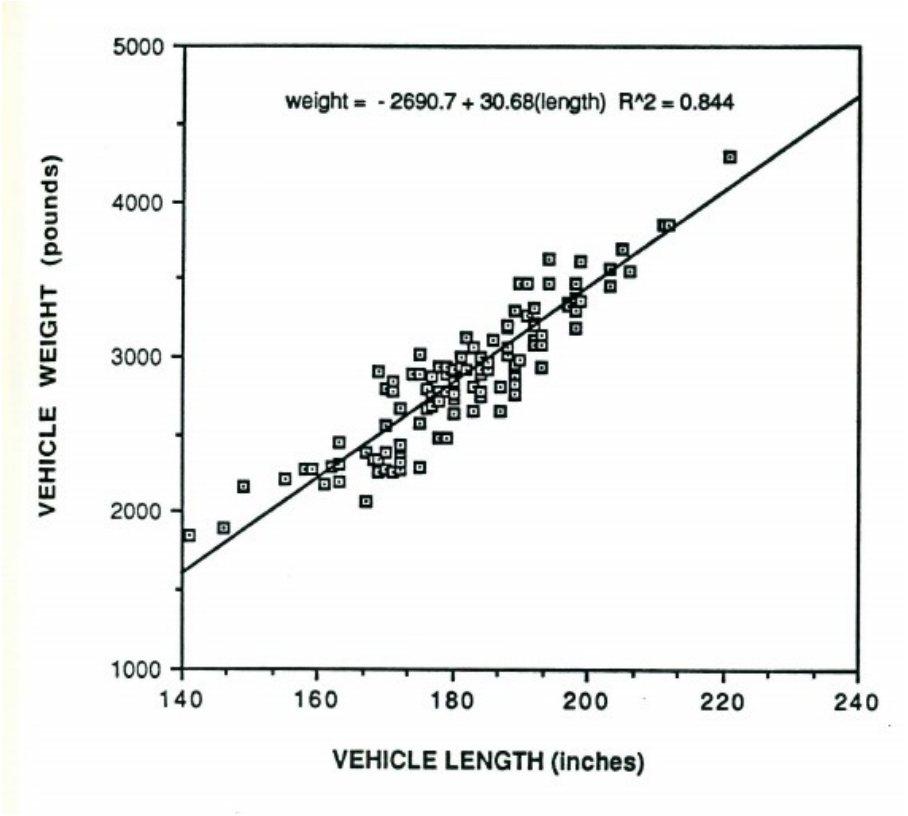

Figure 3.7: Vehicle Weight (lb) vs. Vehicle Length (inches) [11]

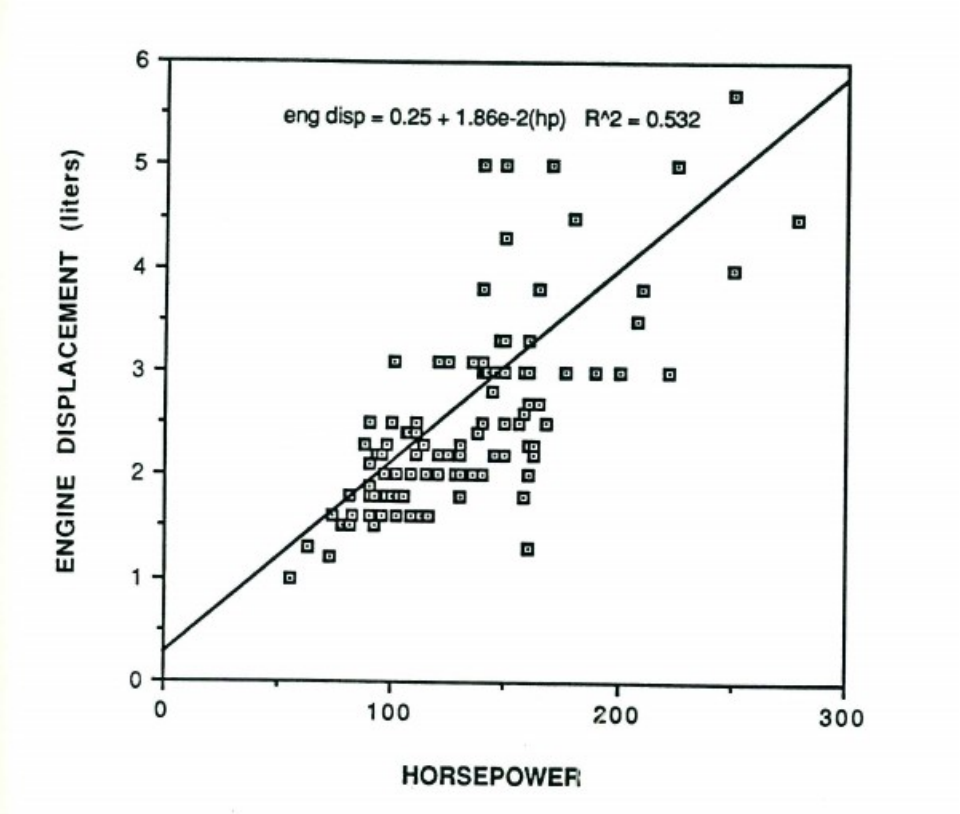

Figure 3.8: Engine Displacement vs. Horsepower [11]

Colton et al. spend significant time describing the development of an object-oriented computer program to support design modeling, calculation and graphics; they also focus on the requirements development for such a program with implementation as a future project.

ICAD (Integrated Computer Aided Design) is discussed as a candidate parametric 3-D modeling system. ICAD has not been available commercially since 2005 after the company of the same name was acquired by Dassault Systemes. Several robust 3-D modeling software packages are currently available, including CATIA, Unigraphics and SolidWorks. These and other commercially available packages can perform many of the

requirements specified for visualization with ICAD as well as database management, expert systems and analysis functions.

Colton et al. develop useful customer-driven requirements for object-oriented design and methods for automotive heirarchical decomposition and design; some areas of design, however, such as occupant packaging and interfaces with the vehicle, are not as well defined as other topics. Some design topics, including side door impact and underhood packaging, are expanded to illustrate specific concepts of the design methodology. Key aspects of QFD and Voice of the Customer are incorporated as the principal drivers of design direction and functional weighting for trade-offs in the final vehicle design.

Design for Manufacture is mentioned in the report but no method is presented for incorporating it into the design optimization. Design for service is considered based on hand / tool access criteria. Work on an optimization strategy is focused on "...the definition of needed parameters to help the multi-disciplinary coordination" [11]. Sensitivity of parameters is also explored.

The work done by Colton et al. provides many useful inputs and considerations for the author's current and proposed research work. Colton et al. focus more on the definition of the requirements for integrated, object-oriented design than the final implementation of their design. However, they definitively establish that such an integrated design environment is feasible with technology existing at the time (1990). Solid-based CAD modeling tools now available support object-oriented representations (to varying degrees) compatible with a system such as that described by Colton et al.

Some of the key attributes, such as wheelbase, may need to be further decomposed into base dimensions (Front Wheel Center to Ball of Foot Reference Point L113, Front to Rear Row Coupling Distance L50-2, etc.) in order to capture the vehicle performance effects as those individual values are varied. Developing a vehicle mass or fuel economy target is an alternative to specifying a percentage of different material types; which parameter is the "driving" parameter and which is the resultant parameter will depend on what the user will do with the final information. "Clearance" may need to be broken down to ground clearance, approach angle, etc. The use of functional decomposition to provide design consistency at each level will assist in developing an integrated product. Employing a Quality Function Deployment strategy provides a method for converting subjective customer tastes into quantifiable targets.

Ouelette(1992) [15] expands on the work conducted by Colton et al. in 1990 [11] and focuses on programming methods and technologies to assist in vehicle conceptual design based on the template laid out in the earlier work. Ouellette gives the definition of conceptual design as, "... a process for establishing function structures and the subsequent mapping of these functions into forms". Rinderle is quoted as arguing that,"...a complete functional description and related form translation enables the designer to reveal novel design concepts and a high variety of candidate subsystem configurations." [16]

Ouelette discusses Rodenacker's top-level design loop for mapping system functions to form (Figure 3.9) [17]. This schematic does not illustrate the fact that the

process can be bidirectional and the forms must also be mapped to functions, as discussed by Ouellette.

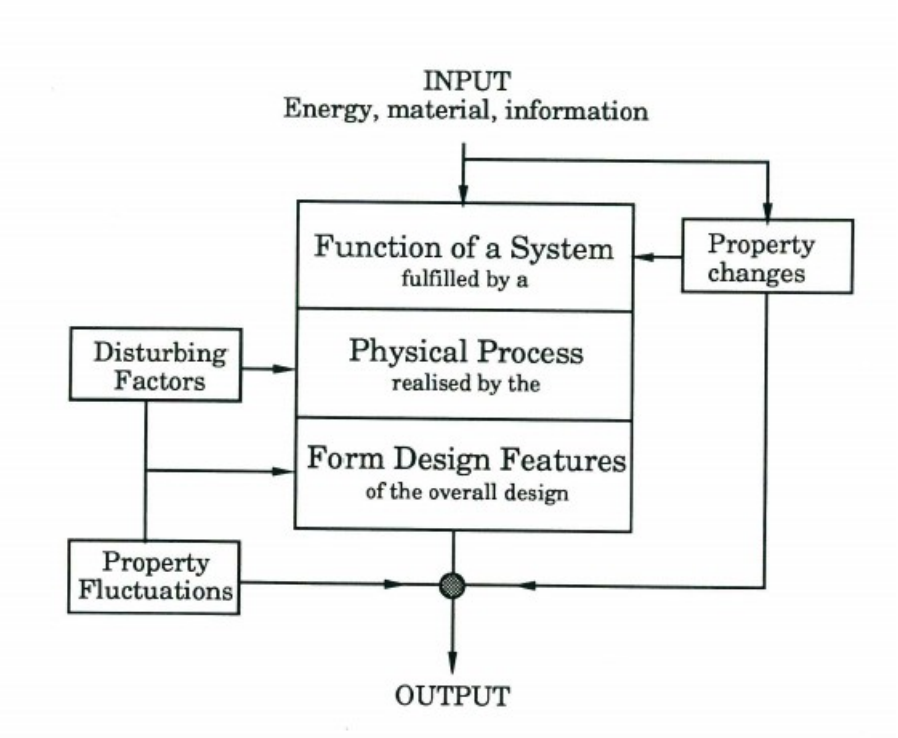

Figure 3.9: Rodenacker's Top Level Loop for Mapping Systems Functions to Form [17]

An example of vehicle mappings between functions and forms is given by Ouellette (Figure 3.10). Mappings will occur between functions and form at each level and in both directions. As with base parameters, there will be a level of subjectivity in defining and providing hierarchical order to both functions and forms.

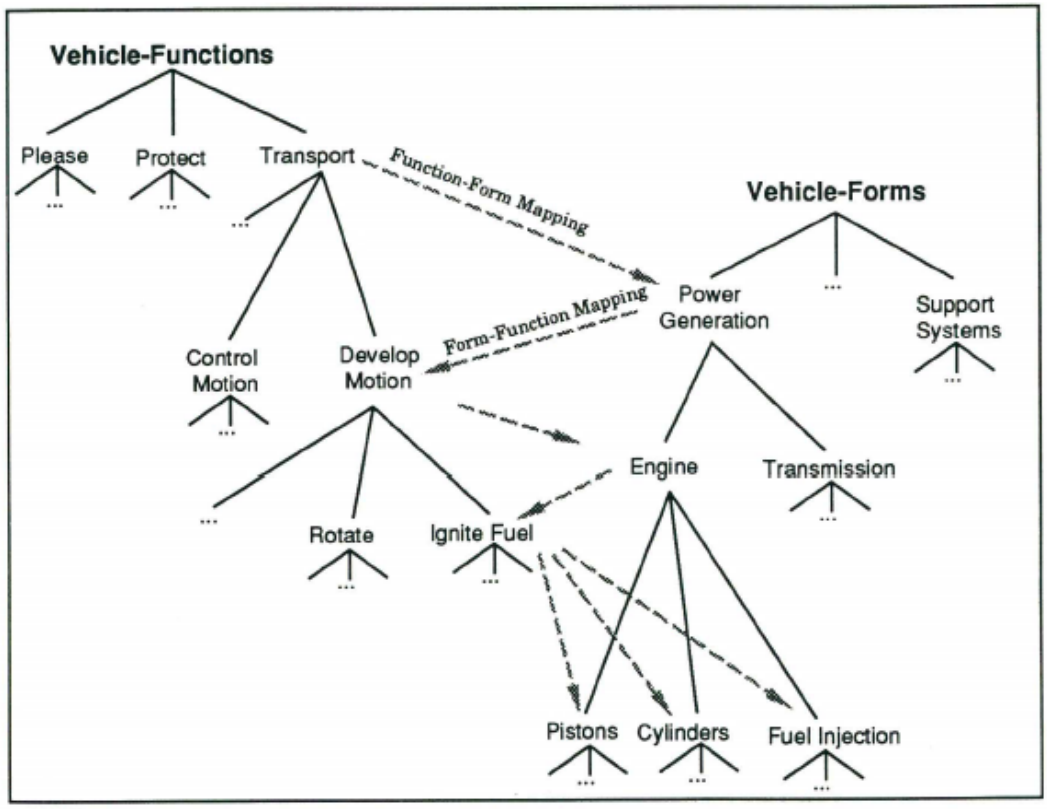

Figure 3.10: Ouellette's Example of Bidirectional Function-Form Mapping [15]

Ouellette discusses the concept of a "blackboard, " or global data structure, which forms part of a blackboard model for opportunistic problem solving. The system is analogous to the activities of a project leader who coordinates and integrates the activity of multiple functional groups (Figure 3.11).

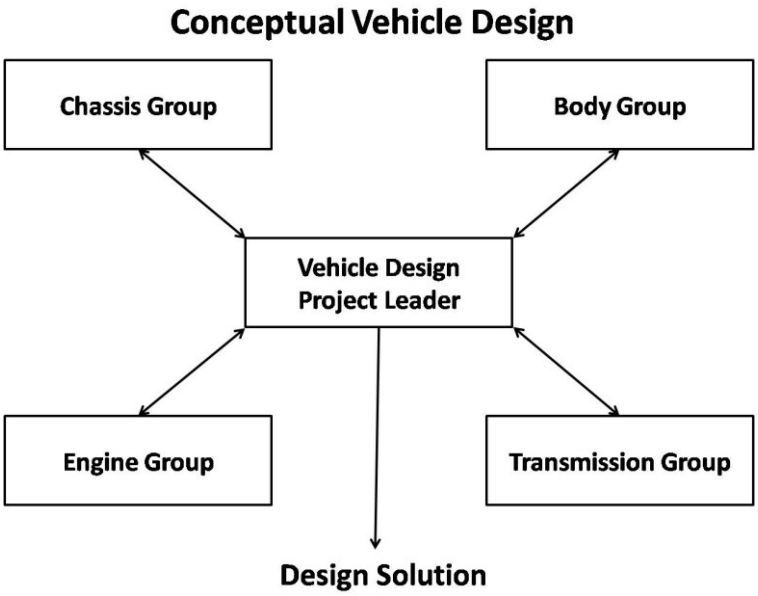

Figure 3.11: Conceptual Vehicle Design with Project Leader as Integrator [15]

In similar fashion, the Blackboard controller coordinates and integrates the knowledge inputs of multiple functional or system knowledge sources to perform a similar role (Figure 3.12).

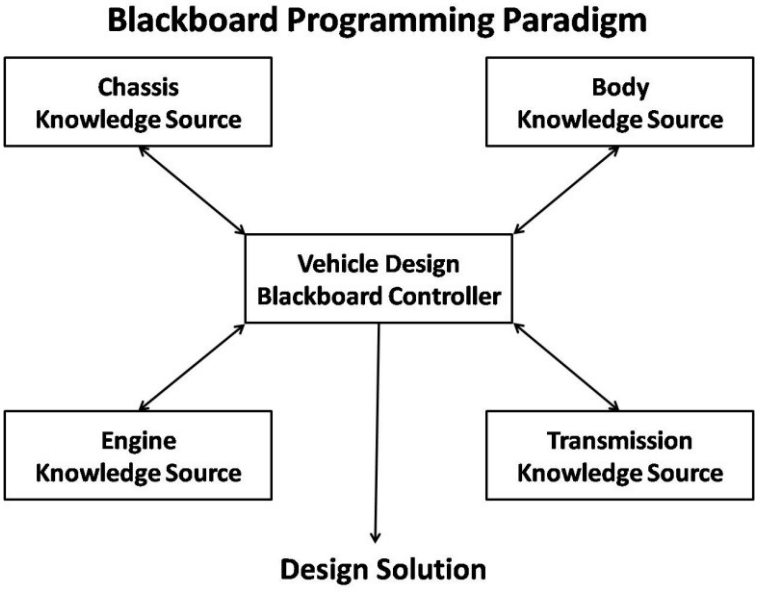

Figure 3.12: Conceptual Vehicle Design with Blackboard Controller as Integrator [15]

The bulk of Ouellette's dissertation is focused on the specific implementation of a specific object-oriented program (VROOM) which links an object-oriented modeling program to a 3-D visualization program (ICAD). In order to build an ICAD model of the vehicle, Ouellette divides the model into separate functional areas (Figure 3.13); this division is used in defining different vehicle types discussed in the next section.

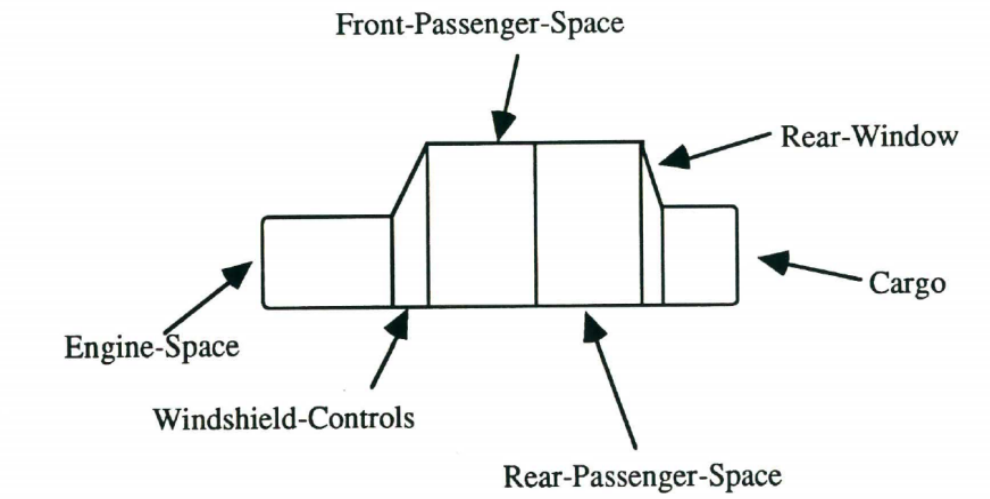

Figure 3.13: Ouellette's Division of Vehicle Zones by Function [15]

It should be noted that the above definition of vehicle divisions enforces certain assumptions and constraints in the vehicle design. It assumes that the engine is always in the front of the vehicle; storage is always in the rear, etc. Another assumption is that these zones are distinct and exclusive of each other when overlap occurs in most actual vehicle designs. It is not possible to avoid making assumptions in developing a simplified vehicle model; the developer must, however, be conscious of the assumptions they are making and how those assumptions will affect the final analysis and optimization result.

Ouellette's work focuses more on the implementation of a knowledge-based system; it is not a comprehensive final suite of design tools to create a production level vehicle design. Customer metrics are included but will need further definition to create a complete conceptual design. Safety is discussed, but compliance with specific OEM or government regulations is not enumerated. Rather, his work treats a few design aspects in greater depth to illustrate what can be accomplished with knowledge-based parametric design tools. Optimization issues are discussed but the final optimization method implementation and weighting is not included. As with the work of Colton et al. [11], many of the same issues and considerations are faced by the author in his research; the implementation will be different due to technology and tools currently available and the foundation of the new work springing from an occupant-centric approach to all vehicle functions.

Colton and Fadel (1992) [18] carry on from their work in 1990 [11] and that of Ouellette in 1992 [15], demonstrating the graphical display of an object-oriented vehicle model (Figure 3.14). They elaborate on the modeling of the conceptual design process as a mapping between the functions and the forms of the system discussed by Ouellette. The report expands on the use of QFD touched on in 1990 along with the use of a combination of data and knowledge representations to encompass a vehicle design.

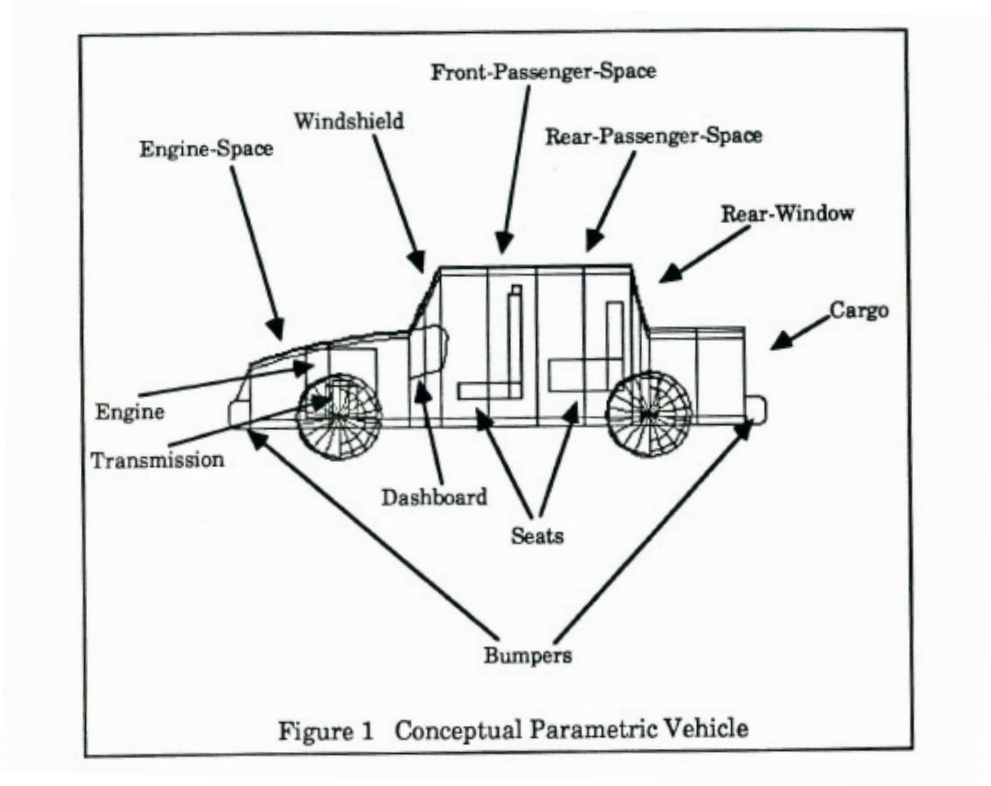

Figure 3.14: Display of Conceptual Vehicle Model in ICAD [18]

The program (VROOM) incorporates the Voice of the Customer through ten vehicle characteristics and the importance rankings assigned to them by the customer (Table 3.1):

VROOM Inputs	**Customer Importance (High, Medium, Low, Not Important)**
Body Style	Body Style Rating
Vehicle Size	Vehicle Size Rating
Cargo Capacity	Cargo Capacity Rating
Number of Side Doors	Number of Doors Rating
Vehicle Value	Value Rating
Fuel Economy	Fuel Economy Rating
0 to 60 Acceleration	Acceleration Rating
Silhouette	Silhouette Rating
Passenger Capacity	Passenger Capacity Rating
Passenger Volume	Passenger Volume Rating

Table 3.1: VROOM Inputs and Importance Rankings [18]

The VROOM input screen for customer QFD inputs is shown below in Figure 3.15:

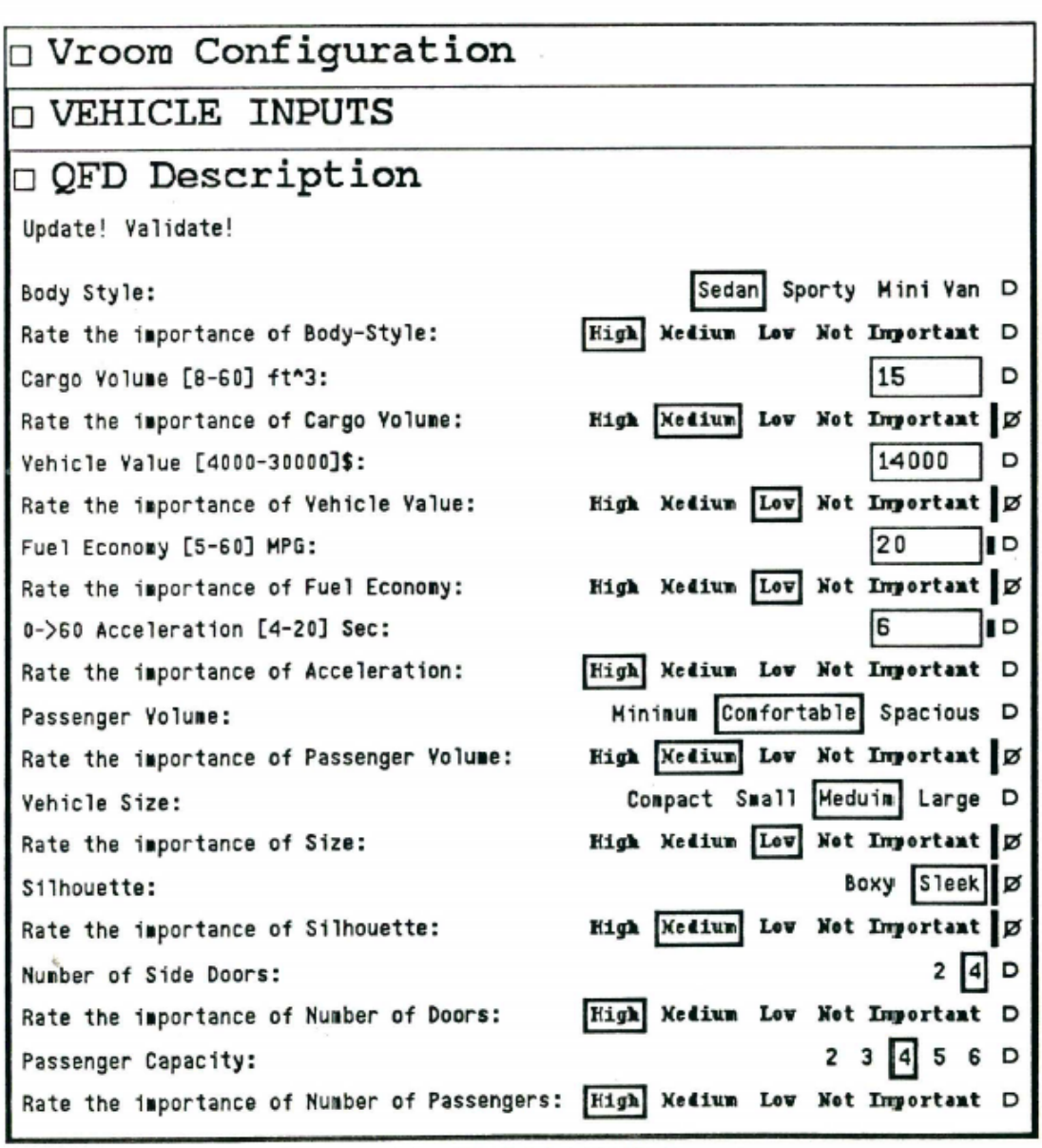

Figure 3.15: VROOM QFD Input Screen [14]

The VROOM QFD input screen illustrates one of the problems encountered in converting customer values and desires into engineering specifications: it is difficult to separate questions establishing values and preferences from those directly asking for

specific technical performance measures or targets (0 to 60 mph acceleration time, etc.). A customer will know that they want more or less cargo volume; they will have difficulty providing a quantity in cubic feet (ft^3) or liters, which is more meaningful for the engineer. General Motors at one time used an informal, "4-golf-bag" standard for Cadillac vehicle luggage compartment storage; this was a roughly quantifiable value, which reflected one value segment for a potential customer.

From the aggregated user inputs the parameters are weighted and an initial vehicle configuration is displayed graphically (Figure 3.16). Updates to the graphical representation are made as the weighting of customer inputs occurs, iterating to produce a final graphical representation of the parametric design.

The VROOM program is configured to represent 6 vehicle categories: sports cars, vans, station wagons, utilities vehicles trucks and sedans. This division of vehicle categories may also constrain the outcome of the conceptual design process. Additional categories of vehicles have emerged since 1992; the most notable addition is the crossover sport utility vehicle (CSUV) segment, which combines attributes of station wagons and truck-based sport utility vehicles. Structural construction methods such as unibody (monococque) or body-on-frame must also be taken into consideration in evaluating performance of a given design optimization.

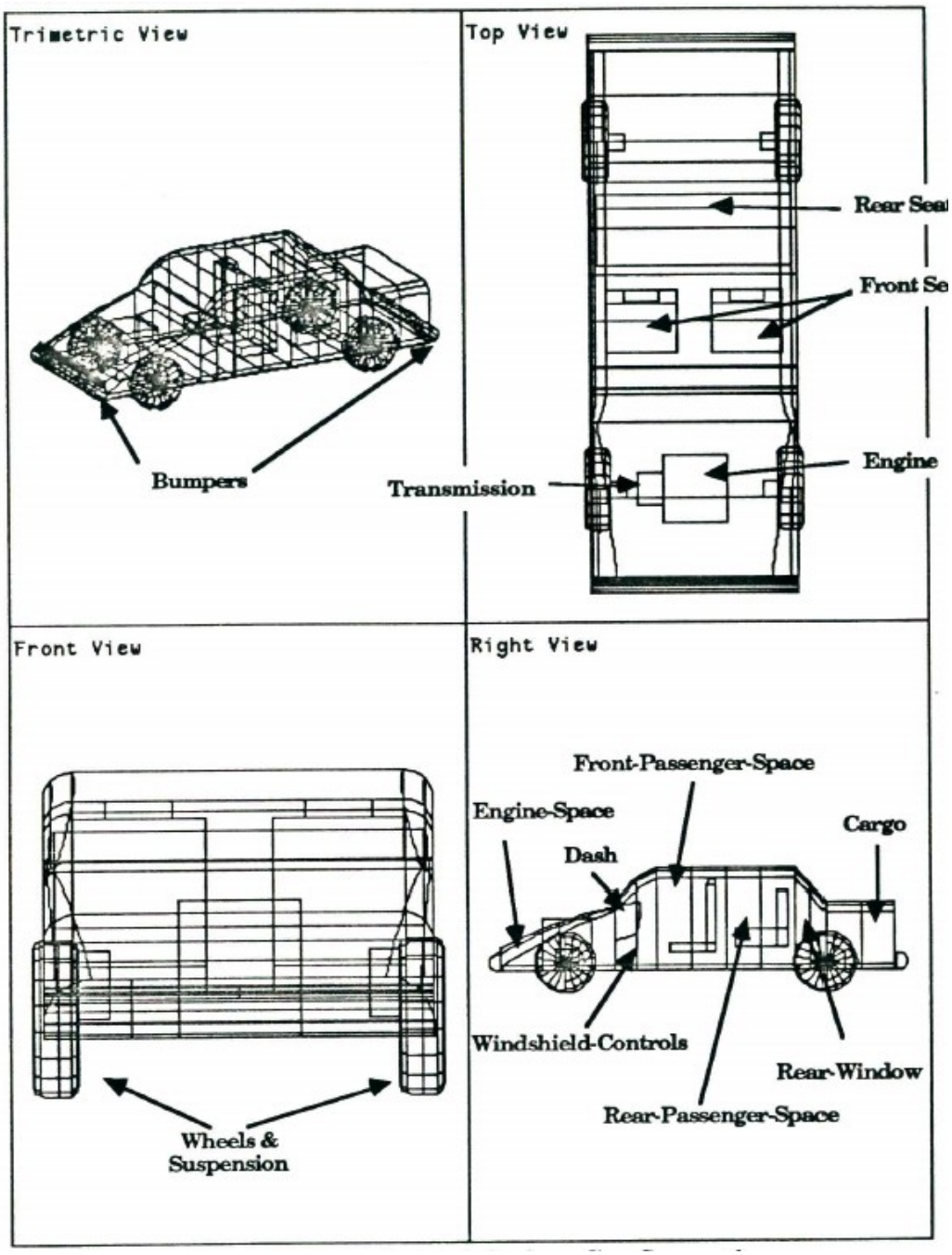

Figure 3.16: ICAD Display of Conceptual Design [18]

Colton and Fadel add additional characteristics to further define the 6 segments: people-to-cargo ratio and off-road-to-surface-ratio. These ratios may be difficult to

extract from a QFD input as they are not intuitive for a customer to define. The ratio of off-road use may be less important than whether a vehicle needs to handle off-road conditions or not. A vehicle that is 50% configured to handle such conditions may be inadequate for both uses and unsatisfying to all potential customers. The initial graphical representation for each vehicle class is shown in Figure 3.17:

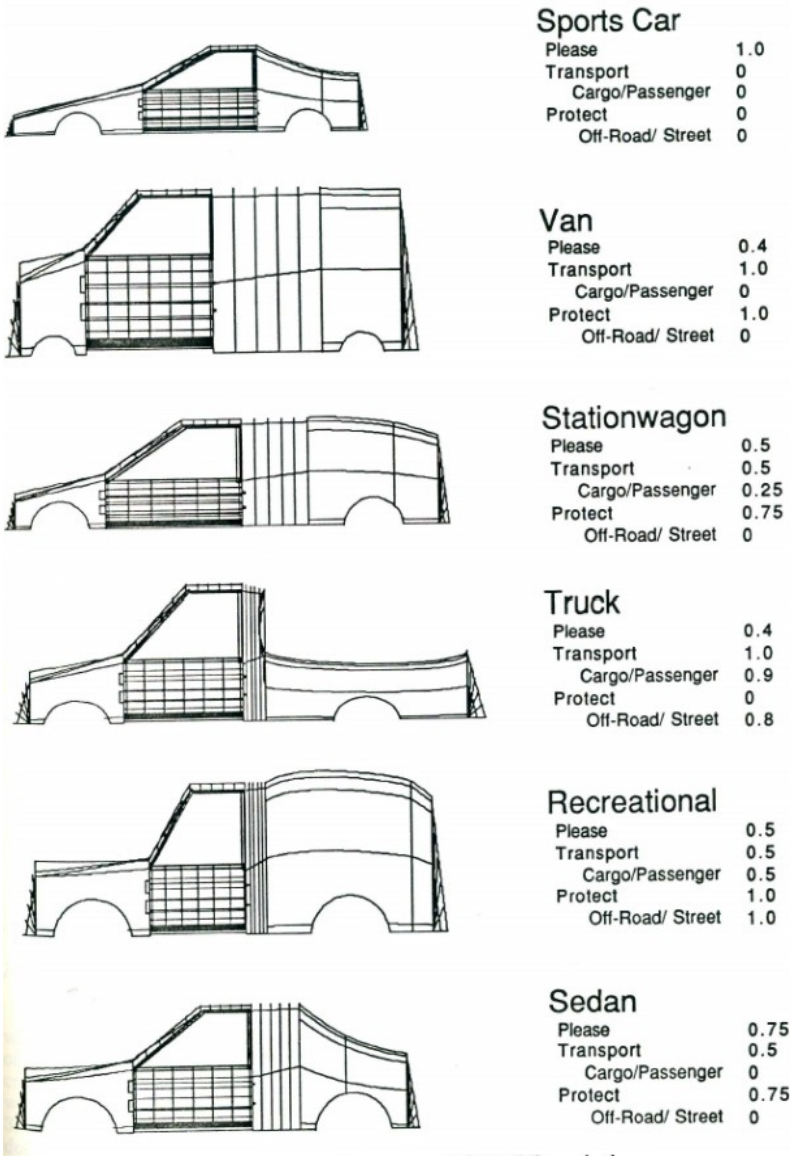

Figure 3.17: VROOM Vehicle Segments [18]

Each segment model is parametrically described using the length and height dimensions shown in Figure 3.18. Eight cross-sections are then generated to develop surface contours within and between the vehicle divisions.

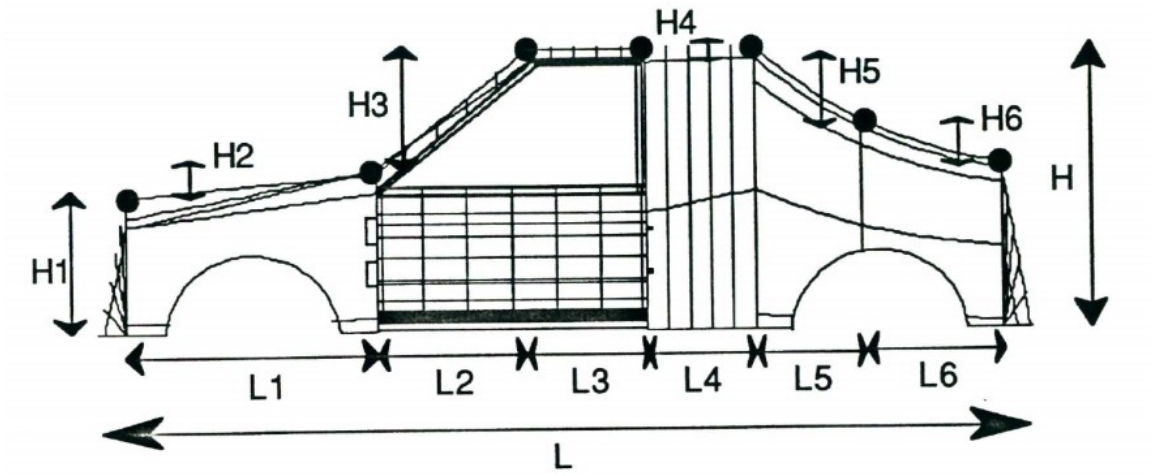

Figure 3.18: Vehicle Parametric Geometry Model [18]

The length and height parameters used above do not correspond to standard industry practice; as a result, it may be difficult to easily transfer such a parametric design into standard industry CAD and design templates. Future work should begin with standard dimensional measures such as those defined in the SAE J1100 vehicle standard [1] to be compatible with industry and government practice.

Colton and Fadel develop the next level of conceptual design with the parametric generation of a door model to analyze side impact. Once again, a standardized structural construction is assumed in order to generate a model which supports a first-order analysis. Assumptions are necessary but require caution in each stage of a design. Any activities to build a simple analysis model require significant assumptions in order to develop a beam-based or other model that can be tested and quantified. This is

unavoidable; in doing so, it is critical to recognize the assumptions which are made and their potential effect on the final result. One way to address concerns over assumptions used in modeling is to include a documentation section listing all assumptions made and the expected impact (good and bad) of those assumptions in determining the validity and fidelity of the model.

Colton and Fadel approach the optimization problem in two ways: in the development and weighting of objective functions and in the implementation of a multi-objective optimization strategy. They use ratios of functional results to target values to create a value for each function between 0 and 1. Each function is weighted and summed into a single high-level functional value*F* as shown in Equation (1) [18]:

$$F = \sum_{i=1}^{n} W_i^* \cdot F_i \qquad \text{Equation (1)}$$

W_i : Weighting of function i

F_i : Value of sub-function i

It is not specified how this value will be used in the optimization; whether all values are specified to yield a minimum, a maximum or other value in establishing an optimum final result.

Colton and Fadel mention that certain individual functions will be evaluated separately and others collected together into a group evaluation. They develop functional measures for specific areas using motor compartment aspects such as compactness, serviceability in terms of access and vibrational characteristics of the compartment.

Colton and Fadel approach optimization as a multi-disciplinary problem based on the work of Sobieski [19, 20] and Fadel et al. [21]. The optimization is treated as a non-hierarchical system with varying levels of coupling between the functions to be optimized. Sensitivity calculations are used to determine the level of coupling. The sensitivities are approximated to represent the derivatives of the functions due to the design variables. This is similar to the Jacobian or Gradient matrix used by Venkataraman [22] as discussed in a later section of this document. Fadel's work uses exponents to evaluate the move limits of a function to converge on an optimized value. It should be noted that many of the techniques used are designed to reduce needed computing time and resources; higher levels of computing power and more powerful optimization codes now available make multi-objective optimization easier to approach than when Fadel et al. performed this work.

New tools such as Optistruct [23] can be used to "grow" or develop structures to meet applied loading and packaging constraints, NVH and safety conditions such as those addressed in ColtonandFadel's work. The specified approach, however, may not be completely achievable from a fully parametric and automated standpoint with the current level of technology available. Such analysis may still be relegated to the detailed design phase for some time to come.

Ontology

Gruber (1993) [24] uses the idea of a conceptualization to then build a definition for what comprises an ontology. He defines a conceptualization as, "...an abstract, simplified view of the world that we wish to represent for some purpose." He asserts that

all knowledge-based systems or agents cannot function without some level of conceptualization.

He then defines an ontology as "an explicit specification of a conceptualization." He further expresses it as defining the syntax in which "queries" and "assertions" are exchanged among agents in knowledge-based systems. The ontology provides a medium for information exchange even if the individual components or “agents” of the system hold different levels of information.

Gruber presents 6 design criteria for effective ontologies: clarity, coherence, extendibility, minimal encoding bias (implementation independent) and minimal ontological commitment (defining the fewest terms necessary). This implies trade-offs and a level of optimization strategy independent from the actual engineering problem. He provides a distinction between the ontology and the knowledge base: "A shared ontology need only describe a vocabulary for talking about a domain, whereas a knowledge base may include the knowledge needed to solve a problem or answer arbitrary queries about a domain." [24]

Gruber focuses on ontology as applied to the development of artificial intelligence and knowledge-based systems. He does not give specific application-dependent examples, instead addressing higher level concepts. Ontology is one tool used in building specifications for a system. Gruber states that, "In conventional data modeling, one would define ontologies with data-type declarations or a database schema." He proposes that knowledge-level specifications would define sets of "classes, relations,

functions and object constants for some domain of discourse...The resulting language is a domain specific specification of a conceptualization" [24].

While Gruber's work is at a more abstract level with few examples, the 6 design criteria may be considered when developing design vocabulary, data structures, definition of design variables and parameters and the manner in which they are used in a design and optimization tool. A limited level of ontology focusing on standard industry definitions and naming conventions is used in the author's work where practical.

Zisko (1990) [25] touches on aspects of integrated conceptual design for tall buildings but focuses primarily on developing an ontology (representation of design components and relationships in machine readable or machine processible code/syntax in his definition). It must be kept in mind that the concept of an ontology will vary with each user and implementation.

In developing his ontology Zisko presents the tall building design process flow as shown in Figure 3.19. Zisko addresses two different delivery models: a design-bid-build model (where construction activities are contracted out) and design-build (where the constructor also develops the design). He then develops the integration relationships for a tall building, a portion of which is shown in Figure 3.20.

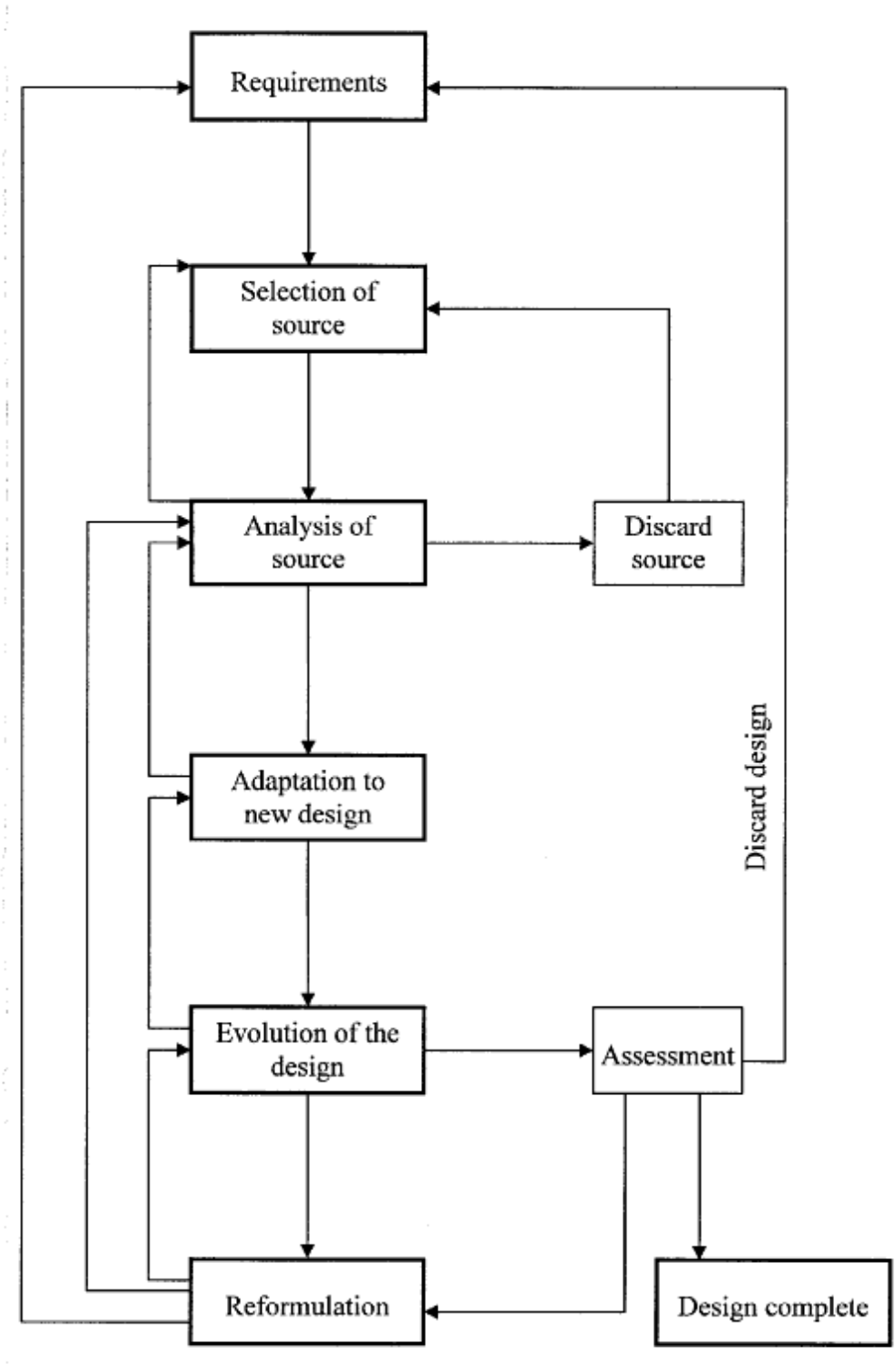

Figure 3.19: Tall Building Design Process Flow [25]

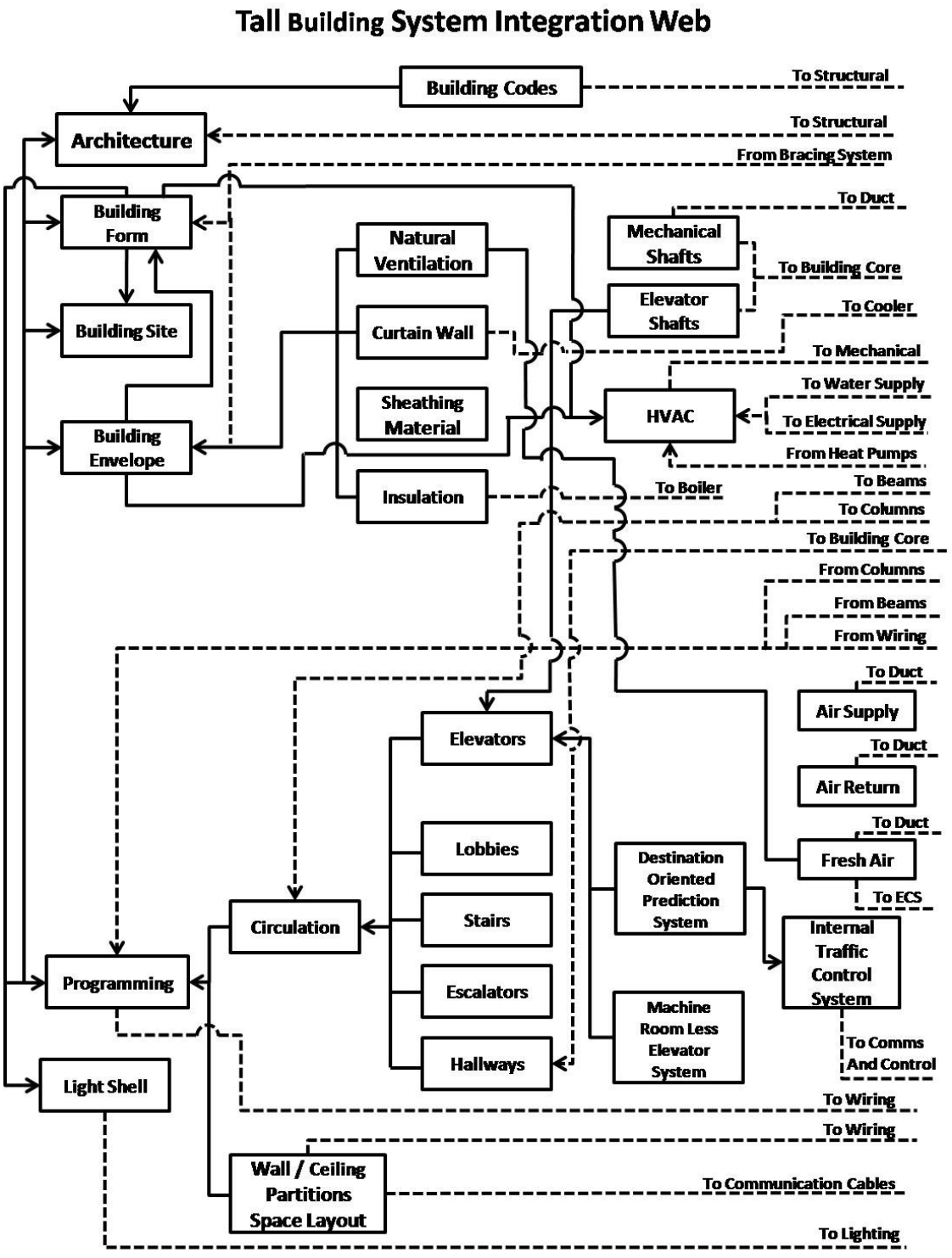

Figure 3.20: Tall Building Integration Web Part A [25] (Re-Drawn for Clarity)

Literature reviewed in Zisko's dissertation shows examples of an integrated construction ontology, which captures all relationships between the design components. These examples are similar to efforts made at DaimlerChrysler [26] to create an automotive naming convention with relationships encoded in the entity names (described later in this section).

Mocko, 2006 [27] not only develops an ontology but additionally develops information models and coding which use the ontology in mechanical design problem examples. He formalizes the process of building information models and ontologies and encoding them to solve a given problem (Figure 3.21).

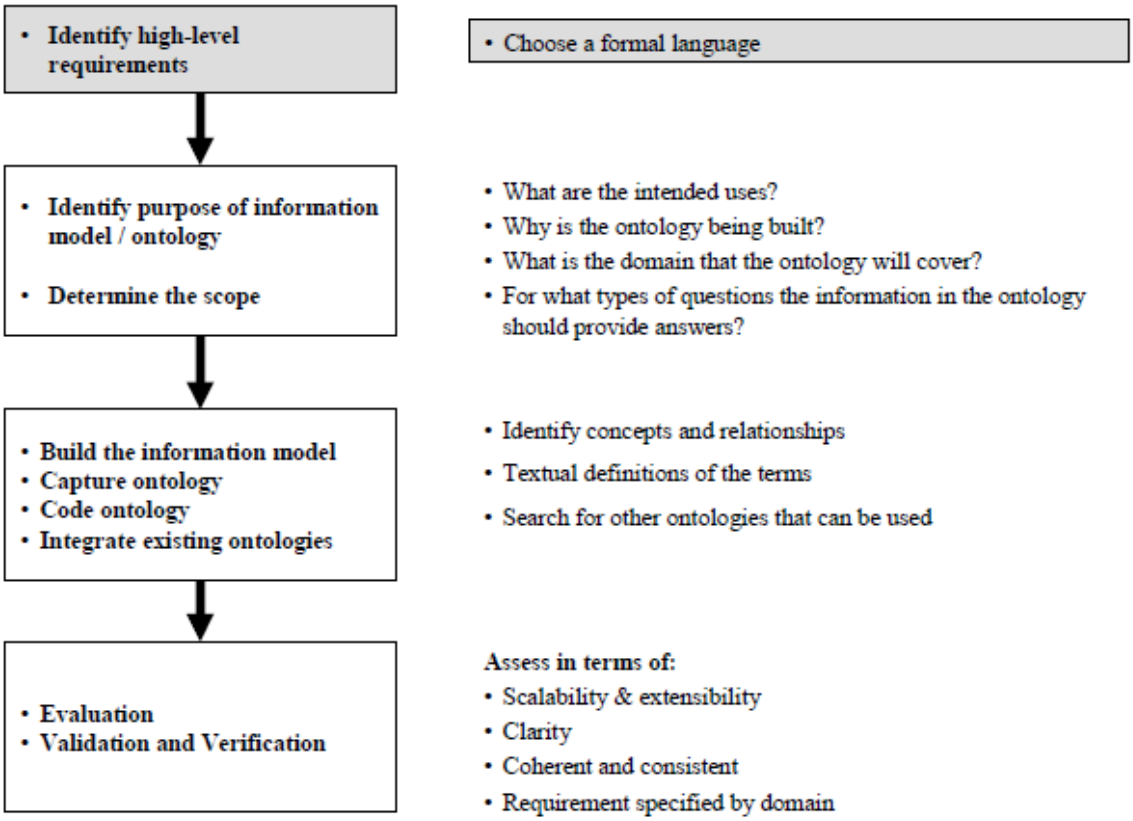

Figure 3.21: Ontology/Information Model and Coding Process Flow [27]

Mocko envisions that design problems which overlap design disciplines will be easier to handle with a common vocabulary and that the commonality will carry over to models used for separate types of analysis. He models the information flow from the conceptual information model to the user (Figure 3.22) to show the development of commonly understood models and relationships.

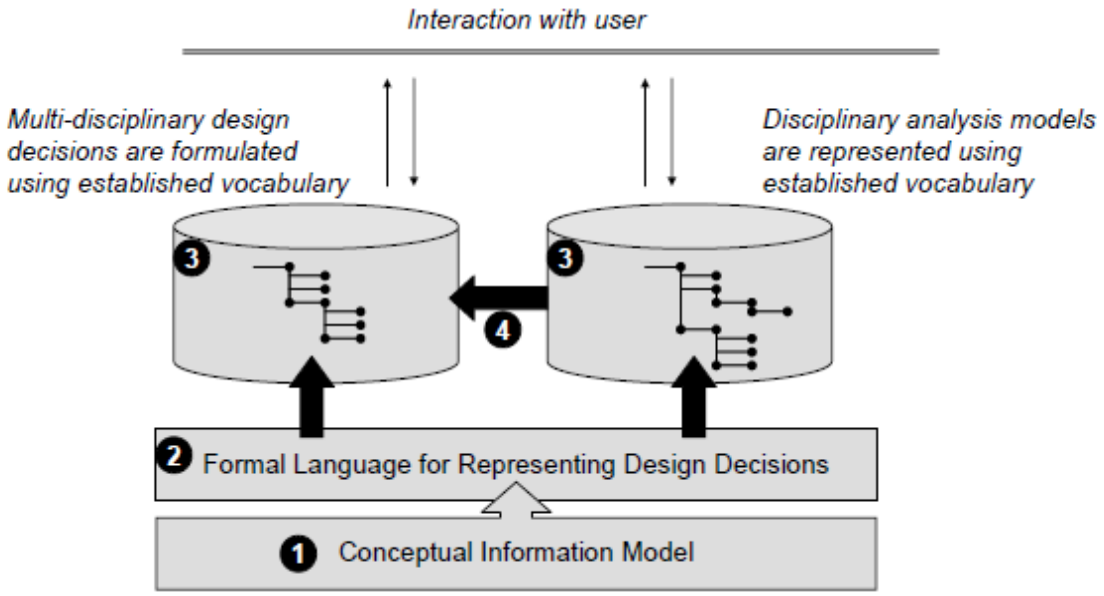

Figure 3.22: Information Flow from a Conceptual Model to the User [27]

Mocko uses ontology as a starting point for the main focus of his thesis: capturing information coming from several sources and then providing a computational integration of that information in a decision-centric design methodology. As with the other examples in this section, ontology serves as a starting point to accomplish other aspects of multi-disciplinary optimization and integrated design.

Mocko's work explores the use of ontology to a greater degree than the author plans to during the current research work. The general encoding strategies, howver, are

useful to follow when developing the framework and code used to implement an integrated optimization environment using a parametric approach. The strategies outlined by Mocko are still beneficial even if a full ontology is not implemented in a development project. The author also does not intend to develop specialized data types and classes based on their ontology. Instead, the design of specific functions, structures and data relationships follow some of the "best practices" enumerated by Mocko and Gruber in their work.

SAE Standard J1100 [1] incorporates some aspects of an automotive ontology in that it designates common automotive dimensional measures in terms of other standardized measures and creates standardized designations for each dimension. While this does not create a comprehensive automotive ontology, it does create a geometric parameter subset to be used in parametric vehicle modeling.

The 2009 revision of SAE J1100 is harmonized with the International Standards Organization, U.S. Environmental Protection Agency, National Highway Traffic Safety Administration and Global Car Manufacturer's Information Exchange. In doing so it provides a standard for representing common vehicle measures and their relationships as shown in Figure 3.23:

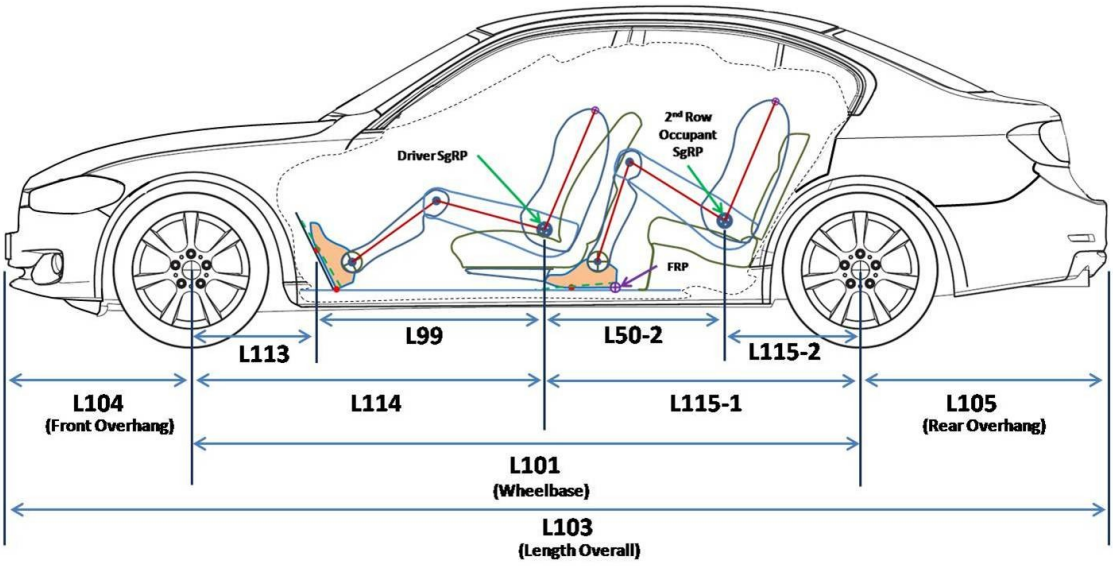

Figure 3.23: Example of SAE J1100 Vehicle Dimensions and Relationships [1, 54]

Wherever possible, standardized dimensions / values from SAE J1100 are used in this work to facilitate understanding and provide a common syntax when discussing vehicle-related parameters such as wheelbase, shoulder room, coupling distance, etc. Measures such as passenger volume are defined as the sum of first, second and (where applicable) third row passenger volume indices (PV1, PV2, etc.), which are each made up of simpler parametric measures. This provides a functional and parametric decomposition of the higher-level measures.

The author has found some missing (but necessary) dimensional parameters during vehicle measurement activities and information gathering. The additional parameters are included to provide a continuum of vehicle overall dimensional parameters. For these dimensions, terminology similar to that in SAE J1100 is used to provide consistency in dimensional descriptions. A summary of parameters used in this work and its associated software framework is covered in Appendix A.

Cumming and Lu (2003) [26] develop examples of standard naming design conventions for use with CATIA V5 at DaimlerChrysler Corporation. Most parametric CAD design packages (CATIA and SolidWorks are examples) do not provide the "design context" which provides the next level of knowledge-based design beyond whether an entity is a part, assembly, geometrical element, etc. The term as used by these two authors roughly correlates with an ontology for vehicle development. This requires adding a level of information encoding to the various fields of a part or entity name to establish functions and relationships. The use of SAE naming conventions for standard dimensions is also mentioned.

They also explore the use of Component Object Model (COM) and Common Object Request Broker Architecture (CORBA) technology to handle part naming and management. The overall intent is to add levels of automation to package drawing generation. Cumming and Lu do not try to develop a fully automated knowledge-based system but rather work to add a level of automation to existing parametric CAD technology. One example of a naming convention is shown in Figure 3.24.

While this convention is repeatable and communicates information about the entity being described, it can be cumbersome in actual use and particularly in writing computer code. The particular parsing cues incorporated into the name (capital letter at the start of each field in the entity name) can lead to data entry errors.

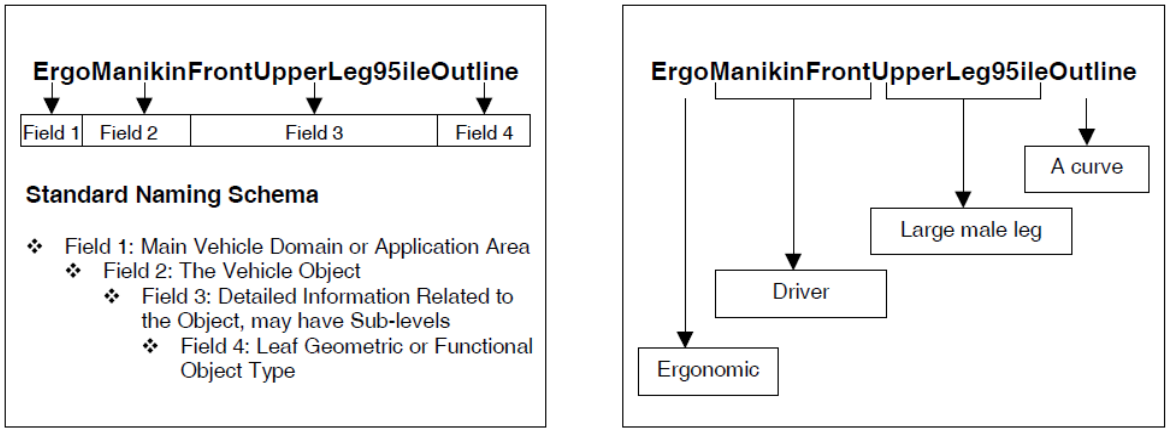

Figure 3.24: Standard Naming Schema (left) and Occupant Definition (right) Reflected in Naming Convention [26]

In the author's work shorter entity names such as common vehicle dimensions listed in SAE J1100 are used with an array index or other differentiator if multiple entries of the same entity type are used or compared. Current programming languages are particularly well suited for the use of structures or arrays of entities in matrix form in iterative or comparative calculations.

Knowledge Based Engineering and Multi-Objective Optimization

Chapman and Pinfold (2001) [28, 29] discuss the use of knowledge based engineering concepts in rapid design and analysis of automotive structures, focusing on Body-in-White (BiW) development. They describe the use of a Design Analysis Response Tool (DART) developed to accomplish this goal [28]. Chapman and Pinfold cite several sources [30, 31, 32] in asserting that the creation of an analysis model, and finite element models in particular, is the most time consuming step of the analysis. One factor is the current need for numerous manual decisions on the part of the individual building the models. The current means of generating analysis models usually result in

the analyst creating a separate, duplicate model which is not logically linked to the source CAD model. Design modifications for analysis are usually performed in the analysis model, leading to a disconnect with the original CAD.

Chapman and Pinfold propose that Body in White design lends itself to knowledge based methods as, "...the same generic problem is faced over and over again, the design requirements are understood, including the knowledge needed but the specific design solution and the pattern of use of the knowledge is repetitive" [28].

Their proposed solution utilizes existing models ("donor cases") where possible and provides a rapid meshing tool where and when these samples are not applicable. The DART system structure is shown in Figure 3.25 below:

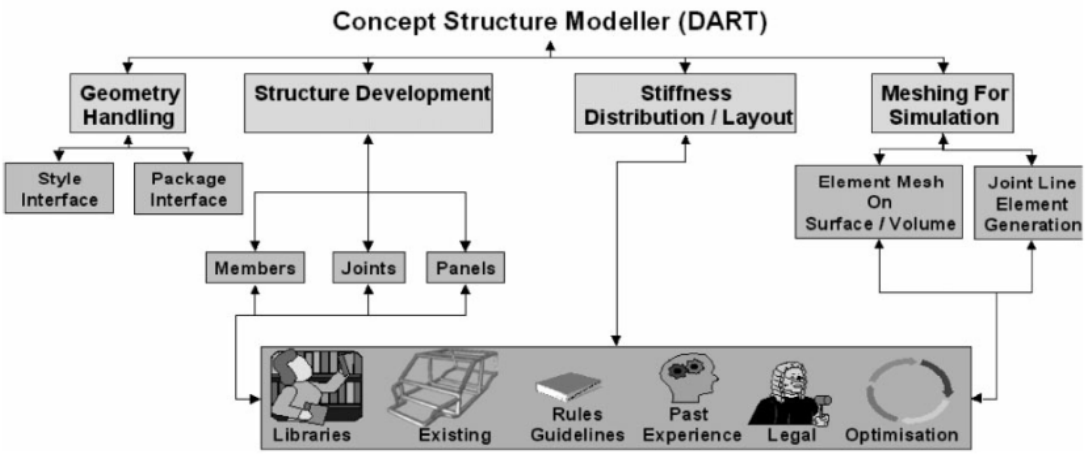

Figure 3.25: DART Structure [28]

DART is constructed using the Adaptive Modeling Language (AML), which is used by other applications cited in this chapter. One difference Chapman and Pinfold raise between a knowledge-based engineering system and traditional procedural programming is that values modified by changes are computed only as needed, whereas

the procedural systems re-compute all values at each change. Such re-computations in the knowledge-based system are triggered by demand events such as a graphical screen redraw event or a query for an updated mass computation.

Another assertion made by Chapman and Pinfold is that the knowledge-based engineering systems will evolve over time. This assumes that, for a given engineering problem, the knowledge-based system will have to be developed along with the problem being developed and analyzed. A key goal in the development of any knowledge-based system must be to ensure that addition of additional knowledge entities and manipulations will not invalidate all previous models in the knowledge base prior to the change. An example of destruction of an existing knowledge base occurs when a company makes a change in CAD software. Standard translators such as Standard Exchange of Product Model Data (STEP) or Initial Graphics Exchange Specification (IGES) often results in the loss of product "intelligence." Forethought and flexibility in defining and relating the interaction of the knowledge entities can permit a forward- as well as backward-compatible implementation.

Chapman and Pinfold claim that development of a vehicle structure in DART can reduce finite element modeling from 15 man-weeks to minutes and will prevent model duplication [28]. They cite examples in aircraft wing and fuselage design using knowledge based systems [33, 34]. This assertion requires validation in an actual commercial vehicle program; savings attained in controlled conditions are not always realized in a production engineering environment. The method used to generate a finite element mesh also assumes a specific structural topology (beam and join structure

defined first before panels are added). Such assumptions constrain both the design space and resulting set of solutions for optimization. While assumptions and constraints cannot be completely avoided, they must be examined carefully for their impact on the end product outcome.

The authors frequently state the time savings and avoidance of duplication possible with the DART system. However, an objective study under industry conditions with the entire vehicle development benchmarked (not just BiW) is necessary to validate claimed savings. It is often possible to optimize one aspect of a vehicle development at the expense of the overall vehicle program (sub-optimization).

Some aspects of Chapman and Pinfold's conclusions can be used in this author's research work. Existing vehicle dimensional data can be used as a "donor work" establishing statistical norms for specified vehicle classes, particularly those classes specified by the Environmental Protection Agency for fuel economy reporting. While this data is not meant to constrain the final design, it can give a more accurate starting point for a multi-objective optimization. In some cases this data can be used to establish constraint requirements (for example, a "midsize" passenger vehicle using the U.S. Environmental Agency definition must have a total interior volume--passenger and cargo--between 110 and 120 cubic feet). Other aspects of knowledge-based engineering can be incorporated using high level computing languages which can graphically represent output in a number of useful formats and perform operations based on data context.

While DART appears to be a useful tool, it is focused on one aspect of vehicle design (Body in White). To support a vehicle development program the knowledge-based tools must encompass whole-vehicle design to avoid sub-optimizing the vehicle development process.

It is important to be cautious in inferring that gains seen in the aerospace industry (which constitute many of the examples given by Chapman and Pinfold) translate directly to automotive design. Many of the functional modules in aerospace design can be treated as orthogonal to each other and designed / optimized in relative isolation from each other. Aircraft cockpit design does not have to consider extensive linkage with wing or structural design in most cases. An automotive design has stronger coupling in all areas which may reduce some of the gains or require approaches different from those of aerospace.

The DART tool is focused on the rapid development and management of finite element analysis (FEA) models. FEA tools should most properly be used in the detailed design phase of vehicle development. While some of the principles explored by Chapman and Pinfold may be useful in the author's current work, it is not desirable to use FEA tools in the Concept Development phase in this current project.

El-Sayed and Song (1998) [35] develop a computer program to provide an optimized balance between 0 to 60 mph vehicle acceleration time and overall vehicle fuel economy with gear shift strategy, tire slip and several other factors taken into account. This work includes a number of vehicle parameters with two optimization targets (acceleration and fuel economy). The article presents the mathematical models used for 0

to 60 mph acceleration time and fuel economy computation. One shortcoming of the fuel economy equation is that it assumes steady-state operation rather than the urban driving (UDDS) and highway driving (FWFET) cycles used in EPA computation of combined miles per gallon fuel economy. The optimization uses Design Optimization Tool (DOT) software from Vanderplaats Research & Development, Inc. coded in FORTRAN 77 to develop a composite objective function [36]. Such an optimization calculation can also be run efficiently and easily using software such as MATLAB with built-in optimization functions. If a more detailed acceleration model is required for aspects of the author's work, the shift strategy enumerated by El-Sayed and Song can be used as one potential input. Other algorithms for gear shift and acceleration strategies are also available in literature [37].

Parametric Design and Concept Design

Calkins, Su and Chan (1998) [4] equate rule-based design with knowledge-based engineering. Rule-based design is more properly a subset of knowledge-based engineering and design. They assert that automotive design is less defined in the conceptual design stage than for aircraft or ship design. In their article they propose the Automotive Decision Support System (AutoDSS) system as a knowledge- or rule-based tool to rapidly develop and visualize an automotive concept level design.

Calkins et al. describe the rule-based portion of knowledge-based engineering in three categories: physical laws or principles, legal constraints and corporate cultural factors ("best practices"). They do not give an example of a completed design rule or how it is implemented in the AutoDSS system. Their system uses ICAD as the graphics

engine as do several other systems cited in this chapter. The product decomposition used shows different levels of detail at successive design stages (Figure 3.26).

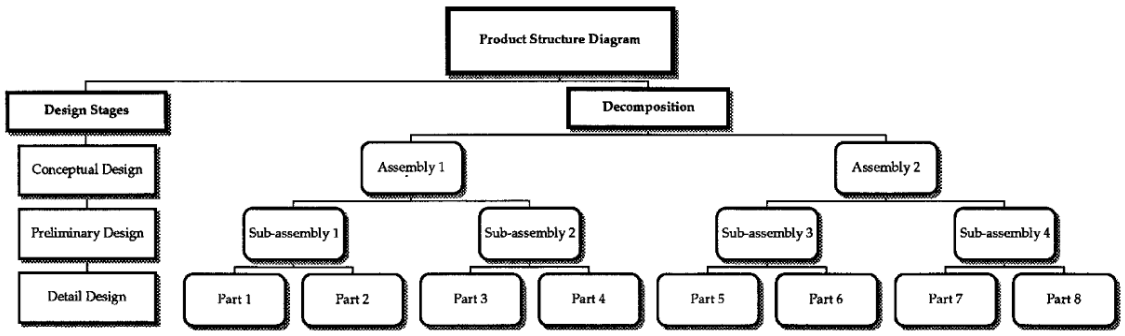

Figure 3.26: Product Structure Decomposition at Respective Design Phases [4]

One limitation of this detail level by design phase approach is that some aspects of the design may require more detail at an earlier stage than those shown above. The product structure should not in itself dictate when these activities should occur; rather, the level of detail should be dictated by the decisions required at a given point in the process (decision-based design).

The AutoDSS Architecture is shown in Figure 3.27 below:

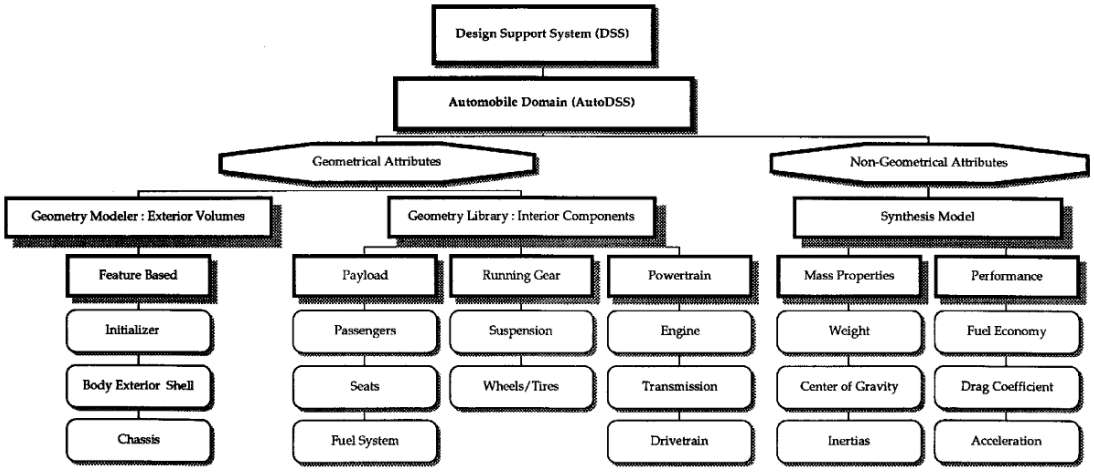

Figure 3.27: AutoDSS Architecture [4]

One outdated aspect of this architecture is that most solid-based CAD programs (CATIA, SolidWorks, etc.) can now store model attributes such as mass, center of gravity and inertial properties as part of the geometric model or readily calculate / update this information as needed. Other system and subsystem groupings (running gear separate from chassis) affect how the software is used and how the program utilizes the design space. AutoDSS uses a surface-based CAD system, which limits the ability to incorporate mass or inertia based properties directly into the CAD model.

Vehicles are initially modeled from the outside "bounding box," and defined as "1-box," "2-box" or "3-box" designs based on whether distinct motor compartment, passenger compartment and trunk divisions are present. The wheels are added and then the box corners rounded with control curve tools. These curves can be further refined to provide detailed surface contours.

A major drawback of this "outside-in," design approach is that it may arbitrarily constrain the occupant layout and space in the vehicle--the aspect of vehicle design with the greatest impact on the end customer. Modern design practice tends to take an "inside-out" approach, setting the occupant positioning and ergonomic envelopes and packaging the rest of the vehicle outward from the occupant volume.

The parametric performance calculations highlighted in the article (0 to 60 mph acceleration time, fuel economy and mass) tend to be uni-dimensional. The 0 to 60 mph acceleration time is given solely as an inverse function of engine power to vehicle weight, ignoring traction limits, weight distribution or aerodynamic factors. Mass is given as a function of vehicle class (sport coupe, coupe or sedan) and overall vehicle

length. Fuel economy is a function of average speed, vehicle weight, width and horsepower, ignoring acceleration, braking and other factors in the EPA urban (UDDS) and highway (FWFET) fuel economy driving cycles. More comprehensive parametric models are currently available as discussed elsewhere in this chapter.

AutoDSS incorporates several useful aspects of a knowledge-based system but suffers some serious technology limitations. A surface based CAD system is more limited for capturing engineering parameters such as mass, inertia, etc. directly from the model. An optimal CAD system handles a mixture of solid- and surface-based CAD within the model. Altair Corporation has developed a modular version of SolidThinking (Surface or Solid-based), which can be incorporated within SolidWorks CAD software [38]. A hybrid CAD system may be able to overcome some of the limitations posed by ICAD within AutoDSS.

Bhise et al. (2004) [39] present an unnamed vehicle design program at the University of Michigan in Dearborn meant to automatically generate a vehicle model covering multiple vehicle functional areas. This program, announced in 2004, would develop the modules shown in solid outline in Figure 3.28.

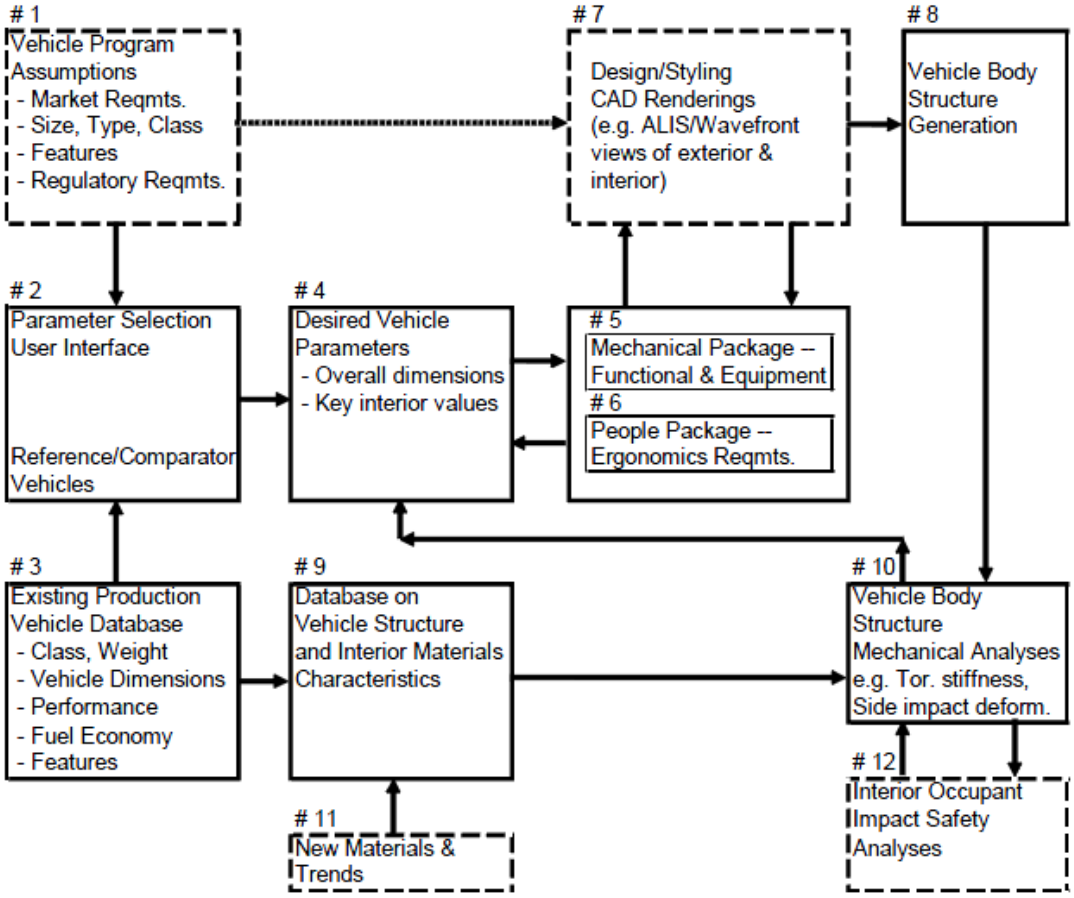

Figure 3.28: U of M Dearborn Proposed Vehicle Development Program [39]

Additional modules shown in dashed outline are not comprehended as part of the initial vehicle development. The article describing this system states that all 8 planned modules have been completed in whole or in part but have not yet been integrated. No additional literature concerning this program or integration of the modules was found. It appears that the integration effort was not pursued but some of the separate modules were developed as stand-alone applications. One lesson learned from this work is that the integration of the functional modules should be defined prior to detailed design and implementation of the modules.

The Project as defined starts at box #2 with a designer / engineer selecting key vehicle characteristics such as overall length, width, height, overhangs, driver heel point to seating reference point height (SAE H30), etc. The program appears to begin with selection of the vehicle exterior dimensions and then works inward to package the occupants. It compares the selected dimensions with a database of existing production vehicles. The program then proceeds with mechanical and occupant packaging before generating body structure based on pre-configured parametric models for finite element model generation. The developed structure is a beam-element space frame and does not generate any sheet metal surfaces or structures other than the beams. Finite element meshing of the models for crashworthiness and NVH analysis appear to be manually generated from parametric models created in IDEAS (Integrated Design and Engineering Analysis Software).

Tasks that are proposed but not executed in this program in addition to the overall integration include:

- A means for developing a functional specification for proposed vehicles
- Selection of software for beam model analysis
- Interface with commercial CAD systems
- User interfaces
- Ergonomics, including driver positioning, primary controls location, maximum comfortable reach, minimum comfortable reach, eye ellipse location, head clearance contours, visibility and obscuration, wiping zones, forward and indirect field of view of targets

- Development of a database of selected vehicle sizes and body types
- Development of mechanical analysis routines for exterior dimensions, overhangs, engine and transmission envelopes, suspension/chassis envelopes, spare tire and gas tank envelopes.

This proposed project was successful in identifying essential functions for an automated vehicle generation program, but two issues may have been key to the lack of progress beyond the initial announcement and modules. First, the integration requirements and interfaces of module inputs / outputs should be defined before the individual modules are created. A stand-alone module will function very differently from an integrated one. Second, the program as described appears to size a vehicle from the outside in and does not explicitly express known relationships between wheelbase and overall length, etc. A better practice is to set key vehicle parameters beginning with the occupant positioning / packaging and working outward using parametric relationships, vehicle type and size class information. This issue is also seen in the AutoDSS program and may have been due to letting the technology available dictate the vehicle generation process.

Bhise and Pillai [40] continued work on a subset of the above software. This subset permits the user to create an exterior vehicle package that represents certain classes of vehicles ("one-box, two-box, three-box," similar to the AutoDSS approach) and specify maximum external length, height and width dimensions. A sample visualization from one of the program input menus is shown in Figure 3.29.

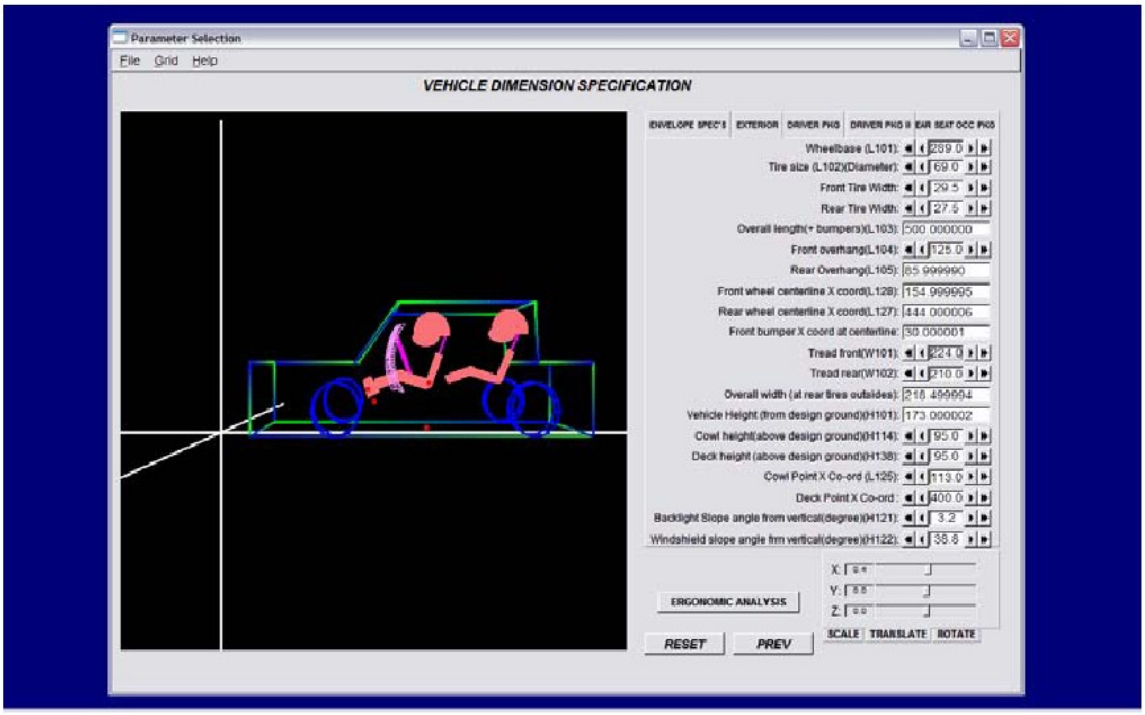

Figure 3.29: Packaging Program Exterior Vehicle Parameters Menu [35]

The program as described dynamically updates other parameters changed by modifying a given parameter value. However, the selection panel appears to require significant knowledge on the operator's part for typical values of occupant parameters such as L50-2 (first to second row coupling distance). The program should give a typical starting value for a vehicle type and size class so that the user has a realistic starting point to adjust from. Parameters such as wheelbase, track width, etc. should be developed first from occupant packaging and optimized for occupant considerations and vehicle performance targets. Otherwise, the software user is required to follow trial and error methods of vehicle sizing and optimization. The software, and the graphics implementation in particular, is stand-alone and is not integrated with common CAD

packages in current use in industry. This may make it difficult for a model to be imported into other software packages without significant manual manipulation.

Anemaat, Kaushik, Hale and Ramabadran (2006)[41] and **Anemaat (2007)** [42] describe an Aircraft Automated Analysis (AAA) program which integrates all common aspects of aircraft design into one package. The program has been developed over a 20-year span and has undergone several revisions, including conversion to an object-oriented programming language (AML) in 2007 [42]. Many of the engineering design processes and required flight factor calculations are delineated in Federal Aviation Rules FAR 23 [43], FAR 25 [44] and various Military Specifications (MILSPECS). One of the stated values and purposes of AAA is to capture engineering knowledge and experience that will be lost when senior aircraft engineering personnel retire or leave. The decomposition of the high-level aircraft and supporting models are shown in Figure 3.30.

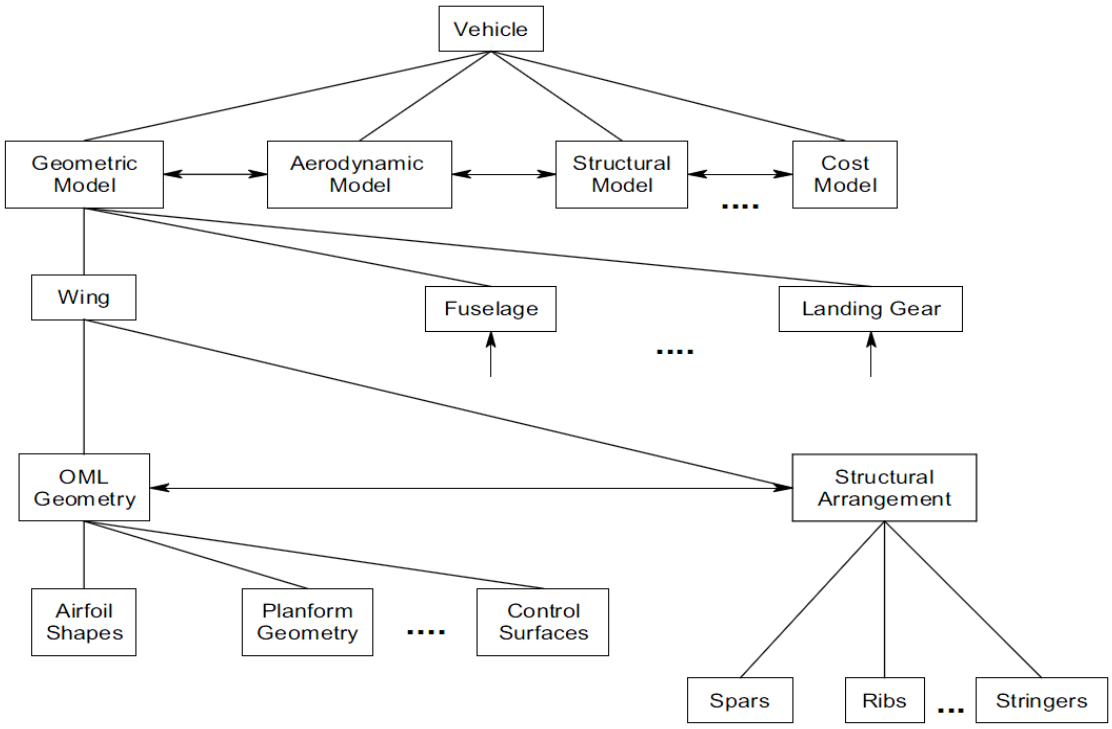

Figure 3.30: Model Decomposition Diagram [41]

They discuss the importance of performing the appropriate analyses at the correct time in the process [41]. The AAA program modules and process flow are shown in Figure 3.31. Note that these are functions common to most fixed-wing aircraft; non-traditional or new functions due to a revolutionary design are not included and are not integrated in this process. The ability of such a program to integrate or accommodate revolutionary design strategies will determine its effectiveness in permitting early validation and inclusion of game-changing designs and technologies.

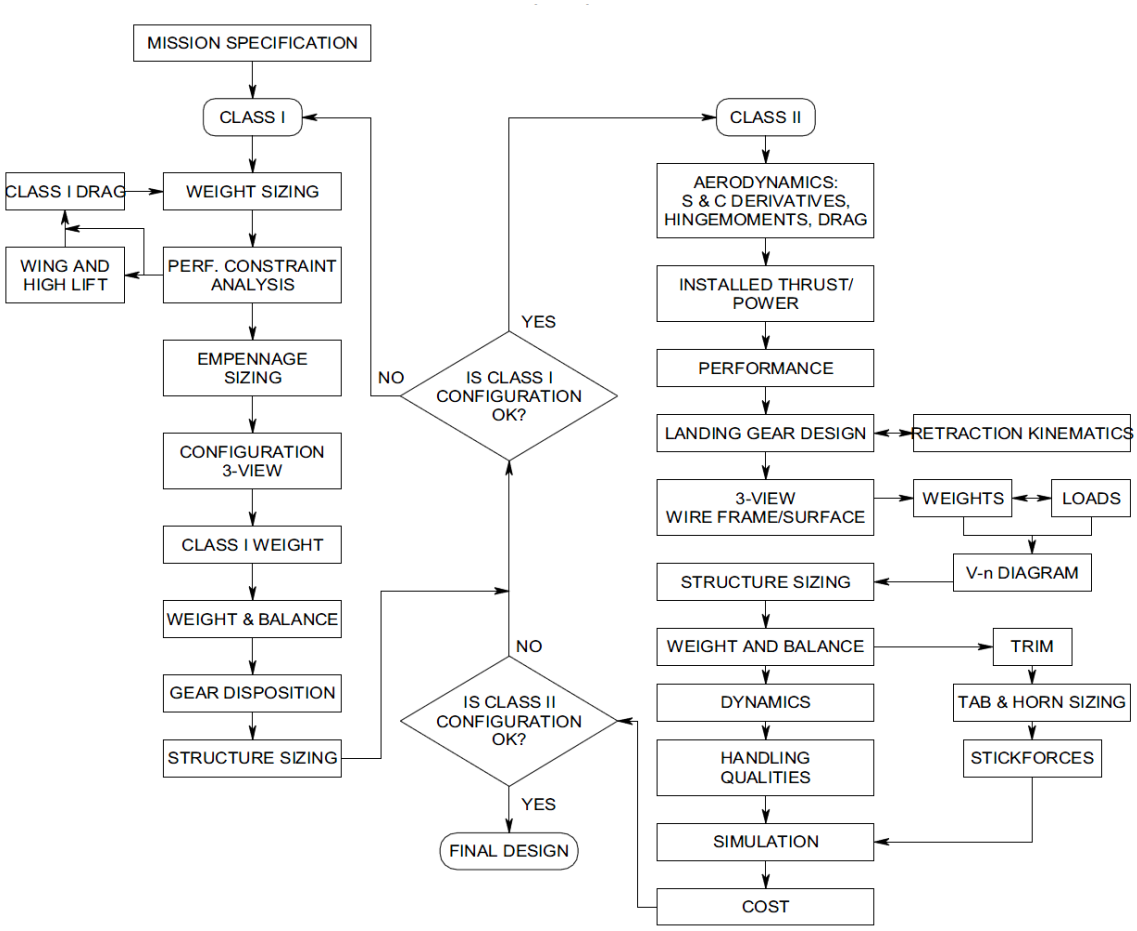

Figure 3.31: AAA Functional Modules and Process Flow [41]

It is important to note that aircraft functional requirements and required calculations are delineated in great detail in FAA regulations. This makes the regulatory aspect of design and validation one of the most important aspects of aircraft development. The actual users of the aircraft (pilots, crewand passengers) are not typically viewed in the aviation industry (for commercial aircraft) as the "customer." At this point the AAA program appears to require an extensive set of specifications as a starting point. It also appears that several modules such as computational fluid dynamics (CFD) analysis are

still under development 15 years later. This shows how complicated and difficult an integrated, layered development program can be to execute.

Huang (2006) [45] focuses on the concept design of a generic Space Access Vehicle (SAV). He notes that the design problem for an SAV differs from that of general aircraft and automotive design due to the differences in design space available (Figure 3.32). The SAV problem is limited to a handful of solution classes, whereas an automotive design has an extremely large quantity of potential viable solutions. This is one of the key reasons that multi-objective optimization can be more difficult in the automotive discipline.

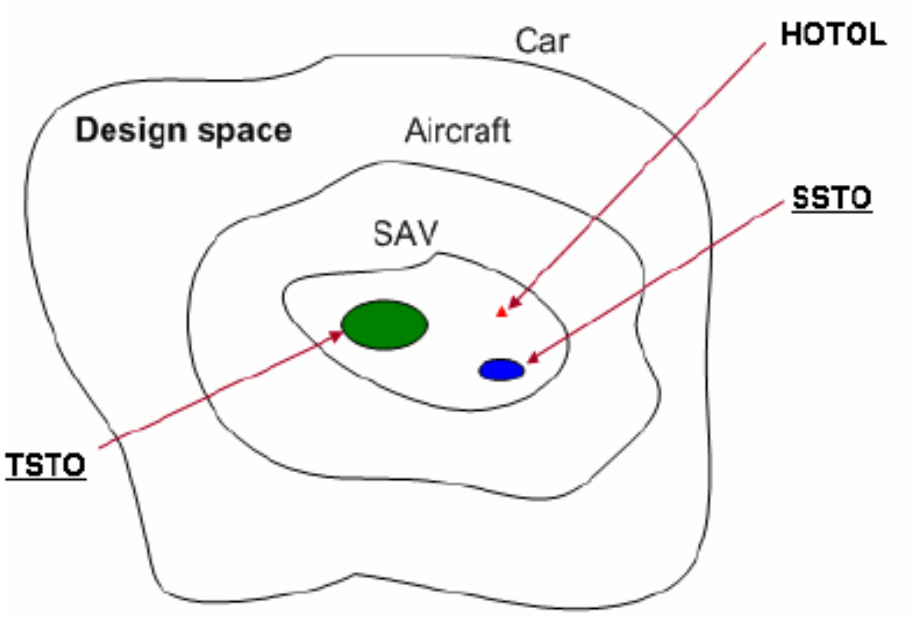

Figure 3.32: Relative Design Space in Automotive, Aircraft and SAV Design [45]

Huang notes that SAV designs often fail after exiting the Conceptual Design phase due to engineers, in the words of Chudoba, "...falling in love with a flight vehicle geometry too early and successively analyzing it to death with high fidelity tools" [46].

This is consistent with the emphasis on decision planning and conducting the proper design activities at the proper stage in development. Such early "lock-in" to a single design is common in the automotive industry and results in sub-optimized designs as a vehicle goes into production.

Huang presents a roadmap for SAV concept design methodology (Figure 3.33). Even though relatively few SAV designs (the Space Shuttle, Spaceship 1) have actually flown, experience with rocketry, supersonic and transonic aircraft have built up a body of knowledge as to performance parameters and flight performance requirements. The amount of funding applied to space vehicle research has also helped to define in detail the expected parameters and design requirements for SAV's.

Many of the analyses cited or proposed by Huang for the Conceptual Design phase of an SAV might be considered detailed design for an automotive vehicle project. One reason for this may be that the design space for an SAV is much smaller and that design option branches narrow down far more quickly. An automotive design must consider many more options in converging to a detailed design (this does not imply that an automobile has more design parameters; rather, the automotive design parameters may have many more values and combinations which provide an "acceptable" vehicle design).

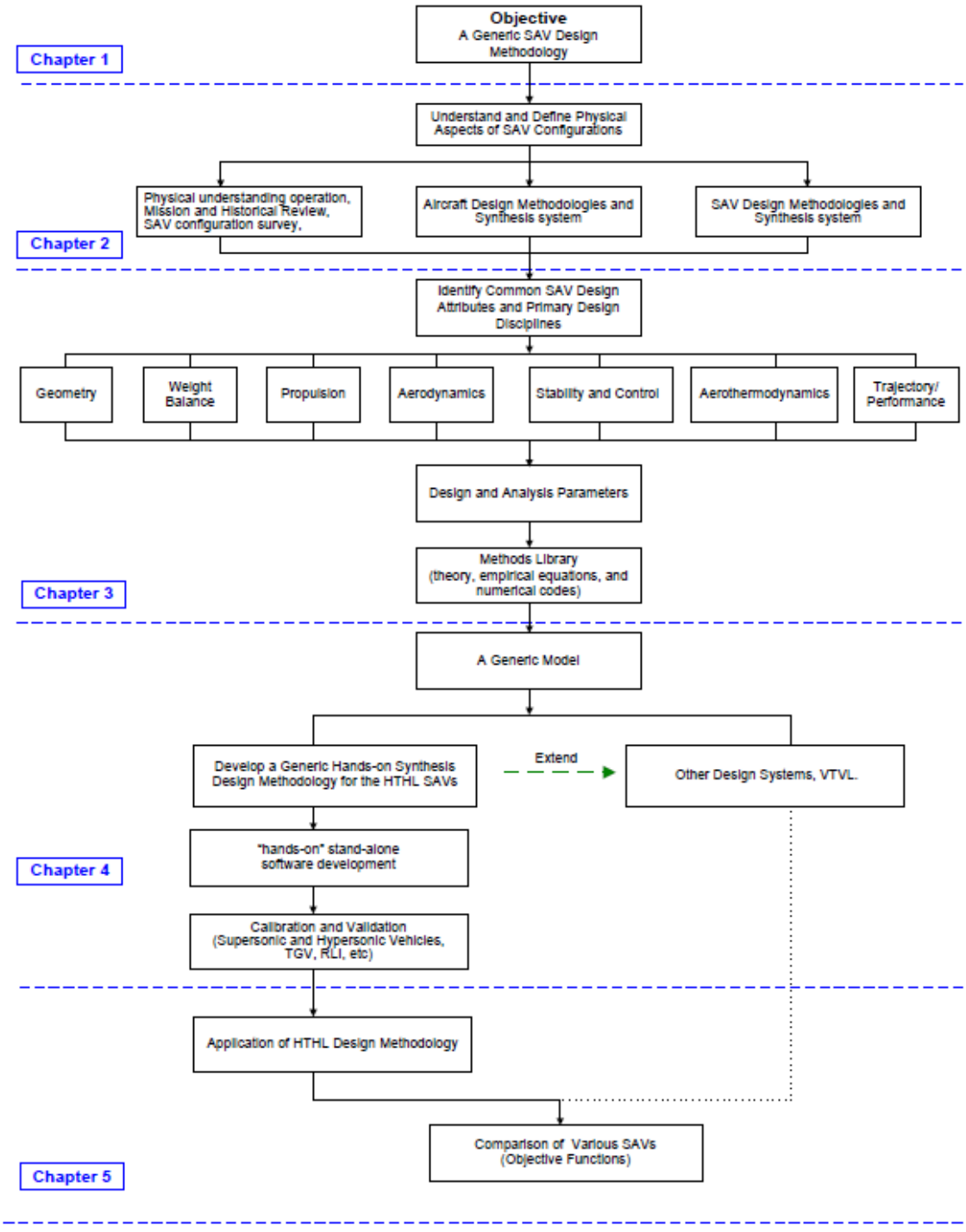

Figure 3.33: SAV Design Methodology Structure [45]

Huang reviews existing analysis tools and methods: he is focused more on an overarching methodology approach than advocating or developing specific tools for that methodology. Several of the points that Huang makes are of use in the author's current research. Ensuring that the correct level of analysis and optimization is performed during the Preconfiguration and Analysis/Optimization stages in the optimization environment will ensure that the most useful trade-offs made and vehicle parameters output for the engineer are generated while minimizing the level of design "noise." In any engineering discipline, many problems can be avoided if the engineer refrains from "falling in love," with a specific vehicle geometry or configuration early in the Concept Design phase.

Khalid (2006) [3] investigates the use of multi-objective optimization in rotorcraft preliminary design. He begins with a discussion of relative cost, knowledge and freedom of decision making during different phases of the design process as previously shown in Figure 1.1. His conclusions are consistent with other authors previously discussed and reinforce the importance of effective decision-making in the concept design stage of any project.

Khalid bases his proposed methodology on the Georgia Tech Integrated Product and Process Development (IPPD) and Product Lifecycle Management (PLM) Rotorcraft Preliminary Design Methodology (Figure 3.34). This methodology specifies activities along with prescribed analysis tools and methods at each stage of the conceptual design. A major difference between aviation and aircraft design is that there are prescribed calculations and documented analysis activities during the concept design phase for FAA approval of an aircraft; automotive certification documents are typically developed in the

detailed design phase and are far less extensive than those for aircraft. It is often stated in the aviation community that, "...the documentation always outweighs the plane before it can fly." Khalid proposes a methodology (Figure 3.35), which is a modification of that in Figure 3.34.

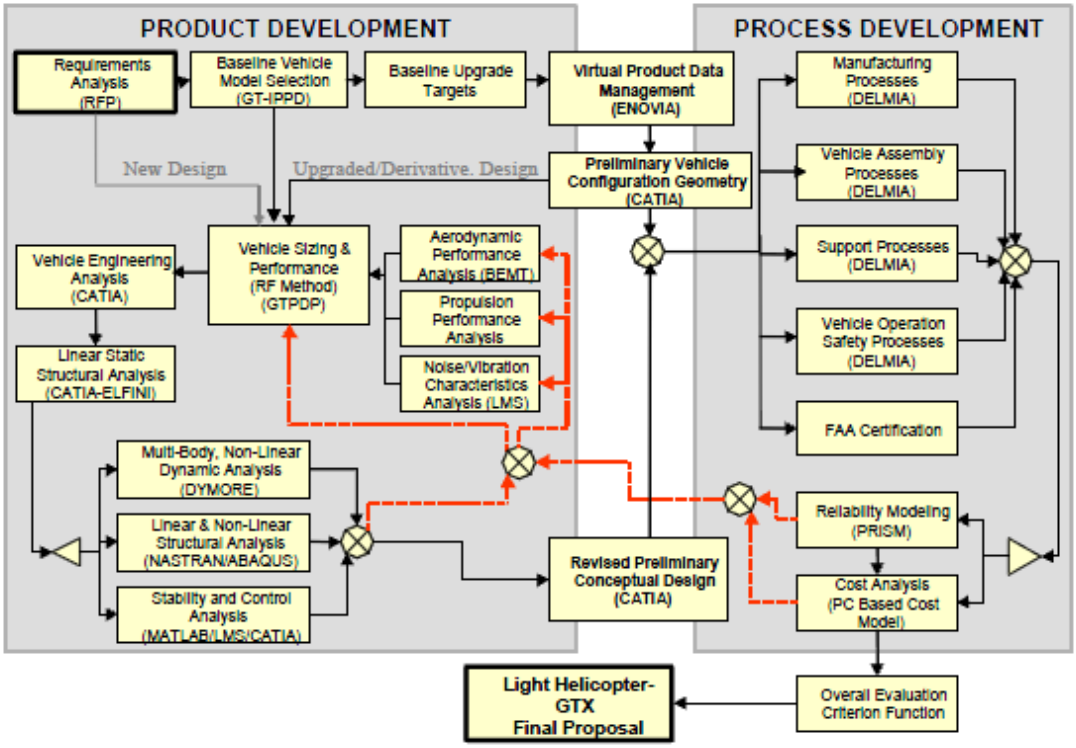

Figure 3.34: IPPD/PLM Methodology [2]

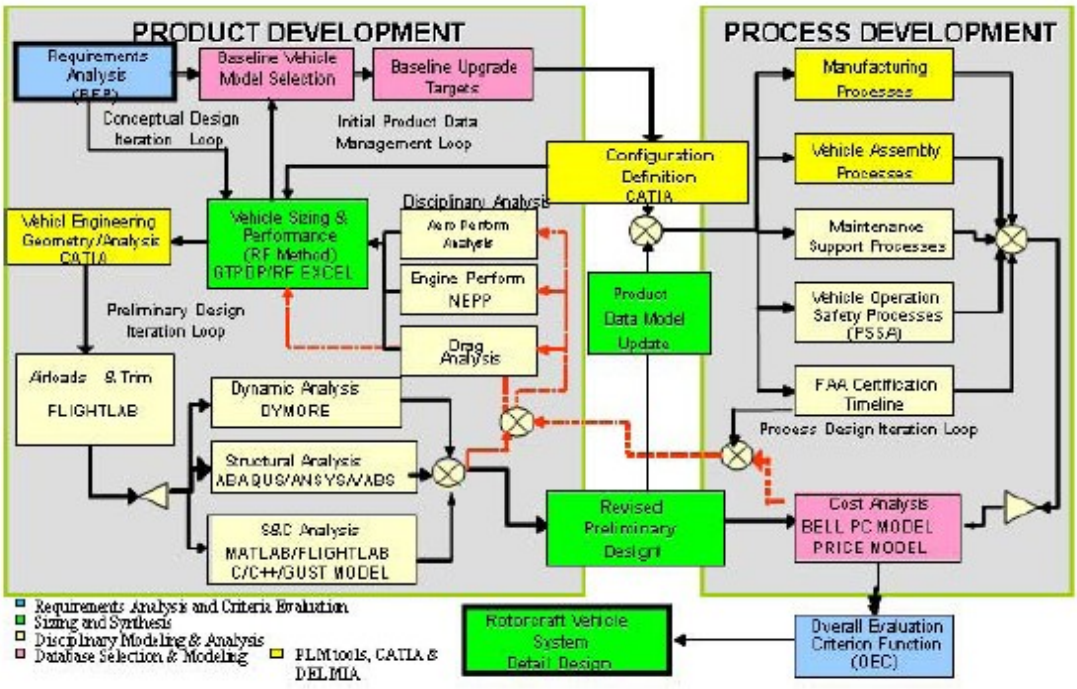

Figure 3.35: Khalid's Proposed Methodology for Rotorcraft Concept Design [3]

Khalid's proposal is a modification of a highly developed methodology (IPPD / PLM) for aircraft development at the Georgia Institute of Technology. Much of this is due to the more detailed and imposed nature of aircraft specifications compared to those of automotive. The structured methodologies and legislated analysis activities lend themselves to a more automated approach, but limit the design options which may be explored. Automotive designs have a higher level of design freedom that increases options but makes the automation of tasks more difficult. Khalid's discussion of cost, product freedom and design knowledge is directly applicable to the automotive design process. The design methodology Khalid advocates for rotorcraft may dive into details in the concept development phase which are best addressed in the detailed design phase in automotive design activities.

Multi-Disciplinary Multi-Objective Optimization Tools and Methods

Venkataraman (2009) [22] defines optimization as "A search for the best *objective* when operating within a set of constraints." He further describes optimization as, "the process of search for the solution that is more useful than several others... Qualitatively, this assertion implicitly recognizes the necessity of choosing among alternatives." The process of optimization produces quantitative values which delineate the specific design and function. Venkataraman defines this quantitative description of the problem as a mathematical model.

Venkataraman asserts that, "The development of a suitable mathematical model presupposes knowledge of content in the particular design area that the optimization problem is being formulated" [22]. Implicit in this statement is the fact that assumptions must also be made as to the relevant design factors, their level of characterization in the model and the impact that these assumptions will have on the result. Many of these assumptions can then be validated or modified based on analysis of the optimization output. He delineates the elements of problem formulation to include design variables, design parameters and design functions, and states that, "It is also a good idea to recognize that optimization is a procedure for searching the best design among candidates, each of which can produce an acceptable product" [22].

Design variables are the unknown quantities in the problem being solved. Venkataraman asserts that the set of design variables must be linearly independent (not related through scalar or additive operations). The processing in obtaining a solution will be a function of an integer power of the number of variables.

He defines design parameters as "constants which will not change as different designs are generated and compared during optimization." Examples given of design parameters are material properties and applied loads. Venkataraman states that design parameters "have no role to play in determining optimal design." Other authors use the term "design parameters" to describe the design variables in a problem. It is perhaps easier to carefully define entities as "design variables" or constant "properties" when defining a mathematical model. Some entities which can vary are nonetheless completely defined by design variables and constant properties such that their value is predetermined or dependent. It is often the conscious selection of the set of independent variables that determines which are independent and which are determinant.

Design functions are separated by Venkataraman into objective functions and constraint functions that establish the mathematical model of the design problem. The design objective or objectives "drive the search for the optimal design" [22]. Satisfaction of the constraints determines the validity of the design. Objective functions are usually expressed as a minimization function; a maximization function can easily be inverted to a minimization function using a reciprocal or negative multiplier.

Multi-Objective or Multiple-Objective Design uses several different design functions as objectives in the search for an optimal design. They permit the math model to represent design functions from several different disciplines. They are generally expected to be conflicting objectives driving trade-offs, though some or all may be cooperating objectives.

Venkataraman describes two approaches to Multi-Objective Design. The first uses a weighted linear combination of the multiple objectives. He asserts that the first approach is not widely embraced, primarily due to the difficulty of establishing the correct weighting factors. The second approach establishes a "premier" objective to solve, with additional constraints based on the remaining objective functions. These two approaches tend to use standard optimization procedures as with a single objective. One hazard of extending standard optimization approaches to multi-objective designs is the higher likelihood of numerous local minimums. Global optimization functions to overcome this problem require significantly greater computing time and resources than traditional optimization methods in most cases.

Venkataraman also discusses the use of a Jacobian matrix to "organize" the gradients of several functions. If an optimization function has variables x_1 and x_2 and constraint functions $g_1(x_1,x_2)$ and $g_2(x_1,x_2)$, the variables and functions are related through the Jacobian Matrix [*J*] as shown in Equation (2) [22].

$$\begin{bmatrix} \partial g_1 \\ \partial g_2 \end{bmatrix} = [J] \begin{bmatrix} dx_1 \\ dx_2 \end{bmatrix} \qquad \text{Equation (2)}$$

The Jacobian is defined in Equation (3) [22].

$$[J] = \begin{bmatrix} \frac{\partial g_1}{\partial x_1} & \frac{\partial g_1}{\partial x_2} \\ \frac{\partial g_2}{\partial x_1} & \frac{\partial g_2}{\partial x_2} \end{bmatrix} \qquad \text{Equation (3)}$$

This can be used in scaling constraint functions to provide equal weighting of constraint functions and their impact on the objective function.

The Jacobian matrix can also be used to understand the sensitivity of an array of objective functions f to the variation of each variable [22]:

$$\begin{bmatrix}\partial f_1 \\ \partial f_2\end{bmatrix} = [J]\begin{bmatrix}dx_1 \\ dx_2\end{bmatrix} \quad \text{Equation (4)}$$

Quantifying the sensitivity can help to determine which variables have the greatest effect on the objective functions. This is important in multi-objective optimization where the number of variables needs to be minimized.

Rao (1996) [47] Does not appear to share Venkataraman's concern for using a linear combination of objective functions as a method of solving multi-objective design problem. He presents the final objective function as a weighting of the individual objectives shown in Equation (5) [47]. Some problems can occur in selecting the "best point" along a non-convex pareto front using this method [53]. This is discussed in a later section.

$$f(\boldsymbol{X}) = \alpha_1 \cdot f_1(\boldsymbol{X}) + \alpha_2 \cdot f_2(\boldsymbol{X}) \quad \text{Equation (5)}$$

In this case $f_1(\mathbf{X})$ and $f_2(\mathbf{X})$ are the individual objective functions and α_1 and α_2 are their respective weightings (or importance) for each objective function in the combined multi-objective function $f(\mathbf{X})$. The solution value of each variable will form a solution vector $\mathbf{X}$ where $\mathbf{X_i}$ is the i^{th} design variable value for the optimized solution vector. Rao discusses the concept of a Pareto Optimum Solution in dealing with multi-objective optimization problems. He states that there is, in general, "...no one solution which satisfies all of the individual objective functions at the same time" [47]. A feasible solution is called Pareto Optimal if there is no other feasible solution which reduces one of the objective functions without increasing one of the other objective functions.

Rao then presents several common methods for dealing with multi-objective optimization problems:

Utility Function Method (also called the Weighting Function Method)

A utility function $U_i(f_i)$ is defined for each objective function with an importance weight established for each function [47]:

$$U = \sum_{i=1}^{k} U_i(f_i) = -\sum_{i=2}^{k} w_i f_i(\boldsymbol{X}) \qquad \text{Equation (6)}$$

In this applicationw_i is the i^{th} weighted scaling factor for the i^{th} objective function. The solution vector **X*** will have the value which gives the smallest value of U which satisfies the set of constraints such that $g_j(\mathbf{X}) \leq 0$ where j = 1, 2, ...m.

Global Criteria Method

The optimum solution vector **X*** is found by minimizing a global criterion function F(**X**) such that [47]:

$$F(\boldsymbol{X}) = \sum_{i=1}^{k} \left\{ \frac{F_i(\boldsymbol{X}_i^*) - F_i(\boldsymbol{X})}{F_i(\boldsymbol{X}_i^*)} \right\}^p \qquad \text{Equation (7)}$$

Where $F(\boldsymbol{X})$ satisfies the constraint set [47]:

$$f_r(\boldsymbol{X}) = minimum \qquad \text{Equation (8)}$$

Exponent p is a constant (usually of value 2).

Bounded Objective Function Method

Minimum and maximum acceptable values for each objective function f_i are specified as $L^{(i)}$ and $U^{(i)}$. The most important objective function $f_r(\mathbf{X})$ is minimized to find **X*** where [47]:

$$f_r(\boldsymbol{X}) = minimum$$ Equation (9)

Such that [47]:

$$L(i) \leq f_i \leq U(i), \qquad i = 1,2, \dots k, \qquad i \neq r$$ Equation (10)

And [47]:

$$L(i) \leq f_i \leq U(i), \qquad i = 1,2, \dots k, \qquad i \neq r$$ Equation (11)

Lexicographic Method

This method ranks and minimizes objective functions in their order of importance, from $f_1(\mathbf{X})$ to $f_k(\mathbf{X})$, where objective function k is the least important. Thus the first objective function is minimized so that [47]:

$$f_1(\boldsymbol{X}) = minimum$$ Equation (12)

Such that [47]:

$$g_j(\boldsymbol{X}) \leq 0, \qquad j = 1,2, \dots m$$ Equation (13)

The resulting solution $\mathbf{X}_1$* and function [47]:

$$f_1^* = f_1(\boldsymbol{X}^*)$$ Equation (14)

Is obtained and used as an equality constraint for the second function [47]:

$$f_2(\boldsymbol{X}) = minimum$$ Equation (15)

Such that [47]:

$$g_j(\boldsymbol{X}) \leq 0, \qquad j = 1,2, \dots m$$ Equation (16)

And [47]

$$f_1(\boldsymbol{X}) = f_1^*$$ Equation (17)

This is repeated for all k objectives [47]:

$$f_i(\boldsymbol{X}) = minimum$$ Equation (18)

Such that [47]:

$$g_j(\boldsymbol{X}) \leq 0, \qquad j = 1,2,\dots m$$ Equation (19)

And [47]:

$$f_l(\boldsymbol{X}) = f_l^*, \quad l = 1,2,\dots i-1$$ Equation (20)

Goal Programming Method

This method defines the optimum solution **X*** as the one with the minimum deviation from set goals for each objective function. A minimum and maximum deviation from each goal is given as a constraint set. This method requires the ability to define the minimum / maximum deviations from the target goals for each objective which may not be possible for this author's research. This method will not be used but some aspects of the method may be considered in formulating inequality constraint functions.

Fadel (2012) [53] cautions against using the weighting method indiscrimately, particularly when applied to gradient-based optimization methods. Weighting can be used with non-gradient methods such as genetic algorithms or particle swarm optimization. If the problem is convex, then weighting can be used in all cases. The other caution is that an evenly distributed set of weights does not necessarily produce an evenly distributed representation of the Pareto optimal set [53]. Alternative methods of selecting a "best" or at least "better" point include the Distance and Tchebychev methods for points along the Pareto front [53].

Summary of Multi-Objective Optimization

A non-gradient (genetic algorithm) method is used by the author for optimization in this work. While the objective functional value for each objective in this research provides a convex pareto front, the functions are not all necessarily continuous in nature (particularly for engine functional and dimensional parameters as formulated in this work). Weighting does not occur in the genetic algorithm optimization itself; rather, weighting is used in conjunction with the distance method in selecting the "better" point from a final generation of points at the completion of the optimization run. There are a number of component objectives (12 for a hybrid powertrain vehicle, 9 for a non-hybrid powertrain vehicle) which are used in the optimization. The optimization provides an array of objective values for each point (one value for each objective in the multi-objective optimization. For a given point with resulting functional values F(X), where F(X) is the array of component objective functional values $f_i(X)$ and X is the "point" or array of design variable values that result in F(X), the weighted distance to each point is expressed as [54]:

$$D_X = \sqrt{\sum_{i=1}^{n} w_i \cdot f_i(X)^2} \qquad \text{Equation (21)}$$

D_X: Weighted "distance" of point from objective origin (0,0,...0)

w_i: Weighting factor--exponential from $(0.5)^P$ to $(2.0)^P$ where P = integer > 1

$f_i(X)$: Objective functional value for the i^{th} objective in the optimization at a given point X

This approach uses weighting in the selection of points from the Pareto front rather than the weighting changing the objective vectors during the genetic algorithm optimization; it also does not change the distribution of the pareto point set.

The weighting approach described above is structured to reflect preferences due to Voice of the Customer / Company / Legislator to reflect attribute requirements or emphases (Brand "DNA"). Each weighting factor may be a combination of more than one componentv_i if the brand "DNA" factor has multiple inputs:

$$w_i = (v_1 \cdot v_2 \cdot v_3)_i \qquad \text{Equation (22)}$$

One brand attribute (such as "Performance") may also be reflected in multiple target weighting factors; additionally, more than one attribute may influence a given target weighting factor, resulting in the above combination of weighting factor components. It is necessary to scale the weighting factors (through exponents, etc.) for them to have significant influence on the weighted distance calculation in Equation (21).

It should be noted that there must be linkage between the Voice of the Customer-based targets and the brand "DNA" weighting factors to provide a consistent vehicle development definition. The targets have the greatest impact on managing optimization trade-offs; the weighting factors have influence on trade-off balance when two targets are opposite in direction/outcome from each other. If a vehicle design is able to meet all objective function targets, there are no trade-offs to manage or influence. If the objective targets and the weighting factors have no linkage to each other, the resulting design optimization and trade-offs are not likely to be meaningful.

It may be argued that the expression of the distance to the weighted point in Equation (21) represents a goal-programming approach as opposed to a true multi-objective optimization; it aggregates the separate objective attainment measures into a single "score" in seeking the "better" point from the genetic algorithm optimization results.

Developing Low Order Parametric Models

In order to perform rapid analysis and optimization of vehicles in the conceptual design phase, the use of simplified lower-order models is preferred. These models are typically generated by simplified mechanics analysis and modeling or by correlation fitting to a known body of vehicle data. These models, while simplified, can be accurate enough to describe vehicle properties and behaviors to an acceptable level of correlation to actual vehicle behavior.

Malen (2011) [48] develops first-order models to describe vehicle body structure design. These simplified models cover aspects of structural performance which include bending, torsion, crashworthiness and vibration. A number of equations and relations are developed using a mix of solid mechanics theory and empirical tables and charts developed from experimental data and published literature. A point-based estimation of vehicle drag coefficient vs. generic body shape (adapted from MIRA, Ltd.) [49] can be used directly to estimate vehicle drag as influenced by vehicle styling. Other relationships are useful for information but cannot be used directly as a math model; instance-specific geometry or properties are required. With a few exceptions such as the

aerodynamic estimator, this reference is a starting point for developing math models rather than a comprehensive model source.

Venhovens and Yanni (2010) [13] develop a number of useful correlations for modeling vehicle fuel mileage as a function of vehicle outside dimensions and engine power. Their work parameterizes standard EPA test cycles into coefficients of a first-order mileage equation. Venhovens and Yanni also reference other useful correlation sources such as Allen et al. [56], who develop an empirical relationship between vehicle roof height (SAE H100) and center of gravity height (H_{cg}) for typical passenger vehicles.

Malen and Reddy (2007) [50] correlate vehicle curb mass and gross vehicle mass to vehicle plan area. They then correlate 13 vehicle subsystems as a fraction of the gross vehicle mass. This permits the mass estimation of a large number of subsystems with the trade-off of lower correlations for each detailed subsystem.

Developing Knowledge-Based Information for Models and Constraints

One of the more challenging aspects of building an automotive knowledge base is that information of interest to the researcher is typically considered proprietary from the viewpoint of an automotive manufacturer. While public sources for vehicle data are available, they are rarely complete or consistent. Some public sources are listed below.

Automotive Magazines carry some useful information but may measure data in different ways or using different procedures [71, 72]. One example is braking distance, which is measured using different initial velocity and start time events (reaction time may or may not be considered). Useful data from these sources include:

- Shoulder room (W3-1, W3-2)

- Engine power (horsepower or kilowatts)
- Passenger volume (ft^3 in U.S. publications)
- Cargo volume (trunk volume in ft^3 or liters)
- 0 to 60 mph acceleration time in seconds (or 0 to 100 kph time)
- Curb weight (lbs or kg)
- First to second row coupling distance (L50-2; found only for a limited number of vehicles)
- 60 mph to 0 or 70 mph to 0 braking distance (feet or meters)
- Headroom (H61-1 and H61-2)
- Driver legroom (L34) and second row legroom (L51-2)

NHTSA Vehicle Database. Available on the internet through the University of Michigan Transportation Research Institute (UMTRI) [51], this database is heavily redacted but still has some useful measurements for vehicle height, rocker thickness, etc. which cannot be found from other public sources. This information is limited to vehicles sold previous to 2002 and does not include newer vehicle classes such as Crossover SUV's, etc. It can, however, be used to develop critical relationships in establishing vehicle height and width dimensions by general vehicle classifications (body-on-frame, unibody, etc.). This is also one of the few resources for finding typical headliner thickness values.

The Motor Vehicle Manufacturer's Association (MVMA) [52] is a useful source of vehicle dimensional and equipment specification documents on a variety of vehicle models up until 1999. The author developed a number of statistical correlations

of common vehicle dimensions (with standard deviation values) for standard vehicle classes based on a combination of MVMA data and field measurements of vehicle seat width and seat spacing.

The MVMA data sheets suffer from a number of issues. Although ostensibly a public document for each vehicle through 1999, only a small number (~140) are available for vehicles from 1990 to 1999; others are offered by commercial information providers at significant cost. These documents are also not evenly distributed among EPA-defined vehicle classes, (large, midsized, compact, subcompact and mini-compact) and do not reflect European Union vehicle classes which are seen in the U.S. with increasing frequency. Some vehicle classes, such as Crossover SUV's, were not in widespread production prior to 1999.

Summary of the State of the Art

Many of the issues faced by the automotive industry in improving conceptual design and multi-objective optimization have been previously explored in the aviation community due to the higher units costs of aircraft vs. automobiles. The more prescribed legislative and industry requirements for aircraft have facilitated automation and optimization approaches, although the two disciplines have very different design spaces.

While many of the approaches and tools utilized in aviation translate well to automotive engineering, the approach must differ slightly in comprehending the different "customers" and influence that each engineering customer exerts on the final product. The need to make accurate and optimized decision early in the design process is equally critical to both industries.

CHAPTER FOUR

GAP ANALYSIS

Review of the State of the Art determined a number of opportunities for new research and development of a multi-objective optimization environment to support automotive conceptual design. Five key areas ("gaps") are discussed in this section. Note that not all of these gaps were noted in each of the projects reviewed.

Gap 1: Tools Applied are Inappropriate for Conceptual Design

Several aspects of this gap area are discussed below. Several publications cited above referenced the fact that either true concept design tools do not exist or detailed design tools tend to be used in the concept design phase.

Tools are Not Open for Integration in an Optimization Framework

Many design tools either do not consider optimization, have a built-in optimization environment with a focus on a single engineering domain or are otherwise constructed in such a way that the integration of external optimization tools is difficult or impractical. Common computer aided engineering (CAE) software packages are proprietary, using self-developed CAE graphics or file formats which are not compatible with commercially available CAE or analysis software.

Iteration Time too Slow

Common CAE tools either employ detailed models (such as finite element or multi-body models) or meta-models derived from detailed design tools (e.g., using response curves/maps) or other detailed analysis tools. A number of the projects cited above focus on accelerating the rate of analysis of detailed design models instead of

seeking a more succinct analysis method. Reducing analysis design iterations from weeks to days does not meet concept development needs; rather, the ability to run numerous multi-objective optimizations and make needed trade-off decisions in one day is needed to rapidly mature the product design.

Focus on Iteration Rather than Optimization

Some projects (such as the Aircraft Automated Analysis program [41]) focus on increased speed of iteration in place of optimization as the path to a mature product design. In focusing on iteration speed and quantity, however, it is difficult to assess whether the most optimal configurations have been included in the analysis process. The iterative emphasis also makes it difficult to ensure that all necessary trade-offs have been consciously considered and selected. It is possible that trade-offs are occurring by default due to the particular design iterations analyzed.

Gap 2: Models Used are Often too Detailed for Conceptual Design

The use of finite element or detailed multi-body dynamics models is usually not suitable for conceptual design. To develop useful models of this type often requires making detailed design decisions which are often "locked in" to future designs for a particular project. Furthermore, these models require hundreds or thousands of functional and geometric parameters which are not available in the conceptual design phase. The danger of "falling in love with a design," cited by Chudoba [46] is increased when detailed design tools are used too early in the process.

The time and cost investment in building large or complex models also reduces the number of configurations which may be analyzed or considered for trade-offs and

optimization. Detailed design tools may converge on a detailed product definition sooner but inhibit product maturity; they effectively limit the design space which may be considered in the analysis. The effort in building detailed models also promotes a "carryover mentality," as it is easier and faster to adapt preliminary detailed design models from an existing body of work (Chapman and Pinfold's "donor cases" [28]).

Gap 3: Values of Starting Parameters may be Arbitrary

Many of the design tools have similar data entry panels requesting specific vehicle dimensions. Some of the input menus do not couple dimensions to each other that are dependent in the overall vehicle design. Some of the analysis tools check dimensions for consistency after the fact or after subsequent dimensions are entered. This requires significant knowledge or experience on the part of the user to ensure consistent and meaningful inputs.

Additionally, many of the dimensions requested for user input should properly be determined as part of the optimization process in meeting customer / company / regulatory targets, constraints and desires. Initial inputs should reflect key aspects of vehicle character, configuration and targets rather than detailed dimensions which are a single aspect of vehicle design. Arbitrary or inconsistent starting parameters may have two effects as detailed in the following sections.

Analysis May Start outside Optimization Constraint Boundaries

If the analysis begins outside the valid solution space defined by inequality constraints, it becomes more difficult to ensure that the "best" or global optimization solution has been reached. As full global search optimization methods require more

extensive and time-consuming analysis methods, more commonly used optimization methods will benefit from starting inside the valid design space.

Analysis May be More Likely to Converge to a Local or Non-Optimal Result

If an optimization begins with initial parameters outside the valid solution space defined by the constraint set, it may increase the likelihood of the solution converging to a local or non-optimal final result (for example, if an optimization ends due to exceeding the maximum number of iterations allowed). Starting parameters which are logically consistent and valid for the defined solution space will increase the likelihood of converging on an optimal solution in a smaller number of iterations of the optimization process. If starting parameters are not logically consistent, it is possible that no optimal solutions may be found.

Gap 4: The Compromised Solutions are Brand Neutral (Nothing is Driving Trade-Offs)

Using optimization in a multi-disciplinary / multi-objective environment almost always leads to a solution that is a trade-off between all objectives / targets. Usually, the direction of the trade-offs can be steered by changing the targets or weighting factors in the cost function (sometimes in unreasonable magnitudes). None of the literature found so far incorporates the “Brand DNA"--the traits and emphases that distinguish one vehicle brand over another to steer this compromise. For example, a design problem for two identical vehicle concepts with identical targets at two different OEMs (e.g. BMW and Lexus. for example) should result in two different compromised solutions which need to align closely with the Brand DNA (sporty vs. comfort).

Used properly, Brand DNA should both qualify and quantify characteristics and values that reflect three "Voices" in the design evalution process: Voice of the Customer, Voice of the Company and Voice of the Legislator. Efforts to include Voice of the Customer include customer clinics, feedback from trade periodicals and surveys such as those conducted by AutoPacific Group [77]. These seek to determine what the customer values in terms of lifestyle, driving experience and perceived value of vehicle traits and attributes. These must then be translated into quantitative measures that the vehicle design engineer can use to evaluate performance to customer values and relative evaluations in trading off performance to often conflicting targets.

While Voice of the Company should be closely aligned with the Voice of the Customer to provide a vehicle the customer desires, conflicts and trade-offs will occur. Voice of the Company must approach vehicle design within an overall business model for the company. A successful vehicle from a company viewpoint meets or exceeds a targeted return on investment. Development time and resources must be balanced within a portfolio of (sometimes competing) company projects. Manufacturing capacity and individual factory volume limits must be balanced between existing and proposed new vehicle models; if a new manufacturing plant is required, the new and existing vehicle profit margins and volume in the new plant must justify the added expense. Sales and marketing must assess potential market volume and share for a new or re-designed vehicle model. The purchasing and human resource groups must determine the number of engineering and supporting staff required to develop and execute a new vehicle design; these costs must be factored against the potential financial return. Measured against these

financial and resource considerations, a trait or feature which the customer desires in a vehicle but is not willing to pay for (desired but not "valued") may not be worth pursuing for an automaker.

Although Voice of the Customer and Voice of the Company should be closely aligned in an ideal vehicle design, Voice of the Regulator / Legislator may pose direct conflicts with both of them. Legislative and Due Care Requirements form a large portion of the source of vehicle targets and specifications. Vehicles which do not meet federal and state legislative requirements will not pass the required homologation procedures required before commercialization.. The U.S., Japan, Europe and Canada are major drivers of legislative requirements for vehicles sold or manufactured in the United States. This author's research will focus on U.S. regulatory requirements to serve as the Voice of the Legislator; European Union and other regulatory inputs may be considered for future enhancements to this effort.

The Code of Federal Regulations (CFR), Part 49 [61] contains the majority of U.S. Federal regulations governing safety, environmental and other pertinent aspects of motor vehicle operation. Some states (such as California) impose additional emissions restrictions which effectively must be met by all high-volume vehicle models [79]. Specific aspects of CFR 49 include Federal Motor Vehicle Safety Standards (FMVSS) which specify test conditions and minimum performance requirements.

The U.S. Environmental Protection Agency (EPA) sets minimum Corporate Average Fuel Economy (CAFE) standards for passenger vehicles sold in the United States [73]. The EPA also defines standardized fuel economy test methods and cycles to

be used in fuel mileage calculations. Noncompliance with fuel economy standards currently results in a financial penalty against noncompliant OEM for each vehicle sold. It is expected that future regulations may bar the sale of noncompliant vehicles.

Voice of the Regulator (or Legislator) may be more difficult to capture than Voice of the Customer. Safety requirements are a "hard floor"; vehicles which do not meet the minimum requirements will not receive homologation approval. These requirements are best expressed as an inequality constraint to a multi-objective optimization function. Automakers selling vehicles in the United States must conduct vehicle tests according to Federal Motor Vehicle Safety Standards (FMVSS) procedures and minimum requirements and certify these results (along with compliance to standards) to the National Highway Transportation and Safety Administration (NHTSA). Vehicles sold in the European Economic Community (EEC) must meet similar legislative requirements.

The New Car Assessment Program (NCAP) is a series of government-run tests to assess vehicle performance separate from FMVSS compliance testing. Results are published using a "Star" rating system. In a frontal NCAP test the star rating measures occupant Head Impact Criteria (HIC) vs. Chest G's to determine the likelihood of serious injury as shown in Figure 4.1 [67]. These ratings are usually shown in comparison with other vehicle models in a market segment (large, midsize, compact, etc.). Vehicles with a lower star rating can still be sold; the perception of relative vehicle safety, however, may strongly influence buyer preferences. In this way the NCAP test, while conducted by the government, may be considered a part of Voice of the Customer inputs.

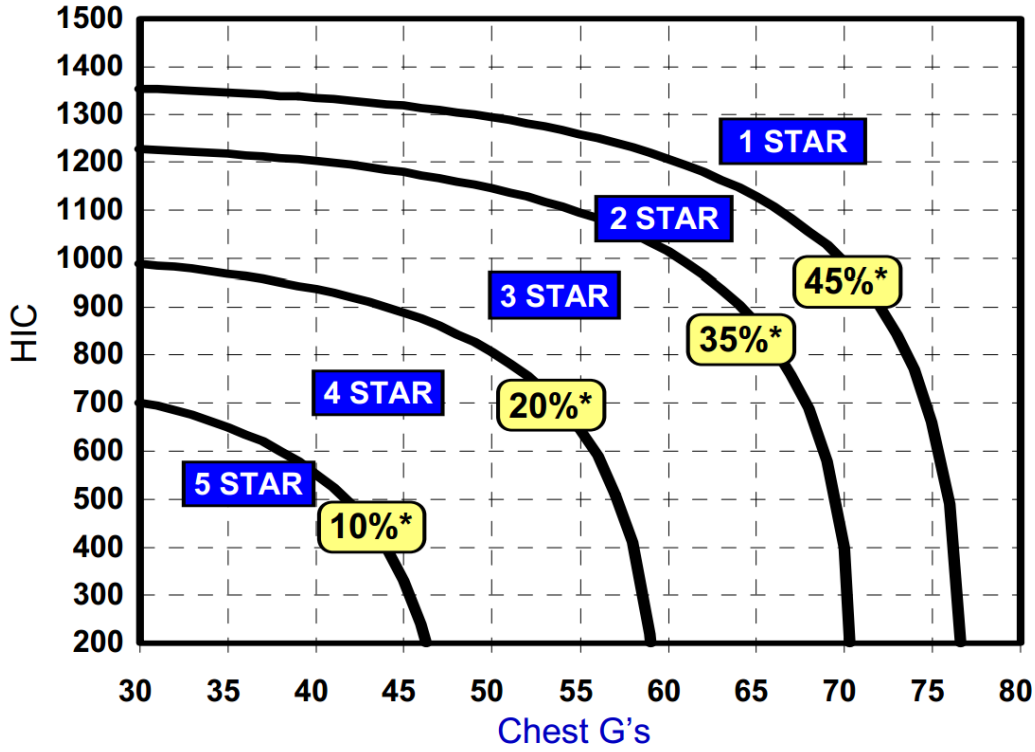

Figure 4.1 Frontal NCAP Star Rating vs. HIC and Chest G's (*: % Chance of Serious Injury for Star Rating) [67]

Other attributes, such as fuel economy, can also be quantified (there is a minimum fuel economy enforced by financial penalties; future targets or proposed mileage goals can be implemented as a function weighting in the optimization functions). As with NCAP results, fuel economy may reflect both the Voice of the Legislator (as a minimum requirement) and Voice of the Customer (as a cost of ownership / operation).

For the purpose of this work, it is contemplated that specific targets will be specified either by the customer or by an engineer with inputs from customers, marketing, manufacturing, regulations, etc.

Gap 5: Solvers are not Transparent

An optimization result is more meaningful if the user can understand the influence and interaction of the input vehicle traits, targets and constraints on the optimization analysis and the resulting body of vehicle design parameters. The lack of transparency may occur in two key areas discussed below.

Sensitivity Analysis and Validation Missing

Venkataraman [22] and Rao [47] spend significant time discussing optimization sensitivity measures such as the Jacobian Matrix. However, none of the works discussed in the State of the Art review in Chapter Three include measures of sensitivity in their discussion with the exception of Colton and Fadel [18]. Colton and Fadel show the user a weighted score for each of several selected vehicle function areas based on target achievement in the calculation process.

Taking a "black box" approach to the optimization process in understanding how trade-offs are made limits the user's understanding of the final optimization result. The type and strength of coupling between design variables, targets and constraints on optimization sensitivities can help the user validate their inputs and whether those inputs are consistent with resulting trade-offs.

Trade-Off Management Tools Missing

With the exception of Colton and Fadel noted above, there are few measures or visual indicators to show the trade-offs resulting from the optimization (or analysis iteration) process. This makes it difficult for the user to intuitively grasp the relative impact or "cost" of target trade-offs. A simple, intuitive trade-off visualization assists the

user in understanding and validating the trade-offs made in reaching an optimization result.

CHAPTER 5

STRATEGY AND IMPLEMENTATION METHOD

Proposed Solutions

A summary of the solution for each identified gap is briefly summarized below. They will be discussed in detail in the following sections.

Gap 1: Tools Applied are Proprietary or Inappropriate for Conceptual Design

- Rapid iteration of simplified models in a multi-objective optimization environment
- Development of an open-source software environment with a plug-and-play architecture
- Develop results output usable in common commercial CAD and spreadsheet software

Gap 2: Models Used are often Too Detailed for Conceptual Design

- Use first-order (or low-order) and knowledge-based mathematical models
- Develop and use models which capture underlying physical/functional principles in place of detailed designs
- Develop a continuum of dimensional and functional parameters which capture relevant vehicle characteristics and performance in line with desired vehicle targets

Gap 3: Starting Parameters with Arbitrary Values

- Use knowledge-based parameters and relationships which are consistent and relevant

- Use this knowledge envelope to set valid, coherent constraints
- Implement a "scenario validation" module which can quickly provide a determinate result for a fixed set (determinate) set of input parameter values. This can permit comparison of input values and resultant parameters and performance to known values of benchmark vehicles. This can be used to build confidence in the range of input parameters explored in provide more targeted inputs in the optimization module.
- Handle the interactions and dependencies between model parameters within the software framework to reduce the number of parameter values which must be specified or validated by the user.

Gap 4: Compromised Solution is Brand-Neutral (Nothing is Driving Trade-Offs)

- Use visually intuitive brand “DNA” inputs to steer the compromised solution by altering weighting factors. Note that weighting factors must be applied at the right point in the optimization process depending on the optimization method used.

Gap 5: Solvers are not Transparent

- Develop and provide sensitivity analysis tools for the user
- Develop and provide visually intuitive trade-off management tools for the user

Implementation Summary

The vehicle development and optimization environment which implements these strategies has two key components. A Scenario Builder module permits the user to input specific values for a set of parameters (including those which will be design variables in

the Optimization Module) to quickly obtain a specific solution including resultant parameters (overall and subsystem mass) and vehicle performance parameters. This is used to assess specific configurations/inputs and provide validation for the models used in both the Scenario Builder and Optimization Module. In addition, the user can quickly test the impact of modifications to the parameters and configurators resulting from a given optimization session. A "session" is defined as one complete iteration of either the Scenario Builder or Analysis / Optimization modules which begins with parameter / configurator inputs and ends with final module results, returning to the environment main menu.

The Analysis and Optimization module performs optimization of the vehicle design configuration. In addition it provides sensitivity gradient measures of parameters vs. design variables along with the sensitivity of resultant parameters to selected input parameters. Optimization targets cover vehicle safety, performance, efficiency, cargo volume and vehicle dynamics. Targets specific to hybrid electric vehicles are also included. Provisions are made to enable incorporating additional functional modules in the future. Scenario Builder and Analysis/Optimization Modules are outlined in subsequent sections. Implementation of this optimization environment is discussed in order of the identified Gap Areas and their proposed solutions.

A third module is included to assess the target vs. target sensitivity and correlation levels for a specific Analysis and Optimization session. This module takes the configurator / parameter inputs for a given optimization session and performs a Design of Experiments (DOE) analysis to assess target vs. target trade-offs.

Gap 1 Strategy Implementation:
Need for Appropriate, Non-Proprietary Tools and Architecture

Rapid Iteration of Simplified Models in a Multi-Objective Optimization Environment

This work is focused on optimization as a preferred approach (over iteration) to rapidly mature the product design in the Conceptual Design phase. This approach helps to ensure that all relevant design variables, user preferences, vehicle configurators, input parameters and constraints have been considered in the optimization process. Trade-offs are managed in a transparent manner in assessing target achievement. A conceptualization of the Vehicle Design, Analysis and Optimization Environment is shown in Figure 5.1 below [54].

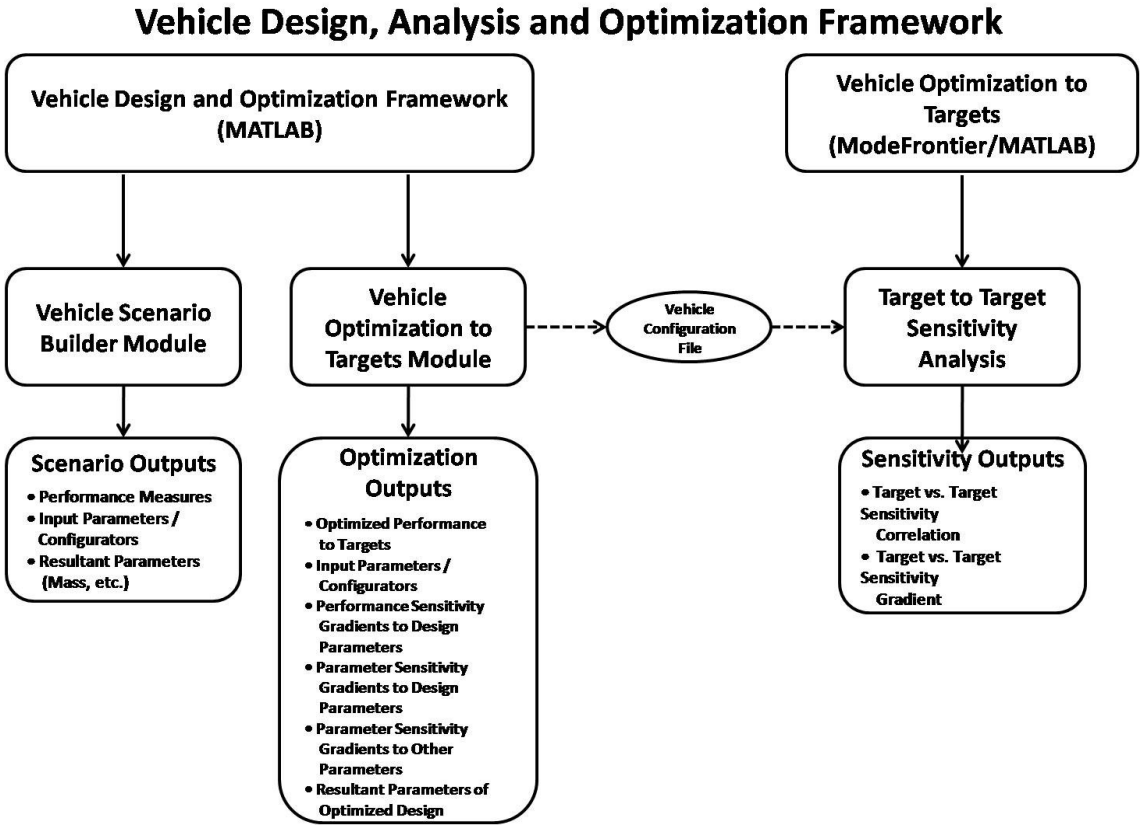

Figure 5.1: Vehicle Development and Optimization Environment [54]

Optimization Strategy

The optimization strategy began with gradient-based optimization methods. While this provided rapid solution convergence, it presented a number of issues.

- In order to converge on an optimal solution, the functional problem must be convex. It is difficult to prove that the objective space is convex for each target objective function. Additionally, future functional models and modules added to this environment may not have convex objective functions.
- Using a weighted-sum method with gradient-based optimization methods may not converge on a global optimum.
- Due to the difficulty of either visualizing or quantifying the full objective function space, it is difficult to determine if an optimized solution is a local or global optimum.

As a result of the above, an NSGA-II (non-dominated sorting genetic algorithm) optimization code has been adopted. While it solves some of the problems posed by the gradient-based methods, it introduces other issues:

- The computation time for a genetic algorithm is typically higher than those for gradient methods.
- Parameter vs. target or parameter vs. parameter sensitivity gradients cannot be rapidly determined as the genetic algorithm does not follow a continuous progression in developing a Pareto front. This requires other methods to approximate the sensitivity gradients.

• A genetic algorithm does not provide a single "best" optimization solution. If all end solution points are on or near a Pareto front, the solutions are considered "equal." Selection of a "better point" can be automated using a distance method or Tchebychev approach; however, the "best point" is still a matter of subjective interpretation. Weighting can still be used, but it should be applied after the genetic algorithm run is completed (in the point selection method) [53].

Development of an Open-Source Software Environment with a Plug-and-Play Architecture

MATLAB has been selected as the primary implementation software for this environment for several reasons:

• MATLAB has defined interfaces with numerous software applications including JAVA, C and C++, Excel, ModeFrontier, VisualDoc and CARSIM along with many others.

• It can be readily compiled into C / C++ code (.mex files) for faster execution and protection of intellectual property when the software is used in a production environment.

• It has an organic optimization toolbox which simplifies optimization activities

• It is a common software in the academic and industrial communities with a large body of coding expertise.

• It can be used to perform the functional evaluation activities inside other optimization software such as ModeFrontier and VisualDoc.

• It has built-in graphical user interface (GUI) functions to create user input menus and results displays. It also has built-in graphing capabilities.

For the target vs. target sensitivities and correlations, ModeFrontier is used in conjunction with MATLAB. When an optimization session is conducted, the input configurations and parameters are written to a Mat-file in a specified directory folder. ModeFrontier can then call up a MATLAB function evaluation file which opens the MAT-files and uses the same functional evaluation modules as the MATLAB NSGA-II algorithm. The resulting ModeFrontier Design of Experiments (DOE) information can be used to determine target vs. target correlations and sensitivities.

Develop Results Output Usable in Common Commercial CAD and Spreadsheet Software

In addition to being able to read Excel and formatted data files, MATLAB can output data to Excel spreadsheets or other output file formats. Common CAE software such as CATIA, SolidWorks and Ramsis can read this data and create 3-D models from it using automated scripts. It is not in the intended scope of this research to develop the scripts for specific CAE software import. The optimization environment, however, provides user options to output Excel or other formatted data files which can be used in such a manner.

Gap 2 Strategy Implementation: Need for Simplified Models which Capture Physical Principles

Use First-Order and Low Order Mathematical Models which Capture Underlying Principles

In place of detailed physical or CAD models, simplified mathematical models and relationships are used to describe the vehicle design, underlying relationships and physical/functional principles which govern achievement of vehicle targets. These

models, while more approximate than detailed models, can provide a high level of fidelity in capturing a broad range of vehicle physical and functional behavior.

The math models used in this work are a combination of relationships found in literature and new relationships generated by the author. Some existing relationships have been combined, modified or refined to develop needed inputs to the optimization models. Existing and author-developed relationships are described in the Validation and Results Section (Chapter Six) and in various Appendices.

An initial effort in this correlation process was to create a spreadsheet presenting the degree of relationship and correlating equations for a diagonal matrix of approximately 80 vehicle parameters (Figure 5.2). The matrix shows 5 levels of correlation from a "1" (direct proportional relationship--green blocks) to a "5" (no effective relationship or correlation--red blocks).

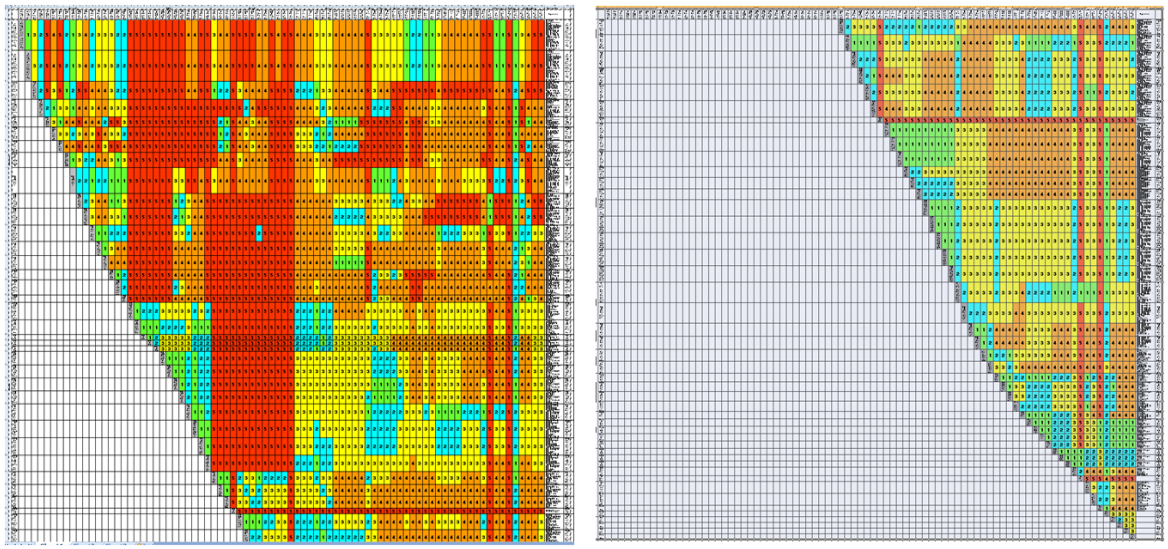

Figure 5.2: Parameter Relationship and Math Model Matrix [54]

This effort has been hampered by several factors. The current number of parameters (dimensional, functional, resultant and resultant target) and configurators

(non-scalar qualitative or quantitative descriptors) has exceeded a count of 200 in this work as shown in Appendix A. For the Spreadsheet shown in Figure 5.2 or software such as Loomeo, a user-input numeric coupling must be supplied for each cell (20,000 + cells). The time required to do this is prohibitive; an alternate approach has been to determine sensitivity gradients for parameters and targets of interest versus each other based on rapid iterations in the Analysis and Optimization Module both pre- and post-optimization. Target vs. target sensitivities are explored in separated software using a combination of the Analysis / Optimization Module code and ModeFrontier software to determine sensitivity gradient values.

Develop a Continuum of Dimensional and Functional Parameters which Capture Relevant Vehicle Characteristics and Performance in Line with Desired Vehicle Targets

Vehicle configurators and parameters used in this work are listed in Appendix A. A continuum of dimensional and functional parameters has been developed by the author to conduct this work; the dimensional parameters are discussed in Appendix B. Functional / geometric domains addressed in this work using these parameters include:

- Interior packaging (passenger / cargo volume and occupant measures)
- Front crashworthiness
- Fuel economy
- Vehicle acceleration
- Vehicle braking
- Vehicle turn radius
- Vehicle weight distribution (front / rear, C_g location)
- Vehicle overall (curb) and subsystem mass and location

- Vehicle overall (length, width, height) and component dimensions
- Tire selection based on dimensional and functional criteria (size, load rating, speed rating)

Functional and geometric domains not addressed in this work include:

- Side / rear / rollover crashworthiness
- Noise, vibration and harshness (NVH)
- Durability
- Serviceability
- Access / egress
- Reach and ergonomics
- Vision angles and envelopes

This continuum of parameters uses a mixture of industry standard dimensional nomenclature with author-supplied parameters which fill gaps in the component dimensions which add up to overall vehicle length, width and height values. Examples of the mix of parameters which make up overall vehicle width are shown in Figure 5.3. Missing dimensions include the lateral gap between the first row seat cushion edge and the door trim (WG-1) and the door belt width (WB-1). In similar fashion, a number of height parameters (HH-1, HC-1 and HR1) are supplied by the author to provide component height parameters from ground to the top of the vehicle body which sum up to the value for the vehicle body height H100 as shown in Figure 5.4.

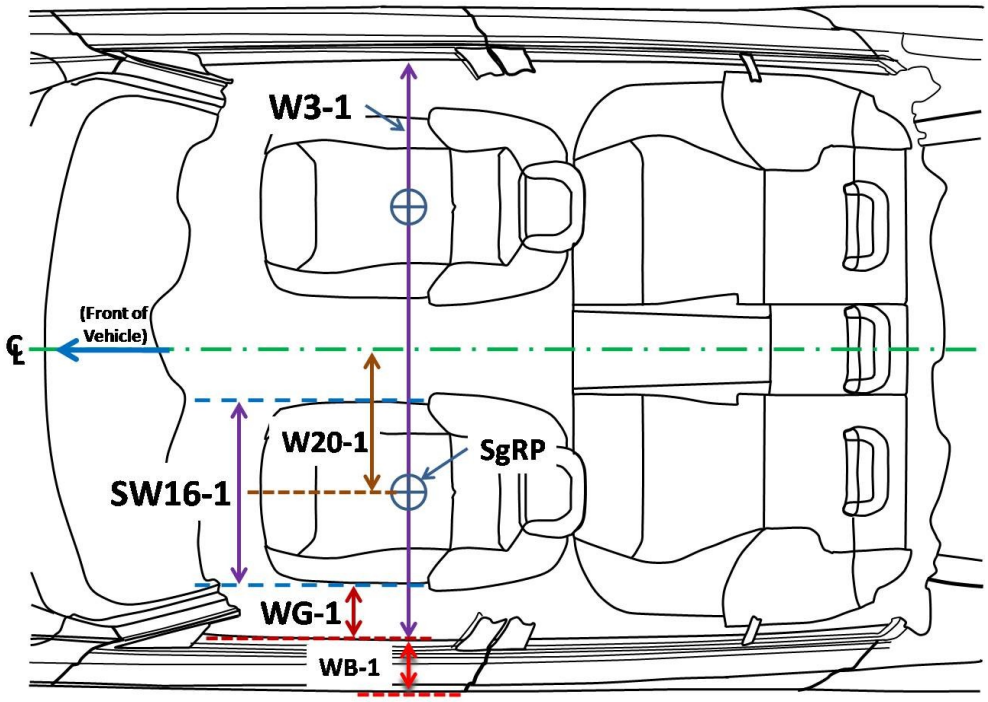

Figure 5.3: Vehicle Width Parameters [54]

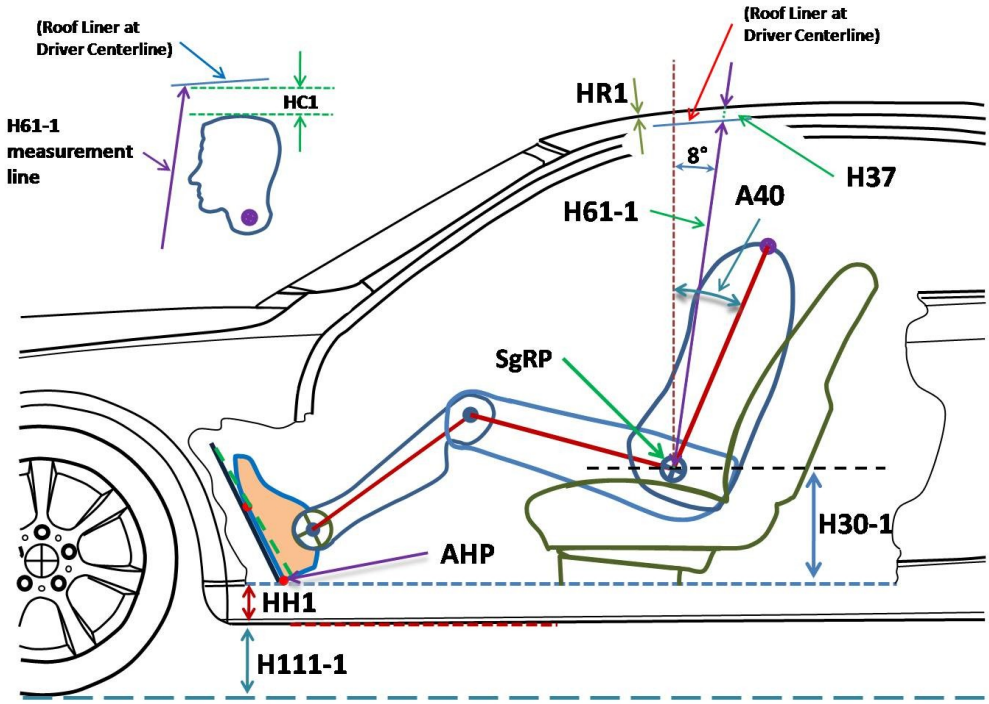

Figure 5.4: Vehicle Height Parameters [54]

A continuity of dimensional and functional parameters has also been implemented to permit an engine to be dynamically sized based on engine configuration and peak engine power for each optimization functional evaluation. Coupled with knowledge-based relations between the cylinder span shown in Figure 5.4 and overall engine length for different engine types and layouts, the engine length can be estimated with sufficient accuracy to estimate longitudinal crush space in the engine bay and other properties related to engine sizing and packaging. Engine dimensional and functional relations are discussed in Appendix C.

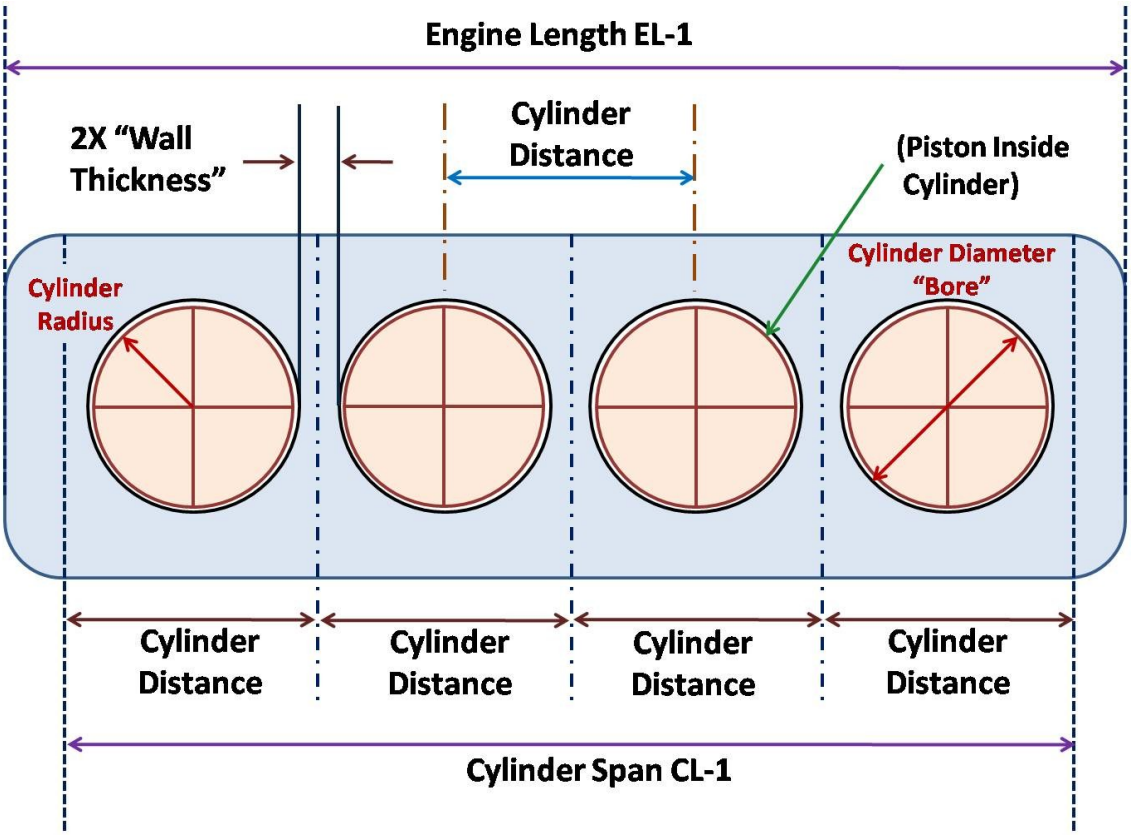

Figure 5.5: Engine Sizing [54]

Develop and Use Models and Relations which Capture Underlying Physical / Functional Principles in Place of Detailed Designs

In addition to developing a continuum of vehicle dimensional parameters, a series of models and relationships have been developed in this work for modeling and developing key aspects of the vehicle model such as frontal New Car Assessment Program (NCAP) crashworthiness, engine sizing and packaging, vehicle turn radius, wheelhouse packaging and mass estimation. An illustration of the front crashworthiness model is shown in Figure 5.6.

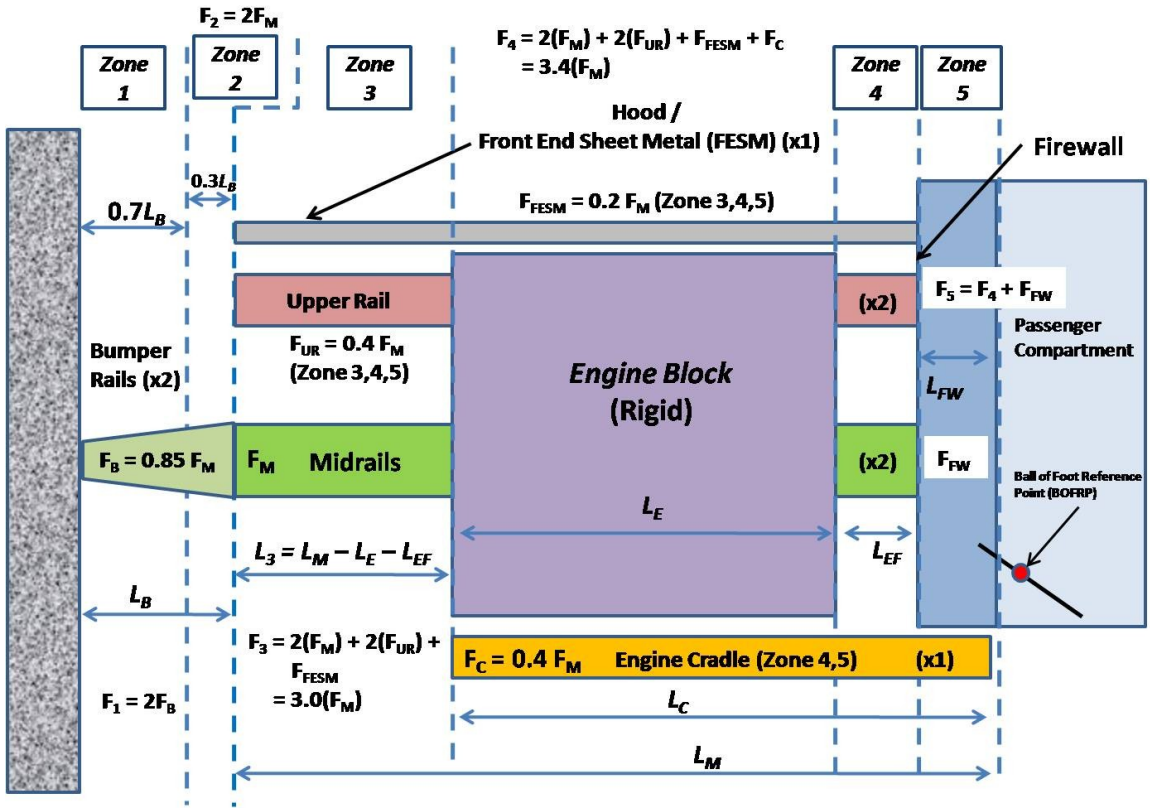

Figure 5.6: Front NCAP Structural Model[54]

Note that other structural configurations can also be modeled and used. By expressing all structural component crush forces as a fraction of the average midrail crush

force, the total forces involved in structural crush can be rapidly formulated and permits calculation of crash accelerations in each of the four crush zones shown above. The ability to add and select structural configurations is a potential for future work. This model is further discussed in Appendix D.

The different methods of expressing turn radius measurement are shown in Figure 5.7.

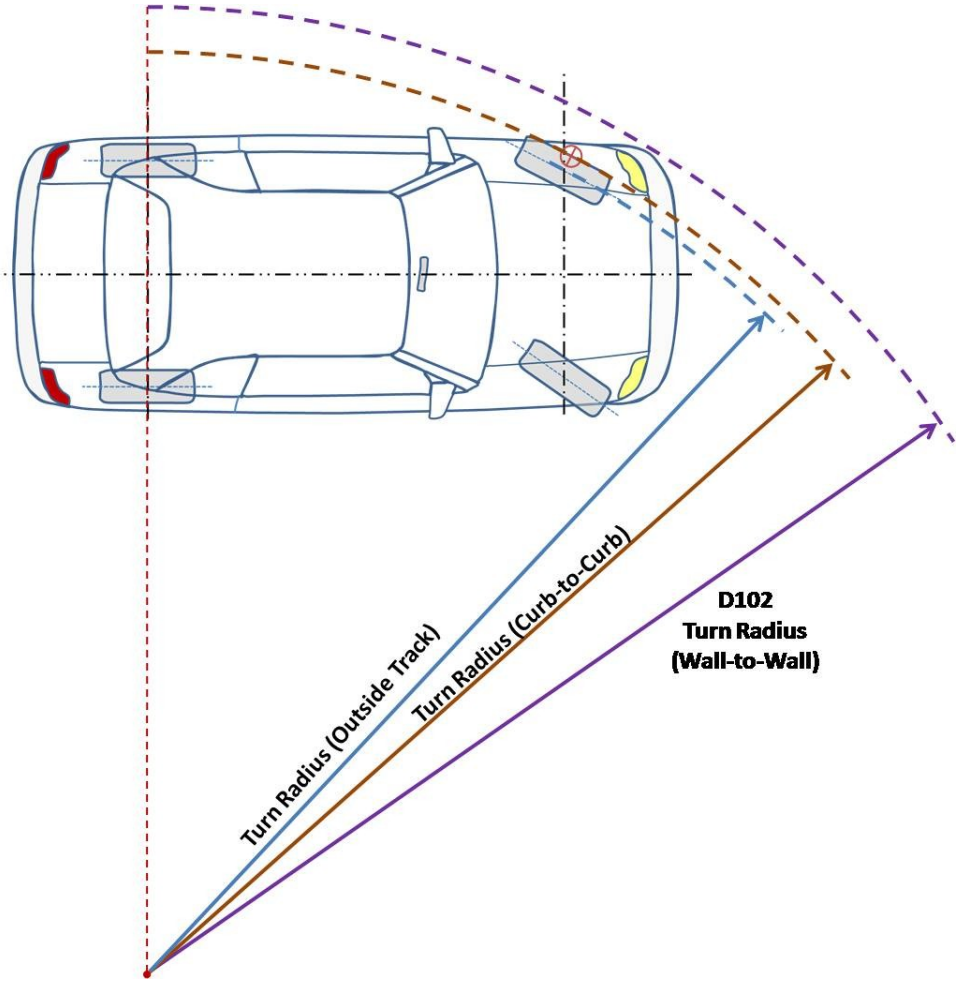

Figure 5.7 Vehicle Turn Radius[62]

Many authors such as Genta calculate turn radius by assuming an averaged value

of inside and outside steer wheel radius in calculating vehicle turn radius [63]. While this approximation may be adequate for many vehicle performance measures, this author has developed a turn radius model based on the relation between inside and outside steer wheel angles assuming Ackerman steering [54]. In addition to increasing calculation accuracy, the expanded model provides more information which can be used in establishing wheelhouse clearances and packaging. When the Outside Track turn radius is calculated, the Curb-to-Curb turn radius (a common industry measure) is found by adding one-half of the tire width (if camber angle is ignored). Wall-to-Wall turn radius, although dependent on vehicle styling, can be approximated by author-developed relationships to the Curb-to-Curb turn radius based on a body of current vehicle knowledge by vehicle size class. The turn radius model and knowledge-based relations in addition to wheelhouse packaging are detailed in Appendix E.

Accurate vehicle curb mass values are usually not available in vehicle design until detailed CAD models are created. Initial vehicle mass estimates often are based on comparison to existing vehicle designs. Parametric vehicle mass estimation tends to be highly simplified [13] or estimates a large number of subsystems at the cost of lower correlation confidence [50]. This work uses a mass estimation model with a moderate number of vehicle subsystems while retaining a reasonable level of correlation confidence for each subsystem. An example of the high level of correlation possible between parametric estimation relationships and actual vehicle curb mass values is shown in Figure 5.8. Further discussion of vehicle parametric mass estimation is found in Appendix F.

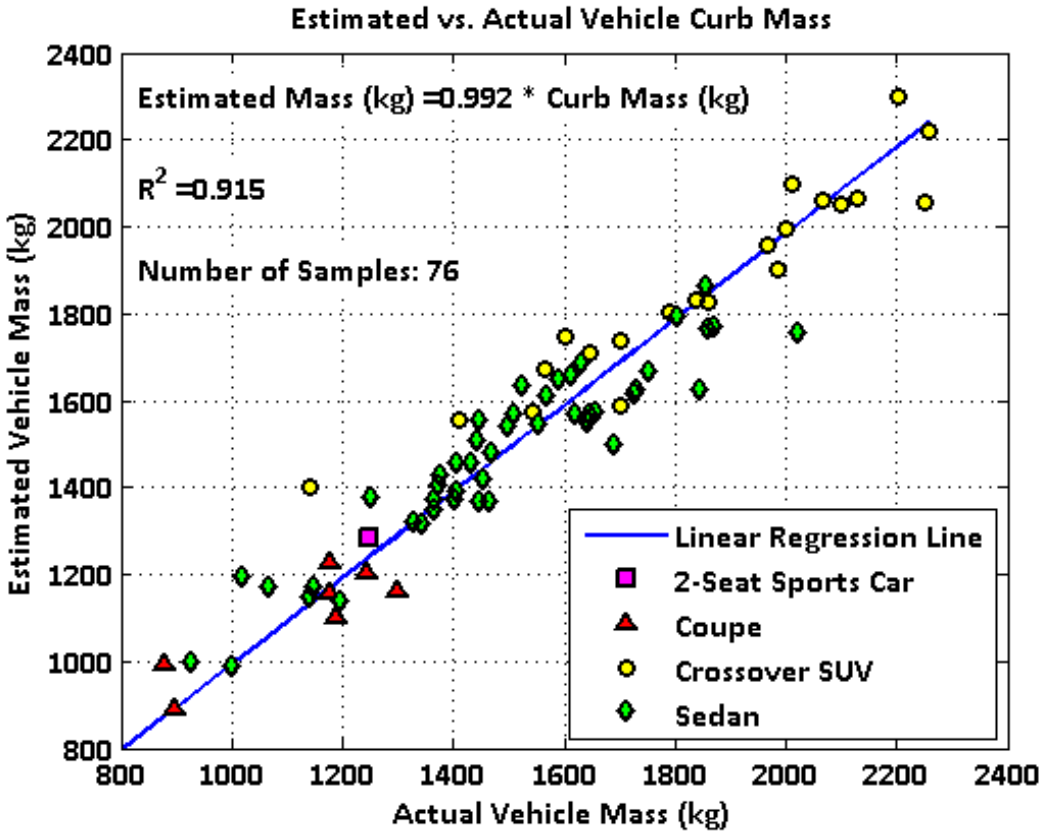

Figure 5.8 Vehicle Mass Estimation Correlation Results[54]

One key approach in developing the vehicle models used in this work is to size and lay out the vehicle starting with the vehicle occupant positioning and packaging and working progressively outward to develop consistant vehicle dimensional relationships and to eliminate the need to check for conflicts between internal and external vehicle dimensions. Examples of occupant-related dimensional parameters are shown in Figure 5.9; these are discussed in Appendix B.

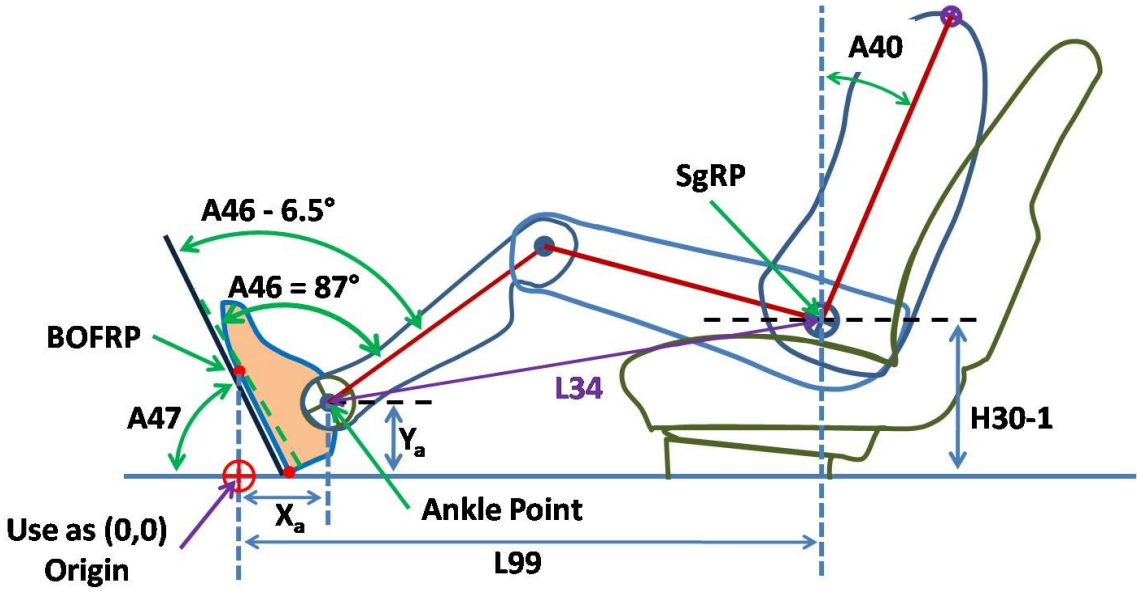

Figure 5.9 Example Occupant Parameters and Relationships[54]

Fuel economy calculations are in Appendix G along with models and calculations related to hybrid electric vehicle performance. Acceleration and braking models and equations are in Appendix H. Vehicle maximum velocity (without electronic speed limiting) is covered in Appendix I. Center of gravity location modeling is discussed in Appendix J. Vehicle constraints are addressed in Appendix K.

Gap 3 Strategy Implementation:
Need for Relevant and Consistent Starting Parameters and Relations

Use Knowledge-Based Parameters and Relationships which are Consistent and Relevant

One of the methods for improving convergence to a global optimization minimum is to begin optimization with a feasible and consistent set of starting parameter and design variable values. This should also promote more rapid convergence to a global minimum. Through a combination of automotive information sources and conducting field measurements of current vehicles, the author has developed a body of data for assorted

vehicle types and size classes. This information includes vehicle dimensional, functional and performance data which can be used to generate typical parameter and design variable values for a given vehicle type and size class. These values have the advantage of being consistent with each other in their relationships to each other. They are useful to a user of the vehicle development, analysis and optimization framework as they provide typical values to provide them with a valid and relevant starting point in the process.

These values also cover a broad variety of vehicle subsystems which a given user may not be familiar with in terms of behavior or typical parameter values. A table of useful functional parameters by engine types is shown in Figure 5.10. An enlarged view of a portion of the table is shown in Figure 5.11. Additional engine data is found in Appendix C. Note that there is no clean separation between the knowledge base and the low-order models as the models are often developed from correlations to various aspects of the knowledge base. Many of the values in the knowledge base may change with time; it will be necessary to continually update the knowledge base in order for it to be relevant for current and future automotive designs and technologies. For hybrid electric vehicles, advances in high-voltage battery materials and technology drive a need for continual updates as well.

	Gasoline													Diesel	
	Naturally Aspirated						Turbo							Turbo	
Metric	I4	I6	V-6	V-8	V-10	V-12	I2	I4	I6	V-6	V-8	V-10	V-12	I4	I6
Specific Power (kw/L Displacement)	60	60	60	60	60	60	85	85	85	75	75	75	75	65	65
Specific Torque (n-m/L Displacement)	100	100	105	105	105	105	155	155	155	135	135	135	135	180	180
Specific Weight (kg/kw)	1.0	1.0	0.7	0.7	0.7	0.7	1.0	1.0	1.0	0.8	0.8	0.8	0.8	1.1	1.1
Specific Volume (L Engine Volume/n-m)	1.19	1.3		0.95	0.9		0.59	0.78	0.89	-	0.58		0.65	0.68	0.55
Weight/Displacement (kg/L displacement)	71.31	58		50.5	48		97.1	71.7	65.1	58.3	52		66.2	74.8	65.1
Volume/Displacement (L Engine Volume/L Displacement)	116.15	126.7		95.2	93.3		104.6	125.6	119.5	-	84.6		78.8	118.3	104.18
Engine Volume / Power (L / kw)	2.13	2.15		1.23	1.25		1.463	1.388	1.58	-	1.06		1.21	1.88	1.57
Engine Length / Power (m / kw)	5.46	4.54		2.32	2.1		4.912	3.59	3.34	-	1.93		1.95	4.54	3.8
Cylinder Span / Engine Length	0.69	0.73	0.48	0.55	0.63	0.72	0.57	0.63	0.73	0.48	0.59	0.64	0.74	0.64	0.73
Engine Length - Cylinder Span (m)	0.157	0.205		0.324	0.294		0.132	0.218	0.205	-	0.275		0.212	0.206	0.206
Max Volume/ Cylinder (CC)	500	500	633 *	550	550	550	550	565	550	633 *	550	550	550	500	500
Min Volume / Cylinder (CC)	350	415	500	500	500	500	440	400	500	500	500	500	500	350	415
Max Bore (mm)	84	85	97 *	94	94	94	87	88	87	93	89	91	89	84	84
Min Bore (mm)	77	82	91	92	92	92	86	77	84	88	88	88	89	75	79
Max Stroke (mm)	90	88	86*	79	79	79	93	94	93	87	88	85	88	90	90
Min Stroke (mm)	72	78	76	75	75	75	88	81	90	83	83	83	80	80	85
Average Bore/ Stroke Ratio	1.00	1.00	1.2	1.2	1.2	1.2	0.95	0.95	0.95	1.05	1.05	1.05	1.05	0.95	0.95

Figure 5.10 Engine Parameter Table [54]

	Naturally Aspirated					
Metric	I4	I6	V-6	V-8	V-10	V-12
Specific Power (kw/L Displacement)	60	60	60	60	60	60
Specific Torque (n-m/L Displacement)	100	100	105	105	105	105
Specific Weight (kg/kw)	1.0	1.0	0.7	0.7	0.7	0.7
Specific Volume (L Engine Volume/n-m)	1.19	1.3		0.95	0.9	
Weight/Displacement (kg/L displacement)	71.31	58		50.5	48	
Volume/Displacement (L Engine Volume/L Displacement)	116.15	126.7		95.2	93.3	
Engine Volume / Power (L / kw)	2.13	2.15		1.23	1.25	
Engine Length / Power (m / kw)	5.46	4.54		2.32	2.1	
Cylinder Span / Engine Length	0.69	0.73	0.48	0.55	0.63	0.72

Figure 5.11 Enlarged View of a Portion of the Engine Parameter Table [54]

Use this Knowledge Envelope to set Valid, Coherent Constraints

In addition to providing a valid starting point for vehicle design and optimization, the knowledge base can be used to constrain initial parameters, configurators and design variables to a valid regime resulting in fully usable design and optimization outputs. The use of standard government and industry standards ensures that the resulting design configuration meets constraints imposed by EPA vehicle class size designations [73] and other common standards. EPA Fuel Economy targets were previously set as fixed values for passenger vehicles and trucks through Model Year 2011; subsequent model years are subject to targets based on the EPA footprint value for that vehicle as shown in Figure 5.12 [54, 73]. This constraint will have an impact on the final dimensional parameters selected in the design of future vehicles.

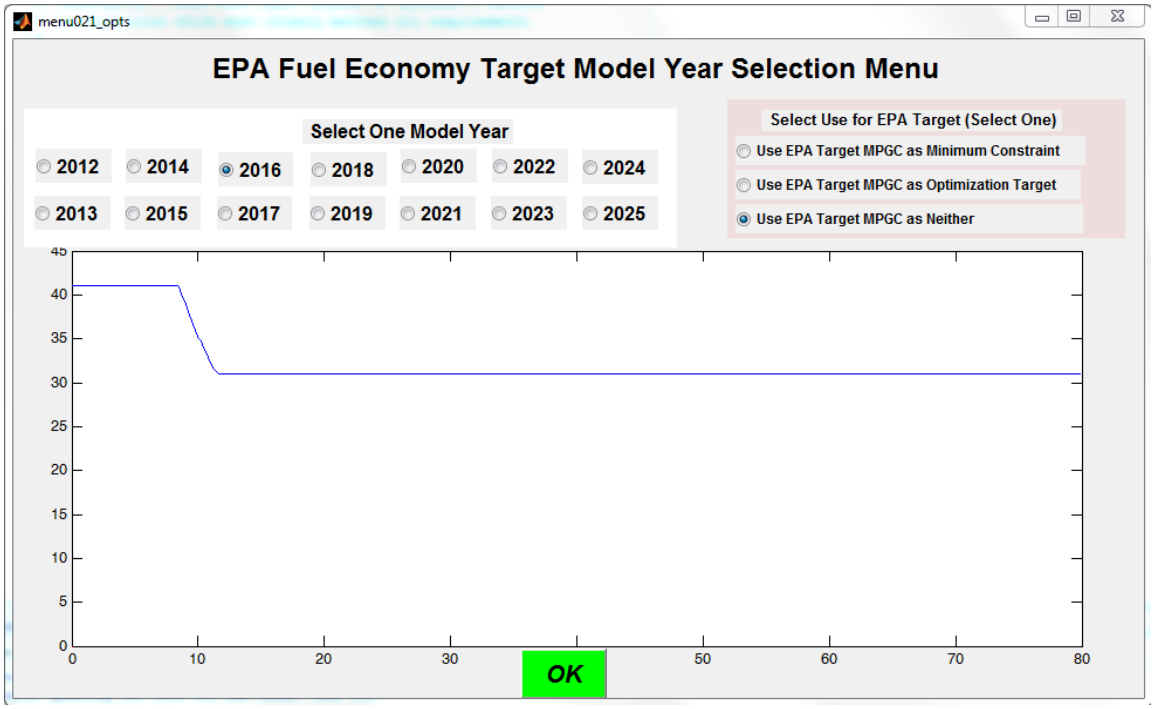

Figure 5.12 EPA Fuel Economy Target Function for Model Year 2016 (Target MPG vs. Vehicle Footprint in ft^2) [54, 73]

Implement a "Scenario Validation" Module which Can Quickly Provide a Determinate Result for a Fixed Set of Input Parameter Values

The Scenario Validation module performs a number of useful functions. It permits the user to supply a full set of specified vehicle configurators and input parameters to obtain a single determinate design with all accompanying output parameters and performance values. The Scenario Validation performs the same functional value calcualations as each iteration of the Optimization Module; this permits validation of both modules by comparing Scenario run outputs to known inputs, configurators and resultant parameters derived from benchmarking of known vehicles. The results of a series of such validation activities is discussed in Chapter 6.

Another function of the Scenario Builder is to permit the user to explore the impact of modifications to an optimized design. This will show how much the design can be modified before the benefits of a particular optimized design are lost (for example, in trying to implement two unique vehicle models on a common platform). Depending on the optimization method used, two optimized "best" solutions along a Pareto front may be different from each other in which optimization targets are most closely met. The Scenario builder can be used to assess which solution is more robust in responding to small changes in various input parameters (this can also be done using Optimization Module sensitivity and trade-off measures).

Handle the Interactions and Dependencies between Model Parameters Within the Software Framework to Reduce the Number of Parameter Values which Must be Specified or Validated by the User

A single iteration of the Optimization or Scenario Builder modules can involve the input, calculation, evaluation and output / display of approximately 200 parameters. This is obviously too large a number of parameters for a user to evaluate or manipulate using manual methods. The software framework is intended to minimize the number of input configurators, parameters and targets which the user must specify. The remainder of the parameters are handled internally through model relationships and interactions.

The necessary user inputs in the software framework are simplified and aided by visual representations of the parameter / configurator in question in input menus in conjunction with the display of typical type/size class values for that parameter. This give the user an intuitive feel for desired input values and what constitutes a realistic input value for the desired vehicle type. A sample input menu with typical input values for a large sedan is shown in Figure 5.13. The typical values shown in each input box can be accepted for use or they can modified by the user before proceeding to the next input menu.

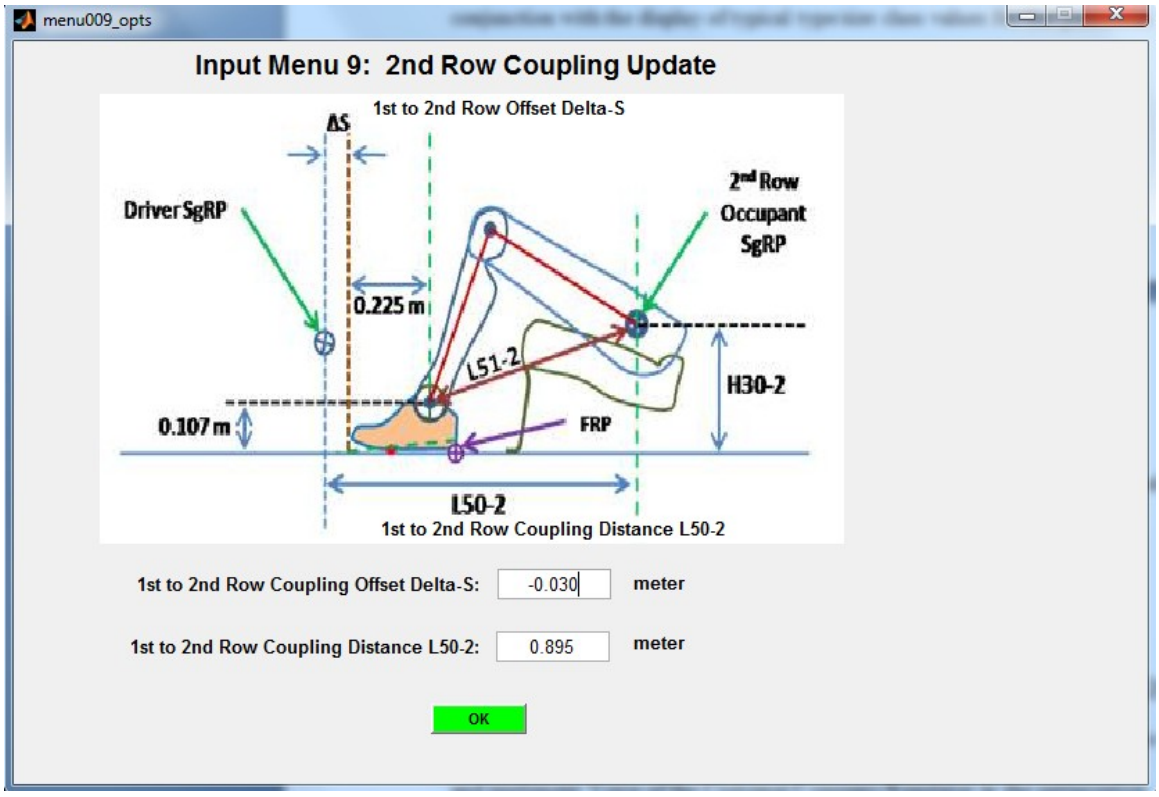

Figure 5.13 Input Menu for First to Second Row Coupling Parameters with Typical Class Values for a Large Sedan

Gap 4 Strategy Implementation:
Compromised Solution Brand Neutral (Nothing Driving Trade-Offs)

Use Visually Intuitive Brand "DNA" Inputs to Steer the Compromised Solution

One method being implemented in the Optimization Module of the software framework is the use of a visual tool to capture relative weighting of a general set of customer values or attributes. A sample of this input method is shown in Figure 5.14 based on customer survey weightings of BMW and in Figure 5.15 for weightings of Lexus perceived brand attributes scaled from the original survey to the scaling of the Brand DNA menu ratings [81].

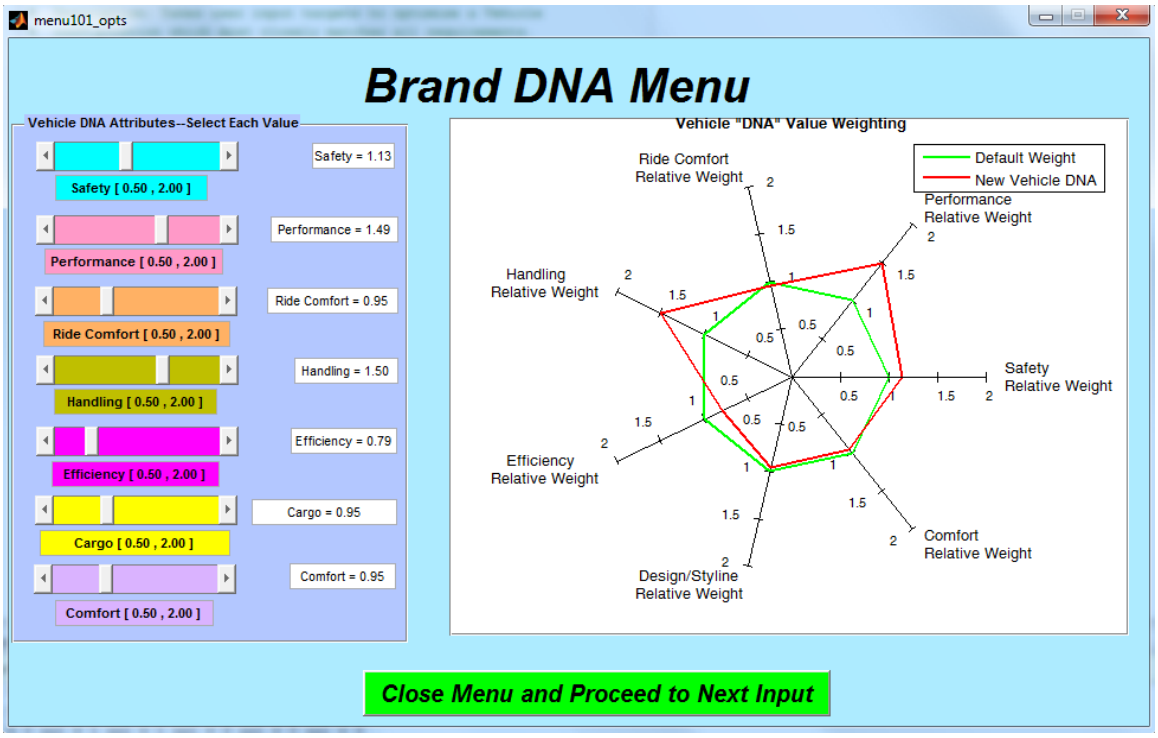

Figure 5.14 Visual Brand DNA Input Menu Representation for BMW Brand [54, 81, 82]

The weighting values are selected by moving the associated "slider" button on the menu. The spider diagram in the graph display window then immediately updates to reflect the new value. When all values are set by the User, the Green "Close Menu and..." button is pressed to move to the next input menu.

Note that the optimization effect of weighting is relative; if all factors are assigned a value of 2.00, it will have the same effect as if they all had an identical value of 1.00. As each rating factor is raised to an exponent as discussed with regard to Equation (21), the separation between DNA factors is enhanced. A rating factor of 0.5 will have an order of magnitude weighting difference compared to a rating factor of 2.0.

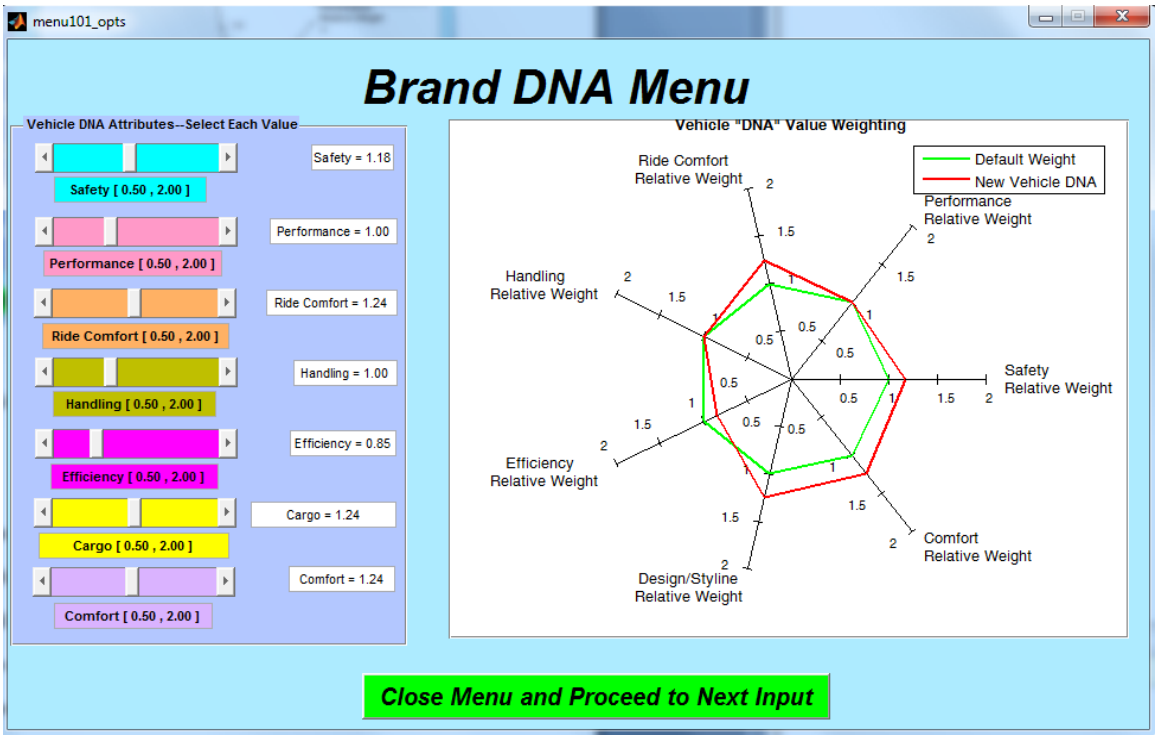

Figure 5.15 Visual Brand DNA Input Menu Representation for Lexus Brand [54, 81, 82]

Various aspects (components) of the Brand DNA inputs are linked to specific targets through the associated weighting factors. For example, the Safety attribute weighting is linked to the Frontal NCAP performance target. Zero to 60 mph acceleration time and 60 mph to zero braking distance are linked to performance,fuel economy is tied to efficiency and so on.

This menu gives a method to provide weighted preferences for higher level vehicle attributes such as safety, ride comfort and efficiency without requiring specific target values to be traded off. This "DNA Spider" gives the user an intuitive feel for what characteristics they desire most in a vehicle and what they are willing to "give up" in trade in order to obtain the most desired traits. The DNA spider provides a method for developing the weighting factors used in the optimization environment. In that role they

provide the "brand influence" on the optimization trade-offs, particularly in balancing targets which are parametrically opposed to each other. Another way to approach the attribute trade-off by vehicle branding is shown in Figure 5.16 using the previous BMW vs. Lexus brand attribute results from a 2013 AutoPacific survey with plus / minus scaling [81, 82]. A "minus" value is something given up from the industry average for a given trait to purchase a vehicle of this brand. A "plus" value is something gained above the industry average for that vehicle segment by purchasing this particular brand of vehicle.

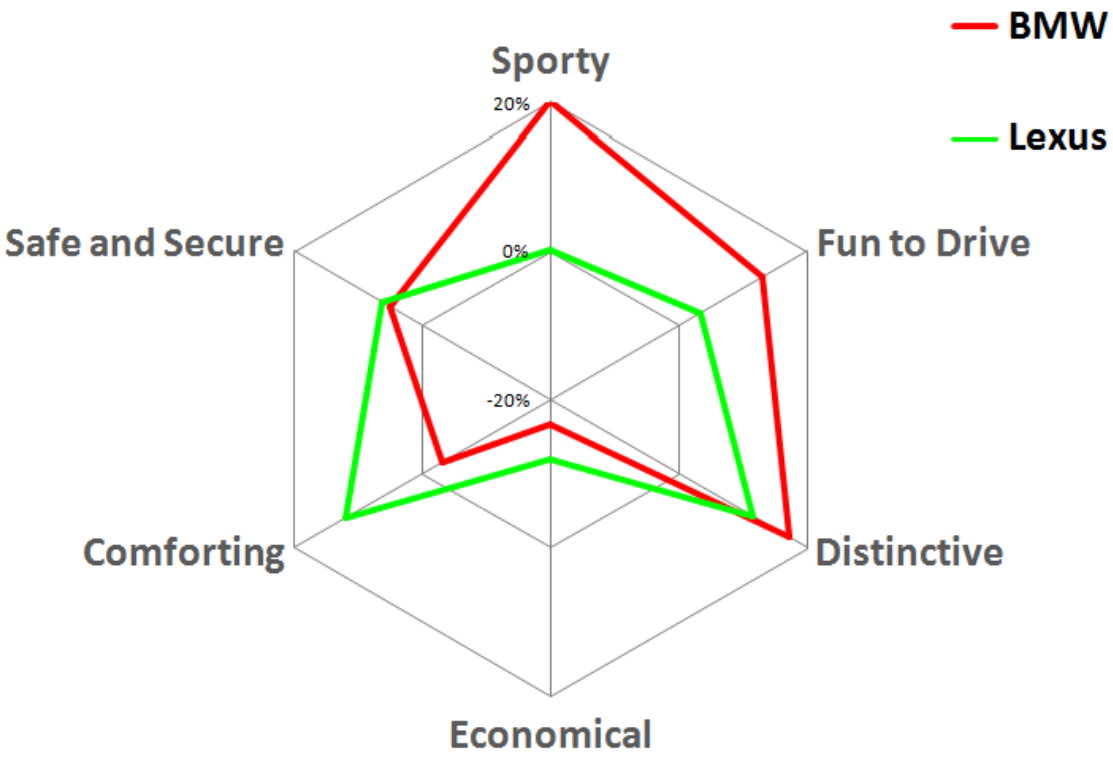

Figure 5.16 Plus / Minus Scaling of BMW and Lexus Brand DNA vs. Industry Averages [81, 82]

The brand DNA must have consistent linkage with vehicle targets and parameters

in order to provide an effectively optimized design with valid trade-offs.. If all targets can be achieved, the brand DNA weightings will have no influence in the final design variable values and resulting vehicle parameters.

It is possible to have separate Brand DNA inputs reflecting a customer's view of the Brand attribute mix and the views of an OEM or other internal entity. When used in this manner, the inputs can be combined into composite weighting factors in the optimization process as described previously. Future work may include an "OEM DNA" input menu.

Gap 5 Strategy Implementation:
Solvers not Transparent (Sensitivity / Trade-Offs)

Develop Sensitivity Analysis Tools and Displays

In understanding trade-offs between various design variables and input parameters vs. target achievement and resultant parameters such as subsystem and vehicle mass, it is important to be able to quantify these influences. The Optimization Module in the software environment incorporates both pre- and post- optimization sensitivity gradient results in tabular form for performance to target vs. design parameters, resultant parameters vs. design and input parameters, etc. These give the user a feel for what resultant quantity is being gained or lost for each unit change in the given input parameter or variable. An example of the pre-optimization sensitivity to design variables is shown in Figure 5.17 [54].

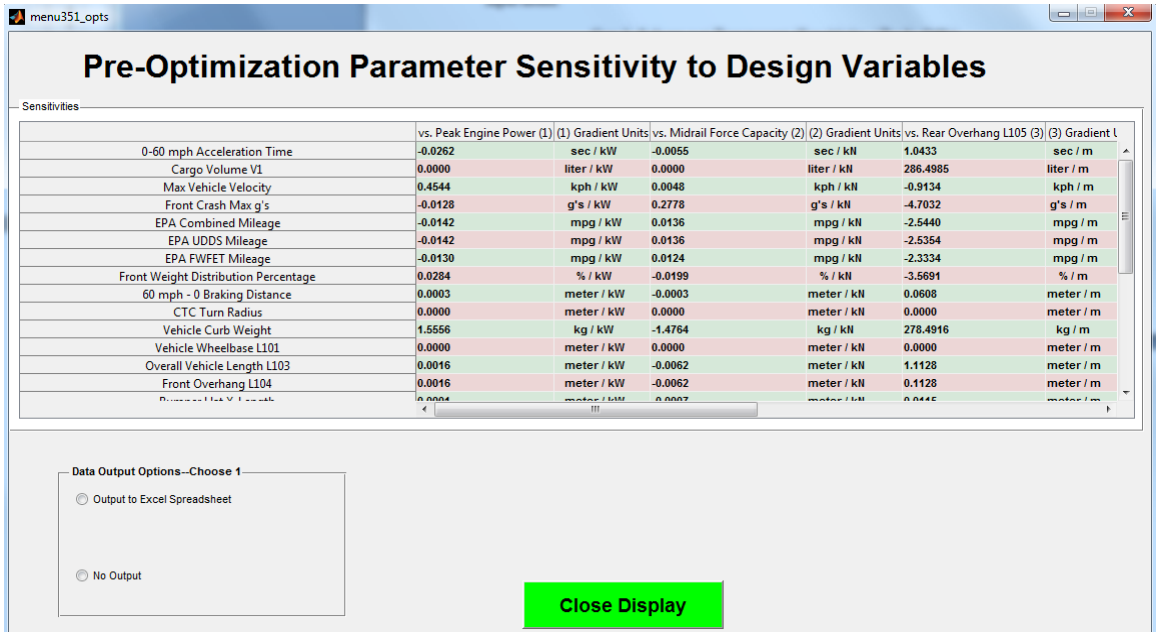

Figure 5.17 Pre-Optimization Parameter Sensitivity to Design Variables Display Menu [54]

An enlarged view of the first row is shown in Figure 5.18 (targets and parametes vs. peak engine power) [54]. This shows the gradient value (resultant parameter units vs. engine power units in kW). Some gradients may show large values if a typical parameter variation is on the order of a few millimeters or centimeters; this is magnified by orders of magnitude when meter units are used in this software.

	vs. Peak Engine Power (1)	(1) Gradient Units
0-60 mph Acceleration Time	-0.0262	sec / kW
Cargo Volume V1	0.0000	liter / kW
Max Vehicle Velocity	0.4544	kph / kW
Front Crash Max g's	-0.0128	g's / kW
EPA Combined Mileage	-0.0142	mpg / kW
EPA UDDS Mileage	-0.0142	mpg / kW
EPA FWFET Mileage	-0.0130	mpg / kW
ront Weight Distribution Percentage	0.0284	% / kW
60 mph - 0 Braking Distance	0.0003	meter / kW
CTC Turn Radius	0.0000	meter / kW
Vehicle Curb Weight	1.5556	kg / kW
Vehicle Wheelbase L101	0.0000	meter / kW
Overall Vehicle Length L103	0.0016	meter / kW
Front Overhang L104	0.0016	meter / kW

Figure 5.18 Enlarged View of Parameter Sensitivity Values and Gradient Units [54]

The sensitivity gradients are generated by performing two iterations of the Scenario Builder evaluation process. The starting value of input parameters and the design variables is used to obtain "baseline" resultant values. The inputs are then perturbed (typically by +5% or a unit amount, depending on the variable / parameter) and the new resultant values obtained. These are then compared to obtain the sensitivities scaled in gradient units). These sensitivity analysis tools and results may require some use and practice on the part of the user in order to understand their influence on design outcomes and to use them to best advantage.

Develop Trade-Off Evaluation Tools

While the generated sensitivity results represent one form of trade-off evaluation and management, the ability to trade off one target versus another is a valuable capability.

It is not possible to generate target vs. target sensitivities in the same manner as the above parameter sensitivities. The target vs. target sensitivities require a design of experiments be run using a range of design variables which generate performance to target results during optimization iterations. This requires more time than the determinate methods used to generate the other sensitivities. The design of experiments approach is best conducted in ModeFrontier using the MATLAB optimization module as the functional evaluation engine.

In assessing the overall effectiveness of the optimization framework, the ability to generate optimal trade-offs in order to satisfy all or most of the targets is to be evaluated. One of the intents of optimization is to optimize trade-offs between conflicting or opposed objective targets while satisfying all of the constraints.

CHAPTER 6

VALIDATION AND RESULTS

Scenario Builder Module Validation

Scenario Builder Inputs

The Scenario Builder module inputs generally match the inputs of the Optimization module; in the Scenario Builder module, however, inputs which are design variables in the Optimization module must be input as fixed values. Conversely, no target values (used in the Optimization module) are input in the Scenario Builder. Scenario builder inputs include:

- Body style (large sedan, etc.)
- Drive wheel type (FWD / RWD / AWD)
- Occupant seating (4 or 5 occupants)
- Body in White material (steel / aluminum)
- Closure material (steel / aluminum)
- Second row ankle angle constraint (adhere to comfort angle limits or not)
- First to second row coupling offset (ΔS)
- First to second row coupling distance L50-2
- First row cushion width SW16
- First row SgRP offset from centerline W20-1
- First row seat cushion edge to shoulder room trim point WG-1
- First row door belt width WB-1
- Front rocker height H111-1

- "Heel Height" distance HH-1
- First row seat height H30-1
- Second row seat height H30-2
- Front torso angle A40-1
- Driver head to headliner vertical clearance HC1
- Headliner thickness H37
- Accelerator shoe plane angle A47
- Engine type (inline / v-type, gasoline / diesel, naturally aspirated / turbocharged for internal combustion engine; parallel electric hybrid with internal combustion engine types)
- Internal Combustion engine power in kW (Optimization module design variable -- designated with ** for subsequent design variables)
- Maximum vehicle velocity (without electronic speed control)
- Electric motor power in kW (for hybrid electric vehicles) **
- Battery capacity in kWh (for hybrid electric vehicles) **
- Battery type (Lithium, Nickel-metal hydride)
- Tire selection (wheel / rim diameter, tire width, tire height %)
- Front wheel center to ball of foot reference point (BOFRP) L113 **
- Second row SgRP to rear wheel center L115-2 **
- Rear overhang L105 **
- Front midrail average crush force **
- Maximum inside steer wheel angle (δ_i)

- Vehicle aerodynamic drag coefficient C_d
- Vehicle maximum driveline torque
- Tire rolling resistance coefficient f_r
- Tire dry pavement friction coefficient μ
- Average (front and rear) track width W102
- Engine distance forward of BOFRP
- Engine distance forward of firewall
- Firewall average crush force
- Average firewall crush distance

While this is a large number of inputs, each scalar-value input box is initially populated with class-representative typical values for the selected vehicle type. These values are derived from the knowledge base used in developing modeling correlations and average parameter values. The default values can be accepted as-is or modified by the user as desired.

Scenario Builder Validation Using Benchmark Vehicles

A sample of six benchmark sedan vehicles of assorted size classes, engine type / layout and drive configuration (RWD and FWD) are used for comparison with outputs from the Scenario Builder module. The Scenario Builder Module uses the same functional evaluations for performance and output parameters as the Optimization Module. The results shown below thus serve as a validation of both the Scenario Builder and Optimization Module outputs. Selected results are displayed in this section; additional results are shown in Appendix L. A summary of the Scenario Builder module

input and output menus is shown in Appendix M. Results for Scenario Builder values vs. actual vehicle performance for 0 to 60 mph acceleration time are shown in Table 6.1.

Vehicle	Scenario Value (sec)	Actual Value (sec)	Difference (sec)	% Difference
BMW 328i	**6.8**	**6.9**	**-0.1**	**-1.4**
Mercedes CLS550	**4.3**	**4.3**	**0.0**	**0.0**
Mercedes E350W	**5.5**	**6.2**	**-0.7**	**-11.3**
Chrysler 300	**6.0**	**6.3**	**-0.3**	**-4.8**
Cadillac XTS	**6.0**	**6.4**	**-0.4**	**-6.3**
Ford Crown Victoria	**7.9**	**8.1**	**-0.2**	**-2.5**
Average Difference (Absolute Value for Each Vehicle)				**4**
Standard Deviation				**4.1**

Table 6.1 Scenario Builder Estimated vs. Actual 0 to 60 mph Acceleration Time (Sec)

The Scenario Builder inputs assume a tire friction coefficient (μ) of 1.0 (this may be modified by the user). This is reasonable for most tires on dry pavement [74]. The friction coefficient for a given tire brand and model is difficult to obtain; these values are not typically published for passenger car tires. Tires designed for high-performance vehicles may have a higher friction coefficient ("stickier") to achieve better acceleration times. Vehicle test mass may also vary according to the testing publication/activity providing published values for the sample vehicles.

Scenario Builder values vs. actual values for trunk cargo volume (V1) are shown in Table 6.2. The Scenario Values provide reasonable correlation for vehicles of three different size classes (large, midsize and compact). Styling differences and placement of

bulky content such as low-voltage batteries in the trunk area of the vehicle may also affect actual cargo volume.

Vehicle	Scenario Value (liter)	Actual Value (liter)	Difference (liter)	% Difference
BMW 328i	**376.7**	**339.8**	**36.9**	**10.9**
Mercedes CLS550	**448.5**	**433.3**	**15.2**	**3.5**
Mercedes E350W	**442.7**	**453.1**	**-10.4**	**-2.3**
Chrysler 300	**454.2**	**461.6**	**-7.4**	**-1.6**
Cadillac XTS	**490.6**	**509.7**	**-19.1**	**-3.7**
Ford Crown Victoria	**550.9**	**583.3**	**-32.4**	**-5.6**
Average Difference (Absolute Value for Each Vehicle)				**5**
Std. Deviation				**3.4**

Table 6.2 Scenario Builder Estimated vs. Actual Cargo Volume V1 (liters)

Scenario Builder values vs. actual vehicle braking distances are shown in Table 6.3. As with 0 to 60 mph acceleration times, the tire friction coefficient used to generate each result may have a significant effect on published results when compared with the Scenario Builder values. Some results may also include driver reaction distance in the published values; this is not currently factored into the Scenario Builder calculation.

Vehicle	Scenario Value (meter)	Actual Value (meter)	Difference (meter)	% Difference
2007 BMW 328i*	**49.3**	**49.1**	**0.2**	**0.4**
2014 Mercedes CLS550	**36.4**	**37.0**	**-0.6**	**-1.6**
2014 Mercedes CLS550*	**49.4**	**49.7**	**-0.3**	**-0.6**
2014 Mercedes E350	**36.4**	**34.4**	**2.0**	**5.8**
2014 Mercedes E350*	**49.5**	**53.0**	**-3.5**	**-6.6**
2013 Chrysler 300*	**49.3**	**53.0**	**-3.7**	**-7.0**
2013 Cadillac XTS	**36.4**	**38.7**	**-2.3**	**-5.9**
2013 Cadillac XTS*	**49.4**	**50.6**	**-1.2**	**-2.4**
2007 Ford Crown Victoria	**36.4**	**41.5**	**-5.1**	**-12.3**
2007 Ford Crown Victoria*	**49.3**	**56.1**	**-6.8**	**-12.1**
Average Difference (Absolute Value for Each Vehicle)				**6**
Standard Deviation				**4.2**

Table 6.3 Scenario Builder Estimated vs. Actual Braking Distance (meter) (*: 70 mph to 0 Braking; Others Are 60 mph to 0 Braking)

Scenario Builder values for vehicle front weight distribution vs. actual vehicle values are shown in Table 6.4. The method for determining vehicle center of gravity location and resulting front weight distributionas shown in Figure 6.1 is discussed in Appendix . Published values for a given vehicle model may vary considerably depending upon the source. Where available, data from trade publications [71, 72] are used as they often provide the test data sheet with on-scale vehicle front and rear axle mass. It may be possible to provide more accurate estimation of the front weight distribution by vehicle size class as more data becomes available to better locate typical subsystem centers of gravity.

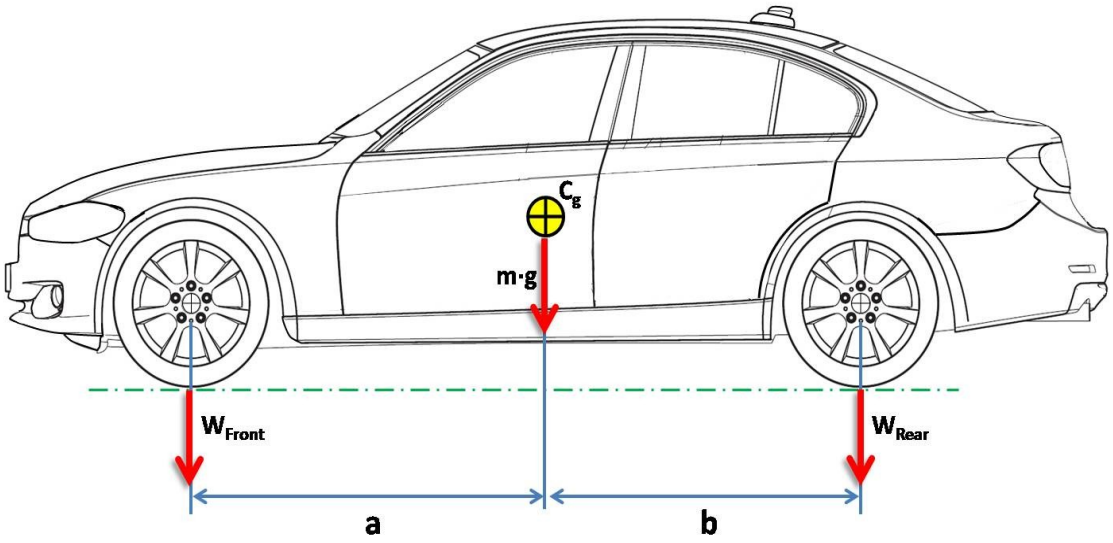

Figure 6.1 Vehicle Center of Gravity Location and Front / Rear Weight Distribution [54]

As seen in Table 6.1 and Table 6.3, the generated values for front weight distribution are sufficiently accurate to generate reasonable results for vehicle acceleration and braking measures which are dependent on vehicle front / rear weight distribution.

Vehicle Curb-to-Curb Turn Radius results are shown in Table 6.5. As the Scenario Builder input for maximum inside steer wheel angle is derived from the known vehicle turn radius value assuming Ackerman steering, the results in Table 6.5 are more of a measure of how closely a vehicle conforms to Ackerman steering assumptions. Note that many vehicles have different turn radius values for right and left turns. Some results show the smaller of the two values; others publish the average value.

Vehicle	Scenario Value (percent)	Actual Value (percent)	Difference (percent)	% Difference
2007 BMW 328i	54.0	51.1	2.9	5.7
2014 Mercedes CLS550	53.5	53.8	-0.3	-0.6
2014 Mercedes E350	52.3	52.0	0.3	0.6
2013 Chrysler 300	53.0	53.0	0.0	0.0
2013 Cadillac XTS	54.4	56.0	-1.6	-2.9
2007 Ford Crown Victoria	50.6	52.0	-1.4	-2.7
Average Difference (Absolute Value for Each Vehicle)				2
Standard Deviation				2.1

Table 6.4 Scenario Builder Estimated vs. Actual Front Weight Distribution (%)

Vehicle	Scenario Value (meter)	Actual Value (meter)	Difference (meter)	% Difference
2007 BMW 328i	5.51	5.50	0.0	0.2
2014 Mercedes CLS550	5.65	5.64	0.0	0.2
2014 Mercedes E350	5.58	5.58	0.0	0.0
2013 Chrysler 300	5.92	5.91	0.0	0.2
2013 Cadillac XTS	5.91	5.90	0.0	0.2
2007 Ford Crown Victoria	6.16	6.14	0.0	0.3
Average Difference (Absolute Value for Each Vehicle)				0.2
Standard Deviation				0.1

Table 6.5 Scenario Builder Estimated vs. Actual Curb-to-Curb Turn Radius (m)

Results for EPA combined mileage are shown in Table 6.6. A number of factors may affect the correlation of these results. Tire rolling resistance (F_r) is not readily available for most OEM-supplied tires on passenger cars. Published values for vehicle drag coefficients (C_d) vary depending on the source and determination method; they may

also be unique to a specific vehicle loading and option content. The tank-to-wheel efficiency η_{t2w} is also assumed in the software framework to be the same for similar engine and fuel configurations. All of these factors in addition to vehicle test mass will affect the values obtained versus published values. It is expected that the Scenario Builder values, reflecting "ideal" conditions, will be slightly higher than actual vehicle values. With a sufficiently large body of estimated vs. actual results, the amount of mileage over-estimation can be determined on average and compensated for.

Vehicle	Scenario Value	Actual Value	Difference (mpg)	% Difference
2007 BMW 328i	**25.4**	**24.3**	**1.1**	**4.5**
2014 Mercedes CLS550	**23.5**	**21.2**	**2.3**	**10.8**
2014 Mercedes E350	**24.9**	**24.6**	**0.3**	**1.2**
2013 Chrysler 300	**23.1**	**23.0**	**0.1**	**0.4**
2013 Cadillac XTS	**22.4**	**20.7**	**1.7**	**8.2**
2007 Ford Crown Victoria	**21.2**	**19.9**	**1.3**	**6.5**
Average Difference (Absolute Value for Each Vehicle)				**5**
Standard Deviation				**4.0**

Table 6.6 Scenario Builder Estimated vs. Actual EPA Combined Mileage (mpg)

Scenario-generated frontal NCAP time-averaged crash g's vs. vehicle NCAP performance values are shown in Table 6.7. Note that the Scenario Builder uses a numeric input (in kN) for the average front midrail crush force; this is a design variable in the Optimization Module. The frontal crashworthiness model is discussed in Appendix D. Only the NCAP acceleration values estimated for the BMW 328i sedan are above the

threshold for actual NCAP performance. While a vehicle exceeding the target threshold for 4- / 3-Star performance can be configured to meet the 4-Star rating (within limits), it will require a more extensive seating and restraints design.

Vehicle	Scenario Builder Value (g's)	Scenario Builder Rating (Stars)	Actual Vehicle NCAP Rating (Stars)	Correlated Value (Maximum) of NCAP Rating (g's)	% Difference
2007 BMW 328i	**32.1**	**2-Star**	**4-Star**	**30 ± 0.5**	**7.0**
2014 Mercedes CLS550	**21.2**	**5-Star**	**5-Star**	**25 ± 0.5**	**-15.2**
2014 Mercedes E350	**25.1**	**5*- / 4- Star**	**5-Star**	**25 ± 0.5**	**0.4**
2013 Chrysler 300	**20.2**	**5-Star**	**5-Star**	**25 ± 0.5**	**-19.2**
2013 Cadillac XTS	**22.9**	**5-Star**	**5-Star**	**25 ± 0.5**	**-8.4**
2007 Ford Crown Victoria	**20.3**	**5-Star**	**5-Star**	**25 ± 0.5**	**-18.8**
Average Difference (Absolute Value for Each Vehicle)					**12**
Standard Deviation (%)					**7.5**

Table 6.7 Scenario Builder Estimated vs. Actual Front NCAP Crash Accelerations (g's) (5-*/4-: Values on the Threshold for 5-Star / 4-Star Performance)

Estimated vs. actual curb mass for these vehicles is shown in Table 6.8. Note that published curb mass values for a vehicle model may vary significantly from the value for a specific vehicle of that model. Vehicle mass values used in EPA mileage testing may reflect all options available to that model rather than the actual vehicle makeup. Actual curb mass values in the tables above reflect a mix of published OEM values and weighings of actual vehicles for trade publication testing. Vehicle mass estimation is treated in detail in Appendix F.

Vehicle	Scenario Value (kg)	Actual Value (kg)	Difference (kg)	% Difference
2007 BMW 328i	**1510**	**1515**	**-5.0**	**-0.3**
2014 Mercedes CLS550	**1722**	**1886**	**-164.0**	**-8.7**
2014 Mercedes E350	**1644**	**1712**	**-68.0**	**-4.0**
2013 Chrysler 300	**1725**	**1887**	**-162.0**	**-8.6**
2013 Cadillac XTS	**1807**	**1817**	**-10.0**	**-0.6**
2007 Ford Crown Victoria	**1802**	**1875**	**-73.0**	**-3.9**
Average Difference (Absolute Value for Each Vehicle)				**4**
Standard Deviation				**3.7**

Table 6.8 Scenario Builder Estimated vs. Actual Vehicle Curb Mass (kg)

As shown above and in Appendix L, key vehicle attributes and performance characteristics can be accurately estimated using the Scenario Builder module. Each functional evaluation iteration of the Optimization Module optimization process uses the same process as one "session" iteration of the Scenario Builder module; this serves to validate the functional values generated in the optimization session runs. In similar fashion, the same process is used to generate comparative results in determining parameter sensitivity gradients, which are discussed later in this chapter.

Scenario Builder Module Case Study Results

The usefulness of the Scenario Builder Module is demonstrated in the following set of case studies. While the Optimization Module is used to generate an "all at once" solution optimizing all vehicle targets, the Scenario Builder can examine the impact of modifying a single parameter / configurator value -- or the effect of several modified inputs in combination. This can be used to progressively modify a vehicle design from a

known baseline configuration. It can also be used to develop a design where the knowledge base supplies typical parameter values for a vehicle type and size class which can then be adjusted by the user to give a feel for a typical range of parameter inputs and resulting vehicle behaviors. This provides the means to explore, "what if...?" scenario case studies.

The Scenario Builder module case studies which follow are progressive in nature; the results of one case study are used to guide the values and changes utilized in the next case study evaluation. This illustrates a feasibility evaluation of modifying existing vehicles to meet current and future requirements. An entirely new vehicle design configuration can be evaluated in the same manner.

Case Study 1: Light-weighting 2007 Ford Crown Victoria with Material Changes

The first case study changes the Body in White and closure materials for a larget sedan from steel to aluminum. The intent is to save vehicle weight and increase EPA combined mileage from the current value of 21.2 miles per gallon (Scenario Builder value, actual vehicle is 19.9 mpg). Two follow-up case studies look at the impact of converting it to a hybrid vehicle; initially as a hybrid with steel Body in White and closures and then the combination of hybrid and aluminum BiW / closures to show the contribution of each parameter change. Changes for Case Study 1 target achievement versus the Scenario Builder vehicle baseline values are shown in Table 6.9. The increase in EPA combined mileage is 7.5%. Vehicle curb mass is reduced 10.1% as shown in Table 6.10. NCAP frontal accelerations increase as the midrail crush force remains the same while the vehicle mass being decelerated has decreased significantly. This

indicates that the front midrails can be slightly downsized to adjust for the decreased mass. The results in this case study indicate that, in spite of the mileage gains from lightweighting, additional measures are required to achieve significantly higher EPA fuel economy targets.

Target	Case Study 1 Results	Baseline Scenario Builder Values	Units	% Difference
0 - 60 Time	7.1	7.9	Second	-10.1
V1	551	551	Liter	0.0
Max Velocity	248	247	kph	0.4
60-0 Braking	36.3	36.4	meter	-0.3
Front Weight Distribution	50.3	50.6	%	-0.6
CTC Turn Radius	6.16	6.16	meter	0.0
EPA Mileage Combined	22.8	21.2	MPG	7.5
EPA Mileage UDDS	19.8	17.0	MPG	16.5
EPA Mileage FWFET	27.8	26.4	MPG	5.3
NCAP Crash Stars	5	5	Stars	0
NCAP Crash Average G's	22.8	20.3	G's	12.3

Table 6.9 2007 Ford Crown Victoria Case Study 1 Target Achievement vs. Vehicle Baseline

These results also show some of the trade-offs which can be assessed and managed. While NCAP frontal g's increase due to the changes, they are still well within the stated criteria for the top 5-star NCAP performance. If material and process costs can be applied to each change, the trade-offs can be approached as a business decision as well as an engineering evaluation.

Parameter	Case Study 1 Results	Baseline Scenario Builder Values	Difference	Units	% Difference
M_{Curb}	1621	1802	-181	kg	-10.0
IV1	128	128	0	ft^3	0
W103	1.964	1.964	0.000	m	0
L101	2.913	2.913	0.000	m	0
L103	5.297	5.387	-0.090	m	-1.7
L104	0.934	1.024	-0.090	m	-8.8
H100	1.460	1.460	0.000	m	0
Midrail Length	1.356	1.440	-0.084	m	-5.8
M_{BiW}	274	389	-115	kg	-29.6
M_{Int}	83	83	0	kg	0
M_{Susp}	242	266	-24	kg	-9.0
M_{Drv}	122	122	0	kg	0
M_{Uncat}	697	709	-12	kg	-1.7
M_{Cls}	67	95	-28	kg	-29.5

Table 6.10 2007 Ford Crown Victoria Case Study 1 Parameters vs.Vehicle Baseline

Case Study 2: Converting Baseline 2007 Ford Crown Victoria to a Hybrid Electric Vehicle

This case study examines the effect of converting the baseline vehicle into a hybrid electric vehicle with an electric motor of 40 kW peak power and a lithium battery of 5 kiloWatt-hour (kWh) capacity. The internal combustion engine peak power is reduced to the minimum value of 161 kW for a gasoline V-type naturally aspirated engine (GVNA) available in the Scenario Builder module. All other input parameters remain the same. The primary gain of the hybrid electric vehicle conversion is the recovery of vehicle braking energy and the higher efficiency of combining an electric motor with the internal combustion engine. Some of the gains in fuel economy are offset by increased vehicle weight due to the added hybrid electric components.

Target achievement changes for Case Study 2 are shown in Table 6.11. The hybrid electric conversion results in a 31% increase in fuel economy to 27.8 combined mpg; this still does not meet the 2013 EPA fuel economy target of 28.5 mpg for a vehicle with a footprint (F101) of 4.77 m^2.

Target	Case Study 2 Results	Baseline Scenario Builder Values	Units	% Difference
0 - 60 Time	7.1	7.9	Second	-10.1
Electric 0-30 Time	8.2		Second	
V1	551	551	liter	0
Max Velocity	261	247	kph	5.7
Electric Max Velocity	146		kph	
60-0 Braking	36.4	36.4	meter	0
Front Weight Distribution	48.4	50.6	%	-4.3
CTC Turn Radius	6.16	6.16	meter	0
EPA Mileage Combined	27.8	21.2	mpg	31.1
EPA Mileage UDDS	27.8	18.3	mpg	51.9
EPA Mileage FWFET	27.8	26.4	mpg	5.3
All-Electric Range	46.2		km	
NCAP Crash Stars	5	5	Stars	0
NCAP Crash Average G's	19.1	20.3	G's	-5.9

Table 6.11 2007 Ford Crown Victoria Case Study 2 Target Achievement vs. Vehicle Baseline

All-electric range shown in Table 6.11 is computed using the EPA fuel economy UDDS cycle to simulate urban driving requirements. The UDDS cycle has a known

distance travelled and energy requirement per UDDS cycle for the given vehicle parameters. The vehicle all-electric range is then the battery capacity (converted from kWh to joules) multiplied by the UDDS cycle distance and divided by the UDDS cycle energy.

Due to the already large vehicle footprint, increasing vehicle footprint to reduce the target value is ineffective. Increasing vehicle footprint, however, can be an effective strategy in meeting EPA fuel economy targets for compact and midsize passenger cars, depending on the model year (this is explored in Case Studies 4 through 6). Parameters of interest for Case Study 2 are shown in Table 6.12.

The decrease (improvement) in 0 to 60 mph acceleration time is due to the minimum value of 161 kW for V-type engines available in the Scenario Builder module vs. 172 kW for the baseline vehicle internal combustion engine. With a 40 kW traction motor, this results in a net gain of 29 kW in traction power. Maximum vehicle velocity also increases for the same reason. This shows that engine sizing is not necessarily a continuous process. There is a net decrease in the internal engine combustion mass as engine power is decreased. If an inline engine is used in place of the V-type internal combustion engine, more mass can be removed while maintaining the original vehicle traction power of 172 kW. Conversely, engine bay length (and front overhang L104) may increase or decrease depending on the length of a new engine configuration.

Parameter	Case Study 2 Results	Baseline Scenario Builder Values	Difference	Units	% Difference
MCurb	**1894**	**1802**	**92**	**kg**	**5.1**
IV1	**128**	**128**	**0**	**ft^3**	**0**
W103	**1.964**	**1.964**	**0**	**m**	**0**
L101	**2.913**	**2.913**	**0**	**m**	**0**
L103	**5.424**	**5.387**	**0.037**	**m**	**0.7**
L104	**1.061**	**1.024**	**0.037**	**m**	**3.6**
H100	**1.460**	**1.460**	**0**	**m**	**0**
Midrail Length	**1.473**	**1.440**	**0.033**	**m**	**2.3**
M_{BiW}	**392**	**389**	**3**	**kg**	**0.8**
M_{Int}	**83**	**83**	**0**	**kg**	**0**
M_{Susp}	**280**	**266**	**14**	**kg**	**5.3**
M_{Drv}	**122**	**122**	**0**	**kg**	**0**
M_{Uncat}	**714**	**709**	**5**	**kg**	**0.7**
M_{Cls}	**96**	**95**	**1**	**kg**	**1.1**
M_{Engine}	**129**	**138**	**-9**	**kg**	**-6.5**
M_{Trans}	**58**	**58**	**0**	**kg**	**0**
M_{Motor}	**30**	**0**	**30**	**kg**	
$M_{Battery}$	**49**	**0**	**49**	**kg**	

Table 6.12 2007 Ford Crown Victoria Case Study 2 Parameters vs.Vehicle Baseline

Curb mass in Case Study 2 is increased due to several factors: addition of an electric motor and battery, increased midrail and bumper rail length and resulting increased front overhang L104. Body in White and uncategorized mass increase due to the increased front overhang as well. Suspension mass also increases due to the overall added sprung vehicle mass. Occupant-based parameters are all unchanged in this case study.

Case Study 3: 2007 Crown Victoria with Material Change, Hybrid Conversion, Improved Rolling Resistance and Improved Drag Coefficient

This case study combines the changes made in Case Studies 1 and 2 along with improved rolling resistance (F_r) and aerodynamic drag coefficient (C_d). The rolling resistance coefficient is improved (decreased) by 25% for a value of 0.0070 which is close to the best current value for commercially available tires. The aerodynamic resistance is decreased from 0.34 to 0.32. A greater decrease in drag coefficient most likely requires a complete re-styling effort. The impact of these combined changes on vehicle target achievement is shown in Table 6.13.

Target	Case Study 3 Results	Baseline Scenario Builder Values	Units	% Difference
0 - 60 Time	6.4	7.9	Second	-19.0
Electric 0-30 Time	7.5		Second	
V1	551	551	liter	0.0
Max Velocity	266	247	kph	7.7
Electric Max Velocity	150		kph	
60-0 Braking	36.4	36.4	meter	0.0
Front Weight Distribution	48.2	50.6	%	-4.7
CTC Turn Radius	6.16	6.16	meter	0.0
EPA Mileage Combined	33.8	21.2	mpg	59.4
EPA Mileage UDDS	34.3	18.3	mpg	87.4
EPA Mileage FWFET	33.1	26.4	mpg	25.4
Electric Range	49.1		km	
NCAP Crash Stars	5	5	Stars	0.0
NCAP Crash Average G's	21.4	20.3	G's	5.4

Table 6.13 2007 Ford Crown Victoria Case Study 3 Target Achievement vs. Vehicle Baseline

These changes provide a 59% increase in combined mileage; acceleration

time is also improved due to a net reduction in vehicle mass as shown in Table 6.14. Front weight distribution is reduced due to the battery mass (located over the rear axle) and mass shifts due to a lighter Body in White and closures. With the same midrail force capacity, NCAP crash g's increase but are still in the 5-star target range.

Note that with all of these changes (many of which are drastic revisions), the vehicle can only meet EPA passenger vehicle fuel economy targets through the 2016 model year (30.96 mpg for this vehicle footprint of 4.77 m^2 / 51.34 ft^2). The 2017 fuel economy target of 35.4 mpg for this vehicle footprint is difficult to achieve as most significant parameter changes which are available to improve vehicle EPA fuel economy have been explored in these three case studies.

An additional possible configuration change is to switch to front wheel drive; while this typically decreases vehicle weight, it also potentially degrades some performance qualities such as 0 to 60 mph acceleration time. Such a change limits the vehicle's usefulness in law enforcement applications, which comprise a large portion of the vehicle's sales. Ford Crown Victoria production was discontinued in 2011; from 2008 onward it was only offered for corporate fleet or police sales. The requirement for all vehicles to have stability control systems (ESC) by 2011 along with fuel economy requirements previously discussed were factors in discontinuing the vehicle [78].

Parameter	Case Study 3 Results	Baseline Scenario Builder Values	Difference	Units	% Difference
MCurb	1710	1802	-92	kg	-5.1
IV1	128	128	0	ft^3	0.0
W103	1.964	1.964	0.000	m	0.0
L101	2.913	2.913	0.000	m	0.0
L103	5.329	5.387	-0.058	m	-1.1
L104	0.966	1.024	-0.058	m	-5.7
H100	1.460	1.460	0.000	m	0.0
Midrail Length	1.385	1.440	-0.055	m	-3.8
M_{BiW}	275	389	-114	kg	-29.3
M_{Int}	83	83	0	kg	0.0
M_{Susp}	254	266	-12	kg	-4.5
M_{Drv}	122	122	0	kg	0.0
M_{Uncat}	702	709	-7	kg	-1.0
M_{Cls}	67	95	-28	kg	-29.5
M_{Engine}	129	138	-9	kg	-6.5
M_{Trans}	58	58	0	kg	0.0
M_{Motor}	30	0	30	kg	
$M_{Battery}$	49	0	49	kg	

Table 6.14 2007 Ford Crown Victoria Case Study 3 Parameters vs.Vehicle Baseline

Case Study 4: Lightweighting 2007 BMW 328i Sedan for Fuel Economy

For a vehicle with a footprint F101 of the 2007 BMW 328i (4.164 m^2 / 44.82 ft^2), the 2013 EPA fuel economy target is 28.5 mpg. The current EPA mileage for the 328i is 25.3 mpg as determined in the Scenario Builder module (24.3 actual). With the 2013 fuel economy target coefficients, increasing vehicle footprint will not improve the vehicle target as it is at the "floor" value (coefficient "b" in the EPA calculation). The next step is to change the Body in White and closure materials from steel to aluminum to meet the

2013 target. All other parameters are kept the same as the baseline vehicle in the Scenario builder module. The target achievement results are shown in Table 6.15.

Parameter	Case Study 4 Results	Baseline Scenario Builder Vehicle Values	Units	% Difference
0 - 60 mph Acceration Time	6.2	6.8	Second	-8.8
Cargo Volume V1	377	377	Liter	0
Maximum Vehicle Velocity	267	266	kph	0.4
60 mph -0 Braking Distance	36.3	36.4	meter	-0.3
70 mph - 0 Braking Distance	49.3	49.3	meter	0
Front Weight Distribution	54.1	54.0	%	0.2
CTC Turn Radius	5.51	5.51	Meter	0
EPA Mileage Combined	27.0	25.4	MPG	6.3
EPA Mileage UDDS	23.3	21.8	MPG	6.9
EPA Mileage FWFET	33.4	32.0	MPG	4.4
NCAP Crash Rating	2	2	Stars	0
NCAP Crash Average G's	35.5	32.1	G's	10.6

Table 6.15 2007 BMW 328i Sedan Case Study 4 Target Achievement vs. Vehicle Baseline

Even with a mass reduction from the material change, the vehicle still does not meet the 2013 fuel economy target. Additionally, the vehicle NCAP crash accelerations increase 11%, requiring a change in the vehicle front structure design to recover the actual vehicle 4-Star performance. Acceleration time improves (decreases due to the mass reduction of 8%.

The switch to aluminum Body in White and closure materials reduces vehicle curb mass by 123 kg as shown in Table 6.16.

Parameter	Case Study 4 Results	Baseline Scenario Builder Values	Difference	Units	% Difference
M_{Curb}	1387	1510	-123	kg	-8.1
M_{Engine}	169	169	0	kg	0
$M_{Transmission}$	62	62	0	kg	0
IV1	107	107	0	ft^3	0
PV	93.7	93.7	0	ft^3	0
PV1	52.1	52.1	0	ft^3	0
PV2	41.6	41.6	0	ft^3	0
L34	1.063	1.063	0	m	0
L51-2	0.878	0.878	0	m	0
W3-1	1.409	1.409	0	m	0
W3-2	1.391	1.391	0	m	0
H61-1	0.985	0.985	0	m	0
H61-2	0.965	0.965	0	m	0
W101	1.508	1.508	0	m	0
W103	1.817	1.817	0	m	0
L101	2.761	2.761	0	m	0
L103	4.518	4.566	-0.048	m	-1.1
L104	0.746	0.795	-0.049	m	-6.2
H100	1.417	1.417	0	m	0
Peak Engine Torque	281	281	0	Nm	0
Engine Length	0.752	0.752	0	m	0
Midrail Length	1.190	1.235	0	m	-3.6
Mbiw	210	296	-86	kg	-29.1
Mint	70	70	0	kg	0
Msusp	207	226	-19	kg	-8.4
Mdrv	127	127	0	kg	0
Muncat	534	540	-6	kg	-1.1
Mcls	57	82	-25	kg	-30.5

Table 6.16 2007 BMW 328i Sedan Case Study 4 Parameters vs.Vehicle Baseline

There are also savings in the suspension mass due to lower vehicle sprung mass. Most other parameters do not change significantly. As these changes do not meet 2013 fuel economy targets, drastic changes such as converting to a hybrid drivetrain are required to meet more stringent future targets. This is examined in Case Study 5.

Case Study 5: Conversion of 2007 BMW 328i Sedan to Parallel Hybrid

This study examines the impact of implementing a parallel hybrid powertrain in the 2007 328i sedan (with Aluminum BiW and Closures) to meet current and future fuel economy targets. A battery of 2 kWh capacity and a motor of 30 kW peak power is used; the internal combustion engine power is reduced by the same 30 kW amount. The impact of this change on vehicle target achievement is shown in Table 6.17.

The EPA combined mileage for this configuration meets the 2013 fuel economy target. NCAP crash g's still require front structure modifications to meet the original 4-Star baseline vehicle performance. Front weight distribution improves slightly.

Additional parameters are shown in Table 6.18. Net curb mass is decreased from the baseline vehicle due to the material changes. The added motor mass is offset by the corresponding decrease in the internal combustion mass; the battery mass results in a net curb mass increase from Case Study 4. Decreased engine length also helps offset increased midrail length. Occupant-related parameters remain unchanged.

Parameter	Case Study 5 Results	Baseline Scenario Builder Values	Units	% Difference
0 - 60 mph AccelerationTime	6.1	6.8	second	-10.3
All-Electric 0-30 mph Acceleration Time	8.3		second	
Cargo Volume V1	377	377	liter	0
Maximum Velocity	271	266	kph	1.9
All-Electric Maximum Velocity	143.2		kph	
60 mph - 0 Braking Distance	36.3	36.4	meter	-0.3
Front Weight Distribution	52.8	54.0	%	-2.2
CTC Turn Radius	5.51	5.51	meter	0
EPA Mileage Combined	36.0	25.4	mpg	41.7
EPA Mileage UDDS	36.1	21.8	mpg	65.6
EPA Mileage FWFET	35.8	32.0	mpg	11.9
All-Electric Range	23.0		km	
NCAP Crash Rating	2	2	Stars	0
NCAP Crash Average G's	34.5	32.1	G's	7.5

Table 6.17 2007 BMW 328i Sedan Case Study 5 Target Achievement vs. Vehicle Baseline

Although the configuration in Case Study 5 meets 2013 fuel economy targets, the vehicle will not meet the 2017 EPA fuel economy target of 40.17 mpg for this vehicle footprint. Due to the model year 2017 footprint-related coefficients ("c" and "d" in the calculation), increasing the vehicle footprint may help in meeting future targets. This is explored in Case Study 6.

Parameter	Case Study 5 Results	Baseline Scenario Builder Values	Difference	Units	% Difference
M_{Curb}	1394	1510	-116	kg	-7.7
M_{Engine}	147	169	-22	kg	-13.2
$M_{Transmission}$	62	62	0	kg	0.0
Total Internal Volume IV1	107	107	0	ft^3	0.0
W101	1.508	1.508	0.000	meter	0.0
W103	1.817	1.817	0.000	meter	0.0
L101	2.761	2.761	0.000	meter	0.0
L103	4.497	4.566	-0.069	meter	-1.5
L104	0.824	0.795	0.029	meter	3.6
H100	1.417	1.417	0.000	meter	0.0
Peak Engine Torque	245.0	281.0	-36.0	Nm	-12.8
Engine Length	0.720	0.752	-0.032	meter	-4.3
Midrail Length	1.168	1.235	-0.067	meter	-5.4
M_{BiW}	210	296	-86	kg	-29.1
M_{Int}	70	70	0	kg	0.0
M_{Susp}	210	226	-16	kg	-7.1
M_{Drv}	127	127	0	kg	0.0
M_{Uncat}	531	540	-9	kg	-1.7
M_{Cls}	57	82	-25	kg	-30.5
M_{Motor}	23			kg	
$M_{Battery}$	20			kg	

Table 6.18 2007 BMW 328i Sedan Case Study 5 Parameters vs.Vehicle Baseline

Case Study 6: Modifications from Case Study 5 with Increased Vehicle Footprint

This case study explores the usefulness of increasing vehicle footprint F101 to meet future EPA fuel economy targets. Without modifying vehicle body width, the vehicle track width can be increased 0.104 meters with the existing tires (P 205/55 R16).

To increase vehicle wheelbase, the value of L115-2 (second row SgRP to rear

wheel center) is increased 0.100 meters and L113 (front wheel center to Ball of Foot Reference Point) is increased by 0.050 meters. Rear overhang is reduced 0.100 meters to compensate for the increase in L115-2. If the combined mileage does not at least equal the Case Study 5 value of 36.0 mph, it will not meet the 2017 target of 36.0 mpg for the new value of F101. To compensate, the rolling resistance is decreased to 0.0070 as in Case Study 3 for the Ford Crown Victoria. Drag coefficient is kept the same. All other parameters are the same is in Case Study 5. The performance to targets is shown in Table 6.19.

With the use of decreased rolling resistance, a combined mileage of 40.0 mpg is achieved, which meets the 2017 fuel economy target of 36.0 mpg for the new vehicle footprint F101. Note that, even with the above changes for improved fuel economy, the vehicle does not meet the 2017 target of 40.2 mpg if the original vehicle footprint value is maintained as in Case Study 5. With the vehicle footprint used in Case Study 6, the vehicle meets EPA fuel economy targets through model year 2019 (38.6 mpg) and narrowly misses the target for 2020 of 40.2 mpg. At that time additional changes are required to meet the targets.

Note that one consequence of the above changes to meet fuel economy targets is an increase in vehicle turn radius. Coupled with the increased front weight distribution, this may impact the handling performance expected of a sporty luxury vehicle. Note that a minimally-sized electric motor is used in Case Studies 2, 3, 5 and 6 to have the least impact on other vehicle parameters. This results in slow 0 to 30 mph all-electric acceleration times. Using a higher motor peak power may result in a much smaller

internal combustion engine which may further reduce front overhang (L104) and change front weight distribution as well.

Parameter	Case Study 6 Results	Baseline Scenario Builder Values	Units	% Difference
0 - 60 mph AccelerationTime	6.1	6.8	Second	-10.3
All-Electric 0-30 mph Acceleration Time	8.3		Second	
Cargo Volume V1	377	377	Liter	0
Maximum Velocity	271	266	kph	1.9
All-Electric Maximum Velocity	143		kph	
60 mph - 0 Braking Distance	36.4	36.4	meter	0
Front Weight Distribution	53.8	54.0	%	-0.4
CTC Turn Radius	5.82	5.51	meter	5.6
EPA Mileage Combined	40.0	25.4	MPG	57.5
EPA Mileage UDDS	40.6	21.8	MPG	86.2
EPA Mileage FWFET	39.2	32.0	MPG	22.5
All-Electric Range	23.0		km	
NCAP Crash Rating	2	2	Stars	0
NCAP Crash Average G's	34.0	32.1	G's	5.9

Table 6.19 2007 BMW 328i Sedan Case Study 6 Target Achievement vs. Vehicle Baseline

Note that the cargo volume (V1) remains unchanged; it is a function of the sum of L115-2 and rear overhang L105 which remains the same since the amount of increase in L115-2 is subtracted from L105. The front overhang L104 is shortened by the distance that L113 is increased in addition to the decrease in midrail and bumper rail length due to the lighter vehicle mass compared to the baseline Scenario Builder value.

The resultant peak engine power is greater than the specified input value. This is normally due to the engine model adding or removing cylinders to meet the specified peak power for that engine type. This results in discontinuous "jumps" or increases / decreases in engine power to match engine power maximum / minimum ranges for a given number of cylinders.

Parameter	Case Study 6 Results	Baseline Scenario Builder Values	Difference	Units	% Difference
M_{Curb}	1403	1510	-107	kg	-7.1
M_{Engine}	147	169	-22	kg	-13.2
$M_{Transmission}$	62	62	0	kg	0
Total Internal Volume IV1	107	107	0	ft^3	0
W102	1.612	1.508	0.104	meter	6.9
W103	1.817	1.817	0.000	meter	0
L101	2.911	2.761	0.150	meter	5.4
L103	4.503	4.566	-0.063	meter	-1.4
L104	0.681	0.795	-0.114	meter	-14.3
H100	1.417	1.417	0.000	meter	0
Peak Engine Torque	245.0	281.0	-36.0	Nm	-12.8
Engine Length	0.720	0.752	-0.032	meter	-4.3
Midrail Length	1.174	1.235	-0.061	meter	-4.9
M_{BiW}	209	296	-87	kg	-29.4
M_{Int}	74	70	4	kg	5.7
M_{Susp}	212	226	-14	kg	-6.2
M_{Drv}	127	127	0	kg	0
M_{Uncat}	532	540	-8	kg	-1.5
M_{Cls}	59	82	-23	kg	-28.0
M_{Motor}	23		23	kg	
$M_{Battery}$	20		20	kg	

Table 6.20 2007 BMW 328i Sedan Case Study 6 Parameters vs. Vehicle Baseline

Summary of Scenario Builder Module Case Studies

The Scenario Builder Module is useful for conducting vehicle design and modification studies which cover a narrower scope than that of an all-at-once vehicle design optimization activity. It may also be useful to explore limited modifications to a vehicle configuration obtained from an Optimization Module study.

Another use is to explore the feasibility of deriving additional vehicle models based on a commonized platform with a specified set of fixed parameters / configurators. This makes the Scenario Builder module a useful and flexible feature of the vehicle design and optimization framework which can be used to supplement other modules in the framework. The progressive changes and their results in the series of Case Studies also shows the gradient nature of many parameter and configurator changes. The use of parameter sensitivity gradients in assesssing design and optimization trade-offs is explored in the following section of this chapter.

Parameter Sensitivity Gradients

Parameter sensitivity gradients (with the exception of Target vs. Target sensitivities) are calculated as part of the Optimization module within the software framework. Pre-optimization overall vehicle parameters are calculated to populate the information presented in the engine selection menu; these are used in calculating the pre-optimization sensitivity gradients. The optimized vehicle parameter values are used in calculating the final sensitivity gradients.

The gradients are calculated for each parameter by changing a given parameter or design variable by a fixed amount (either by +5% or by a fixed value, such as 1 kN for

midrail crush force). The change in each output parameter between the baseline and "perturbed" second run is then divided by the change in the "perturbed" input parameter being assessed. This gives a reasonable approximate value for a large quantity of sensitivity gradients which are often difficult (if possible) to derive mathematically.

Optimization module input and output menus, including pre- and post-optimization sensitivity gradients, are shown in Appendix N. Due to the quantity of sensitivity gradients calculated in the Optimization module, only selected gradient results are shown in this section. Additional gradient results are shown in Appendix O.

Pre- vs. Post-Optimization Gradient Sensitivities

A sample gradient sensitivity results menu (pre-optimization) is shown in Figure 6.2. There are four pre- and four post-optimization gradient displays of vehicle target and selected parameter sensitivities vs. design variables, width, longitudinal / miscellaneous and height parameters. These gradients help the user to determine the trade-offs in changing vehicle input parameters and the effect of each design parameter on the desired vehicle design. These gradients also help to identify candidates for adding additional optimization design variables.

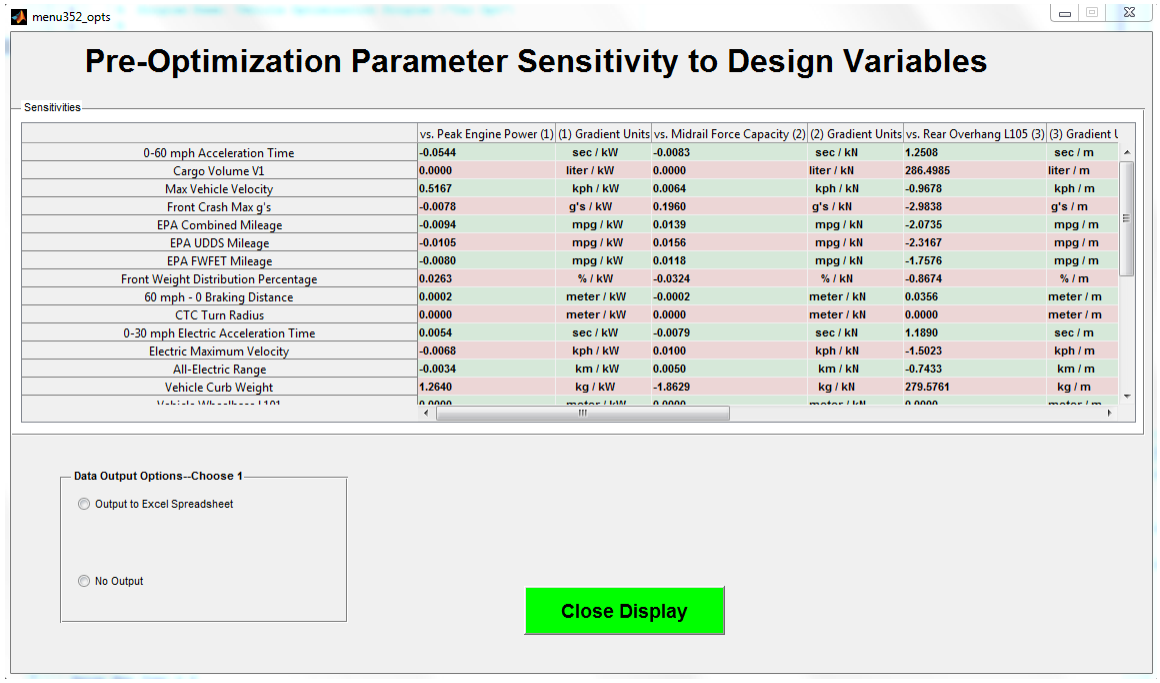

Figure 6.2 Pre-Optimization Parameter Sensitivity Gradient Results Menu

The results for both pre- and post-optimization sensitivity gradients vs. peak engine power are shown in Table 6.21. The pre-optimization gradients use a preliminary estimate of vehicle mass, length, width and height prior to engine selection and final input parameters. As this assumes a single engine type (gasoline inline naturally aspirated) and bases front and rear overhang on typical sedan ratios, it may produce different results compared to optimized design values.

Target / Parameter	Vs. Engine Peak Power Pre-Optimization	Vs. Engine Peak Power Post-Optimization	Gradient Units	% Difference
0 - 60 mph Acceleration Time	-0.027	-0.031	sec / kW	-11.7
Cargo Volume V1	0	0	liter / kW	-
Maximum Vehicle Velocity	0.454	0.457	kph / kW	-0.5
Frontal NCAP Accelerations	-0.0134	-0.0112	g / kW	19.6
EPA Combined Mileage	-0.0114	-0.0098	mpg / kW	16.3
Front Weight Distribution	0.024	0.019	% / kW	27.7
60 mph - 0 Braking Distance	0.0003	0.0002	meter / kW	50.0
CTC Turn Radius	0.0	0.0	meter / kW	-
Mcurb	1.258	1.253	kg / kW	0.4
L101	0.0	0.0	meter / kW	-
L103	0.0004	0.0004	meter / kW	0.0
L104	0.0004	0.0004	meter / kW	0.0
Bumper Rail Length	0.0000	0.0000	meter / kW	-
Midrail Length	0.0004	0.0003	meter / kW	33.3
Maximum Traction Power	0.362	0.313	kW / kW	15.8
MBiW	0.028	0.027	kg / kW	5.7
MCls	0.000	0.000	kg / kW	-
MDrv	0.191	0.191	kg / kW	0.0
Mint	0.000	0.000	kg / kW	-
Msusp	0.187	0.187	kg / kW	0.4
Mtransmission	0.128	0.128	kg / kW	0.0
Muncat	0.051	0.048	kg / kW	5.6

Table 6.21 Parameter Sensitivity Gradient Results vs. Peak Engine Power

For parameters from the sample vehicle used in this section (2007 Ford Crown

Victoria), the pre-optimization mass is 1783 kilograms (kg); the post-optimization value in this case is 1901 kg. Actual vehicle curb mass is 1875 kg. As a result, only the post-optimization results are shown for subsequent gradients in this section and in Appendix O. Additional design variables addressed in Appendix O include:

- Midrail average crush force in kN
- Rear overhang L105 in meters
- Front wheel center to Ball of Foot Reference Point (L113) in meters
- Second row SgRP to rear wheel center L115-2 in meters
- Electric motor peak power (for hybrids) in kW
- High-voltage battery capacity (for hybrids) in kWh

Candidates for Additional Optimization Design Variables

There are several criteria for selecting parameters to be design variables used in the vehicle optimization process. The variables must have a significant influence on the majority of the vehicle targets and resultant parameters of interest. The candidate parameters must have a reasonable valid design space range which can yield different output results in the optimization process. A variable (such as seat width) with significant influence but a limited range of possible values (due to occupant requirements and constraints) is not as effective as one such as W20-1 (cross-car distance of driver SgRP from vehicle centerline). W20-1 can assume a large range of feasible values, has a significant influence on many vehicle targets and parameters and entails fewer inherent limiting constraints. Driver seat height H30-1 has an influence on many other parameters but it is has additional constraints not yet addressed in the Optimization module such as

vision angles and ergonomic / reach envelope factors. Three candidates for use as additional optimization design variables based on sensitivity gradients are:

- First to second row coupling distance L50-2
- Front row SgRP y-coordinate (cross-car coordinate) W20-1
- Front rocker height from ground H111-1

Parameter sensitivity gradients vs. L50-2 and W20-1 are shown in Table 6.22. Gradients vs. H111-1 are shown in Table 6.23. Each of these candidates has a significant impact on several targets and many of the parameters of interest. Each of them force trade-offs between targets. Coupling distance L50-2 is part of passenger volume calculation; increasing the value affects mass, weight distribution and internal volume. This can impact acceleration, braking fuel economy, vehicle mass, turn radius, maximum velocity and the vehicle EPA class size. The latter is important if the vehicle is targeted for a specific vehicle market segment (compact sedan, etc.).

Similarly, W20-1 affects shoulder room, vehicle mass and overall vehicle width. This impacts fuel economy, acceleration, maximum velocity, mass, turn radius and EPA class size. Rocker height H111-1 affects vehicle mass, fuel economy and, less intuitively, C_g location and front overhang--this is due to the lengthening of the midrails to handle front crash energy for increased vehicle mass. This shows that some of the interactions and trade-offs are shaped by the functional model and parameter definitions. The sensitivity gradients for 0 to 60 mph acceleration time vs. the above dimensional parameters and design variables are shown in Figure 6.3 to compare the gradients to each other. EPA combined mileage vs. dimensional parameters is shown in Figure 6.4

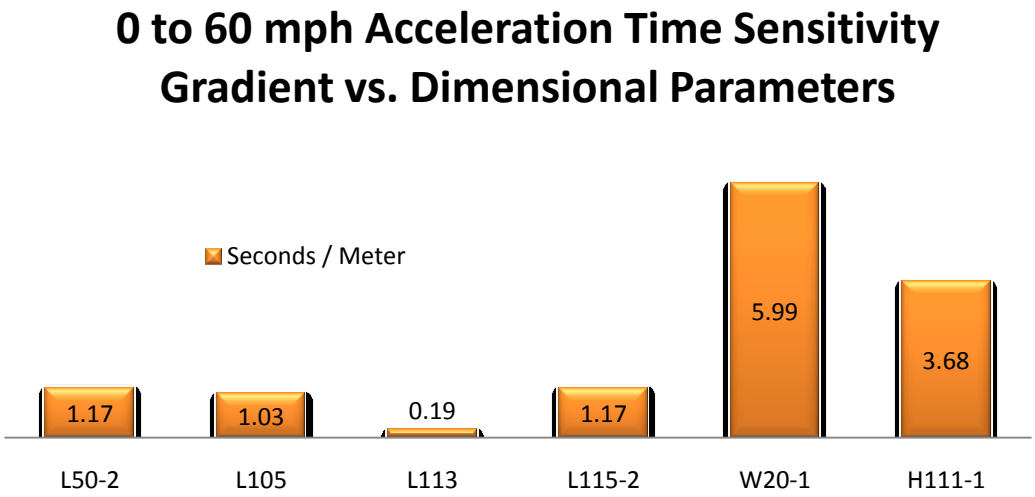

Figure 6.3 Zero to 60 mph Acceleration Time Sensitivity Gradient vs. Dimensional Parameters

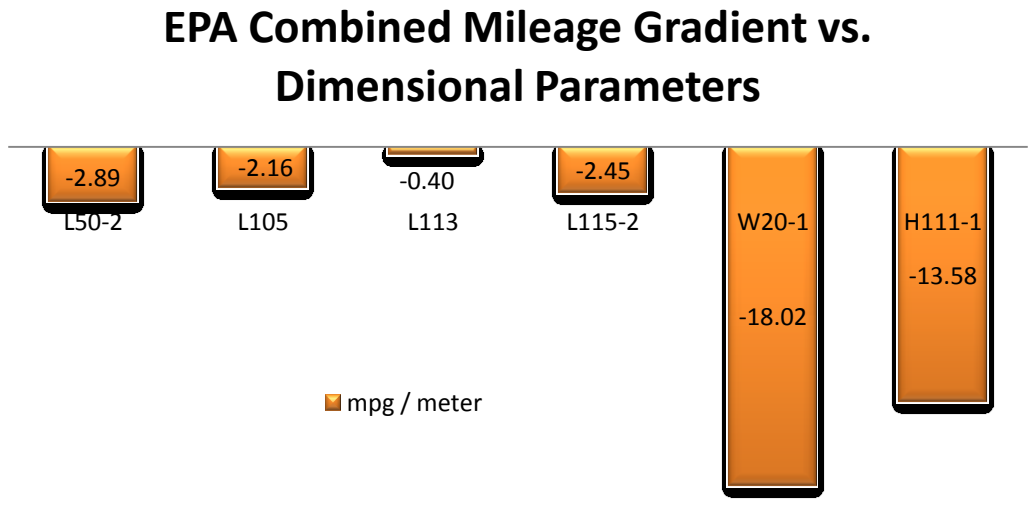

Figure 6.4 EPA Combined Mileage Sensitivity Gradient vs. Dimensional Parameters

Note that the mass impact for changes in W20-1 are generally much greater than for L50-2. W20-1 is doubled (for each side of vehicle centerline) in calculating vehicle width. Additionally, for the same change in value (such as 0.100 meters), W20-1 represents a greater proportional change in overall width W103 than L50-2 does for

overall length L103 (many subsystem mass calculations use the outside volume L103 * W103 * H100).

Target / Parameter	L50-2	Gradient Units	W20-1	Gradient Units
0 - 60 mph Acceleration Time	1.17	sec / kN	5.99	sec / m
Cargo Volume V1	0.0	liter / kN	801.3	liter / m
Maximum Vehicle Velocity	-1.03	kph / kN	-89.18	kph / m
Frontal NCAP Accelerations	-6.53	g / kN	-26.54	g / m
EPA Combined Mileage	-2.89	mpg / kN	-18.02	mpg / m
Front Weight Distribution	-0.05	% / kN	-0.87	% / m
60 mph - 0 Braking Distance	0.069	meter / kN	-0.059	meter / m
CTC Turn Radius	1.58	meter / kN	1.15	meter / m
Mcurb	313.5	kg / kN	1598.8	kg / m
L101	1.000	meter / kN	0.000	meter / m
L103	1.125	meter / kN	0.598	meter / m
L104	0.125	meter / kN	0.598	meter / m
Bumper Rail Length	0.009	meter / kN	0.044	meter / m
Midrail Length	0.116	meter / kN	0.554	meter / m
Maximum Traction Power	31.3	kW / kN	246.4	kW / m
MBiW	80.6	kg / kN	439.3	kg / m
MCls	11.3	kg / kN	26.3	kg / m
MDrv	0.2	kg / kN	0.0	kg / m
Mint	28.1	kg / kN	95.0	kg / m
Msusp	46.7	kg / kN	238.1	kg / m
Mtransmission	0.0	kg / kN	0.0	kg / m
Muncat	146.8	kg / kN	800.2	kg / m

Table 6.22 Parameter Sensitivity Gradients vs. L50-2 and W20-1 (Post-Optimization)

Target / Parameter	H111-1	Gradient Units
0 - 60 mph Acceleration Time	3.68	sec / kN
Cargo Volume V1	0.0	liter / kN
Maximum Vehicle Velocity	-61.07	kph / kN
Frontal NCAP Accelerations	-20.50	g / kN
EPA Combined Mileage	-13.58	mpg / kN
Front Weight Distribution	-1.17	% / kN
60 mph - 0 Braking Distance	-0.04	meter / kN
CTC Turn Radius	0.0	meter / kN
Mcurb	982.5	kg / kN
L101	0.000	meter / kN
L103	0.393	meter / kN
L104	0.393	meter / kN
Bumper Rail Length	0.029	meter / kN
Midrail Length	0.364	meter / kN
Maximum Traction Power	219.2	kW / kN
MBiW	259.7	kg / kN
MCls	46.4	kg / kN
MDrv	0.0	kg / kN
Mint	57.0	kg / kN
Msusp	146.3	kg / kN
Mtransmission	0.0	kg / kN
Muncat	473.1	kg / kN

Table 6.23 Parameter Sensitivity Gradients vs. H111-1 (Post-Optimization)

Summary of Sensitivity Gradients

The sensitivities can be used for several purposes. As shown above, they can be used to identify trade-offs between parameters vs. design variables and parameters vs.

each other. They also show the sensitivity of vehicle target achievement to design variables and parameters. They indicate which parameters and targets can be readily modified and optimized; conversely, they show which targets are relatively insensitive to the designated design variables (such as braking distance) and thus will not benefit much from optimization efforts.

A by-product of sensitivity analysis is that a user applying the Scenario Builder module may find a key parameter that is not a useful design variable and yet profoundly affects a single vehicle target. For example, the largest single influence on braking distance appears to be the tire friction coefficient. Another factor is the availability of data for a parameter and design variable. A knowledge base for most dimensional parameters can be readily developed based on publicly available information or field research. Functional parameters may be difficult to gather for inclusion in a knowledge base; tire rolling resistance and friction coefficient by tire model is rarely promulgated by tire manufacturers and the testing to acquire such data is difficult and resource intensive.

Vehicle Optimization Results

Optimization examples in this section use the base parameters for a 2007 BMW 328i sedan with targets modified slightly to ensure that all targets cannot be simultaniously met and resulting optimization trade-offs must occur. The modified targets vs. actual vehicle performance are shown in Table 6.24. Some targets, such as front weight distribution and braking distance, are more difficult to modify significantly than others.

Target / Parameter	Actual Vehicle Value	Optimization Targets	Units	Change from Actual (%)
0 - 60 mph Acceleration Time	6.9	5.5	seconds	-20.3%
Cargo Volume V1	340	400	liters	17.6%
Maximum Vehicle Velocity	209	250	kph	19.6%
Frontal NCAP Accelerations	30 (4-Star)	25 (5-Star)	g's	-16.7%
EPA Combined Mileage	24.3	30	mpg	23.5%
Front Weight Distribution	51.1	50	%	-2.2%
60 mph - 0 Braking Distance	36.4	36	meters	-1.1%
CTC Turn Radius	5.5	5.5	meters	0.0%

Table 6.24 Optimization Example Targets vs. Actual Vehicle Performance

The first optimizations are run with the default "DNA" weighting of 1.0 for each factor (Unweighted Optimization). The next set of optimizations are run with a single weighting factor increased (efficiency, safety) to a factor of 2.0. Optimizations are then run with two factors increased (efficiency / safety) by a factor of 1.50 each. The results are shown in the following sections.

Unweighted Optimization Examples

Six unweighted optmization runs are conducted; results for the "better" two runs are shown below. For the optimization targets shown in Table 6.24, using the 2007 BMW 328i parameters, the estimated engine power required as shown in the engine selection menu (Figure 6.5) exceeds the available maximum for the gasoline inline normally aspirated engine found in the 328i. As a result, the gasoline inline turbocharged engine is selected instead (this is one function of the engine selection menu--to ensure

that the user has the option of selecting an engine with the appropriate power range to reach optimization targets).

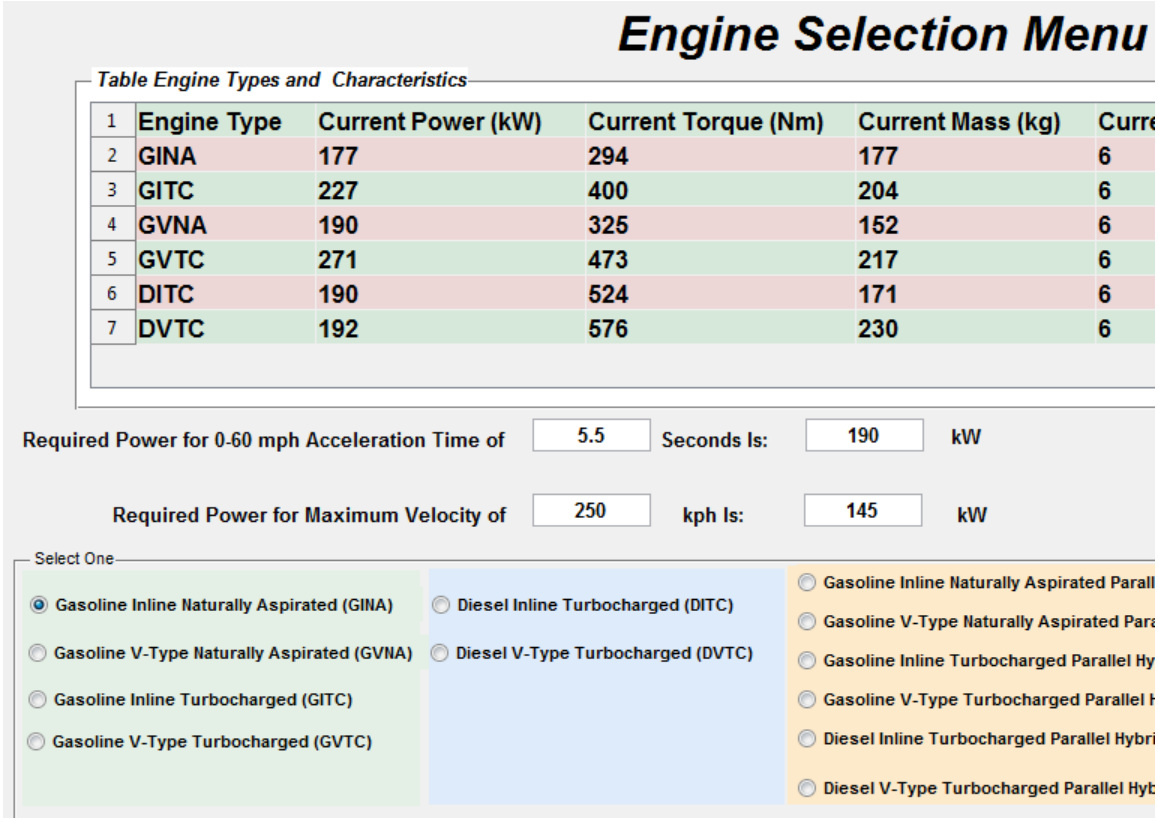

Figure 6.5 View of Portion of Engine Selection Menu with Engine Power Requirement Estimates (to Achieve Acceleration Time / Maximum Velocity Targets)

The spider diagram for displayed optimization run 1 is shown in Figure 6.6. Results for displayed optimization run 2 are shown in Figure 6.7. The performance to target results are also shown in Table 6.25.

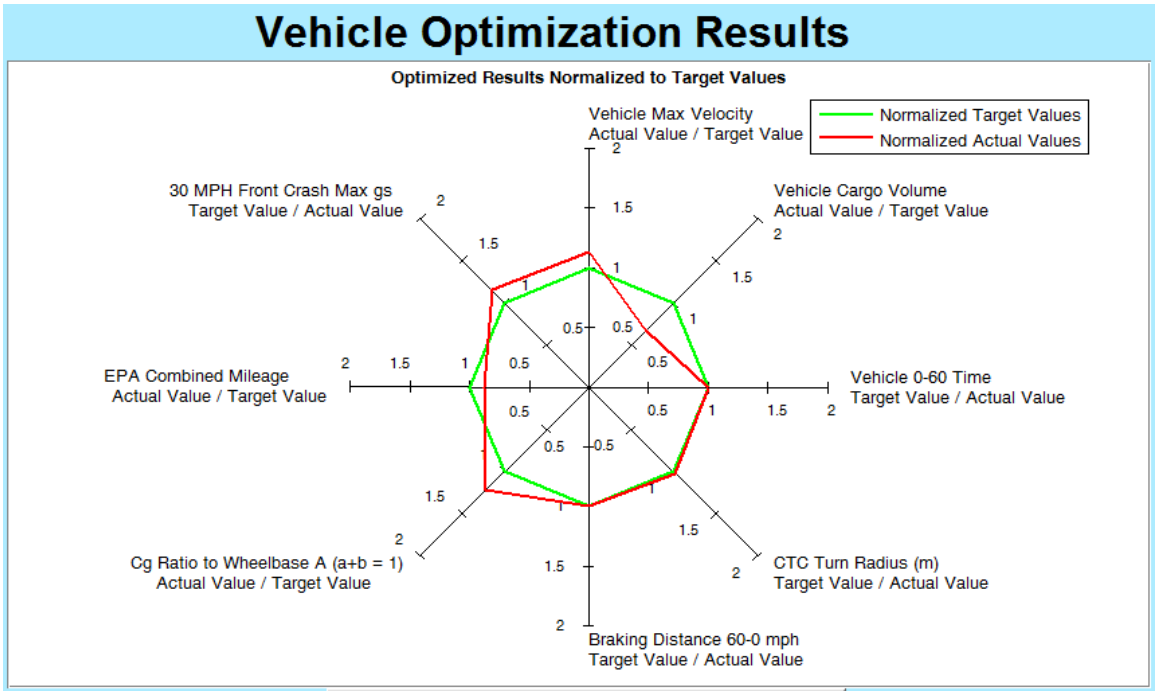

Figure 6.6 Unweighted Optimization Run 1 Performance to Targets Spider Chart

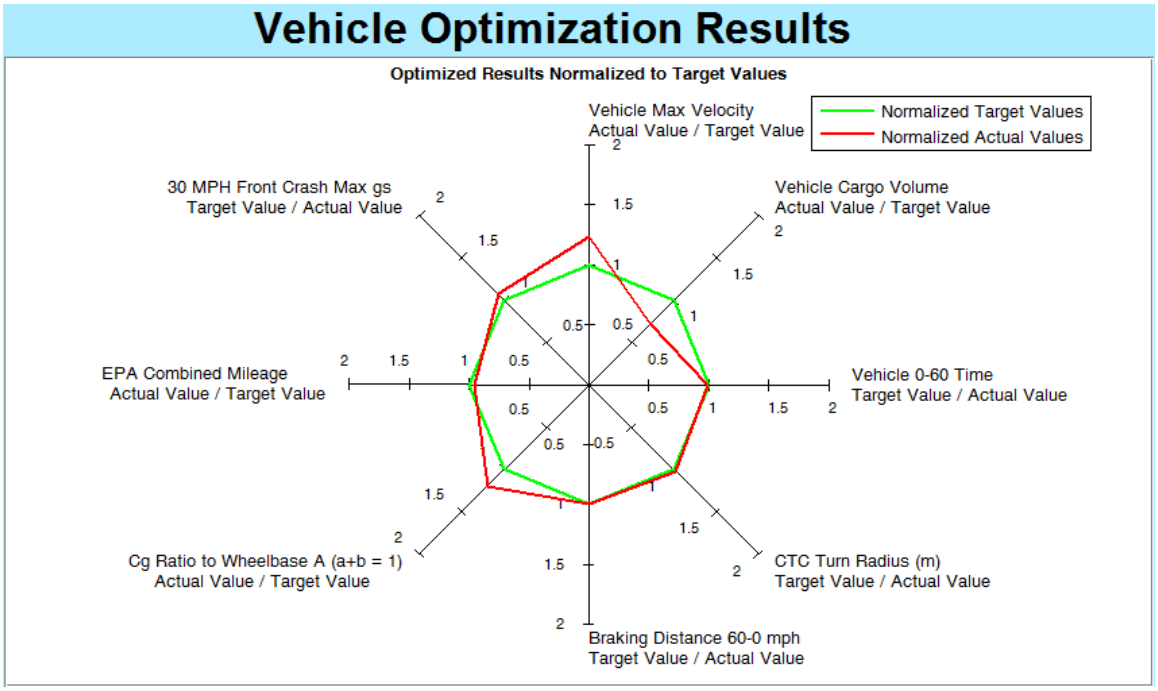

Figure 6.7 Unweighted Optimization Run 2 Performance to Targets Spider Chart

Target / Parameter	Target	Optimization Run 1	Optimization Run 2	Units
0 - 60 mph Acceleration Time	5.5	5.5	5.5	seconds
Cargo Volume V1	400	270	289	liters
Maximum Vehicle Velocity	250	283	284	kph
Frontal NCAP Accelerations	25	21.8	25.0	g's
EPA Combined Mileage	30.0	26.3	25.8	mpg
Front Weight Distribution	50.0	61.1	59.7	%
60 mph - 0 Braking Distance	36	36	36	meters
CTC Turn Radius	5.5	5.4	5.5	meters
Functional Value of "Better Point"	0.0	0.5	0.4	

Table 6.25 Unweighted Optimization Runs Performance to Targets

Of the six unweighted runs, one has a functional value of 0.4. Two have a value of 0.5. one has a value of 0.6, one has a value of 0.7 and one has a value of 1.1; this gives an average functional value of 0.63 for all six runs.

In the unweighted case, the two "better" optimization runs are similar in performance to target and in the design variable values used to achieve that performance. The primary difference was in the midrail crush force for each run. The "better point" from each run is selected from the final generation of 300 points per generation (to a maximum of 300 generations) with current optimization settings. The effect of adding points per generation is explored later in this chapter.

In both runs, the acceleration time targets are met; optimized cargo volume is far below the target value and that for the actual vehicle (340 liters). The frontal NCAP acceleration target is met in both runs and run 1 achieves a value less than 25 g's. EPA combined mileage is improved for both but falls short of the target. Front weight

distribution increases drastically in both optimization runs, due to increased front overhang L104 and decreased rear overhang L105 which occur to meet the front NCAP target. Frontal NCAP g's in all runs ranged from 21.8 (5-Star) to 50.1 g's (worse than 2/1-Star). Front weight distribution ranged from 51.8 % to 62.6 %.

Optimization final design variable values vs. actual vehicle values are shown in Table 6.26. Peak engine power for all runs was less than the potention maximum of 227 kW (with a range from 160 to 224 kW). 0 to 60 acceleration times for all runs ranged from 5.5 to 6.8 seconds.

Design Variable	Actual Vehicle	Optimization Run 1	Optimization Run 2	Units
Peak Engine Power	**169.3**	**200**	**203**	**kW**
Midrail Crush Force	**115 (est.)**	**55**	**67**	**kN**
L105	**1.011**	**0.531**	**0.564**	**meter**
L113	**0.612**	**0.442**	**0.511**	**meter**
L115-2	**0.430**	**0.494**	**0.539**	**meter**

Table 6.26 Unweighted Optimization Design Variable Values vs. Actual Vehicle

The two "better" optimization runs gave similar results in reaching and optimized vehicle configuration. Midrail crush force runs from 55 to 125 kN for all runs. Rear overhang L105 was between 0.521 and 1.168 meters. L113 was between 0.397 and 0.766 meters; L115-2 between 0.419 to 0.623 meters.

In current design practice in industry, values of some of these parameters such as L113 and L115-2 may be the resultant of engineering design decisions in other areas rather than being treated as a design-enhancing parameter in themselves. Using this

optimization method in industry with such design variables requires the ability to attach a cost basis to different design variable values or changes in value.

Vehicle overall dimensional and mass parameters for the two better optimizations are shown in Table 6.27. Overall vehicle length L103 ranges from 4.077 to 4.760 meters. Wheelbase varies from 2.534 to 3.087 meters due to combinations of design variables L113 and L115-2. Total interior volume IV1 ranges from 102 to 109 cubic feet, remaining within the definition of a compact sedan for all six runs. Front overhang varies from 0.722 to 1.646 meters for all runs; the two runs shown in Table 6.27 are near the midpoint of the overall range. The increase of front overhang to meet frontal NCAP accelerations and decrease in L105 to reduce curb mass for fuel economy are major influences in the drastic increase in front weight distribution.

Parameter	Actual Vehicle	Optimization Run 1	Optimization Run 2	Units
Mcurb	**1515**	**1504**	**1502**	**kW**
Internal Volume IV1	**107**	**103**	**104**	**kN**
L101	**2.761**	**2.654**	**2.769**	**meter**
L103	**4.598**	**4.467**	**4.381**	**meter**
L104	**0.827**	**1.282**	**1.048**	**meter**

Table 6.27 Unweighted Optimization Vehicle Parameters vs. Actual Vehicle

The unweighted runs show that the actual vehicle design does not have a significant amount of "free" design space to increase achievement of one target without sacrificing achievement of other targets. Maximum vehicle velocity in the optimization runs will typically exceed the target value except at extremely high target velocities; most vehicles are now electronically speed-limited below the vehicle's actual capability due to

tire speed ratings and safety / due care considerations.

Vehicle DNA Weighting Effects on Optimization--Efficiency DNA Factor Emphasized

For the same targets as in the unweighted optimization, the weighting for efficiency is increased to 2.0 while all other DNA factors remain at the default value of 1.0. Performance to target results are shown in Table 6.28. The optimized values for EPA combined mileage have increased compared to the unweighted results but they do not achieve the 30 mpg target; they are, however, 10% higher than the actual vehicle fuel economy.

Target / Parameter	Target	Optimization Run 1	Optimization Run 2	Units
0 - 60 mph Acceleration Time	5.5	5.4	6.3	seconds
Cargo Volume V1	400	250	250	liters
Maximum Vehicle Velocity	250	283	268	kph
Frontal NCAP Accelerations	25	17.7	22.4	g's
EPA Combined Mileage	30.0	26.7	26.7	mpg
Front Weight Distribution	50.0	62.5	62.6	%
60 mph - 0 Braking Distance	36	36	36	meters
CTC Turn Radius	5.5	5.2	5.2	meters
Functional Value of "Better Point"	0.0	0.8	0.8	

Table 6.28 Performance to Target for Optimization with "Efficiency" DNA Factor at 2.0

Both runs displayed have frontal NCAP accelerations which are lower than the target NCAP value; this is due to midrail crush forces of 42 and 55 kN respectively vs. 115 kN for the actual vehicle. Both have a high front weight distribution due to a rear overhang; that is, on average, 48% shorter than the actual vehicle. The longer front

overhang as the front midrails (with lower crush capacity) are lengthened to absorb the NCAP crash energy also adds to front weight distribution. Cargo volume is 38% lower than the target due to shortened rear overhang.

Vehicle Parameters of interest are shown in Table 6.30. Spider charts showing performance to target for efficiency-biased optimization runs 1 and 2 are shown in Figure 6.8 and Figure 6.9, respectively.

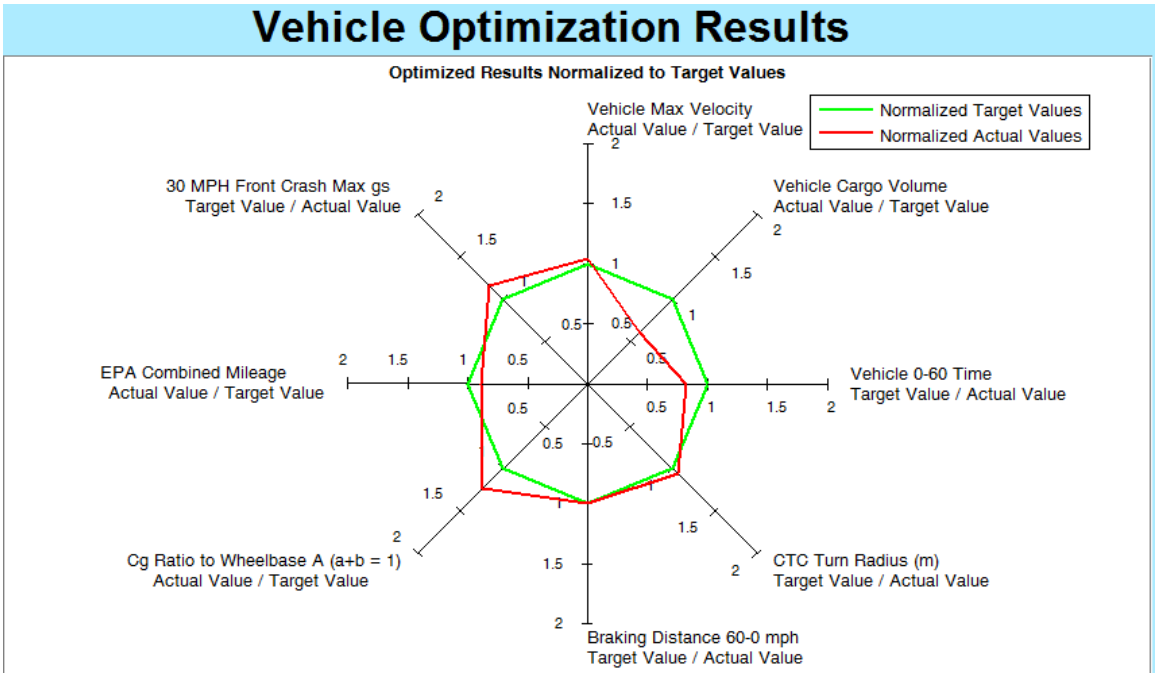

Figure 6.8 Optimization Performance to Target Spider Diagram for Efficiency Weighted Run 1

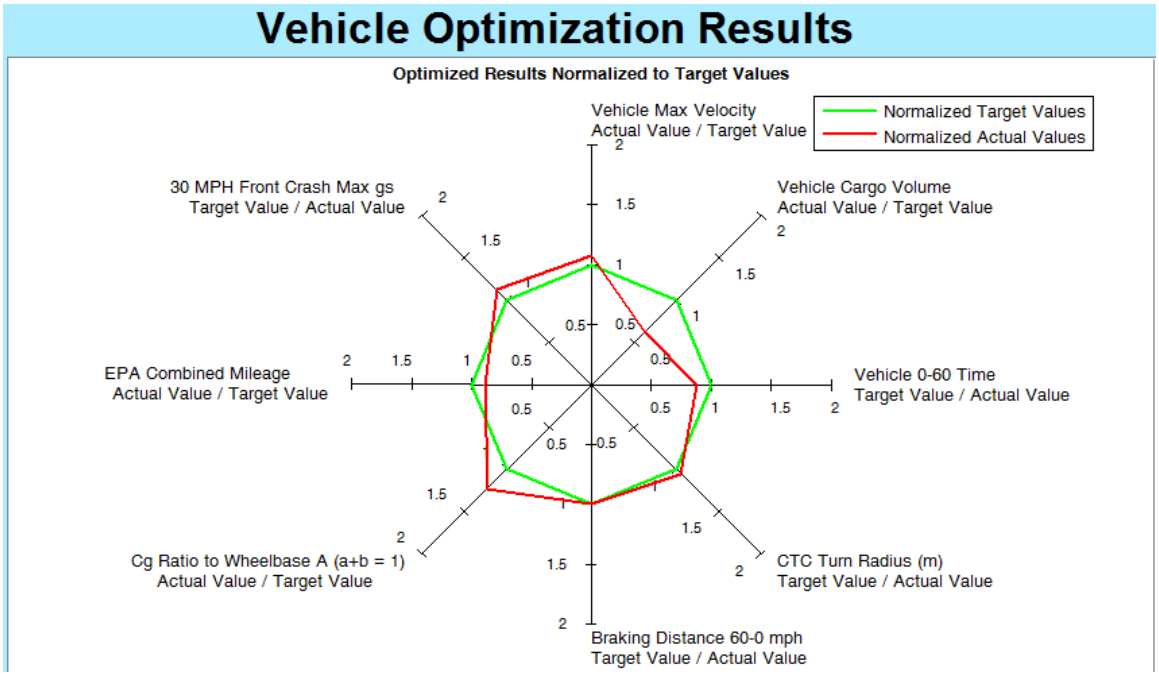

Figure 6.9 Optimization Performance to Target Spider Diagram for Efficiency Weighted Run 2

The optimized values for the design variables are shown in Table 6.29.

Design Variable	Actual Vehicle	Optimization Run 1	Optimization Run 2	Units
Peak Engine Power	**169.3**	**201**	**171**	**kW**
Midrail Crush Force	**115 (est.)**	**42**	**55**	**kN**
L105	**1.011**	**0.535**	**0.523**	**meter**
L113	**0.612**	**0.402**	**0.394**	**meter**
L115-2	**0.430**	**0.419**	**0.433**	**meter**

Table 6.29 Design Variable Values for Efficiency-Weighted Optimization Runs

The two optimization examples for the efficiency weighted runs do not show a dramatic difference from each other. For all efficiency weighted optimization runs, peak engine power ranges from 88 to 201 kW. Rear overhang L105 only ranges from 0.516 to

0.535 meters for all of the runs. Midrail crush force ranged from 42 to 62 kN; this indicates that the NCAP rating target appears to have more influence than other factors such as front weight distribution. Front weight distribution and cargo volume (both affected by L105) seem to be sacrificed in attaining the other targets. Note that these optimization runs also use the turbocharged gasoline inline engine in place of the naturally aspirated inline engine in the actual vehicle in order to have the potential to achieve a 0 to 60 mph acceleration time of 5.5 seconds.

Parameter	Actual Vehicle	Optimization Run 1	Optimization Run 2	Units
Mcurb	**1515**	**1539**	**1480**	**kW**
Internal Volume IV1	**107**	**103**	**103**	**kN**
L101	**2.761**	**2.539**	**2.545**	**meter**
L103	**4.598**	**4.697**	**4.375**	**meter**
L104	**0.827**	**1.621**	**1.307**	**meter**

Table 6.30 Vehicle Parameters for Efficiency-Weighted Optimization Runs

While the weighted distance method appears to be effective in biasing the results in favor of the higher-weighted Efficiency DNA factor at the expense of other targets, it is difficult to directly quantify the bias. This trade-off depends on a number of factors which require detailed study. The difference in effect based on which DNA factor is given an exaggerated weighting is explored in the next section by changing the weighting to favor the "Safety," DNA factor which influences frontal NCAP accelerations.

Vehicle DNA Weighting Effects on Optimization--Safety DNA Factor Emphasized

As with the last example, the DNA factor for "Safety" is set to a value of 2.0; the other factors are left at the default value of 1.0. The Safety DNA factor currently affects

the front NCAP acceleration (in g's) target achievement. The achievement to target for two optimization runs is shown in Table 6.31.

Note that the maximum weighting for a DNA factor does not ensure exact attainment of a specific target. As seen above, the weighting strongly biases the optimization toward the heavily weighted targets; as the performance to target vs. target gap decreases, however, the weighting of the other factors has more influence than when the gap to the preferred target is significant. In order to guarantee exact attainment of a specific goal, an alternative method of optimization is required.

Target / Parameter	Target	Optimization Run 1	Optimization Run 2	Units
0 - 60 mph Acceleration Time	5.5	7.9	7.3	seconds
Cargo Volume V1	400	271	289	liters
Maximum Vehicle Velocity	250	249	257	kph
Frontal NCAP Accelerations	25	23.9	25.0	g's
EPA Combined Mileage	30.0	26.1	25.8	mpg
Front Weight Distribution	50.0	59.9	59.2	%
60 mph - 0 Braking Distance	36	36	36	meters
CTC Turn Radius	5.5	5.4	5.5	meters
Functional Value of "Better Point"	0.0	0.6	0.5	

Table 6.31 Performance to Target for Optimization with "Safety" DNA Factor at 2.0

As with the previous optimization examples, the two "better" optimization runs are reasonably close to each other; there are no drastically different optimizations yielding a similar functional value. This may imply that the optimization is exploring all of the available design space to provide the better solutions. Initial optimization runs with fewer generations and points per generation (200 / 200) produced more widely varying

optimization results. The functional values for runs in this example range from 0.5 to 1.5. All of the runs in this example met or were lower than the 25-g frontal NCAP target, ranging from 21.5 to 25 g's. Note that an NCAP acceleration value drastically below the target is not necessarily desirable; the difference may represent available design space to be used in meeting other targets. Ideally, all targets should be exactly met for a resulting optimization functional value of 0.0.

Cargo volume is once again below the target value of 400 liters in the two "better" optimization runs, although it ranges from 250 to 607 liters over all of the runs. Maximum vehicle velocity is close to the target value for both runs shown here. EPA combined mileage is higher than the actual vehicle (24.3 mpg), but less than the efficiency-weighted better result of 26.7 mpg. A spider diagram for the Optimization Run 1 is shown in Figure 6.10; for Run 2 the results are shown in Figure 6.11.

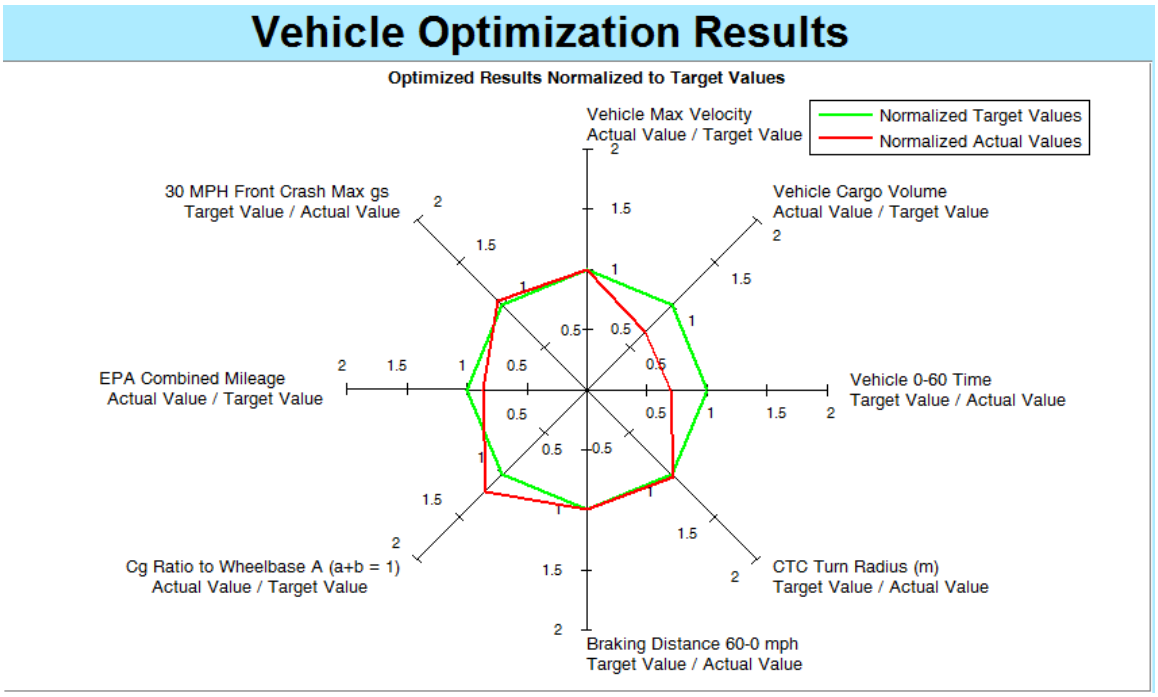

Figure 6.10 Optimization Performance to Target Spider Diagram for Safety-Weighted Run 1

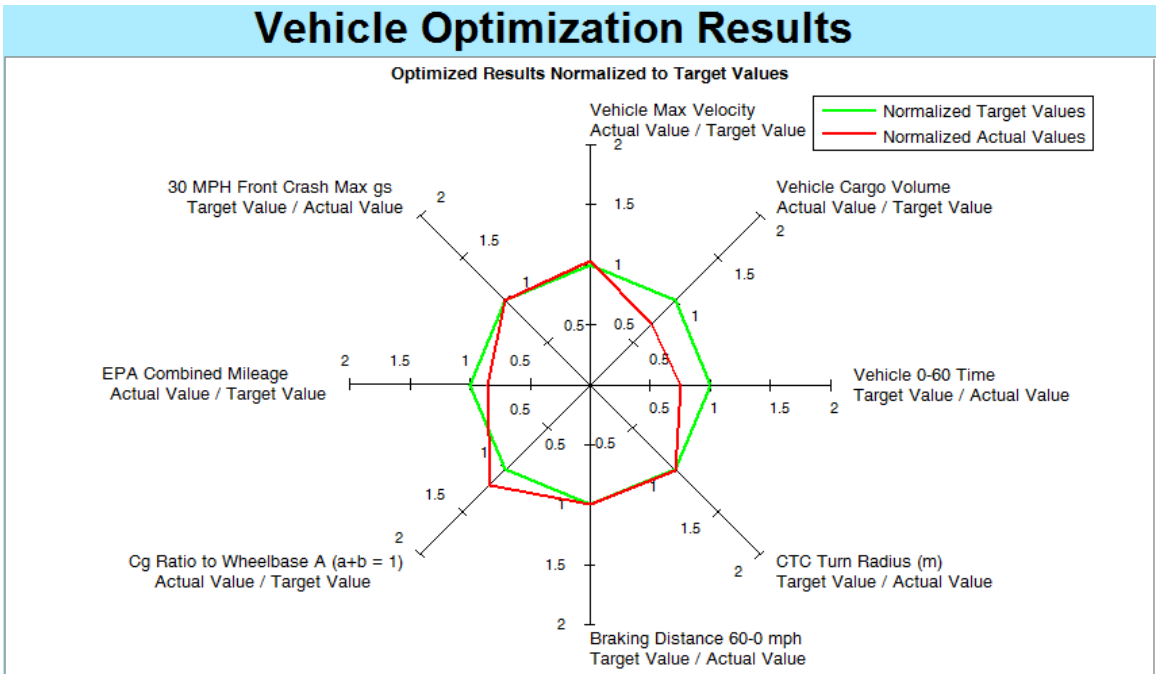

Figure 6.11 Optimization Performance to Target Spider Diagram for Safety-Weighted Run 2

These two spider diagrams are similar to each other, giving a visual confirmation of the similarity noted in Table 6.31. Values of optimized design variables are shown in Table 6.32. Vehicle parameters of interest are shown in Table 6.33.

Design Variable	Actual Vehicle	Optimization Run 1	Optimization Run 2	Units
Peak Engine Power	**169.3**	**140**	**154**	**kW**
Midrail Crush Force	**115 (est.)**	**62**	**67**	**kN**
L105	**1.011**	**0.586**	**0.618**	**meter**
L113	**0.612**	**0.485**	**0.520**	**meter**
L115-2	**0.430**	**0.451**	**0.487**	**meter**

Table 6.32 Design Variable Values for Safety-Weighted Optimization Runs

Parameter	Actual Vehicle	Optimization Run 1	Optimization Run 2	Units
Mcurb	**1515**	**1491**	**1501**	**kg**
Internal Volume IV1	**107**	**103**	**104**	**ft^3**
L101	**2.761**	**2.655**	**2.726**	**meter**
L103	**4.598**	**4.370**	**4.383**	**meter**
L104	**0.827**	**1.130**	**1.039**	**meter**

Table 6.33 Vehicle Parameters for Safety-Weighted Optimization Runs

For a given midrail crush force, increasing the vehicle mass lowers the NCAP accelerations (requiring longer midrails / front structure to absorb added energy). Another approach is to lower midrail crush force to permit lower vehicle mass (although the increase in front overhang due to longer resulting midrails will add some mass back in). Both of the better optimization runs in this example lower midrail crush force with about the same curb mass as the actual vehicle (1510 kg). Internal volume is lower due to a much shorter rear overhang but remains within the bounds for the compact vehicle

class. Wheelbase is shortened, primarily due to decreased values of L113 compared to the actual vehicle. Peak engine power in all runs for this example ranged from 115 to 203 kW.

Vehicle DNA Weighting Effects on Optimization--Efficiency and Safety DNA Factors Emphasized

This optimization is conducted as before with two of the DNA factors set to 1.5 (Efficiency and Safety) and all others at the default value of 1.0. Performance to target for two optimization runs are shown in Table 6.37. Both optimization runs shown in Table 6.37 meet the acceleration time target; they also shown NCAP accelerations lower than the 25-g target value. Cargo volume, while greater than in previous examples, still falls short of the target for these two runs. EPA combined mileage, while exceeding the actual vehicle value of 24.3 mpg, is lower than the performance in the efficiency-only-weighted examples (26.7 mpg). This shows some of the trade-offs occurring with the new weighting combination.

Target / Parameter	Target	Optimization Run 1	Optimization Run 2	Units
0 - 60 mph Acceleration Time	**5.5**	**5.5**	**5.5**	**seconds**
Cargo Volume V1	**400**	**327**	**310**	**liters**
Maximum Vehicle Velocity	**250**	**288**	**284**	**kph**
Frontal NCAP Accelerations	**25**	**24.6**	**23.8**	**g's**
EPA Combined Mileage	**30.0**	**26.1**	**25.8**	**mpg**
Front Weight Distribution	**50.0**	**57.4**	**58.8**	**%**
60 mph - 0 Braking Distance	**36**	**36**	**36**	**meters**
CTC Turn Radius	**5.5**	**5.7**	**5.3**	**meters**
Functional Value of "Better Point"	**0.0**	**0.5**	**0.5**	

Table 6.34 Performance to Target for Optimization with Efficiency and Safety

Design variable values are shown in Table 6.38.

Design Variable	Actual Vehicle	Optimization Run 1	Optimization Run 2	Units
Peak Engine Power	**169.3**	**213**	**204**	**kW**
Midrail Crush Force	**105 (est.)**	**70**	**63**	**kN**
L105	**1.011**	**0.745**	**0.709**	**meter**
L113	**0.612**	**0.644**	**0.444**	**meter**
L115-2	**0.430**	**0.504**	**0.476**	**meter**

Table 6.35 Design Variable Values for Optimization with Efficiency and Safety Emphasized

With the exception of L113, the design variable final values are similar for both optimization runs shown above. The shortening of rear overhang (L105) is not as severe as in the efficiency-only weighted example; however, fuel economy suffers slightly as a result of the additional vehicle mass.

The performance to targets spider chart for Run 1 is shown in Figure 6.12. The spider chart for Run 2 is shown in Figure 6.13. As before, the spider charts appear similar, indicating that there are not a large number of available optimization solutions available to obtain the desired target achievement. These show graphically that the cargo volume (V1) tends to be sacrificed to meet the target factors receiving higher weighting.

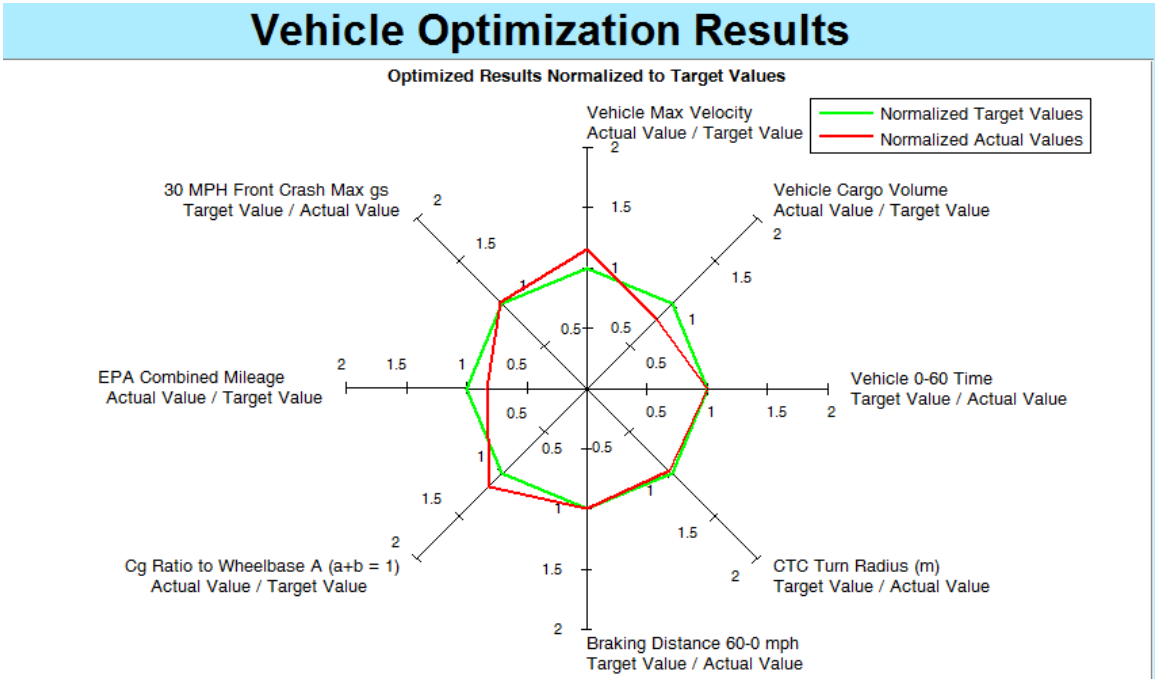

Figure 6.12 Performance to Target -- Efficiency and Safety Emphasized (1.5 Weighting) Run 1 Results

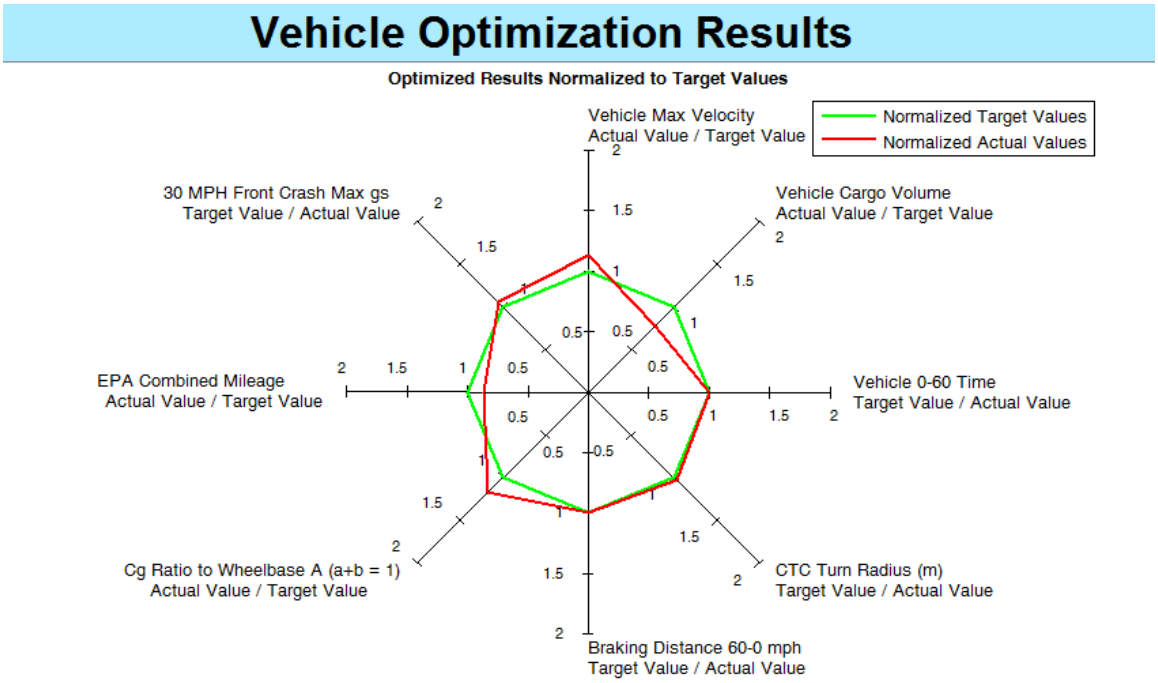

Figure 6.13 Performance to Target -- Efficiency and Safety Emphasized (1.5 Weighting) Run 2 Results

Parameters values of interest are shown in Table 6.39. Vehicle mass in both optmizations shown exceed the actual vehicle value. The lowest optimized vehicle mass in 6 optimization runs is 1486 kg. Internal volume for all runs ranges from 102 to 105 ft^3. Overall vehicle length decreases only slightly from the actual vehicle. Front overhang increases in all cases (between 0.920 and 1.399 meters over six optimization runs) to meet the more stringent 5-Star frontal NCAP target.

Parameter	Actual Vehicle	Optimization Run 1	Optimization Run 2	Units
Mcurb	**1515**	**1546**	**1522**	**kW**
Internal Volume IV1	**107**	**105**	**105**	**kN**
L101	**2.761**	**2.866**	**2.638**	**meter**
L103	**4.598**	**4.531**	**4.518**	**meter**
L104	**0.827**	**0.920**	**1.170**	**meter**

Table 6.36 Vehicle Parameter Values for Optimization with Efficiency and Safety Emphasized

The performance to targets results in this example indicate that the DNA factors for efficiency and safety have some common attainment factors (lighter curb mass through reduction of rear overhang) and some which conflict (front overhang distance which lengthens to lower NCAP accelerations and shortens to reduce curb mass for fuel economy). This shows some of the trade-offs which occur to satisfy vehicle targets which have overlap and potential conflicts within the vehicle design space. The combination of weighting factors requires practice and evaluation by the user to effectively steer optimization trade-offs in the conceptual design process.

Better Optimization Result vs. Number of Points / Generations in Genetic Algorithm Runs

One of the trade-off assessments in the optimization process is to determine (for a genetic algorithm) how many generations and points per generation are most effective and efficient in finding the "better" solution with the fewest iterations (smallest time consumed per optimization run for the best result). Using the unweighted optimization example in this chapter, a series of optimization runs are conducted starting at 50 points per generation and increasing the number of points by 50 for each successive run. The number of generations remains constant at 300 generations. The resulting functional values vs. number of points per generation are shown in Figure 6.14.

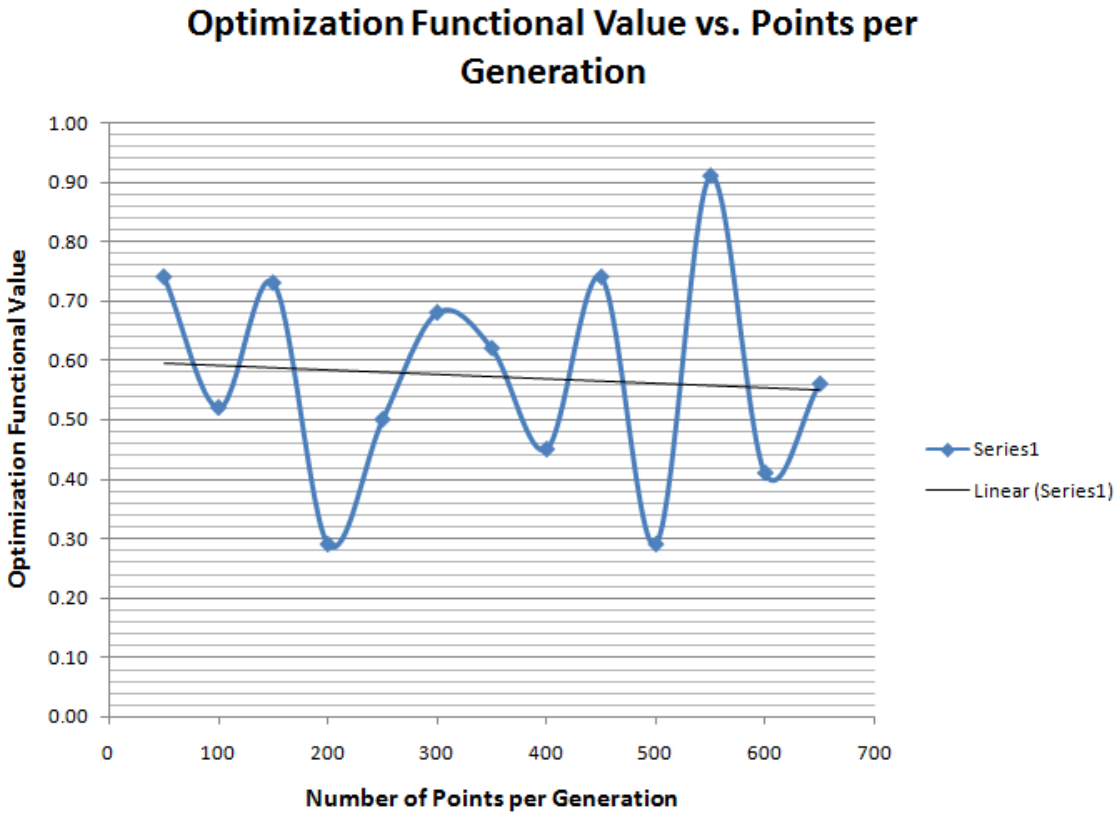

Figure 6.14 Optimization Functional Values vs. Number of Points per Generation

As shown in Figure 6.14, the trend shows a slightly decreasing trend in the functional value with increasing points per generation; however, the values vary drastically between increments in the number of points per generation. This does not guarantee that a single increase in point size increment will provide a "better" solution than the previous increment. It does, however, indicate that an increased number of points in the optimization will tend to provide a solution with a lower optimization functional value. The minimum functional values of 0.29 occur at 200 and 500 points per generation. The performance to target for these samples are shown in Figure 6.15 and Figure 6.16.

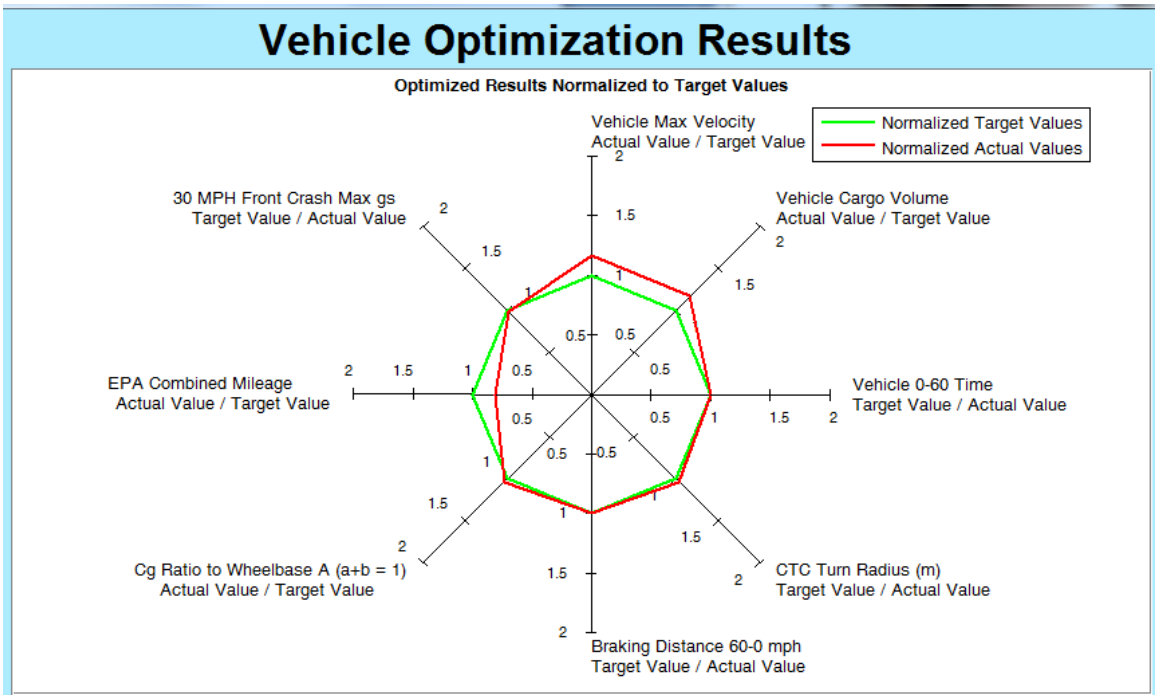

Figure 6.15 Performance to Target Results for Unweighted Optimization (200 Points per Generation, Unweighted)

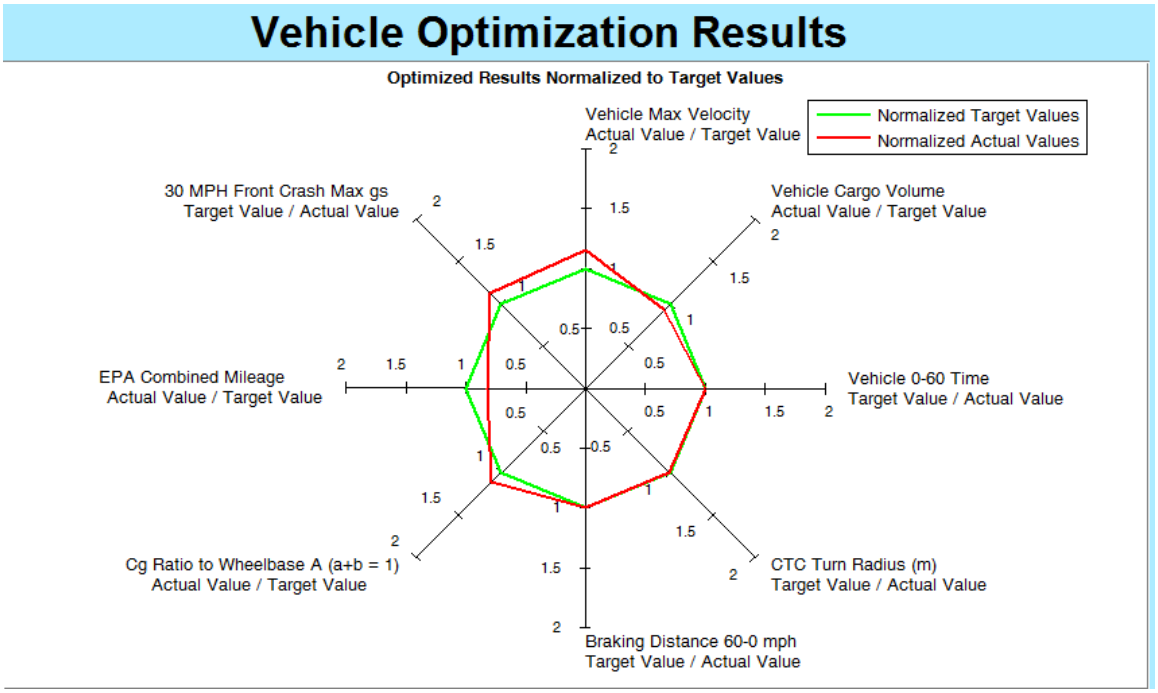

Figure 6.16 Performance to Target Results for Unweighted Optimization (500 Points per Generation, Unweighted)

One insight from the results in Figure 6.14 is that the functional value can vary dramatically between optimization runs. An effective practice in using the genetic algorithm is to run an optimization with the same inputs multiple points, and then pick the "better" point for that configuration.

Optimization Summary

The above examples show that multi-objective optimization can be a powerful tool in the conceptual design process. However, practice and a body of experience are required to effectively steer trade-offs using the vehicle DNA weighting factors. Future incorporation of additional optimization methods will give the user multiple ways to approach design optimization and trade-offs to find the best approach for a given vehicle design project.

CHAPTER 7

SUMMARY AND CONCLUSIONS

Gap 1 Implementation: Need for Appropriate Tools and Architecture

The examples in chapter 6 show that the developed software framework incorporates appropriate tools to develop and optimize vehicle designs in the conceptual design phase. The Scenario Builder and Optimization modules give different ways to understand vehicle designs parametrically to assess and manage trade-offs for improved target achievement. The software development in MATLAB permits open development and can interface with industry-standard optimization and CAD software. The outputs can be readily formatted for import in CAD and spreadsheet software for additional processing and analysis of results.

Gap 2 Implementation: Need for Simplified Models which Capture Physical Principles

The usefulness and accuracy of the simplified models is demonstrated in the Scenario Builder correlation with a sample of validation vehicles shown in Chapter 6. The models combine physical principles and a knowledge base of geometric and functional relations to capture vehicle characteristics and behaviors using low-order models for rapid calculation, iteration and optimization. The consolidation of existing knowledge databases and development of new vehicle knowledge bases through field measurement provide modeling capability for a range of vehicle types and size classes.

Optimization sensitivity gradients provide a method for evaluating trade-offs between not only design variables and targets or design variables and resultant parameters, but also between other parameters of interest and resultant parameters such

as vehicle mass. These gradients provide a rapid method for quantifying gradients which may be difficult to calculate mathematically.

In order to create a theoretical and software framework, the author has developed a continuum of dimensional and functional parameters to enable comprehensive vehicle modeling and optimization. This continuum uses industry-standard dimensional and functional values to the maximum extent possible; however, a number of missing dimensional and functional values are defined and populated as described in the appendices of this work through research and field measurement. A set of mass correlation models developed by the author as shown in Appendix F accurately quantify vehicle curb mass and subsystem mass to permit accurate vehicle center of mass and weight distribution (Appendix J). Engine parameters permit an engine to be dynamically re-sized as peak engine power increases or decreases during optimization or iteration in the Scenario Builder module as detailed in Appendix C.

A simplified frontal NCAP crashworthiness model described in Appendix D provides rapid calculation of acceleration values which might otherwise require finite element modeling and detailed design. Turn radius models shown in Appendix E incorporate existing Ackerman steering models for curb-to-curb turn radius and use the developed knowledge base for estimating vehicle wall-to-wall turn radius. Occupant calculations using parametric relations shown in Appendix B replace detailed occupant positioning in a vehicle CAD model.

In creating this work, key elements to successfully execute the parametric modeling framework include:

- Developing a continuum of common vehicle spatial and functional parameters used by all models in the framework.
- There must be significant interaction between the models to describe vehicle characteristics, functional behavior and required trade-offs.
- Models must be of sufficient detail and accuracy to predict valid vehicle curb mass and subsystem mass and the center of mass location for each subsystem.
- The level of complexity (order) of the models must be sufficient to accurately capture the physical and functional principles. How much accuracy is sufficient to validate the model is a matter of judgment. However, a higher order model which adds complexity while contributing little additional accuracy should be avoided due to the amount of information which must be collected and input to support such a model.
- An integrated set of physics and knowledge-based models permit the assessment of the feasibility of resulting designs. However, the knowledge base must not restrict the ability to investigate revolutionary design implementations.

Gap 3: Need for Relevant and Consistent Starting Parameters and Relations

One method for improving optimization and design iteration results is to begin the process within feasible and consistent parameter boundaries. The development of a vehicle knowledge base of dimensional values and relationships provides valid starting points for vehicle design and optimization and enables more rapid convergence on better vehicle designs. The strategy of parametrically building up a vehicle model from the

inside (occupant-relevant relationships) outward prevents the use of inconsistent vehicle dimensions and relationships (such as the interior packaging exceeding exterior dimensions). This, combined with the knowledge base, sets valid constraints on optimization variables and resultant parameters.

Gap 4: Compromised Solution Brand Neutral

The use and impact of using DNA weighting factors in steering the optimization based on brand attributes and related achievement of vehicle targets is shown in the examples in Chapter 6. The DNA factors are effective in steering target achievement in factor of more highly value targets; however, the weighting factors do not guarantee exact achievement of a given target.

The DNA factors can show the effect of new legislation or customer requirements on the current vehicle's perceived character. If a "sporty" vehicle biased toward performance characteristics must meet new safety or fuel economy regulations, the weighted optimization can show how much is lost in terms of acceleration time, turn diameter or optimal vehicle weight distribution. Similarly, a luxury-branded vehicle model may need to trade off cargo volume to reduce mass for fuel economy or extend the front overhang for crash energy absorption

Gap 5: Solvers Not Transparent (Sensitivity / Trade-Offs)

. The optimization sensitivity gradients give a direct measure of parameter vs. design variable or parameter vs. parameter sensitivity and response to changes in input values. This can be used to calculate changes to fixed parameter inputs in subsequent optimization runs and more quickly develop a design with the best possible compromises

and trade-offs. It is also a useful tool to determine new candidate design variables for vehicle optimization or to eliminate variables which do not have significant impact on optimization outcomes. The ability to make rapid trade-offs and to understand the impact of incremental or drastic design changes reduces the time required to converge on an optimized and effective vehicle design.

The Scenario Builder module can also be effective in assessing trade-offs due to changes in an optimized design. Input parameters can be modified from an optimized design to determine how much variation can be introduced before the benefits of the optimized design are lost. It can also be used to determine if the best aspects of two optimized designs can be blended (as in two vehicle models sharing a common platform) without losing the unique benefits of each design.

Conclusions

The use of parametric and knowledge-based vehicle modeling provides an effective and useful framework for vehicle development and optimization in the conceptual design phase. The speed, flexibility and ability to manage design trade-offs provide a better means of maturing the vehicle design in this phase in contrast to commonly used detailed design tools. The ability to capture complex vehicle behavior and interactions with a set of simplified models enables better understanding and management of design trade-offs and benefits. The use of simplified models sharing a common and continuous set of dimensional and functional vehicle parameters makes it easier to add additional functional models, design variables and vehicle targets in future work. The use of DNA factors is effective in steering vehicle performance toward

achievement of more highly desired targets, but does not guarantee exact target achievement.

The use of optimization in parametric vehicle design does not guarantee achievement of all vehicle targets; rather, it provides the means to understand and manage trade-offs in achieving the "better" compromise available within the available vehicle design space. Familiarity and practice with the software framework is necessary to develop a body of experience and to use it most effectively in developing a mature conceptual designwhichwill require few if any significant modifications in the detailed design phase.

CHAPTER 8

FUTURE WORK

There are many possibilities for continuing and adding to this work. Key items include:

- Inclusion of parameters and knowledge base for serial hybrid vehicles
- Adding additional vehicle types to the software framework. The knowledge base covers additional vehicle types not currently used in the framework.
- Inclusion of knowledge base and relations for transversely mounted engines
- Inclusion of "batch" runs (multiple optimization iterations for the same inputs) and display of results for different runs vs. each other.
- Inclusion of additional optimization design variables. Three candidates are identified in this work.
- Inclusion of additional vehicle targets for optimization.
- Inclusion of additional DNA weighting factors
- Inclusion of additional optimization methods (particle swarm optimization, analytical target cascading, etc.).
- Adding additional vehicle functional models (such as handling and vehicle dynamics measures and targets).
- Addition of vertical center of gravity vehicle and subsystem calculation.

Many additional features can be added to the knowledge base and the software framework. The above examples illustrate the potential for expanding the scope and usefulness of parametric modeling, design and optimization.

APPENDICES

Appendix A
Summary of Vehicle Parameters and Configurators

Definitions

Parameter: A scalar (possibly integer) value which defines a vehicle characteristic (dimensional, functional or resultant parameter).

Dimensional Parameter Example: L101 = Wheelbase in meters

Functional Parameter Example: Eng_kW = Engine Peak Power in kW

Resultant Parameter Example: Mcurb = Vehicle Curb Mass in kg

Target Resultant Parameter Example: 0 to 60 mph acceleration time in seconds

Configurator: A qualitative (non-scalar) value or descriptor which defines a vehicle characteristic or configuration (may be an integer).

Configurator Example 1: Vehicle Class (Compact Sedan, etc.)

Configurator Example 2: Rows of seating (integer value)

Configurator Example 3: Sunroof (yes / no)

Configurator Example 4: Fuel Type (gasoline / diesel / electric)

Configurators Used in this Work

General Vehicle Configurators:

Vehicle Class (Compact Sedan, etc.)

- Vehicle Type (sedan, coupe, SUV, CSUV, MPV, 2-Seater)
- Vehicle Size (Large, Midsize, Compact, Subcompact, Mini-Compact or Large, Medium, Small for non-EPA definitions)

Body Type (Unibody, Body on Frame)

Sunroof (Yes / No)

Convertible (Yes / No)

Number of Doors (Linked to vehicle type for coupe / sedan)

Drive Type (AWD / FWD / RWD)

Rows of Seating (1, 2, 3, ...)

- Number of Row 1 Occupants
- Number of Row 2 Occupants
- Number of Row 3, etc. Occupants as required

Hybrid Type (Parallel / Serial / Non-Hybrid)

Vehicle Model Year (Currently sets EPA fuel economy target parameters a, b, c and d for target calculation in conjunction with vehicle footprint).

Vehicle Engine / Driveline Configurators:

Engine Orientation (Longitudinal / Transverse)

Cylinder Layout (Inline / V-Type)

Number of (Internal Combustion) Engine Cylinders

Transmission Type (Automatic / Manual / Automated Manual)

Internal Combustion Engine Fuel Type (Gasoline / Diesel)

Internal Engine Aspiration Type (Normally Aspirated / Turbocharged)

Materials:

Body in White Material (Aluminum / Steel / Composite)

Closure Materials:

- Door Materials (Aluminum / Steel / Composite)
- Hood Materials (Aluminum / Steel / Composite)

- Decklid / Liftgate Materials (Aluminum / Steel / Composite)

Engine Block (Aluminum / Cast Iron)

Hybrid High-Voltage Battery (Li-Ion, Li-Po, Ni-MH, etc.)

Tire / Wheel Configurators:

Tire Type Designator (P = Passenger Vehicle Tire)

Tire Speed Rating (Letter Designation)

Tire Load Rating Index (Integer Value)

Parameters Used in this Work

Occupant / Internal Length Parameters:

L31-1: Ball of Foot Reference Point (BOFRP) "x" Coordinate [1]

L34: Effective Legroom -- Accelerator (Driver) [1]

L50-2: SgRP Couple Distance, First to Second Row [1]

L51-2: Effective Legroom, Second Row [1]

L99-1: Driver BOFRP to SgRP -- Front Row [1]

X_a: Ankle Point X-Distance from BOFRP

X_h: Accelerator Heel Point (AHP) X-Distance from BOFRP

Occupant / Internal Width Parameters:

SS-1: Row 1 Seat Span (Lateral Distance between Driver / Passenger side Seat Cushion Edges for Bucket Seats) (Used in vehicle field measurements)

SW16: Averaged Driver / Passenger Row 1 Maximum Seat Cushion width[1]

SW16-1: Cushion Width -- Front (Driver Side) [1]

SW16-1-PS: Cushion Width -- Front Passenger Side [1]

W3-1: First Row Shoulder Room [1]

W3-2: Second Row Shoulder Room [1]

W20-1: SgRP Y-Coordinate -- Front [1]

WB-1: First Row Belt Width (W3-1 trim point to outside of door along W3-1 / W117 vector)

WG-1: First Row Gap Width (Lateral Distance from Row 1 Cushion Edge to W3-1 trim point)

Occupant / Internal Height Parameters:

H5-1: SgRP to Ground -- Front [1]

H5-2: SgRP to Ground -- Second [1]

H30-1: Seat Height -- Front [1]

H30-2: Seat Height -- Rear [1]

H30D-2: Seat Height Difference -- First to Second (*H30-2* - *H30-1*)

H37: Roof Liner Thickness along H61-1 Vector [1] (Not currently used in SAE J1100)

H38: Roof Liner Thickness along H61-2 Vector [1] (Not currently used in SAE J1100)

H61-1: Effective Headroom -- Front [1]

H61-1: Effective Headroom -- Second [1]

H61-1V: Vertical component of H61-1

H61-2V: Vertical component of H61-2

H67-1: Undepressed Floor Covering Thickness -- Front [1]

H67-2: Undepressed Floor Covering Thickness -- Rear [1]

HC-1: Vertical Clearance from Top of Manikin (95th) to Headliner -- Front

HH-1: Vertical Distance from H111-1 Rocker Point to AHP

HR-1: Roof Panel Thickness at Driver H61-1 vector contact point

HV-1: Vertical Distance from Front SgRP to Roof Liner. (Used in field measurements)

HV-2: Vertical Distance from Second Row SgRP to Roof Liner (Used in field measurements)

HVD-1: Vertical Difference between HV-1 and HV-2 (*HV-2* - *HV-1*)

Y_a: Vertical Distance from AHP to Driver Ankle Point

Occupant / Internal Angle Parameters:

A40-1: Torso Angle -- Front [1]

A40-2: Torso Angle -- Second [1]

A42-1: Hip Angle -- Front [1]

A42-2: Hip Angle -- Second [1]

A44-1: Knee Angle -- Front [1]

A44-2: Knee Angle -- Second [1]

A46-1: Ankle Angle -- Front [1]

A46-2: Ankle Angle -- Second [1]

A47: Shoe Plane Angle [1]

A48-2: Floor Plane Angle -- Second [1]

A57-1: Thigh Angle -- Front [1]

A57-2: Thigh Angle -- Second [1]

Vehicle (External) Length Parameters:

a: Longitudinal Distance from Front Wheel Center (FWC) to Vehicle Center of Gravity (C_g)

b: Longitudinal Distance from C_g to Rear Wheel Center (RWC)

L101: Wheelbase Distance [1]

L102: Average Tire Diameter (Uncompressed) [1]

L102-1: Tire Size -- Front [1]

L102-2: Tire Size -- Rear [1]

L103: Vehicle Length [1]

L104: Overhang -- Front [1]

L105: Overhang -- Rear [1]

L113: Longitudinal Distance FWC to BOFRP [1]

L114: Longitudinal Distance FWC to SgRP -- Front [1]

L115-1: SgRP -- Front to RWC [1]

L115-2: SgRP -- Second to RWC [1]

L128-1: Wheel Centerline "X" Coordinate -- Front [1]

L128-2: Wheel Centerline "X" Coordinate -- Rear [1]

Vehicle (External) Width Parameters:

W101: Tread Width (Average of Front and Rear) [1]

W101-1: Tread Width -- Front [1]

W101-2: Tread Width -- Rear [1]

W102: Track Width (Average of Front and Rear) [1]

W102-1: Track Width -- Front [1]

W102-2: Track Width -- Rear [1]

W103: Vehicle Width Maximum (without Side Mirrors) [1]

W117: Vehicle Body Width at SgRP -- Front [1]

Vehicle (External) Height Parameters:

H100: Vehicle Height -- Body [1]

H101: Vehicle Height -- Maximum [1]

H111: Rocker Panel Height (Average of *H111-1* and *H111-2*) [1]

H111-1: Rocker Panel Height -- Front [1]

H111-2: Rocker Panel Height -- Rear [1]

H156: Ground Clearance [1]

H_{cg}: Vehicle C_g height from Ground

Vehicle (External) Angle Parameters:

A106-1: Angle of Approach [1]

A106-2: Angle of Departure [1]

A147: Ramp Breakover Angle [1]

δ_i: Maximum Inside Steer Wheel Angle (may be different for Right / Left turns)

δ_o: Outside Steer Wheel Angle for corresponding δ_i assuming Ackerman Steering

γ: Camber Angle (Nu)

Caster: Caster Angle

Toe: Toe Angle

Volume Parameters:

IV1: Passenger Vehicle Interior Volume Index [1]

PV: Total Passenger Volume Index [1]

PV1: Passenger Volume Index -- Front [1]

PV2: Passenger Volume Index -- Second [1] (Similarly for Additional Rows)

V1: Hidden Cargo Volume (Trunk) [1]

Area Parameters:

A_s: Vehicle Frontal Surface Area

F101: Vehicle Footprint (SAE) [1]

F101-EPA: Vehicle Footprint (EPA) [] (CFR 49)

S101: Windscreen Surface Area [1]

Radius (Radial) Parameters:

D102: Vehicle Wall-to-Wall Turn Radius [1]

D102-R: Vehicle Wall-to-Wall Turn Radius -- Right Turn [1]

D102-L: Vehicle Wall-to-Wall Turn Radius -- Left Turn [1]

R-CTC: Curb-to-Curb Turn Radius

R-CTC-R: Curb-to-Curb Turn Radius -- Right Turn

R-CTC-L: Curb-to-Curb Turn Radius -- Left Turn

R-OT: Vehicle Outside Track Turn Radius

R-OT-R: Vehicle Outside Track Turn Radius -- Right Turn

R-OT-L: Vehicle Outside Track Turn Radius -- Left Turn

Vehicle Mass Parameters:

M_{Accel}: Vehicle Acceleration Test Mass

M_{Batt}: Vehicle Battery Mass (for Hybrids)

M_{BiW}: Body in White Mass

M_{Cls}: Closure Mass (Doors, Hood, Decklid/Liftgate)

M_{Curb}: Vehicle Curb Mass

M_{Drv}: Driveline Mass

M_{Eng}: Engine Mass

M_{EPA}: EPA Mileage Vehicle Test Mass

M_{gwvr}: Gross Vehicle Weight Rating

M_{Int}: Vehicle Interior Mass

M_{Motor}: Mass of Electric Traction Motor (Hybrid / Electric Vehicles)

M_{Prop}: Mass of Prop Shaft (Rear Wheel Drive and All-Wheel Drive)

M_{Susp}: Mass of Vehicle Suspension

M_{Trans}: Transmission Mass

M_{Uncat}: Mass of "Uncategorized" Vehicle Subsystem

Engine and Driveline Parameters:

Cyl_Bank_Ang: Cylinder Bank Angle

Cyl_Bore:	Cylinder Bore (Diameter)
Cyl_Dist:	Cylinder Spacing Distance (Center to Center) (Note that Some Engines do not have uniform cylinder spacing along a bank of cylinders)
Cyl_Stroke:	Cylinder Stroke Distance
Cyl_Volume:	Per-Cylinder Volume
Cyl_Wall_Thick:	Average Cylinder Wall Thickness
CL-1:	Engine Cylinder Span
EL-1:	Engine Length
Eng_Displ:	Engine Displacement (Total Cylinder Volume in Liters)
Eng_kW	Peak Engine Power in kW
Eng_Spec_Power:	Engine Specific Power (kW / Liter Displacement)
Eng_Spec_Torque:	Engine Specific Torque (Nm / Liter Displacement)
Eng_Spec_Volume:	Engine Specific Volume (kg / Liter Displacement)
Eng_Spec_Weight:	Engine Specific Weight (kg / kW)
Eng_Torque:	Engine Peak Torque (Nm)
Power_to_Torque:	Engine Peak Power to Peak Torque Ratio (kW / Nm)
R_{BS}:	Ratio of Bore to Stroke
Trans_Max_Torque:	Transmission Maximum Torque Rating (Nm)
$V_{Cylinder}$:	Cylinder Volume

Hybrid Vehicle Motor / Battery Parameters:

Motor_Torque: Peak Traction Motor Torque (Nm)

Batt_kWh: High-Voltage Battery Capacity (kWh -- kiloWatt-hour)

Wheel / Tire Parameters:

Tire_Aspect: Ratio of Tire Wall Height to Tire Width

Tire_Diameter: Nominal Rim Diameter in Inches

Tire_Width: Tire Width

Vehicle Performance Target Parameters:

T_0_30_mph_Electric:	All-Electric 0 to 30 mph Acceleration Time (sec)
T_0_60_mph_IC:	IC Engine 0 to 60 mph Acceleration Time (seconds)
T_0_60_mph_Comb:	Combined Electric/IC Engine 0 to 60 mph Acceleration Time (seconds)
T_0_100_kph_IC:	IC Engine 0 to 100 kph Acceleration Time (sec)
T_0_100_kph_Comb:	Combined Electric / IC Engine 0 to 100 kph Acceleration Time (seconds)
T_60_mph_0_Brake:	60 mph to 0 Vehicle Braking Distance (meters)
T_70_mph_0_Brake:	70 mph to 0 Vehicle Braking Distance (meters)
T_Cargo_V1_Liter:	V1 Hidden Cargo Volume (liters)
T_Front_Crash_g:	Front NCAP Maximum Crash g's (by NCAP Star Rating)
T_Elec_Max_Vel:	All-Electric Vehicle Maximum Velocity (kph)

T_Elec_Range: All-Electric Vehicle Maximum Range (kph) (Using UDDS cycle)

T_EPA_MPGC: EPA Combined (UDDS and FWFET) Fuel Economy (mpg)

T_Frt_Weight_Dist_Pct: Front Weight Distribution (Percentage)

T_Max_Vel: Vehicle Maximum Velocity (kph)

T_Turn_Rad_CTC: CTC Turn Radius (Assumes same value for Right / Left Turns)

T_Turn_Radius_WTW: WTW Turn Radius (Assumes same Left / Right)

T_Lateral-g: Maximum Lateral g's (future use)

Vehicle Coefficient / Ratio Parameters

Cd: Vehicle Drag Coefficient

Cg_Ratio: Ratio of Cg distance "a" to Wheelbase L101 (L101 = a + b)

F_r: Tire Rolling Resistance Coefficient

μ: Tire Friction Coefficient ("Mu")

η_{t2w}: Tank to Wheel Efficiency ("Eta")

η_{b2w}: Battery to Wheel Efficiency ("Eta")

Coordinate Parameters (X: Longitudinal, Y: Lateral, Z: Vertical Axis)

Cg_X_Macc: Vehicle Acceleration / Braking Test Mass C_g X-Coordinate

Cg_X_Batt: Vehicle Battery (for Hybrids) C_g X-Coordinate

Cg_X_BiW: Vehicle Body in White C_g X-Coordinate

Cg_X_Cls: Vehicle Closure Subsystem C_g X-Coordinate

Cg_X_Drv: Vehicle Driveline Subsystem C_g X-Coordinate

Cg_X_Eng: Engine C_g X-Coordinate

Cg_X_Int: Interior Subsystem C_g X-Coordinate

Cg_X_Mcurb: Vehicle Curb Mass C_g X-Coordinate

Cg_X_Motor: Vehicle Traction Motor C_g X-Coordinate

Cg_X_Prop: Vehicle Prop Shaft C_g X-Coordinate

Cg_X_Susp: Vehicle Suspension Subsystem C_g X-Coordinate

Cg_X_Trans: Vehicle Transmission C_g X-Coordinate

Cg_X_Uncat: Uncategorized Subsystem C_g X-Coordinate

Cg_Z_Batt: Vehicle Battery C_g Z-Coordinate (future use)

Cg_Z_BiW: Vehicle Body-in-White C_g Z-Coordinate (future use)

Cg_Z_Cls: Closure Subsystem C_g Z-Coordinate (future use)

Cg_Z_Drv: Driveline Subsystem C_g Z-Coordinate (future use)

Cg_Z_Eng: Engine C_g Z-Coordinate (future use)

Cg_Z_Int: Interior Subsystem C_g Z-Coordinate (future use)

Cg_Z_Macc: Vehicle Acceleration / Braking Test Mass C_g Z-Coordinate
(Currently assumed = 0.39 * *H100*)

Cg_Z_Mcurb: Vehicle Curb Mass C_g Z-Coordinate
(Currently assumed = 0.39 * *H100*)

Cg_Z_Motor: Traction Motor C_g Z-Coordinate (future use)

Cg_Z_Prop: Prop Shaft C_g Z-Coordinate (future use)

Cg_Z_Susp: Suspension Subsystem C_g Z-Coordinate (future use)

Cg_Z_Trans: Transmission C_g Z-Coordinate (future use)

Cg_Z_Uncat: Uncategorized Subsystem C_g Z-Coordinate (future use)

Coordinate Systems Used in this Work

Coordinate X-Axis Reference Systems:

Coord_X_BOFRP: Uses Ball of Foot Reference Point as "X" Origin

Coord_X_FWC: Uses Front Wheel Centerline (FWC) as "X" Origin

Coord_X_Front: Uses Front of Vehicle as "X" Origin (not currently used)

Coordinate Y-Axis Reference Systems:

Coord_Y_CL: Uses Vehicle Longitudinal Centerline as "Y" Origin

Coordinate Z-Axix Reference Systems:

Coord_Z_Grd: Uses Ground Reference as "Z" Origin

Appendix B
Development of a Consistent Continuum of Vehicle Dimensional Parameters for Optimization and Simulation

Introduction

Parametric vehicle modeling permits rapid iteration and optimization of vehicles in the conceptual design phase. A significant portion of vehicle design can be optimized parametrically without knowing specific Computer Aided Design (CAD) based details. Many overall vehicle characteristics can be assessed and improved at the parametric level. Vehicle performance can also be determined to a high level of confidence.

In developing vehicle dimensions for a parametric model it is recommended to build up a vehicle using an "inside-out" approach centered on effective, knowledge-based occupant packaging. This appendix develops a continuum of dimensional parameters which tie vehicle internal and external dimensions together; it employs a combination of industry standard and author-defined component dimensions, which make up overall vehicle outside dimensions.

In order to develop and optimize models for a desired vehicle type and size class, a knowledge base of vehicle typical values for key dimensional parameters has been compiled using a combination of data sources and field measurements. These values provide a useful starting point for the vehicle design and optimization process. They also increase optimization effectiveness, reducing the likelihood of local minima / maxima, and ensure that the optimization begins within a valid design space.

Typical vehicle parametric models are a series of relationships based on a specified set of vehicle dimensional and functional components such as length, width,

height and engine power. From a reasonable set of parameters, the majority of vehicle characteristics and performance to desired targets can be assessed and improved.

The results shown in this appendix serve to:

• Provide a continuum of consistent length, width and height parameters, which make up overall vehicle length, width and height dimensions.

• Provide a series of relationships, which logically tie the vehicle interior and exterior design together and identify candidate design variables for parametric vehicle optimization.

• Using sedans (3-box design) as an example vehicle class, provide typical / average values of key parameters by vehicle size category to serve as a valid starting point for parametric vehicle optimization.

The continuum of parameters developed in this appendix ties the interior and exterior vehicle dimensions together in a proper relationship and develops overall vehicle length, width and height as the sum of realistic component dimensions. Typical values for a number of component dimensional parameters by vehicle type are shown as they are discussed.

It should be noted that other combinations of subordinate dimensions and relationships can be developed and used to build up overall vehicle length, width and height. The combination of parameters selected for use in this work is specific to desired vehicle optimization goals and available data. Tabulated values in this work are derived from a number of sources, including public and private vehicle databases, public

documents such as Motor Vehicle Manufacturer's Association data sheets and field measurements [54, 52, 51, 55, 56].

Occupant related measures discussed in the results utilize an SAE standard 95th percentile male manikin for occupant positioning [57]. This work only addresses positioning of the 95th percentile manikin in parametric optimization; the SAE H-point manikin is used in determining legroom (L34, L51-2), headroom (H61-1), passenger volume and other standard industry measures. Designing for the largest occupant envelope ensures that other occupant ranges (male / female, 50th percentile, 5th percentile) can be accommodated; optimizing for all possible occupant sizes and proportions, however, requires additional steps to ensure that joint comfort angles, driver vision and similar imperatives are met for each occupant size.

Continuum of Parameters

Key longitudinal vehicle dimensions of interest in this work are shown in Figure B.1 [1, 54]. Dimensions are defined below as their relationships are delineated. Dimensional values are given in meter units unless otherwise noted.

The driver ball of foot reference point (BOFRP) to first row seating reference point (SgRP) distance L99 is determined from the height of the driver accelerator heel point (AHP) to driver SgRP H30-1 shown in Figure B.2 [1, 54].

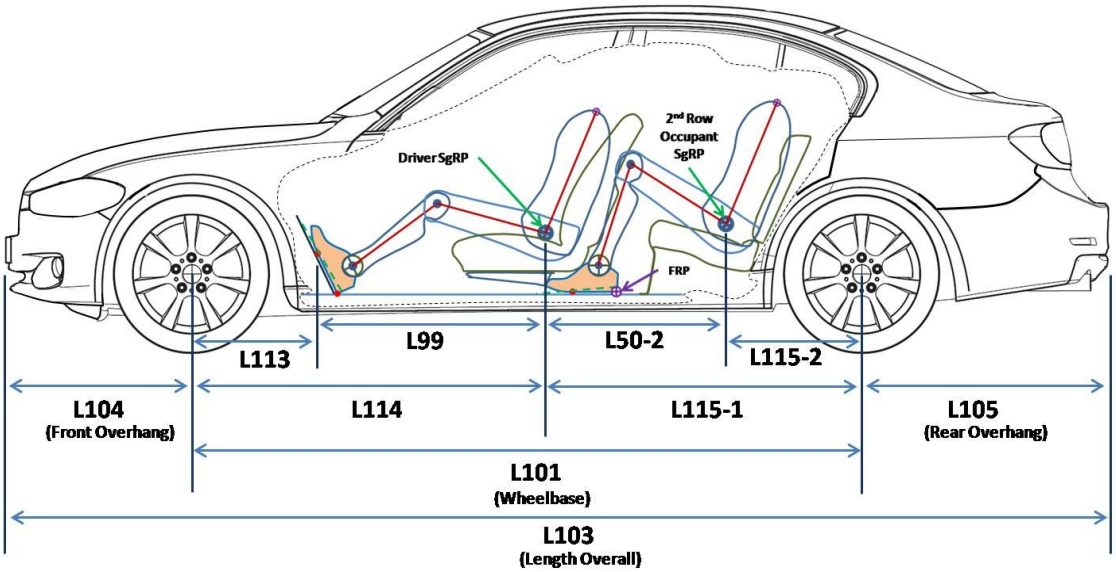

Figure B.1 SAE J1100 Standard Vehicle Longitudinal Dimensions (Terms/Abbreviations Defined Below) [1, 54]

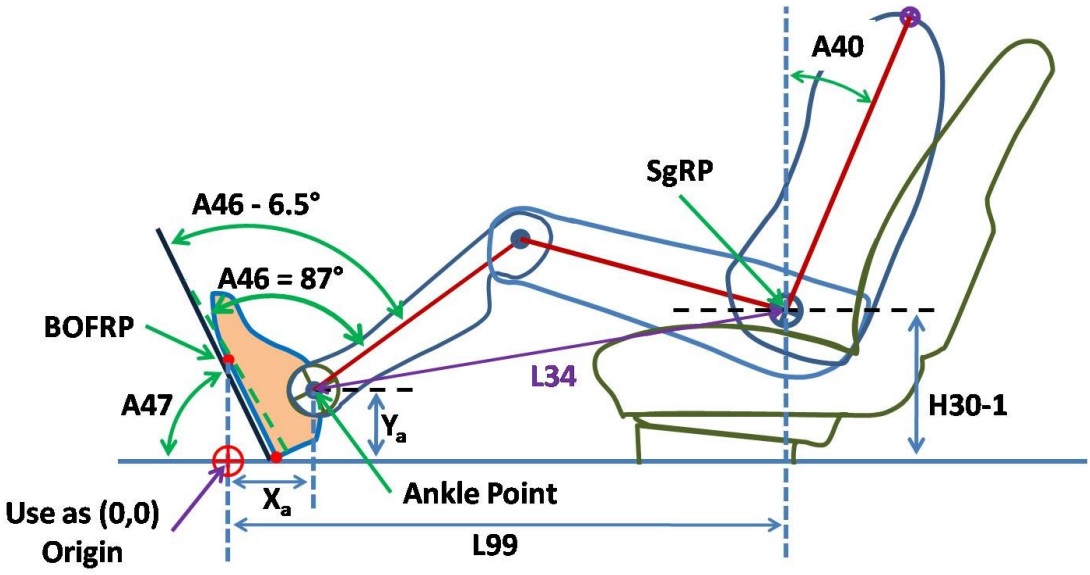

Figure B.2 Seated Driver Geometry for Calculation of L99-1 and L34 (Abbreviations Defined Below) [1, 54]

Calculation of the distance L99 in meters for a 95th percentile male is based on the geometry shown in Figure B.2 using an ankle angle A46 of 87° as the minimum angle

which meets comfort limits [58]. The resulting calculation of L99 is given in Equation (B.1) which is converted from millimeter to meter units from SAE J1517 [54, 59]:

$$L99 = 0.9137 + 0.67231 \cdot (\text{H30-1}) - 1.94433 \cdot (\text{H30-1})^2 \text{ meters} \qquad \text{Equation (B.1)}$$

Driver legroom L34 can then be determined from the relationships shown in Figure B.2 and known 95th percentile male manikin dimensions [1, 54, 58, 57]. Accurate initial estimates can be determined through average values of driver seat height H30-1 and driver accelerator shoe plane angle A47 by vehicle type. Average values of H30-1 by vehicle type are shown in discussion of height parameters. Driver legroom L34 is used in the calculation of first row passenger volume PV1 [1].

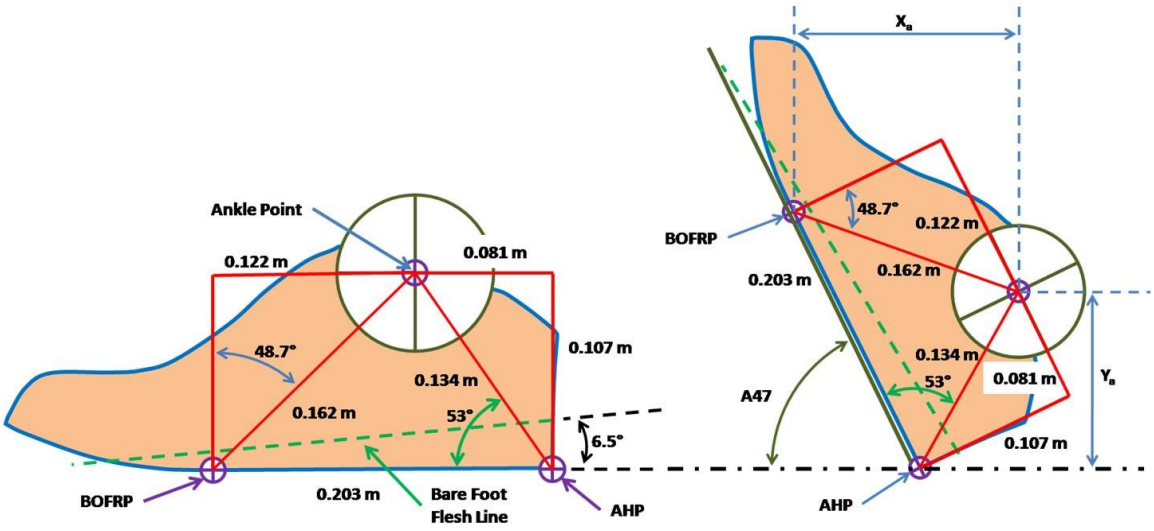

Figure B.3 Shoe Dimensions and Ankle Point Position for 95th Percentile Male Manikin [1,54, 58, 57]

If the foot is rotated by angle A47 for positioning on the accelerator pedal as shown in Figure B.3, the values of X_a and Y_a (not SAE dimensions) from the origin shown in Equation (B.2) and Equation (B.3) are [54, 58, 57]:

$$X_a = 0.162 \cdot \sin(A47 + 48.7°) \text{ metres} \quad \text{Equation (B.2)}$$

$$Y_a = 0.134 \cdot \sin(A47 + 53.0°) \text{metres} \quad \text{Equation (B.3)}$$

X_a and Y_a are the ankle point X- and Y-distance from the Ball of Foot Reference Point (BOFRP) and A47 is the shoe plane angle in degrees. With known values for H30-1, X_a, Y_a and L99, driver legroom L34 (in meters) as defined in SAE J1100 can be calculated as [1, 54]:

$$L34 = \sqrt{(L99 - X_a)^2 + ([H30\text{-}1] - Y_a)^2} + 0.254 \text{ metres} \quad \text{Equation (B.4)}$$

If typical values of A47, H30-1 and L99 are used by vehicle type, the resulting values for L34 are shown in Table B.1 [54, 58].

Vehicle Type	**Typical A47 (Degrees)**	**Range of H30-1 (meters)**	**Typical H30-1 (meters)**	**Typical L99-1 (meters)**	**Typical L34 (meters)**
Sports Car	**71.0**	**0.130 - 0.200**	**0.175**	**0.971**	**1.087**
Passenger Car	**64.0**	**0.230 - 0.270**	**0.250**	**0.960**	**1.075**
Minivan / Sport Utility Vehicle (SUV)	**55.0**	**0.270 - 0.400**	**0.325**	**0.926**	**1.048**

Table B.1 Typical A47, H30-1, L99-1 and L34 Values by Vehicle Type [54, 58]

Angles relevant to calcuation of length parameters shown shown in Figure B.4.

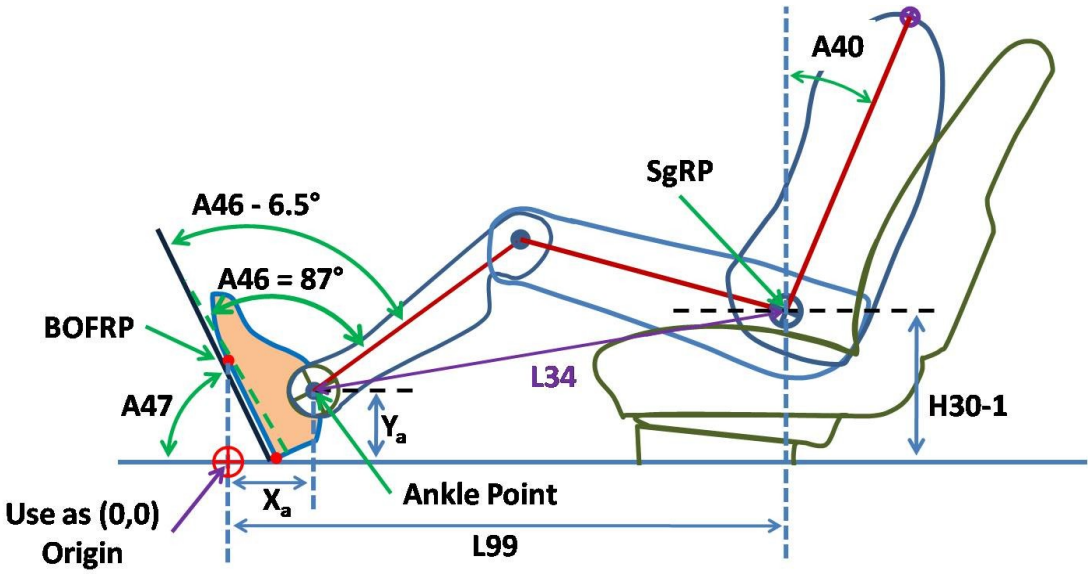

Figure B.4 Occupant Dimensions and Angles for L34 and L99-1 Calculation [1, 54]

A40**:** Torso Angle, measured from vertical (has a value between 15° and 40° for Class A vehicles) [1].

Typical Values for the torso angle A40 are shown in Table B.2

Vehicle Type:	**Torso Angle A40 (Degrees)**
Sports Car	**25**
Passenger Car	**22**
Minivan/MPV, SUV	**21**

Table B.2 Typical Values for Torso Angle A40 by Vehicle Type [58]

A46: Ankle Angle (Angle from Bare Foot Flesh Plane in Shoe to Tibia Axis).

- The minimum comfort angle for A46 is 87°.
- The maximum comfort angle for A46 is 130°.

(A46 – 6.5°): Ankle Angle with the Bare Foot Flesh Plane Angle of 6.5° subtracted.

A47: Shoe Plane Angle

First to second row coupling distance L50-2 may be used as an engineering design variable in the development of a vehicle; second row legroom L51-2 and other dimensions are a result of the selected value of L50-2. The value of L50-2 can result in three types of coupling: short coupling, standard coupling and long couplingas defined in SAE J1100 [1].

Short Coupling occurs when the selected value of L50-2 results in the 2nd row H-Point device (dimensional assessment dummy) interfering with the seat in front of it. The shoe is located as far forward as possible without interference. An example of short coupling is shown in Figure B.5. (If the 2nd row occupant shoe cannot fit in the foot well, the Floor Reference Point "FRP" is located at the rearmost level point in the foot well).

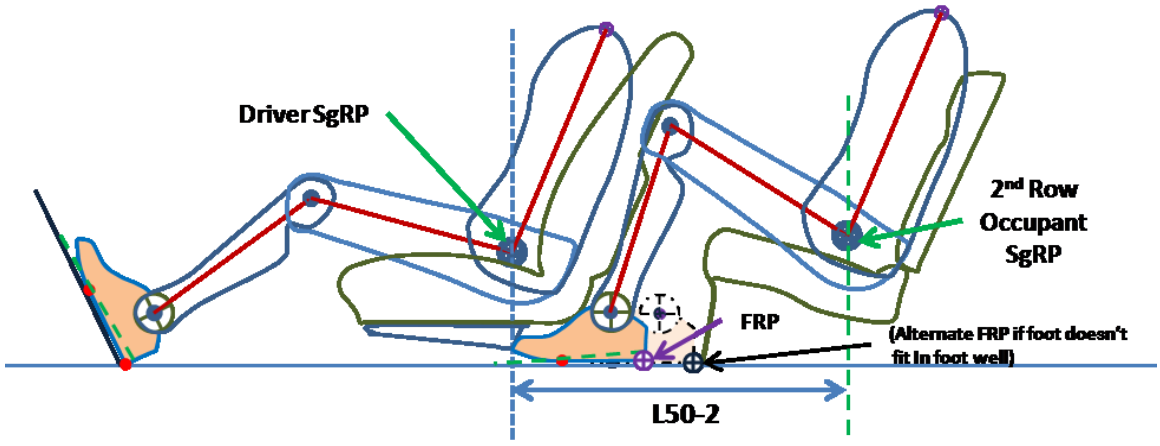

Figure B.5 Short-Coupled Seating (FRP: Floor Reference Point, SgRP: Seating Reference Point) [1, 54]

Standard Coupling as shown in Figure B.6 occurs when the design value of L50-2 is such that the H-Point occupant device can be placed without interference with the seat in front of it and the ankle angle is between 78° and 130° (ankle angle comfort limits).

The Floor Reference Point is located at the occupant heel point.

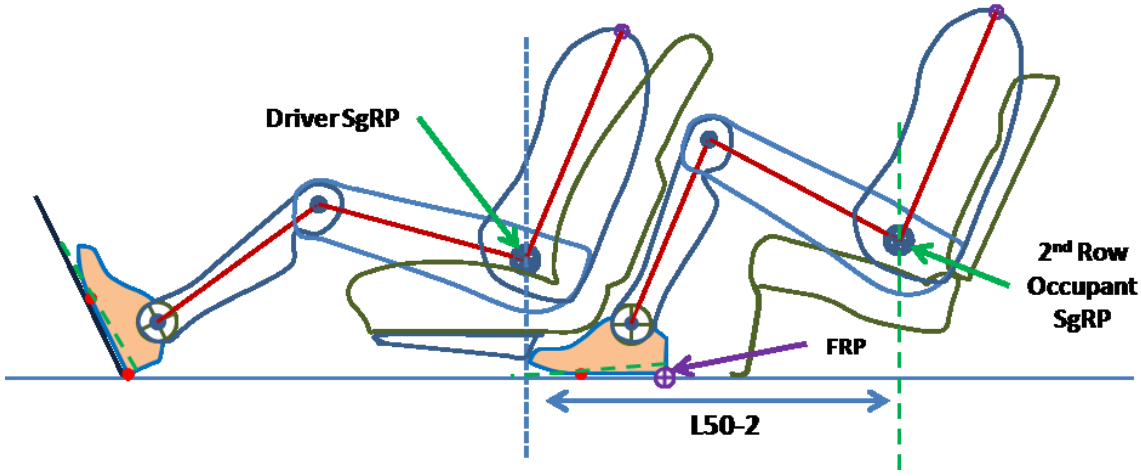

Figure B.6 Standard Coupling (FRP: Floor Reference Point, SgRP: Seating Reference Point)[1, 54]

Long coupling occurs when the second row ankle angle A46-2 will exceed 130° when placing the shoe as far forward as possible in the foot well. In this case the forward-most shoe location without interference is noted and the ankle angle is set at 130° for the comfort limit. The FRP is at the heel point with the ankle angle set at 130°. The difference in the two shoe locations is ΔX_{LC} as shown in Figure B.7.

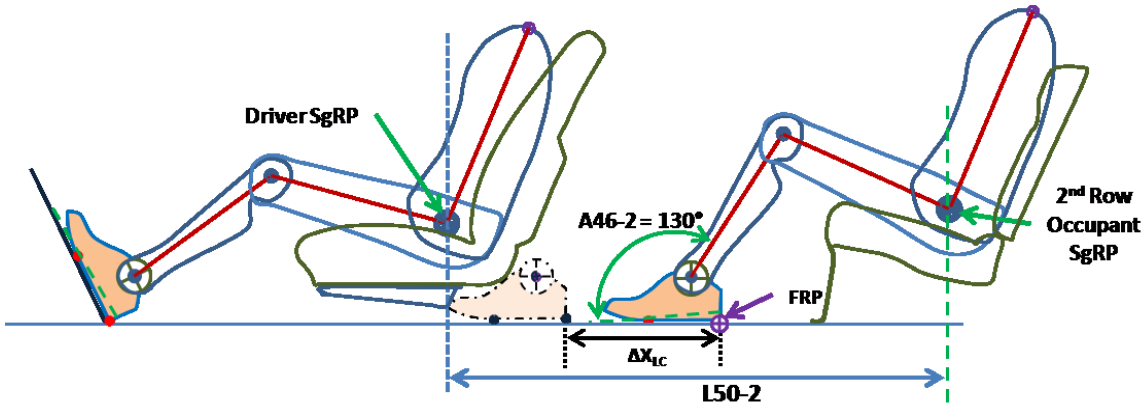

Figure B.7 Long Coupling (FRP: Floor Reference Point, SgRP: Seating Reference Point) [1] [54]

With the exception of Long Coupling, the FRP as located in the above coupling

scenarios determines the final value of the second row legroom (L51-2) measure. If optimization of L50-2 as a design variable is not desired, the statistical average value for a vehicle class/type may be used instead for this dimension as shown in Table B.3.

Vehicle Type	Samples	Average L50-2 (meters)	Std. Deviation for L50-2 (meters)
Large Minivan	2	0.937	0.049
Large Traditional SUV	-	-	-
Large Sedan/Coupe	5	0.846	0.081
Large Sedan	3	0.882	0.000
Large Coupe	2	0.792	0.128
Midsize Traditional SUV	1	0.715	-
Midsize Sedan/Coupe	24	0.816	0.029
Midsize Sedan	17	0.818	0.029
Midsize Coupe	7	0.812	0.029
Midsize Wagon	1	0.786	-
Compact Sedan/Coupe	33	0.753	0.021
Compact Sedan	21	0.750	0.023
Compact Coupe	12	0.758	0.016
Subcompact Traditional SUV	-	-	-
Subcompact Sedan/Coupe	24	0.681	0.056
Subcompact Sedan	4	0.724	0.023
Subcompact Coupe	23	0.673	0.057
Small Wagon	2	0.736	0.008
Mini-Compact Traditional SUV	-	-	-
Mini-Compact Coupe	3	0.573	0.094
2-Seater Sports Car/Roadster	N/A	N/A	N/A

Table B.3 L50-2 Average Values by Vehicle Type [54, 52]

The couple type affects the location of the second row Floor Reference Point (FRP) in calculating second row legroom L51-2. Only standard coupling (Figure B.6) is

addressed in this work. As previously discussed, L50-2 is a suitable candidate for use as a design variable in vehicle design optimization. Average values for typical sedan size classes shown in Table B.4 can be used as an optimization starting point [54, 52].

For a given value of L50-2, Second row legroom L51-2 can be calculated using the relationships for a 95th percentile male manikin as shown in Figure B.8 [1, 54]. H30-2 is second row seat height. The coupling offset ΔS is the distance from the driver SgRP to the toe of the second row manikin shoe; this value can be positive or negative depending on the seat design [1, 54, 58].

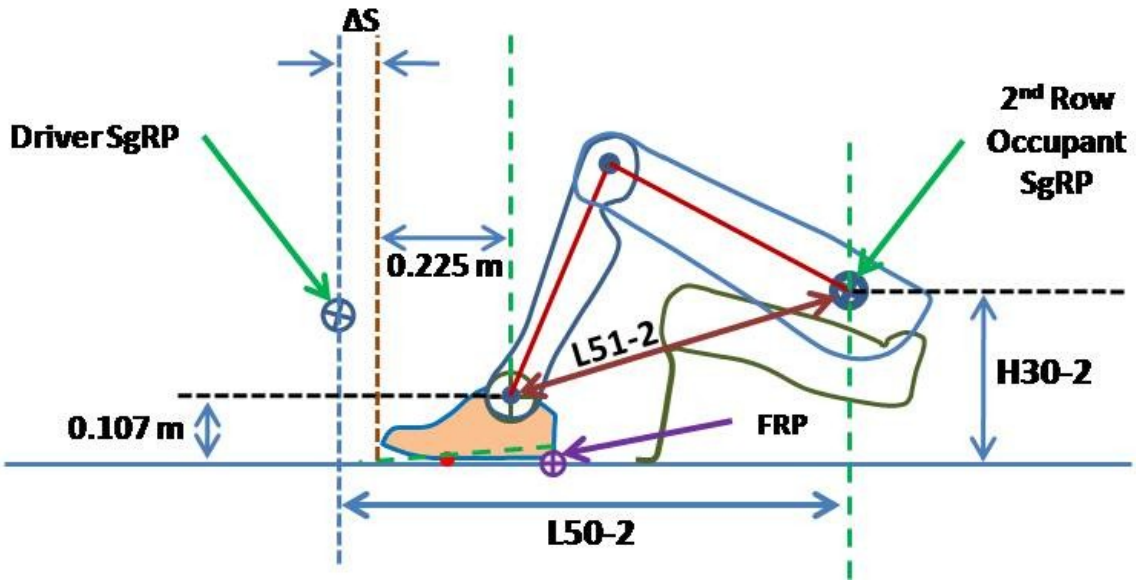

Figure B.8 Second Row Geometry for L51-2 Calculation [1, 54]

The resulting calculation of L51-2 is shown in Equation (B.5) [1, 54].

$$\text{L51-2} = \sqrt{(\text{L50-2} - 0.225 - \Delta S)^2 + (\text{H30-2} - 0.107)^2} + 0.254 \text{ meters} \quad \text{Equation (B.5)}$$

For vehicles with a third row of seating, second to third row coupling (L50-3) and third row effective legroom (L51-3) can be determined in the same manner as shown

above for L50-2 and L51-2 [1]. L51-2 is used in calculating second row passenger volume PV2. Note that longitudinal occupant packaging dimensions for manikins other than 95th percentile males can be similarly calculated using the desired size / gender manikin component dimensions in the parametric models.

Wheel diameter L102 (Figure B.9) is used in calculating minimum values for front wheel centre to ball of foot reference point L113 and second row SgRP to rear wheel centre L115-2 [1, 54]. Dimension L102-1 designates front wheel diameter, L102-2 the rear wheel diameter [1].

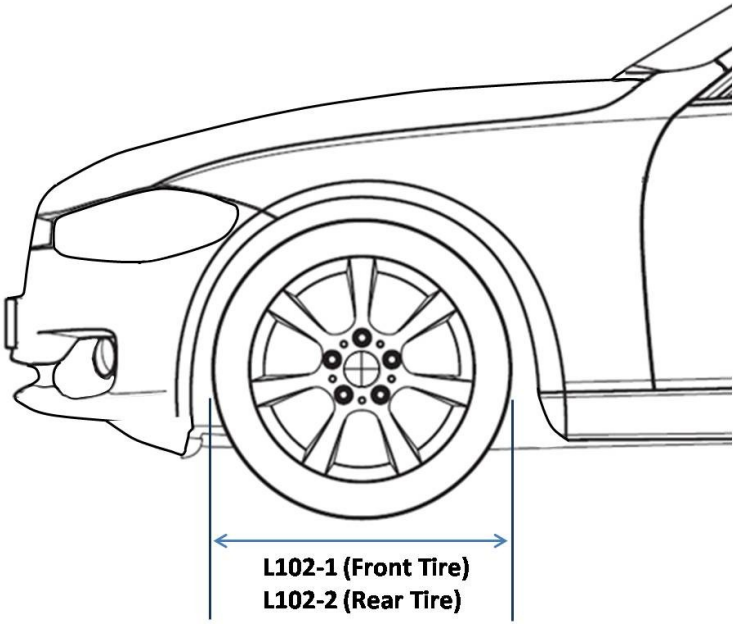

Figure B.9 Longitudinal Tire Dimensions [1,54]

Distance L113 affects vehicle centre of gravity location, frontal crash safety, wheelhouse clearance and other target-related parameters. This makes it a candidate for use as a design variable in vehicle design optimization. While no direct correlation of L113 to other dimensional parameters has been found by the author, surveys of vehicle

datas how that L113 is generally greater than the wheelhouse radius plus a desired tire-to-wheelhouse clearance distance [54, 52]. As L113 is a component of vehicle overall length (L103), which impacts vehicle curb mass, L113 should typically be made as small as possible while still meeting clearance, packaging, safety and turn radius imperatives. Average values for L113 and for L113 less the tire radius are shown in Table B.4 [52, 54].

Vehicle Type	Samples	Average Front Tire Diameter (meters)	Average L113 (meters)	Average of L113 - Tire Radius (meters)	Std. Deviation σ for difference (meters)
Large Sedan	**3**	**0.693**	**0.588**	**0.242**	**0.005**
Midsize Sedan	**16**	**0.633**	**0.398**	**0.082**	**0.049**
Compact Sedan	**17**	**0.610**	**0.373**	**0.068**	**0.042**

Table B.4 Average Values for L113 and L113 Less Tire Radius [52, 54]

As with L113, the second row SgRP to rear wheel centre distance L115-2 is suitable for use as an optimization design variable. As shown in Table B.5, L115-2 is typically greater than rear tire radius plus a clearance distance [54, 52]. For both L113 and L115, snow chain clearance is a consideration which is addressed in snow chain standard NACM-92805 [60]. For L113, additional clearance for maximum wheel turn angle must also be considered.

Vehicle Type	Samples	Average Rear Tire Diameter (meters)	Average L115-2 (meters)	Average of L115-2 - Tire Radius (meters)	Std. Deviation σ for difference (meters)
Large Sedan	**3**	**0.693**	**0.515**	**0.168**	**0.005**
Midsize Sedan	**17**	**0.607**	**0.496**	**0.193**	**0.062**
Compact Sedan	**19**	**0.605**	**0.466**	**0.164**	**0.050**

Table B.5 Average Values for L115 and L115 Less Tire Radius [52] [54]

From the above dimensions, vehicle wheelbase L101 can be expressed as [1]:

$$L101 = L113 + L99 + L50\text{-}2 + L115\text{-}2 \qquad \text{Equation (B.6)}$$

Front vehicle overhang L104 will largely be determined by space requirements for engine bay packaging and front crush space to meet crash safety requirements. Rear overhang L105 will be a function of desired rear cargo storage space (V1) in addition to rear crash safety concerns. Reasonable starting values for L104 and L105 in vehicle optimization can be estimated from existing vehicle data.Using MVMA data sheets, average ratios for L101, L104 and L105 versus L103 specific to sedan size classes are shown inTable B.6 [52, 54].

Sedan Size Class	Average Ratio L101 / L103	L101 / L103 Std. Dev. σ	Average Ratio L104 / L103	L104 / L103 Std. Dev. σ	Average Ratio L105 / L103	L105 / L103 Std. Dev. σ
Large	**0.544**	**0.003**	**0.192**	**0.003**	**0.264**	**0.001**
Midsize	**0.557**	**0.016**	**0.214**	**0.013**	**0.229**	**0.015**
Compact	**0.576**	**0.023**	**0.210**	**0.011**	**0.215**	**0.017**

Table B.6 L101, L104 and L105 vs. L103 [52] [54]

This provides a starting value for optimization of front overhang L104 and rear overhang L105. Cargo volume estimation for sedans (and conversely, the minimum value of L105 for a prescribed cargo volume) is addressed after discussion of vehicle width parameters.

Outside vehicle width dimensions of interest are shown in Figure B.10 [1, 54]. Using correlations derived from Motor Vehicle Manufacturer's Association (MVMA) data sheets, an initial estimation of maximum vehicle width without mirrors W103 can be derived from vehicle outside width at the driver SgRP point W117 [54, 52].

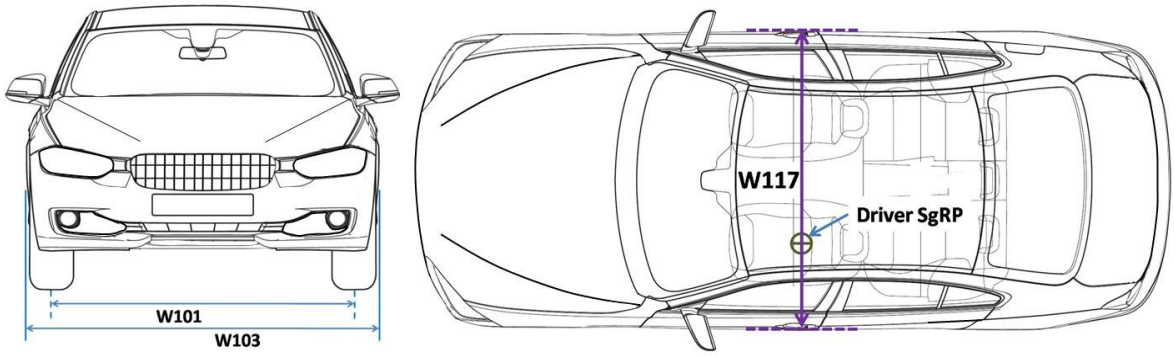

Figure B.10 Vehicle External Width dimensions [1, 54]

Vehicle width is used in calculations of vehicle frontal surface area (A_s) and vehicle volume / mass. While maximum body width (W116) is a more appropriate measure to use in these calculations, it is difficult to find vehicle data which includes W116. Maximum vehicle width (W103) is readily available in literature and vehicle databases for the majority of passenger vehicles. In this work W103 is used in place of W116, accepting the resulting difference in calculations of width, vehicle surface area and vehicle mass. This difference should be manageable due to current trends toward

flush or recessed door hardware and reduced use of moldings and cladding in vehicle design.

Correlations have been derived in this work using information found in Motor Vehicle Manufacturer's Association (MVMA) vehicle data forms for numerous vehicles [52]. These relationships have been developed as shown in Table B.7. Relationships for vehicles not found in the above sources (such as Crossover SUV's) must be extrapolated from known correlated vehicle classes. [51, 52, 54].

Vehicle Class	Samples	Correlation Equation (m)	Correlation R^2
All Vehicles	**112**	**W103 = 0.960 * W117 + 0.048 m**	**0.916**
Passenger (non-SUV / Truck / Minivan)	**107**	**W103 = 0.964 * W117 + 0.041 m**	**0.923**
Sedans	**47**	**W103 = 0.954 * W117 + 0.063 m**	**0.944**
Coupes	**48**	**W103 = 0.934 * W117 + 0.930 m**	**0.913**
2-Seater Sports Car / Roadster	**10**	**W103 = 1.110 * W117 - 0.222 m**	**0.924**
SUV/Truck/Minivan	**9**	**W103 = 1.155 * W117 - 0.324 m**	**0.959**

Table B.7 Correlation of W103 to W117 by vehicle type [52, 54}

Vehicle tread width W101 and track width W102 are shown in Figure B.11 along with camber angle γ [1, 54].

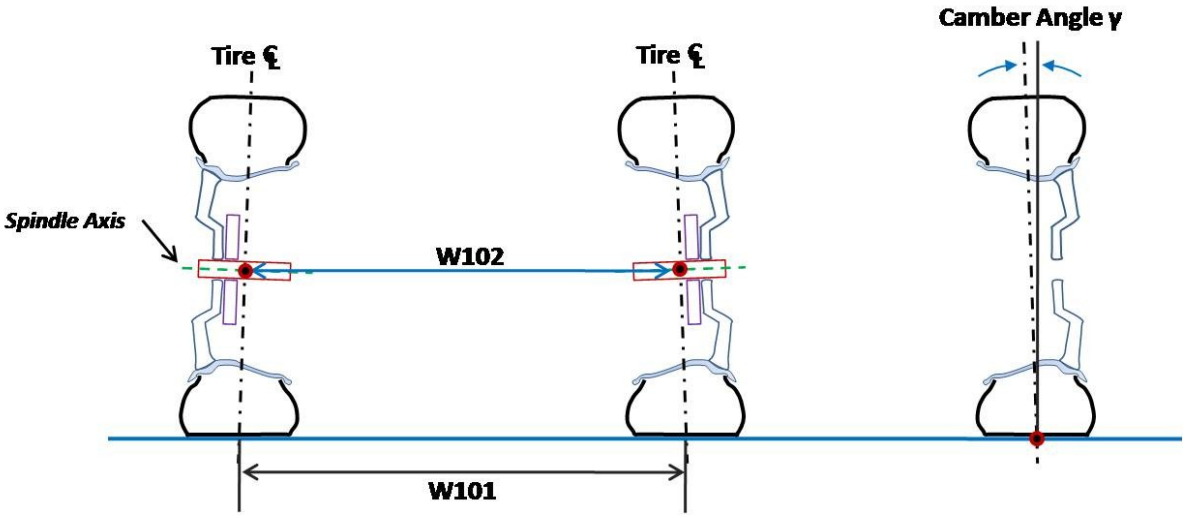

Figure B.11 W101, W102 and Camber Angle [1, 54]

Once a value for W103 is established, typical vehicle tread width W101 can be estimated from a correlation based on 2160 passenger vehicles from a NHTSA databaseshown in Table B.8 [51, 54].

Vehicle Class	**Samples**	**Correlation Equation (m)**	**Correlation R^2**
Passenger Vehicles	**2160**	**W101 = 0.664 * W103 + 0.310 m**	**0.822**
Passenger Vehicles	**2160**	**W101 = 0.842 * W103 m**	**0.763**

Table B.8 Correlation of W101 to W103 for Passenger Vehicles [51] [54]

Tread width is the lateral distance between tire tread centres; track width is the lateral distance between wheel centres.Tread width W101 and track width W102 are occasionally used interchangeably or confused with each other. They are used in determining vehicle footprint, vehicle turn radius and various vehicle dynamics measures. For a given front or rear axle, tread width for a tire of radius "***r***" can be expressed as (ignoring tire deflection) [1, 54]:

$$W101 = W102 + 2 \cdot r \cdot \sin \gamma$$ Equation (B.7)

For a camber angle of 0°, W101 and W102 will be equal to each other. The typical difference between W101 and W102 was examined for several vehicle classes. Results are shown inTable B.9 [54, 52].

Vehicle Class	**Samples**	**Average Camber Angle (degrees)**	**Standard Deviation of Camber Angle (degrees)**	**Average Difference *W101 - W102* (m)**	**Standard Deviation of Average Difference *W101 - W102* (m)**
Large Sedan / Coupe	**5**	**0.32**	**0.44**	**0.005**	**0.005**
Midsize Sedan / Coupe	**24**	**0.21**	**0.36**	**0.004**	**0.004**
Compact Sedan / Coupe	**35**	**0.03**	**0.57**	**0.001**	**0.005**

Table B.9 Vehicle Camber Angle and Influence on W101 [52, 54]

SAE J1100defines vehicle footprint F101 as the product of wheelbase L101 and tread width W101 as shown in Figure B.12 [1, 54]. The U.S. National Highway and Traffic Safety Administration (NHTSA) and Environmental Protection Agency (EPA) fuel economy regulations define vehicle footprint in 49 CFR 523.2 as the product of wheelbase L101 and track width W102, rounding track width to the nearest tenth of an inch (0.003 meters) [61]. For most vehicles the average difference between W101 and W102 will be less than or equal to 0.005 meters, with the majority of vehicles having a difference less than or equal to 0.01 meters. This results in an average error of up to 0.3% for a vehicle with a track width of 1.5 meters; the majority of vehicles will vary by less than 0.7% if W101 and W102 are used interchangeably. The decision to include

camber angle in parametric vehicle models will depend on selected optimization targets in addition to the level of detail and accuracy desired in modeling and optimization results.

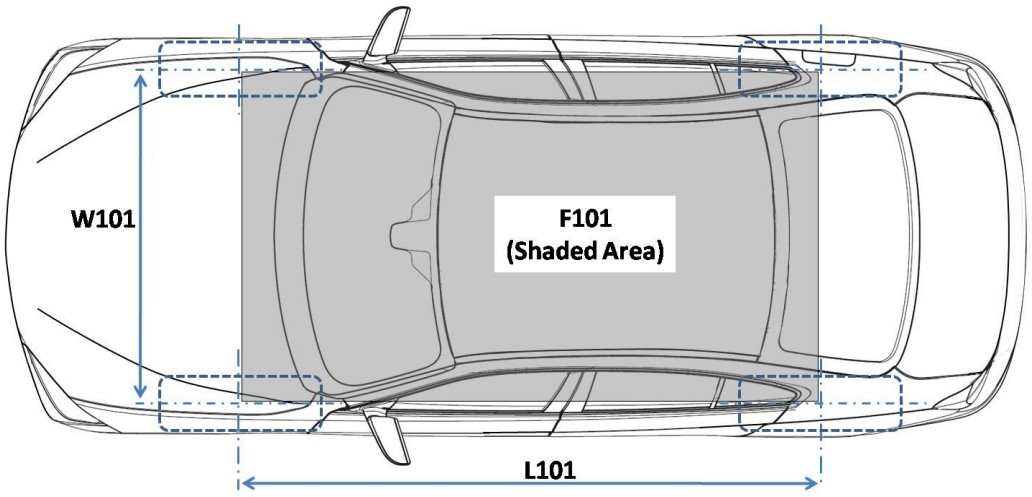

Figure B.12 SAE J1100 Vehicle Footprint F101 [1, 54]

Vehicle internal width dimensions (SAE J1100 and author-defined) are shown in Figure B.13 [1, 54, 58].

It is important to ensure that the component dimensions which add up to overall vehicle width W103 are consistent in their relationships and construction using an "inside out" approach beginning with occupant-based dimensions.

At the driver SgRP, width dimension W117 is the sum of interior vehicle dimensions [1, 54]:

$$W117 = W3\text{-}1 + 2 \cdot WB\text{-}1 \qquad \text{Equation (B.8)}$$

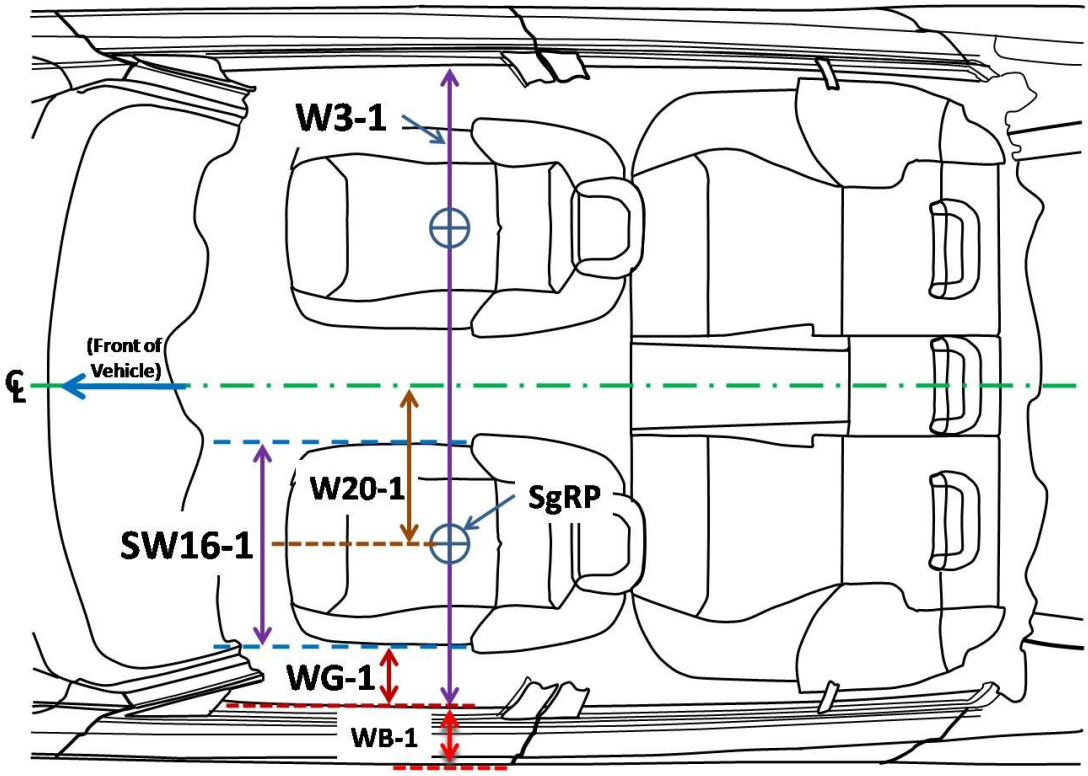

Figure B.13 Vehicle Internal Width Dimensions [1,54, 58]

Dimension W3-1 is first row shoulder room and WB-1 (not an SAE dimension) is the "belt width," or the distance from the shoulder room trim point to the vehicle outside point along the W3-1 reference line shown in Figure B.14 [1, 54].

The axis line defined for W3-1 is also used as the reference axis in defining WG-1 ("gap width"--not an SAE dimension). Width W117 uses a line in the Y-axis (cross-car axis) that passes through the X-axis (longitudinal axis) point of the driver seating reference point (SgRP). Seen in plan (top) view, these dimensions are all collinear.

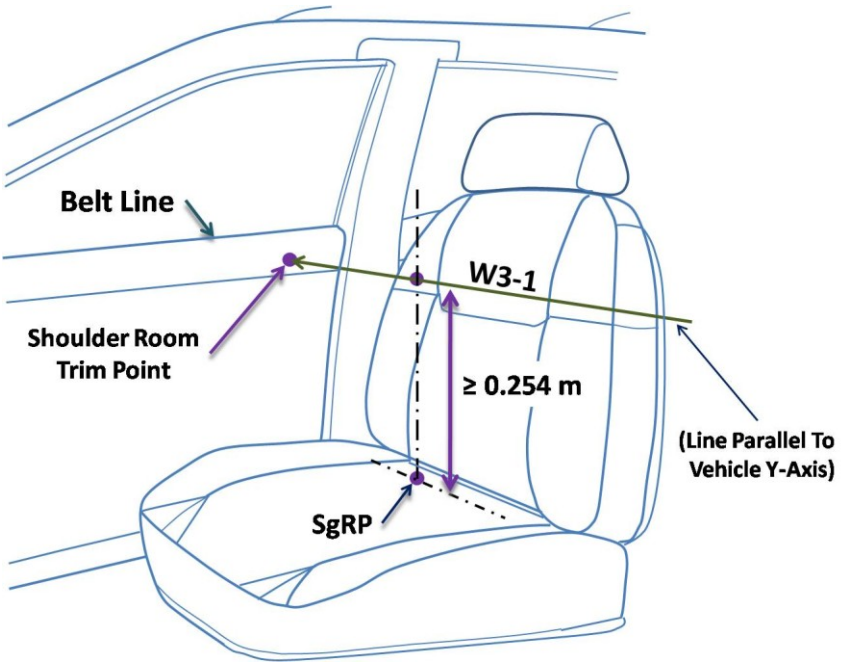

Figure B.14 W3-1 Locator Reference Point [1, 54]

Shoulder room W3-1 is made up of component dimensions SW16 (driver seat cushion width), seating cross-car coordinate W20-1 and WG-1 as shown in Equation (B.9) [1, 54, 58].

$$W3\text{-}1 = SW16 + 2 \cdot (W20\text{-}1 + WG\text{-}1) \qquad \text{Equation (B.11)}$$

Averaged driver and passenger side values are used in this work for SW16, W20-1 and WG-1 if they are different. W20-1 is another candidate for use as an optimization design variable. In order to begin an optimization with viable width dimensions, average values for component dimensions have been found through literature search and by conducting field measurements by vehicle type. Values for sedans are shown in Table B.10 [54, 52, 51]. While there is a slight variation in average WG-1 value by class size, the values are generally close to each other. The most likely size determinant for WG-1

is providing proper occupant shoulder belt positioning and sufficient clearance for side airbag inflation.

Sedan Size Class	Average SW16 (m)	SW16 Std. Dev.Σ (m)	Average W20-1 (m)	W20-1 Std. Dev.Σ (m)	Average WG1 (m)	WG1 Std. Dev.Σ (m)
Large	**0.524**	**0.019**	**0.379**	**0.005**	**0.093**	**0.030**
Midsize	**0.523**	**0.013**	**0.362**	**0.010**	**0.089**	**0.015**
Compact	**0.509**	**0.013**	**0.355**	**0.014**	**0.086**	**0.013**

Table B.10 SW16, W20-1 and WG-1 by Sedan Size Class [51, 52, 54]

In order to bridge the gap between vehicle internal and external dimensions, it is necessary to develop values for the belt width WB-1. Using vehicles with documented values for W117 and W3-1, values for WB-1 are calculated from the relation in Equation (B.10) [1, 54].

$$\text{WB-1} = 0.5 \cdot (\text{W117} - \text{W3-1}) \qquad \text{Equation (B.10)}$$

Average values of WB-1 have been determined from two sources: a NHTSA databaseand data from MVMA data sheets for various vehicles [51, 52, 54]. Values from the two sources are generally close to each other as shown in Table B.11 [51, 52, 54]. WG-1 and WB-1 can also be used in developing parametric models for vehicle side impact calculations [58].

Vehicle Type	Data Source	Samples	Average WB-1 (m)	Std. Deviation σ (m)
All Vehicles	**NHTSA**	**4996**	**0.165**	**0.024**
All Vehicles	**MVMA**	**112**	**0.163**	**0.021**
Passenger Vehicles (non-SUV, non-Minivan, non-Truck)	**NHTSA**	**4302**	**0.165**	**0.024**
Passenger Vehicles (non-SUV, non-Minivan, non-Truck)	**MVMA**	**107**	**0.165**	**0.020**
SUV's / Trucks	**NHTSA**	**333**	**0.138**	**0.034**
Minivans	**NHTSA**	**354**	**0.158**	**0.014**
Sedans	**MVMA**	**47**	**0.162**	**0.013**
Coupes	**MVMA**	**49**	**0.166**	**0.020**
2-Seater Sports Cars / Roadsters	**MVMA**	**10**	**0.183**	**0.033**

Table B.11 Average Values of WB-1 by Vehicle Type [51,52, 54]

Field Measurement of Occupant Width Parameters

Data for dimensions W20-1, SW16-1 and WG-1 are difficult to find in literature and public documents. In order to develop statistical data by vehicle type, field measurements of vehicles were conducted to obtain the values shown in Figure B.15. Only the shoulder room (W3-1, W3-2) dimensions are readily available in literature.

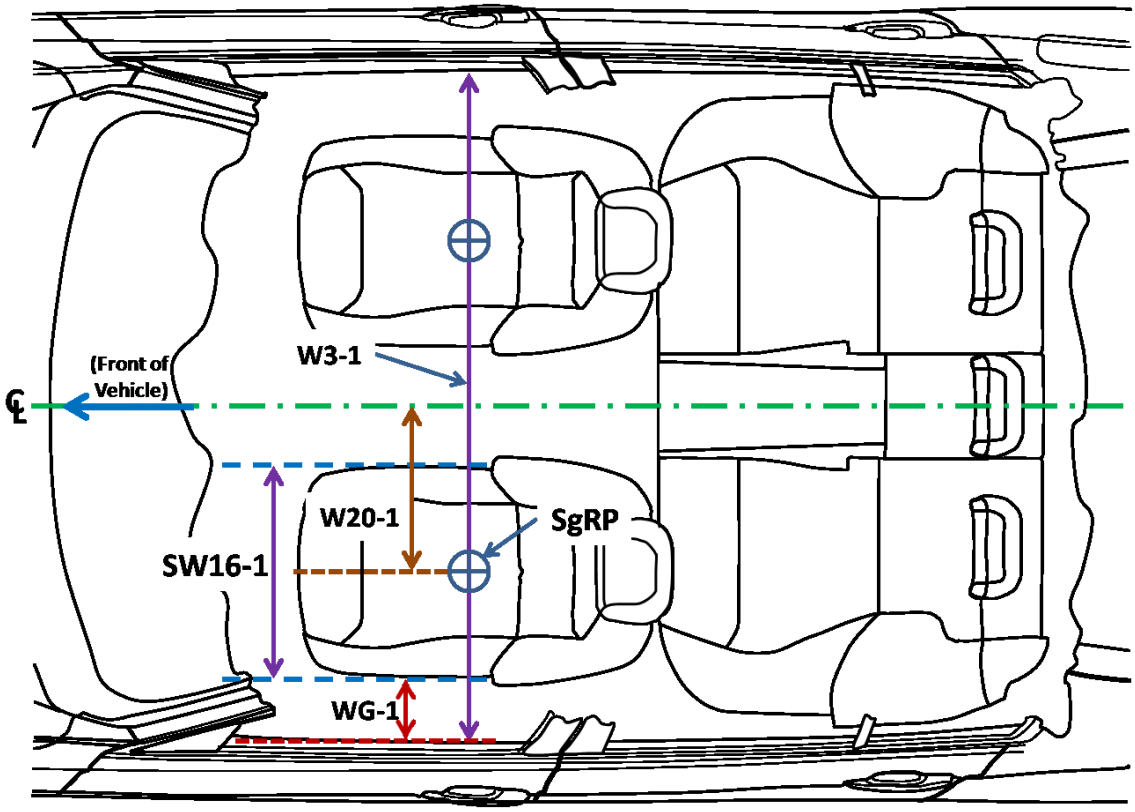

Figure B.15 Front Row Shoulder Room (W3-1) Component Parameters [1, 54]

Front row shoulder room W3-1 is thus the sum of the component parameters as shown in Equation (B.11).

$$W3\text{-}1 = 2 \cdot W20\text{-}1 + SW16\text{-}1 + 2 \cdot WG\text{-}1 \qquad \text{Equation (B.11)}$$

W3-1: First Row Shoulder Room

W20-1: SgRP Y-Coordinate -- Front

SW16-1: First Row seat cushion width

WG-1: Seat Cushion edge to Shoulder Room Trim Point lateral distance

Note that this assumes that the 1st row driver and passenger seat cushions are the same with and that the driver and front passenger SgRP are the same. If the driver and passenger values are different, they can be averaged for the purpose of determining W3-

1. As the component parameters are hard to find in literature, a field measurement approach is used by taking measurements of the parameters SW16-1, WG-1 and WC-1 shown in Figure B.16.

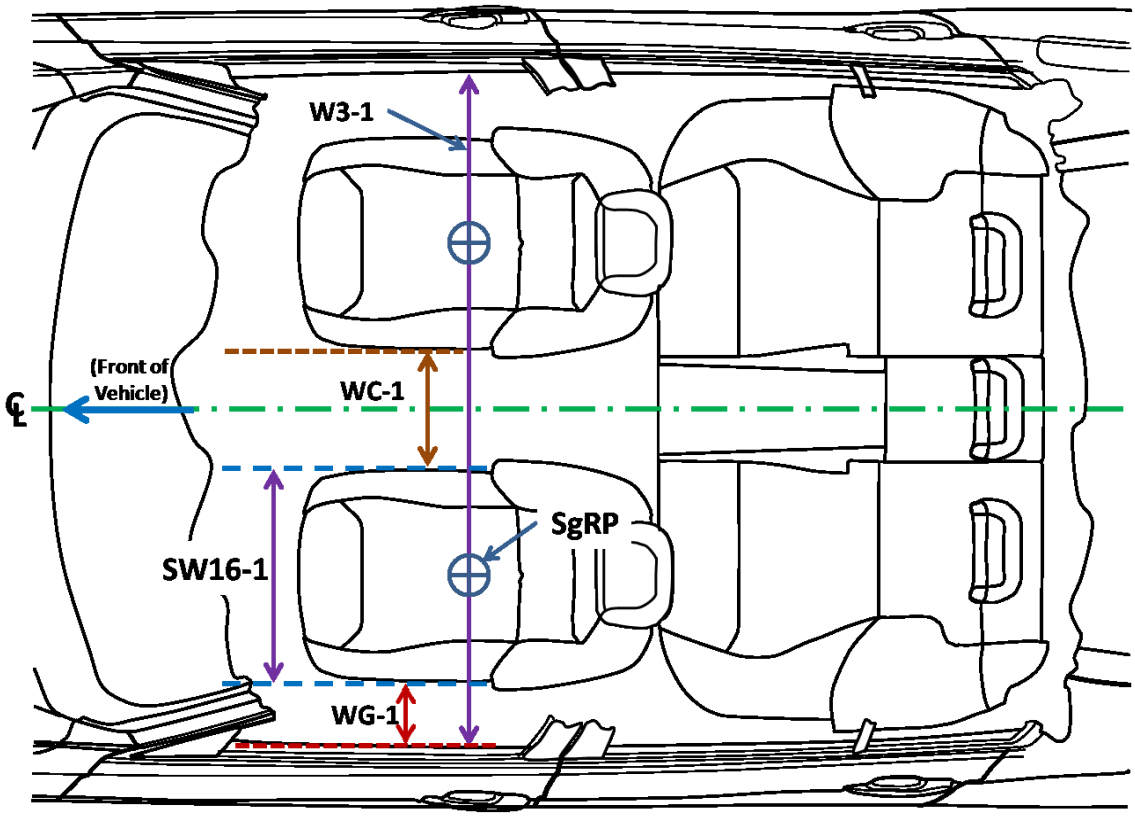

Figure B.16 Field Measurement Parameters Used to Determine WG-1, SW16-1 and W20-1 [1, 54]

In Figure B.17, measurement WC-1 (first row seat cushion lateral distance) is used as it is easily obtainable in field surveys. The seat cushion width SW16-1 is averaged for the driver and passenger seats and WG-1 is assumed to be equal for the driver and passenger sides (this is not always true but represents an average value for the two sides). With measurements for WC-1 and SW16-1, the gap distance WG-1 can be determined for the front row as:

$$\text{WG-1} = \frac{1}{2} \cdot (\text{W3-1} - 2 \cdot \text{SW16-1} - \text{WC-1}) \qquad \text{Equation (B.12)}$$

A minimum seat width of 0.5 meters is recommended by a University of Michigan Transportation Research Institute (UMTRI) survey [55]. Recommended minimum seat dimensions from the survey are shown in B.17.

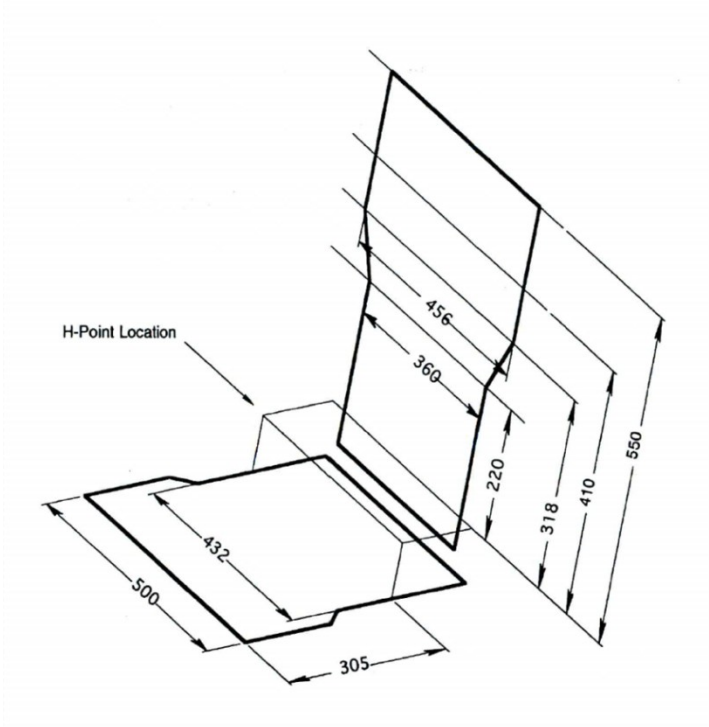

Figure B.17 Recommended Minimum Seat Dimensions [55]

A field survey of 213 vehicles has been performed to get actual cross-car dimension values as tabulated below. Values for SW16-1 by general vehicle type are shown in Table B.12 .

Vehicle Class	Sample Size	DS / PS SW16-1 Average (m)	DS / PS SW16 Standard Deviation σ (m)
All Vehicles (Cars and Trucks)	213	0.527	0.021
All Passenger Cars and Crossovers	149	0.521	0.018
All Trucks and SUV's	53	0.545	0.020
All Passenger Cars	120	0.519	0.017
All Crossovers	34	0.526	0.019
All Pickup Trucks	28	0.551	0.021
All SUV's	25	0.539	0.018

Table B.12 Seat Cushion Width SW16-1 by General Vehicle Type [54]

Values of WG-1 by general vehicle type are shown in Table B.13.

Vehicle Class	Sample Size	WG1 Average (m)	WG1 Std. Dev. (m)
All Vehicles (Cars and Trucks)	213	0.086	0.021
All Passenger Cars and Crossovers	149	0.084	0.021
All Trucks and SUV's	53	0.090	0.017
All Passenger Cars	120	0.081	0.022
All Crossovers	34	0.093	0.013
All Pickup Trucks	28	0.088	0.020
All SUV's	25	0.093	0.015

Table B.13 First Row Values for WG-1 by General Vehicle Type

Typical values of SW16-1 by specific vehicle class are shown in Table B.14.

These are field measurements of new and recent model year vehicles.

Vehicle Class	Sample Size	DS/PS SW16 Average (m)	DS/PS SW16 Standard Deviation σ (m)
Large Sedans and Crossovers	22	0.538	0.021
Large Sedans	14	0.534	0.023
Large Luxury Sedans	8	0.542	0.024
Large Standard Sedans	6	0.524	0.019
Large Crossovers	7	0.548	0.017
Large MPV's	9	0.536	0.016
Midsize Sedans, Coupes, Crossovers	56	0.524	0.014
Midsize Sedans/Coupes	38	0.524	0.014
Midsize Sedans	36	0.523	0.013
Midsize Luxury Sedans	18	0.523	0.012
Midsize Standard Sedans	18	0.523	0.015
Midsize Coupes	2	0.531	0.016
Midsize Crossovers	18	0.524	0.016
Midsize Luxury Crossovers	5	0.516	0.011
Midsize Standard Crossovers	13	0.527	0.017
Small Wagons	3	0.520	0.009
Mini-MPV's	1	0.495	-
Compact Sedans/Coupes/Crossovers	39	0.511	0.012
Compact Sedans/Coupes	30	0.511	0.013
Compact Sedans	20	0.509	0.013
Compact Coupes	10	0.516	0.012
Compact Crossovers	9	0.512	0.010
Subcompact Sedan/Coupes	10	0.513	0.011
Subcompact Sedans	2	0.503	0.004
Subcompact Coupes	8	0.515	0.010
Mini-Compact Coupes	6	0.518	0.009
2-Seater Sports Cars/Roadsters	10	0.499	0.016
Large SUV's	9	0.540	0.022
Midsize SUV's	16	0.538	0.016
Large (Standard) Pickups	20	0.558	0.020
Midsize Pickups	3	0.535	0.005
Compact (Small) Pickups	5	0.533	0.011

Table B.14 Seat Cushion Width SW16-1 Values by Specific Vehicle Class [54]

Typical values of WG-1 by specific vehicle class are shown in Table B.15.

Vehicle Class	Sample Size	WG-1 Average (m)	WG-1 Std. Dev. (m)
Large Sedans and Crossovers	22	0.097	0.028
Large Sedans	14	0.090	0.030
Large Luxury Sedans	8	0.088	0.032
Large Standard Sedans	6	0.093	0.030
Large Crossovers	7	0.104	0.004
Large MPV's	9	0.106	0.017
Midsize Sedans, Coupes, Crossovers	56	0.089	0.016
Midsize Sedans/Coupes	38	0.088	0.016
Midsize Sedans	36	0.087	0.016
Midsize Luxury Sedans	18	0.085	0.016
Midsize Standard Sedans	18	0.089	0.015
Midsize Coupes	2	0.095	0.026
Midsize Crossovers	18	0.092	0.017
Midsize Luxury Crossovers	5	0.099	0.006
Midsize Standard Crossovers	13	0.090	0.020
Small Wagons	3	0.085	0.010
Mini-MPV's	1	0.078	-
Compact Sedans/Coupes/Crossovers	39	0.085	0.013
Compact Sedans/Coupes	30	0.085	0.014
Compact Sedans	20	0.086	0.013
Compact Coupes	10	0.083	0.016
Compact Crossovers	9	0.085	0.010
Subcompact Sedan/Coupes	10	0.061	0.018
Subcompact Sedans	2	0.079	0.007
Subcompact Coupes	8	0.056	0.017
Mini-Compact Coupes	6	0.056	0.015
2-Seater Sports Cars/Roadsters	10	0.063	0.019
Large SUV's	9	0.102	0.007
Midsize SUV's	16	0.088	0.013
Large (Standard) Pickups	20	0.095	0.015
Midsize Pickups	3	0.078	0.015
Compact (Small) Pickups	5	0.067	0.026

Table B.15 Typical Values of WG-1 by Specific Vehicle Class [54]

Values for W20-1 by general vehicle type are shown in Table B.16.

Vehicle Class	Sample Size	W20-1 Average (m)	W20-1 Std. Dev. (m)
All Vehicles (Cars and Trucks)	**213**	**0.385**	**0.034**
All Passenger Cars and Crossovers	**149**	**0.371**	**0.020**
All Trucks and SUV's	**53**	**0.421**	**0.039**
All Passenger Cars	**120**	**0.367**	**0.019**
All Crossovers	**34**	**0.385**	**0.017**
All Pickup Trucks	**28**	**0.433**	**0.041**
All SUV's	**25**	**0.407**	**0.032**

Table B.16 Values for W20-1 by General Vehicle Type [54]

Values of W20-1 by specific vehicle class are shown in Table B.17.

Vehicle Class	Sample Size	W20-1 Average (m)	W20-1 Std. Dev. (m)
Large Sedans and Crossovers	**22**	**0.389**	**0.016**
Large Sedans	**14**	**0.385**	**0.016**
Large Luxury Sedans	**8**	**0.390**	**0.020**
Large Standard Sedans	**6**	**0.379**	**0.005**
Large Crossovers	**7**	**0.399**	**0.010**
Large MPV's	**9**	**0.408**	**0.015**
Midsize Sedans, Coupes, Crossovers	**56**	**0.376**	**0.016**
Midsize Sedans/Coupes	**38**	**0.371**	**0.014**
Midsize Sedans	**36**	**0.372**	**0.014**
Midsize Luxury Sedans	**18**	**0.381**	**0.010**
Midsize Standard Sedans	**18**	**0.362**	**0.010**
Midsize Coupes	**2**	**0.366**	**0.013**
Midsize Crossovers	**18**	**0.387**	**0.017**
Midsize Luxury Crossovers	**5**	**0.389**	**0.014**
Midsize Standard Crossovers	**13**	**0.387**	**0.018**
Small Wagons	**3**	**0.357**	**0.021**
Mini-MPV's	**1**	**0.338**	**-**
Compact Sedans/Coupes/Crossovers	**39**	**0.363**	**0.017**
Compact Sedans/Coupes	**30**	**0.360**	**0.017**
Compact Sedans	**20**	**0.355**	**0.014**
Compact Coupes	**10**	**0.372**	**0.017**
Compact Crossovers	**9**	**0.371**	**0.013**
Subcompact Sedan/Coupes	**10**	**0.361**	**0.023**
Subcompact Sedans	**2**	**0.348**	**0.021**
Subcompact Coupes	**8**	**0.365**	**0.023**
Mini-Compact Coupes	**6**	**0.343**	**0.023**
2-Seater Sports Cars/Roadsters	**10**	**0.369**	**0.015**
Large SUV's	**9**	**0.442**	**0.018**
Midsize SUV's	**16**	**0.386**	**0.017**
Large (Standard) Pickups	**20**	**0.457**	**0.012**
Midsize Pickups	**3**	**0.378**	**0.015**
Compact (Small) Pickups	**5**	**0.370**	**0.014**

Table B.17 Typical Values of W20-1 by Specific Vehicle Class [54]

Vehicle cargo volume for sedans is determined by fitting defined pieces of luggage into the trunk as specified in SAE J1100 [1]. However, an analysis of MVMA vehicle data provides a correlation for hidden (trunk) cargo volume V1 shown in Equation B.13 [1, 52, 54]. SAE dimension W3-2 is second row shoulder room [1].

$$V1 = 0.188 \cdot W3\text{-}2 \cdot (L115\text{-}2 + L105)(R^2 = 0.76) \qquad \text{Equation (B.13)}$$

If second row shoulder room is not otherwise determined by design considerations, a review of 106 sedans provides a correlation based on front row shoulder room shown in Equation B.14 [52, 54].

$$W3\text{-}2 = 0.987 \cdot W3\text{-}1 \qquad (R^2 = 0.86) \qquad \text{Equation (B.14)}$$

Outside vehicle dimensions are shown in Figure B.18 [1, 54]. H101 (overall vehicle height) is readily available in literature; H100 (vehicle body height) is more useful in vehicle mass calculations. The difference due to roof-mounted antennae and hardware will have to be accounted for when using outside vehicle height in parametric optimization.

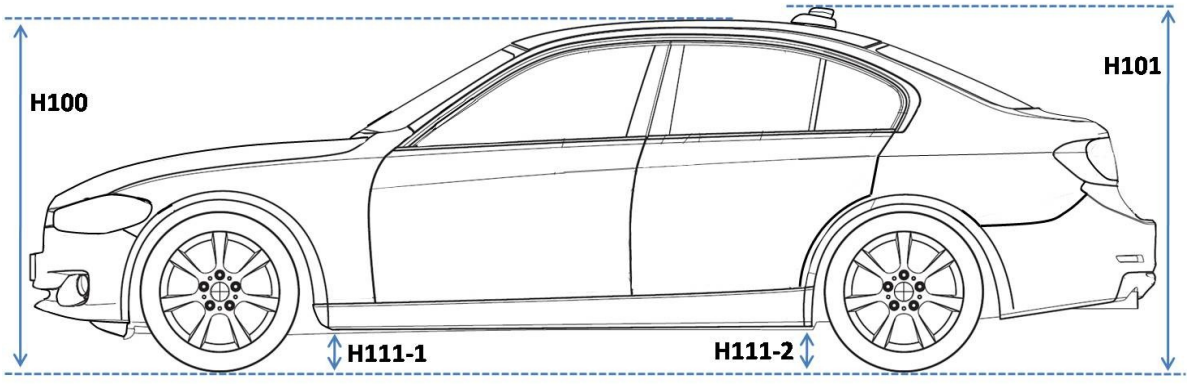

Figure B.18 Outside Vehicle Height Dimensions [1, 54]

H111-1 and H111-2 are vehicle front and rear rocker height (distance from ground to bottom of the rocker), respectively [1]. H111-2 and H111-1 differ significantly only for pickup trucks in the vehicles surveyed for this work [54]. For most equations, H111-1 is used due to its proximity to the Accelerator Heel Point (AHP). Statistical data developed from a NHTSA database yields average values for Front Rocker Height H111-1 by vehicle body type shown in Table B.18 [51, 54].

Vehicle Type	Average H111-1 (m)	σ (m)	Average H111-2 (m)	σ (m)	Total Samples
Unibody Non-SUV	**0.199**	**0.024**	**0.196**	**0.029**	**2297**
Body on Frame Non-SUV	**0.213**	**0.041**	**0.214**	**0.051**	**244**

Table B.18 Average Values of H111-1 and H111-2 by Body Type [51, 54]

Statistical data developed from a NHTSA database yields average values for front rocker height H111-1 by vehicle type shown in Table B.19 [51, 54].

Vehicle Type	Average H111-1 (m)	Standard Deviation σ (m)	Samples
Unibody Non-SUV Non-Sport	**0.199**	**0.024**	**2297**
Unibody Sports Car	**0.180**	**0.019**	**208**
Unibody SUV (Crossover SUV)	**0.284**	**0.007**	**19**
Body-on-Frame Non-SUV	**0.213**	**0.041**	**244**
Traditional SUV	**0.325**	**0.077**	**146**
Pickup Truck	**0.348**	**0.068**	**101**
Minivan/MPV	**0.254**	**0.027**	**336**

Table B.19 Values of H111-1 by Vehicle Type [51, 54]

Values of Rear Rocker Height are shown in Table B.21 [52, 54].

Vehicle Type	Average H111-2 (m)	Standard Deviation σ (m)	Samples
Unibody Non-SUV Non-Sports	**0.196**	**0.029**	**2297**
Unibody Sports Car	**0.180**	**0.024**	**208**
Unibody SUV (Crossover SUV)	**0.294**	**0.007**	**19**
Body-on-Frame Non-SUV	**0.214**	**0.051**	**244**
Traditional SUV	**0.334**	**0.080**	**146**
Pickup Truck	**0.392**	**0.088**	**101**
Minivan/MPV	**0.266**	**0.029**	**336**

Table B.21 Values of H111-2 by Vehicle Type [52, 54]

Vehicle interior vertical dimensions of interest are shown in Figure B.19 [1, 54].

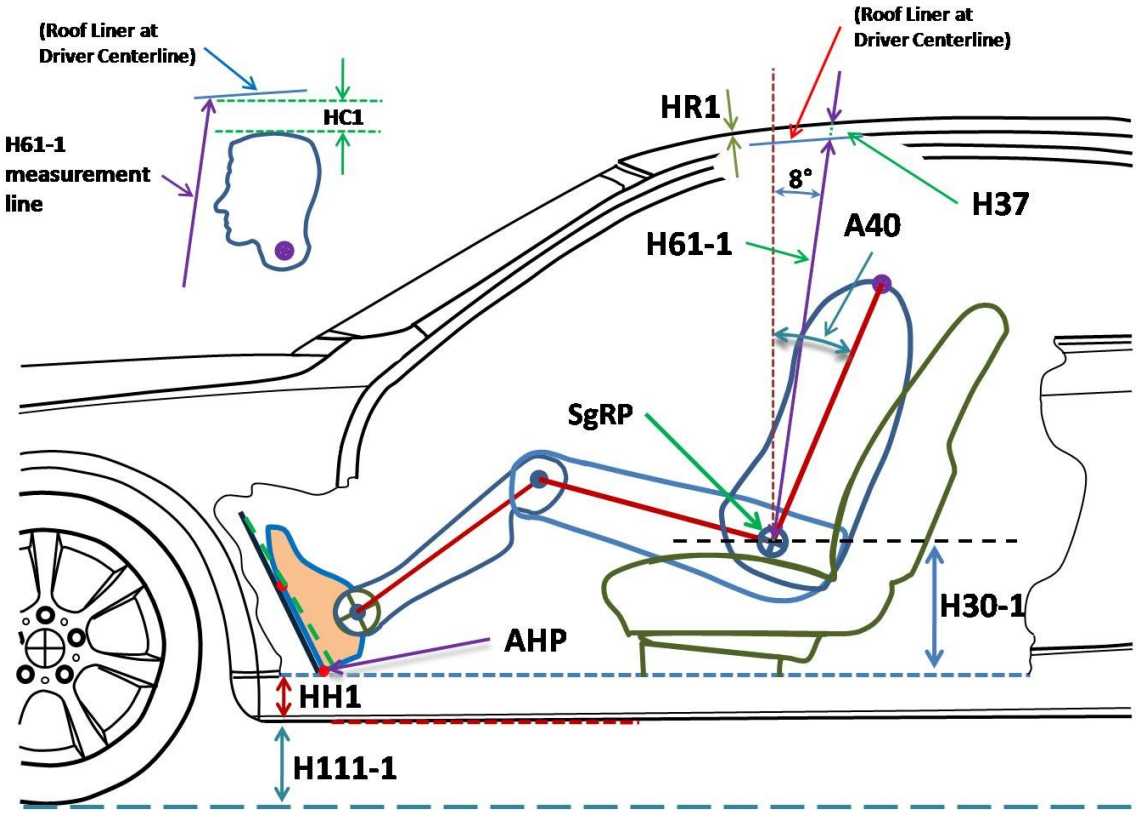

Figure B.19 Interior Vertical Dimensions: HH-1, H30-1, H61-1, H37, HC-1 and HR1 [1, 54]

H30-1 is the "seat height," or the vertical distance of the driver seating reference point (SgRP) above the accelerator heel point (AHP) [1]. H30-1 values from NHTSA data is shown in Table B.21. Values of H30-1 for vehicle classes from MVMA data sheets are shown in Table B.22.

Vehicle Type	Average H30-1 Value (m)	Standard Deviation σ (m)	Number of Samples
Unibody Non-SUV Non-Sports Car	0.243	0.021	2297
Unibody Sports Car	0.178	0.012	208
Unibody SUV (Crossover SUV)	0.332	0.016	19
Body-on-Frame Sedan/Coupe/Wagon	0.227	0.015	244
Body-on-Frame SUV	0.298	0.038	146
Body-on-Frame Truck	0.254	0.016	101
Minivan / MPV	0.352	0.020	336

Table B.21 NHTSA Database H30-1 Values by Vehicle Type [51, 54]

Vehicle Class	Average H30-1 Value (m)	Standard Deviation σ (m)	Number of Samples
Large Sedan / Coupe Body-on-Frame	0.217	N/A	2
Large Sedan / Coupe Unibody	0.221	0.002	3
Midsize Sedan	0.249	0.018	23
Midsize Coupe	0.237	0.022	6
Midsize Coupe Body-on-Frame	0.228	N/A	2
Midsize Coupe Unibody	0.241	0.027	4
Midsize Wagon	0.258	N/A	1
Compact Sedan	0.254	0.017	20
Compact Coupe	0.246	0.018	12
Small Wagon	0.239	N/A	2
Subcompact Sedan	0.238	0.013	3
Subcompact Coupe	0.222	0.035	22

Table B.22 Average H30-1 Values by Detailed Vehicle Class [52, 54]

H61-1 is driver headroom; it is the distance along an 8° line from vertical between the SgRP and the vehicle headliner plus 0.102 meters [1]. MVMA data provides the following average H61-1 values by general vehicle class as shown in Table B.23 [1, 54]. H61-1 values by detailed vehicle class are shown in Table B.24 [52, 54]

Vehicle Class	Average H61-1 Value (m)	Standard Deviation σ (m)	Number of Samples
Large Sedan / Coupe	**0.984**	**0.034**	**3**
Midsize Sedan / Coupe / Wagon	**0.982**	**0.024**	**17**
Compact Sedan / Coupe	**0.971**	**0.013**	**27**
Subcompact Sedan / Coupe	**0.961**	**0.018**	**22**
Mini-Compact (Coupe Only)	**0.957**	**N/A**	**1**
Large Minivan	**0.990**	**N/A**	**1**
Subcompact Traditional SUV	**0.925**	**N/A**	**1**

Table B.23 MVMA H61-1 Values by General Vehicle Type [52, 54]

Vehicle Class	Average H61-1 Value (m)	Standard Deviation σ (m)	Number of Samples
Large Sedan / Coupe Body-on-Frame	**1.003**	**N/A**	**2**
Large Sedan / Coupe Unibody	**0.944**	**N/A**	**1**
Midsize Sedan	**0.980**	**0.011**	**12**
Midsize Coupe	**0.988**	**0.044**	**5**
Midsize Coupe Body-on-Frame	**0.967**	**N/A**	**2**
Midsize Coupe Unibody	**1.002**	**0.055**	**3**
Compact Sedan	**0.975**	**0.015**	**15**
Compact Coupe	**0.965**	**0.009**	**11**
Small Wagon	**0.968**	**N/A**	**2**
Subcompact Sedan	**0.978**	**0.015**	**3**
Subcompact Coupe	**0.959**	**0.018**	**19**

Table B.24 MVMA H61-1 Values by Detailed Vehicle Class [52, 54]

H37 is the headliner thickness; H37 has been discontinued as an official SAE dimension but remains useful in this work [1]. Roof panel thickness HR1 is not an SAE dimension; it is typically between 0.8 and 1.2 mm for steel panels [54]. Aluminium and composite panels will have different thickness values compared to steel.

"Heel height" HH1 is not an SAE dimension; it is the vertical distance from the bottom of the front rocker to the accelerator heel point (AHP). Along with H111-1, these component parameters provide a continuous set of dimensions, which add up to vehicle body height H100 shown in Equation (B.15) [1, 54]. This assumes that the high point of the vehicle body is close to the H61-1 vector intersection with the roof panel, which is a

plausible assumption. Non-SAE dimension HC1 is the vertical distance from the top of the driver manikin head to the H61-1 reference line intersection with the roof liner. With known manikin dimensions and positioning (A40), the height from the SgRP to the top of the manikin (with head form) to HC1 will equal the vertical component of H61-1 less 0.102 m [54] .

$$H100 \approx H111\text{-}1 + HH1 + H30\text{-}1 + HR1 + H37 + (H61\text{-}1 - 0.102) \cdot \cos(8°)$$ Equation (B.15)

An average value of H37 for all vehicle types is approximately 0.016 m with standard deviation of 0.006 meters based on 693 samples from a NHTSA database [51, 54]. Vehicle center of gravity (CG) height will not be explored in this work, although studies have shown that the CG height tends to be approximately 39% of total body height H100 [56].

Heel height HH1 is a height dimension created by the author for use in calculating overall vehicle height in vehicle conceptual design and optimization. As all other height dimensions in this work can be found in literature or calculated from known dimensional values, HH1 is determined by subtracting the other factors from vehicle body height H100 as shown in Equation (B.16) [51, 52, 54].

$$HH1 = H100 - HR1 - H37 - (H61\text{-}1 - 0.102) \cdot \cos(8°) - H30\text{-}1 - H111\text{-}1$$ Equation (B.16)

Using NHTSA data, typical Values of HH-1 by vehicle type are shown in Table B.25 [51, 54].

Vehicle Class	HH-1 Average (m)	HH-1 Standard Deviation σ (m)	Sample Size
Unibody Non-SUV Non-Sports	**0.043**	**0.028**	**2297**
Unibody Sports Car	**0.059**	**0.037**	**208**
Unibody Crossover SUV	**0.092**	**0.021**	**19**
Body-on-Frame Non-Truck Non-SUV	**0.119**	**0.037**	**244**
Body-on-Frame SUV	**0.164**	**0.048**	**146**
Body-on-Frame Truck	**0.137**	**0.051**	**101**
Minivan / MPV	**0.162**	**0.062**	**336**

Table B.25 Average Value of HH-1 by Vehicle Type [51, 54]

H30-1 and H30-2 were previously discussed in determining first and second row legroom. Average values for sedans are shown in Table B.26 [52, 54].

Sedan Size Class	H30-1 (m)	σ (m)	H30-2 (m)	σ (m)
Large	**0.221**	**0.002**	**0.292**	**0.000**
Midsize	**0.249**	**0.018**	**0.278**	**0.013**
Compact	**0.254**	**0.017**	**0.286**	**0.025**

Table B.26 Average Values for H30-1 and H30-2 [52, 54]

Second row seats tend to be positioned slightly higher than first row seating for visibility. This can be accomplished by raising the rear floorpan and thus the height of the FRP or by increasing the value of H30-2. Second row seat height H30-2 is shown in Figure B.20

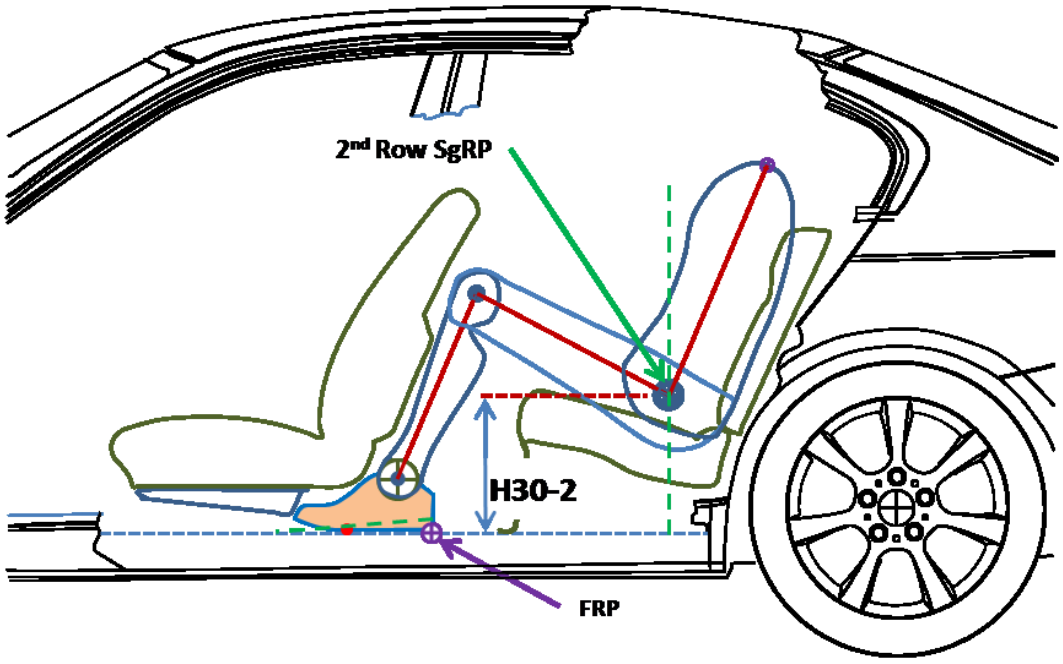

Figure B.20 Second Row Seat Height H30-2 [1, 54]

Typical values of H30-2 by vehicle class from MVMA vehicle data is shown in Table B.27 [52, 54].

Vehicle Class	Average H30-2 Value (m)	Standard Deviation σ (m)	Number of Samples
Large Sedan / Coupe	**0.283**	**0.016**	**5**
Midsize Sedan	**0.277**	**0.015**	**17**
Midsize Coupe	**0.277**	**0.012**	**7**
Compact Sedan	**0.286**	**0.025**	**21**
Compact Coupe	**0.278**	**0.019**	**12**
Subcompact Sedan	**0.304**	**0.015**	**4**
Subcompact Coupe	**0.266**	**0.040**	**23**
Mini-Compact Coupe	**0.272**	**0.030**	**3**

Table B.27 Typical Values of H30-2 by Vehicle Class from MVMA Data [52, 54]

The average difference between H30-2 and H30-1 (H30-2 less H30-1) by specific

vehicle class from MVMA data is shown in Table B.28 [52, 54].

Vehicle Class	Average H30-2 Less H30-1 Value (m)	Standard Deviation σ (m)	Number of Samples
Large Sedan / Coupe	0.064	0.019	5
Midsize Sedan	0.024	0.020	17
Midsize Coupe	0.042	0.020	7
Compact Sedan	0.032	0.021	21
Compact Coupe	0.029	0.017	12
Subcompact Sedan	0.060	0.002	4
Subcompact Coupe	0.045	0.027	23
Mini-Compact Coupe	0.095	0.036	3

Table B.28 Average Difference of H30-2 Less H30-1 by Vehicle Class [52, 54]

Second row headroom H61-2 is measured similarly to H61-1 as shown in Figure B.21 [1, 54].

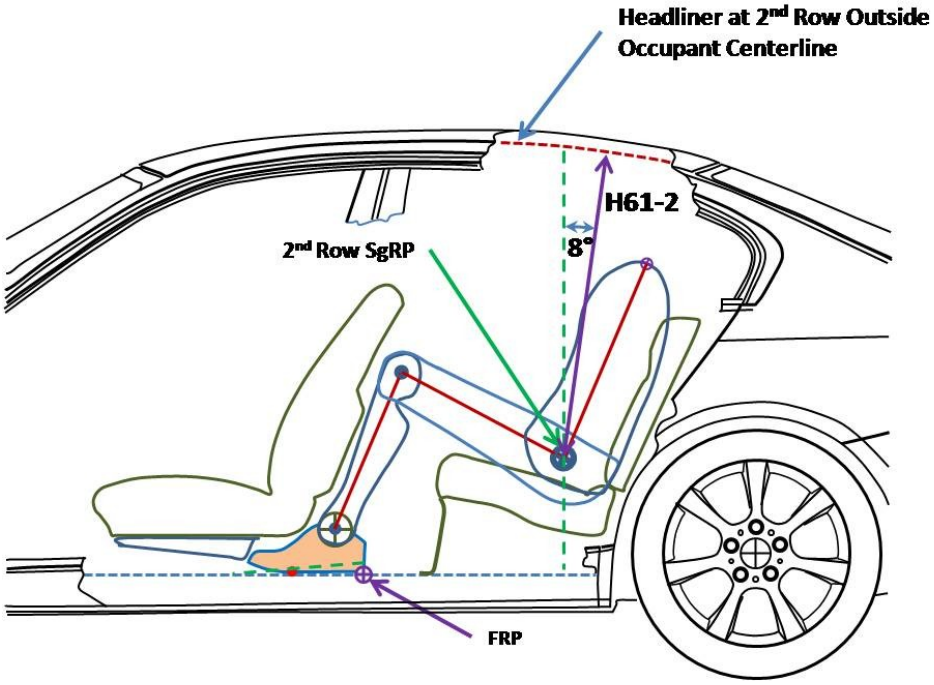

Figure B.21 Second Row Headroom H61-2 [1, 54]

Average H61-2 values by general vehicle type from MVMA data are shown in Table B.29 [52, 54].

Vehicle Class	Average H61-2 Value (meter)	Standard Deviation σ (m)	Number of Samples
Large Sedan / Coupe	**0.955**	**0.046**	**3**
Midsize Sedan / Coupe / Wagon	**0.953**	**0.008**	**17**
Compact Sedan / Coupe	**0.941**	**0.017**	**26**
Subcompact Sedan / Coupe	**0.906**	**0.041**	**22**
Mini-Compact (Coupe Only)	**0.813**	**N/A**	**1**
Large Minivan	**0.969**	**N/A**	**1**

Table B.29 Average H61-2 Values by General Vehicle Type [52, 54]

Average values of H61-2 by detailed vehicle class are shown in Table B.30.

Vehicle Class	Average H61-2 Value (m)	Standard Deviation σ (m)	Number of Samples
Large Sedan / Coupe Body-on-Frame	0.981	N/A	2
Large Sedan / Coupe Unibody	0.904	N/A	1
Midsize Sedan	0.955	0.006	12
Midsize Coupe	0.947	0.010	5
Midsize Coupe Body-on-Frame	0.958	N/A	2
Midsize Coupe Unibody	0.941	0.001	3
Compact Sedan	0.943	0.012	15
Compact Coupe	0.939	0.022	11
Small Wagon	0.963	N/A	2
Subcompact Sedan	0.958	0.016	3
Subcompact Coupe	0.898	0.038	19

Table B.30 Average H61-2 Values by Detailed Vehicle Class [52, 54]

Vehicle Center of Gravity (C_g) Height

Vehicle center of gravity height is an important parameter in vehicle performance measures such as acceleration time, braking distance and roll stability. Center of gravity height is shown in Figure B.22 [54]

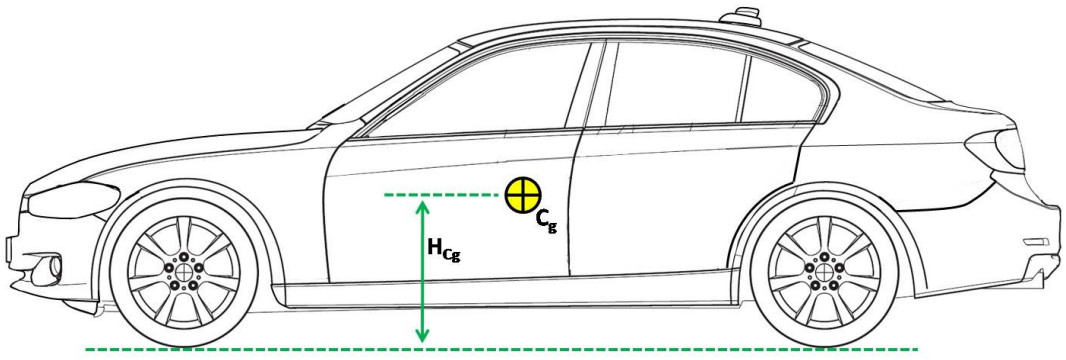

Figure B.22 Vehicle Center of Gravity Height [54]

While many longitudinal center of gravity locations for major vehicle subsystems can be either calculated or extrapolated from vehicle data, it is more difficult to determine the exact C_g height of the vehicle or subsystems parametrically from the existing body of public data. Some vehicle enthusiast publications now include measured values of vehicle C_g height; these tend, however, to be focused on performance and luxury vehicles rather than the vehicle population at large [71, 72].

Allen, Klyde et al. have developed a correlation between vehicle roof height (H100) and Center of Gravity Height (in feet) [56]:

$$H_{Cg} = 0.389 \cdot H100 + 0.0113 \text{ feet}$$

Equation (B.17)

Converting to meters yields:

$$H_{Cg} = 0.389 \cdot H100 + 0.003 \text{ m}$$

Equation (B.18)

This correlation can be used as a starting point early in conceptual design when details of vehicle system, subsystem and component masses and location are not yet determined. It is useful for initial parametric vehicle definition, pre-configuration and optimization. In practice, the relation can be simplified to H_{Cg} = 0.39 x H100 with little loss of accuracy.

The above continuum of parameters for vehicle length, width and height dimensions can be used to determine vehicle mass and volume characteristics along with estimation of vehicle performance to desired targets. Estimation of vehicle curb mass

and subsystem mass values is treated in Appendix F.

Vehicle interior volume (IV1 for passenger cars) is defined in SAE J1100 as shown in Equation (B.19) [1]:

$$IV1 = PV1 + PV2 + V1 \qquad \text{Equation (B.19)}$$

PV1 and PV2 are first and second row passenger volume as shown in Equation (B.20) [1]. Cargo volume V1 and the correlation of estimated cargo volume for sedans were previously discussed in this appendix.

$$PV1 = L34 \cdot W3\text{-}1 \cdot H61\text{-}1\ ; \qquad PV2 = L51\text{-}2 \cdot W3\text{-}2 \cdot H61\text{-}2 \qquad \text{Equation (B.20)}$$

Vehicle interior volume is used in determining U.S. Environmental Protection Agency vehicle size classification and as one measure of vehicle comfort published in many automotive trade publications [61].

Yanni and Venhovens provide a parametric means for calculating vehicle EPA (Environmental Protection Agency) mileage for a variety of specified test cycles, which correlate well with actual vehicle EPA test data [13]. They use a simpler mass calculation than that described in this work, utilizing peak engine power, L103, W103 and H100.

A reasonable estimate of CAD-dependent values such as vehicle wall-to-wall turn radius can be made based on vehicle correlations between curb-to-curb turn radius and resulting wall-to-wall turn radius from MVMA data [52, 54]. If Ackerman steering is used, vehicle turn radius can be calculated parametrically at the outside front wheel track [54, 58, 62, 63]. The relationship between vehicle outside track, curb-to-curb and wall-to-wall turn radii are shown in Figure B.23 [1, 52, 54, 58]. Curb-to-curb turn radius is the

outside track turn radius plus one-half of the tire width. Wall-to-wall turn radius is based on the outermost vehicle point describing a turn circle; this will be dependent on the vehicle geometry resulting from detailed CAD design.

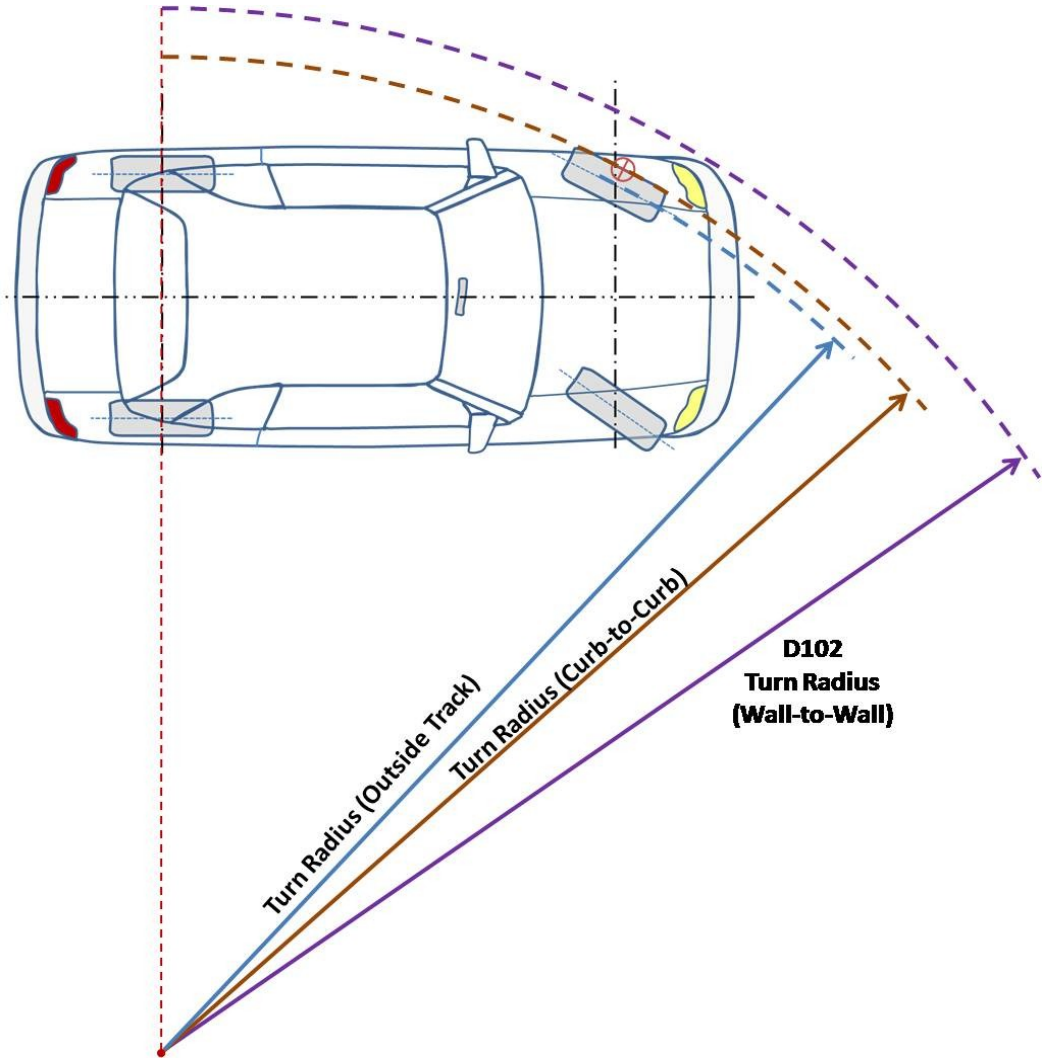

Figure B.23 Outside Track, Curb-to-Curb and Wall-to-Wall Turn Radius [1, 52, 54, 62]

If vehicle wheelbase L101, track width W102 and maximum inside wheel turn angle $\boldsymbol{\delta_i}$ are specified, the outside track turn radius can be calculated [54]. For a given tire width, the curb-to-curb turn radius is then obtained. Using information from MVMA

data sheets, typical ratios of wall-to-wall (WTW) to curb-to-curb (CTC) turn radius can be found as shown in Table B.31 [52, 54].

Vehicle Class	Samples	Average Wheelbase (m)	Average Track Width (m)	Average Maximum δ_i (degrees)	Average CTC Turn Radius (m)	Average WTW / CTC Ratio
Large Sedan / Coupe	**5**	**2.87**	**1.54**	**38.1**	**6.05**	**1.15**
Midsize Sedan / Coupe	**24**	**2.69**	**1.48**	**39.2**	**5.60**	**1.09**
Compact Sedan / Coupe	**35**	**2.55**	**1.44**	**39.2**	**5.25**	**1.07**

Table B.31 Curb-to-Curb (CTC) vs. Wall-to-Wall (WTW) Vehicle Turn Radius [52, 54]

These values are computed using the actual Ackerman values for outside wheel angle $\boldsymbol{\delta_o}$ resulting from the given inside wheel angle $\boldsymbol{\delta_i}$. Many low-speed turn radius calculations use an average of the inner and outer front wheel steer angles [63, 64]. This simplification generally has a low error compared to using the true $\boldsymbol{\delta_i}$ and $\boldsymbol{\delta_o}$ values [54, 63].

In similar fashion, performance targets such as 0-60 mph / 0-100 kph acceleration, braking distance, lateral g's, maximum velocity and other factors can be calculated parametrically with a high degree of accuracy [54, 58, 62, 63, 64]. This permits rapid and accurate calculation and optimization of overall vehicle design prior to the detailed design phase, greatly reducing design iterations and changes in the detailed design phase.

Some aspects of modeling cannot be determined without knowing detailed design and styling information, such as vehicle drag coefficient. However, typical drag

coefficients may be estimated for a class of vehicles (approximately 0.27 to 0.32 for most sedans) [52, 54, 62]. Additionally, the Motor Industry Research Association (MIRA) has developed a table for estimating drag coefficient based on general vehicle external shape [65]. Such estimates will necessarily affect the accuracy of the parametric calculations; the designer will have to account for the possible error. Conversely, these parameters can be used as a design variable in which the designer validates the upper and lower boundaries used for that variable in the optimization.

Appendix C
Engine and Transmission Modeling Dimensional and Functional Relations

Internal Combustion Engine Sizing Dimensions and Parameters

Engine outside volume is defined by engine external maximum width, length and height as shown in Figure C.1.

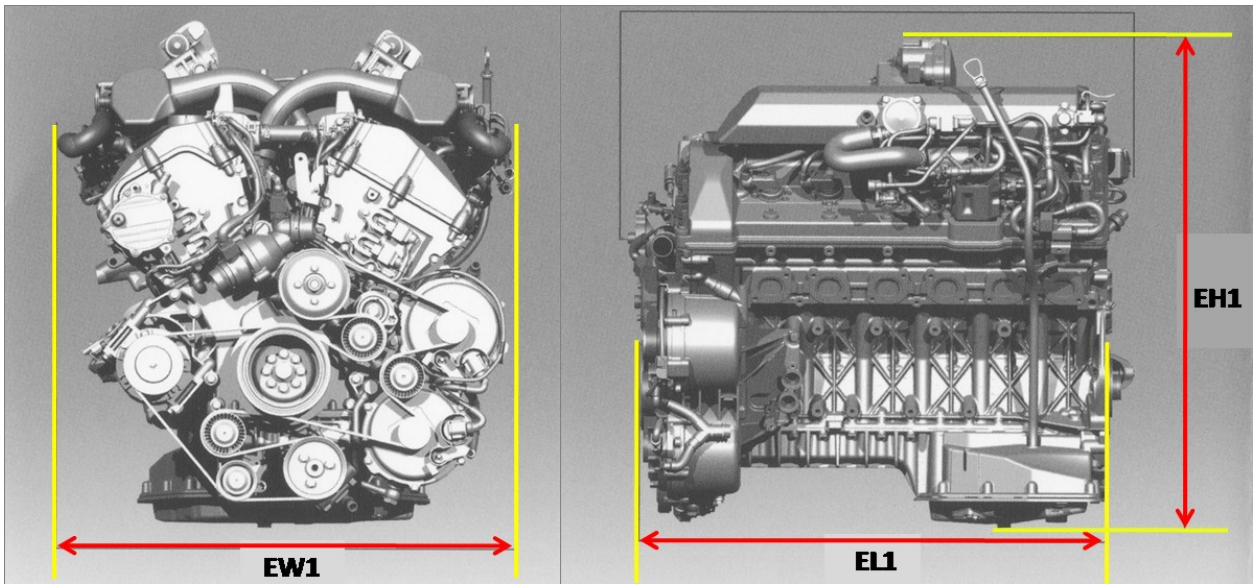

Figure C.1 External Engine Dimensions [54]

The dimensional parameters in Figure C.1 are:

- EW1: External Engine Width; The maximum distance across the engine (normal to the cylinder axis)
- EL1: External Engine length; The distance along the line of cylinders from the transmission attachment to the accessory pulleys
- EH1: External Engine height: The maximum distance measured in a vertical line from the top of the engine to the bottom point.

Dimensions used in sizing an inline internal combustion engine (or one bank of a

V-type engine) are shown in Figure C.2 [54]:

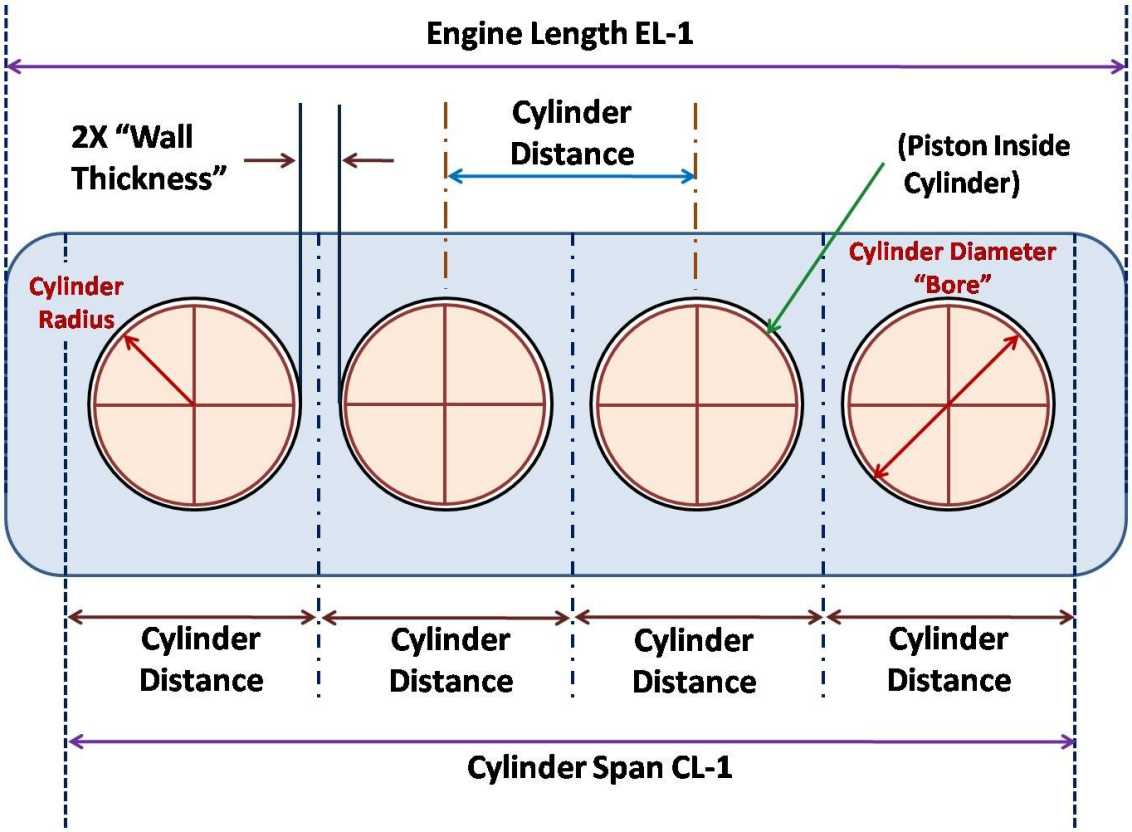

Figure C.2: Engine Bank Sizing [54]

Parameters used in Figure C.2 include:

- Cylinder distance: The distance along the center axis of the line of cylinders from one cylinder/piston center to the next (assumed to be the same between all adjacent cylinders). This distance can also be used to determine "wall thickness" between adjacent cylinders

- Cylinder Diameter: The distance along a diameter of an engine cylinder.

- Cylinder Radius: The distance along a radius of an engine cylinder

• Cylinder Span (CL-1) = Number of cylinders x Cylinder distance. This will be used to calculate total engine length.

From available sources, typical values by engine type can be calculated for Engine Length and Cylinder Span. The typical resulting ratio CL1 / EL1 can then be found for each engine type. As cylinder span changes due to bore and stroke optimization, a new overall engine length can be estimated from the known Span/Length ratio for that engine type.

Cylinder Bore and Piston Stroke distances are shown in Figure C.3 where:

• Cylinder Bore: The diameter of the cylinder

• Piston Stroke: The distance along the cylinder axis from the top of the piston travel to the bottom point of piston motion in the engine cylinder.

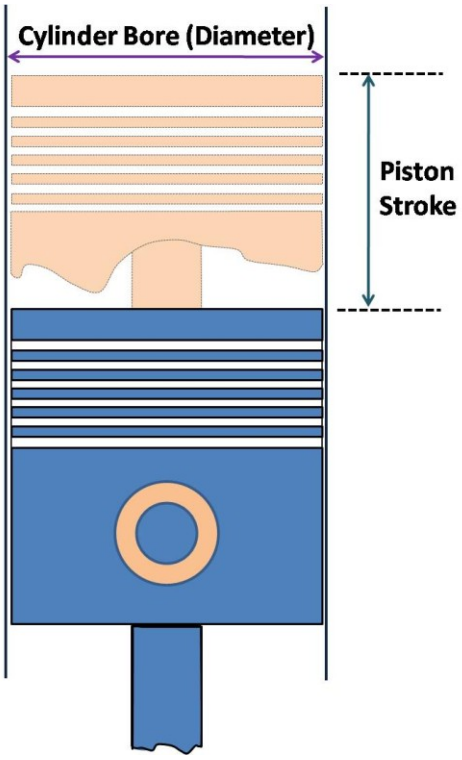

Figure C.3 Cylinder Bore and Stroke [54]

Cylinder Volume is the volume enclosed by the piston travel in the engine cylinder measured from the top surface of the piston head. This volume can be expressed as shown in Equation (C.1):

$$V_{Cylinder} = \pi \cdot \left(Radius_{Cylinder}\right)^2 \cdot Stroke \quad \text{Equation (C.1)}$$

$V_{Cylinder}$: Per-cylinder volume

Cylinder volume is typically expressed in units of cubic centimeters (cc or cm^3). For consistency within this work units of liters or m^3 will be used as appropriate.

The ratio of bore to stroke (R_{BS}) is a commonly used engine parameter. This ratio is shown in Equation (C.2):

$$R_{BS} = \frac{Bore}{Stroke} \quad \text{Equation (C.2)}$$

R_{BS}: Bore to stroke ratio

In literature, the bore-to-stroke ratio and cylinder bore are usually given; the resulting stroke distance is:

$$Stroke = \frac{Bore}{R_{BS}} \quad \text{Equation (C.3)}$$

If cylinder volume (in cm^3) and bore/stroke ratio are given, cylinder bore can be calculated as:

$$Bore = \left(\frac{4 \cdot V_{Cylinder} \cdot [R_{BS}]^2}{\pi}\right)^{\frac{1}{3}} \quad \text{Equation (C.4)}$$

$V_{Cylinder}$: Per-cylinder volume

The stroke distance can be calculated as above for Bore and bore/stroke ratio.

$$Distance_{Cyl} = Bore_{Cyl} + 2 \cdot t_{Wall}$$ Equation (C.5)

$Distance_{Cyl}$: Cylinder distance

$Bore_{Cyl}$: Cylinder bore

t_{Wall}: Cylinder wall thickness

The typical value for wall thickness (t_{Wall}) is about 3.0 mm (0.003 m).

Using the above relationships, parameters have been calculated/extrapolated by engine type in order to generate engine values, packaging and mass distribution within a motor compartment. Averaged values for gasoline inline naturally aspirated engines are shown in Table C.1. Engine volume refers to the external engine dimension volume. Displacement refers to total cylinder volume. Maximum and Minimum cylinder volume are based on maximum / minimum bore and stroke values for an engine type using the "class" value for bore-to-stroke ratio. Parameter values for inline turbocharged gasoline engines are shown in Table C.2. Inline diesel engine values are shown in Table C.3. Corresponding values for V-type engines are shown in Tables C.4, C.5 and C.6.

Parameter	3-Cylinder (3 Samples)	4-Cylinder (27 Samples)	5-Cylinder (1 Sample)	6-Cylinder (6 Samples)
Specific Power (kW / liter Displacement)	48	55	51	59
Specific Torque (Nm / liter Displacement)	94	98	97	98
Specific Weight (kg / liter Displacement)	1.4	1.2	1.1	1.0
Specific Volume (liter Engine Volume / Nm)	1.7	1.3	1.8	1.3
Engine Weight / Displacement (kg / liter Displacement)	69	64	58	58
Volume / Displacement (L Engine Volume / L Displacement)	158	127	175	127
Engine Volume / Power (Liter Engine Volume / kW)	3.6	2.3	2.2	2.2
Engine Length / Power (m / kW)	0.0093	0.0056	0.0051	0.0045
Cylinder Span / Engine Length Ratio	0.60	0.65	0.60	0.73
Maximum Volume / Cylinder (cc) (1000 cc = 1 liter)	333	589	490	500
Minimum Volume / Cylinder (cc)	332	311	490	416
Maximum Cylinder Bore (mm) (1000 mm = 1 meter)	75	92	83	85
Minimum Cylinder Bore (mm)	71	71	83	82
Maximum Stroke (mm)	84	99	91	88
Minimum Stroke (mm)	76	72	91	78
Average Bore / Stroke Ratio	0.89	0.95	0.90	0.99
Cylinder Wall Thickness (mm)	3.5	3.5	3.5	3.5

Table C.1 Values of Parameters for Inline Naturally Aspirated Gasoline Engines

Parameter	2-Cylinder (1 Sample)	3-Cylinder (2 Samples)	4-Cylinder (16 Samples)	6-Cylinder (2 Samples)
Specific Power (kW / liter Displacement)	71	83	83	76
Specific Torque (Nm / liter Displacement)	177	170	158	134
Specific Weight (kg / liter Displacement)	1.4	1.2	1.0	0.9
Specific Volume (liter Engine Volume / Nm)	0.6	0.7	1.0	0.9
Engine Weight / Displacement (kg / liter Displacement)	97	97	74	65
Volume / Displacement (L Engine Volume / L Displacement)	105	121	150	120
Engine Volume / Power (Liter Engine Volume / kW)	1.5	1.6	1.9	1.6
Engine Length / Power (m / kW)	0.0049	0.0047	0.0047	0.0033
Cylinder Span / Engine Length Ratio	0.57	0.59	0.60	0.73
Maximum Volume / Cylinder (cc) (1000 cc = 1 liter)	438	333	565	497
Minimum Volume / Cylinder (cc)	438	333	341	497
Maximum Cylinder Bore (mm) (1000 mm = 1 meter)	438	333	341	497
Minimum Cylinder Bore (mm)	86	72	90	84
Maximum Stroke (mm)	88	82	94	90
Minimum Stroke (mm)	88	82	81	90
Average Bore / Stroke Ratio	0.94	0.88	0.95	0.94
Cylinder Wall Thickness (mm)	3.5	3.5	3.5	3.5

Table C.2 Values of Parameters for Inline Turbocharged Gasoline Engines

Parameter	3-Cylinder (1 Sample)	4-Cylinder (2 Samples)	5-Cylinder (16 Samples)	6-Cylinder (2 Samples)
Specific Power (kW / liter Displacement)	49	54	66	76
Specific Torque (Nm / liter Displacement)	138	164	175	209
Specific Weight (kg / liter Displacement)	2.4	1.6	1.1	0.9
Specific Volume (liter Engine Volume / Nm)	1.1	1.0	1.1	0.5
Engine Weight / Displacement (kg / liter Displacement)	117	84	71	68
Volume / Displacement (L Engine Volume / L Displacement)	199	167	184	104
Engine Volume / Power (Liter Engine Volume / kW)	4.2	3.2	2.8	1.4
Engine Length / Power (m / kW)	0.0085	0.0070	0.0044	0.0034
Cylinder Span / Engine Length Ratio	0.45	0.58	0.50	0.73
Maximum Volume / Cylinder (cc) (1000 cc = 1 liter)	560	550	482	500
Minimum Volume / Cylinder (cc)	560	312	482	500
Maximum Cylinder Bore (mm) (1000 mm = 1 meter)	75	86	81	84
Minimum Cylinder Bore (mm)	75	70	81	84
Maximum Stroke (mm)	85	97	94	90
Minimum Stroke (mm)	85	80	94	90
Average Bore / Stroke Ratio	0.90	0.92	0.87	0.93
Cylinder Wall Thickness (mm)	3.5	3.5	3.5	3.5

Table C.3 Values of Parameters for Inline Diesel Engines

Parameter	6-Cylinder (14 Samples)	8-Cylinder (5 Samples)	10-Cylinder (1 Sample)	12-Cylinder (*)
Specific Power (kW / liter Displacement)	58	56	75	79
Specific Torque (Nm / liter Displacement)	99	94	104	104
Specific Weight (kg / liter Displacement)	0.8	0.6	0.6	0.5
Specific Volume (liter Engine Volume / Nm)	0.9	0.9	0.9	0.9
Engine Weight / Displacement (kg / liter Displacement)	48	48	48	48
Volume / Displacement (L Engine Volume / L Displacement)	93	93	93	93
Engine Volume / Power (Liter Engine Volume / kW)	1.9	1.3	1.3	1.3
Engine Length / Power (m / kW)	0.0049	0.0023	0.0021	0.0020
Cylinder Span / Engine Length Ratio	0.42	0.55	0.63	0.74
Maximum Volume / Cylinder (cc) (1000 cc = 1 liter)	621	876	500	550
Minimum Volume / Cylinder (cc)	462	500	500	500
Maximum Cylinder Bore (mm) (1000 mm = 1 meter)	96	105	92	-
Minimum Cylinder Bore (mm)	85	92	92	-
Maximum Stroke (mm)	93	102	75	-
Minimum Stroke (mm)	80	75	75	-
Average Bore / Stroke Ratio	1.09	1.10	1.22	1.26
Cylinder Wall Thickness (mm)	4.5	4.5	4.5	4.5

Table C.4 Values of Parameters for V-Type Naturally Aspirated Gasoline Engines (*: Interpolated from Other Columns in Table)

Parameter	6-Cylinder (1 Sample)	8-Cylinder (2 Samples)	10-Cylinder (*)	12-Cylinder (2 Samples)
Specific Power (kW / liter Displacement)	78	79	71	65
Specific Torque (Nm / liter Displacement)	136	141	129	122
Specific Weight (kg / liter Displacement)	0.8	0.7	0.9	1.0
Specific Volume (liter Engine Volume / Nm)	0.5	0.7	0.9	1.0
Engine Weight / Displacement (kg / liter Displacement)	58	52	61	66
Volume / Displacement (L Engine Volume / L Displacement)	87	85	82	79
Engine Volume / Power (Liter Engine Volume / kW)	1.0	1.1	1.1	1.2
Engine Length / Power (m / kW)	0.0019	0.0019	0.0019	0.0020
Cylinder Span / Engine Length Ratio	0.51	0.59	0.65	0.74
Maximum Volume / Cylinder (cc) (1000 cc = 1 liter)	583	770	-	550
Minimum Volume / Cylinder (cc)	583	550	-	500
Maximum Cylinder Bore (mm) (1000 mm = 1 meter)	93	103	-	89
Minimum Cylinder Bore (mm)	93	89	-	89
Maximum Stroke (mm)	87	92	-	88
Minimum Stroke (mm)	87	88	-	80
Average Bore / Stroke Ratio	1.07	1.05	1.06	1.06
Cylinder Wall Thickness (mm)	4.5	4.5	4.5	4.5

Table C.5 Values of Parameters for V-Type Turbocharged Gasoline Engines (*: Interpolated from Other Columns in Table)

Parameter	6-Cylinder (3 Samples)
Specific Power (kW / liter Displacement)	64
Specific Torque (Nm / liter Displacement)	192
Specific Weight (kg / liter Displacement)	1.2
Specific Volume (liter Engine Volume / Nm)	0.7
Engine Weight / Displacement (kg / liter Displacement)	75
Volume / Displacement (L Engine Volume / L Displacement)	141
Engine Volume / Power (Liter Engine Volume / kW)	2.1
Engine Length / Power (m / kW)	0.0039
Cylinder Span / Engine Length Ratio	0.35
Maximum Volume / Cylinder (cc) (1000 cc = 1 liter)	500
Minimum Volume / Cylinder (cc)	500
Maximum Cylinder Bore (mm) (1000 mm = 1 meter)	84
Minimum Cylinder Bore (mm)	84
Maximum Stroke (mm)	90
Minimum Stroke (mm)	90
Average Bore / StrokeRatio	0.93
Cylinder Wall Thickness (mm)	4.5

Table C.6 Values of Parameters for V-Type Diesel Engines

Constructing a Parametric Internal Combustion Engine Model

In developing the internal combustion engine model, the following vehicle configurators are initially specified:

- Engine fuel type (Gasoline / Diesel)
- Engine Cylinder Layout (Inline / V-Type)
- Engine Aspiration Type (Naturally Aspirated / Turbocharged)

Note that diesel engines are considered to be turbocharged by the nature of the diesel combustion cycle.

Desired engine power (in kW) is then specified. This is a single input for the Scenario Builder module; in the Optimization module the engine power is a design variable and is updated for each functional evaluation in the optimization process. This may change the number of cylinders in each bank required to supply the required power with successive functional iterations.

Using a gasoline inline naturally aspirated (GINA) engine as an example, the maximum and minimum power in kW for the range of cylinders (3 to 6 for GINA with existing data) is determined. The input menu in the Scenario Builder checks the desired power to the maximum / minimum available values by engine type. If the input power value is outside the specified engine range, an error message is displayed and the user must re-enter a valid value (or select another engine type). The power ranges for each engine type are also displayed in the engine selection menu window as shown in Figure C.4.

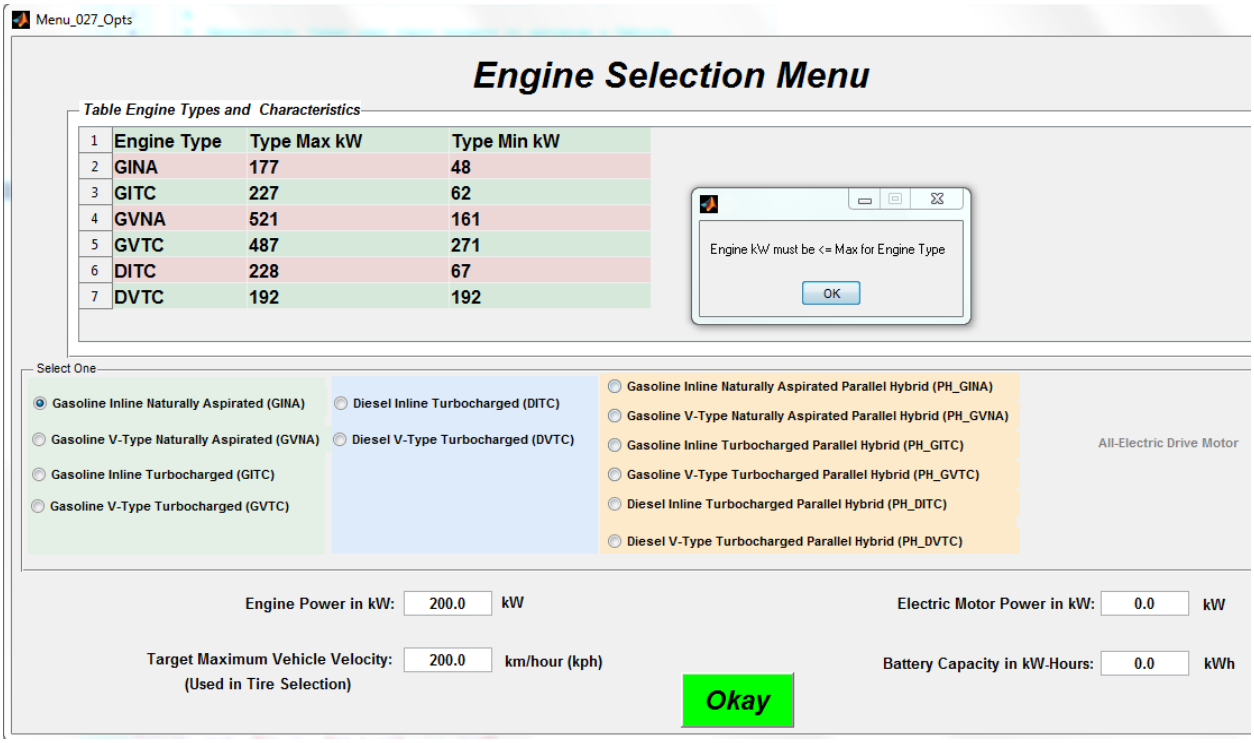

Figure C.4: Scenario Builder Engine Selection Menu [54]

In the Optimization Module, a preliminary calculation determines the starting value for the engine power design variable as shown in Figure C.5. The configurator selections are the same in the menus for both modules. The optimization module selection menu also shows the preliminary estimated power requirements for the vehicle top speed and 0 to 60 mph acceleration time targets; this aids the user in selecting an appropriate engine for the preliminary and final design and optimization iterations. The higher power requirement (maximum velocity or acceleration) is used as the initial input for engine power. If in subsequent optimization iterations the required power exceeds the maximum value for the specified engine type, the power is limited to the maximum for that engine type in the performance to target calculations.

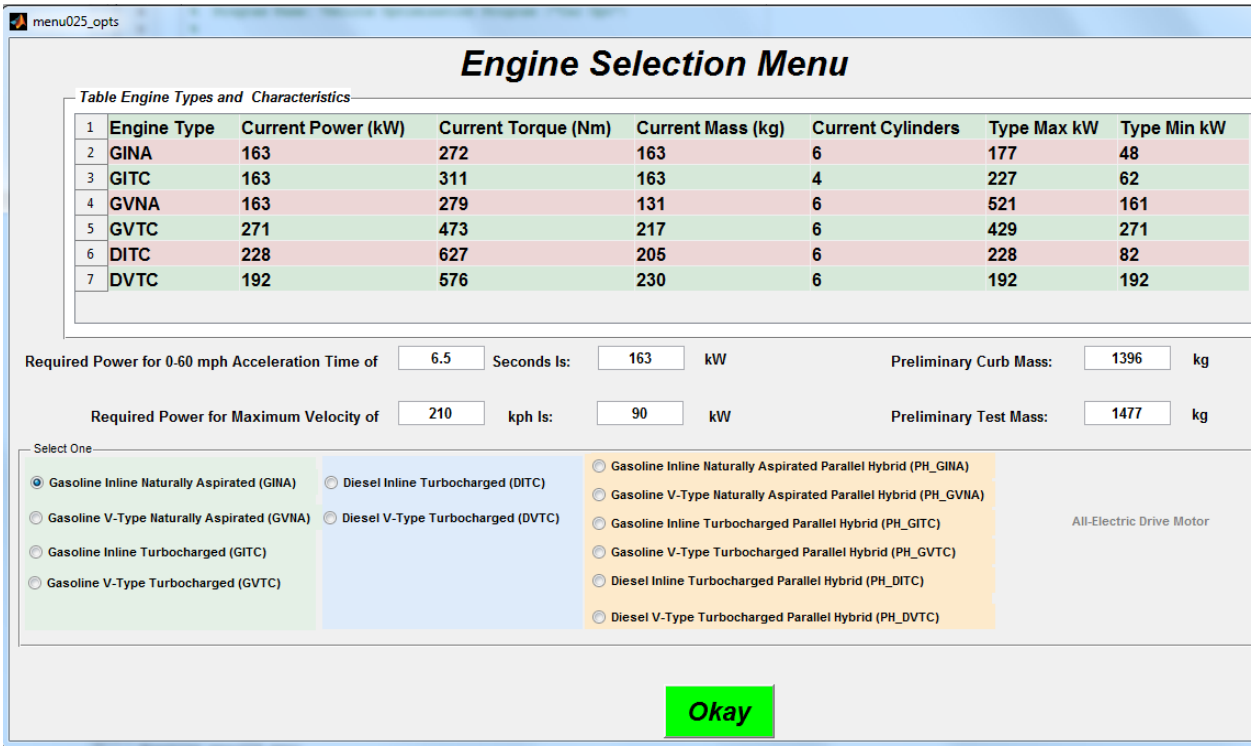

Figure C.5 Optimization Module Engine Selection Menu

The calculation then checks the engine power (in kW) vs. the option with the least number of cylinders (3 for the GINA case). If power is within the 3-cylinder minimum/maximum power range, the resulting engine will have 3 cylinders and the other associated parameter values are loaded into the model structure. In the Optimization module, a power level that would drop below the 3-cylinder minimum (in this case) would be kept at the minimum power value for the 3-cylinder engine.

If the engine power is greater than the 3-cylinder maximum, the engine power is compared to the minimum / maximum power range. If the power is in this range, the 4-cylinder parameters are loaded into the model structure. If not, the next number of cylinders is checked up to the GINA maximum of 6 cylinders. If the power exceeds the

maximum rating for the maximum cylinder count, the power is set to the 6-cylinder maximum.

Once the number of engine cylinders is set, the per-cylinder volume is determined from the engine power and engine specific power (kW / liter displacement) as shown in Equation (C.6).

$$V_{Cylinder} = \frac{P_{Engine}}{P_{Specific} \cdot N_{Cyl}} \quad \text{Equation (C.6)}$$

P_{Engine}: Engine power (in kW)

$P_{Specific}$: Engine Specific Power (kW / liter displacement)

N_{Cyl}: Number of cylinders in engine

The cylinder bore is then determined using Equation C.7.

$$Bore_{Cyl} = \left(\frac{4 \cdot V_{Cyl} \cdot R_{BS}}{\pi}\right)^{\frac{1}{3}} \quad \text{Equation (C.7)}$$

$Bore_{Cyl}$: Cylinder bore

V_{Cyl}: Per-cylinder volume

R_{BS}: Cylinder bore-to-stroke ratio

Note that the bore-to-stroke ratio is an average for all engines of the specified engine type and number of cylinders. While specific engines in industry use may vary from these values, they gives a reasonable value for the engine parameters used in the performance measures utilized in this work

The overall engine cylinder span (CL1) is then determined using Equation C.8.

$$\text{CL1} = N_{Cyl} \cdot Bore_{Cyl} + 2 \cdot t_{Wall} \quad \text{Equation (C.8)}$$

C_{L1}: Engine cylinder span

N_{Cyl}: Engine cylinder count

$Bore_{Cyl}$: Cylinder Bore

t_{Wall}: Cylinder wall thickness

The resulting engine length (EL1) is then determined from Equation (C.9).

$$EL1 = \frac{CL1}{R_{CS2EL}} \quad \text{Equation (C.9)}$$

EL1: Engine Length

CL1: Cylinder Span

R_{CS2EL}: Average ratio of cylinder span to engine length for engine type / cylinder count

Total engine mass is determined from peak engine power and specific weight as shown in Equation (C.10).

$$M_{Eng} = P_{Eng} \cdot W_{Specific} \quad \text{Equation (C.10)}$$

M_{Eng}: Engine mass

P_{Eng}: Peak engine power (kW)

$W_{Specific}$: Engine specific power (kg / kW)

The correlation between estimated and actual engine mass is shown in Figure C.6.

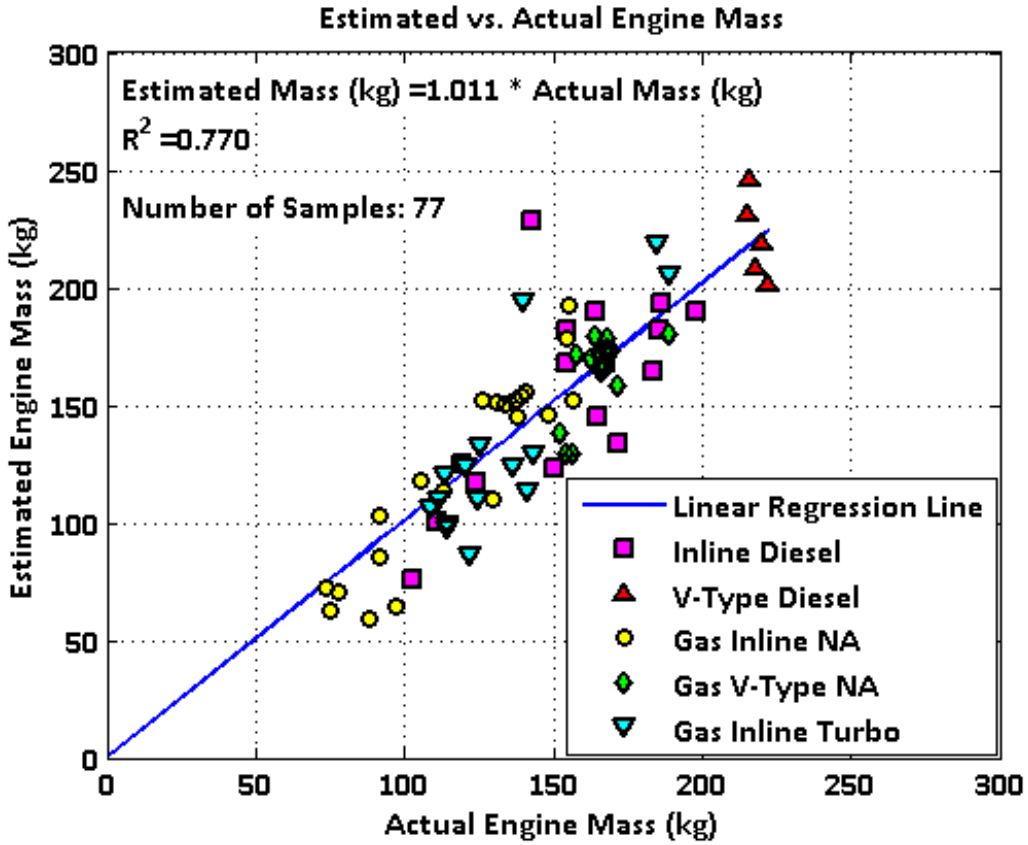

Figure C.6 Estimated vs. Actual Mass for Engine (Gas: Gasoline, NA: Naturally Aspirated) [54]

The mix of gasoline and diesel engines in Figure C.6 includes inline and V-type engines for both fuel options. Inline engines show the greatest variation in estimated vs. actual mass. One source of variation may be a mix of aluminum and steel inline engine blocks in the above sample.

Peak engine torque calculation is shown in Equation (C.11).

$$T_{Eng} = V_{Cyl} \cdot N_{Cyl} \cdot T_{Specific} \qquad \text{Equation (C.11)}$$

T_{Eng}: Peak engine torque (Nm)

V_{Cyl}: Per-cylinder volume (liter)

N_{Cyl}: Number of cylinders

$T_{Specific}$: Engine specific torque (Nm / liter displacement)

Overall engine volume (EL1 * EW1 * EH1) can be obtained from Equation (C.12).

$$V_{Eng} = T_{Eng} \cdot V_{Specific} \quad \text{Equation (C.12)}$$

V_{Eng}: Engine volume (liters or m^3; 1 m^3 = 1000 liters)

TEng: Peak engine torque (Nm)

VSpecific: Engine specific volume (liters engine volume / Nm)

Additional engine measures / parameters can be determined using the values shown in Tables C.1 through C.6.

Driveline and Transmission Relationships

Driveline and transmission mass estimates are a two-step process; transmissions (and the resulting drivelines) are sized by peak engine torque rather than direct engine power. Engine peak power must first be converted to the corresponding peak torque by engine type (although peak power and peak torque may occur at different engine speeds, the relationship between the two can be correlated). Relationships for the driveline and included transmission are then based on the torque value. From the engine database, relationships between peak engine power and peak engine torque have been developed for various engine types as shown in Table C.7 [54]. Some engine types are left blank due to lack of available data for this work.

Cylinder Layout (Inline / V-Type)	Gasoline Naturally Aspirated Torque / Power (Nm/kW)	Gasoline Turbocharged Torque / Power (Nm/kW)	Diesel Torque / Power (Nm/kW)
I-2	**-**	**2.50**	**-**
I-3	**1.85**	**2.10**	**2.85**
I-4	**1.90**	**1.90**	**3.10**
I-5	**1.90**	**-**	**2.65**
I-6	**1.65**	**1.75**	**2.70**
V-6	**1.70**	**1.75**	**3.00**
V-8	**1.70**	**1.85**	**-**
V-10	**1.40**	**1.85**	**-**
V-12	**1.40**	**1.85**	**-**

Table C.7 Engine Maximum Torque vs. Engine Peak Power (I: Inline, V: V-Type) [54]

Values of torque to power ratios from Table C.7 are used to estimate torque values for engines in the vehicle database. A comparison of estimated vs. actual engine torque is shown in Figure C.7 [54]. The trend line is close to the desired value of 1.000 with a high level of correlation.

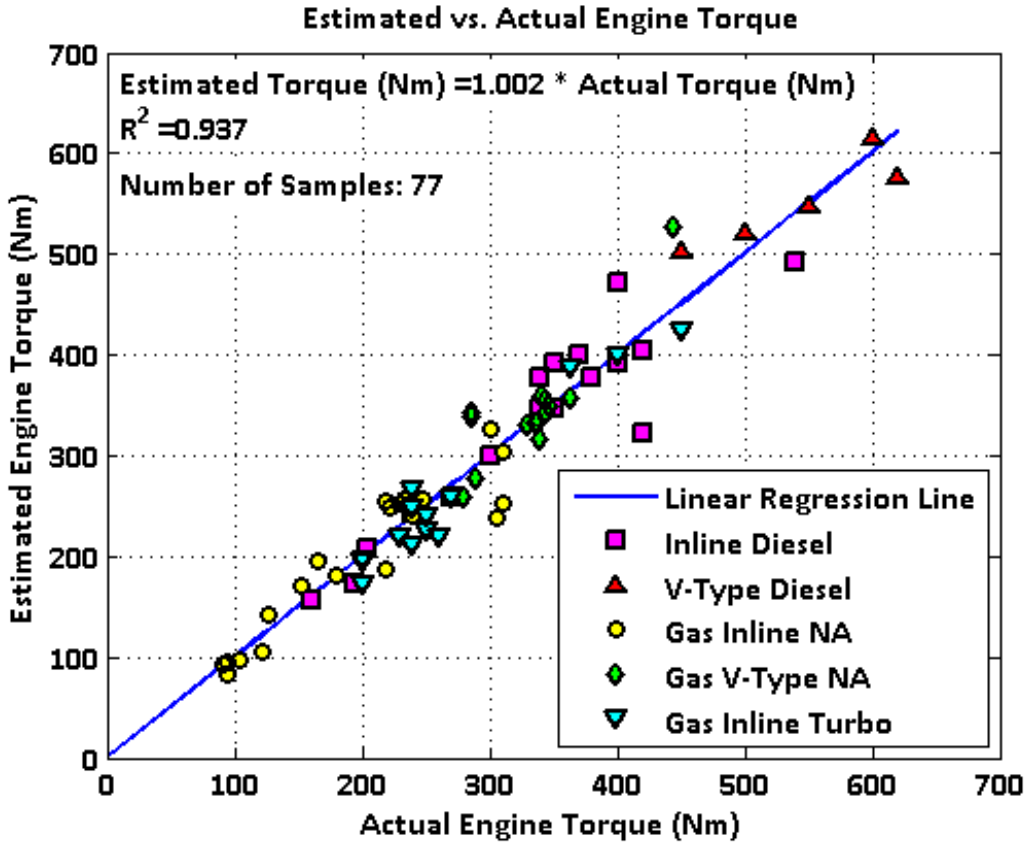

Figure C.7 Estimated vs. Actual Engine Torque (Gas: Gasoline, NA: Naturally Aspirated, Turbo: Turbocharged) [54]

Maximum (peak) torque is then used to develop the driveline mass relationship (and the included transmission mass for center of gravity location calculations). All subsystem relationships except those for engines have been developed using the vehicle database; a series of curb mass case studies using samples outside the vehicle database have also been compared to validate the subsystem and curb mass modeling correlations. Driveline Correlations are shown in Table C.8 according to shift type (automatic or manual) and drive configuration (front- / rear- / all-wheel drive) along with associated correlation confidence (R^2) values for each mass relationship [54].

Driveline Configuration	Driveline Estimated Mass (M_{Drv})	R^2 Value
Automatic Front Wheel Drive	M_{Drv} = 0.241 * (Engine Peak Torque in Nm) + 35.58 kg	**0.779**
Manual Front Wheel Drive	M_{Drv} = 0.102 * (Engine Peak Torque in Nm) + 42.39 kg	**0.783**
Automatic Rear Wheel Drive	M_{Drv} = 0.112 * (Engine Peak Torque in Nm) + 71.34 kg	**0.897**
Manual Rear Wheel Drive	M_{Drv} = 0.123 * (Engine Peak Torque in Nm) + 59.96 kg	**0.939**
Automatic All Wheel Drive	M_{Drv} = 0.102 * (Engine Peak Torque in Nm) + 141.10 kg	**0.623**
Manual All Wheel Drive	M_{Drv} = 0.103 * (Engine Peak Torque in Nm) + 103.0 kg	**0.503**

Table C.8 Driveline Mass Estimation Relationships (M_{Drv}: Driveline Mass in kg) [54]

Driveline estimated mass is compared to actual driveline mass in the vehicle database in Figure C.8 [54]. Some variation is due to the inclusion of a variety of vehicle types (sedan, coupe, crossover sport utility vehicle, 2-seat sports car); however, the correlation of overall vehicle curb mass and limited sample size for some vehicle types dictates against using separate driveline correlations for each vehicle type. The higher trendline value in Figure C.8 may be due to the two-step process in estimating driveline mass.

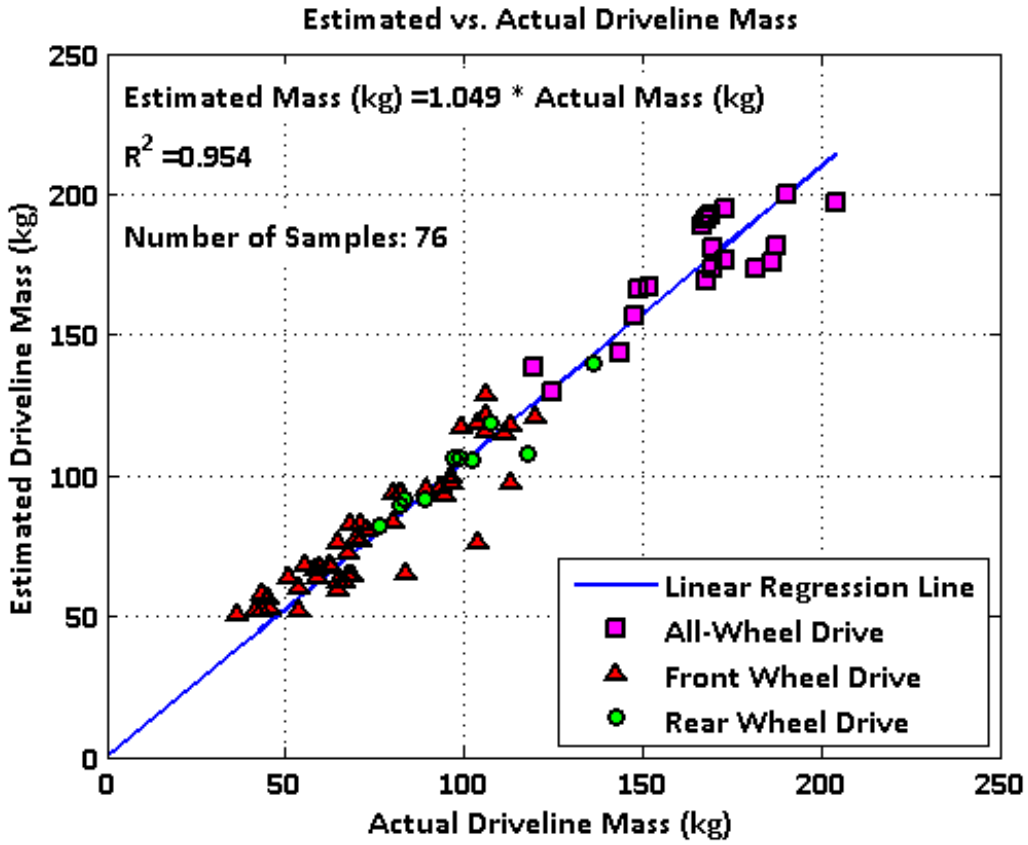

Figure C.8 Estimated vs. Actual Driveline Mass from Estimated Torque [54]

For center of gravity (C_g) location estimation purposes it is desirable to separate the transmission mass from the rest of the driveline. From the engine / transmission database, correlations between peak torque and transmission mass have been developed as shown in Table C.9 [54]:

Transmission Configuration	Transmission Estimated Mass (M_{Tran})	R^2 Value	Sample Size
Manual Front Wheel Drive	**M_{Tran} = 0.092 *(Peak Torque) + 17.81 kg**	**0.975**	**7**
Manual Rear Wheel Drive	**M_{Tran} = 0.084 *(Peak Torque) + 8.75 kg**	**0.886**	**6**
Automatic Front Wheel Drive	**M_{Tran} = 0.148 *(Peak Torque) + 16.20 kg**	**0.563**	**9**
Automatic Rear Wheel Drive	**M_{Tran} = 0.075 *(Peak Torque) + 24.05 kg**	**0.758**	**7**
Automated Manual Transmission (FWD/RWD)	**M_{Tran} = 0.090 *(Peak Torque) + 21.46 kg**	**0.999**	**3**
Dual Clutch Transmissions (FWD/RWD)	**M_{Tran} = 0.014 *(Peak Torque) + 70.62 kg**	**0.498**	**3**

Table C.9 Transmission Mass Estimation Relationships (FWD: Front Wheel Drive, RWD: Rear Wheel Drive, M_{Tran}: Transmission Mass in kg) [54]

A certain level of variation is expected for driveline and particularly for transmission mass estimation. Transmissions are typically not continuously sized for torque; rather they are grouped in families in increments of 20, 50, 100 etc. Nm maximum torque capacity depending on each transmission supplier. As a result, the trend line for estimated vs. actual transmission torque is expected to be less than 1.000 as seen in Figure C.9 [54]. The correlation confidence value R^2 is similarly reduced compared to overall driveline mass estimation. In practice this can be compensated for by rounding estimated torque upward to the nearest desired torque increment prior to estimating the driveline and transmission mass.

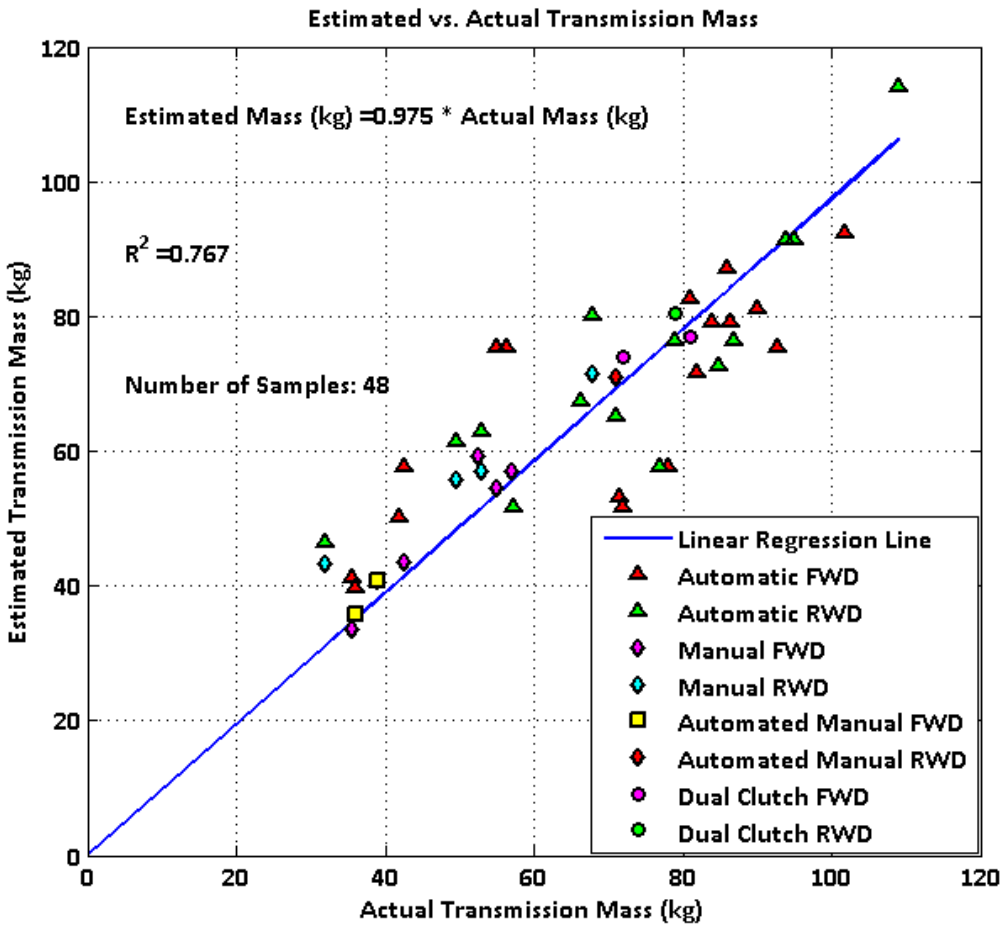

Figure C.9 Estimated vs. Actual Transmission Mass (FWD: Front Wheel Drive, RWD: Rear Wheel Drive) [54]

Appendix D
Frontal Crashworthiness Modeling and Development

A frontal crash surrogate model has been developed to assess one aspect of the Safety functional area frontal New Car Assessment Program (NCAP) crash performance. Development of a front crash model requires that three activities be completed:

- Correlation between vehicle structural accelerations and NCAP star rating
- A representative structural model with all structural elements expressed as a fraction of midrail average crush force
- The ability to solve for accelerations, energy balance and resulting midrail length if average midrail crush force is used as the input parameter or design variable.

Correlation between Accelerations and Frontal NCAP Rating

In order to develop a correlation between vehicle accelerations and the resulting NCAP "Star" rating values, published data for NCAP test results shown in Table D.1 was examined [67, 68]. The star rating assesses the likelihood of the occupant suffering a severe injury based on a combination of the head impact criteria (HIC) and chest g's measured in crash testing. The likelihood of injury vs. these two factors in combination is shown in Figure D.1. The test impact velocity is 35 mph / 56.3 kph into a rigid flat barrier. The maximum allowed HIC value is 1000; the maximum chest g level in a 3-millisecond span is 60 g's [67].

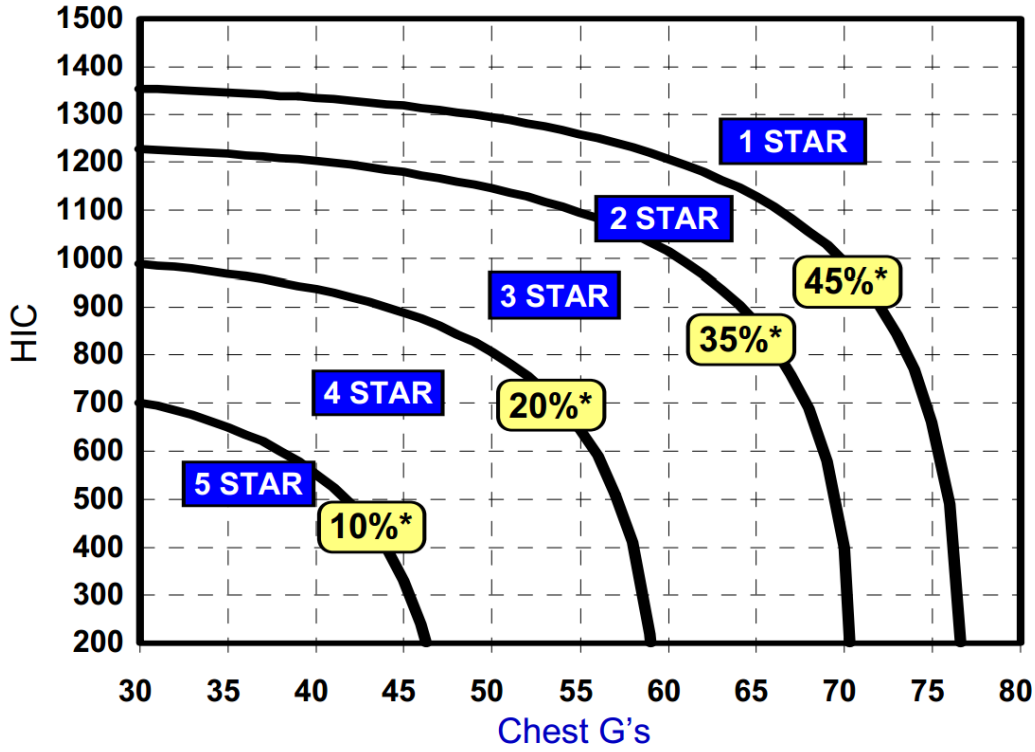

Figure D.1 Frontal NCAP Star Rating vs. HIC and Chest G's (*: % Chance of Serious Injury for Star Rating) [67]

NHTSA NCAP test results are shown in Table D.1 The author has experience with two of these vehicles from analysis and testing performed at General Motors (Buick LeSabre and Chrysler LHS). The LeSabre underwent front structural modifications which increased stiffness (and slightly increased HIC as a result) in order to reduce intrusion and achieve a "Good" rating on the IIHS offset crash test (an intrusion-based test) [69]. This example shows the need to manage trade-offs between different and often conflicting vehicle requirements and targets. Chest g's are measured as the maximum value over a rolling 3 millesecond interval through the test.

Vehicle	Average Acceleration (g)	HIC	Chest G's	Stars	Offset Rating
Buick LeSabre	**24.1**	**467**	**43**	**5**	**Good**
Ford Taurus	**25.8**	**345**	**41**	**5**	**Good**
Volkswagen Passat	**23.1**	**377**	**44**	**5**	
Volvo S70	**25.0**	**259**	**46**	**5**	
Nissan Maxima	**28.4**	**437**	**50**	**4**	**Average**
Toyota Avalon	**25.6**	**504**	**50**	**4**	
Subaru Legacy	**24.6**	**559**	**45**	**4**	**Good**
Mitsubishi Galant	**30.5**	**439**	**50**	**4**	**Average**
Toyota Camry	**26.9**	**525**	**46**	**4**	
Honda Accord	**27.8**	**631**	**49**	**4**	**Good**
Chrysler LHS	**26.6**	**708**	**61**	**3**	
Nissan Altima	**26.3**	**908**	**50**	**3**	

Table D.1 NHTSA NCAP Test Results [68]

While a correlation between vehicle accelerations and chest g's is found as shown in Figure D.2, no meaningful correlation was found between accelerations and HIC. Without both correlations, a direct mapping to the HIC vs. Chest G NCAP star rating curves cannot be made [67].

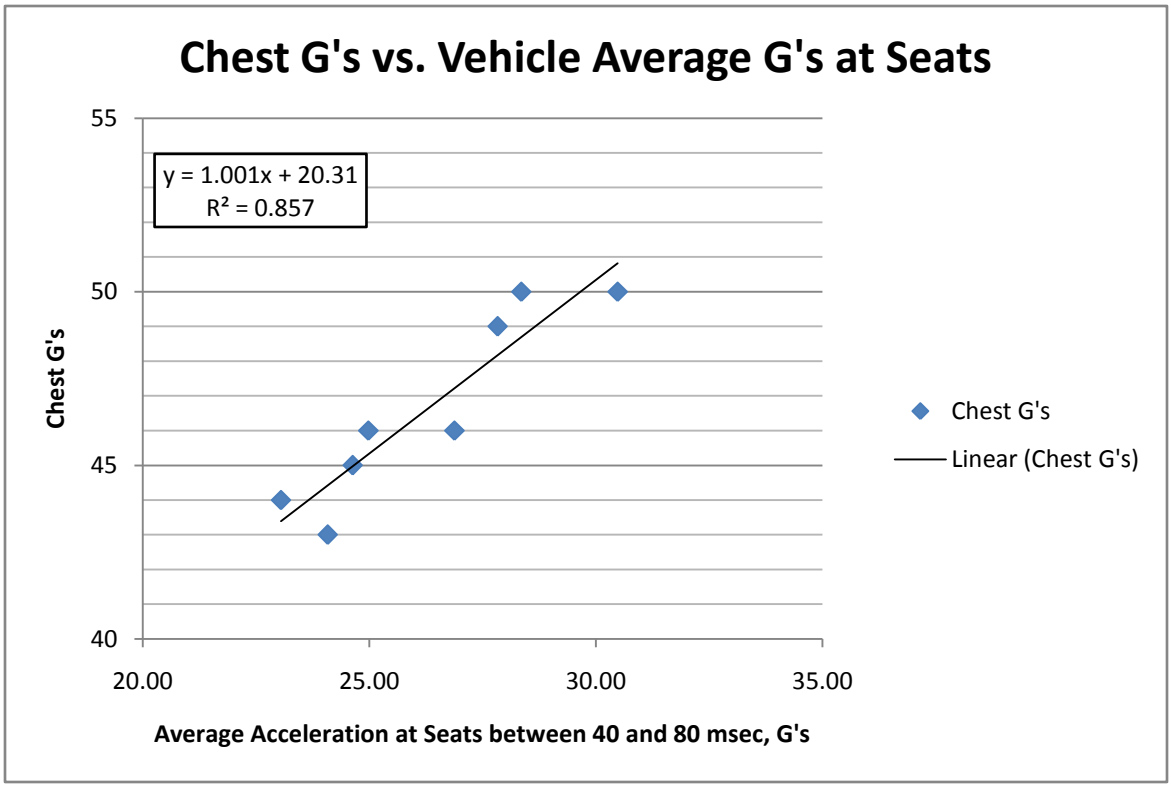

Figure D.2 Frontal NCAP Chest G's vs. Average Vehicle Accelerations

A simpler comparison of NCAP ratings (star values) vs. average vehicle accelerations is shown in Table D.2.

NCAP Performance Rating (Stars)	Average Vehicle Acceleration (g's)	Standard Deviation (g's)	Average HIC Value	HIC Standard Deviation	Average Chest g's	Chest g's Standard Deviation
5	24.5	1.2	362	85.9	43.5	2.1
4	27.3	2.1	516	74.1	48.3	2.3
3	26.4	N/A	808	N/A	55.5	N/A

Table D.2 NCAP Performance Measures by NCAP Star Rating (NCAP: New Car Assessment Program)

The data in Table D.2 indicates a proposed maximum acceleration target for each

star rating:

- 5-Star: Average accelerations less than 25 g's (± 0.5 g)
- 3- / 4-Star: Average accelerations less than 30 g's (± 0.5 g)
- 1- / 2-Star: Average accelerations greater than 30 g's

Note in Table D.1, that there is a vehicle above the 25-g level with a 5-star rating and one above the 30-g level with a 4-star rating. The target for 5-star ratings should be to remain under 25.0 g's, but the ± 0.5g tolerance for evaluation recognizes that other factors may come into play (the same applies to the 4-star rating). However, vehicles which fall in this threshold region should be given additional attention in seating and restraint design if such a design configuration is carried forward into detailed design.

Vehicles with a 3-Star rating have accelerations comparable to those with 4-Star ratings, indicating that other factors contribute to their comparatively worse performance (restraints, seat design, etc.). However, even a 3-Star rating typically requires accelerations less than 30 g's. Potential factors differentiating 3- vs. 4-Star performance may include:

- Seat Design
- Airbag deployment time and single vs. dual stage inflation
- Airbag firing time
- Restraint type (B-pillar anchor or all-belts-to-seats -- ABTS. Some vehicles also use a deformable guide loop with the B-pillar anchor to manage energy distribution over time)

It is important to note that these factors are all finalized in the detailed design

phase. This indicates that if the vehicle accelerations in the conceptual design stage support 4-Star performance, additional detailed design activities are required to avoid the design degrading into the 3-Star performance range (or from 5-star to 4-star range).

An American Iron and Steel Institute (AISI) project to develop a light-weight vehicle structure providing the highest level of NCAP performance, also recommends average accelerations less than 25 g's for a proposed vehicle design which meets 5-star / "Good" test performance[68]. As no vehicles in the test sample have a 1- or 2-Star rating, the 30+ g's value is assumed as no 3-Star vehicles exceeded 30 g's.

The software framework determines the maximum acceleration in each of 4 crush zones (bumper, in front of engine, between engine and firewall, firewall ride-down). To match the above acceleration averages, a time-weighted average of the crush accelerations in zones 3 through 5 shown in Figure D.3 are used. Only 40% of the zone 2 interval is used as this is about the time in a front crash event that an occupant is loading into the restraints; until then they are not tied to the vehicle deceleration. Higher accelerations in Zone 1, 2 and 3 take energy out before occupant ride-down with the vehicle, but progressive crush and low-speed bumper performance considerations may preclude achieving this in practice.

Frontal Crashworthiness Surrogate Model

A schematic diagram of the frontal crash surrogate model is shown in Figure D.3. A simplified surrogate model is used to assess crashworthiness parametrically and at the conceptual design level; one trade-off in avoiding elements of detailed design is the loss

of detailed, time-specific event information due to the use of average values throughout each crush zone. The model must be able to capture several aspects of a crash event:

- Average vehicle accelerations (in the passenger compartment) at each stage (zone) of the crash event
- Average forces in each zone causing structural crush and resulting energy absorption
- Time duration of crush in each zone

Several assumptions must be made in developing the front crash model:

- That the engine is in front of the vehicle in an engine bay (for this model)
- Crush forces are uniform throughout the crush event in each zone.
- Crush is progressive from the front rearward through each crush zone.
- All available crush distance in each zone is used before crush begins in the next zone.
- The bumper hat (rail) will crush up to 70% of its original length (and that the uncrushable portion of the midrails can extend into the zone of the engine block, using all available crush space not "blocked" by the rigid engine).
- That crush of the midrails, engine cradle and hood / sheet metal continues as the engine intrudes into the vehicle firewall.

These assumptions impose limitations on the model. The model cannot find an individual peak acceleration or force in the crash event; only the average value for each zone. Tire interactions are ignored (typically a tire stores and then releases energy when compressed, unless the tire deflates in a crash event). A perfect longitudinal crush with

no structural bending is assumed; this may result in higher energy absorption than in an actual vehicle.

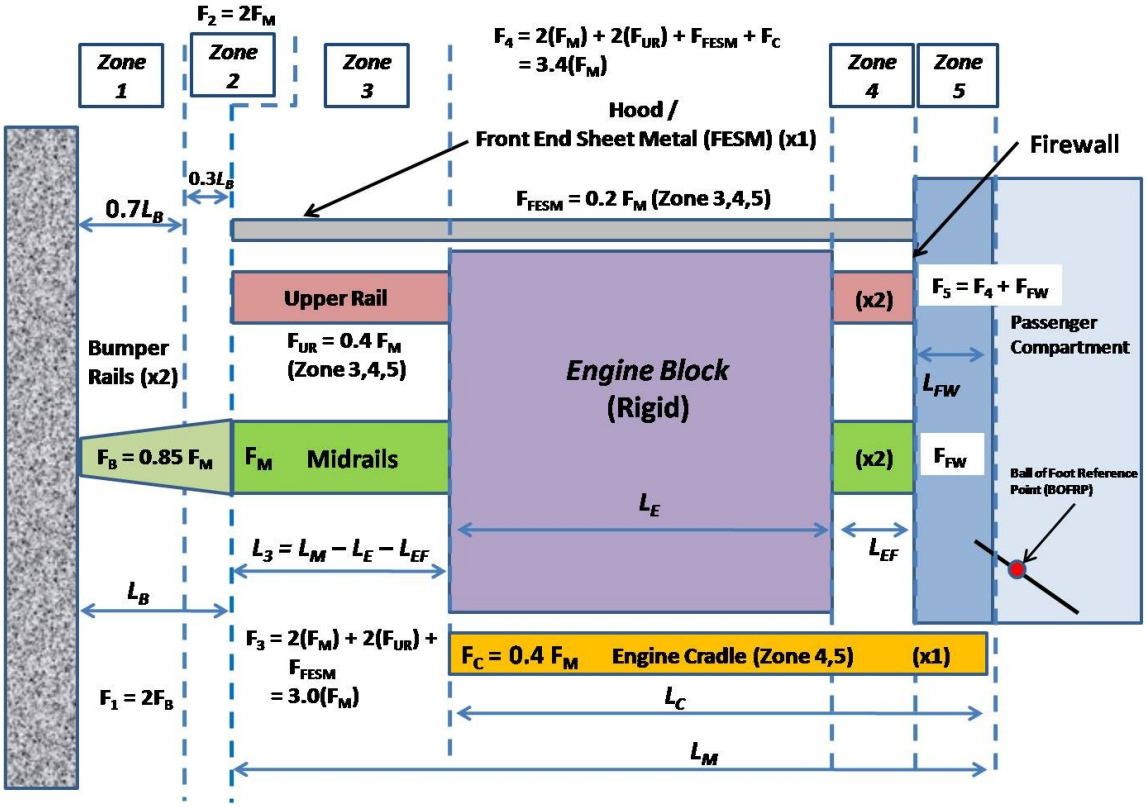

Figure D.3 Schematic Diagram of Frontal Crash Surrogate Model [54, 70]

The frontal crash energy absorption is analyzed in five distinct zones: bumper rail crush (Zone 1), front midrail crush in front of cradle / sheet metal (Zone 2), front midrail / upper rail / sheet metal crush (Zone 3), cradle / midrail / upper rail crush without engine mass (Zone 4) and firewall crush (Zone 5). The average front midrail crush force is used as the design variable. The crush of other structural elements (bumper rails, engine cradle, etc.) are expressed as a typical fraction of the midrail crush force. These ratios are consistent in typical vehicle structures as documented by Malen [48]. This permits all forces to be expressed by a single aggregated variable. Mass is

considered to be lumped in either the engine (M_E) or body of the vehicle (M_B). The amount of crushable (energy absorbing) space in each zone is shown in Figure D.2 as well.

It should be noted that other front structural configurations and crush force proportions are possible. This initial configuration of a typical front layout is used as a proof of concept and applies to many current vehicle models. The inclusion of a selection of front structural configuration options may be potential future work

With this information the crash event can be analyzed by zone in order. The first zone (bumper rail crush) has an additional criteria: in a 10 kph frontal crash, only the bumper beam can deform (no other structural crush). This is to simulate some of the requirements inherent to the Insurance Institute for Highway Safety bumper test and rating protocol [83]. This sets the bumper rail length based on vehicle mass and constrains the maximum bumper rail force to 85% of average midrail crush force to ensure progressive structural crush (70% maximum crush of the bumper rails is also assumed).

Based on the above front structure representation, the calculation of bumper rail and midrail length along with associated average acceleration for each zone can be carried out as described below. Many of the relations shown in the zone calculations are derived from existing sources with slight variation [70]; one of the author's contributions has been to tie the equations for each zone together to derive accelerations and resulting midrail length as a function of midrail average crush force as a single design variable input.

Zone 1 (Bumper Crush) Model Calculations

Crush of the bumper rails is shown in Figure D.4. It is assumed that the bumper rails will crush up to approximately 70% of their initial length.

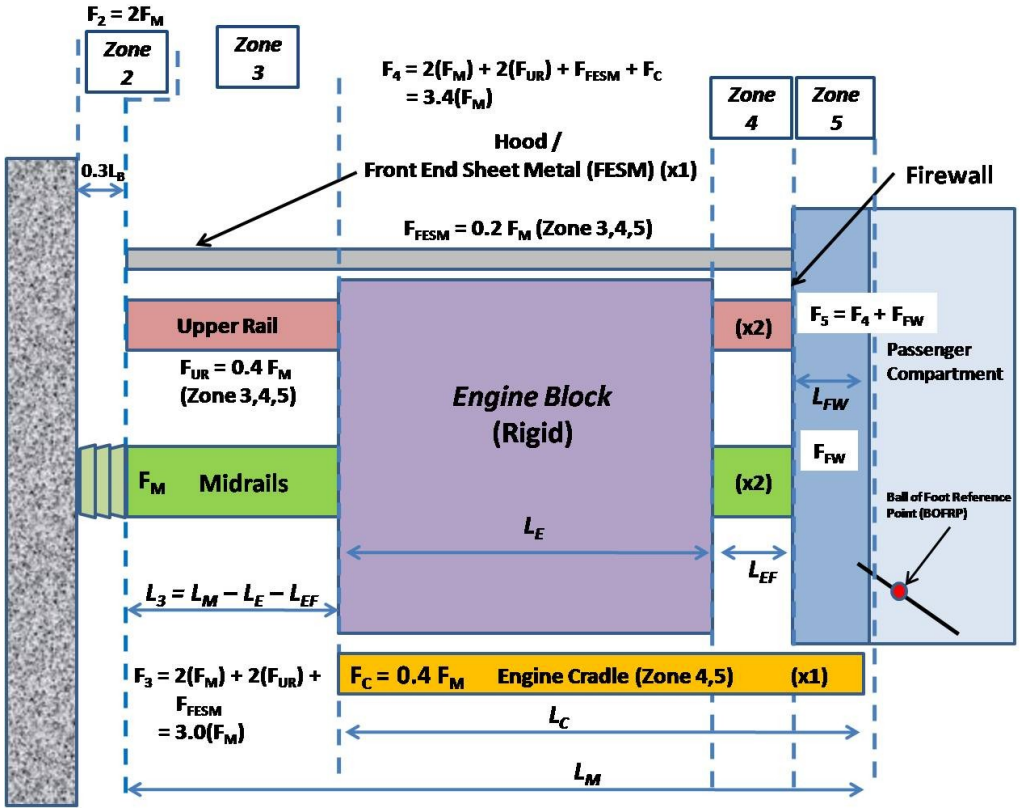

Figure D.4 Zone 1 Crush

The bumper rail length is calculated as a function of total vehicle mass and midrail crush force for a 10 kph impact requirement (bumper crush force limited to 85% of midrail crush force and 70% bumper rail crush) as shown in Equation (D.1). This uses the energy relation $F*d = ½ Mv^2$:

$$L_B = \frac{0.5 \cdot (M_B + M_E) \cdot (2.278\ m/sec)^2}{2 \cdot 0.7 \cdot 0.85 \cdot F_M} = \frac{2.180 \cdot (M_B + M_E)}{F_M} \qquad \text{Equation (D.1)}$$

L_B: Bumper Rail Length (m)

M_B: Body Mass (kg) (Includes 150 kg for two 50th percentile test manikins)

M_E: Engine Mass (kg) (Includes transmission mass as well)

F_M: Average Midrail Force (Newtons) for one midrail (one side of vehicle)

2.778 m/sec = 10.0 kph

2 = Number of Bumper Rails

0.7 = Portion of bumper rail which crushes

0.85 = Ratio of bumper rail average crush force / midrail crush force

Note that in the multi-objective optimization F_M is a design variable and M_B and M_E are resultant parameters which vary due to changes in various vehicle configurators and input variables. With bumper rail length L_B expressed in terms of the midrail force F_M, accelerations during Zone 1 crush are shown in Equation (D.2). This uses the relation F = Ma:

$$a_1 = \frac{F_1}{M_B + M_E} = \frac{2 \cdot 0.85 \cdot F_M}{M_B + M_E} = \frac{1.7 \cdot F_M}{M_B + M_E} \qquad \text{Equation (D.2)}$$

a_1:Zone 1 average acceleration (m/sec^2)

F_1: Average Force during Zone 1 Crush (Newtons)

M_B: Body Mass (kg) (Includes 150 kg for two 50th percentile test manikins)

M_E: Engine Mass (kg) (Includes transmission mass as well)

F_M: Average Midrail Force (Newtons)

2 = Number of bumper rails

0.85 = Fraction of bumper rail average crush force to average midrail crush force

The vehicle velocity will decrease as energy is absorbed by vehicle structure in each stage of the crash event. The resulting energy balance at the start and end of Zone 1 crush is shown in Equation (D.3).

$$\frac{1}{2}M_0V_0^2 = \frac{1}{2}M_1V_1^2 + F_{Crush} \cdot d_{Crush} \qquad \text{Equation (D.3)}$$

M_0: Initial vehicle mass (kg)

V_0: Initial vehicle velocity = 35.0 mph = 15.646 m/sec

M_1: Vehicle mass at end of Zone 1 crush (kg) (= M_0)

V_1: Vehicle velocity at end of Zone 1 crush (m/sec)

F_{Crush}: Average Zone 1 crush force (N)

d_{Crush}: Zone 1 crush distance (m)

If the Zone 1 relations are substituted and the equation solved for V_1, Vehicle velocity at the end of Zone 1 crush may be expressed as:

$$V_1 = \sqrt{V_0^2 - \frac{2 \cdot (2 \cdot 0.85 \cdot F_M) \cdot (0.7 \cdot L_B)}{M_B + M_E}} = \sqrt{244.8 - \frac{2.38 \cdot F_M \cdot L_B}{M_B + M_E}} \qquad \text{Equation (D.4)}$$

V_0: Initial vehicle velocity (m/sec)

V_1: Vehicle velocity at end of Zone 1 crush

F_M: Average midrail crush force (N)

L_B: Bumper rail length (m)

M_B: Vehicle body mass (kg) (Includes 150 kg for two 50th percentile test manikins)

M_E: Vehicle engine mass (kg) (Includes transmission mass as well)

Zone 2 (Midrail In Front of Upper Rail / Sheet Metal) Crush Model Calculations

Zone 2 crush is shown in Figure D.5.

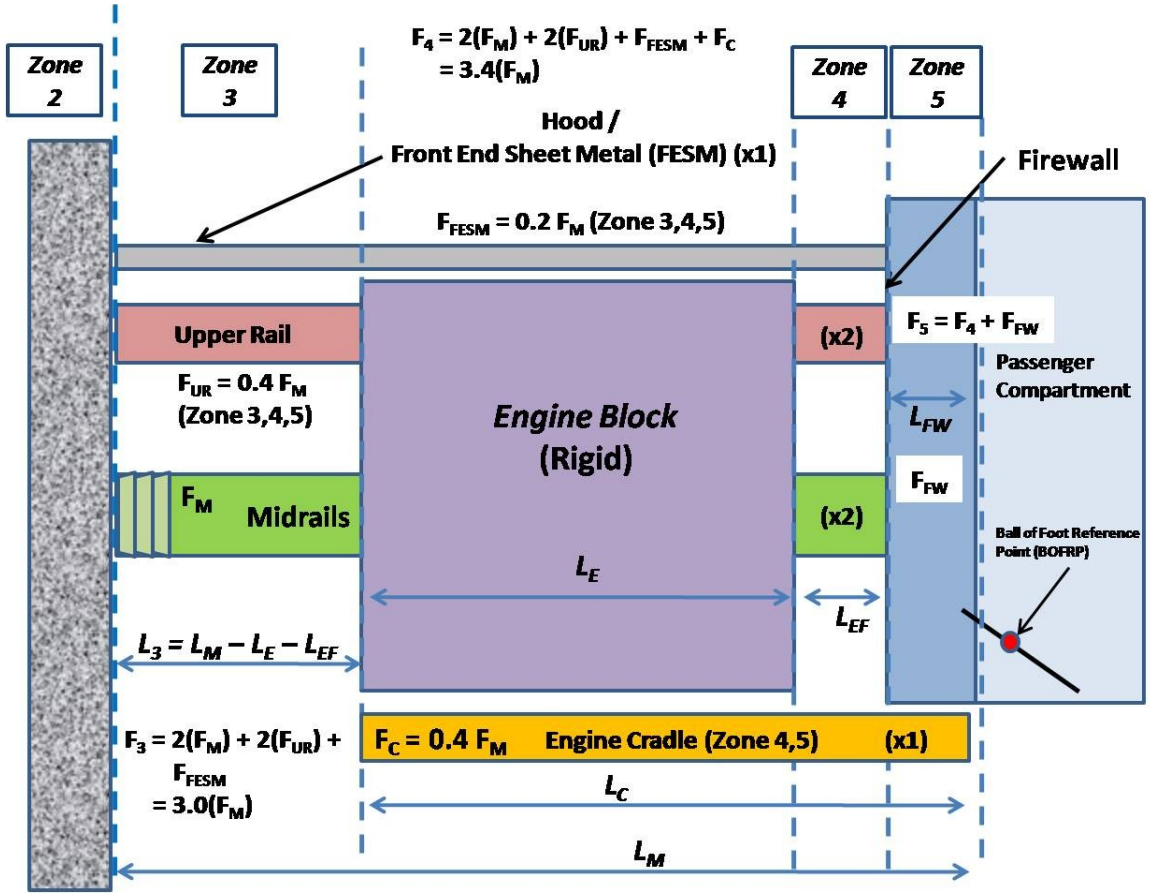

Figure D.5 Zone 2 Crush

Zone 2 average acceleration is calculated similarly to that of Zone 1 with different structural elements (midrails only) crushing and absorbing energy as shown in Equation (D.5).

$$a_2 = \frac{F_2}{M_B + M_E} = \frac{2 \cdot F_M}{M_B + M_E}$$ Equation (D.5)

a_2: Zone 2 average acceleration (m/sec^2)

F_2: Zone 2 crush force (N)

F_M: Average midrail crush force for one side (N)

M_B: Vehicle body mass (Includes 150 kg for two 50th percentile test manikins)

M_E: Vehicle engine mass (kg) (Includes transmission mass as well)

Velocity at the end of Zone 2 crush is also calculated similarly to that of Zone 1 crush as shown in Equation (D.6). The length of the midrail that crushes in Zone 2 is the remaining uncrushed bumper rail distance prior to the upper rails and sheet metal being loaded. If progressive crush from the front of the vehicle is assumed, the result is shown in Equation (D.6).

$$V_2 = \sqrt{V_1^2 - \frac{2 \cdot F_2 \cdot d_2}{M_B + M_E}} = \sqrt{V_1^2 - \frac{2.0 \cdot F_M \cdot (0.3 \cdot L_B)}{M_B + M_E}} = \sqrt{V_1^2 - \frac{0.6 \cdot F_M \cdot L_B}{M_B + M_E}}$$ Equation (D.6)

V_1: Vehicle velocity at end of Zone 1 crush (m/sec)

V_2: Vehicle velocity at end of Zone 2 crush (m/sec)

F_2: Average Zone 2 crush force (N)

d_2: Zone 2 crush distance (m)

M_B: Vehicle body mass (kg) (Includes 150 kg for two 50th percentile test manikins)

M_E: Vehicle engine mass (kg) (Includes transmission mass as well)

F_M: Average midrail crush force for one side (N)

L_B: Bumper rail length (m)

Zone 3 (In Front of Engine) Crush Model Calculations

Zone 3 crush is shown in Figure D.6.

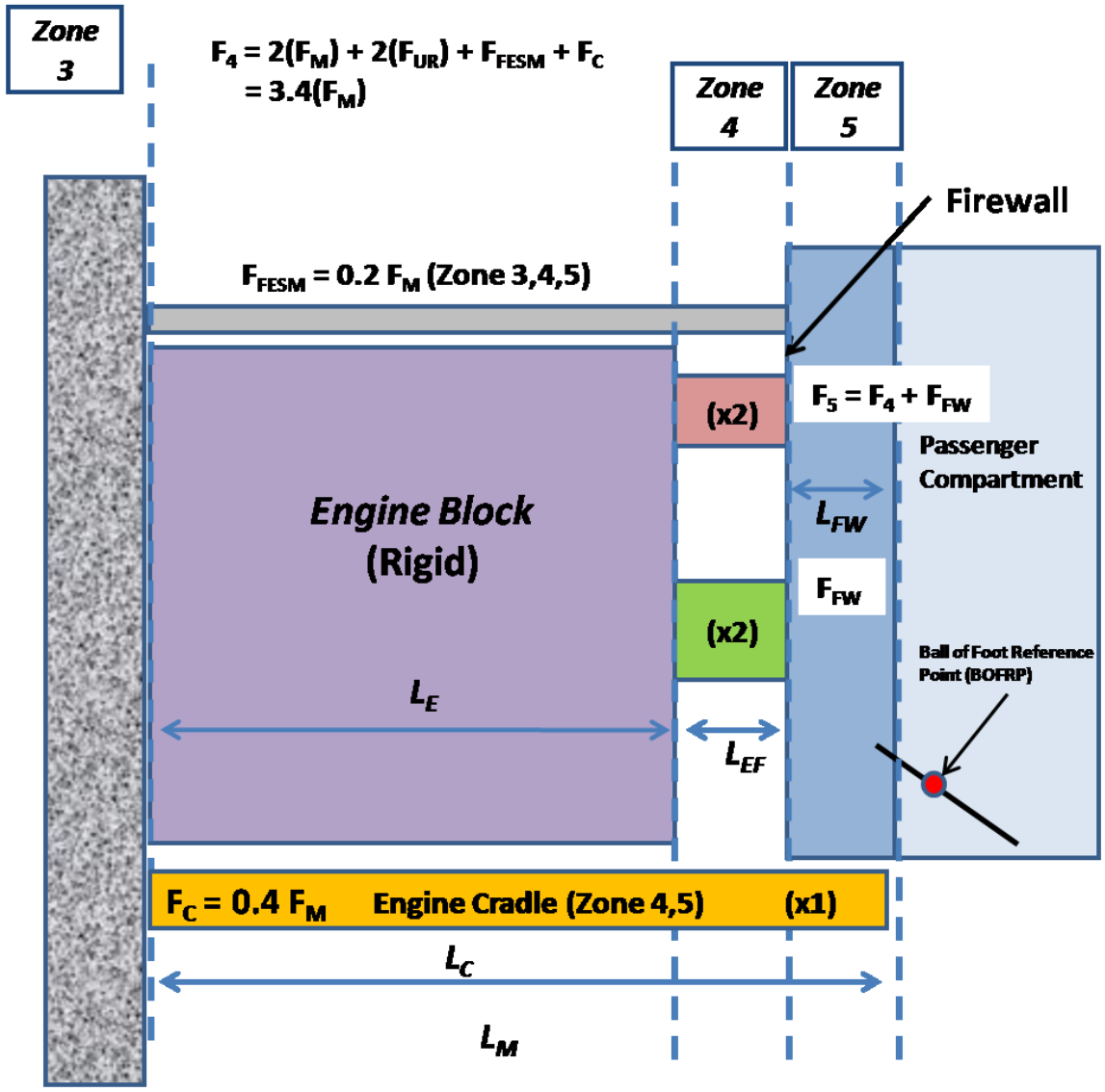

Figure D.6 Zone 3 Crush

Zone 3 average acceleration is calculated similarly to that of Zone 1 and Zone 2 with different structural elements crushing and absorbing energy as shown in Equation (D.7).

$$a_3 = \frac{F_3}{M_3} = \frac{2 \cdot F_M + 2 \cdot 0.4 \cdot F_M + 0.2 \cdot F_M}{M_B + M_E} = \frac{3.0 \cdot F_M}{M_B + M_E} \qquad \text{Equation (D.7)}$$

a_3: Zone 3 average acceleration (m/sec^2)

F_3: Zone 3 crush force (N)

M_3: Zone 3 vehicle crush mass (kg)

F_M: Average midrail crush force for one side (N)

M_B: Vehicle body mass (Includes 150 kg for two 50th percentile test manikins)

M_E: Vehicle engine mass (kg) (Includes transmission mass as well)

There are two midrails in Zone 3 crush. The two upper rails are each rated at 0.4 x midrail crush force. The hood and front end sheet metal is rated at 0.2 x midrail crush force.

Velocity at the end of Zone 3 crush is calculated similarly to that of Zone 1 and Zone 2 crush as shown in Equation (D.5). The length of the midrail that crushes in Zone 3 is the total uncrushed midrail length (L_M) minus the engine length (rigid obstruction) (L_E) minus the distance between the engine and the firewall (L_F). If progressive crush from the front of the vehicle is assumed, all of these length parameters are known values.

$$V_3 = \sqrt{V_2^2 - \frac{2 \cdot F_3 \cdot d_3}{M_B + M_E}} = \sqrt{V_2^2 - \frac{6.0 \cdot F_M \cdot (L_M - L_E - L_{EF})}{M_B + M_E}} \qquad \text{Equation (D.8)}$$

V_2: Vehicle velocity at end of Zone 2 crush (m/sec)

V_3: Vehicle velocity at end of Zone 3 crush (m/sec)

F_3: Average Zone 3 crush force (N)

d_3: Zone 3 crush distance (m)

M_B: Vehicle body mass (kg) (Includes 150 kg for two 50th percentile test manikins)

M_E: Vehicle engine mass (kg) (Includes transmission mass as well)

F_M: Average midrail crush force for one side (N)

L_M: Total midrail length (m) forward of the firewall

L_E: Longitudinal length of engine (m)

L_{EF}:Longitudinal distance from rear of engine to front of firewall (m)

Zone 4 (Between Engine and Firewall) Crush Model Calculations

Zone 4 Crush is shown in Figure D.7.

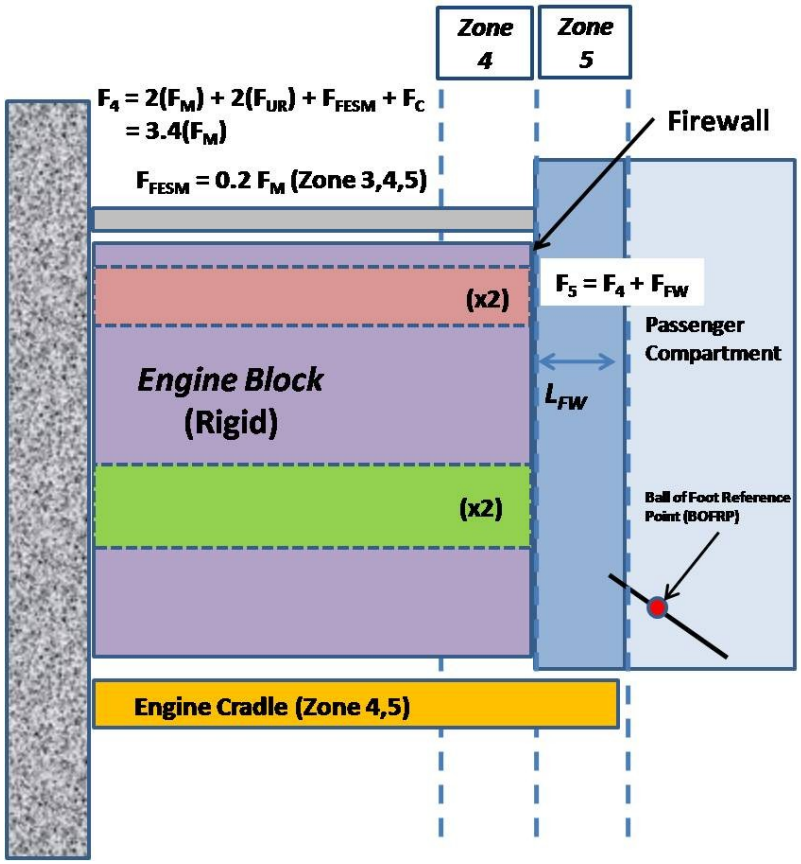

Figure D.7 Zone 4 Crush

Zone 4 acceleration and final velocity are calculated similarly to those of Zone 3with the addition of engine cradle crush (cradle crush force ~0.4 x F_M). Only the body mass is used as the engine motion is now zero. The resulting Zone 4 acceleration is shown in Equation (D.9).

$$a_4 = \frac{F_4}{M_4} = \frac{2 \cdot F_M + 2 \cdot 0.4 \cdot F_M + 0.2 \cdot F_M + 0.4 \cdot F_M}{M_B} = \frac{3.4 \cdot F_M}{M_B} \qquad \text{Equation (D.9)}$$

a_4: Zone 4 acceleration (m/sec^2)

F_4: Zone 4 crush force (N)

M_4: Zone 4 vehicle mass (body mass only)

F_M: Average midrail crush force (N)

M_B: Vehicle body mass (kg) (Includes 150 kg for two 50th percentile test manikins)

The calculation of velocity at the end of Zone 4crush is shown in Equation (D.10).

$$V_4 = \sqrt{V_3^2 - \frac{2 \cdot F_4 \cdot d_4}{M_B}} = \sqrt{V_3^2 - \frac{6.8 \cdot F_M \cdot (L_{EF})}{M_B}} \quad \text{Equation (D.10)}$$

V_4: Velocity at end of Zone 3 crush (m/sec)

V_3: Velocity at end of Zone 2 crush (m/sec)

F_4: Zone 3 crush force (N)

d_4: Zone 3 crush distance (m)

M_B: Body mass (kg) (Includes 150 kg for two 50th percentile test manikins)

F_M: Midrail crush force (N)

L_{EF}: Longitudinal distance between rear of engine and front of firewall

Zone 5 (Firewall Ride-Down) Crush Model Calculations

Zone 5 Crush is shown in Figure D.8

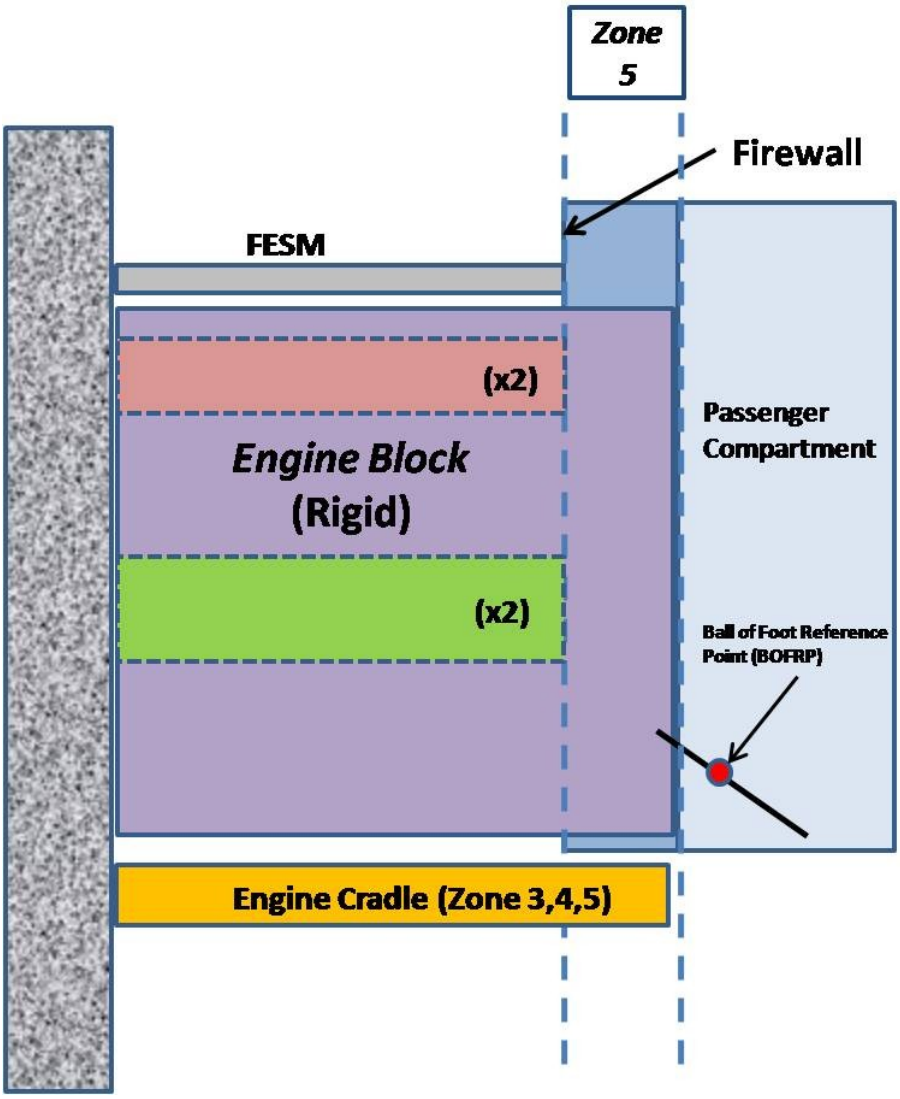

Figure D.8 Zone 5 Crush

In Zone 5, the engine is intruding into the firewall region. During this phase crush of the other elements (midrails, upper rails, engine cradle and hood/sheet metal) still occurs, resulting in higher accelerations in this zone. If a firewall crush force value is expressed as F_{FW}, then the total Zone 5 force is:

$$F_5 = 2 \cdot F_M + 2 \cdot 0.4 \cdot F_M + 0.4 \cdot F_M + 0.2 \cdot F_M + F_{FW}$$
$$= 3.4 \cdot F_M + F_{FW}$$

Equation (D.11)

F_5: Zone 4 crush force (N)

F_M: Midrail crush force (N)

F_{FW}: Firewall crush force (N)

The resulting acceleration a_5 is then:

$$a_5 = \frac{F_5}{M_5} = \frac{3.4 \cdot F_M + F_{FW}}{M_B}$$

Equation (D.12)

a_5: Zone 5 acceleration (m/sec^2)

F_5: Zone 5 crush force (N)

F_M: Midrail crush force (N)

M_B: Vehicle body mass (kg) (Includes 150 kg for two 50th percentile test manikins)

F_{FW}: Firewall average crush force (N)

If an average engine intrusioninto the firewall L_{FW} is assumed (it will typically be greater toward the centerline, less toward the outside edges of the engine bay), the crush distance d_5 is then known. At the end of Zone 5 crush the velocity will be zero. The resulting energy balance is shown in Equation (D.13).

$$V_5 = 0 = \sqrt{V_4^2 - \frac{2 \cdot F_5 \cdot d_5}{M_B}} = \sqrt{V_4^2 - \frac{2 \cdot (3.4 \cdot F_M + F_{FW}) \cdot L_{FW}}{M_B}} = \sqrt{V_4^2 - \frac{(6.8 \cdot F_M + 2 \cdot F_{FW}) \cdot L_{FW}}{M_B}}$$

Equation (D.13)

V_5: Velocity at end of Zone 5 crush (= 0)

V_4: Velocity at end of Zone 4crush (m/sec)

F_5: Zone 5 crush force (N)

d_5: Zone 5crush distance (m)

M_B: Vehicle body mass (kg) (Includes 150 kg for two 50th percentile test manikins)

F_M: Midrail crush force (N)

F_{FW}: Firewall crush force (N)

L_{FW}: Firewall crush distance (m)

It is important to know the midrail length for motor compartment packaging and other vehicle calculations. Substituting values to combine the velocity equations for each Zone results in Equation (D.14):

$$244.8\ m^2/sec^2 - \frac{2.88 \cdot F_M \cdot L_B + 6.0 \cdot F_M \cdot L_M - 6.0 \cdot F_M \cdot L_E - 6.0 \cdot F_M \cdot L_{EF}}{M_B + M_E} - \frac{6.8 \cdot F_M \cdot L_{EF} + (6.8 \cdot F_M + 2 \cdot F_{FW}) \cdot L_{FW}}{M_B} = 0$$

Equation (D.14)

F_M: Midrail crush force (N)

L_B: Bumper rail length (m)

L_M: Midrail length (m)

L_E: Engine length (m)

L_{EF}: Longitudinal distance from rear of engine to front of firewall (m)

M_B: Vehicle body mass (kg) (Includes 150 kg for two 50th percentile test manikins)

M_E: Vehicle engine mass (kg)

The midrail length can be moved to one side of the equation as shown in Equation (D.15):

$$\frac{6.0 \cdot F_M \cdot L_M}{M_B + M_E} = 244.8\ m^2/sec^2 - \frac{2.98 \cdot F_M \cdot L_B - 6.0 \cdot F_M \cdot (L_E + L_{EF})}{M_B + M_E} - \frac{6.8 \cdot F_M \cdot L_{EF} + (6.8 \cdot F_M + 2 \cdot F_{FW}) \cdot L_{FW}}{M_B} = 0 \qquad \text{Equation (D.15)}$$

The value for midrail length can then be solved for as shown in Equation (D.16):

$$L_M = (40.8) \cdot \frac{(M_B + M_E)}{F_m} - 0.497 \cdot L_B + L_E + L_{EF} - 1.133 \cdot L_{EF} \cdot \left(\frac{M_B + M_E}{M_B}\right) - 0.333 \cdot \left(\frac{F_{FW}}{F_M}\right) \cdot L_{FW} \cdot \left(\frac{M_B + M_E}{M_B}\right) - 1.133 \cdot \left(\frac{M_B + M_E}{M_B}\right) \cdot L_{FW} \qquad \text{Equation (D.16)}$$

L_M: Midrail length (kg)

M_B: Vehicle body mass (kg) (Includes 150 kg for two 50th percentile test manikins)

M_E: Vehicle engine mass (kg) (Includes transmission mass as well)

F_M: Midrail crush force (N)

L_B: Bumper rail length (m)

L_E: Engine length (m)

L_{EF}: Longitudinal distance from rear of engine to firewall (m)

L_{FW}: Firewall crush distance (m)

F_{FW}: Firewall crush force (N)

If the value of L_B in Equation (D.1) is substituted, the final calculation of midrail length is shown in Equation (D.17).

$$L_M = (39.717) \cdot \frac{(M_B + M_E)}{F_m} + L_E + L_{EF} - 1.133 \cdot L_{EF} \cdot \left(\frac{M_B + M_E}{M_B}\right) - 0.333 \cdot \left(\frac{F_{FW}}{F_M}\right) \cdot L_{FW} \cdot \left(\frac{M_B + M_E}{M_B}\right) - 1.133 \cdot \left(\frac{M_B + M_E}{M_B}\right) \cdot L_{FW} \quad \text{Equation (D.17)}$$

For a given iteration of the multi-objective optimization process, the Midrail Length L_M is the only unknown and can be solved for from the above equation. Calculation of midrail length is also used to ensure the midrail is long enough to package all motor compartment content (engine, radiator, etc.).

The time interval for each crush zone (and as a result the time duration of the crash event) can also be calculated. The time calculation for crush Zones 1 through 5 is shown in Equation (D.16).

$$t_1 = \frac{V_0 - V_1}{a_1} \; ; \; t_2 = \frac{V_1 - V_2}{a_2} \; ; \; t_3 = \frac{V_2 - V_3}{a_3} \; ; \; t_4 = \frac{V_3 - V_4}{a_4}; \quad t_5 = \frac{V_4 - 0.0}{a_5}$$

Equation (D.18)

As the accelerations during occupant ride-down are of greatest interest for injury criteria, the maximum acceleration is then taken as a time-weighted function of accelerations in Zones 3, 4 and 5:

$$a_{average} = \frac{0.4 \cdot a_3 \cdot t_3 + a_4 \cdot t_4 + a_5 \cdot t_5}{0.4 \cdot t_3 + t_4 + t_5}$$

Equation (D.19)

$a_{average}$: average vehicle acceleration (g's)

a_3: Vehicle acceleration during Zone 3crush (g's)

a_4: Vehicle acceleration during Zone 4crush (g's)

a_5: Vehicle acceleration during Zone 5crush (g's)

t_2: Duration of Zone 3 crush event (sec)

t_3: Duration of Zone 4 crush event (sec)

t_4: Duration of Zone 5 crush event (sec)

The resulting average acceleration during occupant ride-down with the vehicle is then compared to the standard for NCAP performance:

- 5-Star: Target of 25 g's or less, up to 25.5 g's with significant added work in detailed design
- 4-Star / 3-Star: Target of 30 g's or less, up to 30.5 g's with significant added work in detailed design for 4-Star

- 2-Star / 1-Star: In excess of 30.5 g's. As vehicles must meet minimum FMVSS criteria to be saleable in the U.S., an arbitrary limit of 35.0 g's is used in the software framework for these ratings.

Appendix E

Turn Radius Model Development and Relations and Wheelhouse Clearance

Key parameters in calculating vehicle turn radius are show in Figure E.1 for calculation of the vehicle turn radius measured at the outside steer wheel track. Ackerman steering is assumed in this model.

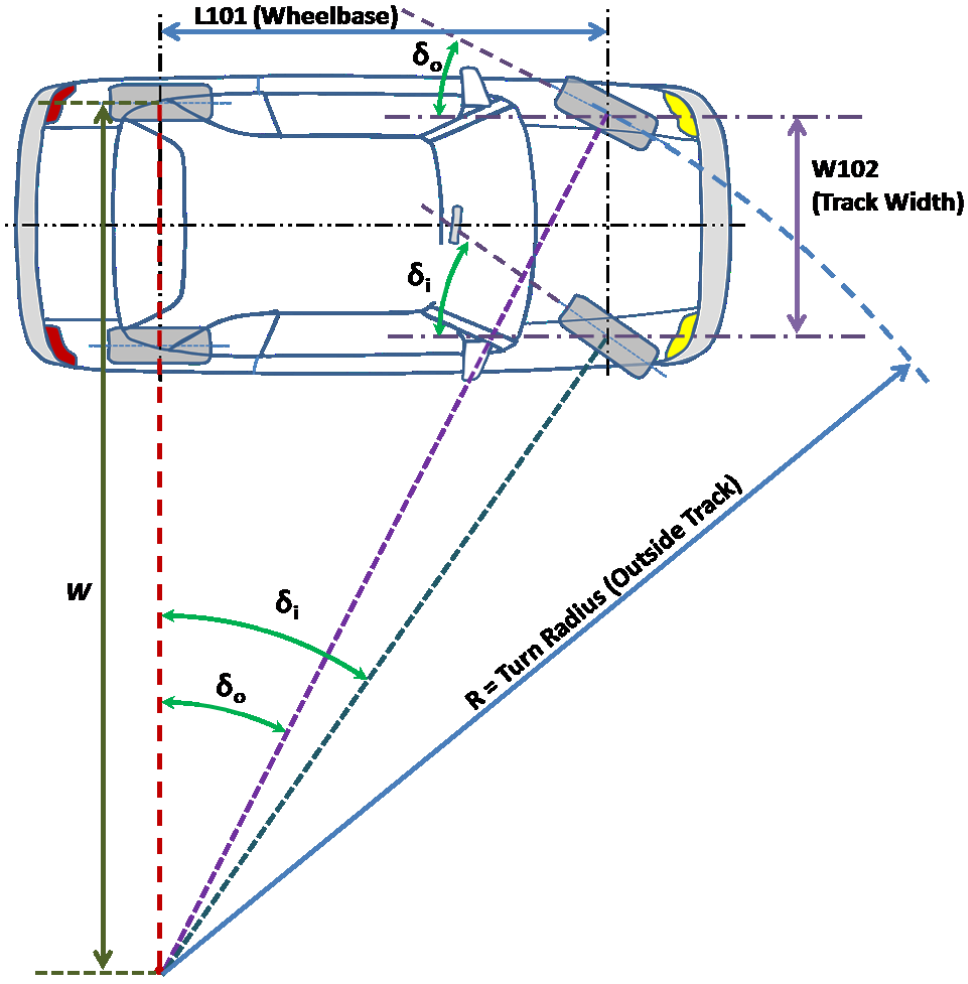

Figure E.1 Vehicle Turn Radius Parameters (Ackerman Steering) [54, 62]

W102 : Vehicle track width [1]

δ_i :Inside Steer Wheel Angle [64]

δ_o :Outside Steer Wheel Angle [64]

L101:Vehicle wheelbase [64]

R: Outside track turn radius [62]

W :Distance from turning circle center to outside wheel centers (average front/rear track width if different). [62]

For Ackerman steering, $\delta_i > \delta_o$. Therefore, for a given value of W102 and L101, the minimum turn radius is determined by the maximum value for the inside wheel turn angle δ_i, typically due to wheelhouse clearance and packaging. The relationships between the inside and outside steer wheel turn radii give sufficient information to solve for *W*, R and δ_o as shown in Figure E.2.

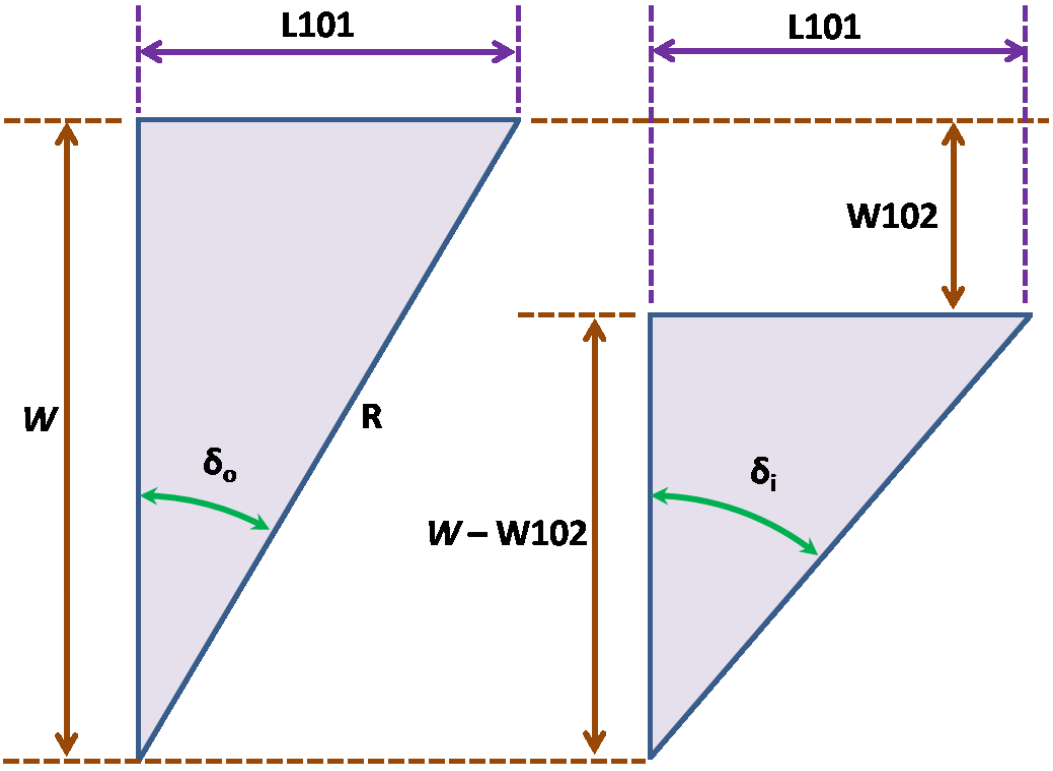

Figure E.2 Turn Radius Relationships

For a given maximum inside wheel turn angle, the turn center to outside track distance W can be found as shown in Equation (E.1).

$$W = \frac{L101}{\tan \delta_i} + W102 \qquad \text{Equation (E.1)}$$

W: Distance from turn center to outside vehicle wheel centers

L101: Vehicle wheelbase

δ_i: Inside steer wheel maximum steer angle

W102: Vehicle track width

With known values for W and L101, R is found as shown in Equation (E.2).

$$R = \sqrt{W^2 + (L101)^2} \qquad \text{Equation (E.2)}$$

R: Turn radius as outside steer wheel track (center)

For Ackerman steering, the resulting outside steer wheel angle δ_o can be computed as shown in Equation (E.3)

$$\delta_o = \sin^{-1}\left(\frac{L101}{R}\right) \qquad \text{Equation (E.3)}$$

The inside and outside steer wheel angles can be found in similar fashion if the tire size, turn radius, wheelbase (L101) and track or tread width (W101 or W102) are available. The outside steer wheel angle is found by the previous equation. The inside steer wheel maximum angle δ_i is found as shown in Equation (E.4).

$$\delta_i = \tan^{-1}\left(\frac{L101}{R \cdot \cos(\delta_o) - W102}\right)$$ Equation (E.4)

Typical values for maximum inside steer wheel angle by vehicle type are shown in Table E.1

Vehicle Type	Average Wheelbase L101 (m)	Average Track Width W102 (m)	Average Maximum δ_i (degrees)	Number of Samples
2-Seater	**2.45**	**1.47**	**36.7**	**10**
Large Coupe / Sedan	**2.87**	**1.54**	**38.1**	**5**
Midsize Coupe / Sedan	**2.69**	**1.48**	**39.2**	**24**
Compact Coupe / Sedan	**2.55**	**1.44**	**39.2**	**35**
Subcompact Coupe / Sedan	**2.49**	**1.45**	**40.5**	**27**
Mini-Compact Coupe	**2.44**	**1.47**	**39.6**	**3**

Table E.1 Average Values of Wheelbase, Track Width and δ_i by Vehicle Type

Turn radius is typically measured as "Curb-to-Curb" (CTC) or "Wall-to-Wall" (WTW) as shown in Figure E.3. Curb-to-Curb turn radius is the radius of the turning circle measured from the circle center to the outside edge of the outside steer wheel as shown in Figure E.3. Once the outside track turn radius is known, Curb-to-Curb turn radius is then:

$$R_{CTC} = R_{OT} + \frac{W_{Tire}}{2}$$ Equation (E.4)

R_{CTC}: Curb-to-Curb Turn Radius

R_{OT}: Outside Track Turn Radius

W_{tire}: Width of outside steer tire

Wall-to-Wall turn radius is the radius of the turning circle measured from the circle center to the outermost projecting portion of the vehicle during the turn as shown in Figure E.3.

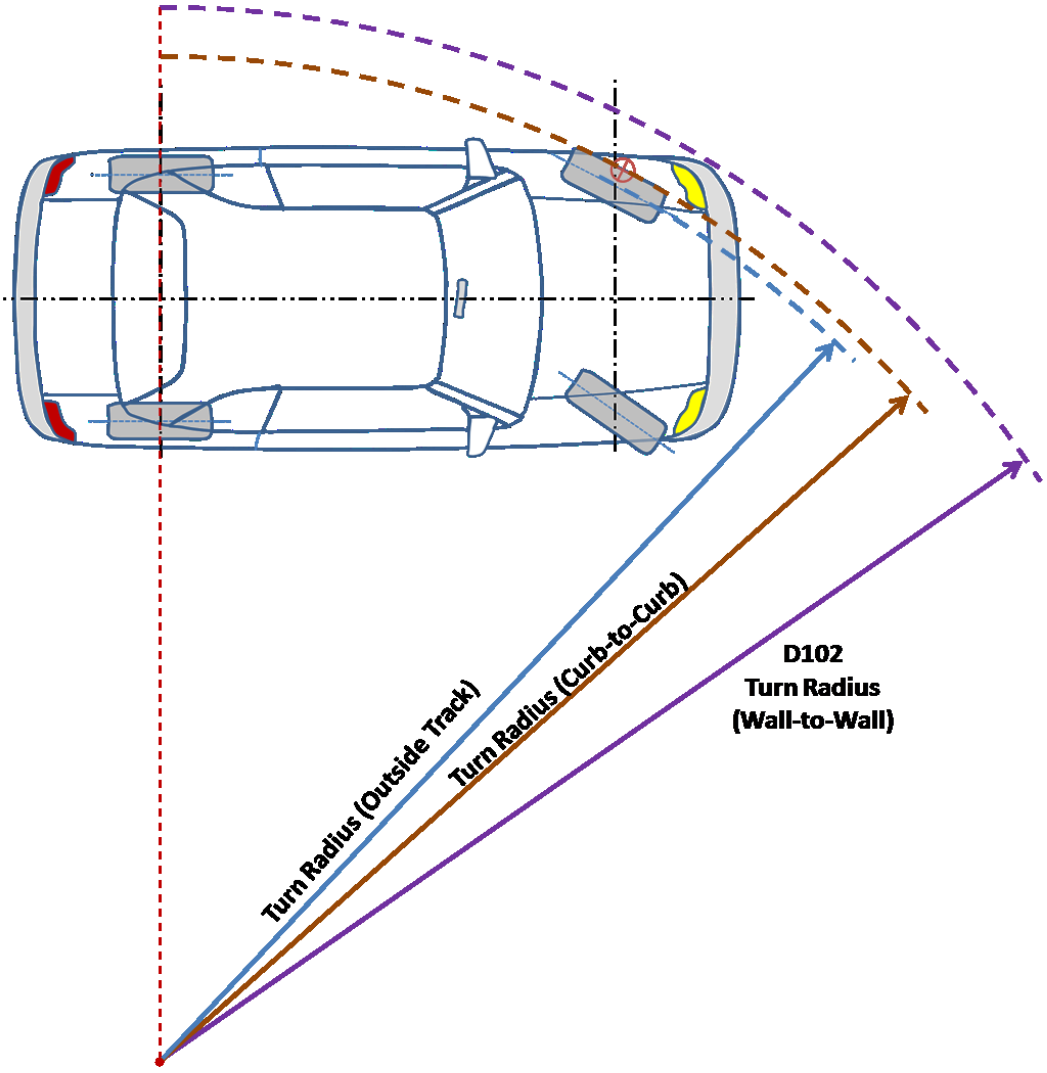

Figure E.3 Turn Radius Measurements

Calculation of Wall-to-Wall turn radius requires knowledge of the actual vehicle exterior geometry. However, for parametric modeling purposes in the conceptual design stage, the average ratio of Wall-to-Wall vs. Curb-to-Curb turn radius values can be used

to approximate the Wall-to-Wall value in the model. Typical ratios and standard deviation by vehicle type are show in Table E.2.

Vehicle Class	Average CTC Turn Radius (m)	Average CTC σ (m)	Average WTW/CTC Ratio	WTW/CTC Ratio σ	Samples
2-Seater (Roadster, Sports Car)	**5.47**	**0.46**	**1.05**	**0.02**	**10**
Large Coupe/Sedan	**6.05**	**0.37**	**1.15**	**0.00**	**5**
Midsize Coupe/Sedan	**5.60**	**0.27**	**1.09**	**0.03**	**24**
Compact Coupe/Sedan	**5.34**	**0.28**	**1.07**	**0.02**	**35**
Subcompact Coupe/Sedan	**5.16**	**0.46**	**1.08**	**0.03**	**27**
Mini-Compact Coupe	**5.15**	**0.27**	**1.07**	**0.01**	**3**

Table E.2 Typical Wall-to-Wall vs. Curb-to-Curb Turn Radius Ratios by Vehicle Type [54, 52]

Note that many authors such as Genta use the average of δ_i and δ_o as a single value δ, reducing turn radius to a single-track model (treating the model as having one centerline steer wheel). As Genta notes, the resulting error tends to be small [63]. His focus, however, is on the turn radius circle of the vehicle center of mass, which the single-track model is well suited to provide. The maximum value of δ_i is a factor in vehicle front wheelhouse packaging and clearances as discussed below. Additionally, the method used in this work gives direct output for vehicle Outside Track, CTC And WTW turn radius; Curb-to-Curb turn radius is one of the vehicle target parameters assessed in validation and optimization activities in this work.

Wheelhouse Clearance

Factors affecting wheel house clearance are shown in Figure E.4. Wheelhouse clearance is tied to the values of L113 and L115-2 Additional average values for L113 and a comparison with tire radius are shown in Table E.3 [52, 54]. Front wheelhouse clearances appear to be a significant factor in the values for L113.

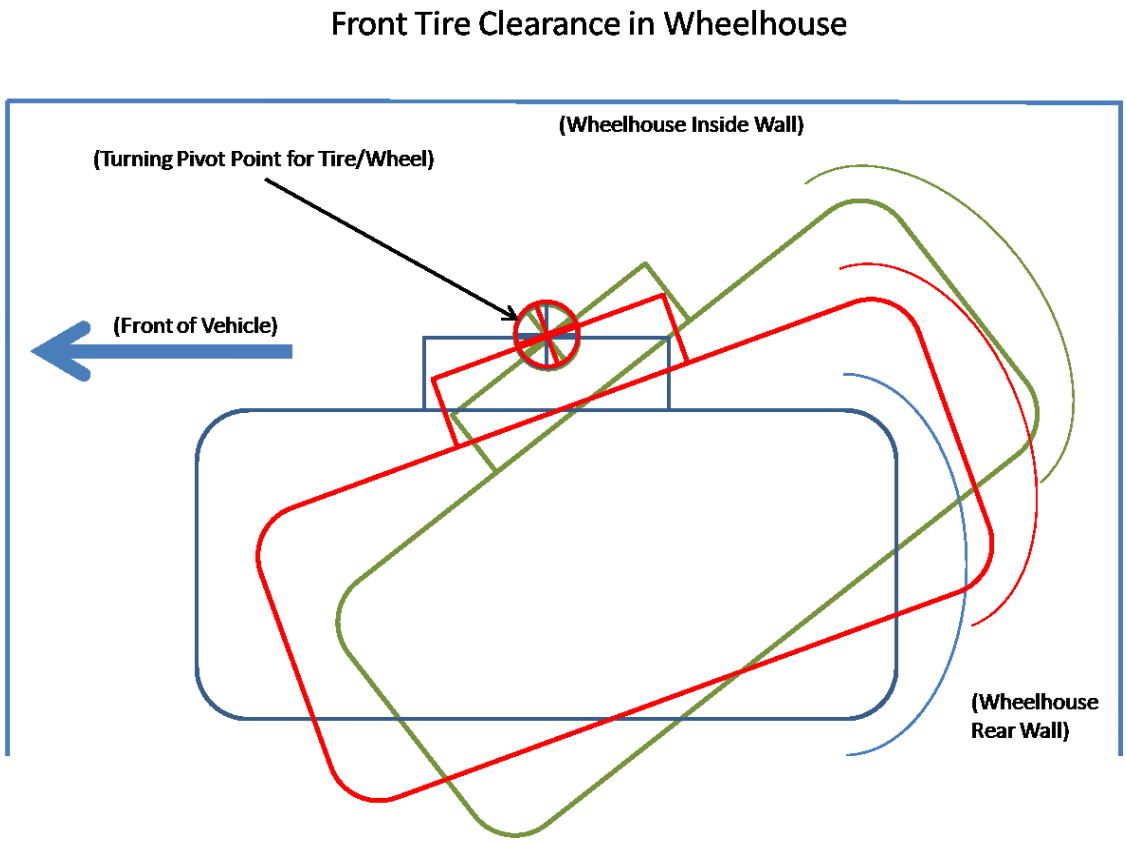

Figure E.4 Front Tire Wheelhouse Clearance (Outline Curve is Snow Chain Envelope) [54, 60]

Vehicle Type	Samples	Average Front Tire Diameter (Meters)	Average L113 (meters)	Average L113 - Tire Radius (meters)	Std. Deviation for difference (meters)
Large Minivan	2	0.661	0.302	-0.028	0.015
Large Traditional SUV	1	0.775	0.579	0.191	-
Large Sedan/Coupe	5	0.680	0.557	0.217	0.057
Large Sedan	3	0.693	0.588	0.242	0.005
Large Coupe	2	0.661	0.510	0.179	0.091
Midsize Traditional SUV	2	0.719	0.522	0.163	0.017
Midsize Sedan/Coupe/Wagon	24	0.639	0.413	0.093	0.052
Midsize Sedan	16	0.633	0.398	0.082	0.049
Midsize Coupe	7	0.651	0.451	0.125	0.053
Midsize Wagon	1	0.648	0.383	0.059	-
Compact Sedan/Coupe	25	0.613	0.376	0.070	0.040
Compact Sedan	17	0.610	0.373	0.068	0.042
Compact Coupe	8	0.618	0.383	0.074	0.037
Subcompact Traditional SUV	1	0.719	0.624	0.265	-
Subcompact Sedan/Coupe	21	0.608	0.408	0.104	0.044
Subcompact Sedan	2	0.604	0.386	0.084	0.006
Subcompact Coupe	19	0.609	0.411	0.106	0.046
Small Wagon	1	0.610	0.370	0.065	-
Mini-Compact Traditional SUV	1	0.674	0.448	0.111	-
Mini-Compact Coupe	3	0.619	0.505	0.195	0.122
2-Seater Sports Car/Roadster	9	0.623	0.530	0.219	0.167

Table E.3 L113 vs. Tire Diameter Relations by Vehicle Type [52, 54]

Standard dimensional parameters for snow chains in a vehicle wheelhouse have

been defined by the National Association of Chain Manufacturers as shown in Figure E.5 [54, 60].

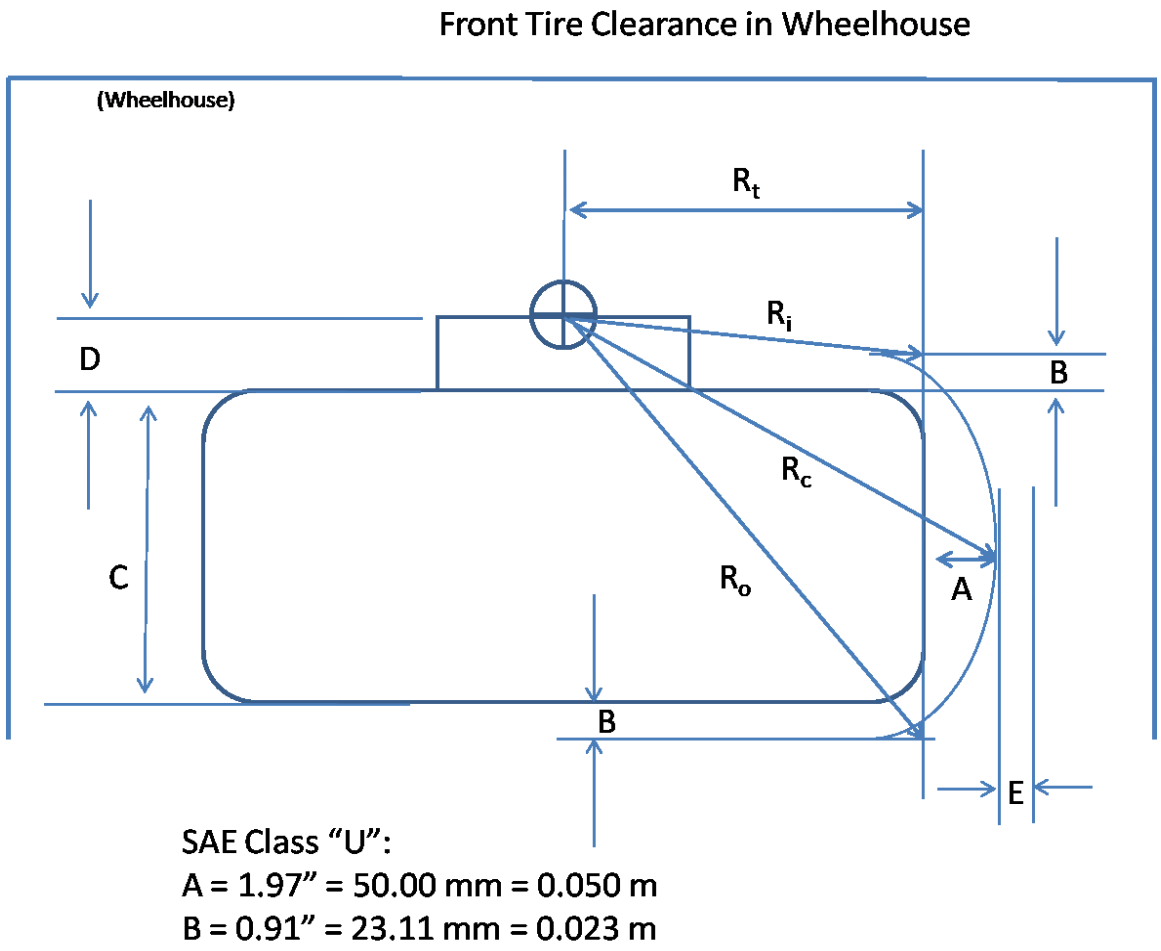

Figure E.5 Front Tire Clearance in Wheelhouse Dimensions for Snow Chains [54, 60]

Parameters affecting front tire clearance to the rear wheelhouse wall as shown in Figure E.5 include [60]:

A: Centerline maximum snow chain X-displacement due to centrifugal motion

B: Lateral clearance required for snow chain retention rings/tensioners

C: Tire Width

D: Tire/Wheel pivot point offset from inside tire edge (may be positive or negative)

E: Required clearance beyond snow chain arc

R_t: Nominal Tire Radius

R_c: Clearance Radius at Tire Centerline with Snow Chains

R_i: Clearance Radius at Tire Inside Edge with Snow Chains

R_o: Clearance Radius at Tire Outside Edge with Snow Chains

Parameters A and B for SAE Vehicle Class "U" (passenger vehicles with clearance for normal snow chains) are [60]:

A = 0.050 meters (1.97")

B = 0.023 meters (0.91")

Parameter "E" is initially assigned a value of 0.010 meters in this work and is used for clearance with the wheel at 0 degrees of turn. This is clearance in addition to that required for snow chains (for packed snow, etc.).

With the tire / wheel at 0 degrees of turn, the minimum required clearance to the rear wheelhouse wall is:

$$Clearance_{0\ degrees} = R_t + A + E \qquad \text{Equation (E.5)}$$

This is also the clearance requirement for the rear wheels (assuming no rear-wheel steering). For maximum wheel clearance to the front wheelhouse rear wall during a turn, the clearance will be R_0 as shown in Equation (E.6):

$$R_o = \sqrt{(B + C + D)^2 + (R_t)^2}$$ Equation (E.6)

With the exception of an extremely narrow tire, R_0 will be greater than the clearance at 0 degrees of wheel turn and should be used to calculate minimum clearance to the rear wall of the front tire wheelhouse. Examples of L113 vs. 0-degree wheel turn clearance are shown in Table E.4 [52, 54, 60]. Examples of L113 vs. R_0 clearance are shown in Table E.5 [52, 54, 60].

Vehicle	**Tire Description**	**0-Degrees Wheel Turn Clearance (m)**	**L113 (m)**	**L113 - Clearance (m)**
2003 Ford Mustang	**P225/55 R16**	**0.387**	**0.466**	**0.079**
2003 Honda Civic	**195/60 R15**	**0.368**	**0.377**	**0.010**
2004 Subaru Impreza	**P205/55 R16**	**0.376**	**0.396**	**0.020**
1994 Ford Thunderbird	**P205/70 R15**	**0.394**	**0.498**	**0.104**
2004 Dodge Durango	**245/70 R17**	**0.447**	**0.579**	**0.131**
1995 Honda Accord	**P185/70 R14**	**0.367**	**0.495**	**0.128**
1991 Chevrolet Corsica	**P185/75 R14**	**0.377**	**0.395**	**0.018**
1987 Dodge Caravan	**P205/70 R14**	**0.381**	**0.319**	**-0.062**
1996 Honda Civic	**P175/70 R13**	**0.348**	**0.450**	**0.102**

Table E.4 L113 vs. 0-Degree Wheel Turn Clearance for Sample Vehicles [52, 54, 60]

With the exception of the 1987 Caravan, L113 is within 10 mm (0.01 m) of meeting or exceeding the R_0 clearance values as shown in Table E.5. This indicates that the R_0 clearance criteria should be used to set a minimum value for L113.

Vehicle	Tire Description	Ro for D = 0 (m)	L113 (m)	L113 - Clearance (m)
2003 Ford Mustang	P225/55 R16	0.420	0.466	0.046
2003 Honda Civic	195/60 R15	0.387	0.377	-0.010
2004 Subaru Impreza	P205/55 R16	0.400	0.396	-0.004
1994 Ford Thunderbird	P205/70 R15	0.414	0.498	0.084
2004 Dodge Durango	245/70 R17	0.481	0.579	0.098
1995 Honda Accord	P185/70 R14	0.381	0.495	0.114
1991 Chevrolet Corsica	P185/75 R14	0.389	0.395	0.006
1987 Dodge Caravan	P205/70 R14	0.404	0.319	-0.085
1996 Honda Civic	P175/70 R13	0.359	0.450	0.091

Table E.5 L113 vs. R_0 Clearance for Sample Vehicles [52, 54, 60]

The value of L113 affects vehicle center of gravity location, frontal crash safety, wheelhouse clearance and other target-related parameters although it appears to have no direct correlation to any given single vehicle dimension. Comparisons of L113 to tire diameter L102 showed no direct correlation.

As with L113, L115-2 shows no direct correlation to rear tire diameter. L115-2 has implications for rear wheelhouse clearances, rear cargo volume and rear crash safety. As seen in Table E.6, L115-2 by vehicle type is greater than average rear tire radius with one exception (mid-size traditional SUV) [52, 54]. This indicates that L115-2 should also be set such that, at a minimum, it is equal or greater to the wheel radius plus tire-to-wheelhouse clearance distance.

Vehicle Type	Samples	Average Rear Tire Diameter (m)	Average L115-2 (m)	Average L115-2 - Tire Radius (m)	Standard Deviation σ for difference (m)
Large Minivan	2	0.661	0.843	0.512	0.058
Large Sedan/Coupe	5	0.680	0.504	0.164	0.012
Large Sedan	3	0.693	0.515	0.168	0.005
Large Coupe	2	0.661	0.487	0.156	0.020
Midsize Traditional SUV	1	0.689	0.320	-0.024	-
Midsize Sedan/Coupe/Wagon	25	0.604	0.500	0.198	0.066
Midsize Sedan	17	0.607	0.496	0.193	0.062
Midsize Coupe	7	0.589	0.503	0.208	0.084
Midsize Wagon	1	0.648	0.535	0.211	-
Compact Sedan/Coupe	29	0.609	0.460	0.156	0.055
Compact Sedan	19	0.605	0.466	0.164	0.050
Compact Coupe	10	0.615	0.448	0.141	0.065
Subcompact Traditional SUV	1	0.719	0.800	0.441	-
Subcompact Sedan/Coupe	26	0.606	0.443	0.140	0.074
Subcompact Sedan	3	0.594	0.443	0.136	0.012
Subcompact Coupe	23	0.607	0.444	0.140	0.079
Small Wagon	1	0.610	0.500	0.195	-
Mini-Compact Traditional SUV	1	0.674	0.656	0.319	-
Mini-Compact Coupe	3	0.617	0.398	0.090	0.052
2-Seater Sports Car/Roadster	8	0.621	0.978	0.668	0.084

Table E.6 L115-2 vs. Tire Radius Average Values by Vehicle Class [52, 54]

Appendix F

Parametric Mass Estimation for Optimization

Mass Estimation Method

The total vehicle curb mass model is broken into several subsystems:

- Engine: this is a fully dressed engine with fluids included.
- Driveline: this includes the transmission, output and prop shafts and differential units along with mounts.
- Body in White: this consists of the painted body structure without closures or removable body / fender panels.
- Closures: this includes doors, hood and rear decklid / liftgate.
- Interior: this includes seating, instrument panel, center console, headliner, carpeting, inside mirror, insulation and interior trim parts.
- Uncategorized: this contains all items not currently in another subsystem including: glazing/wiper systems, lighting, bumpers / fenders / front end assembly, exterior trim, removable reinforcements, electrical system and accessories, seats, exhaust, steering, braking, air system and HVAC (heating, ventilation and air conditioning), fuel and safety systems and all fluids except engine and transmission oil.
- Suspension: this includes shock absorber / spring assemblies, front/rear axles or suspension arms, stabilizer bars and wheel / tire assemblies.

Motor vehicle dimensions defined in SAE Standard J1100 used in this appendix are shown in Figure F.1 [1, 54].

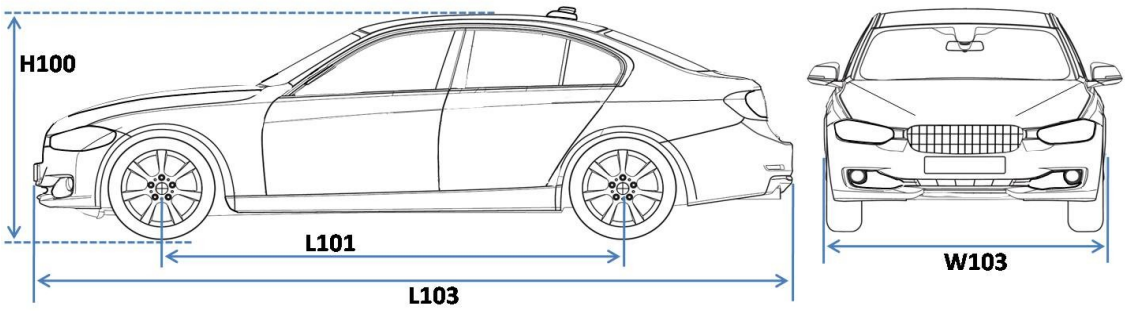

Figure F.1 SAE J1100 Dimensions [1, 54]

These dimensions are:

- L101: Wheelbase; the longitudinal distance between the front and rear wheel centers [1]
- L103: Vehicle length [1]
- W103: Maximum vehicle width without outside mirrors [1]
- H100: Vehicle body height (excludes roof-mounted hardware or antennae) [1]

All dimensions are in meters. Engine power is in kilowatts (kW). Torque is in Newton meters (Nm).

For gasoline and diesel powered vehicles, the estimated vehicle curb mass is a summation of the estimated mass for each subsystem as shown in Equation (F.1):

$$M_{Curb} = M_{Eng} + M_{Drv} + M_{BiW} + M_{Cls} + M_{Int} + M_{Unc} + M_{Sus} \qquad \text{Equation (F.1)}$$

M_{Curb}: Vehicle curb mass

M_{Eng}: Engine mass

M_{Drv}: Driveline mass

M_{BiW}: Body in White mass

M_{Cls}: Closure mass

M_{Int}: Interior mass

M_{Unc}: Uncategorized mass

M_{Sus}: Suspension mass

Parametric Mass Estimation and Correlation by Vehicle Subsystem

Engine mass estimation, along with driveline and transmission estimation, is addressed in Appendix C.

Body in White mass correlations have been developed for steel and aluminum bodies as shown in Table F.5 [54]. With a 66% lower density and 50% lower yield strength than steel, aluminum Bodies in White would be expected to average approximately 33% lower mass compared to steel for an identical body structure. The correlations shown in Table F.5 indicate an average 28% reduction in aluminum body mass compared to steel. Geometry and processing requirements due to the different material properties may account for the difference between theoretical and achieved savings. Higher strength aluminum alloys used in the aircraft industry may improve mass savings, but at significantly higher cost.

Body in White Material	**Mass Relationship**	**R^2 Value**	**Samples**
Steel	M_{BiW} **= 25.195*(L103*W103*H100) kg**	**0.921**	**75**
Aluminum	M_{BiW} **= 18.033*(L103*W103*H100) kg**	**0.972**	**3**

Table F.1 Body in White Mass Estimation Relationships (M_{BiW}: Body in White Mass in kg) [54]

Comparison of estimated vs. actual Body in White mass for steel and aluminum bodies from the vehicle database is shown in Figure F.2 [54]. For both materials, the correlation is based on vehicle external or "block" volume (Vehicle Length L103 x Width W103 x Height H100) using a linear correlation line fit. Vehicles included in the correlation include sedans, coupes, 2-seat sports cars and crossover SUV's (CSUV's). Convertibles are not included in these mass estimation relations.

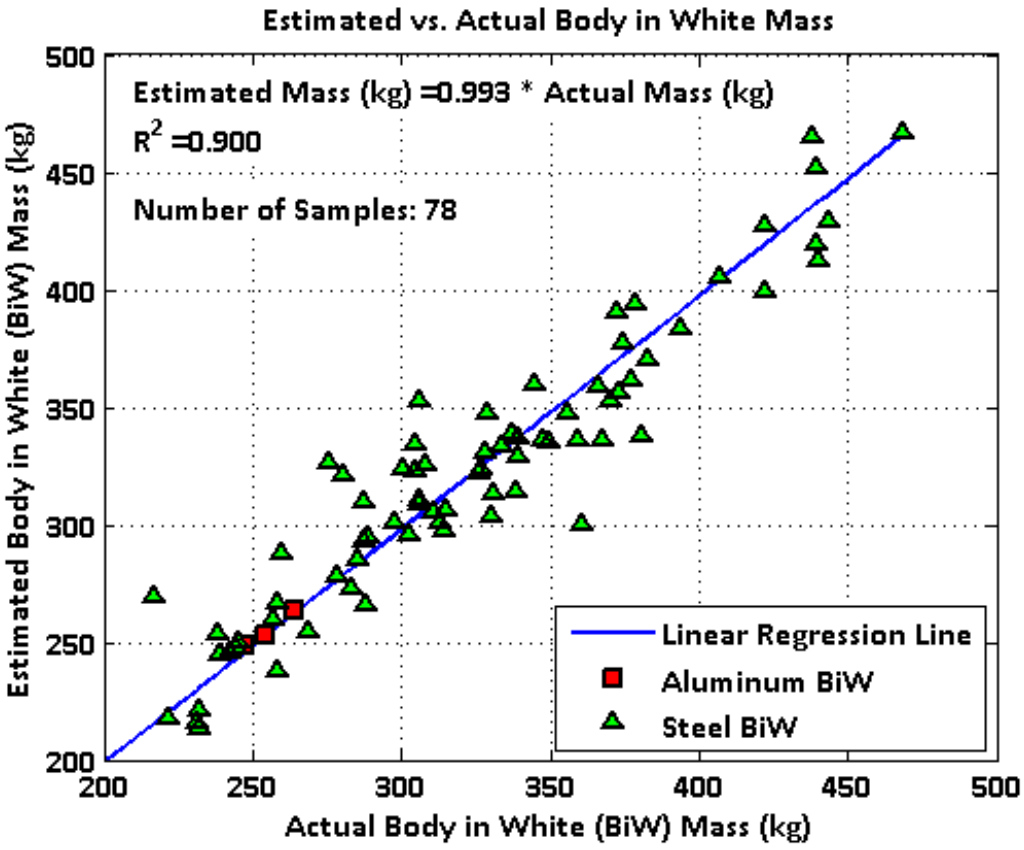

Figure F.2 Estimated vs. Actual Body in White Mass (BiW: Body in White) [54]

Closure mass correlations are shown in Table F.2 [54]. Components of the correlation relationships use the lateral surface area inside the wheelbase (for doors) and a product of width and vehicle overhang for the hood and decklid liftgate. Component

coefficients for both steel and aluminum 4-door vehicles are kept the same (2.0 / 0.75) to compare the effects of material selection. For both 4-door and 2-door vehicles, the component coefficients are selected by empirical fitting of data. Closure mass does not include glazing, which is grouped in the "uncategorized" subsystem.

Closure Material / Configuration	**Mass Estimation Relationship**	**R^2 Value**
Steel / 4 Doors	$M_{Cls} = 7.915 * [2.00 * L101 * H100 + 0.75 * W103 * (L103 - L101)]$ kg	**0.760**
Steel / 2 Doors	$M_{Cls} = 5.494 * [1.70 * L101 * H100 + 2.50 * W103 * (L103 - L101)]$ kg	**0.836**
Aluminum / 4 Doors	$M_{Cls} = 3.655 * [2.00 * L101 * H100 + 0.75 * W103 * (L103 - L101)]$ kg	**0.555**

Table F.2 Closure Mass Estimation Relationships (M_{Cls}: Closure Mass in kg) [54]

Estimated vs. actual closure mass correlation is shown in Figure F.3 [54].

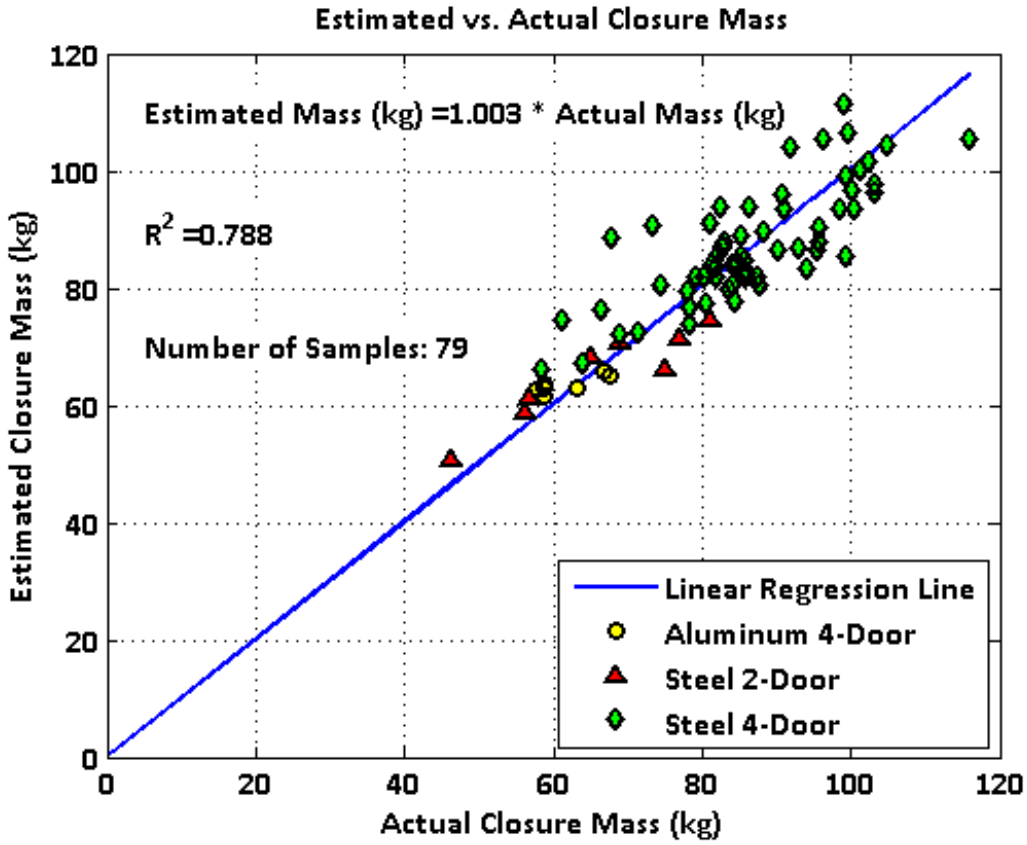

Figure F.3 Estimated vs. Actual Closure Mass [54]

The relations in Table F.2 provide a useful level of correlation, particularly considering the spectrum of vehicle types (from sports cars to crossover sport utility vehicles) and different closure configurations encompassed in the mass estimation for this subsystem.

Interior mass estimation follows the relationship shown in Equation (F.2) with a confidence factor (R^2) of 0.714. As with many of the subsystem correlations, this relation uses the vehicle outside (block) volume.

$$M_{Int} = 9.889 \cdot (\mathrm{L101} \cdot \mathrm{W103} \cdot \mathrm{H100})\ \mathrm{kg} \qquad \text{Equation (F.2)}$$

Estimated vs. actual interior mass correlation is shown in Figure F.4 [54]. This has the lowest correlation of the various subsystems in this work. It is difficult to find a single simplified correlation to provide a best fit for all of the components (seats, instrument panel, center console, trim, headliner, etc.) contained in this subsystem over a broad range of vehicle types. The amount of variation seen in the mass estimation of this subsystem does not, however, appear to have a significant impact on overall curb mass correlations.

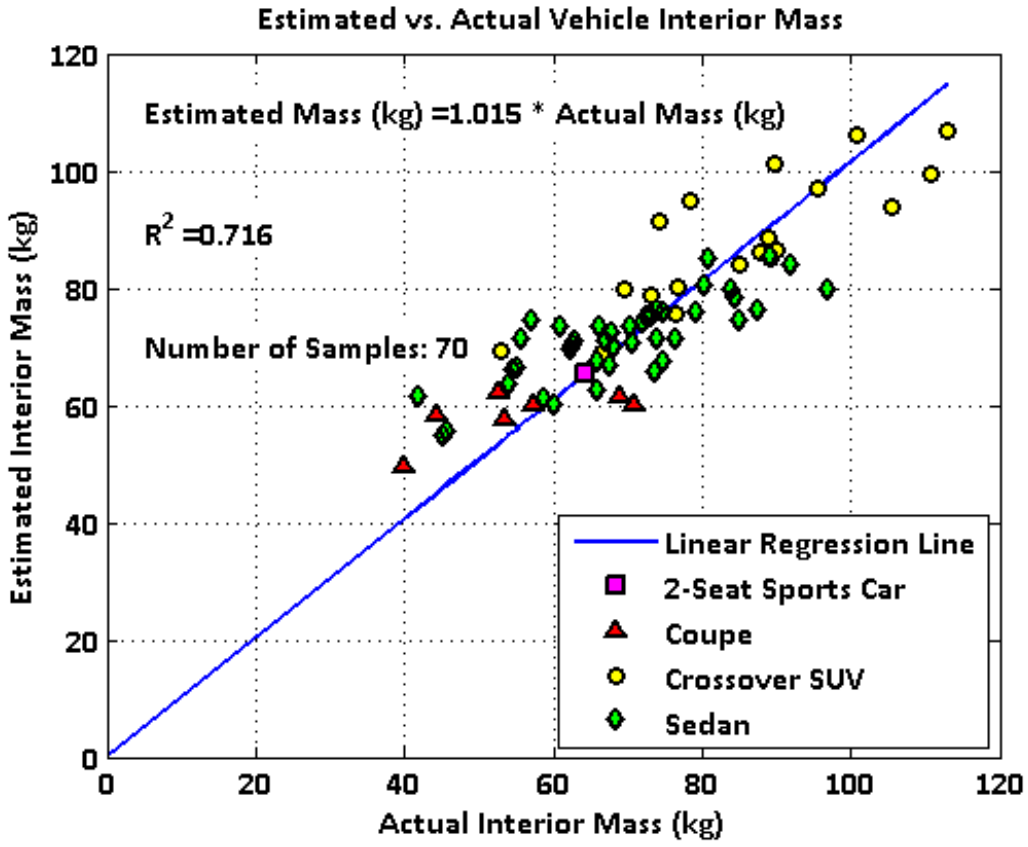

Figure F.4 Estimated vs. Actual Vehicle Interior Mass (SUV: Sport Utility Vehicle) [54]

The "uncategorized mass" subsystem, containing a high diversity of content items, appears to provide an effective level of estimated vs. actual mass correlation. The relation shown in Equation (F.3) has a confidence factor (R^2) of 0.835.

$$M_{Unc} = 45.898 \cdot (\mathrm{L101} \cdot \mathrm{W103} \cdot \mathrm{H100})\ \mathrm{kg} \qquad \text{Equation (F.3)}$$

Estimated vs. actual mass correlation for uncategorized mass is shown in Figure F.5 [54]. This subsystem is a collective of all items not in other subsystems and may be divided into further subsystems at a later date as mass data permits.

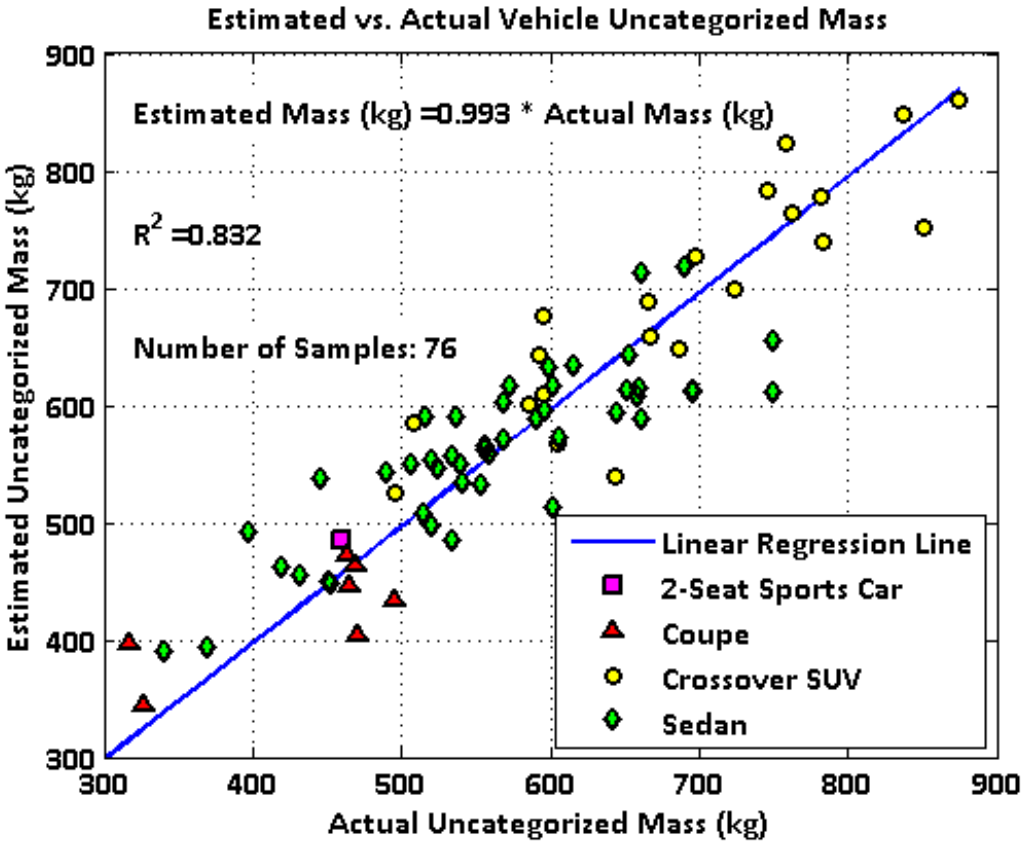

Figure F.5 Estimated vs. Actual Uncategorized Mass (SUV: Sport Utility Vehicle) [54]

Vehicle Sprung Mass consists of all components of curb mass with the exception of the suspension system as shown in Equation (F.4).

$$M_{Sprung} = M_{Eng} + M_{Drv} + M_{BiW} + M_{Cls} + M_{Int} + M_{Unc}$$ Equation (F.4)

The vehicle sprung mass is used to estimate vehicle suspension mass. A comparison of estimated vs. actual vehicle sprung mass is shown in Figure F.6 [54].

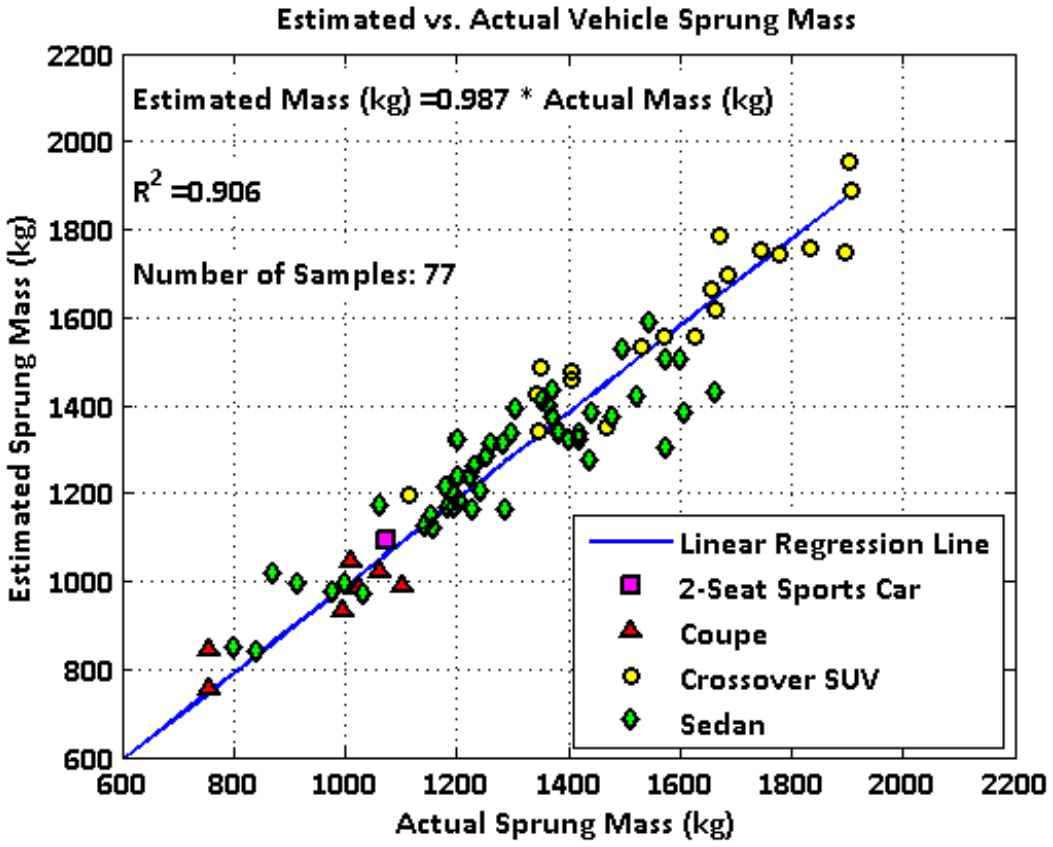

Figure F.6 Estimated vs. Actual Vehicle Sprung Mass (SUV: Sport Utility Vehicle)[54]

The suspension system mass correlation to vehicle sprung mass is shown in Equation (F.5) with a confidence factor (R^2) of 0.807.

$$M_{Sus} = 0.175 \cdot M_{Sprung}$$ Equation (F.5)

Correlation of estimated vs. actual suspension mass is shown in Figure F.7 [54].

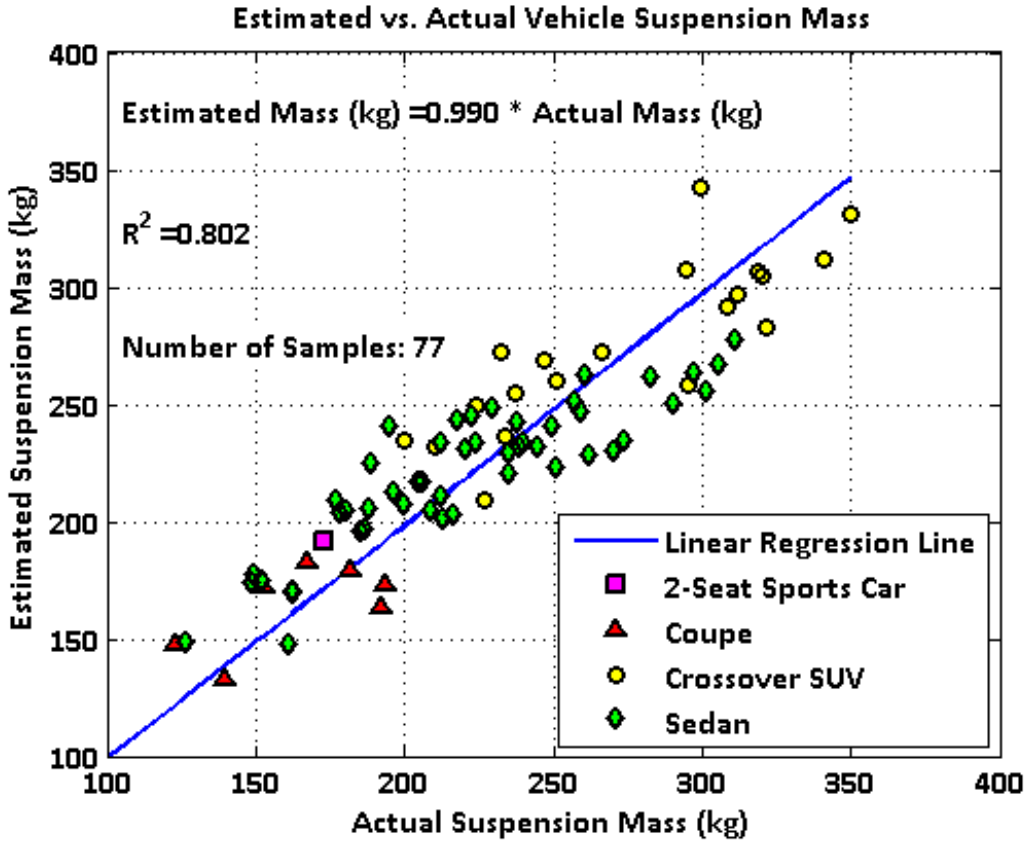

Figure F.7 Estimated vs. Actual Suspension Mass (SUV: Sport Utility Vehicle) [54]

Vehicle Curb Mass Estimation and Correlation

In order to further validate the mass estimation models in this work, a set of "case study" vehicles is assessed to validate the mass estimation models. These vehicles are independent of the vehicle database used to develop most of the subsystem mass estimation correlations. Results are shown in Figure F.8 [54]. These show results that are reasonably close to an ideal trendline value of 1.000 with a high correlation

confidence factor. This validates the ability to provide a reasonable vehicle mass correlation based on a relatively small number of vehicle parameters.

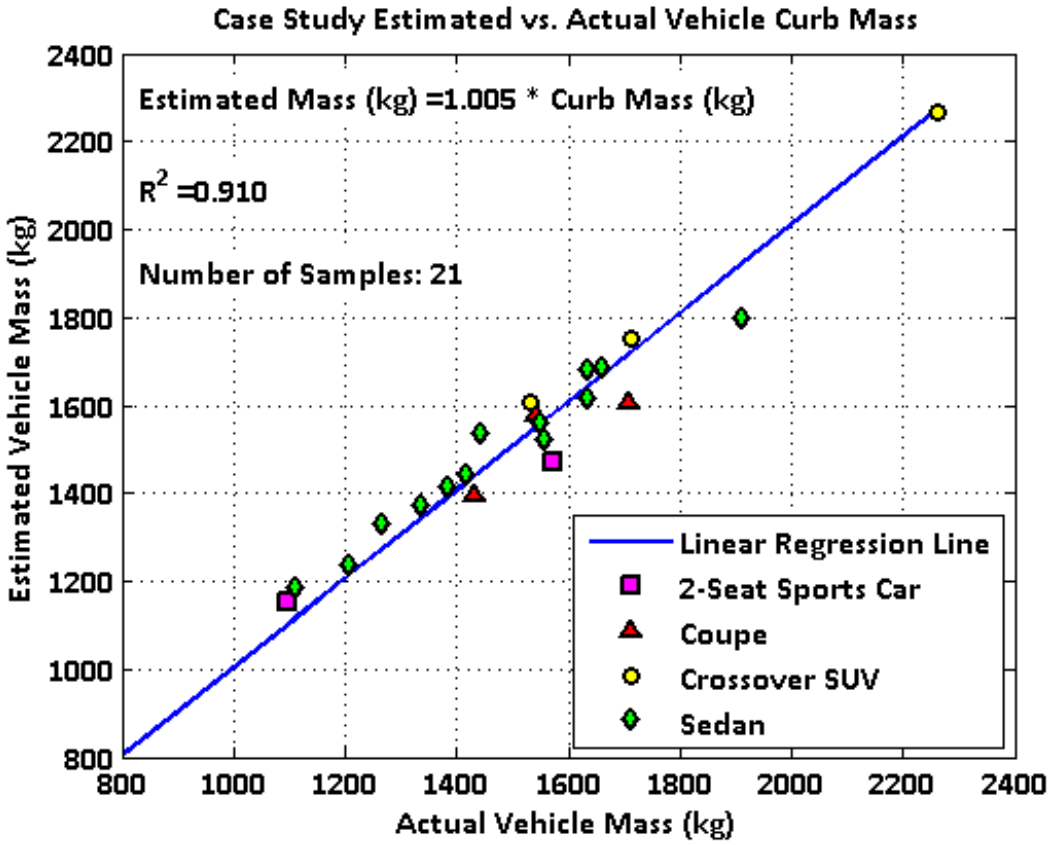

Figure F.8 Estimated vs. Actual Curb Mass for Case Study Vehicles (SUV: Sport Utility Vehicle) [54]

Curb mass is then estimated for a larger population of vehicles (those used for subsystem mass estimation development) and compared with actual vehicle curb mass as shown in Figure F.9 [54].

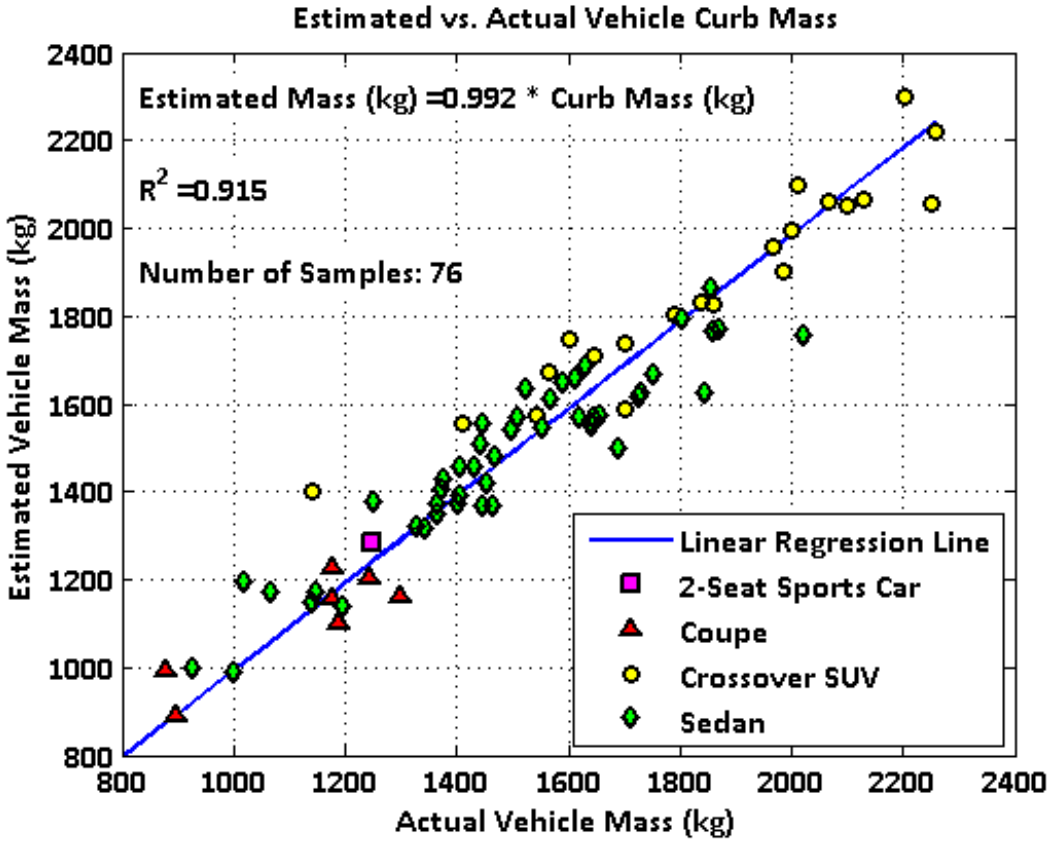

Figure F.9 Estimated vs. Actual Curb Mass (SUV: Sport Utility Vehicle) [54]

The results indicate that vehicle mass calculation based on a limited set of parameters can yield an estimate which is close to actual vehicle curb mass without detailed knowledge of vehicle styling and exact component content yet to be determined in the detailed design phase. Some variation is expected due to individual Original Equipment Manufacturer (OEM) targets and the quantity of transmissions and other standardized components from which they select. Variation in curb mass by vehicle type can also be seen in Figure F.13. A total of 76 Vehicles are evaluated in developing these mass correlations.

Appendix G
Fuel Economy Modeling and Relations

Parametric Fuel Economy Mileage Calculations

EPA combined mileage serves as one of the customer-defined targets in the optimization objective function. This mileage value is posted by law on all vehicles sold in the U.S. [73]

EPA combined gas mileage is defined as [73]:

$$EPA_{Combined} = \frac{1}{\frac{0.55}{EPA_{City}} + \frac{0.45}{EPA_{Highway}}} \qquad \text{Equation (G.1)}$$

EPA_{City}:EPA Mileage using City Driving Cycle (UDDS)

$EPA_{Highway}$:EPA Mileage using Highway Driving Cycle (FWFET)

Forces acting on the vehicle during EPA fuel economy testing are shown in Figure G.1.

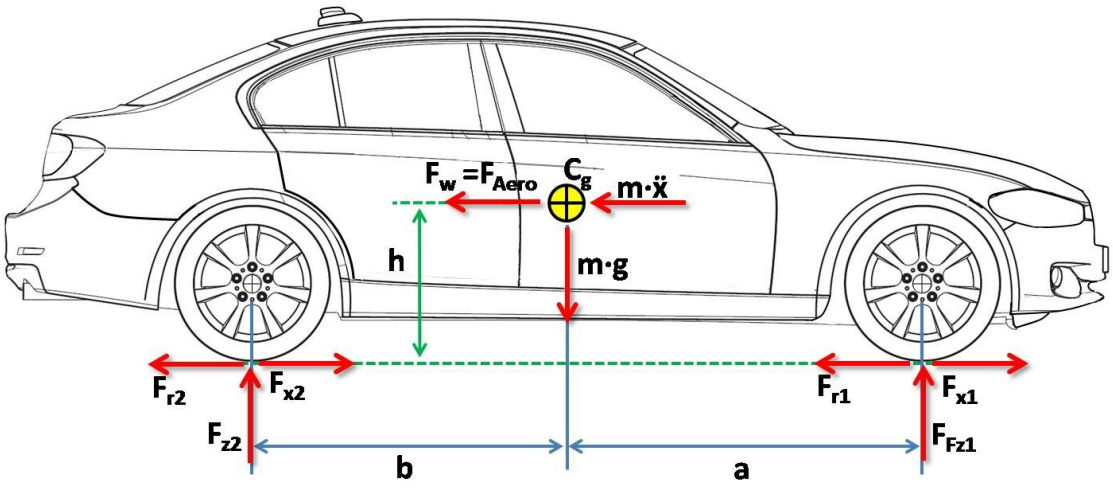

Figure G.1 Forces Acting on Vehicle During EPA Fuel Economy Testing [54, 75]

F_w: Aerodynamic resistance (F_{aero})

m: Vehicle test mass specified by EPA regulations [73]

C_g: Vehicle center of gravity location

h: Vehicle center of gravity height from ground

g: Acceleration due to gravity ≈ 9.81 m/sec2

ẍ: Vehicle acceleration (m/sec^2) = dV/dt

a: Distance from C_g to front wheel center

b: Distance from C_g to rear wheel center

F_{x1}: Vehicle traction force at front axle

F_{x2}: Vehicle traction force at rear axle

F_{z1}: Tire normal load at front axle

F_{z2}: Tire normal load at rear axle

F_{r1}: Tire rolling resistance at front axle

F_{r2}: Tire rolling resistance at rear axle

The aerodynamic resistance force F_w can be expressed as [75]:

$$\boldsymbol{F_w = C_d \cdot A_s \cdot \rho \cdot \frac{V^2}{2}} \qquad \text{Equation (G.2)}$$

Cd: Vehicle drag coefficient

As: Vehicle frontal surface area

ρ: Density of Air at 23° C at Sea Level (kg/m^3) = 1.225 kg/m^3 (or ρ_{air})

V: Vehicle velocity

Tire rolling resistance F_r is expressed as [75]:

$$F_r = f_r \cdot F_z$$ Equation (G.3)

f_r: Tire rolling resistance

F_z: Tire normal load

The force balance equation is then [75]:

$$m \cdot \frac{dV}{dt} + C_d \cdot A_s \cdot \rho \cdot \frac{V^2}{2} + f_r \cdot (F_{z1} + F_{z2}) - F_{x1} - F_{x2} = 0$$ Equation (G.4)

The front tire normal load F_{z1} is [75]:

$$F_{z1} = \frac{m \cdot \left[b \cdot g - h \cdot \frac{dV}{dt}\right]}{a + b}$$ Equation (G.5)

The rear tire normal load F_{z2} is [75]:

$$F_{z2} = \frac{m \cdot \left[b \cdot g + h \cdot \frac{dV}{dt}\right]}{a + b}$$ Equation (G.6)

From Equation (F.3), the traction forces are [75]:

$$F_{x1} + F_{x2} = m \cdot \frac{dV}{dt} + C_d \cdot A_s \cdot \rho \cdot \frac{V^2}{2} + f_r \cdot m \cdot g$$ Equation (G.7)

Power at the wheels (P = F·V) is [75]:

$$P = m \cdot V \cdot \frac{dV}{dt} + C_d \cdot A_s \cdot \rho \cdot \frac{V^3}{2} + f_r \cdot m \cdot g \cdot V$$ Equation (G.8)

The cycle energy is then [75]:

$$\boldsymbol{E = \int_0^{cycle} P \cdot dt = m \cdot \int_0^{cycle} V \cdot \frac{dV}{dt} \cdot dt + \frac{C_d \cdot A_s \rho}{2} \cdot \int_0^{cycle} V^3 dt + f_r \cdot m \cdot g \cdot \int_0^{cycle} V \cdot dt}$$ Equation (G.9)

The portion inside each integral expression in Equation (G.6) is solely dependent on the test cycle and independent of the vehicle parameters. The expression inside each integral expression can be parameterized as β_1, β_2 and β_3. The energy can then be expressed as [75]:

$$E_{cycle} = \beta_1 \cdot M_{EPA} + \beta_2 \cdot \frac{1}{2} \cdot C_d \cdot A_s \cdot \rho_{air} + \beta_3 \cdot f_r \cdot M_{EPA} \cdot g$$ Equation (G.10)

E_{cycle}: Test cycle energy (joules)

β_1: Driving (vehicle acceleration) contribution coefficient for the designated driving cycle (joules / kg)

β_2: Aerodynamic contribution coefficient for the designated driving cycle (m^3/sec^2)

β_3: Rolling resistance contribution coefficient (meters = cycle driving distance in meters)

M_{EPA}: Vehicle EPA test mass in kg (curb mass M_{curb} + Specified added test mass of 136.36 kg) [73]

M_{curb}: Vehicle curb mass (vehicle mass without occupants) in kg.

C_d: Vehicle drag coefficient

A_s: Vehicle Frontal Surface Area (m^2) ≈ 0.84 · (W103) · (H100) []

ρ_{air}: Density of Air at 23° C at Sea Level (kg/m^3) = 1.225 kg/m^3

f_r: Coefficient of Rolling Resistance

For the UDDS and FWFET cycles the β parameters have been calculated as shown in Table G.1 below along with the parameters for several other driving test cycles [13]:

Driving Cycle	**β_1 Driving Contribution (joules/kg)**	**β_2 Aerodynamic Contribution (m^3/sec^2)**	**β_3 Rolling Resistance Contribution (meters)**
UDDS	**2,098**	**2,628,604**	**11,990**
FWFET	**1,165**	**8,539,652**	**16,507**
US06	**2,712**	**9,923,220**	**12,888**
SC03	**1,188**	**1,341,165**	**5,761**
NEDC	**1.227**	**3,980,986**	**10,931**
JC08	**1,442**	**1,560,874**	**8.172**

Table G.1 Driving Cycle Parameters for Common Fuel Economy Test Cycles [13]

Once the Cycle Energy E_{cycle} is calculated for each cycle, the vehicle mileage for each cycle can be calculated as shown in Equation (G.11) [13]:

$$MPG_{cycle} = \eta_{t2w} \cdot \frac{\rho_{fuel}}{E_{cycle}} \cdot \frac{l_{cycle}}{1{,}609.344} \cdot 3.785 \qquad \text{Equation (G.11)}$$

MPG_{cycle}: MPG for specified driving cycle

η_{t2w}: Tank-to-Wheel Efficiency (or η_{b2w}--Battery to Wheel Efficiency--for electric vehicles)

ρ_{fuel}: Energy density of fuel (joules/liter) (Official EPA value for gasoline = 32.052 x 10^6 joule/liter, diesel ≈ 35 x 10^6 joule/liter, no official value) [73]

E_{cycle}: Energy required for Driving Cycle (joules)

l_{cycle}: Distance travelled in Driving Cycle in meters (= β_3 Parameter)

1,609.344: Meters in 1 mile

3.785: Liters in 1 U.S. gallon

From the above equations the final EPA mileage can be calculated. The EPA mileage must be recalculated for each iteration of the optimization process as vehicle mass is affected by many of the optimization design variables. Using actual vehicle data (mass, width, height, EPA urban / highway mileage, drag coefficient, etc.), the tank-to-wheel efficiency η_{t2w} is calculated using a statistical sample for gasoline and diesel engines for UDDS and FWFET cycles as shown in Table G.2 [54]. These values for tank-to-wheel efficiency appear to be independent of engine power.

Fuel Type	**UDDS η_{t2w}**	**UDDS η_{t2w} Standard Deviation σ**	**FWFET η_{t2w}**	**FWFET η_{t2w} Standard Deviation σ**	**Sample Size**
Gasoline	**0.163**	**0.010**	**0.214**	**0.014**	**30**
Diesel	**0.208**	**0.015**	**0.271**	**0.017**	**10**

Table G.2 Tank-to-Wheel Efficiency Values for Gasoline and Diesel Engines [54]

For parallel hybrid vehicles (those with both an electric drive motor and gasoline or diesel engine, either of which can drive the wheels), the energy equation is modified due to recovery of energy during regenerative braking [13]:

$$E_{cycle} = \beta_1 \cdot \left(1 - \eta_{regen}\right) \cdot M_{EPA} \cdot g + \beta_2 \cdot \frac{1}{2} \cdot C_d \cdot A_s \cdot \rho_{air} + \beta_3 \cdot f_r \cdot M_{EPA} \qquad \text{Equation (G.12)}$$

η_{regen}: Percentage of acceleration energy recovered by regenerative braking. All other parameters same as in Equation (G.10).

With known values for all other parameters, the regeneration coefficient can be determined from gas / diesel engine-only EPA mileage information for existing hybrid vehicles (using gas / diesel tank-to-wheel efficiency values for each cycle as appropriate).

A measure of miles per gallon gasoline equivalent (MPGe) can be calculated using Equation (G.13).

$$MPGe_{cycle} = \eta_{b2w} \cdot \frac{\rho_{gasoline}}{E_{cycle}} \cdot \frac{l_{cycle}}{1{,}609.344} \cdot 3.785 \qquad \text{Equation (G.13)}$$

MPGe: Miles per Gallon Gasoline equivalent

η_{b2w}= Battery-to-Wheel efficiency (for electric motor driveline)

All other parameters as in Equation (G.10)

Noting that $\eta_{regen} = \eta^2_{b2w}$ if driveline efficiency is the same for battery charge / discharge, the battery-to-wheel efficiency can be determined once the regeneration coefficient is known as shown in Table G.3 (UDDS) and Table G.4 (FWFET) [54].

η_{regen} UDDS	η_{regen} UDDS Standard Deviation σ	η_{b2w} UDDS	η_{b2w} UDDSStandard Deviation σ	Samples
0.642	**0.139**	**0.790**	**0.091**	**14**

Table G.3 Battery-to-Wheel Efficiency Coefficient for UDDS Cycle [54]

η_{regen} FWFET	η_{regen}FWFET Standard Deviation σ	η_{b2w} FWFET	η_{b2w}FWFETStandard Deviation σ	Samples
0.314	**0.123**	**0.550**	**0.112**	**14**

Table G.4 Battery-to-Wheel Efficiency Coefficient for FWFET Cycle [54]

While this sample has a larger standard deviation than the gasoline/diesel efficiencies previously calculated in Table G.2, these values can still be used to provide a reasonable estimate of hybrid vehicle performance.

Note that EPA test mass and resulting cycle energies can change in each optimization iteration as vehicle longitudinal dimension components change (several longitudinal parameters are currently used as design variables). If width and / or height

dimensional components become design variables, the vehicle frontal surface area will also change with each optimization iteration.

These calculations give a means of determining vehicle EPA mileage for gasoline, diesel and hybrid vehicles along with gasoline mileage equivalents for hybrid vehicles. These can be used in optimization codes with customer- or company-determined mileage objective targets (or to determine if vehicles meet government CAFE mileage requirements as a minimum constraint value).

EPA Fuel Economy Targets

Beginning in 2012, passenger vehicles sold in the U.S. must achieve a fuel economy target (FET) based on vehicle footprint F101. The target is expressed as shown in Equation (G.14) [73].

$$Target_{mpg} = \frac{1}{min\left(max\left(c \cdot F101 + d, \frac{1}{a}\right), \frac{1}{b}\right)} \qquad \text{Equation (G.14)}$$

F101: Vehicle footprint (EPA definition) in ft^2

a: Function upper limit in miles per gallon (mpg)

b: Function lower limit (mpg)

c: Function slope (gpm / ft^2)

d: Function intercept (gpm)

Values of coefficients a, b, c and d by model year (through 2025) are shown in Table G.5 [73].

Model Year	a	b	c	d
2012	**35.95**	**27.95**	**0.005308**	**0.005410**
2013	**36.80**	**28.46**	**0.005308**	**0.005410**
2014	**37.75**	**29.03**	**0.004725**	**0.004725**
2015	**39.24**	**29.90**	**0.003719**	**0.003719**
2016	**41.09**	**30.96**	**0.002573**	**0.002573**
2017	**43.61**	**32.65**	**0.0005131**	**0.001896**
2018	**45.21**	**33.84**	**0.0004954**	**0.001811**
2019	**46.87**	**35.07**	**0.0004783**	**0.001729**
2020	**48.74**	**36.47**	**0.0004603**	**0.001643**
2021	**50.83**	**38.02**	**0.0004419**	**0.001555**
2022	**53.21**	**39.79**	**0.0004227**	**0.001463**
2023	**55.71**	**41.64**	**0.0004043**	**0.001375**
2024	**58.32**	**43.58**	**0.0003867**	**0.001290**
2025	**61.07**	**45.61**	**0.0003699**	**0.001200**

Table G.5 EPA Passenger Vehicle Fuel Economy Target Parameters by Model Year [73]

An example of the Fuel Economy Target function for vehicle Model Year 2021 as calculated in the software framework is shown in Figure G.3 [54].

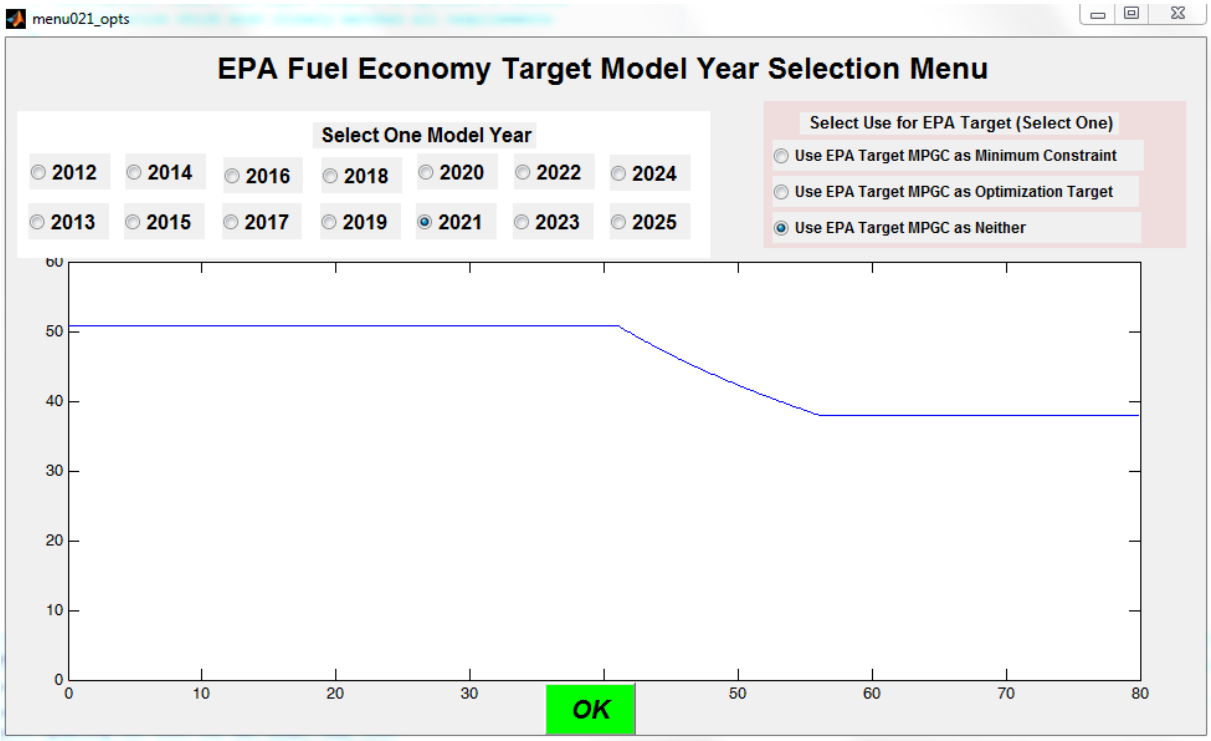

Figure G.2 Sample Fuel Economy Target Function Calculation for MY 2021 [54]

Hybrid Modeling and Relations:
Regeneration Coefficient and Battery-to-Wheel Efficiency by Vehicle Type

Fourteen vehicles of assorted type / class are used in developing the hybrid relations shown above. Regeneration coefficient by vehicle type is shown in Table G.6 [54].

Vehicle Type	η_{regen} (Urban)	Standard Deviation σ	η_{regen} (Highway)	Standard Deviation σ	Samples
Coupe / Sedan	0.67	0.11	0.31	0.12	10
SUV / CSUV	0.58	0.19	0.33	0.14	4

Table G.6 Hybrid Regeneration Coefficient by Vehicle Type [54]

Battery-to-Wheel efficiency by Vehicle Type is shown in Table G.7 [54].

Vehicle Type	η_{B2W} (Urban)	Standard Deviation σ	η_{B2W} (Highway)	Standard Deviation σ	Samples
Coupe / Sedan	**0.82**	**0.07**	**0.54**	**0.11**	**10**
SUV / CSUV	**0.75**	**0.13**	**0.57**	**0.13**	**4**

Table G.7 Hybrid Battery-to-Wheel Efficiency by Vehicle Type [54]

In calculating all-electric range performance to target, the EPA UDDS Cycle is used as the test cycle in this work and in the software framework. The total battery energy (in joules) is divided by the cycle energy (joules/km) to find the vehicle range in kilometers.

Mass vs. Capacity for Hybrid Battery Packs

While the use of hybrid vehicle batteries can extend vehicle mileage, the added mass can affect other vehicle targets such as 0 to 60 mph acceleration time and braking distance. A major factor in the battery size is the target all-electric vehicle range. Calculation of overall battery mass (with electronics) and resulting battery center of gravity location in this work is based on benchmarking results for a number of batteries of different material composition. An example of Lithium battery energy density is shown in Figure G.3 [54, 75]

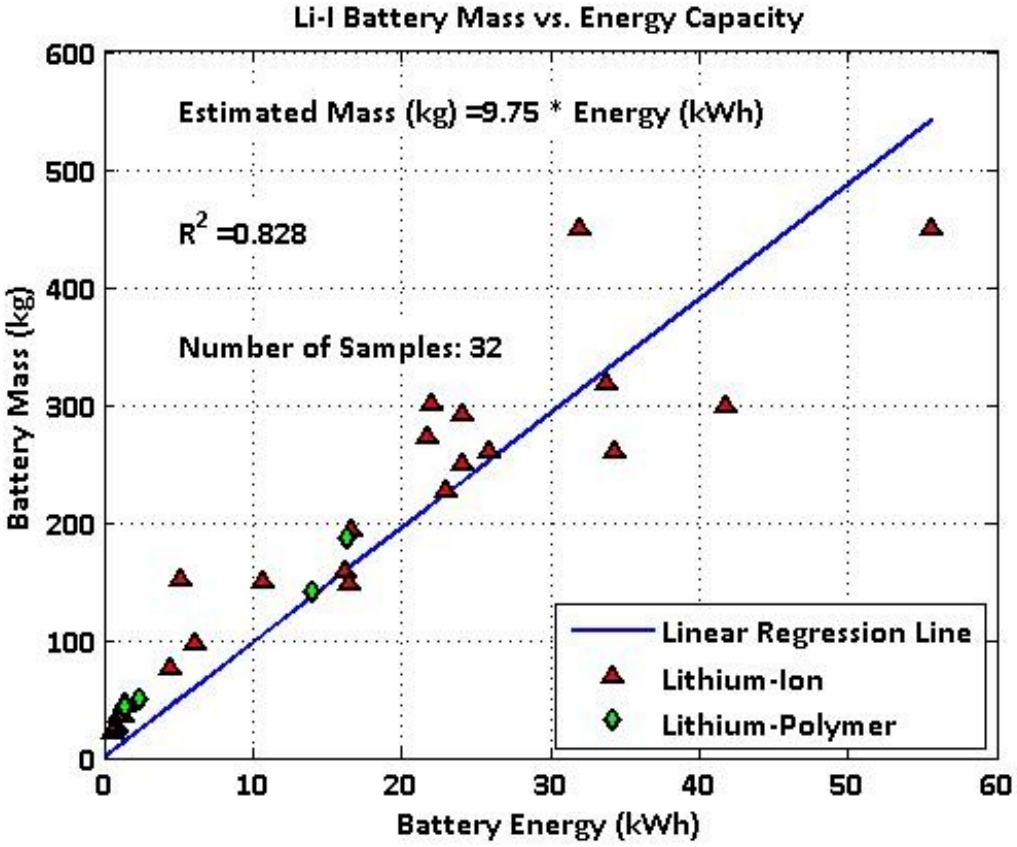

Figure G.3 Lithium Battery Mass vs. Energy Capacity [54]

Energy densities (kg/kWh) are shown for several battery materials in Table G.8 [54, 75].

Battery Type	Correlation	R2	Samples
Lithium (Ion + Polymer)	**M_{Batt} = 0.75 * Energy in kWh (kg)**	**0.828**	**32**
Lithium-Ion	**M_{Batt} = 9.70 * Energy in kWh (kg)**	**0.821**	**28**
Lithium-Polymer	**M_{Batt} = 11.07 * Energy in kWh (kg)**	**0.899**	**4**
Ni-MH ≤ 5 kWh	**M_{Batt} = 36.63 * Energy in kWh (kg)**	**0.734**	**32**
Ni-MH > 5kWh	**M_{Batt} = 13.10 * Energy in kWh + 118.3 (kg)**	**0.991**	**3**

Table G.8 Hybrid Battery Energy Density by Material [54, 75]

Electric Motor Power vs. Mass and Torque

Electric motor power density and Cg location are also important in assessing the impact of hybrid vehicle characteristics on other vehicle target achievements. Benchmarking data for a number of hybrid vehicles and commercially available motors is shown in Table G.9 [54, 75, 76].

Electric Motor	Peak Power (kW)	Total Mass (kg)	Motor Mass (kg)	Inverter Mass (kg)	Peak Torque (Nm)
Mistubishi i-Miev	**49.0**	**64.0**	**49.0**	**15.0**	**196.0**
Nissan Leaf	**80.0**	**71.0**	**55.7**	**15.3**	**280.0**
Deep Orange 1 Vehicle	**125.0**	**71.4**	**37.1**	**34.3**	**300.0**
Deep Orange 1 Generator	**75.0**	**75.0**	**41.0**	**34.0**	**240.0**
Mini E	**150.0**	**80.0**	**50.0**	**30.0**	**225.0**
Tesla	**225.0**	**87.2**	**52.2**	**35.0**	**370.0**
TM4 Motive A Drivetrain	**80.0**	**70.0**	**36.0**	**34.0**	**170.0**
Coda EV	**100.0**	**80.0**	**50.0**	**30.0**	**225.0**
TM4 Motive B Drivetrain	**105**	**44.0**	**33**	**11**	**180**

Table G.9 Hybrid Vehicle Motor Energy Densities and Resulting Torque [54, 75, 76]

Specific ratios of interest derived from Table G.9 are shown in Table G.10. [54, 75, 76]. The key ratios used in this work are peak power density (kW/kg) and peak torque to peak power (Nm/kW). For a given motor power in kW, this gives motor mass and resulting torque.

Ratio of Interest	Average Value	Standard Deviation σ	Units	Samples
Peak Power Density	**1.54**	**0.64**	**kW/kg**	**9**
Sustained Power Density	**0.68**	**0.32**	**kW/kg**	**5**
Peak Torque to Peak Power	**2.48**	**0.89**	**Nm/kW**	**9**
Sustained Torque to Sustained Power	**2.66**	**1.39**	**Nm/kW**	**4**
30-Second Peak Power to Sustained Peak Power	**2.80**	**0.50**	**kW/kW**	**5**
30-Second Peak Torque to Sustained Peak Torque	**2.20**	**0.49**	**Nm/Nm**	**4**

Table G.10 Hybrid Motor Ratios of Interest [54, 75, 76]

Appendix H
Acceleration and Braking Modeling and Relations

Vehicle Acceleration Model

Forces involved in vehicle acceleration time calculation are shown in Figure H.1 below [74, 54].

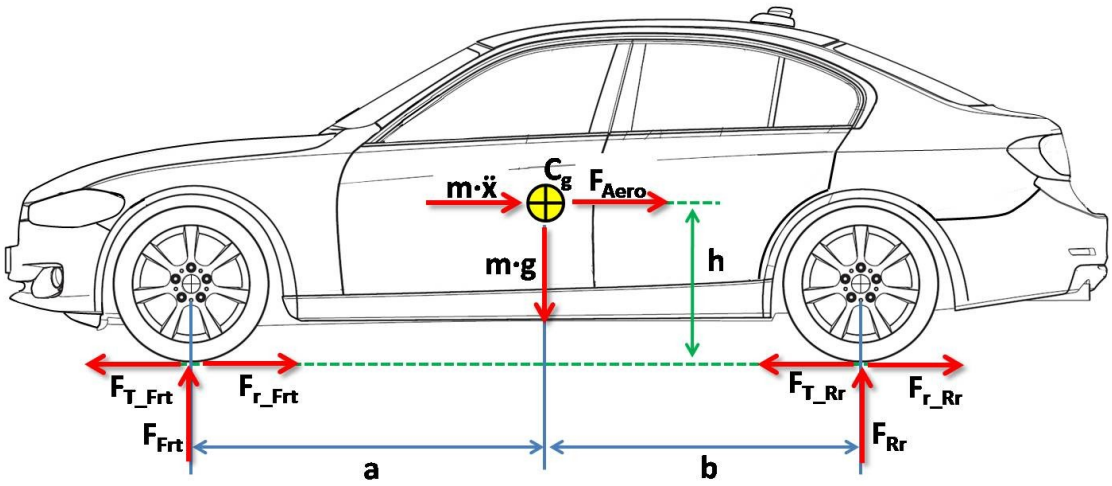

Figure H.1 Vehicle Loads During Acceleration [54, 74]

m•ẍ: Force exerted by acceleration/decleration of vehicle mass (N)

m•g: Downward force due to gravitational acceleration of vehicle mass (N)

C_g: Vehicle center of gravity location

F_{Aero}: The resisting force due to movement of the vehicle through air (N)

h: Vehicle C_g height above ground (m)

F_{T_Frt}: Traction force exerted through the front wheels (N)

F_{r_Frt}: Rolling resistance between the front tires and ground (N)

F_{Frt}: The downward force on the front wheels due to vehicle mass and gravity (N)

a: Longitudinal distance from front wheel center to C_g

b: Longitudinal distance from C_g to rear wheel center

F_{T_Rr}: Traction force exerted through rear wheels (N)

F_{r_Rr}: Rolling resistance between the rear tires and ground (N)

F_{Rr}: The downward force on the rear wheels due to vehicle mass and gravity (N)

The acceleration model used in this work makes several assumptions:

- Rolling resistance (0.0075 to 0.010 of vehicle weight) forces can be excluded with small loss in accuracy.
- For 0 to 60 mph and 0 to 100 kph acceleration times, the aerodynamic drag can also be excluded with small loss in accuracy.
- A constant acceleration model can be used in conjunction with traction limits to describe vehicle acceleration and resulting 0 to 60 mph time.

If a constant acceleration (due to constant power application) is used, the acceleration time is shown in Equation (J.1) [74].

$$t_{0\ to\ 60\ mph} = \frac{v}{a} = \frac{m}{P} \cdot v_{60\ mph}{}^2 \qquad \text{Equation (H.1)}$$

$v_{60\ mph}$: Vehicle final velocity (m/sec) = 26.82 m/sec for 60 mph

a: Vehicle acceleration (m/sec^2)

m: Vehicle test mass (kg) (Curb Mass + 80.6 kg; 1 75 kg driver and 10 lb measuring equipment

P: Vehicle traction power (kW)

For 0 to 100 kph acceleration time, only the vehicle final velocity (27.78 m/sec instead of 26.82 m/sec) will change in Equation (H.1). Traction limits (the maximum power/force which can be applied at the wheels) will be dependent on the vehicle drive configuration (FWD/RWD/AWD). For 0 to 60 mph acceleration, the limiting traction for front wheel drive is shown in Equation (H.2) [74].

$$P_{Max_{FWD}} = \left[\frac{m \cdot g \cdot b \cdot \mu}{a + b + h \cdot \mu}\right] \cdot v_{60\ mph} \qquad \text{Equation (H.2)}$$

P_{MaxFWD}: Maximum traction force available for vehicle acceleration for a front wheel drive (FWD) vehicle

m: Vehicle test mass (kg) (Curb Mass + 80.6 kg; 1 75 kg driver and 10 lb measuring equipment

g: Gravitational acceleration = 9.81 m/sec^2

b: Longitudinal distance from center of gravity (C_g) to rear wheel center (m)

μ: Tire/surface friction coefficient

a: Longitudinal distance from front wheel center to C_g (m)

h: C_g height from ground (m)

$v_{60\ mph}$: Vehicle velocity in m/sec for 60 mph (= 26.82 m/sec)

The limiting traction power for rear wheel drive vehicles is shown in Equation (H.3) [74].

$$P_{Max_{RWD}} = \left[\frac{m \cdot g \cdot b \cdot \mu}{a + b - h \cdot \mu}\right] \cdot v_{60\ mph} \qquad \text{Equation (H.3)}$$

P_{MaxRWD}: Maximum traction force available for vehicle acceleration for a rear wheel drive (RWD) vehicle

All other parameters as for Equation (H.2)

The limiting traction power for all-wheel drive vehicles is shown in Equation (H.4) [74].

$$P_{Max_{AWD}} = m \cdot g \cdot \mu \cdot v_{60\ mph} \qquad \text{Equation (H.4)}$$

P_{MaxAWD}: Maximum traction force available for vehicle acceleration for an all-wheel drive (RWD) vehicle

All other parameters as for Equation (H.2)

In the Scenario Builder and Optimization modules, if a specified engine power is greater than the traction limit, the maximum traction power is used in the 0 to 60 mph and 0 to 100 kph acceleration time calculations.

One of the greatest sources of variation in this calculation is the value used for the coefficient of friction. The default value used in the software framework is 1.0; values of 0.9 to 1.1 are typical for tires on dry pavement [74]. The software framework permits the user to change the default value for the tire friction coefficient to the user-desired input value.

An alternative acceleration equation accounts for gear shifting but not for drive configuration (FWD / RWD / AWD) as shown in Equation (H.5) as curve-fitted from a body of data [37].

$$t_{0-60} = a \cdot \left(\frac{hp}{lb}\right)^{-b} \qquad \text{Equation (H.5)}$$

$t_{0\text{-}60}$: Time to accelerate from 0 to 60 mph in seconds

hp: Vehicle maximum power in horsepower

lb: Vehicle weight in pounds (1 driver at 75 kg + 10 lb equipment)

a: 0.892 for automatic transmission, 0.967 for vehicles with manual transmissions

b: 0.805 for automatic transmission, 0.775 for vehicles with manual transmissions

Vehicle Braking Model

Forces involved in vehicle acceleration time calculation are shown in Figure H.2 below [74, 54].

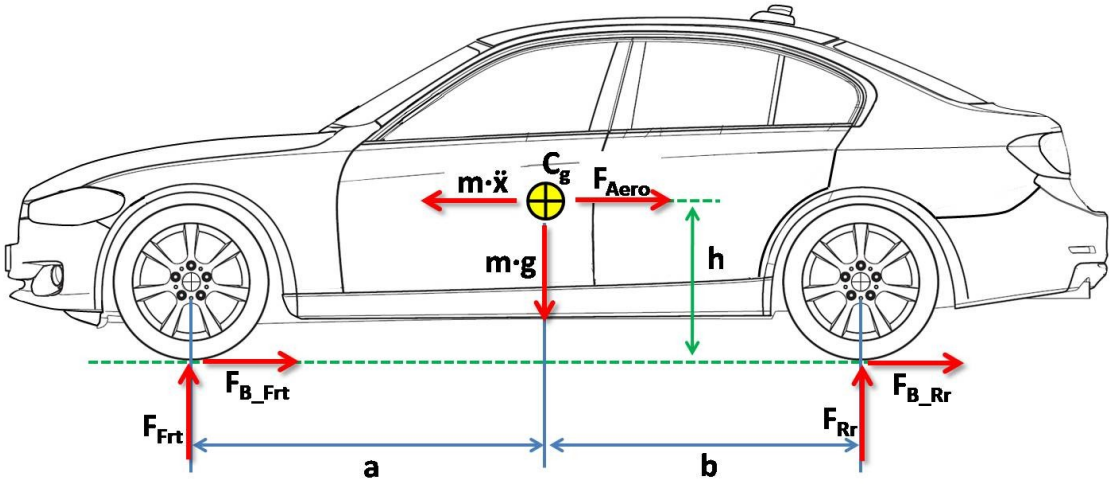

Figure H.2 Vehicle Loads During Braking [54, 74]

Parameters are the same as in Figure H.1.

As with vehicle acceleration, the simplified braking model excludes rolling resistance. It does, however, include aerodynamic forces as shown in Equation H.6 [74]

$$D_{Min} = \frac{m}{C_d \cdot A_S \cdot \rho_{air}} \cdot \ln\left(1 + \frac{\frac{1}{2} \cdot C_d \cdot A \cdot \rho_{air}}{\mu \cdot m \cdot g} \cdot v_0^2\right) \qquad \text{Equation (H.6)}$$

D_{Min}: Minimum vehicle braking distance from initial velocity (m)

m: Vehicle test mass (kg) (Curb Mass + 80.6 kg; one 75 kg driver and 10 lb measuring equipment

C_d: Vehicle drag coefficient

A_S: Vehicle frontal surface area (m^2) ≈ 0.84 x W103 x H100

ρ_{Air}: Density of air at 20° C (= 1.225 kg/m^3)

μ: Coefficient of friction between tires and ground

g: Acceleration due to gravity (= 9.81 m/sec^2)

V_0: Initial vehicle velocity (m/sec). For 60 mph this is 26.82 m / sec.

If aerodynamice forces are ignored, the calculation is simplified as shown in Equation H.7 [74] .

$$D_{Min} = \frac{v_0^2}{2 \cdot \mu \cdot g}$$ Equation (H.7)

Driver reaction time is not included in the results in this work. If reaction time were included, the total stopping distance is shown in Equation (H.8).

$$D_{Tot} = D_{Min} + D_R = D_{Min} + v_0 \cdot t_R$$ Equation (H.8)

D_{Tot}: Total stopping distance (m)

D_{Min}: Minimum stopping distance (m)

D_R: Reaction time distance (m)

v_0: Initial vehicle velocity (m/sec)

t_R: Reaction time (sec)

As with vehicle acceleration time, one of the greatest sources of variation is the value assigned for the coefficient of friction. This value is difficult to find in literature for a given tire model.

Appendix I
Maximum Velocity Modeling and Relations

The forces acting on a vehicle at maximum velocity are shown in Figure I.1 [54, 74].

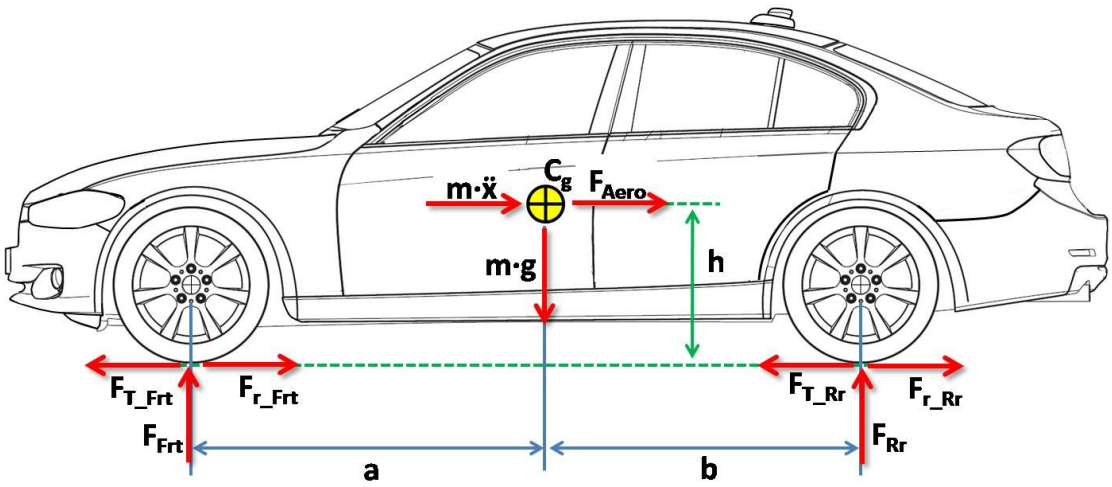

Figure I.1 Vehicle Loads at Maximum Velocity [54, 74]

$m \bullet \ddot{x}$: Force exerted by acceleration/decleration of vehicle mass (N)

$m \bullet g$: Downward force due to gravitational acceleration of vehicle mass (N)

C_g: Vehicle center of gravity location

F_{Aero}: The resisting force due to movement of the vehicle through air (N)

h: Vehicle C_g height above ground (m)

F_{T_Frt}: Traction force exerted through the front wheels (N)

F_{r_Frt}: Rolling resistance between the front tires and ground (N)

F_{Frt}: The downward force on the front wheels due to vehicle mass and gravity (N)

a: Longitudinal distance from front wheel center to C_g

b: Longitudinal distance from C_g to rear wheel center

F_{T_Rr}: Traction force exerted through rear wheels (N)

F_{r_Rr}: Rolling resistance between the rear tires and ground (N)

F_{Rr}: The downward force on the rear wheels due to vehicle mass and gravity (N)

At constant velocity, the force m•ẍ = 0. For a given engine power P at maximum velocity (not electronically speed-limited), the power will be equal to the resisting force multiplied by the velocity as shown in Equation (I.1) [54, 74].

$$P_{Eng} = (F_{Aero} + F_{RR}) \cdot v_{Max} \qquad \text{Equation (I.1)}$$

P_{Eng}: Engine power (kW)

F_{Aero}: Aerodynamic resistance force (N)

F_{RR}: Total vehicle rolling resistance force (N)

v_{Max}: Maximum vehicle velocity (m/sec)

Including the parameters of each force results in Equation (I.2) [54, 74].

$$P_{Eng} = \left(\frac{1}{2} \cdot A_S \cdot \rho_{Air} \cdot C_d \cdot v_{Max}^2 + F_r \cdot m \cdot g\right) \cdot v_{Max} \qquad \text{Equation (I.2)}$$

A_S: Vehicle frontal surface area (m^2)

ρ_{Air}: Density of air at 20°C (= 1.225 kg/m^3)

C_d: Vehicle drag coefficient

v_{Max}: Maximum vehicle velocity (m/sec)

m: Vehicle test mass (kg) (Curb Mass + 80.6 kg; one 75 kg driver and 10 lb measuring equipment

g: Acceleration due to gravity (= 9.81 m/sec^2)

This can be simplified into a cubic equation which can be solved for velocity as shown in Equation (I.3) [74] .

$$\frac{A_S \cdot \rho_{Air} \cdot C_d}{2} \cdot v_{Max}^3 + F_r \cdot m \cdot g \cdot v_{Max} - P_{Eng} = 0 \qquad \text{Equation (I.3)}$$

Note that this assumes that 100% of engine power reaches the wheels; in practice there are driveline inefficiencies / losses.

Appendix J
Vehicle Center of Gravity and Front Weight Distribution Modeling

The relationships between vehicle center of gravity (C_g) location and front / rear weight distribution are shown in diagram J.1 [54].

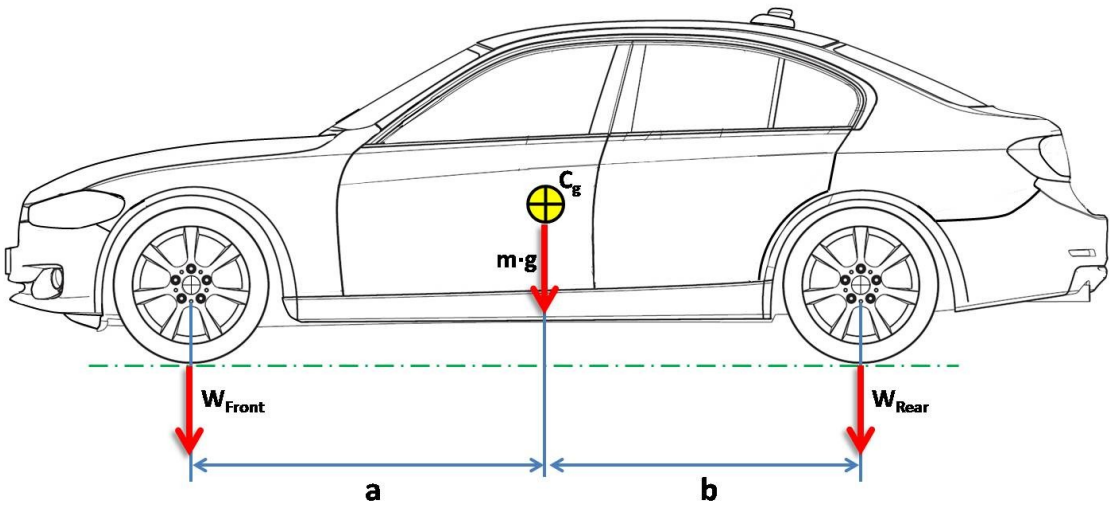

Figure J.1 Relationship between Cg Location and Front/Rear Weight Distribution [54].

a: Longitudinal distance from front wheel center (FWC) to C_g (m)

b: Longitudinal distance from C_g to rear wheel center (RWC) (m)

m·g: Vehicle weight due to gravitational acceleration (N)

Additional longitudinal parameters related to length are shown in Figure J.2 [1, 54]. Several of these parameters will are used to describe the location of specific vehicle subsystems. Figure J.1 dimensions "a" and "b" add up to equal vehicle wheelbase L101.

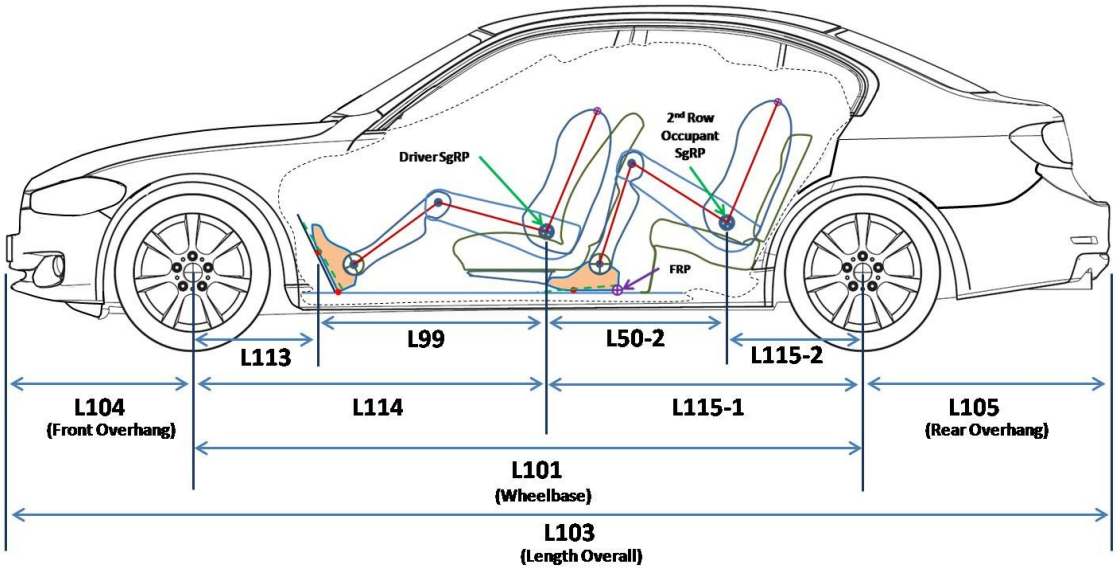

Figure J.2 Vehicle Longitudinal Parameters [1, 54]

Using moments about the wheel centers, the relation for front weight distribution is shown in Equation (J.1) [74]

$$W_{Frt} = \frac{b}{a+b} \cdot (m \cdot g) = \frac{b}{L101} \cdot (m \cdot g) \qquad \text{Equation (J.1)}$$

The corresponding relation for rear weight distribution is shown in Equation (J.2) [74].

$$W_{Rr} = \frac{a}{a+b} \cdot (m \cdot g) = \frac{a}{L101} \cdot (m \cdot g) \qquad \text{Equation (J.2)}$$

If the mass of *n* vehicle subsystems is known, the longitudinal coordinate x_{Cg} of the vehicle can be expressed as shown in Equation (J.3).

$$x_{Cg} = \frac{1}{m_{total}} \cdot \sum_{i=1}^{n} m_i \cdot x_i \qquad \text{Equation (J.3)}$$

x_{Cg}: X-coordinate of vehicle center of gravity (C_g) (m)

m_{total}: Total vehicle mass (kg)

n: Number of vehicle subsystems contributing to total vehicle mass (kg)

m_i: Mass of the i-th subsystem (kg)

x_i: X-coordinate of the i-th subsystem center of gravity

Mass estimation of vehicle subsystems is covered in Appendix F. The mass of hybrid vehicle batteries and motors is covered in Appendix G. While the center of mass for a few subsystems such as the engine and motor may be approximated easily, the mass center for others such as the Body in White, interior, uncategorized, etc. are not intuitive; nor are there readily available sources in public literature for these locations.

Benchmarking of several vehicles was performed as part of the validation portion of this work (Chapter 6, Appendix). While the vehicle front and rear weight distribution are available for each vehicle, subsystem C_g location was not found.

In order to find the key subsystem locations, an optimization analysis was conducted to find the "optimal" location of each major subsystem C_g as a proportion of key length parameters such as wheelbase [54].

The Cg x-coordinates of 9 non-hybrid parameters were established as the design variables in a genetic algorithm (NSGAII) optimization and the difference between actual and optimized front weight distribution fraction used as the functional objective value for each iteration:

$$Norm_i = Actual\ D_{Frt_i} - Calculated\ D_{Frt_i}$$ Equation (J.4)

D_{Frti}: Front weight distribution (WFrt / [m·g]) fractional value for i^{th} validation vehicle

The sums of the squares of the norm for each validation vehicle becomes the functional value for that vehicle for each optimization iteration.

$$Fval_j = \sum_{i=1}^{n} Norm_i{}^2$$ Equation (J.5)

$Fval_j$: The functional value for the j^{th} member of the final generation of points in the genetic algrorithm analysis.

$Norm_i$: The norm of the i^{th} vehicle comparison as shown in Equation (J.3) for one point in the final generation of the analysis.

n: Number of comparisons to separate validation vehicles (number of norms generated) in each point evaluation in the last generation of the genetic algorithm analysis.

The method in which the norms and functional value for each point is defined should result in a convex function in the objective space as shown in Figure J.3 [54]. This along with the definition of the functional value at each point lends itself to using the distance method in selecting a "better" point from the candidate points in the final generation of the genetic algorithm optimization analysis. The Tchebycheff method can also be used for this purpose, but in this case the "distance" of each point is already calculated. Note that the definition of the norm and functional value permit any of the

objectives to have an ideal value of 0.0 (but typically not all objectives at the same time). As a result, the distance can be taken from the origin (0,0,0,0,0,0) of the objective axes [53].

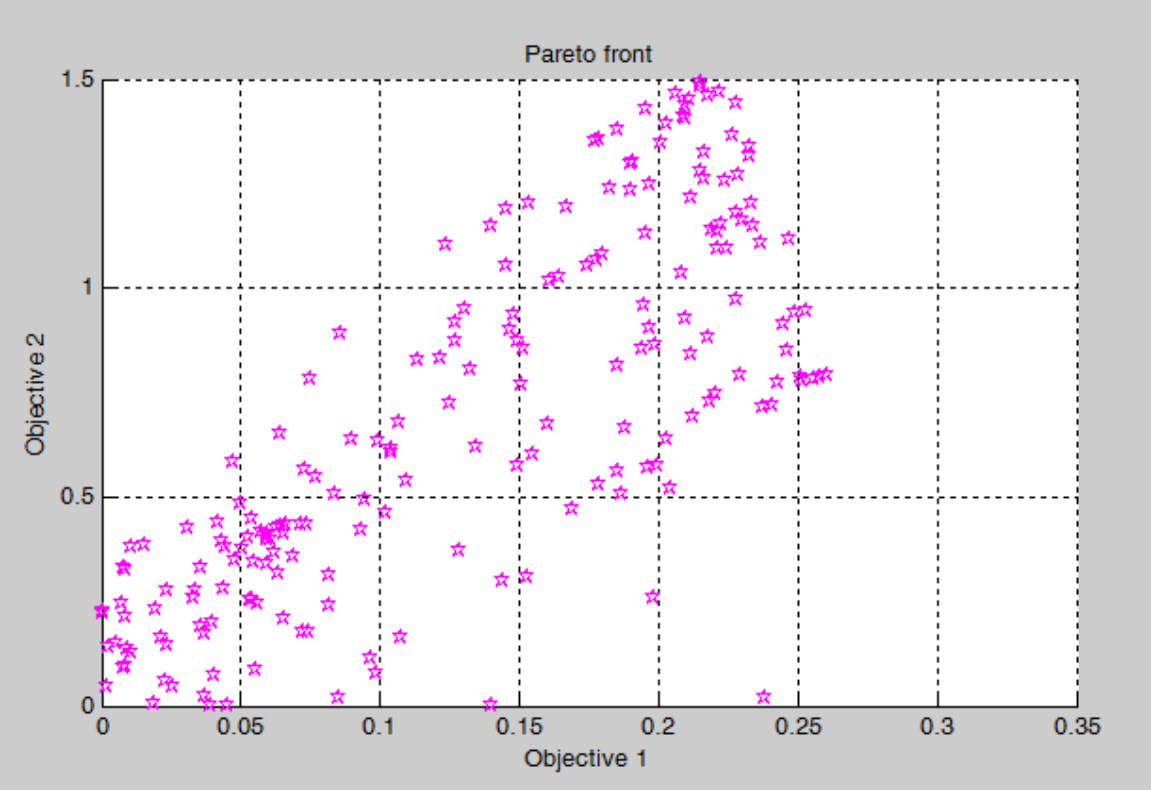

Figure J.3 Pareto Front from One Generation of Genetic Algorithm Optimization with 200 Points per Generation [54]

For the optimization of the subsystem locations, 7 subsystem masses are used:

- Body in White
- Interior
- Suspension
- Engine
- Driveline (including transmission and prop shaft if applicable)

•Uncategorized

• Closures (doors, hood, decklid/liftgate)

Nine subsystem C_g locations are included as design variables. Note that not all are used for each vehicle (due to driveline configuration--FWD/RWD/AWD). These are:

• X(1): BiW C_g location as a fraction of L103 rearward from front of vehicle

• X(2): Interior C_g location as a fraction of L101 rearward from Front Wheel Center (FWC)

• X(3): Suspension C_g location as a fraction of L101 rearward from FWC

• X(4): Engine C_g location as a fraction of engine length forward from rear of engine (EL2 in Figure L.4)

• X(5): Uncategorized C_g location as a fraction of L101 rearward from FWC

• X(6): Closure C_g location as a fraction of L101 rearward from FWC

• X(7): Rear of engine forward from Ball of Foot Reference Point (distance in meters) (LBE1 in Figure L.4)

• X(8): RWD driveline C_g location as a fraction of L101 rearward from FWC

• X(9): FWD driveline C_g location as a fraction of L101 from FWC

No all-wheel-drive sample vehicles were available in the validation vehicle sample. Otherwise, AWD driveline C_g location as a fraction of L101 from FWC can also be included as a design variable in the optimization.

5 separate genetic analysis optimization runs were conducted. The starting point of the design variables (initial guess of location variables), the "better" point selected and the maximum / minimum value of each in the 5 runs is shown in Table J.1 [54].

Design Variable	Starting Value	Fraction of Parameter:	"Better" Point Value	Minimum Value of 5 Runs	MaximumValue of 5 Runs
X(1)	0.55	L103	0.45	0.45	0.45
X(2)	0.40	L101	0.42	0.36	0.50
X(3)	0.45	L101	0.49	0.41	0.49
X(4) (EL2)	0.52	L101	0.50	0.47	0.60
X(5)	0.42	L101	0.53	0.44	0.53
X(6)	0.40	L101	0.56	0.47	0.64
X(7) (LBE-1)	0.150	meter	0.200	0.160	0.200
X(8)	0.50	L101	0.52	0.48	0.79
X(9)	0.05	L101	0.13	0.07	0.13

Table J.1 Optimization Results for Subsystem Cg Location [54]

As seen in Table 6.4, this method provides a reasonable method for estimating subsystem C_g locations. More accurate estimation should be possible with a larger population of vehicle samples which can be separated into specific vehicle types and size classes when developing optimized subsystem C_g locations for each specific vehicle class. Parameters locating the engine Cg based from the Ball of Foot Reference Point (BOFRP) are shown in Figure J.4.

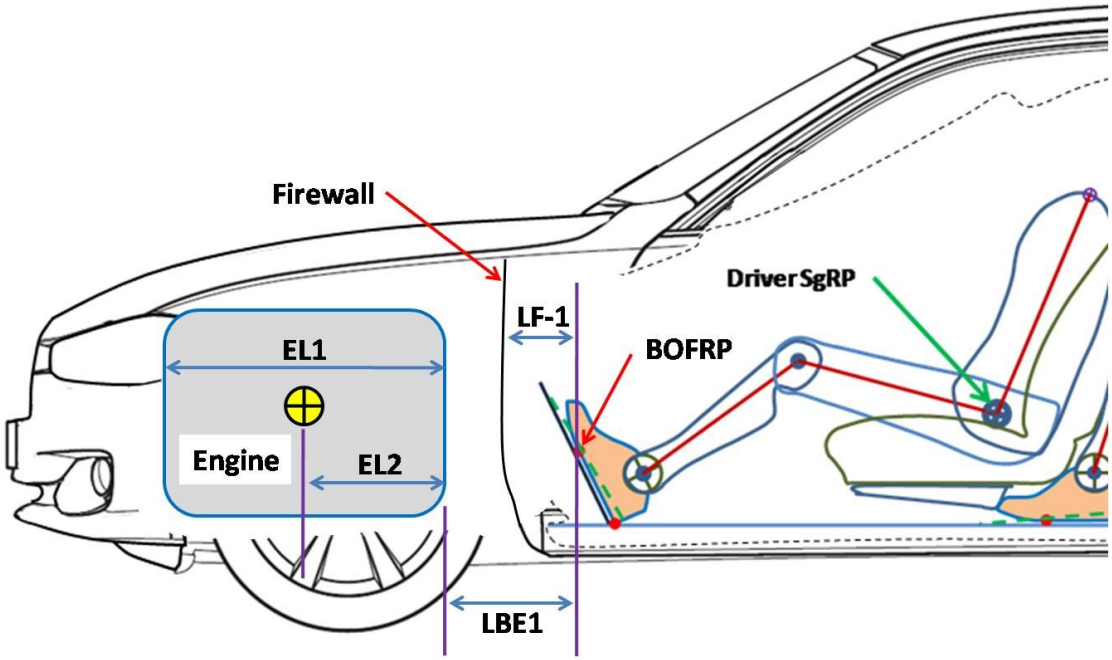

Figure J.4 Engine Cg Location Parameters from Ball of Foot Reference Point [54]

Appendix K
Vehicle Constraints

This appendix discusses constraints encountered in designing and optimizing passenger vehicles. Many of the constraints are due to regulatory requirements and/or definitions. Others are driven by vehicle dimensional and functional relationships. These constraints will be discussed in dimensional and functional groupings.

Vehicle Mass

Maximum vehicle mass/weight rating is one parameter used to define the class of passenger vehicles as defined in U.S. 49 CFR Part 523 [61]:

Passenger Automobile: any vehicle intended for use by up to 10 passengers and with a Gross Vehicle Weight Rating (GVWR) of 6,000 lb / 2722 kg or less [61]. GVWR is defined as vehicle curb mass plus the mass of all passengers plus the mass of all vehicle cargo.

As a consequence of this definition, the maximum number of passengers must be equal or less than 10, providing a second passenger vehicle constraint.

Length Constraints

The U.S. Federal limit on overall vehicle length (L103) is 45 feet (13.72 m) [61]. This is an extreme limit which will not be realized in most passenger vehicle designs. Passenger vehicle maximum mass (GWVR) is more likely to set maximum limits on vehicle length in conjunction with W103 and H100. An alternative approach in design and optimization is to establish a user-defined limit on overall vehicle length L103.

Front overhang L104 must be less than or equal to the sum of the front tire radius plus the front tire wheelhouse longitudinal clearance plus the front bumper rail length.

Similarly, the rear overhang L105 must be less than or equal to the sum of the rear tire radius plus the rear wheelhouse longitudinal tire clearance plus the rear bumper rail length.

Width Constraints

A typical width maximum of 80 inches / 2.032 meters is often quoted for passenger vehicles. Under federal law, the maximum vehicle width without mirrors W103 can be greater than 2.032 meters; the lighting systems requirements, however, change for vehicles wider than 80 inches so that this has become a de facto standard for standard passenger vehicle width [61].

Some U.S. states such as California permit municipalities to restrict passenger vehicle width to 96 inches / 2.438 meters. Texas has a width limit of 96 inches / 2.438 meters as well. In the U.S., the maximum commercial vehicle width is 102 inches / 2.591 meters [61]. Additionally, tires may not project beyond outside vehicle fenders.

For occupant comfort, an UMTRI study recommends that occupant seat width be at least 0.5 meters wide at each seating position [55]. If this is used as a seating requirement, it will impose a minimum width constraint on vehicle shoulder room values (W3-1 first row, W3-2 second row) depending on the designed number of seating positions across each row of the vehicle. For vehicles with 3-across row seating, the center occupant position seat width is often less than that of the outside positions. For bench seats, SAE J1100 defines the minimum width of a designated seating position as 0.300 meters [1].

Height Constraints

U.S. passenger vehicle maximum height is 162 inches / 4.114 meters. This value is unlikely to be attained by most (if any) passenger vehicle designs. It is rare for most passenger vehicles to exceed 2 meters in height. Additionally, the U.S. definition of a passenger car is that the frontal surface area (A_s) does not exceed 45 ft^2 [61].

For ground clearance, the Australian Vehicle Standards Rules (Reg 73) require that the minimum vehicle clearance at the midpoint between the front and rear wheel centers must be greater than or equal to one-thirtieth (1/30) of the wheelbase distance [80].

U.S. standards for vehicle breakover angles were rescinded [62]. SAE automotive standards prescribe a minimum 9-degree approach and departure angle [62].

Vehicle Size Class Constraints

EPA vehicle size class definitions provide a minimum and maximum interior volume for vehicles constained to fit within one of these classes. Standard vehicle size classes are defined by interior volume IV1 (Passenger Volume plus Cargo Volume V1) [73]:

- Large Vehicles: 120 ft^3 (3398 liters) ≤ IV1
- Midsize Vehicles: 110 ft^3 (3115 liters) ≤ IV1 < 120 ft^3 (3398 liters)
- Compact Vehicles: 100 ft^3 (2832 liters) ≤ IV1 < 110 ft^3 (3115 liters)
- Subcompact Vehicles: 85 ft^3 (2407 liters) ≤ IV1 < 100 ft^3 (2832 liters)
- Midsize Vehicles: IV1 <85 ft^3 (2407 liters)

2-Seater vehicles have no size class definitions

Vehicles classified as wagons by the EPA utilize the following size classes based on IV1 (Passenger Volume plus Cargo Volume V2) [73]:

- Large Wagon: 160 ft^3 (4531 liters) ≤ IV1
- Medium Wagon: 130 ft^3 (3681 liters) ≤ IV1 < 160 ft^3 (4531 liters)
- Small Wagon: IV1 < 130 ft^3 (3681 liters)

All other vehicles are classified by vehicle weight (GVWR) []:

- Standard Pickup: 6,000 lb to 8,500 lb.
- Small Pickup: Less than 6,000 lb.
- Passenger Van: Less than 10,000 lb.
- Minivan (MPV): Less than 10,000 lb.
- Sport Utility Vehicle (SUV): Less than 10,000 lb.
- Special Purpose Vehicle: Less than 8,500 lb.

Efficiency Constraints

EPA (or other) fuel economy measures may serve as a constraint. Vehicles sold in the U.S. which do not meet EPA fuel economy targets may face an imposed fine for each noncompliant vehicle sold. It is possible that at a future point in time noncompliant vehicles will not be permitted to be sold in the U.S. From 2012 onward, the EPA defines vehicle fuel economy targets based on vehicle footprint. These targets are outlined in Appendix .

Additional Constraints

In general, nearly all dimensional parameters must have positive values (with a few exceptions such as ΔS in computing first to second row coupling). Dimensional

parameters which can have a negative value are noted where they are initially defined in this work. Similarly, most functional values (such as peak engine power and peak torque) must have positive values except where noted.

Appendix L
Scenario Builder Validation Data

Compiled Results for All Vehicles

The data shown below shows additional Scenario Builder results beyond those discussed in Chapter 6. Results for EPA urban (UDDS) driving cycle mileage vs. actual values are shown in Table L.1. As expected, most scenario-generated results show a higher mileage than the actual. The Mercedes E350W showed conflicting values for drag coefficient (C_d) ranging from 0.24 to 0.28; this may explain some of the variation from other results. While the maximum difference is 11.2% for the Cadillac XTS, the difference in predicted vs. actual performance is less than 2 miles per gallon.

Vehicle	Scenario Value (mpg)	Actual Value (mpg)	Difference (mpg)	% Difference
2007 BMW 328i	**21.8**	**21.0**	**0.8**	**3.8**
2014 Mercedes CLS550	**19.8**	**18.0**	**1.8**	**10.0**
2014 Mercedes E350	**20.9**	**21.0**	**-0.1**	**-0.5**
2013 Chrysler 300	**19.8**	**19.0**	**0.8**	**4.2**
2013 Cadillac XTS	**18.9**	**17.0**	**1.9**	**11.2**
2007 Ford Crown Victoria	**18.3**	**17.0**	**1.3**	**7.6**
Average Difference (Absolute Value for Each Vehicle)				**6**
Standard Deviation				**4.1**

Table L.1 Scenario Validation vs. Actual EPA UDDS Mileage Results

EPA highway (FWFET) driving cycle scenario vs. actual results are shown in Table L.2. The maximum difference between predicted and actual mileage is 3.1 mpg for the Mercedes CLS550.

Vehicle	Scenario Value (mpg)	Actual Value (mpg)	Difference (mpg)	% Difference
2007 BMW 328i	**32.0**	**30.0**	**2.0**	**6.7**
2014 Mercedes CLS550	**30.3**	**27.0**	**3.3**	**12.2**
2014 Mercedes E350	**32.6**	**31.0**	**1.6**	**5.2**
2013 Chrysler 300	**29.0**	**31.0**	**-2.0**	**-6.5**
2013 Cadillac XTS	**28.9**	**28.0**	**0.9**	**3.2**
2007 Ford Crown Victoria	**26.4**	**25.0**	**1.4**	**5.6**
Average Difference (Absolute Value for Each Vehicle)				**7**
Standard Deviation				**3.0**

Table L.2 Scenario Validation vs. Actual EPA FWFET Mileage Results

Predicted vs. actual total internal volume (IV1) is shown in Table L.3. This is the sum of total vehicle passenger and cargo volume. As the occupant dimensions are well defined using standard manikins, it is expected that the greatest variation in estimated vs. actual internal volume will be due to the cargo volume (V1) estimation relations. This appears to be the case in light of the results for first row passenger volume index (PV1) shown in Table L.4 and for second row passenger volume (PV2) shown in Table L.5.

Vehicle	EPA Size Class	Scenario Value (ft^3)	Actual Value (ft^3)	Difference (ft^3)	% Difference
2007 BMW 328i	Compact	107	105	2	1.8
2014 Mercedes CLS550	Compact	109	108	1	1.0
2014 Mercedes E350	Midsize	115	113	2	1.4
2013 Chrysler 300	Large	124	123	1	1.1
2013 Cadillac XTS	Large	124	124	0	0.2
2007 Ford Crown Victoria	Large	128	130	-2	-1.2
Average Difference (Absolute Value for Each Vehicle)					1.1
Standard Deviation (%)					0.5

Table L.3 Scenario Validation vs. Actual Vehicle Total Internal Volume (IV1)

Vehicle	Scenario Value (ft^3)	Actual Value (ft^3)	Difference (ft^3)	% Difference
2007 BMW 328i	52.1	51.2	0.9	1.8
2014 Mercedes CLS550	51.8	51.3	0.5	1.0
2014 Mercedes E350	53.9	52.4	1.5	2.9
2013 Chrysler 300	56.4	55.5	0.9	1.6
2013 Cadillac XTS	57.4	56.6	0.8	1.4
2007 Ford Crown Victoria	59.1	58.8	0.3	0.5
Average Difference (Absolute Value for Each Vehicle)				2
Standard Deviation (%)				0.8

Table L.4 Scenario Builder vs. Actual First Row Passenger Volume Index (PV1)

Vehicle	Scenario Value (ft^3)	Actual Value (ft^3)	Difference (ft^3)	% Difference
2007 BMW 328i	41.6	41.9	-0.3	-0.7
2014 Mercedes CLS550	41.6	41.3	0.3	0.7
2014 Mercedes E350	45.4	45.0	0.4	0.9
2013 Chrysler 300	51.9	50.8	1.1	2.2
2013 Cadillac XTS	49.5	49.3	0.2	0.4
2007 Ford Crown Victoria	49.3	50.2	-0.9	-1.8
Average Difference (Absolute Value for Each Vehicle)				1
Standard Deviation (%)				0.7

Table L.5 Scenario Builder vs. Actual Second Row Passenger Volume Index (PV2)

Estimated vs. actual engine torque is shown in Table N.6.

Vehicle	Scenario Value (Nm)	Actual Value (Nm)	Difference (Nm)	% Difference
2007 BMW 328i	281	271	10	4
2014 Mercedes CLS550	504	443	61	14
2014 Mercedes E350	378	370	8	2
2013 Chrysler 300	378	370	8	2
2013 Cadillac XTS	378	358	20	6
2007 Ford Crown Victoria	294	381	-87	-23
Average Difference (Absolute Value for Each Vehicle)				8
Standard Deviation (%)				8

Table L.6 Scenario Builder vs. Actual Peak Engine Torque

Driver legroom (L34) is one of the inputs (along with W3-1 and H61-1) to the first row passenger volume index (PV1). Estimated vs. actual values are shown in Table L.7.

Vehicle	Scenario Value (m)	Actual Value (m)	Difference (m)	% Difference
2007 BMW 328i	**1.063**	**1.054**	**0.009**	**0.85**
2014 Mercedes CLS550	**1.070**	**1.069**	**0.001**	**0.09**
2014 Mercedes E350	**1.054**	**1.049**	**0.005**	**0.48**
2013 Chrysler 300	**1.063**	**1.062**	**0.001**	**0.09**
2013 Cadillac XTS	**1.072**	**1.069**	**0.003**	**0.28**
2007 Ford Crown Victoria	**1.080**	**1.080**	**0.000**	**0.00**
Average Difference (Absolute Value for Each Vehicle)				**0.30**
Standard Deviation (%)				**0.67**

Table L.7 Scenario Builder vs. Actual Driver Legroom (L34)

As the results in Table L.7 show, it is possible to estimate L34 to a high degree of accuracy if seat height (H30-1) and shoe plane angle (A47) are known.

Driver headroom (H61-1) estimated vs. actual values are shown in Table L.8. Second row estimated vs. actual headroom (H61-2) values are shown in Table L.9. As with driver legroom, these results show the high level of correspondence between the estimated and actual occupant-based dimensional measures.

Vehicle	Scenario Value (m)	Actual Value (m)	Difference (m)	% Difference
2007 BMW 328i	0.985	0.978	0.007	0.72
2014 Mercedes CLS550	0.944	0.937	0.007	0.75
2014 Mercedes E350	0.985	0.963	0.022	2.28
2013 Chrysler 300	0.994	0.980	0.014	1.43
2013 Cadillac XTS	1.028	1.019	0.009	0.88
2007 Ford Crown Victoria	1.003	0.990	0.013	1.31
Average Difference (Absolute Value for Each Vehicle)				1.23
Standard Deviation(%)				0.60

Table L.8. Scenario Builder vs. Actual Driver Headroom (H61-1)

Vehicle	Scenario Value (m)	Actual Value (m)	Difference (m)	% Difference
2007 BMW 328i	0.965	0.963	0.002	0.21
2014 Mercedes CLS550	0.928	0.917	0.011	1.20
2014 Mercedes E350	0.965	0.970	-0.005	-0.52
2013 Chrysler 300	0.976	0.963	0.013	1.35
2013 Cadillac XTS	0.956	0.960	-0.004	-0.42
2007 Ford Crown Victoria	0.954	0.963	-0.009	-0.93
Average Difference (Absolute Value for Each Vehicle)				0.77
Standard Deviation (%)				0.46

Table L.9 Scenario Builder vs. Actual Second Row Passenger Headroom (H61-2)

Outside vehicle dimensions L103 (overall length), W103 (maximum outside width) and H100 (body height) are shown in Table L.10, Table L.11 and Table L.12, respectively. These results show that the overall vehicle dimensions resulting from the summ of the component parameters can also be determined with accuracy. This strengthens the validation of the models which form the foundation of both the Scenario Builder and Optimization modules.

Vehicle	Scenario Value (meter)	Actual Value (meter)	Difference (meter)	% Difference
2007 BMW 328i	**4.557**	**4.526**	**0.031**	**0.68**
2014 Mercedes CLS550	**4.980**	**4.940**	**0.040**	**0.81**
2014 Mercedes E350	**4.881**	**4.879**	**0.002**	**0.04**
2013 Chrysler 300	**5.063**	**5.044**	**0.019**	**0.38**
2013 Cadillac XTS	**5.167**	**5.131**	**0.036**	**0.70**
2007 Ford Crown Victoria	**5.387**	**5.385**	**0.002**	**0.04**
Average Difference (Absolute Value for Each Vehicle)				**0.44**
Standard Deviation				**0.34**

Table L.10 Scenario Builder vs. Actual Vehicle Overall Length (L103)

Vehicle	Scenario Value (m)	Actual Value (m)	Difference (m)	% Difference
2007 BMW 328i	1.817	1.816	0.001	0.06
2014 Mercedes CLS550	1.890	1.882	0.008	0.43
2014 Mercedes E350	1.855	1.854	0.001	0.05
2013 Chrysler 300	1.907	1.905	0.002	0.10
2013 Cadillac XTS	1.863	1.852	0.011	0.59
2007 Ford Crown Victoria	1.964	1.963	0.001	0.05
Average Difference (Absolute Value for Each Vehicle)				0.21
Standard Deviation (%)				0.24

Table L.11 Scenario Builder vs. Actual Maximum Vehicle Width (W103)

Vehicle	Scenario Value (m)	Actual Value (m)	Difference (m)	% Difference
2007 BMW 328i	1.417	1.420	-0.003	-0.21
2014 Mercedes CLS550	1.406	1.417	-0.011	-0.78
2014 Mercedes E350	1.478	1.477	0.001	0.07
2013 Chrysler 300	1.471	1.483	-0.012	-0.81
2013 Cadillac XTS	1.501	1.501	0.000	0.00
2007 Ford Crown Victoria	1.460	1.443	0.017	1.18
Average Difference (Absolute Value for Each Vehicle)				0.51
Standard Deviation				0.48

Table L.12 Scenario Builder vs. Actual Vehicle Body Height (H100)

Additional Parameter Values by Individual Vehicle

Additional parameter values for the 2007 BMW 328i sedan are shown in Table L.13. Values for the 2014 Mercedes CLS550 sedan are show in Table L.14. Values for the Mercedes E350 sedan are shown in Table L.15. Values for the 2013 Chrysler 300 sedan are shown in Table L.16. Values for the 2013 Cadillac XTS sedan are shown in Table L.17. Values for the 2007 Ford Crown Victoria sedan are shown in Table L.18.

Parameter	Scenario Result	Actual Vehicle	Difference	Units	% Difference
Mcurb	1510	1533	-23	kg	-1.5
Mengine	169.3	163.0	6.3	kg	3.9
Mtransmission	62.0	76.0	24.5	kg	-18.4
IV1	107	105	2	ft^3	1.8
PV	93.7	93.1	0.6	ft^3	0.6
PV1	52.1	51.2	0.9	ft^3	1.8
PV2	41.6	41.9	-0.3	ft^3	-0.7
L34	1.063	1.054	0.009	m	0.9
L51-2	0.878	0.879	-0.001	m	-0.1
W3-1	1.409	1.407	0.002	m	0.1
W3-2	1.391	1.400	-0.009	m	-0.6
H61-1	0.985	0.978	0.007	m	0.7
H61-2	0.965	0.963	0.002	m	0.2
W101	1.508			m	
W103	1.817	1.816	0.001	m	0.1
H30-2	0.279	0.279	0.000	m	0
L101	2.761	2.761	0.000	m	0
L103	4.566	4.526	0.040	m	0.9
L104	0.795	0.754	0.041	m	5.4
H100	1.417	1.420	-0.003	m	-0.2
Peak Engine Torque	281	271	10	Nm	3.7
Engine Length	0.752	0.751	0.001	m	0.1
Midrail Length	1.235			m	
Mgvwr		1994.90		kg	
Mbiw	296.00	285.00	11	kg	3.9
Mint	70.00	62.40	8	kg	12.2
Msusp	226.00	208.00	18	kg	8.7
Mdrv	127.00	82.30	45	kg	54.3
Muncat	540.00	568.00	-28	kg	-4.9
Mcls	82.00	82.00	0	kg	0

Table L.13 Individual Vehicle Parameters for 2007 BMW 328i Sedan

Parameter	Scenario Result	Actual Vehicle	Difference	Units	% Difference
Mcurb	1722	1815	-93	kg	-5.1
Mengine	210			kg	
Mtransmission	80			kg	
IV1	109	108	1	ft^3	1.0
PV	93.4	92.6	0.8	ft^3	0.9
PV1	51.8	51.3	0.5	ft^3	1.0
PV2	41.6	41.3	0.3	ft^3	0.7
L34	1.070	1.069	0.001	m	0.1
L51-2	0.886	0.889	-0.003	m	-0.3
W3-1	1.450	1.450	0.000	m	0.0
W3-2	1.431	1.435	-0.004	m	-0.3
H61-1	0.944	0.937	0.007	m	0.7
H61-2	0.928	0.917	0.011	m	1.2
W103	1.890	1.882	0.008	m	0.4
L101	2.875	2.875	0.000	m	0.0
L103	4.980	4.940	0.040	m	0.8
L104	0.940	0.900	0.040	m	4.4
H100	1.406	1.417	-0.011	m	-0.8
Peak Engine Torque	504	443	61	Nm	13.8
Engine Length	0.737			m	
Midrail Length	1.341			m	
Mgvwr		2495		kg	
Mbiw	333			kg	
Mint	76			kg	
Msusp	253			kg	
Mdrv	155			kg	
Muncat	607			kg	
Mcls	86			kg	

Table L.14 Individual Vehicle Parameters for 2014 Mercedes CLS550 Sedan

Parameter	Scenario Result	Actual Vehicle	Difference	Units	% Difference
Mcurb	1644	1712	-68	kg	-4.0
Mengine	135			kg	
Mtransmission	74			kg	
IV1	115.0	113.4	1.6	ft^3	1.4
PV	99.3	97.4	1.9	ft^3	2.0
PV1	53.9	52.4	1.5	ft^3	2.9
PV2	45.4	45.0	0.4	ft^3	0.9
L34	1.054	1.049	0.005	m	0.5
L51-2	0.917	0.909	0.008	m	0.9
W3-1	1.469	1.468	0.001	m	0.1
W3-2	1.450	1.445	0.005	m	0.3
H61-1	0.985	0.963	0.022	m	2.3
H61-2	0.965	0.970	-0.005	m	-0.5
W103	1.855	1.854	0.001	m	0.1
L101	2.875	2.875	0.000	m	0.0
L103	4.881	4.879	0.002	m	0.04
L104	0.857	0.855	0.002	m	0.2
H100	1.478	1.477	0.001	m	0.1
Peak Engine Torque	378	370	8	Nm	2.1
Engine Length	0.672			m	
Midrail Length	1.250			m	
Mgvwr		1994.90		kg	
Mbiw	337			kg	
Mint	78			kg	
Msusp	245			kg	
Mdrv	145			kg	
Muncat	614			kg	
Mcls	89			kg	

Table L.15 Individual Vehicle Parameters for 2014 Mercedes E350 Sedan

Parameter	Scenario Result	Actual Vehicle	Difference	Units	% Difference
Mcurb	1725	1828	-103	kg	-5.6
Mengine	131			kg	
Mtransmission	77	87	-10	kg	-11.5
IV1	124	123	1	ft^3	1.1
PV	108.30	106.30	2.0	ft^3	1.9
PV1	56.40	55.50	0.9	ft^3	1.6
PV2	51.90	50.80	1.1	ft^3	2.2
L34	1.063	1.062	0.001	m	0.1
L51-2	1.008	1.019	-0.011	m	-1.1
W3-1	1.513	1.511	0.002	m	0.1
W3-2	1.493	1.466	0.027	m	1.8
H61-1	0.994	0.980	0.014	m	1.4
H61-2	0.976	0.963	0.013	m	1.3
W101	1.616			m	
W103	1.907	1.905	0.002	m	0.1
H30-2	0.322	0.322	0.000	m	0.0
L101	3.053	3.053	0.000	m	0.0
L103	5.063	5.044	0.019	m	0.4
L104	0.927	0.906	0.021	m	2.3
H100	1.471	1.483	-0.012	m	-0.8
Peak Engine Torque	378	370	8	Nm	2.1
Engine Length	0.672	0.503	0.169	m	33.6
Midrail Length	1.456			m	
Mgvwr		1994.90		kg	
Mbiw	358.00			kg	
Mint	85.00			kg	
Msusp	257.00			kg	
Mdrv	150.00			kg	
Muncat	652.00			kg	
Mcls	94.00			kg	

L.16 Individual Vehicle Parameters for 2013 Chrysler 300 Sedan

Parameter	Scenario Result	Actual Vehicle	Difference	Units	% Difference
Mcurb	1807	1817	-10	kg	-0.6
Mengine	135	157	-22	kg	-14.0
Mtransmission	109	102	7	kg	6.9
IV1	124	124	0	ft^3	0.2
PV	106.9	105.8	1.1	ft^3	1.0
PV1	57.4	56.6	0.8	ft^3	1.4
PV2	49.5	49.3	0.2	ft^3	0.4
L34	1.072	1.069	0.003	m	0.3
L51-2	1.009	1.016	-0.007	m	-0.7
W3-1	1.473	1.471	0.002	m	0.1
W3-2	1.454	1.430	0.024	m	1.7
H61-1	1.028	1.019	0.009	m	0.9
H61-2	0.956	0.960	-0.004	m	-0.4
W103	1.863	1.852	0.011	m	0.6
H30-2	0.312	0.312	0.000	m	0.0
L101	2.837	2.837	0.000	m	0.0
L103	5.167	5.131	0.036	m	0.70
L104	1.055	1.019	0.036	m	3.5
H100	1.501	1.501	0.000	m	0.0
Peak Engine Torque	378	358	20	Nm	5.6
Engine Length	0.672			m	
Midrail Length	1.276			m	
Mbiw	364			kg	
Mint	78			kg	
Msusp	268			kg	
Mdrv	205			kg	
Muncat	663			kg	
Mcls	93			kg	

Table L.17 Individual Vehicle Parameters for 2013 Cadillac XTS Sedan

Parameter	Scenario Result	Actual Vehicle	Difference	Units	% Difference
Mcurb	1802	1875	-73	kg	-3.9
Mengine	138			kg	
Mtransmission	58	77	-19	kg	-24.7
IV1	128	130	-2	ft^3	-1.2
PV	108.4	108.9	-0.5	ft^3	-0.5
PV1	59.1	58.8	0.3	ft^3	0.5
PV2	49.3	50.2	-0.9	ft^3	-1.8
L34	1.080	1.080	0.000	m	0.0
L51-2	0.961	0.963	-0.002	m	-0.2
W3-1	1.544	1.544	0.000	m	0.0
W3-2	1.524	1.532	-0.008	m	-0.5
H61-1	1.003	0.998	0.005	m	0.5
H61-2	0.954	0.963	-0.009	m	-0.9
W101	1.638			m	
W103	1.964	1.963	0.001	m	0.1
H30-2	0.327	0.327	0.000	m	0.0
L101	2.913	2.913	0.000	m	0.0
L103	5.387	5.385	0.002	m	0.0
L104	1.024	1.022	0.002	m	0.2
H100	1.460	1.443	0.017	m	1.2
Peak Engine Torque	294	381	-87	Nm	-22.8
Engine Length	0.655			m	
Midrail Length	1.412			m	
Mbiw	389			kg	
Mint	83			kg	
Msusp	266			kg	
Mdrv	122			kg	
Muncat	709			kg	
Mcls	95			kg	

Table L.18 Individual Vehicle Parameters for 2007 Ford Crown Victoria

Appendix M
Scenario Builder Input and Output Menus

A summary of the input and output menus for the Scenario Builder Module is shown in this appendix. Most of the menus are common between the Scenario Builder and Optimization modules. Differences occur where design variables in the Optimization module are input as fixed values in the Scenario Builder module. These differences will be shown in the following menus. The software framework opening menu is shown in Figure M.1. The program currently uses the working name of "CarOpt." This name is expected to change when the framework is put into production use by CU-ICAR design teams.

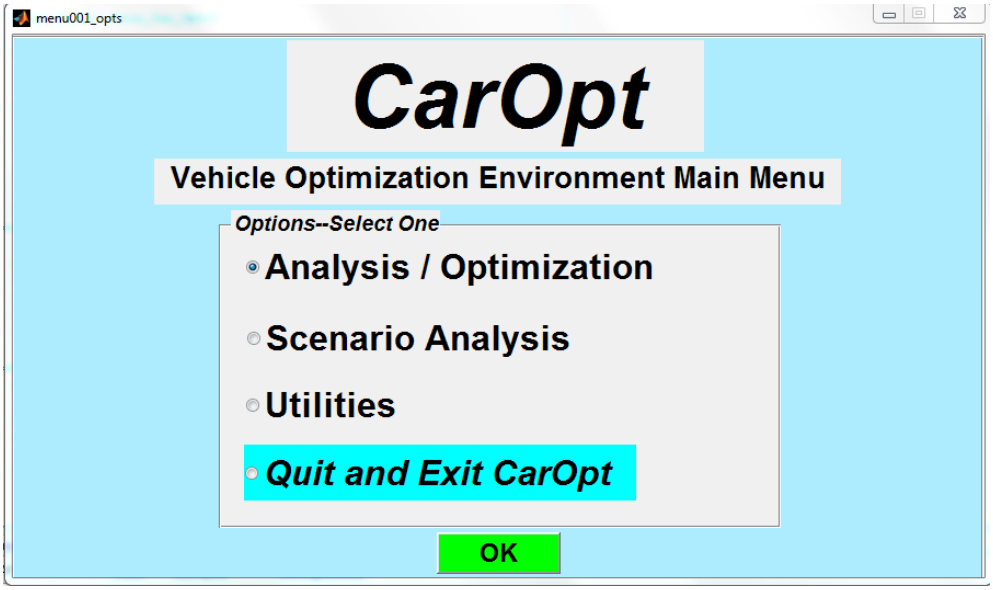

Figure M.1 Software Optimization Framework Opening Menu

When the "Scenario Analysis" option is selected, a Scenario Selection menu appears as shown in Figure M.2. Currently only one method is available -- other methods or variations are envisioned as future work.

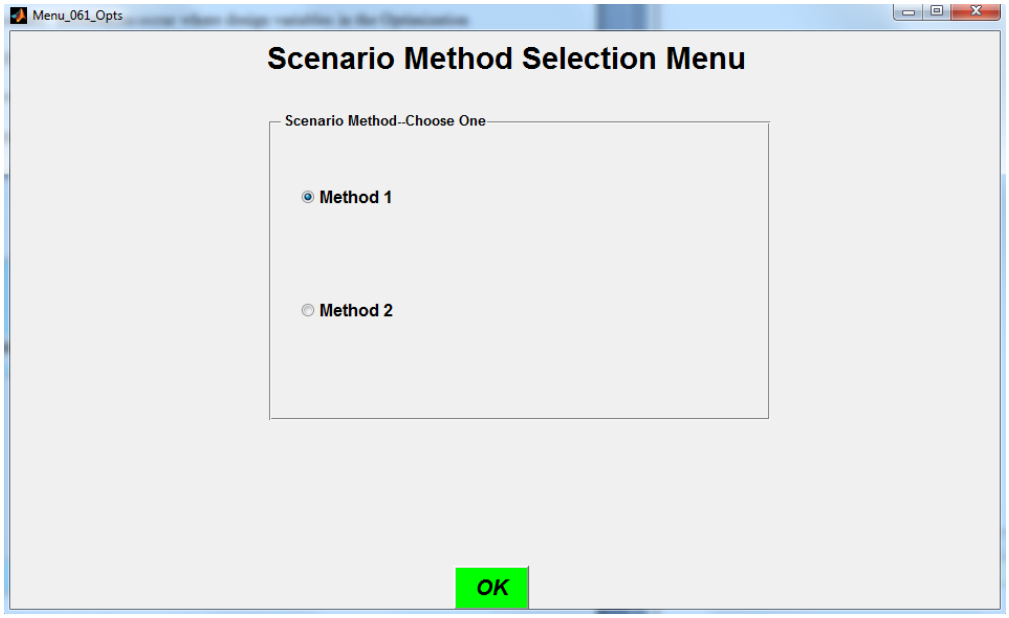

Figure M.2. Scenario Method Selection Menu

The Vehicle Configuration Menu is shown in Figure M.3. This menu is common to the Scenario Builder and Optimization modules

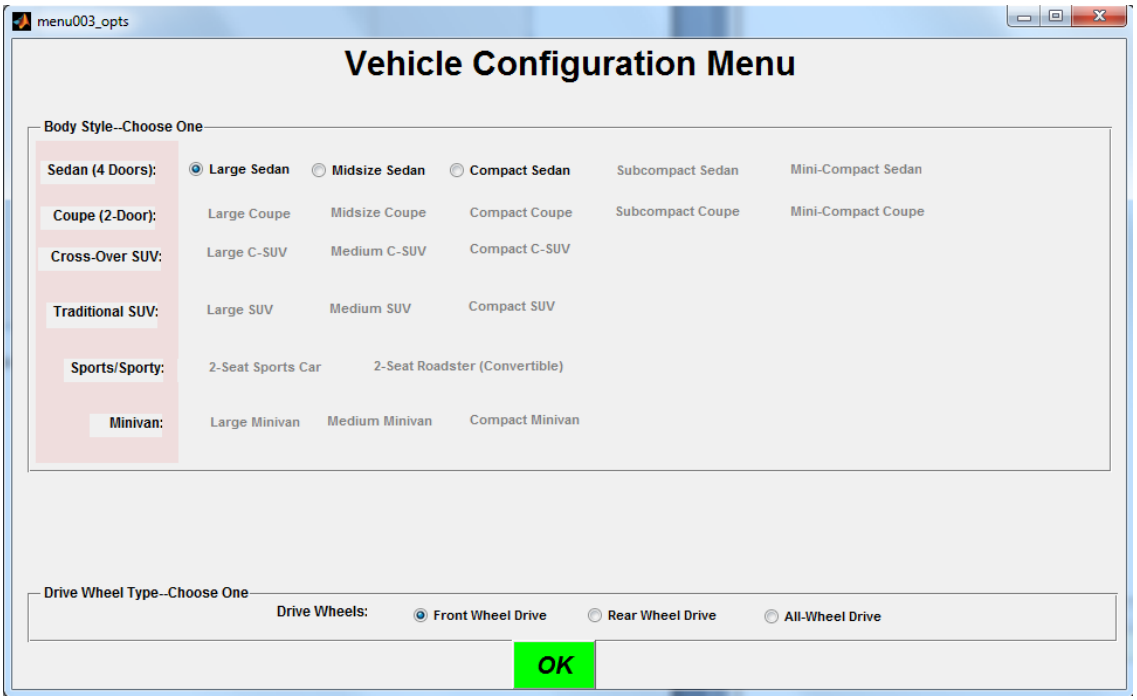

Figure M.3 Vehicle Configuration Menu

The configuration menu permits the selection of vehicle body style (vehicle class) and drive wheel configuration (front, rear or All-wheel drive). Currently only sedans are included, although a knowledge base has been assembled for other vehicle types which may be incorporated as future work.

The Occupant Seating Menu, shown in Figure P.4, is common to both modules. This is included to consider the impact of occupant seating on vehicle targets and paremters. The current use is to ensure a minimum vehicle shoulder room value for three-across seating (W3-1 / W3-2) based on UMTRI-recommended seat width values [55]. Other vehicle classes such as large MPV's (minivans) or sport utility vehicles may have multiple seating configurations which may affect occupant and seating mass distribution.

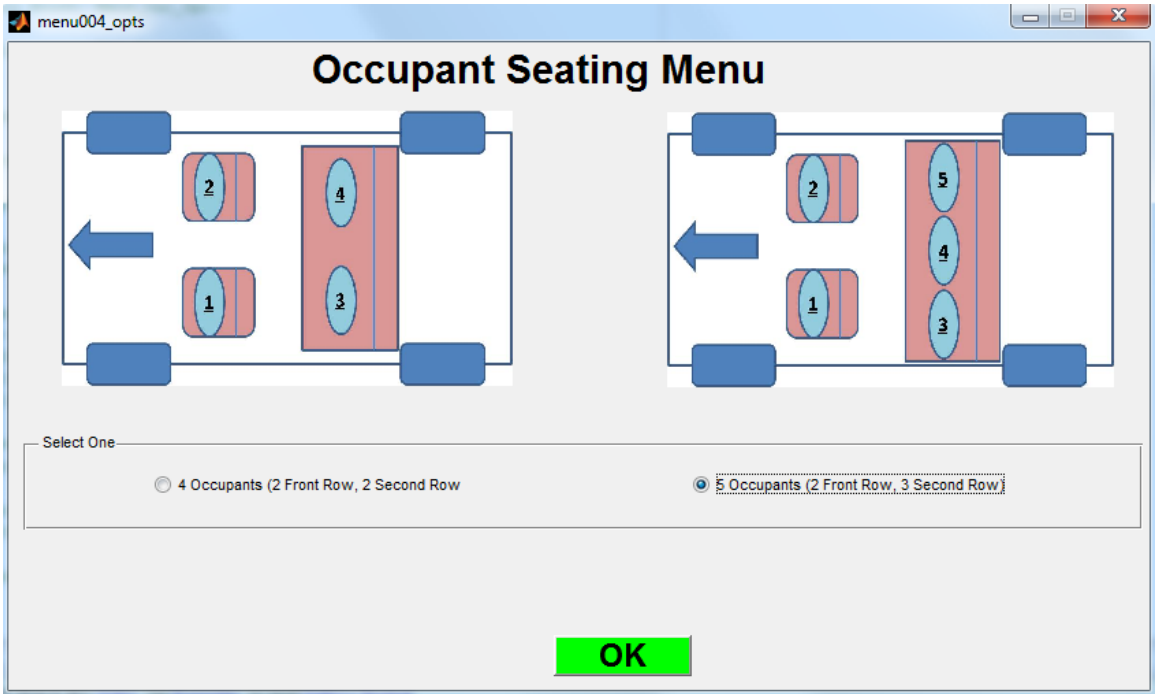

Figure M.4 Occupant Seating Menu

The Vehicle Material Selection Menu is shown in Figure M.5

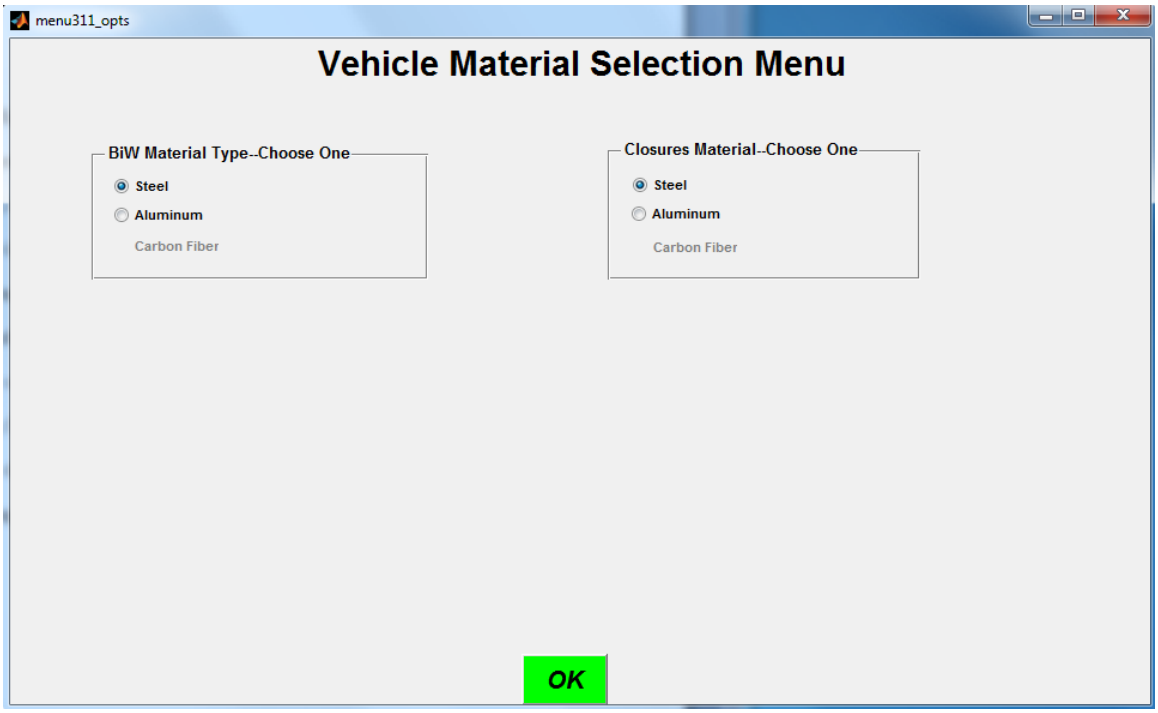

Figure M.5 Vehicle Material Selection Menu

Current options include steel and aluminum for the vehicle Body in White and closures. Composite materials can be added as material data becomes available. Other candidates for material selection options include suspension components and engine blocks, although iron engine blocks are already being superceded by aluminum blocks.

The Vehicle Constraints Update Menu shown in Figure M.6 is used by both modules. The minimum / maximum interior volume constraint is not active in the Scenario Builder as all parameters which determine total interior volume (IV1) are directly specified. If the ankle angle (A46-2) constraint is required to be equal or greater to the minimum comfort angle of 78 degrees, the value of first to second row coupling L50-2 is increased until the minimum angle is achieved.

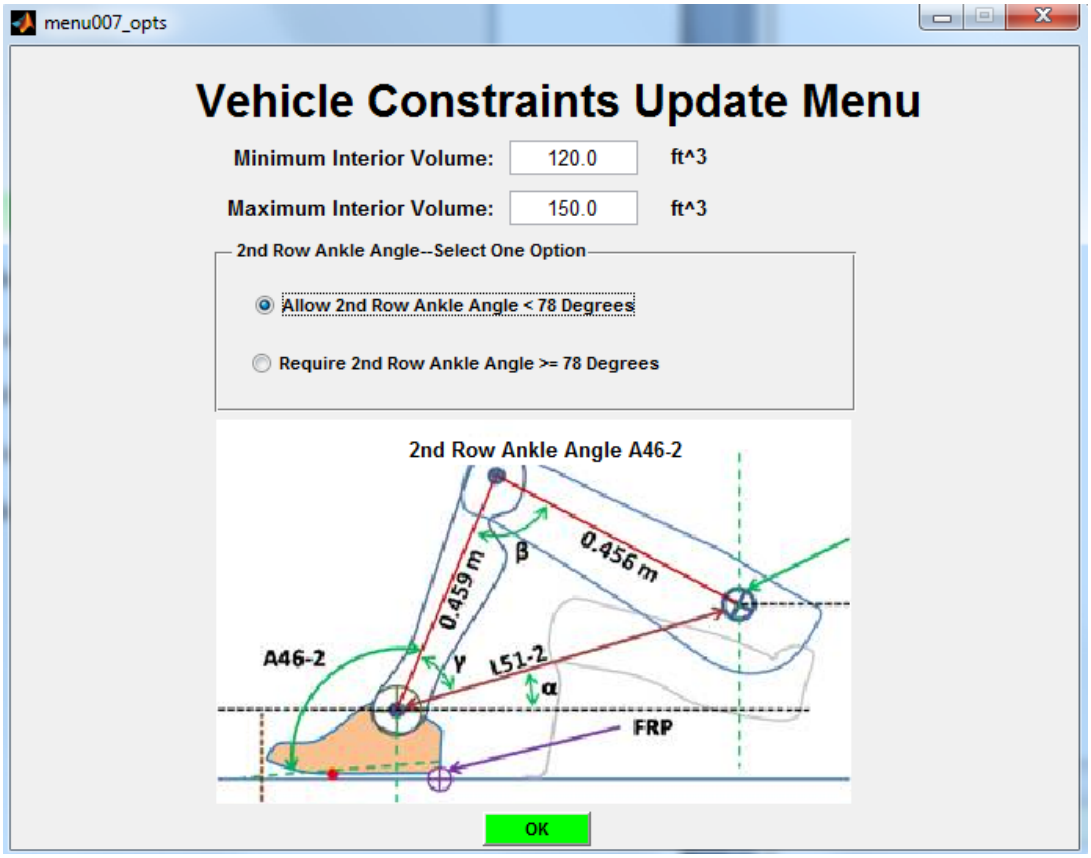

Figure M.6 Vehicle Constraints Update Menu

The Second Row Coupling Menu is shown in Figure M.7. This menu sets the first to second row coupling distance (L50-2) along with the first-to-second row offset which specificies the longtidunal distance between the first row SgRP and the front of the second row manikin shoe. Note that this parameter can be (and typically is) a negative value. These two parameters, combined with second row seat height H30-2, define the value for second row outside passenger legroom L51-2. They are also used to determine the type of coupling (short, standard or long) which affects the manner in which the second row manikin is positioned and legroom measured. Typical parameters by vehicle class are pre-entered in the menu input boxes; these parameters may be modified /

updated by the user typing in a new value.

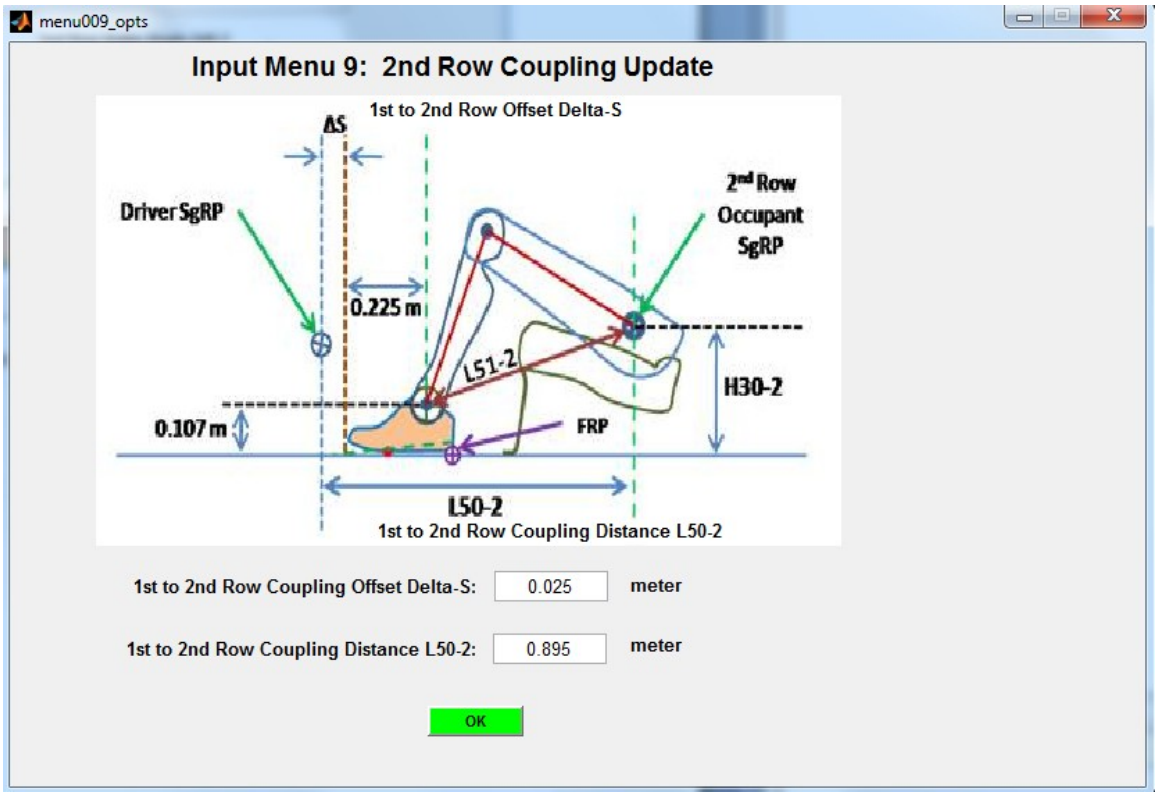

Figure M.7 Second Row Coupling Menu

The Width Parameter Input Menu is shown in Figure M.8. These values determine the front row shoulder room (W3-1), vehicle outside width at the driver SgRP W117 and resulting estimate of vehicle maximumm outside width (without mirrors) W103. All numeric values inside a black-bordered white data entry box may be updated by the user. The value for second row shoulder room is calculated through a correletion relationship to first row shoulder room.

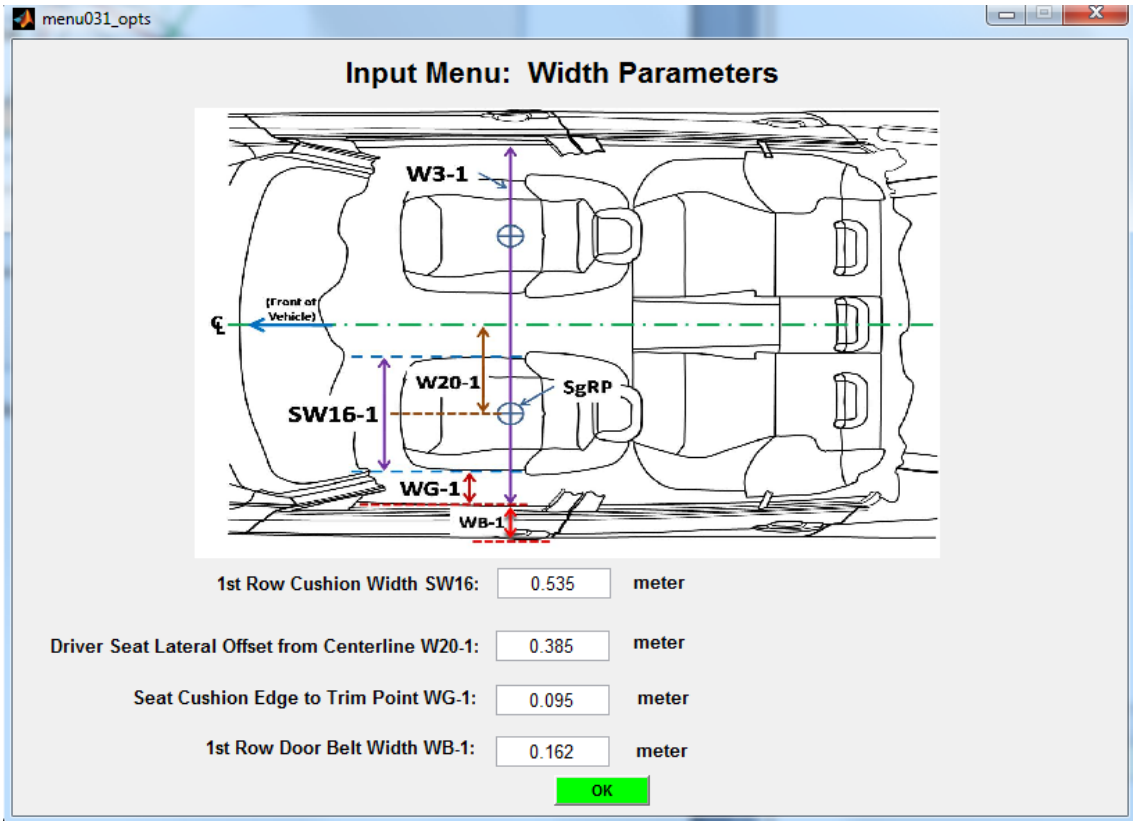

Figure M.8 Width Parameter Input Menu

The Height Parameter Input Menu is shown in Figure M.9. These values set a continuum of vehicle dimensions which define overall vehicle body height H100. The driver seat height H30-1 sets the value of longitudinal parameter L99-1 and resulting driver legroom L34. As previously discussed, H30-2 is used in calculating second row legroom L51-2. The torso angle A40 sets the height to the top of the driver headform; the vertical clearance to the headliner (HC1) along with headliner thickness H37 and roof panel thickness HR1 set the final vehicle body height.

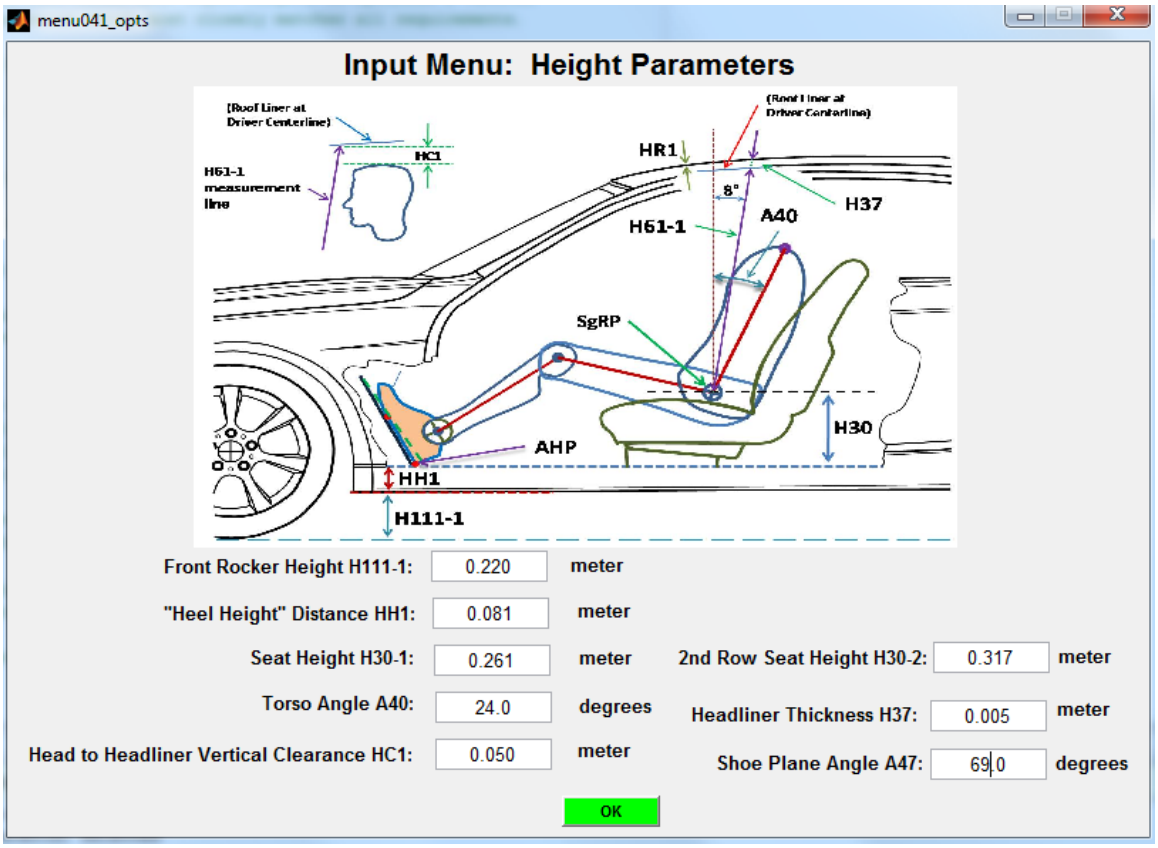

Figure M.9 Height Parameter Input Menu

The Engine Selection Menu for the Scenario Builder is shown in Figure M.10. In the scenario builder specific values are entered for engine power, motor power and battery capacity; in the Optimization module these are determined by optimization to relevant vehicle targets. The target maximum vehicle velocity is used in tire selection. While the vehicle maximum velocity may exceed this value, many current vehicles are electronically speed-limited; the maximum rated tire speed is one reason for this speed limitation. Engine types available include inline / V-type, gasoline or diesel, naturally aspirated / turbocharged and hybrid / non-hybrid combinations of these configurations.

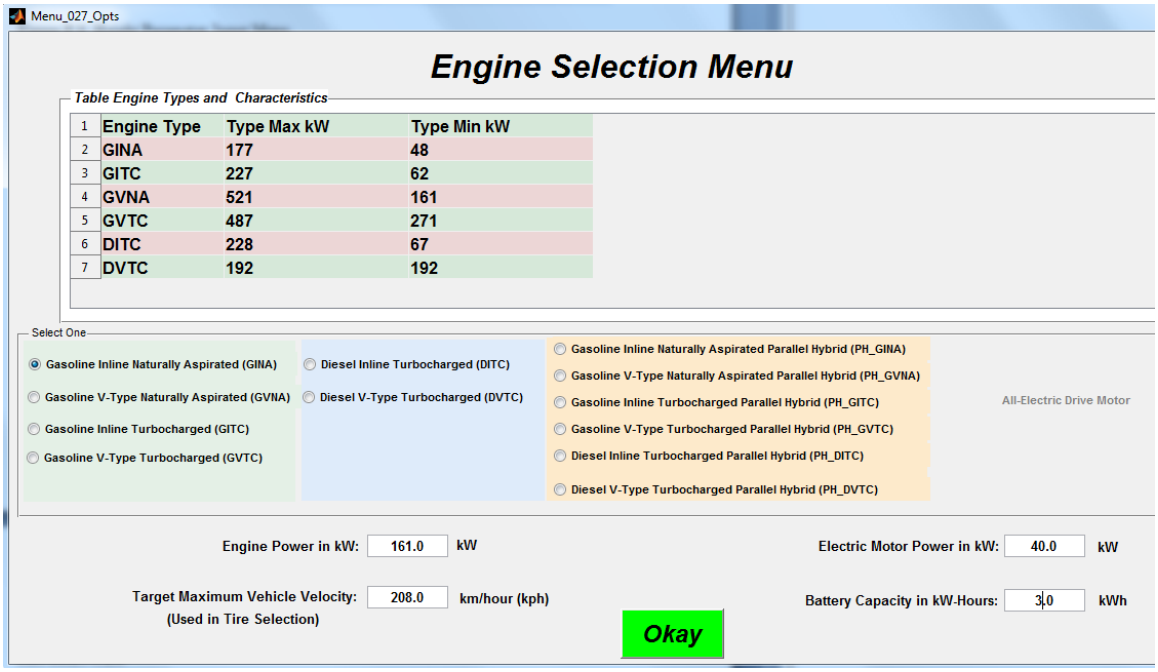

Figure M.10 Scenario Builder Engine Selection Menu

The Hybrid Battery Selection Menu is shown in Figure M.11. This only appears if a hybrid drivetrain configuration has been selected. This is used to select the hybrid battery type to be used and resulting battery mass and energy density. Lead acid batteries are not included due to their low energy density compared to Lithium and Nickel-metal Hydride battery options.

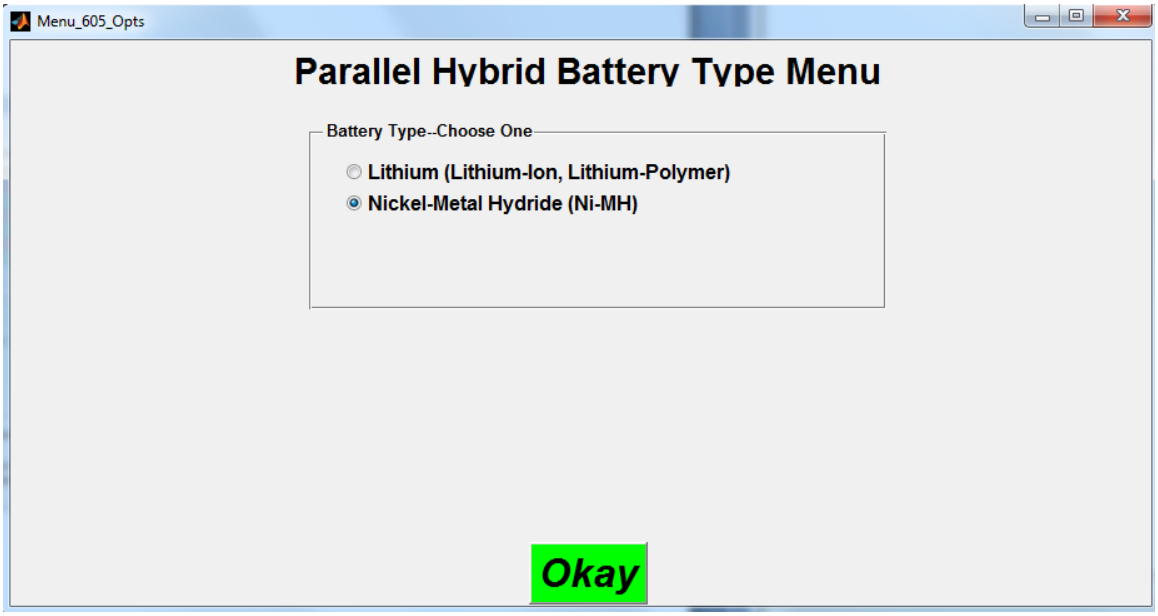

Figure M.11 Hybrid Battery Selection Menu

There are four Tire Selection Menus which are used by both the Scenario Builder and Optimization modules. The first menu, shown in Figure M.12, is used to select the wheel diameter (rim diameter) in inches. The tire speed and load ratings are calculated from target maximum vehicle velocity and gross vehicle weight rating (GVWR). In both modules the GVWR is estimated by correlations to calculated vehicle curb mass by vehicle type. All tire menu inputs consist of value selections from list box entries showing values commercially available for the selected vehicle and tire parameters.

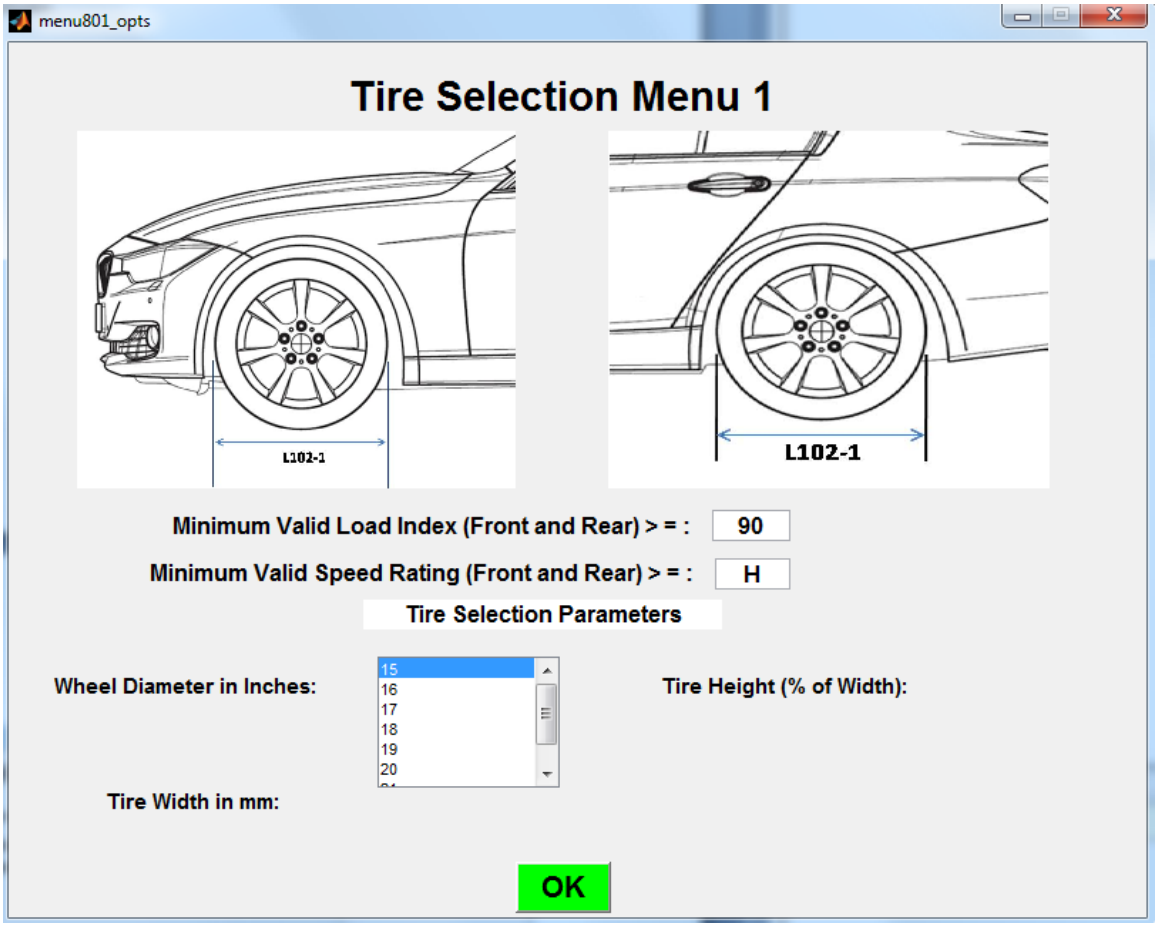

Figure M.12 Tire Selection Menu 1 (Wheel Diameter)

The second Tire Selection Menu is shown in Figure M.13. This is used to select the tire width in millimeters (the used of inch units for wheel diameter and millimeters for width follows standard U.S. industry practice). In both the Scenario Builder and Optimization modules, the tire width is used to calculate vehicle curb-to-curb (CTC) once the Outside Track turn radius is calculated as described in Appendix E.

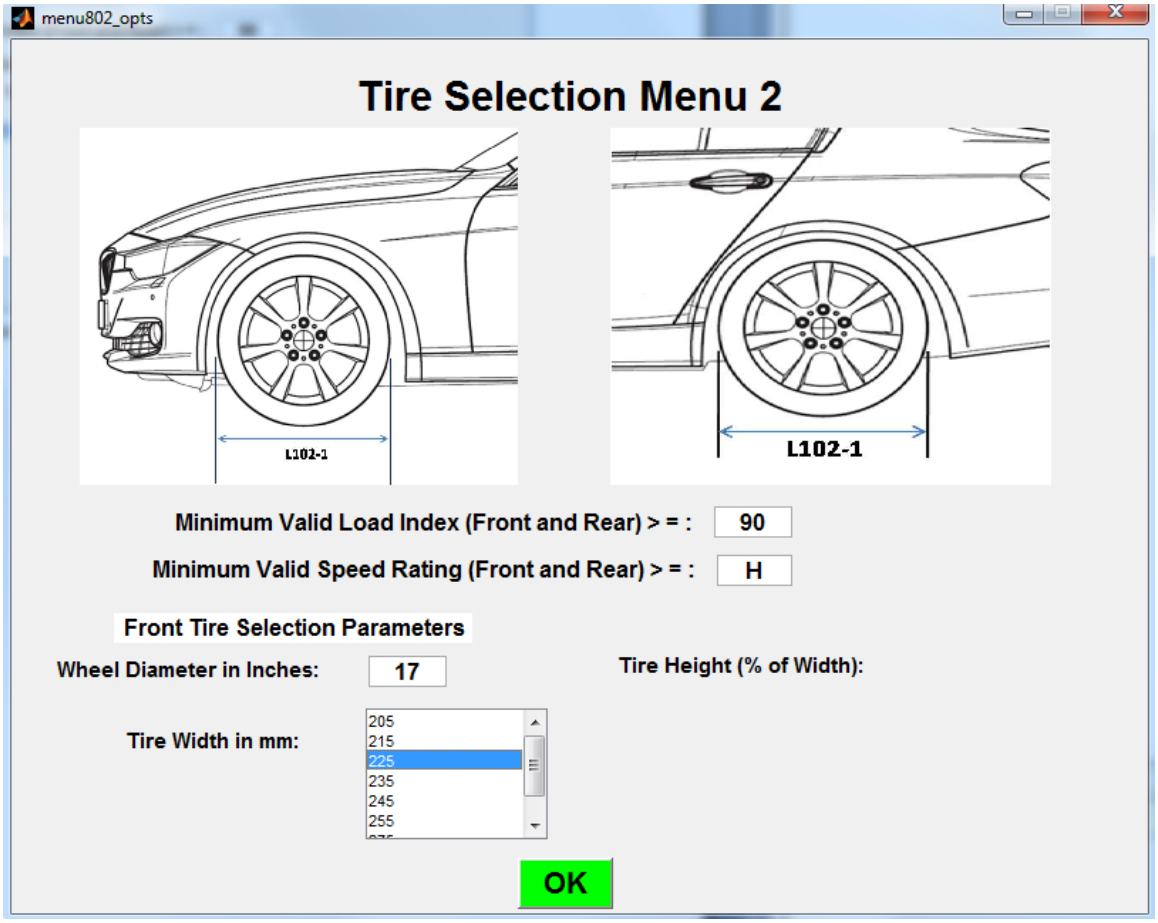

Figure M.13 Tire Selection Menu 2 (Tire Width)

The third Tire Selection Menu is shown in Figure M.14. This is used to select tire height as a percentage of tire width. Note the the number of available selection in successive tire menus tends to decrease as the selection tree narrows to a single combination choice.

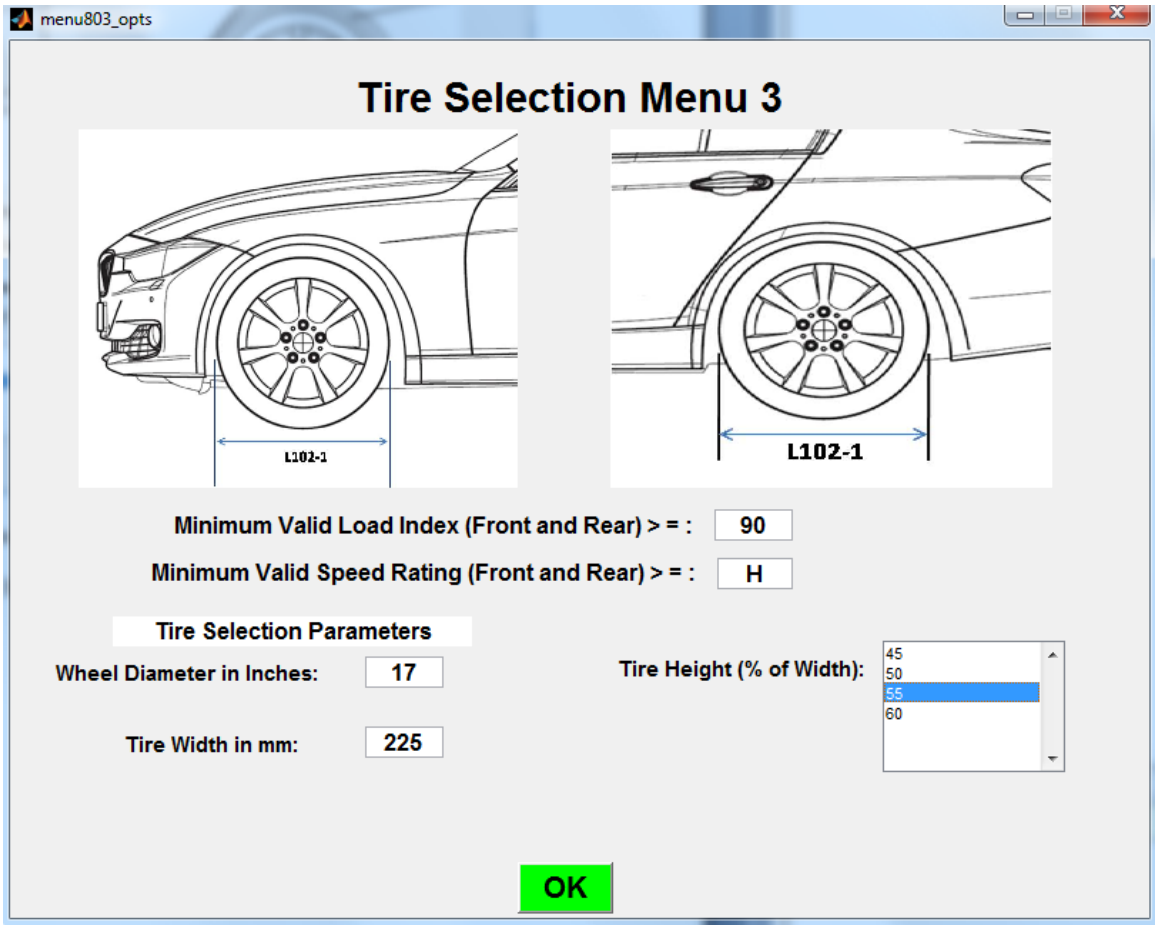

Figure M.14 Tire Selection Menu 3 (Tire Height)

Tire Selection Menu 4, shown in Figure M.15, provides a summary of the tire selection parameters along with uncompressed tire diameter L102. Note that the current tire selection method assumes that the front and rear tires are the same; some of the vehicles surveyed in this work (such as the 2014 Mercedes CLS550) had different front vs. rear tire diameter and width.

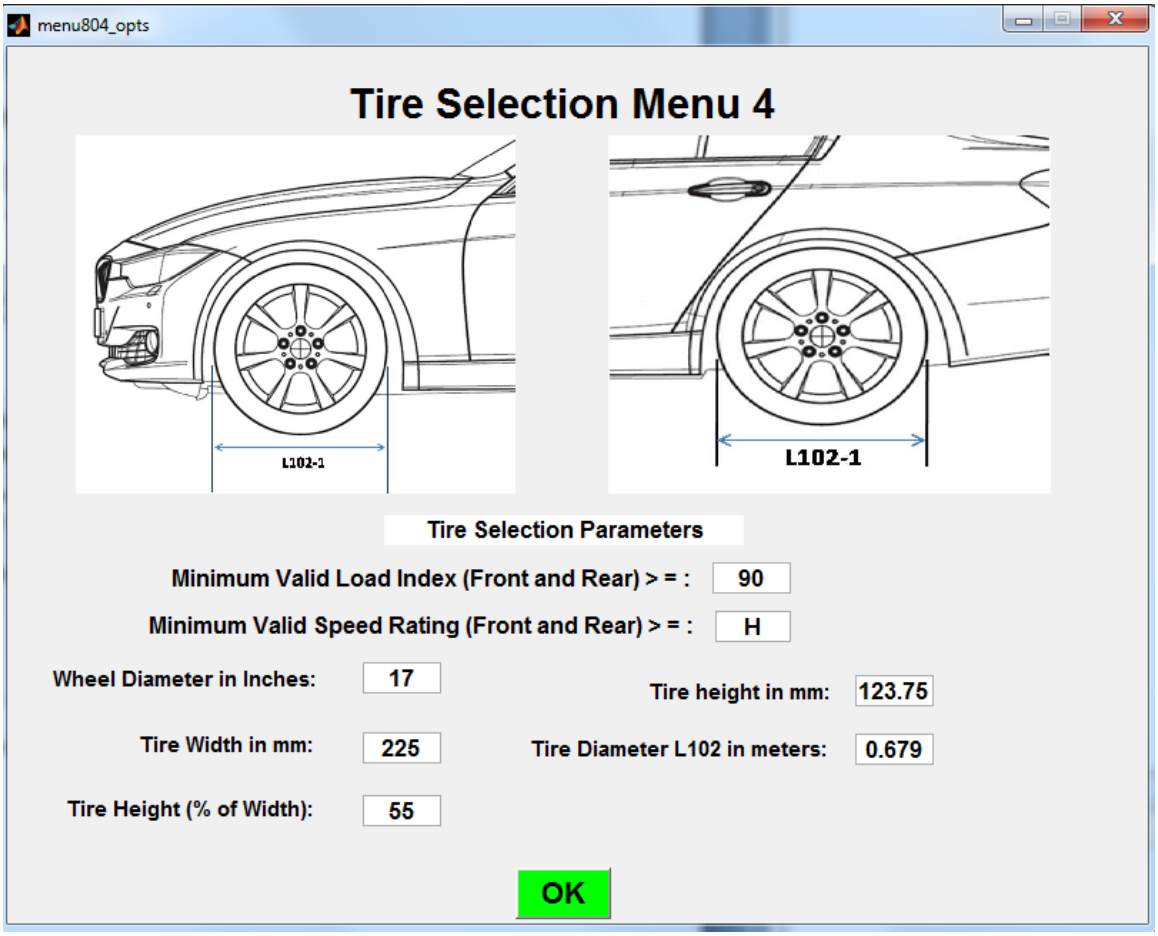

Figure M.15 Tire Selection Menu 4 (Tire Selection Summary)

The Longitudinal Dimensions and Midrail Crush Force Input Menu, shown in Figure M.16, is specific to the Scenario Builder Module; these parameters, along with engine power, are optimization design variables in the Optimization module. The values of L113, L115-2 and L105 affect overall vehicle length, mass and center of mass location. Rear overhang L105 and L115-2 are components of the cargo volume (V1) calculation along with rear shoulder room (W3-2). Front midrail crush force is used to determine front midrail length, frontal NCAP crash performance and front overhang length (L104).

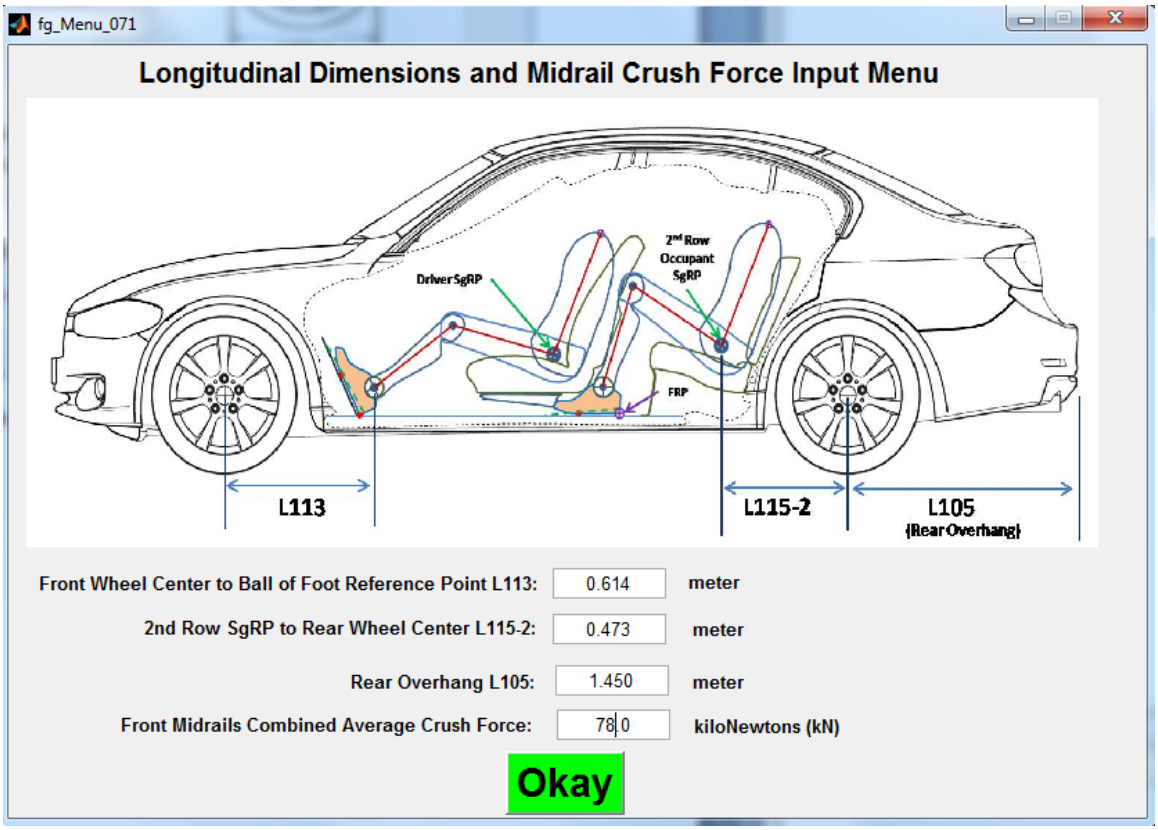

Figure M.16 Longitudinal Dimensions and Midrail Crush Force Input Menu

The Miscellaneous Input Menu is shown in Figure M.17. Vehicle inside steer wheel angle is used to calculate vehicle Outside Track (OT) turn radius. The drag coefficient and rolling resistance are used in calculating vehicle maximum velocity and fuel economy. The default value for maximum driveline torque is the sum of the vehicle peak internal combustion engine and electric motor torque (if a hybrid). This value can be modified to reflect that the actual transmission and driveline may be sized larger to reflect the fact that the vehicle may be designed for a range of engines and motors with different torque output. The maximum driveline torque determines the vehicle transmission and driveline mass. The friction coefficient is used in calculating vehicle acceleration times and braking distances. Average track width is estimated as a

correlation to maximum vehicle outside width W103; there is a logic check which prevents the tire width from extending beyond the vehicle outside width.

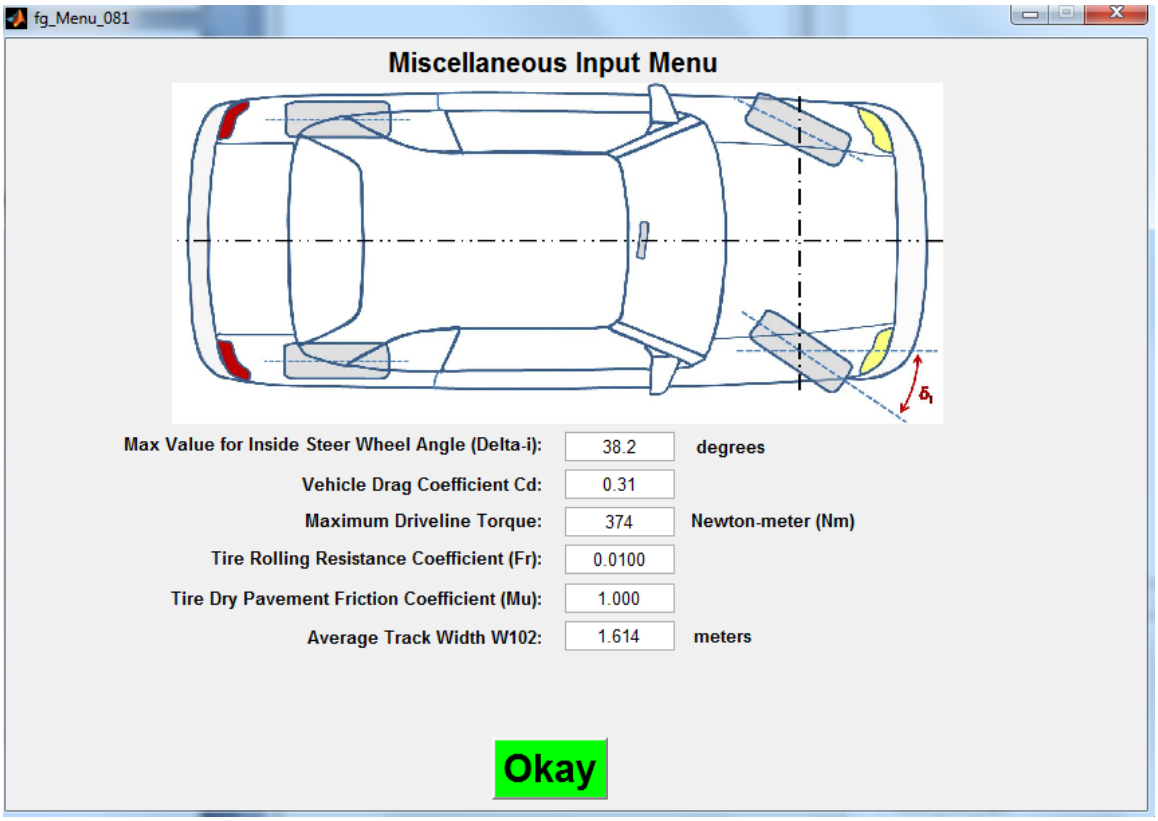

Figure M.17 Miscellaneous Input Menu

The Engine Position Input Menu is shown in Figure M.18. The engine distance parameters set engine location for center of gravity location calculation and distance between the engine and firewall for NCAP crash performance calculation. Firewall crush force and average firewall crush distance are also used in NCAP performance assessment. For the Scenario Builder Module, this is the last input menu.

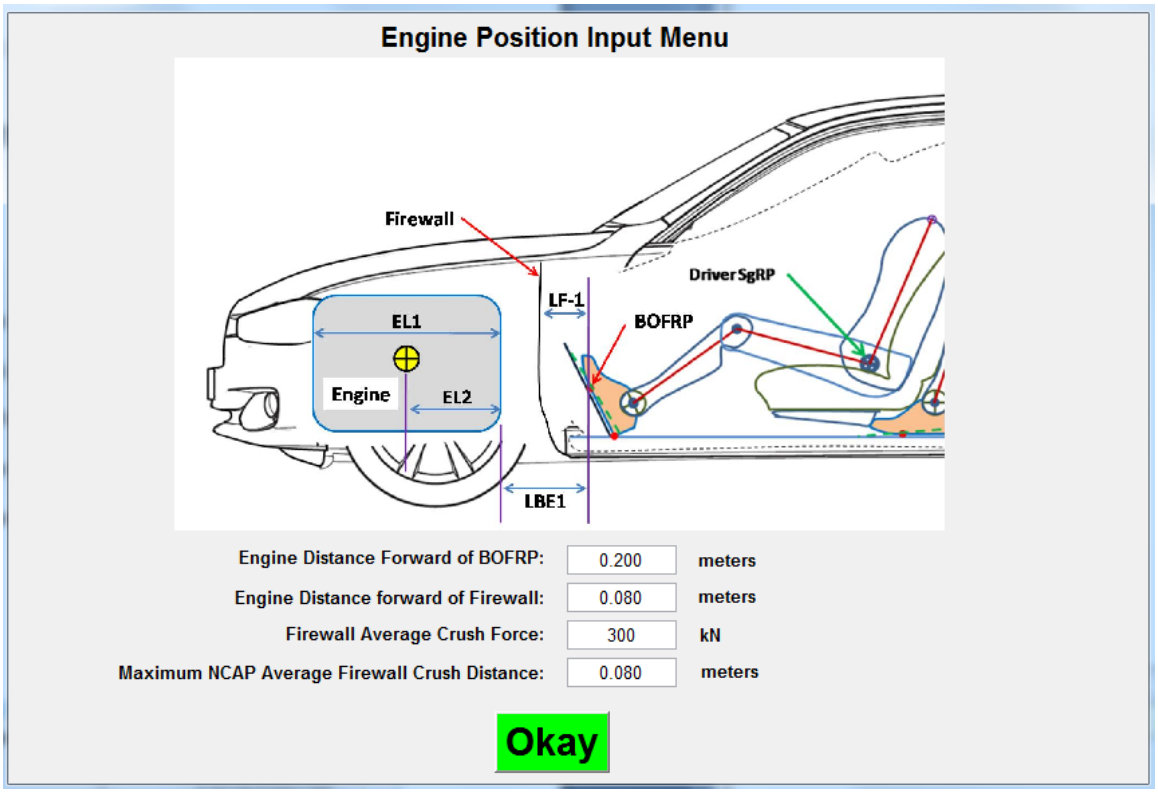

Figure M.18 Engine Position Input Menu

The Scenario Results menu is shown in Figure M.19 (this menu is common to the Scenario Builder and Optimization modules). The upper table shows vehicle performance target results for acceleration, braking, fuel economy, etc. The lower table shows assorted vehicle dimensional and functional resultant parameters of interest. This table provides a summary of the design inputs and outputs which define the vehicle design.

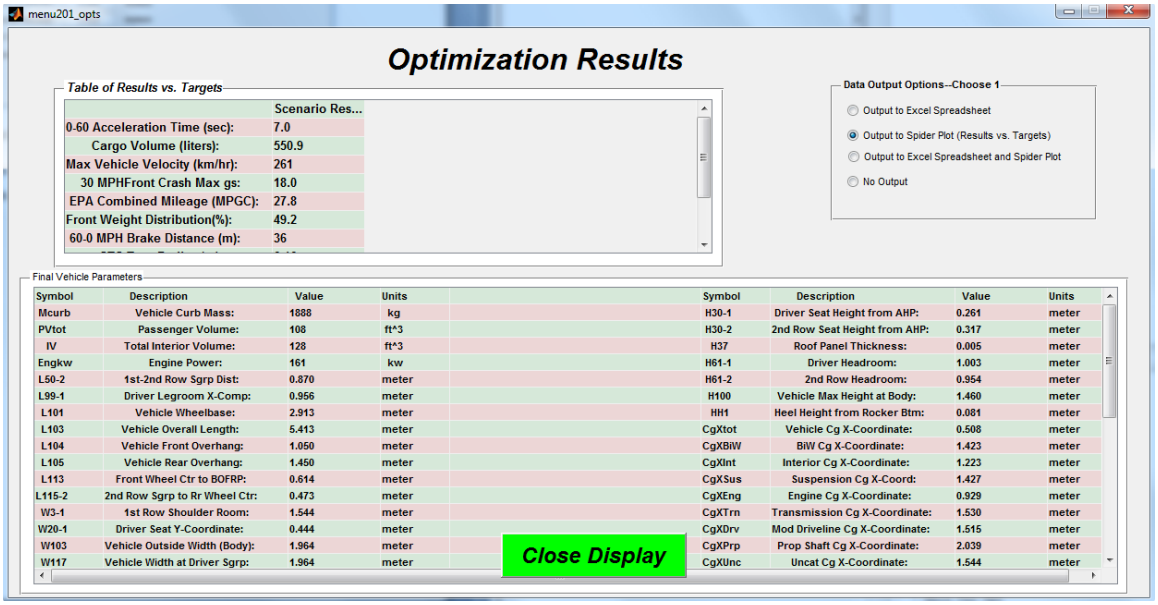

Figure M.19 Scenario Results Menu

The Vehicle Longitudinal Dimensions Results Menu shown in Figure M.20 provides a vehicle side view which displays the longitudinal parameter values in context to each other and overall vehicle length. This is a common menu for the Scenario Builder and Optimization Modules. The Vehicle External Width Dimensions Menu, also common between modules, is shown in Figure M.21. The Vehicle Internal and Occupant Width Dimensions Menu, also a common menu, is shown in Figure M.22. The Vehicle Height Dimensions Results Menu (also common) is shown in Figure M.23. After this menu is displayed the software framework returns to the Main Menu shown in Figure M.1.

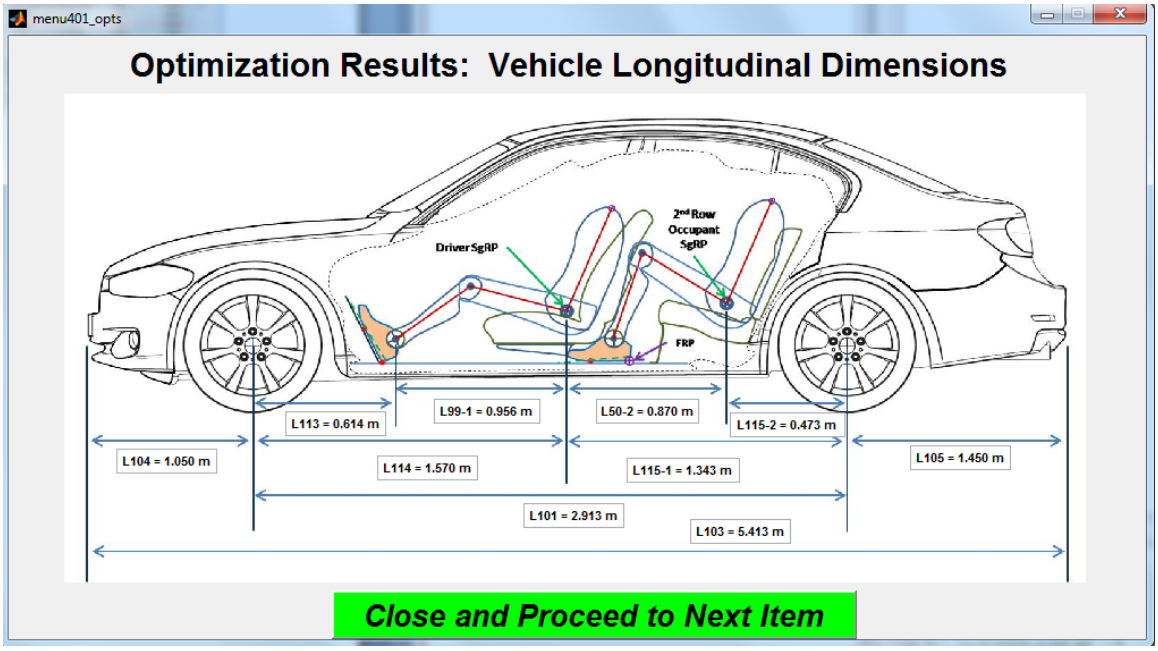

Figure M.20 Vehicle Longitudinal Dimensions Results Menu

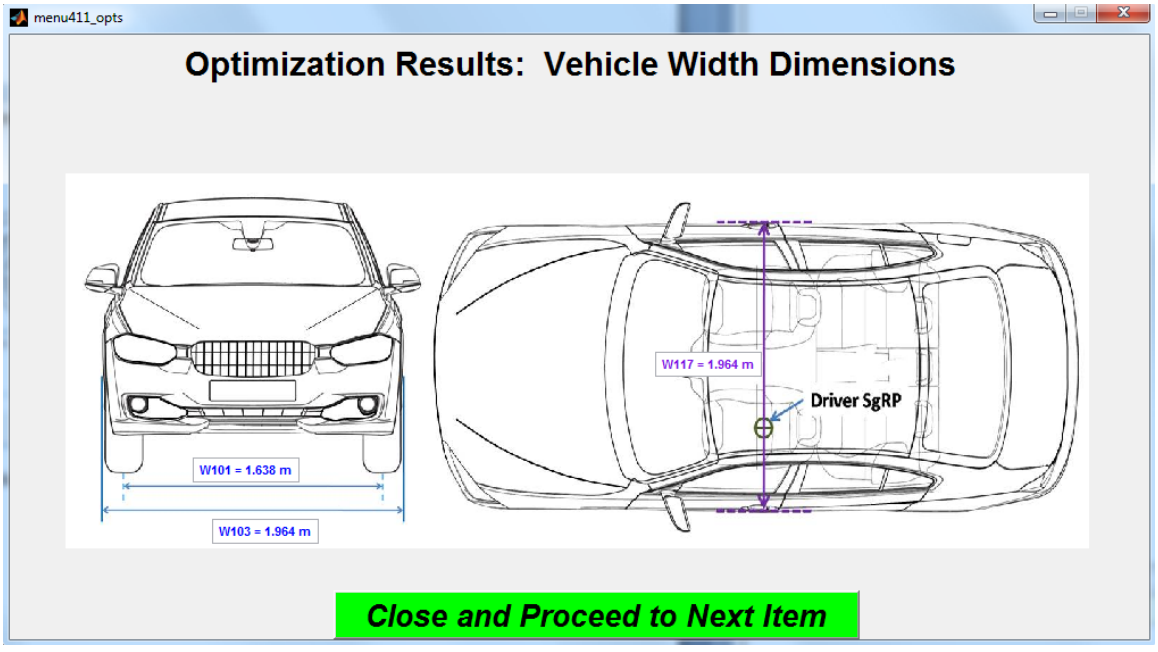

Figure M.21 Vehicle External Width Dimensions Results Menu

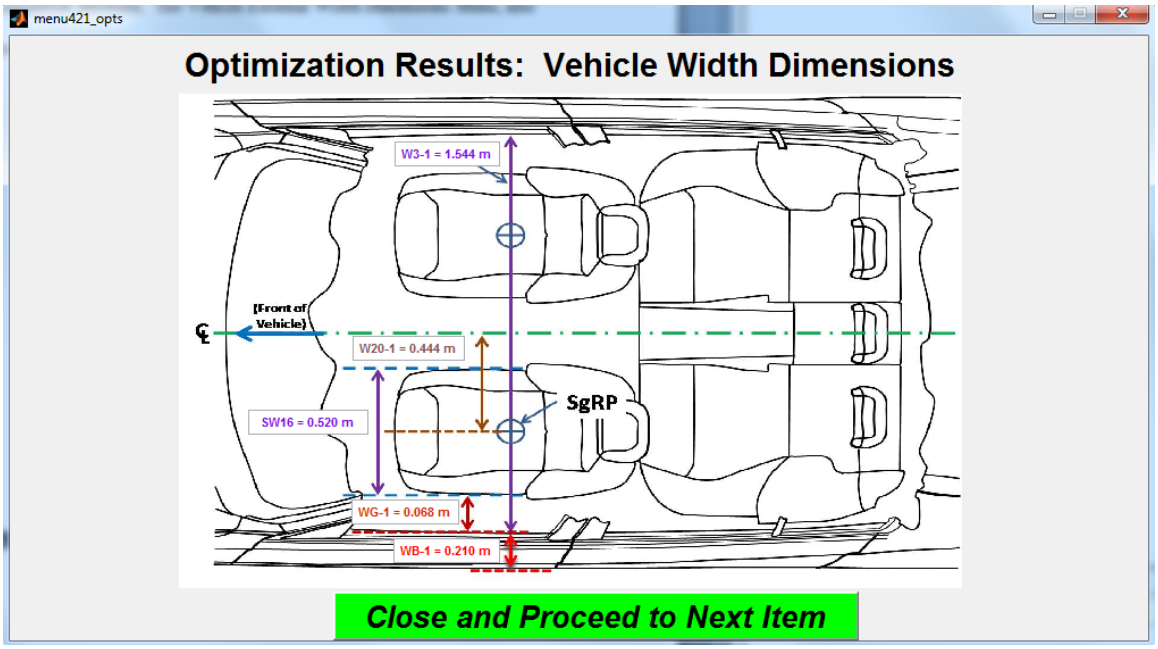

Figure M.22 Vehicle Internal and Occupant Width Dimensions Results Menu

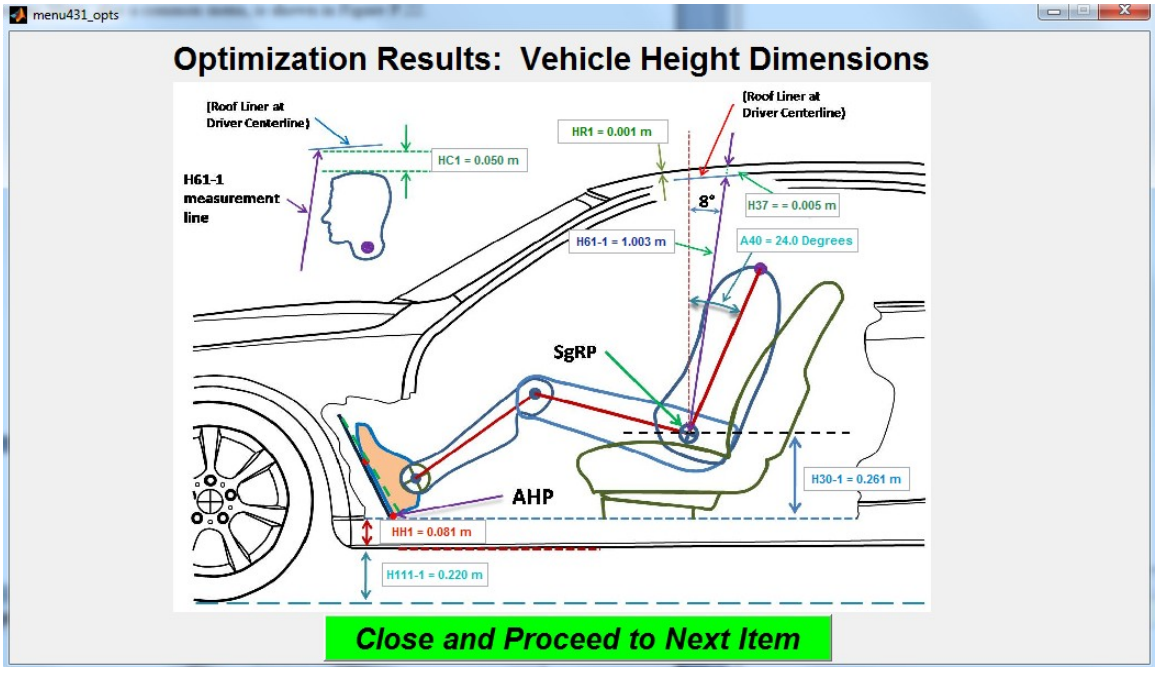

Figure M.23 Vehicle Height Dimensions Results Menu

Appendix N
Optimization Module Input and Output Menus

When the Optimization option is selected in the Main Menu (Figure M.1), the Optimization Method Selection Menu appears as shown in Figure N.1. There are currently two options; a gradient method and a genetic algorithm optimization method. The gradient based method is being phased out; it is expected that additional non-gradient methods will be added in future work.

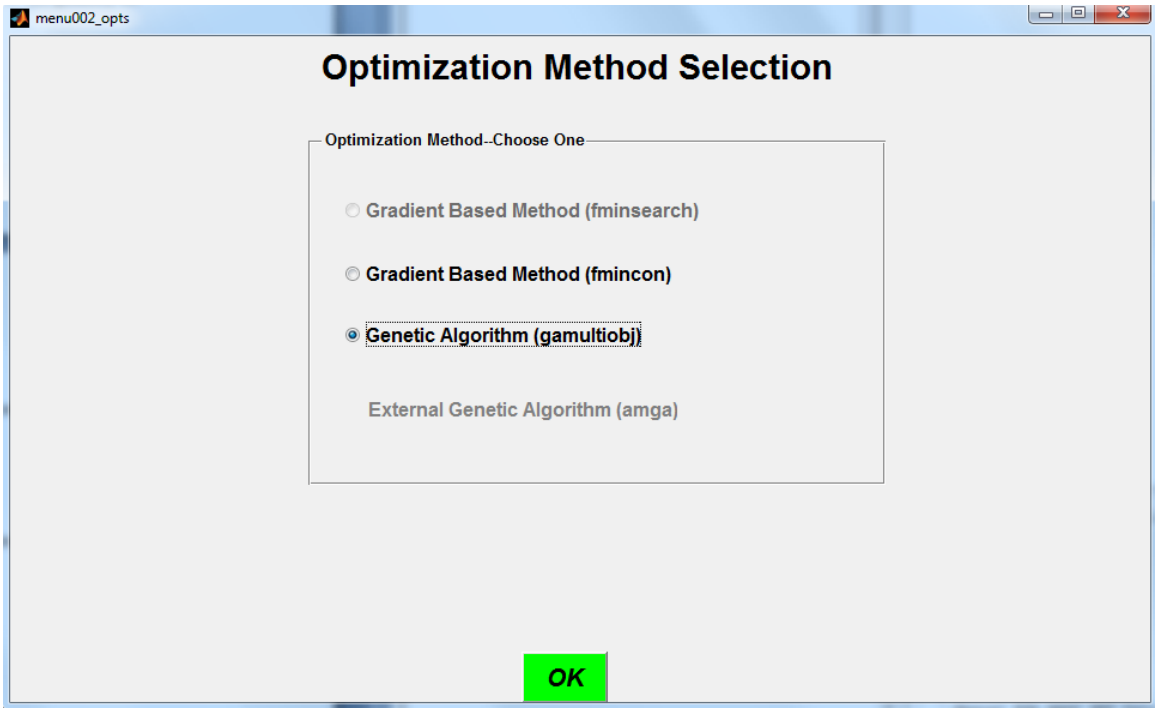

Figure N.1 Optimization Method Selection Menu

The Brand DNA Input Menu is shown in Figure N.2. This menu provides a method for weighting one target over another in priority (note that the weighting does not occur in the optimization itself, but rather in selecting the "better" result in the final generation of optimization points from the genetic algorithm optimization run). The

weighting is exponential in nature -- this is the reason for using a weighting range from 0.5 to 2.0. A weighting value of 1.0 represents a "neutral" priority weighting. Each weighting factor applies to one or more vehicle functional targets such as NCAP crash rating ("Safety" DNA factor), Acceleration ("Performance") and fuel economy ("Efficiency"). Each DNA factor can be adjusted by moving a slider button, the resulting change from the default value is updated on a spider chart in the menu as shown in Figure N.3. Note that if all DNA factors are set at the same value (such as 1.5), it will have the same effect as leaving them all at the neutral default value.

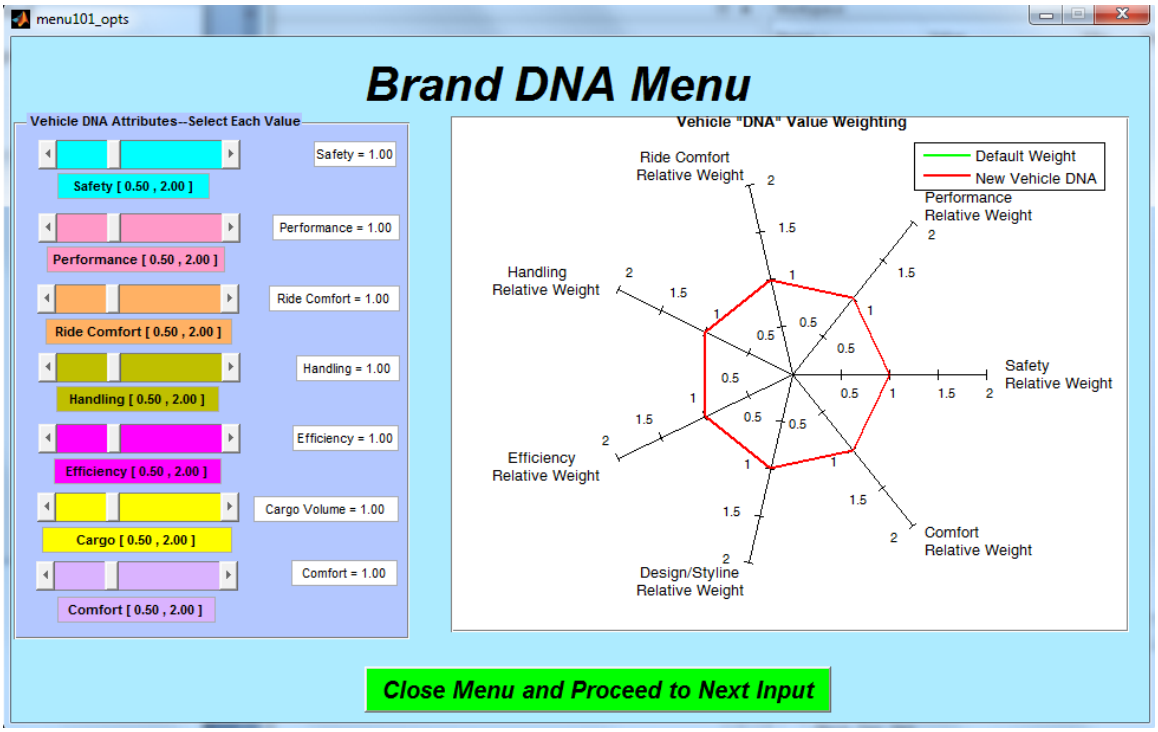

Figure N.2 Brand DNA Input Menu

Input menus shared with the Scenario Builder module are not shown in this appendix. Those menus that are common with the Scenario Builder are noted in Appendix M.

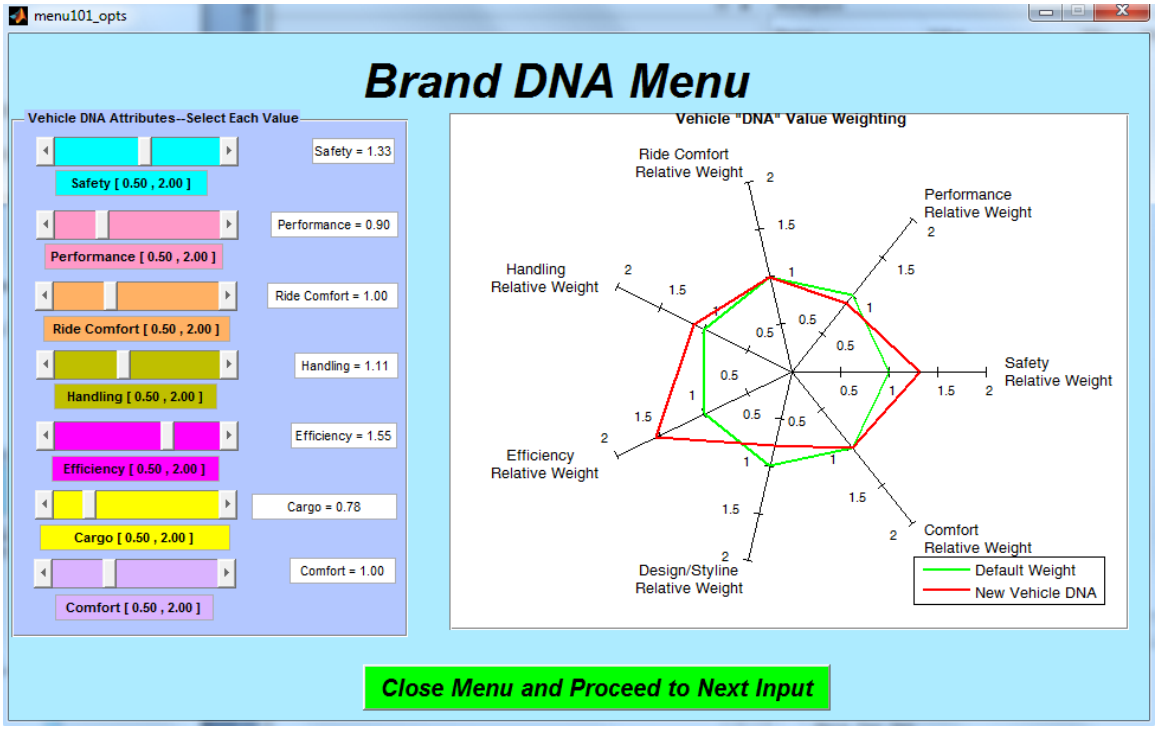

Figure N.3 Brand DNA Menu Showing Updated DNA Factor Values

The next input menu unique to the Optimization Module is the Fuel Economy Target Model Year Selection Menu shown in Figure N.4. The menu shows the EPA Fuel Economy Target (FET) for the selected vehicle model year in EPA combined miles per gallon (mpg) as a function of vehicle footprint F101. Note that the vehicle footprint may change with each iteration of the optimization functional evaluation as design variables vary through the optimization run. The fuel economy target can be used as the optimization target; this creates a situation where the target value used in the functional value component based on fuel economy can also change with each functional evaluation iteration in the optimization. The genetic algorithm appears to be able to handle this dynamic update in the optimization criteria. This is one reason for moving away from gradient-based optimization methods.

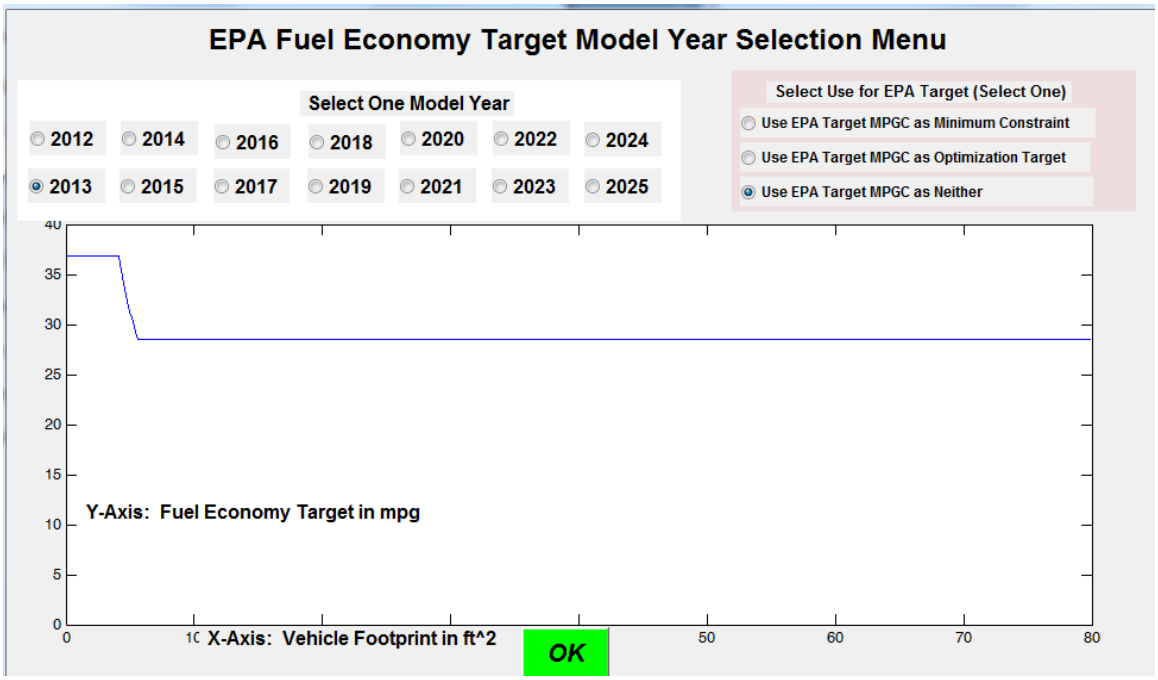

Figure N.4 EPA Fuel Economy Target Model Year Selection Menu

The Vehicle Target Input Menu is shown in Figure N.5. This menu allows the user to input all non-hybrid vehicle targets except for front weight distribution, which has a separate input menu. These targets currently require a reasonable level of vehicle knowledge; some targets can vary depending on whether the vehicle is a luxury, high-performance or economy vehicle. Supplying default values based on additional vehicle DNA inputs may be potential future work as more knowledge base data is collected and assessed. If the EPA fuel economy target is selected as a vehicle target, the user input in this menu will not be used for the optimization target value. The maximum vehicle velocity target is used in the vehicle tire selection menu as well.

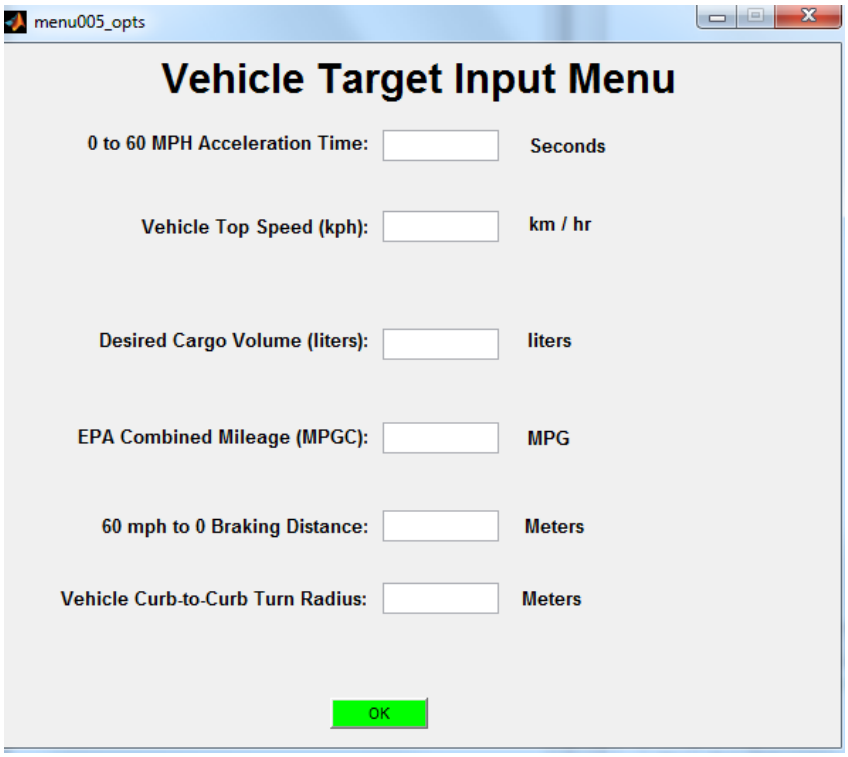

Figure N.5 Vehicle Target Input Menu

The Vehicle Frontal NCAP Performance Target Menu is shown in Figure N.6. Currently, a selected Star-performance level is associated with a specific value for calculated time-weighted accelerations in g's (25 g's for 5-star, 30 g's for 4 / 3-star and 35 g's for 2 / 1-star). Future work may include an input box showing the target in g's and permit the user to enter a different target value. The crash performance input is used to calculate the required midrail length to meet the desired frontal crash acceleration. This midrail length in turn is reconciled with engine bay packaging: the larger value is used in the given optimization functional evaluation. Note that the midrail length changes in turn change vehicle mass, affecting the required midrail length in circular fashion. For this reason, each functional evaluation iteration is repeated in a loop until it converges on a stable value. Even with this midrail sizing method, the optimized NCAP crash g's due

not always achieve the target value depending on DNA weighting and other trade-off factors.

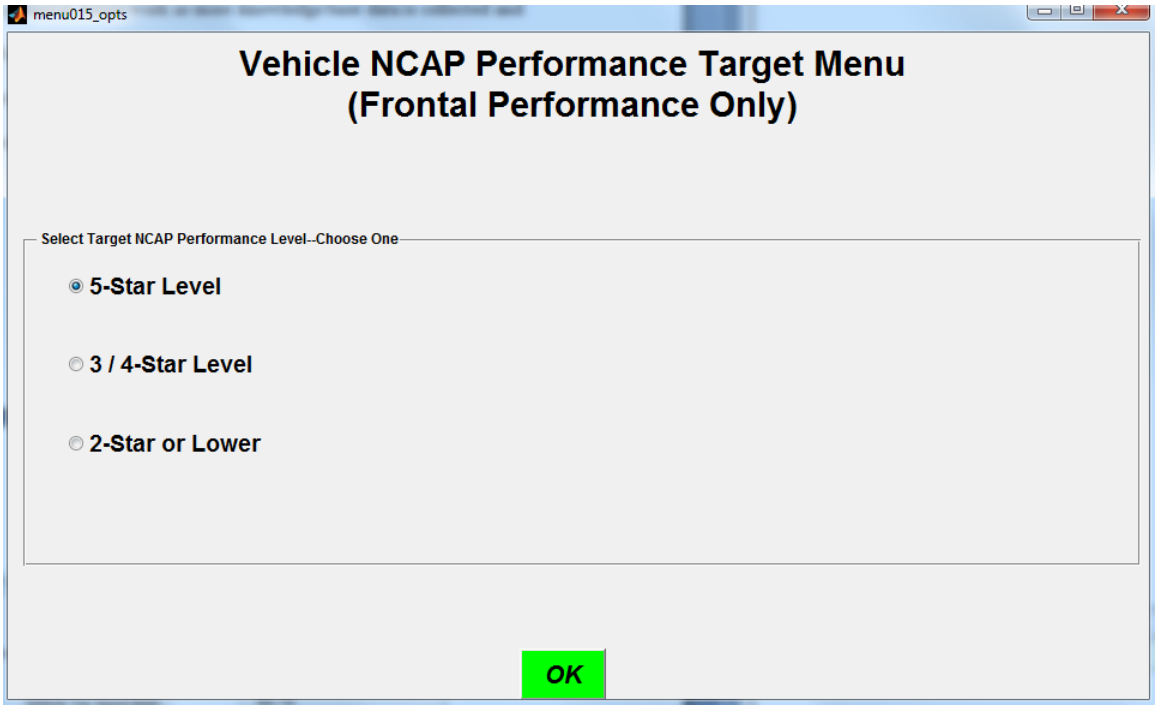

Figure N.6 Vehicle NCAP Performance Target Menu

The Front Weight Distribution Target Input Menu is shown in Figure N.7. The center of gravity (Cg) location is directly related to front weight distribution (or rear distribution). In practice it is simpler to address it in terms of the front weight distribution value. An ideal vehicle would have a 50% front / 50% rear distribution; in practice it is rare to achieve the ideal value. Front-wheel drive vehicles in particular tend to be front-heavy (resulting in vehicle understeer).

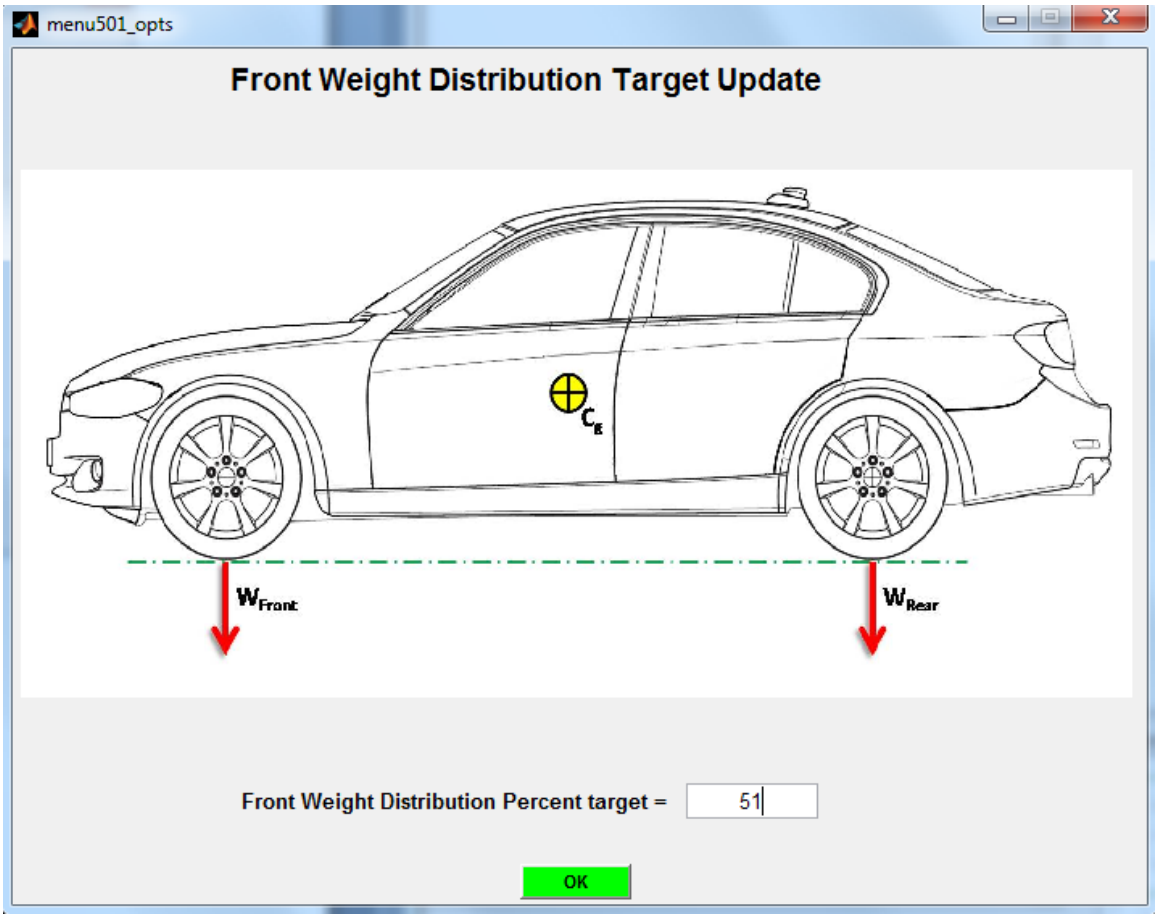

Figure N.7 Front Weight Distribution Target Input Menu

The Optimization Module Engine Selection menu, shown in Figure N.8, differs slightly from the Scenario Builder module equivalent. Required power based on an initial estimate of vehicle mass and mass distribution is calculated by the module and displayed in the menu as a guide for selected engine type. In selecting the engine type, the current and potential optimized engine power must be considered. If the value of the design variable for engine power exceeds the available power level for the selected engine type, engine power applied to traction is limited to the maximum / minimum for that engine configuration. If a hybrid configuration is selected, an additional hybrid

targets menu will be displayed.

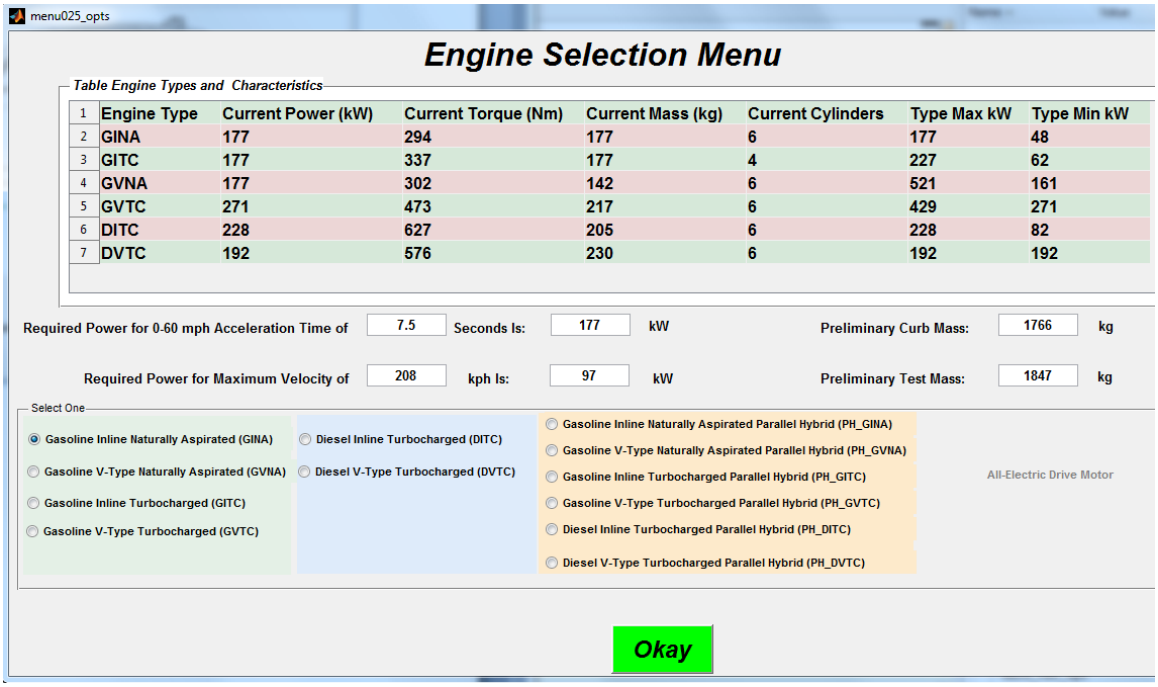

Figure N.8 Scenario Builder Module Engine Selection Menu

The Hybrid Battery and Targets Selection Menu is shown in Figure N.9. This combines the battery selection menu in the Scenario Builder with inputs for three hybrid-relevant targets: 0 to 30 mph all-electric acceleration time, all-electric maximum velocity and all-electric range. The latter determines battery capacity; the first two targets size the electric motor similar to the internal combustion engine power sizing criteria. Note that, with a hybrid configuration, 0 to 60 mph acceleration time and maximum vehicle velocity is now calculated using the combined traction power of the motor and the internal combustion engine.

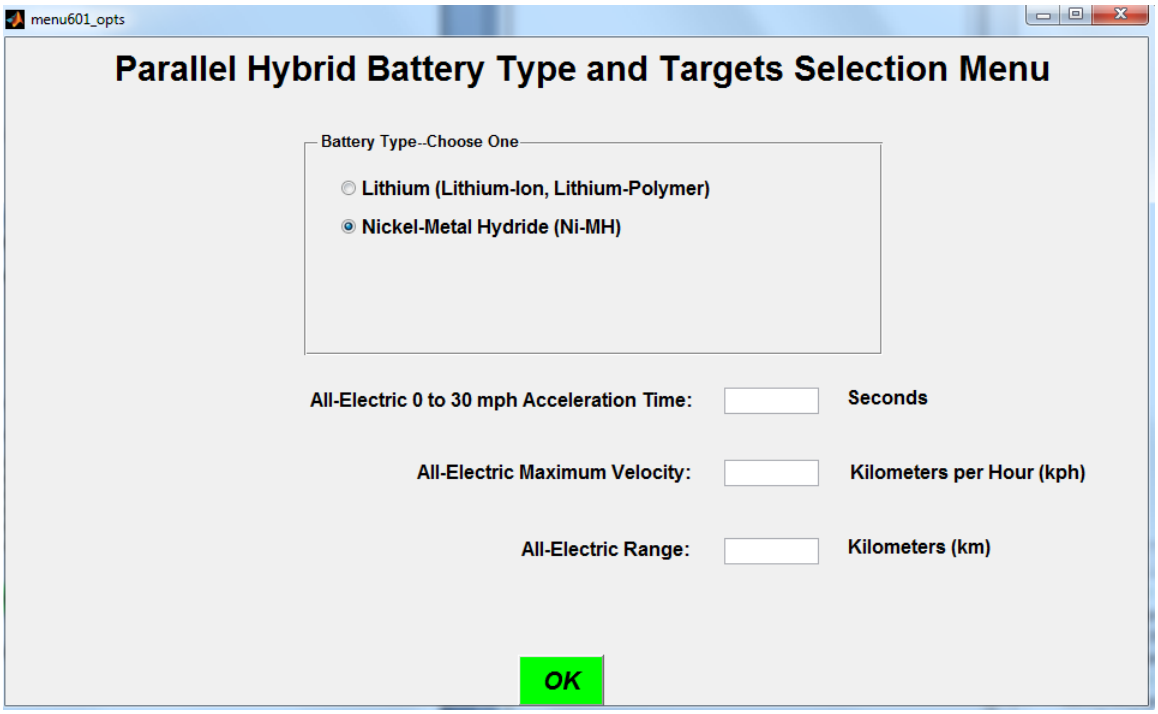

Figure N.9 Hybrid Battery and Targets Selection Menu

The first pre-optimization parameter sensitivity gradient results menu is shown in Figure N.10. Note that if a hybrid configuration is selected, the additional associated design variables are shown in added columns; the hybrid-related performance to hybrid targets is shown in rows added at the bottom of the table. For each design variable there are two columns: the first column gives the gradient value of the target / parameter vs. the variable and the second column gives the gradient units for that specific relation. A similar format is followed for the other sensitivity gradient results tables.

The Sensitivity Gradient vs.Width Parameter Results Menu is shown in Figure N.11. Gradient results are displayed in a format similar to the previous menu.

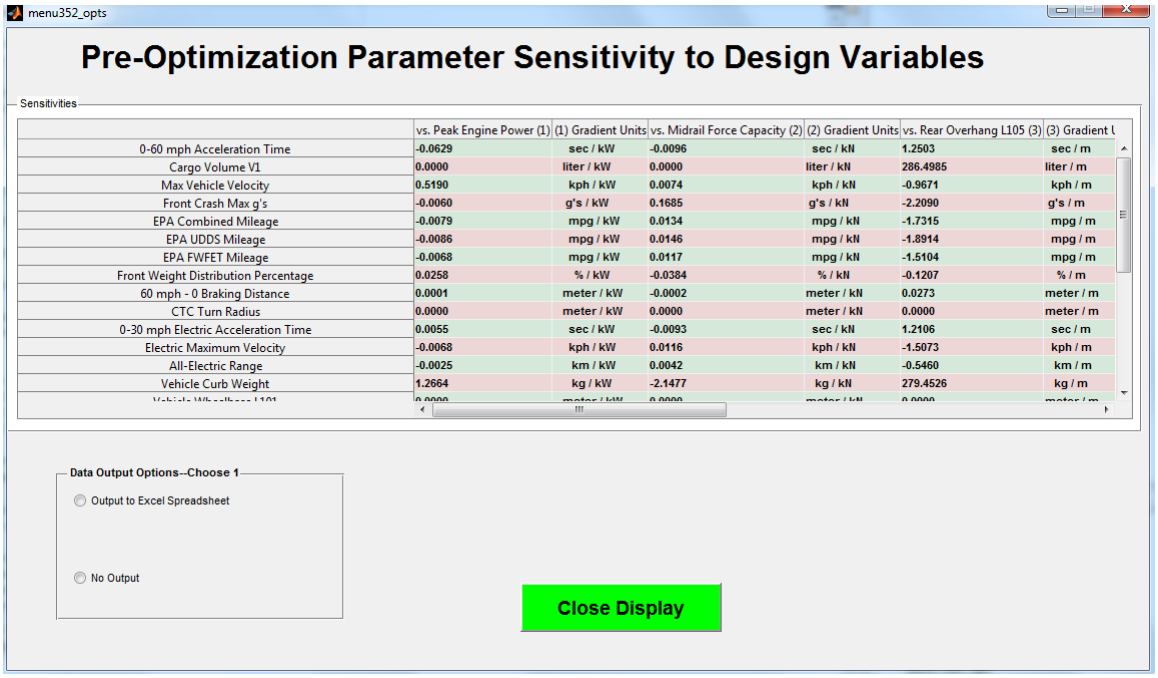

	vs. Peak Engine Power (1)	(1) Gradient Units	vs. Midrail Force Capacity (2)	(2) Gradient Units	vs. Rear Overhang L105 (3)	(3) Gradient U
0-60 mph Acceleration Time	-0.0629	sec / kW	-0.0096	sec / kN	1.2503	sec / m
Cargo Volume V1	0.0000	liter / kW	0.0000	liter / kN	286.4985	liter / m
Max Vehicle Velocity	0.5190	kph / kW	0.0074	kph / kN	-0.9671	kph / m
Front Crash Max g's	-0.0060	g's / kW	0.1685	g's / kN	-2.2090	g's / m
EPA Combined Mileage	-0.0079	mpg / kW	0.0134	mpg / kN	-1.7315	mpg / m
EPA UDDS Mileage	-0.0086	mpg / kW	0.0146	mpg / kN	-1.8914	mpg / m
EPA FWFET Mileage	-0.0068	mpg / kW	0.0117	mpg / kN	-1.5104	mpg / m
Front Weight Distribution Percentage	0.0258	% / kW	-0.0384	% / kN	-0.1207	% / m
60 mph - 0 Braking Distance	0.0001	meter / kW	-0.0002	meter / kN	0.0273	meter / m
CTC Turn Radius	0.0000	meter / kW	0.0000	meter / kN	0.0000	meter / m
0-30 mph Electric Acceleration Time	0.0055	sec / kW	-0.0093	sec / kN	1.2106	sec / m
Electric Maximum Velocity	-0.0068	kph / kW	0.0116	kph / kN	-1.5073	kph / m
All-Electric Range	-0.0025	km / kW	0.0042	km / kN	-0.5460	km / m
Vehicle Curb Weight	1.2664	kg / kW	-2.1477	kg / kN	279.4526	kg / m

Figure N.10 Pre-Optimization Parameter Sensitivity Gradient vs. Design Variables Menu

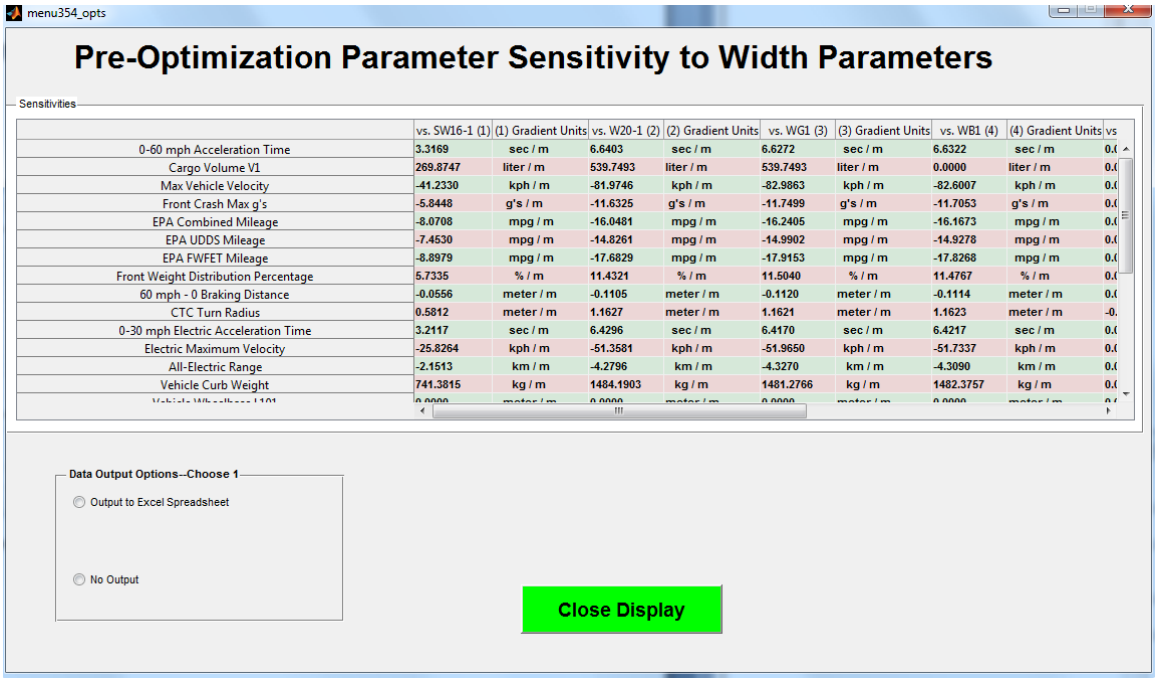

	vs. SW16-1 (1)	(1) Gradient Units	vs. W20-1 (2)	(2) Gradient Units	vs. WG1 (3)	(3) Gradient Units	vs. WB1 (4)	(4) Gradient Units	vs
0-60 mph Acceleration Time	3.3169	sec / m	6.6403	sec / m	6.6272	sec / m	6.6322	sec / m	0.(
Cargo Volume V1	269.8747	liter / m	539.7493	liter / m	539.7493	liter / m	0.0000	liter / m	0.(
Max Vehicle Velocity	-41.2330	kph / m	-81.9746	kph / m	-82.9863	kph / m	-82.6007	kph / m	0.(
Front Crash Max g's	-5.8448	g's / m	-11.6325	g's / m	-11.7499	g's / m	-11.7053	g's / m	0.(
EPA Combined Mileage	-8.0708	mpg / m	-16.0481	mpg / m	-16.2405	mpg / m	-16.1673	mpg / m	0.(
EPA UDDS Mileage	-7.4530	mpg / m	-14.8261	mpg / m	-14.9902	mpg / m	-14.9278	mpg / m	0.(
EPA FWFET Mileage	-8.8979	mpg / m	-17.6829	mpg / m	-17.9153	mpg / m	-17.8268	mpg / m	0.(
Front Weight Distribution Percentage	5.7335	% / m	11.4321	% / m	11.5040	% / m	11.4767	% / m	0.(
60 mph - 0 Braking Distance	-0.0556	meter / m	-0.1105	meter / m	-0.1120	meter / m	-0.1114	meter / m	0.(
CTC Turn Radius	0.5812	meter / m	1.1627	meter / m	1.1621	meter / m	1.1623	meter / m	-0.
0-30 mph Electric Acceleration Time	3.2117	sec / m	6.4296	sec / m	6.4170	sec / m	6.4217	sec / m	0.(
Electric Maximum Velocity	-25.8264	kph / m	-51.3581	kph / m	-51.9650	kph / m	-51.7337	kph / m	0.(
All-Electric Range	-2.1513	km / m	-4.2796	km / m	-4.3270	km / m	-4.3090	km / m	0.(
Vehicle Curb Weight	741.3815	kg / m	1484.1903	kg / m	1481.2766	kg / m	1482.3757	kg / m	0.(

Figure N.11 Pre-Optimization Parameter Sensitivity Gradient vs. Width Parameters Results Menu

The gradient sensitivity to length-related and miscellaneous parameters results menu is shown in Figure N.12. Note that some gradients in all of the results menu may have large values due to retention of the meter / kilogram / second system for results. Some parameters are sensitive to changes on the order of millimeters; dimensionless coefficients will similarly tend to show large values which must be scaled to reasonable change limits in evaluating trade-offs.

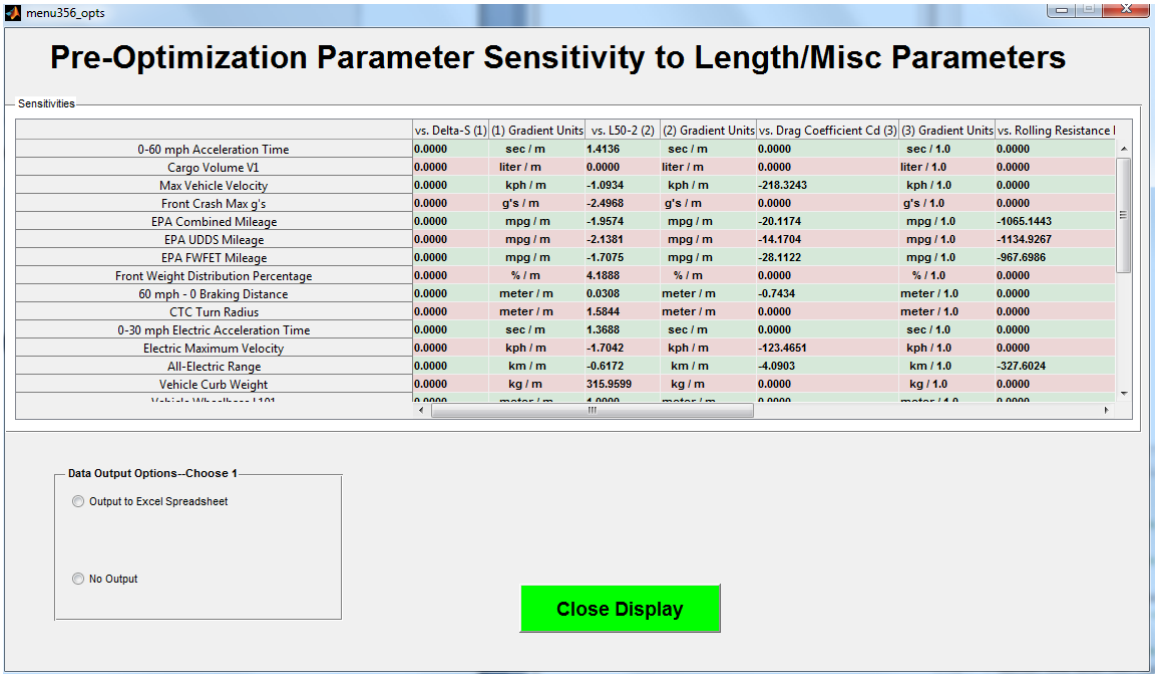

Figure N.12 Pre-Optimization Parameter Sensitivity to Length / Misc Parameters Results Menu

The Pre-Optimization Parameter Gradient Sensitivity to Height Parameters Results Menu is shown in Figure N.13.

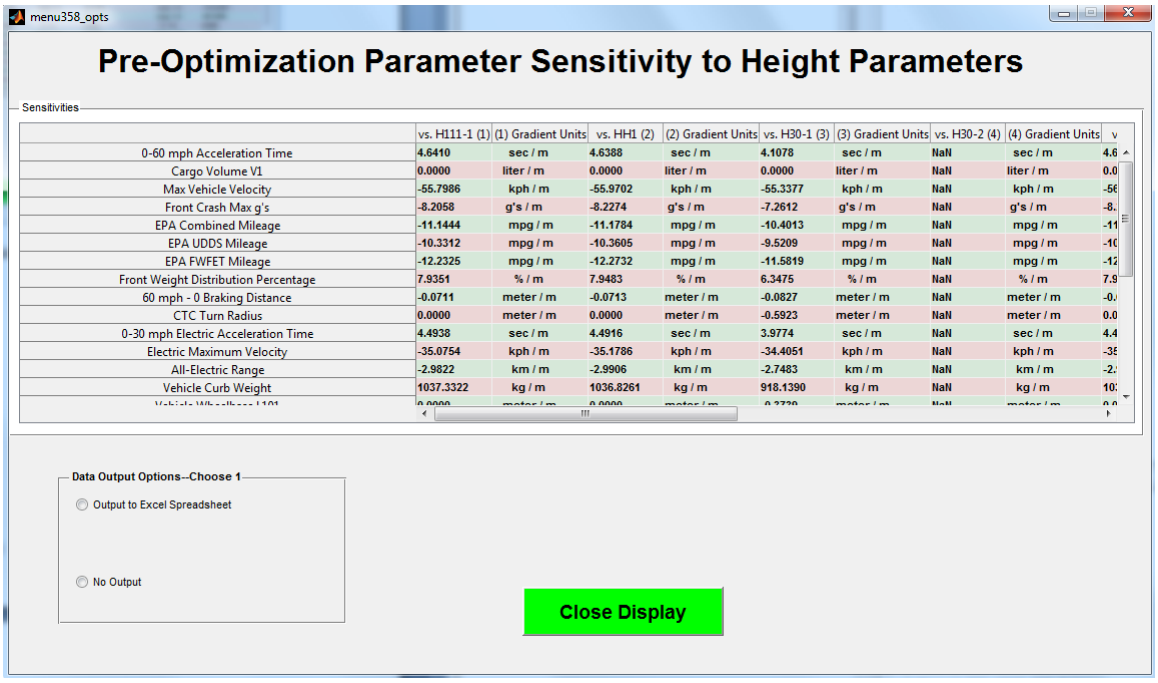

Figure N.13 Pre-Optimization Parameter Gradient Sensitivity to Height Parameters Results Menu

After the menu in Figure N.13 is displayed, the optimization process begins. A status display is updated during the optimization run as shown in Figure N.14. This shows the pareto front for the first two objective axes. The algorithm is currently set for a maximum of 300 generations with 300 points per generation. This is generally sufficient to find optimized solutions for a given vehicle input configuration depending on the amount of conflict between the multiple optimization objectives. More points and a larger generation limit may be used; however, this results in a longer run time.

The Pareto front plot shows the coordinates of points along the first two objective axes (out of the total number of target objectives in the optimization). The distance between individual points in each generation is shown in the upper right histogram. The rank histrogram shows the "rank" or ranked distance from the Pareto front for points.

The lower left plot shows the average spread or distance between point for each generation (a measure of their distribution).

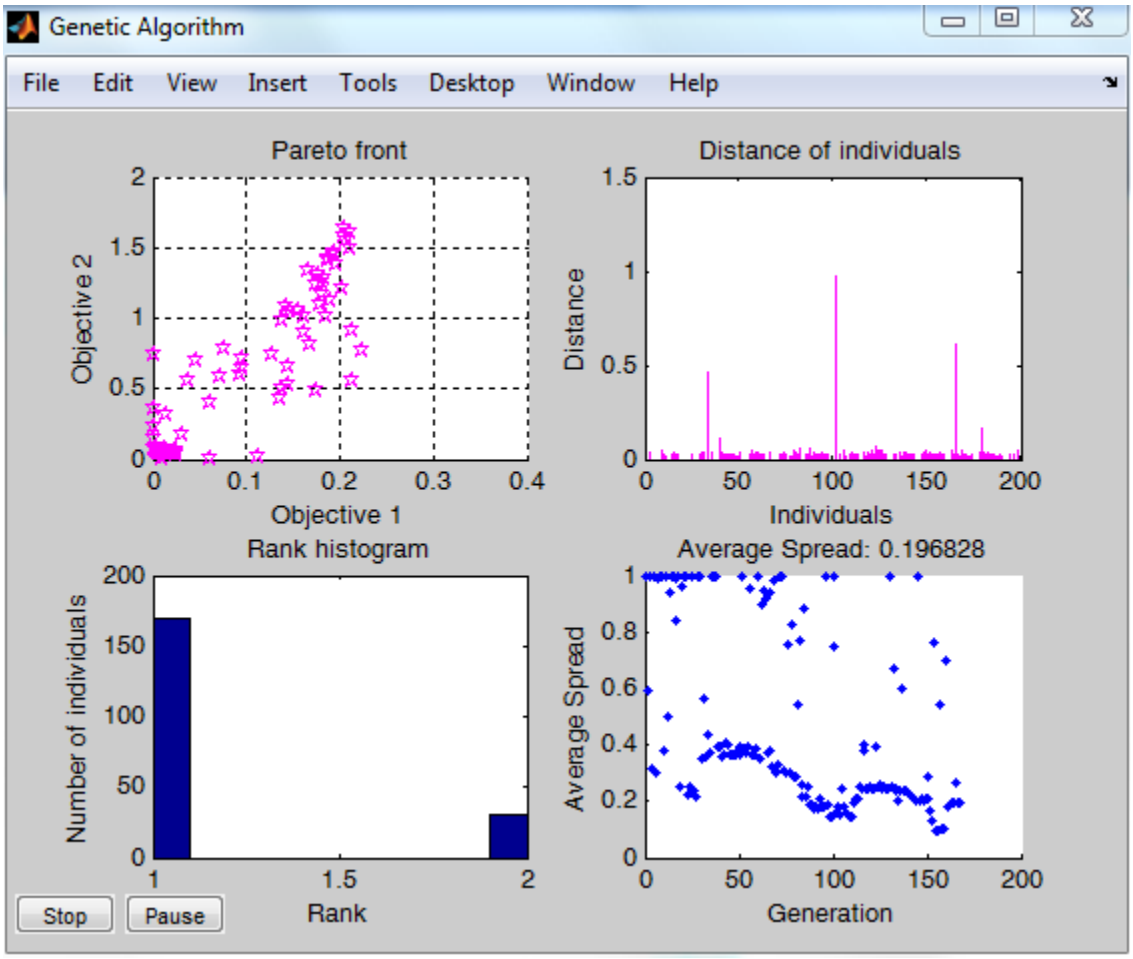

Figure N.14 Genetic Algorithm Run Status Display

At the end of the optimization run, the same Optimization Results Menu is displayed as in the Scenario Builder module (Figure N.15); additional columns in the upper table are shown, however, which show the performance vs. target for the vehicle target performance values. The parameters displayed in the lower table are the same as in the Scenario Builder. The Vehicle Optimization Results Menu displaying performance vs. targets on a spider chart is shown in Figure N.16

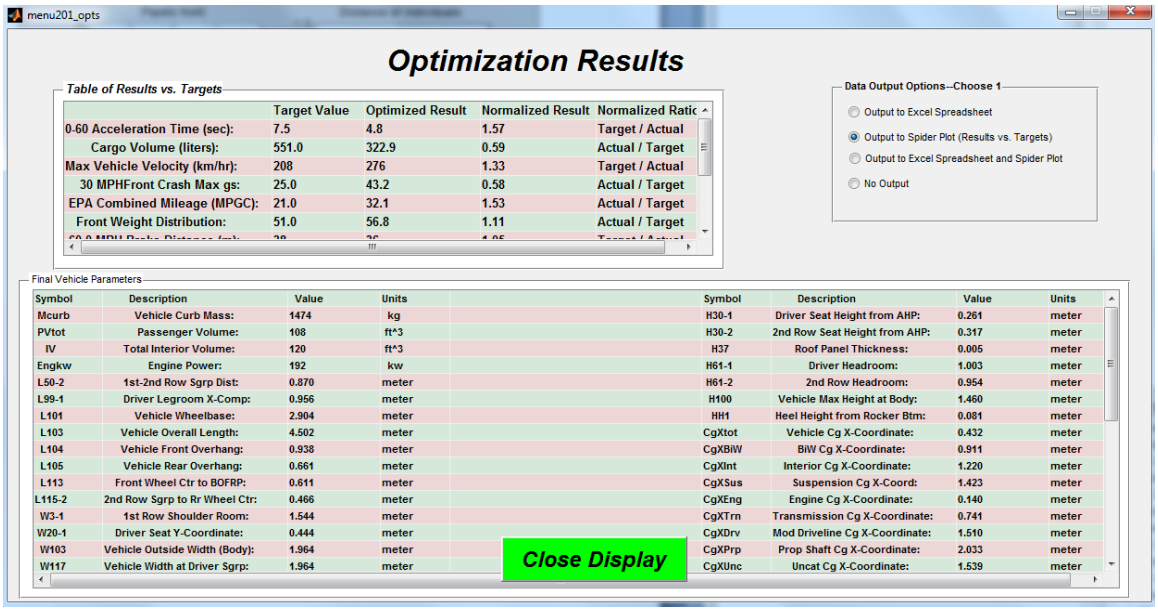

Figure N.15 Optimization Results Menu

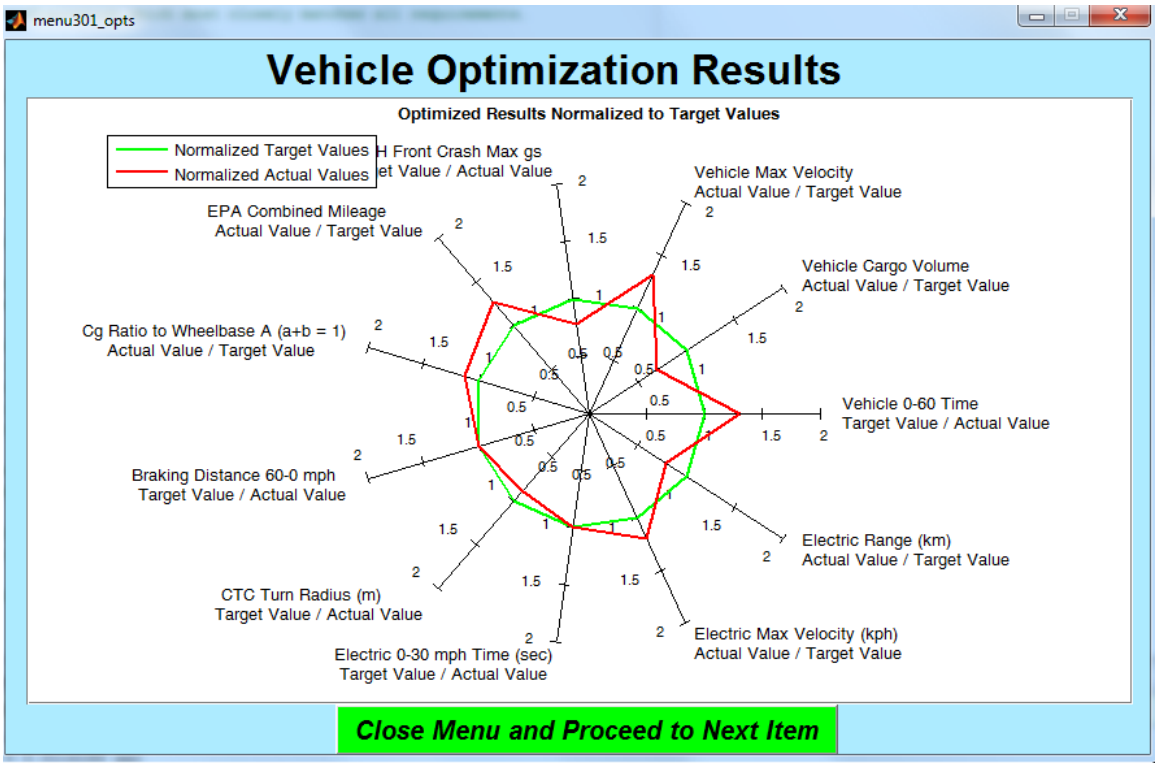

Figure N.16 Vehicle Optimization Results Menu (Spider Chart)

The graphical results display menus which follow the spider chart display are the

same as in the Scenario Builder module. The next set of results menus show post-optimization sensitivity gradients in the same manner as the pre-optimization results. The Post-Optimization Parameter Sensitivity to Design Variables Results Menu is shown in Figure N.17. The remaining three menus are not shown as they are similar to the pre-optimization menus with updated results and menu title.

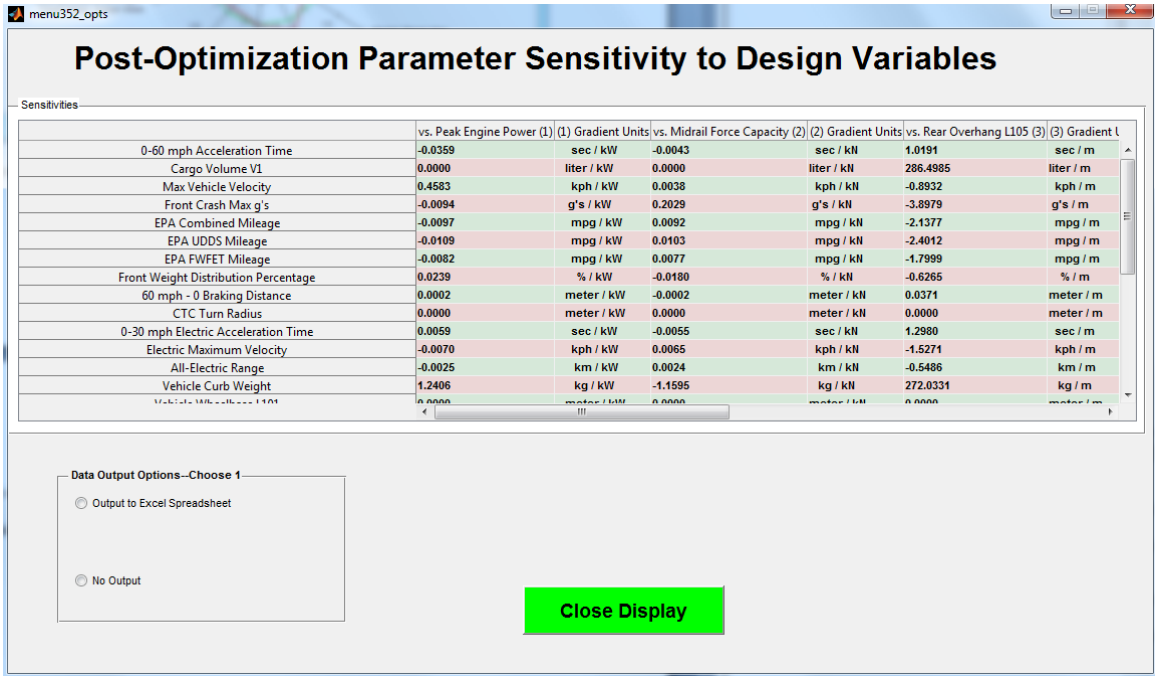

Figure N.17 Post-Optimization Parameter Sensitivity to Design Variables Results Menu

The Batch Optimization Analysis Selection Menu is shown in Figure N.18. The target menu is being replaced with a MATLAB / ModeFrontier interface to use a design of experiments to generate more consistent target-vs.-target sensitivity gradients. The Batch analysis conducts 10 additional optimization runs using the same user inputs as described above for all of the runs. The results are then compared for the "better" solution point from each run.

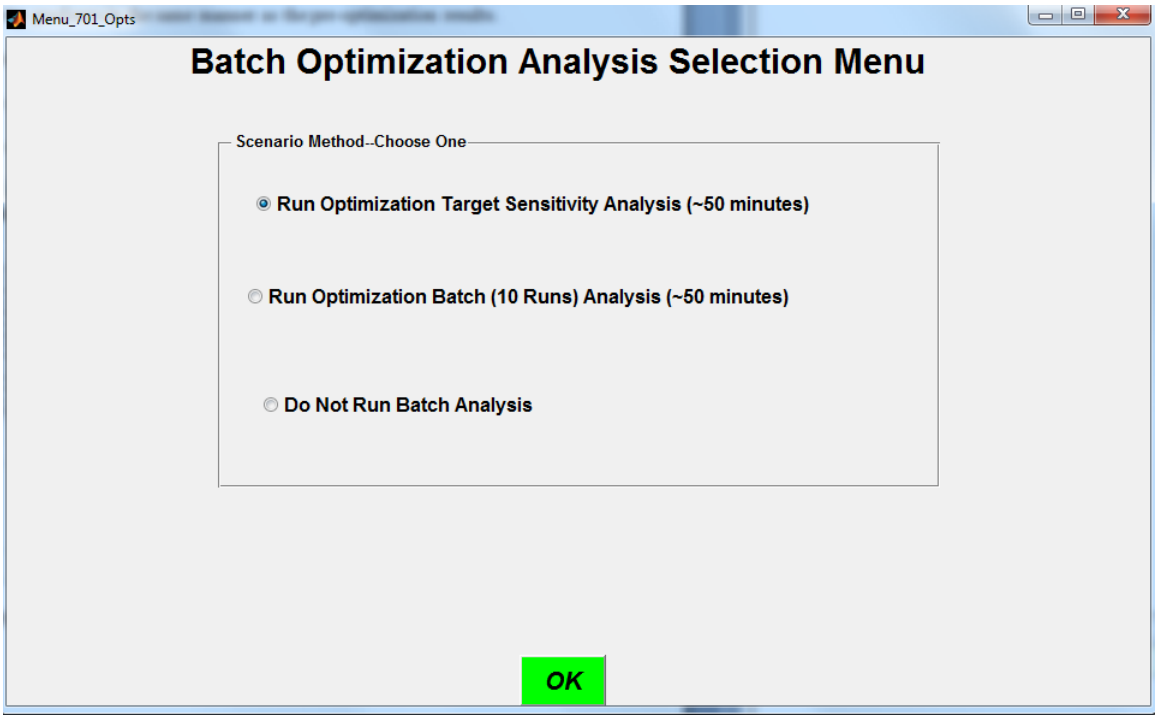

Figure N.18 Batch Optimization Analysis Selection Menu

Appendix O
Additional Parameter Sensitivity Gradient Results

Sensitivity gradient results for design variables midrail crush force and rear overhang L105 are shown in Table O.1. Results for L113 and L115-2 are shown in Table O.2. Results for (hybrid) variables peak motor power and battery capacity are shown in Table O.3.

Note that 0 to 60 mph acceleration time and maximum vehicle velocity only use the internal combustion engine power (and not electric motor power if it is a hybrid). For this reason the added motor and battery mass decrease 0 to 60 time and also decrease vehicle maximum velocity while affecting other parameters due to added mass. Motor peak power and battery capacity are less effective than the non-hybrid design variables; however, they are required to include hybrids in the design trade-offs. A separate acceleration target for total tractive power can also increase linkage and drive trade-offs between internal combustion engine and electric motor power values.

The EPA combined mileage gradient only captures the effect of the added motor and battery mass. There is an added mileage gain due to specifying a hybrid configuration to recapture braking energy; this is not seen in the gradient. An effective gradient measure will have to separately benchmark a hybrid vs. non-hybrid performance value for the same optimization run. This is potential future work.

Target / Parameter	Midrail Crush Force	Gradient Units	Rear Overhang L105	Gradient Units
0 - 60 mph Acceleration Time	-0.005	sec / kN	1.03	sec / m
Cargo Volume V1	0	liter / kN	286.5	liter / m
Maximum Vehicle Velocity	0.005	kph / kN	0.91	kph / m
Frontal NCAP Accelerations	0.24	g / kN	-4.61	g / m
EPA Combined Mileage	0.01	mpg / kN	-2.16	mpg / m
Front Weight Distribution	-0.017	% / kN	-3.18	% / m
60 mph - 0 Braking Distance	-0.0002	meter / kN	-0.048	meter / m
CTC Turn Radius	0.0	meter / kN	0.0	meter / m
Mcurb	-1.36	kg / kN	275.65	kg / m
L101	0.000	meter / kN	0.000	meter / m
L103	-0.006	meter / kN	1.103	meter / m
L104	-0.006	meter / kN	0.103	meter / m
Bumper Rail Length	-0.001	meter / kN	0.077	meter / m
Midrail Length	-0.005	meter / kN	0.096	meter / m
Maximum Traction Power	-0.32	kW / kN	24.01	kW / m
MBiW	-0.41	kg / kN	70.01	kg / m
MCls	0.00	kg / kN	11.66	kg / m
MDrv	0.00	kg / kN	0.00	kg / m
Mint	0.00	kg / kN	0.00	kg / m
Msusp	-0.20	kg / kN	41.05	kg / m
Mtransmission	0.00	kg / kN	0.00	kg / m
Muncat	-0.75	kg / kN	143.93	kg / m

Table O.1 Sensitivity Gradient Results for Midrail Crush Force and L105 (Post-Optimization)

Target / Parameter	L113	Gradient Units	L115-2	Gradient Units
0 - 60 mph Acceleration Time	0.19	sec / m	1.17	sec / m
Cargo Volume V1	0	liter / m	286.5	liter / m
Maximum Vehicle Velocity	-0.17	kph / m	-1.02	kph / m
Frontal NCAP Accelerations	-0.86	g / m	-5.26	g / m
EPA Combined Mileage	-0.40	mpg / m	-2.45	mpg / m
Front Weight Distribution	-5.03	% / m	1.47	% / m
60 mph - 0 Braking Distance	0.01	meter / m	0.05	meter / m
CTC Turn Radius	1.6	meter / m	1.6	meter / m
Mcurb	50.8	kg / m	311.4	kg / m
L101	1.000	meter / m	1.000	meter / m
L103	0.019	meter / m	1.117	meter / m
L104	-0.981	meter / m	0.117	meter / m
Bumper Rail Length	0.001	meter / m	0.009	meter / m
Midrail Length	0.018	meter / m	0.108	meter / m
Maximum Traction Power	-40.6	kW / m	39.5	kW / m
MBiW	1.36	kg / m	79.97	kg / m
MCls	11.25	kg / m	11.25	kg / m
MDrv	0.00	kg / m	0.00	kg / m
Mint	28.11	kg / m	28.11	kg / m
Msusp	7.56	kg / m	46.38	kg / m
Mtransmission	0.00	kg / m	0.00	kg / m
Muncat	2.48	kg / m	145.68	kg / m

Table O.2 Sensitivity Gradient Results for L113 and L115-2 (Post-Optimization)

Target / Parameter	Peak Motor Power	Gradient Units	Battery Capacity	Gradient Units
0 - 60 mph Acceleration Time	0.068	sec / kW	0	sec / kW
Cargo Volume V1	0	liter / kW	0	liter / kWh
Maximum Vehicle Velocity	-0.06	kph / kW	0	kph / kWh
Frontal NCAP Accelerations	-0.13	g / kW	0	g / kWh
EPA Combined Mileage	-0.10	mpg / kW	0	mpg / kWh
Front Weight Distribution	-0.22	% / kW	0	% / kWh
60 mph - 0 Braking Distance	0.00	meter / kW	0	meter / kWh
CTC Turn Radius	0.0	meter / kW	0	meter / kWh
0 to 30 mph Acceleration Time	-0.2	sec / kW	0	sec / kWh
All-Electric Maximum Velocity	1.3	kph / kW	0	kph / kWh
All-Electric Range	-0.023	km / kW	6.7	km / kWh
Mcurb	18.2	kg / kW	0	kg / kWh
L101	0.000	meter / kW	0	meter / kWh
L103	0.007	meter / kW	0	meter / kWh
L104	0.007	meter / kW	0	meter / kWh
Bumper Rail Length	0.001	meter / kW	0	meter / kWh
Midrail Length	0.006	meter / kW	0	meter / kWh
Maximum Traction Power	-0.10	kW / kW	0	kW / kWh
MBiW	0.5	kg / kW	0	kg / kWh
MCls	0.0	kg / kW	0	kg / kWh
MDrv	0.3	kg / kW	0	kg / kWh
Mint	0.0	kg / kW	0	kg / kWh
Msusp	2.7	kg / kW	0	kg / kWh
Mtransmission	0.2	kg / kW	0	kg / kWh
Muncat	0.9	kg / kW	0	kg / kWh

Table O.3 Sensitivity Gradient Results for Motor Power and Battery Capacity (Post-Optimization)

REFERENCES

1. SAE J1100 NOV2009 surface vehicle recommended practice (R): Motor vehicle dimensions(2009). . Warrendale, PA, USA: SAE.
2. Goettlicher, C., & Trecapelli, A. A. (2007). Conditions for significant efficiency improvement in the product development chain by the application of integrated virtual engineering. SAE World Congress, Detroit Michigan, CAD/CAM/CAE Technology, Digital Modeling, Virtual Development and Engineering (SP-2072)
3. Khalid, A. S. (2006). Development and implementation of rotorcraft preliminary design methodology using multidisciplinary design optimization. (Georgia Institute of Technology, Georgia Institute of Technology). ProQuest Dissertations and Theses, Retrieved from http://search.proquest.com/docview/305333271?accountid=6167
4. Calkins, D. E., Su, W., & Chan, W. T. (1998).A design rule-based tool for automobile systems design. SP-1318, SAE International Congress and Exposition
5. Venhovens, P. J., & Mau, R. (2011). Deep orange--A framework for research, education and collaboration for a sustainable automotive industry. SAE Transactions, (SAE 2011 World Congress)
6. Ury, A. B. (2009). The top 10 best-selling cars of all time. Retrieved 11/10, 2011, from http://news.wyotech.edu/post/2009/07/top-10-best-selling-cars
7. Clarke, W. (2011). Top 10 best-selling vehicles for 2010. Retrieved 08/20, 2011, from http://www.edmunds.com/car-reviews/top-10/top-10-best-selling-vehicles-for-2010.html

8. FANG broad agency announcement (BAA)(2011). . Arlington, VA USA: DARPA/Tactical Technology Office (TTO).
9. META-II broad agency announcement (BAA)(2010). Arlington, VA USA: DARPA/Tactical Technology Office (TTO).
10. RAMSIS in CATIA V5 Training Manual. Human Solutions, Kaiserslautern, Germany, 2009.
11. Colton, J. S. et al. (1990). The requirements for an object-oriented vehicle model. Atlanta: School of Mechanical Engineering, Georgia Institute of Technology.
12. Akao, Y. (1994). Development History of Quality Function Deployment. Tokyo, Japan: Asian Productivity Organization.
13. Yanni, T., & Venhovens, P. J. (2010). Impact and sensitivity of vehicle design parameters on fuel economy estimates. SP-2292, SAE 2010 World Congress
14. Allen, R. W., Klyde, D. H., Rosenthal, T. J., & Smith, D. M. (2003). Estimation of passenger vehicle inertial properties and their effect on stability and handling. SAE Transactions, 112(Journal of Passenger Cars--Mechanical Systems)
15. Ouellette, M. P. (1992). Form verification for the conceptual design of complex mechanical systems. (Ph.D., Georgia Institute of Technology).
16. Rinderle, J. R. (1987). Function and form relationships; A basis for preliminary design. Proceedings of the NSF Workshop on the Design Process, , 295-312.
17. Rodenacker, W. G. (1976).Design methodology. Berlin: Springer-Verlag Publishing.

18. Colton, J. S., Fadel, G. M.. (1992). Implementation and testing of an object oriented vehicle for conceptual design. Atlanta: School of Mechanical Engineering, Georgia Institute of Technology.
19. Sobieski, J. (1988). Optimization to decomposition: A step from hierarchic to non-hierarchic systems (NASA memorandum 101494)
20. Sobieski, J. (1991). Optimization by decomposition in structural and multidisciplinary applications
21. Fadel, G. M., Riley, M. F., &Barthelemy, J. M. (1990). Two point exponential approximation method for structural optimization.Structural Optimization, (Structural Optimization 2), 117-124.
22. Venkataraman, P. (2009). Applied optimization with MATLAB programming (2nd ed.). Hoboken, NJ USA: John Wiley and Sons, Inc.
23. RADIOSS / optistruct 9.0 user's guide(2008). . Troy, MI, USA: Altair Engineering
24. Gruber, T. (1993). Toward principles for the design of ontologies used for knowledge sharing.International Journal Human-Computer Studies, 43(5-6), 907-928.
25. Zisko, A. (2008). Knowledge-based model for integrated tall building design factors. (University of Illinois at Urbana-Champaign, University of Illinois at Urbana-Champaign).ProQuest Dissertations and Theses, Retrieved from http://search.proquest.com/docview/304625081?accountid=6167

26. Cumming, H., & Lu, Y. (2003). Computer-aided vehicle design and packaging using standard naming design methodology. SP-1785, SAE 2003 World Congress
27. Mocko, G.,M. (2006). A knowledge framework for integrating multiple perspectives in decision-centric design. (Georgia Institute of Technology, Georgia Institute of Technology). ProQuest Dissertations and Theses, Retrieved from http://search.proquest.com/docview/305330388?accountid=6167
28. Chapman, C. B., & Pinfold, M. (2001). The application of a knowledge based engineering approach to the rapid design and analysis of an automotive structure.Advances in Engineering Software, 32(12), 903-912.doi:DOI: 10.1016/S0965-9978(01)00041-2
29. Pinfold, M., & Chapman, C. (2001).The application of KBE techniques to the FE model creation of an automotive body structure.Computers in Industry, 44(1), 1-10.doi:DOI: 10.1016/S0166-3615(00)00079-8
30. Robertson, T., Prasad, B., &Duggirala, R. (1994).A knowledge based engineering method to integrate metal forming process design and simulation. Proceedings of the ASME Database Symposium, Engineering Data Management: Integrating the Engineering Enterprise, 41-50.
31. Haghighi, K., & Kang, E. (1995). A knowledge based approach to the adaptive finite element analysis.IMA Volumes in Mathematics and its Applications, 75, 267-276.

32. Jones, M., Price, M., &Butlin, G. (1995).Geometry management support for automeshing. Proceedings of the 4th International Meshing Roundtable, , 153-164.
33. Heinz, A. (1996). 777 rule based design: Integrated fuselage system. International ICAD Users Group Conference
34. Gay, P. (2000). Achieving competitive advantage through knowledge-based engineering--A best practise guide. London, UK: DTI.
35. El-Sayed, M., & Song, D. Automotive performance optimization. SP1324 SAE Transactions, 107(SAE International Congress and Exposition Journal of Passenger Cars)
36. Vanderplaats Research & Development, Inc. (VR&D) (2013). Design Optimization Tools (DOT) informational brochure retrieved from http://www.vrand.com/sites/default/files/pub/DOT%20Brochure.pdf
37. EPA (2009).Light-Duty Automotive Technology, Carbon Dioxide Emissions, and Fuel Economy Trends: 1975 through 2009.
38. SolidThinking user manual: Modeling(2011). SolidThinking Inc.
39. Bhise, V., Kridli, G., Mamoola, H., Devaraj, S., Pillai, A., &Shulze, R. (2004). Development of a parametric model for advanced vehicle design. SP-1858, SAE 2004 World Congress and Exhibition
40. Bhise, V., &Pillai, A. A parametric model for automotive packaging and ergonomics design

41. Anemaat, W., Kaushik, B., Hale, R. D., &Ramabadran, N. (2006).A knowledge-based design framework for aircraft conceptual and preliminary design. SAE Transactions, 115
42. Anemaat, W. A. J. (2007).A knowledge-based design framework for airplane conceptual and preliminary design. (University of Kansas, University of Kansas). ProQuest Dissertations and Theses, Retrieved from http://search.proquest.com/docview/304846662?accountid=6167
43. Code of Federal Regulations, Title 14, Part 23 -- Airworthiness Standards: Normal, Utility, Acrobatic and Commuter Category Airplanes, Code of Federal RegulationsU.S.C. (2011).
44. Code of Federal Regulations Title 14, Part 25--Airworthiness Standards: Transport Category Airplanes, (2011).
45. Huang, X. (2006). A prototype computerized synthesis methodology for generic space access vehicle (SAV) conceptual design. (The University of Oklahoma, The University of Oklahoma).ProQuest Dissertations and Theses, Retrieved from http://search.proquest.com/docview/305303083?accountid=6167
46. Chudoba, B. (2004). Managerial implications of generic flight vehicle synthesis.
47. Rao, S. S. (1996).Engineering optimization: Theory and practice (3rd ed.). New York, NY USA: John Wiley & Sons, Inc.
48. Malen, D. E. (2011).Fundamentals of automobile body structure design. Warrendale, PA USA: SAE International.

49. Table for estimating aerodynamic drag based on visual characteristics.(1969 (Reprinted in Industrial Design, 1977)). Society of Automotive Engineers Journal, (June 1969)

50. Malen, D.E., Reddy K (2007). Preliminary vehicle mass estimation using empirical subsystem influence coefficients. Auto/Steel Partnership. Southfield, Michigan

51. NHTSA vehicle parameter database., 2011, from http://mreed.umtri.umich.edu/mreed/downloads.html#vehicle_parameter_database

52. Motor Vehicle Manufacturers Association (1980 - 2006). Vehicle information sheets for assorted vehicles. MVMA: Troy, MI USA.

53. Fadel, G. (2012). Multi-criteria optimization and decision making. Course notes for ME 871: Engineering Optimization. Clemson University, Clemson, SC USA.

54. Mau, R.J. (2012). Vehicle parametric modeling and target assessment. Unpublished Notes, CU-ICAR, Greenville, South Carolina, USA.

55. Reed MP Schneider LW Ricci LL. Survey of auto seat design recommendations for improved comfort. Report, University of Michigan Transportation Research Institute, Ann Arbor, Michigan, USA, 1994

56. Allen, R. W., Klyde, D. H., Rosenthal, T. J., & Smith, D. M. (2003). Estimation of passenger vehicle inertial properties and their effect on stability and handling. SAE Transactions, 112(Journal of Passenger Cars--Mechanical Systems)

57. SAE J826:2008. Devices for use in defining and measuring vehicle seating accommodation.

58. Venhovens PJ. Systems integration concepts and methods: vehicle interior/occupant packaging (course notes). CU-ICAR, Greenville, South Carolina, USA, 2011.

59. SAE J1517:2011. Driver selected seat position.

60. NACM-92805 (TC):2005. Tire chain specifications.

61. Code of Federal Regulations, Title 49 Part 523.2:2012 Definitions

62. Venhovens PJ. Systems integration concepts and methods: vehicle exterior packaging (course notes). CU-ICAR, Greenville, South Carolina, USA, 2011.

63. Genta G. Motor vehicle dynamics modeling and simulation. Singapore: World Scientific, Singapore, 1997.

64. Gillespie TD. Fundamentals of vehicle dynamics. Warrendale: Society of Automotive Engineers, 1992.

65. Motor Industry Research Association (MIRA). Table for estimating aerodynamic drag based on visual characteristics. SAE Int. J. 1969.

66. Mau, R.J., Venhovens, P.J. (2013). Development of a consistent continuum of vehicle dimensional parameters for optimization and simulation. IMechE Part D: Journal of Automotive Engineering.

67. Hershman, L.L. (2001). The U.S. new car assessment program (NCAP): past, present and future. Paper No. 390, National Highway Traffic and Safety Administration (NHTSA). Washington D.C., USA.

68. Lightweight Front End Structure: Phase I & II -- Final Report. 2005, Auto/Steel Partnership, Southfield, MI USA.

69. IIHS (2012). Moderate overlap frontal crashworthiness evaluation crash test protocol (version XIV). Insurance Institute for Highway Safety, Arlington, VA USA.

70. Venhovens P.J(2009). Systems integration concepts and methods: safety part I (course notes). CU-ICAR, Greenville, South Carolina, USA.

71. Road and Track Magazine. http://www.roadandtrack.com/

72. Car and Driver Magazine. http://www.caranddriver.com/

73. Code of Federal Regulations, Title 40 Part 600--Fuel Economy of Motor Vehicles

74. Venhovens P.J. (2009). Automotive Systems and Functions: Performance (course notes). CU-ICAR, Greenville, South Carolina, USA.

75. Venhovens P.J. (2011). Automotive Systems and Functions: Energy Efficiency (course notes). CU-ICAR, Greenville, South Carolina, USA.

76. Mau, R.J., Venhovens, P.J. (2010). Deep Orange Pilot Project Final Team Evidence Document. CU-ICAR, Greenville, South Carolina, USA.

77. AutoPacific Group (2013). www.autopacific.com

78. Hyde, J. (2011). The death of the Ford Crown Victoria is a sad day for America. http://jalopnik.com/5840709/the-death-of-the-ford-crown-victoria-is-a-sad-day-for-america

79. California Air Pollution Control Laws--2012 Blue Book. www.arb.ca.gov/bluebook/bb12/bb12htm.

80. Australian Vehicle Standards Rules 1999. http://www.ntc.gov.au/filemedia/Reforms/AustralianVehicleStandardsRules1.pdf

81. AutoPacific Survey Results (2013). http://www.autopacific.com.

82. Venhovens, PJ (2013). Analysis of AutoPacific Survey Results (Unpublished notes).

83. Insurance Institute for Highway Safety (2010). Bumper Test and Rating Protocol. Arlington, VA, USA.